

PROGRESS TOWARD THE TOTAL SYNTHESIS OF HMP-Y1 AND HIBARIMICINONE

By

Ian M. Romaine

Dissertation

Submitted to the Faculty of the
Graduate School of Vanderbilt University
in partial fulfillment of the requirements

for the degree of

DOCTOR OF PHILOSOPHY

in

Chemistry

May, 2011

Nashville, Tennessee

Approved:

Professor Gary A. Sulikowski

Professor Michael P. Stone

Professor Piotr Kaszynski

Professor Brian O. Bachmann

For Amber and J.R.

ACKNOWLEDGEMENTS

Many people have aided and lifted me up along my graduate career. So much so, I cannot possibly thank everyone; but there are several people that I need to thank. First and foremost is Professor Gary Sulikowski. You have always pushed me to become a better chemist and provided me with a pathway to achieve that goal. I am truly grateful for the members of my committee, Brian Bachmann, Petro Kaszynski, and Michael Stone. Each have always had an open door policy and have been great resources for information and advice. I am also truly grateful to Craig Lindsley for open access to instrumentation. I owe many thanks to Prasad Polavarapu for conversations on atropisomers and the assignment of absolute stereochemistry about the biaryl bond.

There have been several that have helped me greatly throughout this process. Don Stec has always been ready and willing to assist in any and all needs concerning NMR. Chris Denicola and Nathan Kett have been invaluable with support in chiral chromatography. Electronic Circular Dichroism (ECD) and Vibrational Circular Dichroism (VCD) would not have been possible without Ana Petrovic and Ganesh Shanmugam. You (Sonny) Du has spent many hours teaching me the skill set of fermentation.

I have had a great cast of group members working along beside me on the hibiramicin project, Daren Engers, Jonathon Hempel, and Kwango Kim. I would like to single out Kim as he started me in the right direction and taught me a great many things about chemistry. I would also like to thank the entire Sulikowski group, who have made a truly unique and enjoyable work environment. Among other I would like to thank Brian Smith, Jingqi Wang, Steve Townsend, Brandon Dorah, Qingsong Liu, Aleksandra Baranczak, Stephen Chau, Shawn Deguire, Hiroki Tanimoto. Jesse Teske, Bruce Melancon, Victor Ghidu, and Weidong Zang. All have played a great role in helping me along the path to becoming a better scientist.

I would not have made it through any of this process without the love and support of my family. Thank you for always giving me the strength to venture out by knowing you will always be there to help pick me up. Lastly I want to thank Amber Romaine for riding the rollercoaster that is research with me and for providing me perspective on what is our life together.

TABLE OF CONTENTS

	Page
DEDICATION	ii
ACKNOWLEDGEMENTS	iii
LIST OF FIGURES	viii
LIST OF SCHEMES	xiii
Chapter	
I. BIARYL AND RELATED SYMMETRICAL DIMERS IN NATURE	1
Structure and Nomenclature	1
Atropisomerism within Dimeric Natural Products	3
Related aromatic dimers that have not been synthesized	4
Totosachryson Dimers in Nature	4
Viriditoxin	5
Related aromatic dimers that have been synthesized	5
Turriane	5
Masticophorenes A and B	6
Gossypol	9
Crisamicin A	11
Biphyscion	13
Cardinalin 3	14
Bioxanthracene ES 242	16
Nigerone	17
Calphostin D	19
Michellamine A and B	21
Rugulosin A	23
Isolation, Structure and Biological Activity of Hibarimicins	27
Angelmicin B	27
Isolation and Biological Activity of the Hibarimicins	27
Structure Elucidation	28

Biosynthesis	29
Models that demonstrate Hibiramicin Atropisomers	33
Hydroxyisodiospyrin	33
Roush's Model of the Angelmicin Core	34
Sulikowski Model of the Hibarimicin Core	35
II. SYNTHETIC METHODS DIRECTED TOWARD DIMERIC BIARYL NATURAL PRODUCTS.....	38
Synthetic Methods for Formation of Biaryl Carbon-Carbon Bonds.	38
Ullmann Coupling.....	38
Other Oxidative Coupling	39
Methods to Arrive at a Single Atropisomer.....	41
Resolution	41
Auxiliary Assisted Resolution	41
Desymmetrization	43
Dynamic Resolution	44
Dynamic Kinetic Resolution	44
Dynamic Thermodynamic Resolution	46
Direct Asymmetric coupling.....	48
Structural Restraints.....	48
Chiral Tethers.....	49
Oxazolidine Coupling.....	50
Copper / Diamine Complex	51
Asymmetric Suzuki Coupling	53
Synthetic Analysis of HMP-Y1 / Hibarimicins and Precursors Studies.....	54
Conversion of HMP-Y1 to Hibarimicinone	54
Synthetic Approaches to Dimeric Natural Products	55
Analysis of Two Directional Approach	56
Previous Work on Decalin	57
Roush	57
Mootoo.....	59
Sulikowski/Lee	61
Sulikowski/Kim	62
Sulikowski/Engers/Hempel.....	64
Two Directional Approach.....	66

Annulation Approach.....	66
Annulation Studies	67
Racemic Biaryl Formation	71
Sequential Two Annulation Approach.....	73
Sequential Two Annulation Studies.....	74
Resolution of Atropisomers and Assignment of Absolute Stereochemistry	76
Mosher Ester Formation.....	76
Separation of Atropo-enantiomers.....	79
Approaches to a Single Atropisomer	81
Copper diamine	81
Kozlowski Coupling	82
Dynamic Thermodynamic Resolution	83
Tentative Assigning the Absolute Stereochemistry of HMP-Y6	85
III. A BIOMIMETIC APPROACH TO HMP-Y1	89
Problems in Oxidative Coupling	89
Regioselectivity in Oxidative Coupling.....	89
Enzymatic solution to Stereochemistry in Biaryl Coupling	92
Over Oxidation in Coupling	94
Preliminary Studies Directed Toward HMP-Y1.....	95
Approaches to Oxidative coupling of Phenol	95
Silicon Tether	97
Attempts at Naphthol Coupling.....	98
IV. ANALYSIS AND PROGRESS TOWARD ABCD RING SYSTEM	101
Summary and proposed future directions	101
Diels-Alder Route to Tetracycle	102
Approach to Aryl Bromide	102
V. EXPERIMENTAL	106
REFERENCES.....	155
APPENDIX	170

LIST OF FIGURES

Figure	Page
1. Nomenclature for <i>aR/aS</i> and <i>M/P</i> Determination of Atropisomers.	2
2. Examples of Atropisomers Found in Nature.	3
3. Torosachryson Dimers in Nature.	4
4. Proposed and Revised Structure of Viriditoxin.	5
5. Structures of the Hibarimicins.	29
6. Benzyl Protons of 2.189 in CDCl ₃ and D ₆ -DMSO.	78
7. X-ray Crystal Structure of the Faster Eluting bis-Mosher Ester.	78
8. ECD Spectra of Phenol (<i>aS</i>)- 2.190 and (<i>aR</i>)- 2.190	79
9. Trace of Chiral Separation of bis-Phenyl Ester 2.172 on OD Chiral Column ...	80
10. ¹ H NMR Analysis of an Isomeric Mixture of (<i>aS</i>)- 2.204 and (<i>aR</i>)- 2.204	85
11. CD Spectra of (<i>aR</i>)- 2.187 (<i>aS</i>)- 2.187	86
12. CD Spectra of (<i>aS</i>)- 2.187 and Crude HMP-Y6 (1.147) in MeOH.	87
13. Proposed Silicon Tether to Direct Coupling in HMP-Y1	92
A1 300 MHz ¹ H NMR of 3-Bromo-4-hydroxy-5-methoxybenzaldehyde in CDCl ₃	170
A2 75 MHz ¹³ C NMR of 3-Bromo-4-hydroxy-5-methoxybenzaldehyde in CDCl ₃	171
A3 300 MHz ¹ H NMR of 2.149 in CDCl ₃	172
A4 75 MHz ¹³ C NMR of 2.149 in CDCl ₃	173
A5 300 MHz ¹ H NMR of 2.150 in CDCl ₃	174
A6 75 MHz ¹³ C NMR of 2.150 in CDCl ₃	175
A7 300 MHz ¹ H NMR of 5-(Benzyloxy)-1-bromo-2,3-dimethoxybenzene in CDCl ₃	176
A8 75 MHz ¹³ C NMR of 5-(Benzyloxy)-1-bromo-2,3-dimethoxybenzene in CDCl ₃	177

A9	300 MHz ^1H NMR of 2.151 in CDCl_3	178
A10	75 MHz ^{13}C NMR of 2.151 in CDCl_3	179
A11	300 MHz ^1H NMR of 2.152 in CDCl_3	180
A12	75 MHz ^{13}C NMR of 2.152 in CDCl_3	181
A13	300 MHz ^1H NMR of 2.153 in CDCl_3	182
A14	300 MHz ^1H NMR of 2.154 in CDCl_3	183
A15	75 MHz ^{13}C NMR of 2.154 in CDCl_3	184
A16	300 MHz ^1H NMR of Phenyl 6-hydroxy-3,4-dimethoxy-2-methylbenzoate in CDCl_3	185
A17	75 MHz ^{13}C NMR of Phenyl 6-hydroxy-3,4-dimethoxy-2-methylbenzoate in CDCl_3	186
A18	300 MHz ^1H NMR of 2.158 in CDCl_3	187
A19	75 MHz ^{13}C NMR of 2.158 in CDCl_3	188
A20	300 MHz ^1H NMR of 2.159 in CDCl_3	189
A21	75 MHz ^{13}C NMR of 2.159 in CDCl_3	190
A22	300 MHz ^1H NMR of 2.156 in CDCl_3	191
A23	300 MHz ^1H NMR of 2.157 in CDCl_3	192
A24	300 MHz ^1H NMR of Phenyl 6-(tert-butoxycarbonyloxy)-3,4-dimethoxy-2- methylbenzoate in CDCl_3	193
A25	25. 300 MHz ^1H NMR of Phenyl 6-(tert-butyldimethylsilyloxy)-3,4-dimethoxy-2- methylbenzoate in CDCl_3	194
A26	400 MHz ^1H NMR of 2.160 in CDCl_3	195
A27	100 MHz ^{13}C NMR of 2.160 in CDCl_3	196
A28	400 MHz ^1H NMR of 2.161 in CDCl_3	197
A29	100 MHz ^{13}C of 2.161 in CDCl_3	198
A30	400 MHz ^1H NMR of 2.164 in CDCl_3	199

A31	400 MHz ^1H NMR of 2.160 in CDCl_3 .	200
A32	100 MHz ^{13}C of 2.165 in CDCl_3 .	201
A33	400 MHz ^1H NMR of 2.166 in CDCl_3 .	202
A34	100 MHz ^{13}C NMR of 2.166 in CDCl_3 .	203
A35	400 MHz ^1H NMR of 5,8,9-trihydroxy-6-methoxy-3,4-dihydroanthracen-1(2H)-one in CDCl_3 .	204
A36	400 MHz ^1H NMR of 2.167 in CDCl_3 .	205
A37	400 MHz ^1H NMR of 2.168 . in CDCl_3 .	206
A38	100 MHz ^{13}C NMR of 2.168 in CDCl_3 .	207
A39	400 MHz ^1H NMR of 2.169 . in CDCl_3 .	208
A40	100 MHz ^{13}C NMR of 2.169 in CDCl_3 .	209
A41	400 MHz ^1H NMR of 2.170 in CDCl_3 .	210
A42	100 MHz ^{13}C NMR of 2.170 in CDCl_3 .	211
A43	400 MHz ^1H NMR of 2.171 in CDCl_3 .	212
A44	100 MHz ^{13}C NMR of 2.171 in CDCl_3 .	213
A45	400 MHz ^1H NMR of 2.172 in CDCl_3 .	214
A46	100 MHz ^{13}C NMR of 2.172 in CDCl_3 .	215
A47	400 MHz ^1H NMR of 2.176 in CDCl_3 .	216
A48	400 MHz ^1H NMR of 2.177 in CDCl_3 .	217
A49	75 MHz ^{13}C NMR of 2.177 in CDCl_3 .	218
A50	400 MHz ^1H NMR of 2.178 in CDCl_3 .	219
A51	400 MHz ^1H NMR of 2.179 in CDCl_3 .	220
A52	75 MHz ^{13}C NMR of 2.179 in CDCl_3 .	221
A53	400 MHz ^1H NMR of 2.181 in CDCl_3 .	222
A54	400 MHz ^1H NMR of 2.182 in CDCl_3 .	223
A55	400 MHz ^1H NMR of 2.183 in CDCl_3 .	224

A56	600 MHz ^1H NMR of 2.186 in CDCl_3	225
A57	150 MHz ^{13}C NMR of 2.186 in CDCl_3	226
A58	400 MHz ^1H NMR of 2.187 in CDCl_3	227
A59	100 MHz ^{13}C NMR of 2.187 in CDCl_3	228
A60	400 MHz ^1H NMR of 2.189 in CDCl_3	229
A61	100 MHz ^{13}C NMR of 2.189 in CDCl_3	230
A62	400 MHz ^1H NMR of 2.190 in CDCl_3	231
A63	100 MHz ^{13}C NMR of 2.190 in CDCl_3	232
A64	400 MHz ^1H NMR of Faster Eluting 2.191 in CDCl_3	233
A65	282 MHz ^{19}F NMR of Faster Eluting 2.191 in CDCl_3	234
A66	300 MHz ^1H NMR of Slower Eluting 2.191 in CDCl_3	235
A67	282 MHz ^{19}F NMR of Slower Eluting 2.191 in CDCl_3	236
A68	300 MHz ^1H NMR of (<i>aS</i>)- 2.192 in CDCl_3	237
A69	100 MHz ^{13}C NMR of (<i>aS</i>)- 2.192 in CDCl_3	238
A70	282 MHz ^{19}F NMR of (<i>aS</i>)- 2.192 in CDCl_3	239
A71	400 MHz ^1H NMR of (<i>aR</i>)- 2.192 in CDCl_3	240
A72	100 MHz ^{13}C NMR of (<i>aR</i>)- 2.192 in CDCl_3	241
A73	282 MHz ^{19}F NMR of (<i>aR</i>)- 2.192 in CDCl_3	242
A74	400 MHz ^1H NMR of 2.197 in CDCl_3	243
A75	100 MHz ^{13}C NMR of 2.197 in CDCl_3	244
A76	400 MHz ^1H NMR of 2.198 in CDCl_3	245
A77	100 MHz ^{13}C NMR of 2.198 in CDCl_3	246
A78	400 MHz ^1H NMR of 2.199 in CDCl_3	247
A79	100 MHz ^{13}C NMR of 2.199 in CDCl_3	248
A80	300 MHz ^1H NMR of 2.201 in CDCl_3	249
A81	100 MHz ^{13}C NMR of 2.201 in CDCl_3	250

A82	400 MHz ^1H NMR of 2.202 in CDCl_3	251
A83	100 MHz ^{13}C NMR of 2.202 in CDCl_3	252
A84	400 MHz ^1H NMR of 2.203 in CDCl_3	253
A85	400 MHz ^1H NMR of 2.203 in d_6 -Benzene.....	254
A86	100 MHz ^{13}C NMR of 2.203 in CDCl_3	255
A87	400 MHz ^1H NMR of (<i>aS</i>)- 2.204 in CDCl_3	256
A88	100 MHz ^{13}C NMR of (<i>aS</i>)- 2.204 in CDCl_3	257
A89	400 MHz ^1H NMR of (<i>aR</i>)- 2.204 in CDCl_3	258
A90	100 MHz ^{13}C NMR of (<i>aR</i>)- 2.204 in CDCl_3	259
A91	400 MHz ^1H NMR of 3.38 in CDCl_3	260
A92	100 MHz ^{13}C NMR of 3.38 in CDCl_3	261
A93	400 MHz ^1H NMR of 3.39 in CDCl_3	262
A94	100 MHz ^{13}C NMR of 3.39 in CDCl_3	263
A95	400 MHz ^1H NMR of 3.40 in CDCl_3	264
A96	100 MHz ^{13}C NMR of 3.40 in CDCl_3	265
A97	400 MHz ^1H NMR of 3.41 in CDCl_3	266
A98	100 MHz ^{13}C NMR of 3.41 in CDCl_3	267
A99	400 MHz ^1H NMR of 3.47 in CDCl_3	268
A100	100 MHz ^{13}C NMR of 3.47 in CDCl_3	269
A101	400 MHz ^1H NMR of 3.48 in CDCl_3	270
A102	100 MHz ^{13}C NMR of 3.48 in CDCl_3	271
A103	400 MHz ^1H NMR of 3.49 in CDCl_3	272
A104	100 MHz ^{13}C NMR of 3.49 in CDCl_3	273
A105	400 MHz ^1H NMR of 3.51 in CDCl_3	274
A106	400 MHz ^1H NMR of 3.52 in CDCl_3	275
A107	100 MHz ^{13}C NMR of 3.52 in CDCl_3	276

A108	400 MHz ^1H NMR of 4.8 in CDCl_3 .	277
A109	100 MHz ^{13}C NMR of 4.8 in CDCl_3 .	278
A110	400 MHz ^1H NMR of 4.9 in CDCl_3 .	279
A111	100 MHz ^{13}C NMR of 4.9 in CDCl_3 .	280
A112	400 MHz ^1H NMR of 4.11 in CDCl_3 .	281
A113	100 MHz ^{13}C NMR of 4.11 in CDCl_3 .	282
A114	400 MHz ^1H NMR of 4.12 in CDCl_3 .	283
A115	100 MHz ^{13}C NMR of 4.12 in CDCl_3 .	284
A116	400 MHz ^1H NMR of 4.13 in CDCl_3 .	285
A117	100 MHz ^{13}C NMR of 4.13 in CDCl_3 .	286

LIST OF SCHEMES

Schemes	Page
1. Biaryl Coupling Leading to the Turriane.	6
2. Bringmann's First Synthesis of Mastigophorenes A and B.	7
3. Bringmann's Dynamic Kinetic Resolution Approach to the Mastigophorenes.	8
4. Meyers Oxazoline Approach to the Mastigophorenes.	9
5. Edward's Synthesis of Gossypol.	10
6. Meyer's Synthesis of Gossypol.	11
7. Mechanism for Palladium Catalyzed Alkoxy carbonylative Annulations.	12
8. Yang's Synthesis of Crisamicin A.	13
9. Hauser's Synthesis of Biphyscion.	14
10. Brimble's Approach to the Cardinalins.	15
11. De Koning's Total Synthesis of Cardinalin 3.	16
12. Tatsuta's Synthesis of Bioxanthracene ES-242-4.	17
13. Asymmetric Synthesis of Nigerone by Kozłowski.	18
14. Broka's Approach to Calphostin D.	19
15. Proposed Lewis Acid Catalysed Dimerization.	21
16. Lipshutz Synthesis of Korupensamine A.	22
17. Convergent Total Synthesis of the Michellamines.	23
18. The Multistep "Cytoskryin Cascade."	25
19. Snider's Approach to Rugulosin Analogs.	26
20. The Proposed Biosynthesis of the Hibarimicins.	30
21. Plausible Pathway for Skeletal Rearrangement in the Hibarimicins.	32
22. Block Mutants that Describe the Biosynthetic Timeline of Hibarimicins.	33

23. Sargent's Synthesis of Aryl Quinone by a Meyers Oxazoline.	34
24. Roush's Model of Atropisomerism in Angelmicin.	35
25. Sulikowski Model of Atropisomerism in Hibarimicins.	36
26. Absolute Configuration of HMP-Y1 is Retained in Hibarimicinone.	37
27. A Mechanistic View of the Ullmann Coupling	38
28. Proposed Mechanism for the One Electron Oxidation of β -Naphthol (2.6).....	39
29. Mechanism of PIFA Oxidative Coupling.	40
30. Oxidative Coupling of Cuprates.....	40
31. Spring's Direct Lithiation and Cuprate Oxidation.	41
32. Example of Auxiliaries used in the Resolution of Atropisomers.	43
33. Desymmetrization and Kinetic Resolution Using Enzymatic and Non-Enzymatic methods.....	44
34. Mechanistic Analysis of Dynamic Kinetic Resolution.....	46
35. Proposal for the Mechanism of Dynamic Thermodynamic Resolution.	48
36. Atropo-diastereoselectivity under substrate control	49
37. Chiral Tethers of Miyano and Lipshutz.	50
38. Mechanism of Selectivity in the Meyers Chiral Oxazolidine Coupling.	51
39. Brussee's First Observed Enantioenriched Coupling of BINOL.	51
40. Proposed Catalytic Cycle of Kozlowski Coupling.....	53
41. Buchwald's Asymmetric Suzuki Coupling.....	54
42. Proposed Oxidative Conversion of HMP-Y1 to Hibarimicinone B.	55
43. Strategic Analysis of HMP-Y1.	56
44. Single Bis-Annulation Approach to HMP-Y1.....	57
45. Roush's Route to the <i>cis</i> -Decalin of the Hibarimicins.	59
46. Mootoo's Route to the <i>cis</i> -Decalin of the Hibarimicins.....	60
47. First Attempt of an Intramolecular Diels-Alder Reaction to Form the <i>cis</i> -Decalin.	62

48. Intermolecular Diels-Alder Route to <i>cis</i> -Decalin.	63
49. Kim's Progress Toward the <i>cis</i> -Decalin Ring System.	64
50. Engers/Hempel Approach to the <i>cis</i> -Decalin.	66
51. Original Annulations Performed by Hauser, Kraus, Staunton, and Weinreb.	67
52. Synthesis of Staunton-Weinreb Annulation Precursor.	68
53. Effect of Protecting Group on the Staunton-Weinreb Annulation.	69
54. Selective Demethylation Followed by Oxidation to Naphthyl Ring System.	70
55. Possible Mechanism for the Alpha Halogenations of Phenol 2.157	70
56. Oxidation and Demethylation to Naphthol Ring system 2.164	71
57. Biaryl Formation.	72
58. Methods to Form the bis-Phenyl Ester 2.170	73
59. Two bis-Annulation Approaches to HMP-Y1.	74
60. Attempts at a Two-Annulation Approach.	75
61. Synthesis of BCD-EFG Rings Model of HMP-Y1.	76
62. Synthesis of the Mono-Mosher's Ester.	77
63. Separation of Bis-Mosher Ester and Retention of Optical Activity.	79
64. Synthesis of Enantiopure bis-Phenyl Ester.	80
65. Spring Coupling with Chiral Diamines.	81
66. Biaryl Kozlowski Coupling.	82
67. Improved Route to Biaryl Phenol.	83
68. Dynamic Thermodynamic Resolution Conditions.	84
69. Synthesis of (<i>aS</i>)- 2.187 with Known Configuration about the Biaryl Axis.	86
70. Conversion of HMP-Y1 to a Single Atropo-diastereomer through Dynamic Thermodynamic Resolution.	88
71. Brimble's Studies Directed Toward Cardinalin 3.	90
72. Müller's Advantageous Unselective Phenolic Coupling.	91

73. Silicon Tether to Direct Regioselectivity in Oxidative Coupling.	91
74. Unsymmetrical Biaryl Coupling Through a Silicon Tether.	92
75. Cytochrome p-450 Oxidation to Provide Salutaridinone 3.18	93
76. Laccase Enzymatic Dimerization of Phenols.....	94
77. Over Oxidation and Side Products in Oxidative Coupling.....	95
78. Biomimetic Approach to HMP-Y1	96
79. Oxidative Coupling of the Phenol 3.19	97
80. Mechanistic Understanding of the Aluminum Phenolate Coupling.....	97
81. Unexpected Furan Formation and Possible Mechanism	98
82. Oxidative Coupling of Naphthyl Ring Systems	99
83. Biomimetic Oxidative Coupling Followed by Deracemization.	100
84. Biomimetic Approach to HMP-Y1	102
85. Two Routes to the Allyl Bromide 4.18	103
86. Hempel's Work Toward the Formation of the C17/C18 Bond	104
87. Future approaches to the Diels Alder.	105

CHAPTER I

BIARYL AND RELATED SYMMETRICAL DIMERS IN NATURE

Structure and Nomenclature

The number of natural products and biologically significant molecules identified that contain an axis of chirality has grown rapidly in recent history. The utility of axially chiral compounds range from medicinal uses like the antibiotic vancomycin¹ to asymmetric transformations using BINOL derivatives. Axially chiral compounds were first termed atropisomers in 1933 by Kuhn for the Greek words representing “knot” and “turn.” Atropisomers have piqued the interest of many in the scientific community since 1922 when Christie and Kenner² isolated the first stable biaryl atropisomer with the crystallization of 6,6'-dinitrobiphenyl-2,2'-dicarboxylic acid.

The ability to separate and isolate atropisomers depends on the rate of their interconversion. Atropisomers are observed on the nuclear magnetic resonance (NMR) time scale at room temperature if the half life exceed 10^{-2} seconds; while they are isolable at room temperature if the half life is above 1000 seconds.³ The nature, position, and number of substituents all affect the rate of interconversion of atropisomers. In general, biaryls that have tetra-*ortho*-substituents are stable at room temperature while biaryls with tri-*ortho*-substitution typically racemize just above room temperature.

There are two different sets of nomenclature commonly employed to assign the absolute configuration of a chiral biaryl compound⁴. The most common convention is the *R/S* nomenclature, denoted as *aR* and *aS* in axially chiral compounds. In this system the configuration is determined by first viewing a Newman projection down the biaryl bond as indicated in Figure 1. The front biaryl is vertical and assigned Conn-Ingold-

Prelog (CIP) priorities one and two, while the biaryl in the back is given CIP priorities three and four. Drawing an arc from the substituent with first priority to the substituent with the third priority, while passing through the second in a clockwise direction would be assigned *aR configuration* while, if the arc is in a counter clockwise direction, the configuration is assigned as *aS*. A second set of nomenclature is derived from protein nomenclature and designates an atropisomer as *M* (minus) or *P* (positive). The model for this system also looks down a Newman projection of the biaryl bond; however, moving from the highest priority on the front aryl ring directly to the highest priority on the back aryl ring in a 90° arc assigns *M* or *P* configuration.⁵ If the arc's movement is in a clockwise motion, the configuration is defined as *P* (positive) and, if it is a counterclockwise motion, the configuration is defined as *M* (minus). Relating the two assignments, the *aR* designation corresponds to *M* and the *aS* to the *P* configuration.

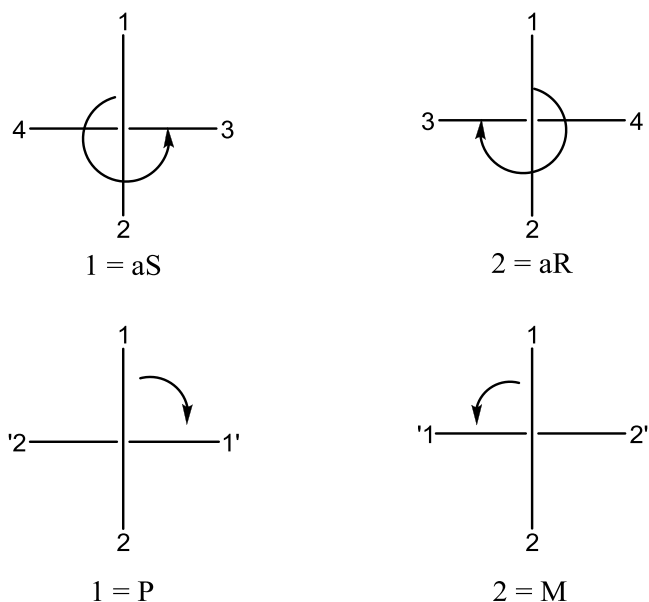


Figure 1: Nomenclature for *aR/aS* and *M/P* Determination of Atropisomers.

Atropisomerism within Dimeric Natural Products

Atropisomers in nature are seen in many different forms of chirality (eg. carbon-heteroatom, carbon-carbon bond). Two of the most common functionalities that show hindered bond rotation are biaryls and tri-substituted amide bonds. Nature continues to be a rich source for many different biaryl compounds that have significant uses either in their biological properties or structural novelty. Many examples of atropisomers in nature have been identified over the years (Figure 2). These examples vary from the hindered rotation of the ether linked chlorobenzene in the antibiotic vancomycin (**1.1**) to the nitrogen carbon bond in murrastifoline F (**1.2**). Other examples have varied from the simple biaryl linkage of gossypol (**1.3**) to that of the antiviral sanguiin H-5 (**1.4**). For the purpose of this dissertation we limit the discussion to natural products that are hypothetically derived in nature by the dimerization of monomers leading to symmetric dimers.

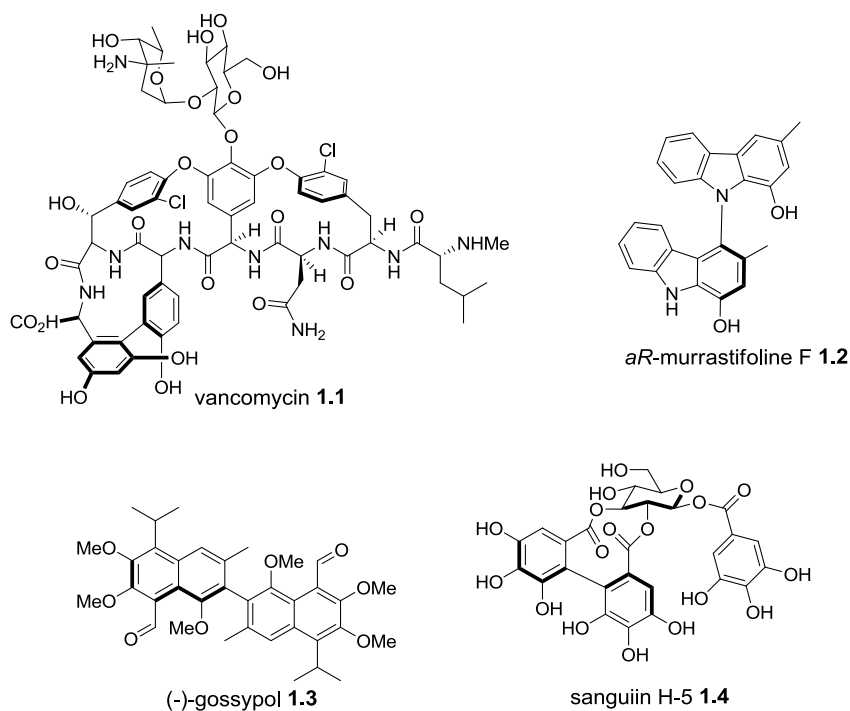


Figure 2. Examples of Atropisomers Found in Nature.

Torosachryson (1.5) has been isolated from several different natural sources. This molecule is interesting in that its dimer has also been isolated from a variety of natural sources, and the site of carbon-carbon bond formation leading to dimerization varies based on the source (Figure 3). When isolated from the Australian toadstool *Dermocybe* sp. WAT 24272,⁶ flavomannin (1.6) is symmetrically coupled at the C7 position. The toadstool *Dermocybe icterinoides* produces the symmetrically coupled atrovirin (1.7)⁷ via connection at the C5 position. The unsymmetrical phlegmacin B (1.8), produced through a coupling at the C5 and C7 positions, was first observed in the *Cortinarius* (*Phlegmacium*) *odorifer* Britz,⁸ and was later isolated from the seeds of the *Cassia torosa* Cavanilles plant.⁹ Each of these natural products is produced as racemic mixtures of atropisomers. Following resolution of each natural product, the individual enantiomers were assigned by analysis of their circular dichroism (CD) spectra.¹⁰

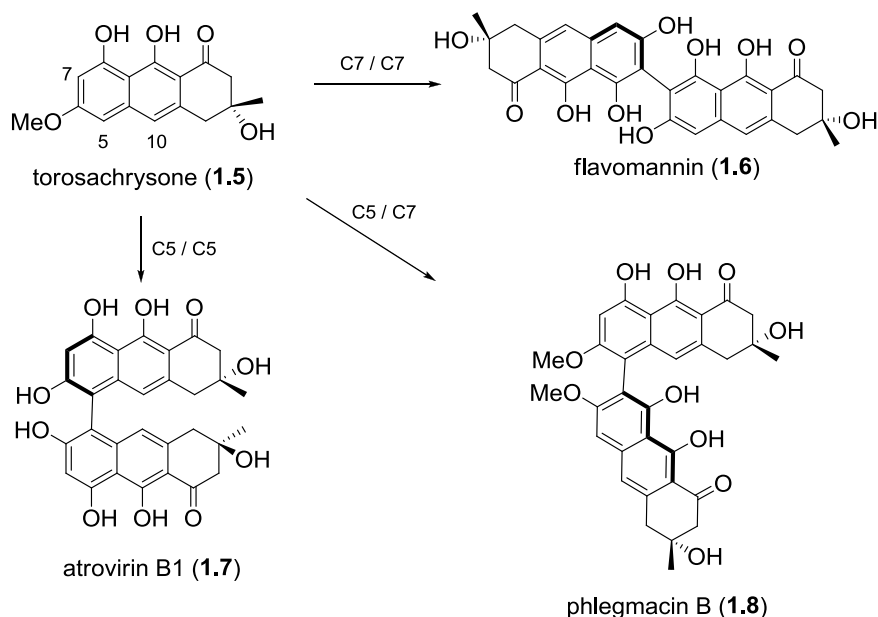


Figure 3. Torosachryson Dimers in Nature.

In screening for toxins isolated from *Aspergillus Viridi-nutans*, Lillehoj isolated a compound toxic to mice termed viriditoxin (**1.10**).¹¹ The structure was assigned based on NMR analysis, elemental analysis and infrared spectroscopy (Figure 4). In 1990, the structure was revised, moving the binaphthyl linkage from a 8,8' linkage to that of a 6,6' linkage based on observed NOE correlations between the proton at the 8 position and the two methyl ethers.¹² During the correction of the structure, viriditoxin was shown to be a single atropisomer and assigned the *aR* configuration. Viriditoxin was shown to inhibit FtsZ polymerization with an IC₅₀ of 8.2 μg/mL.¹³ Inhibition of FtsZ polymerization can lead to cell death, by inhibiting cell from division. Viriditoxin was also shown to exhibit broad-spectrum antibacterial activities against methicillin-resistant and vancomycin-resistant strains.

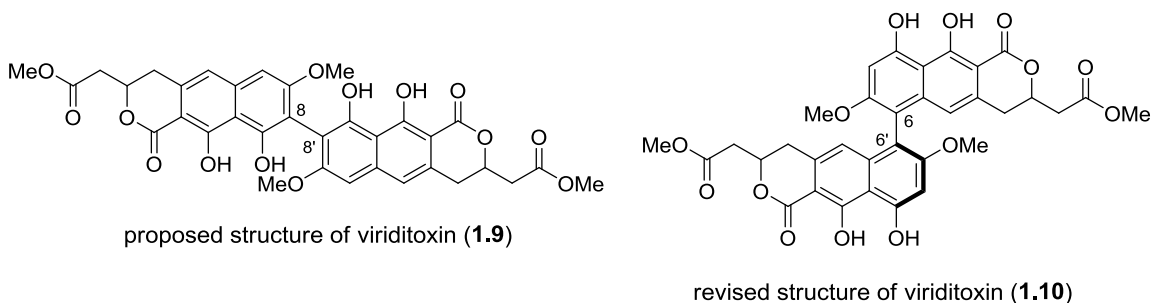
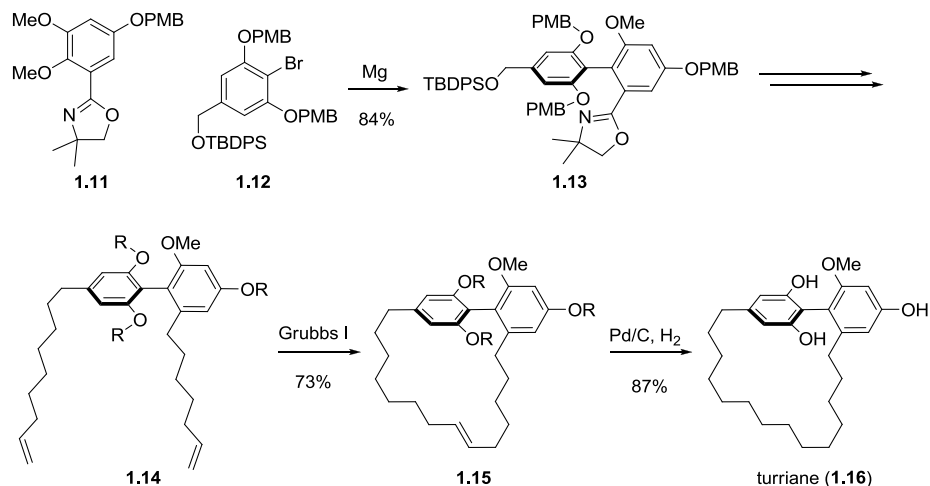


Figure 4. Proposed and Revised Structure of Viriditoxin.

The turrianes were isolated from the stem wood of the Australian tree *Grevillea striata* R. Br.¹⁴ and were shown to be potent DNA cleaving agents in the presence of Cu^{II}.¹⁵ This family of natural products, although not chiral due to the symmetry of the bisphenol, remains a synthetic challenge due to the tetra *ortho* substituted biaryls. This problem was solved by Fürstner with the aryl Grignard derived from **1.12** coupling with oxazoline **1.11** (Scheme 1). The coupling provided the biaryl **1.13** that was elaborated in

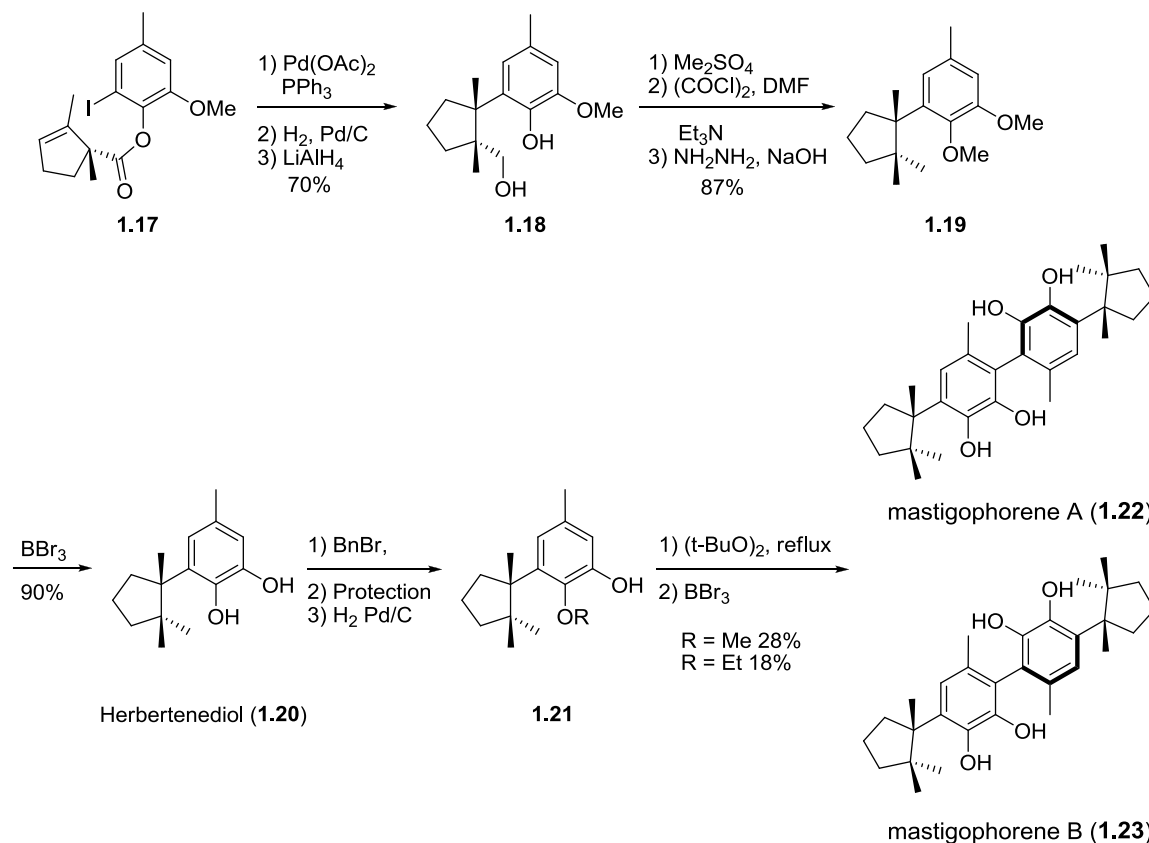
several steps to the bis-alkene **1.14**. Turriane **1.16** was then completed by ring closing metathesis, followed by concurrent reduction of the alkene and benzyl ethers.



Scheme 1. Biaryl Coupling Leading to the Turriane.

The biaryls mastigophorene A and B were isolated from the liverwort *Mastigophora diclados*.¹⁶ These compounds were found to have neurotrophic properties at 10^{-5} – 10^{-7} M. Mastigophorene A and B were determined to differ in configuration about the central biaryl bond. The mastigophorenes have been proposed to be derived from a one electron oxidative coupling of the natural product herbertenediol (**1.20**). Bringmann's¹⁷ first synthesis of the mastigophorene began with an intramolecular Heck reaction followed by reduction of the alkene and the lactone to provide the primary alcohol **1.18** (Scheme 2). The phenol was methylated, and the primary alcohol was reduced via the derived aldehyde under Wolff-Kishner conditions. Herbertenediol (**1.20**) was then completed by cleavage of the methyl ethers. The oxidative coupling substrate was then prepared by selective benzylation of a phenol to avoid quinone formation (**1.21**). The oxidative coupling was then accomplished with di-*t*-butyl peroxide, followed

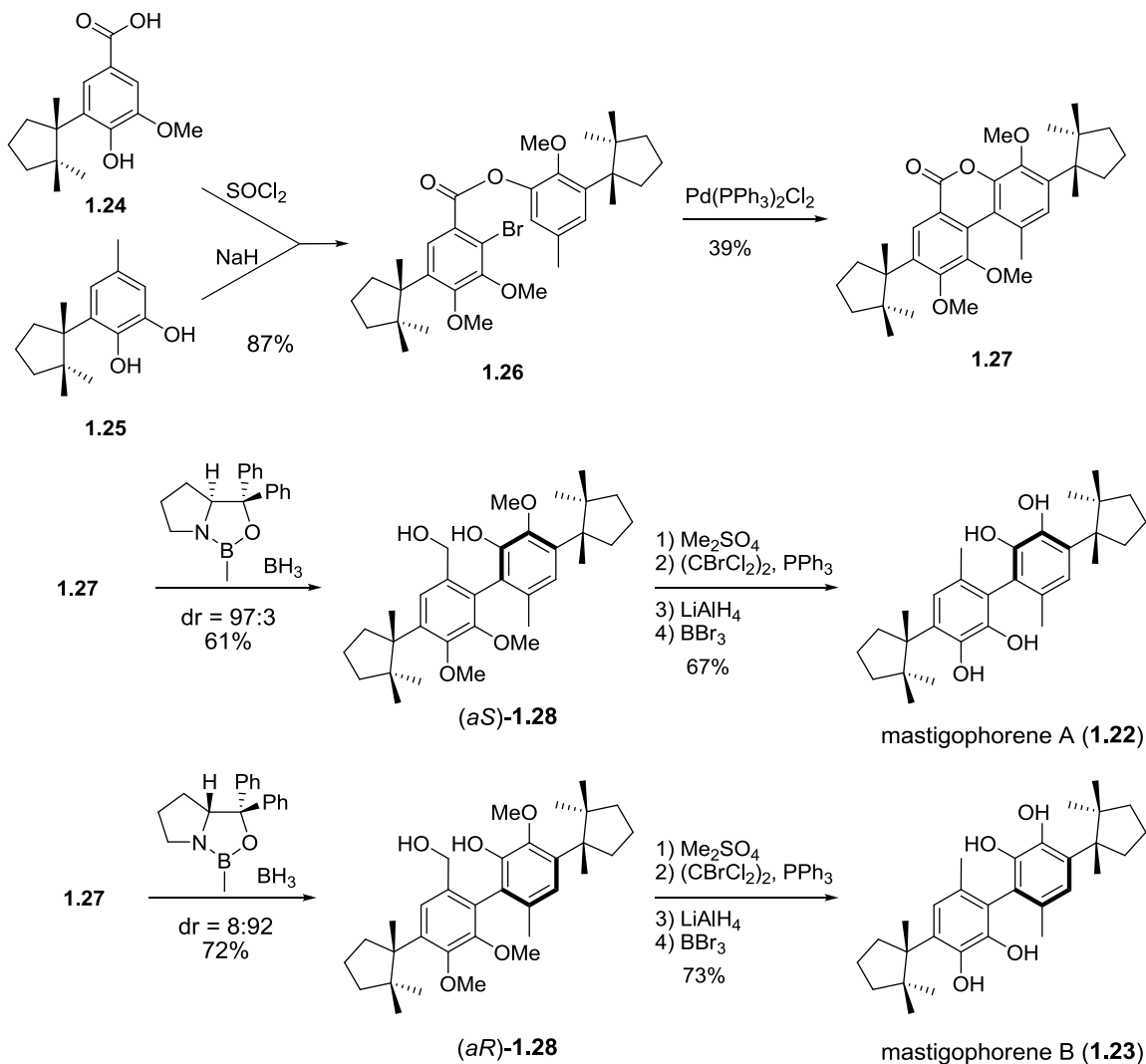
by BBr_3 mediated removal of the alkyl ethers. This sequence led to a mixture of mastigophorene A (**1.22**) and B (**1.23**).



Scheme 2. Bringmann's First Synthesis of Mastigophorenes A and B.

In a second approach to the mastigophorenes, Bringmann¹⁸ used a dynamic kinetic resolution to arrive at each individual atropo-diastereomer. The formation of the biaryl lactone **1.27** by a Pd-catalyzed intramolecular biaryl coupling furnished rapidly inter-converting atropisomers (Scheme 3). The rapidly converting atropisomers allow for the resolution of atropisomers through a stereoselective reduction using the Corey-Bakshi-Shibata (CBS) catalyst. The CBS reduction with *S*-oxaborolidine led to (*P*)-**1.28** with a *dr* of 97:3. Reduction of lactone **1.27** with *R*-oxaborolidine led to (*aR*)-**1.28** with a

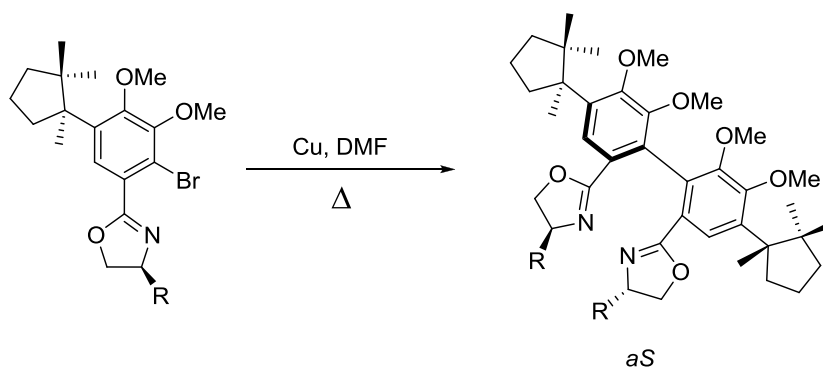
dr of 92:8. Then, as before, the atropisomer was taken forward to mastigophorene A (**1.22**) and B (**1.23**).



Scheme 3. Bringmann's Dynamic Kinetic Resolution Approach to the Mastigophorenes.

Following the Bringmann syntheses of the mastigophorenes, Meyers¹⁹ applied his oxazoline chemistry to the synthesis of the mastigophorenes (Scheme 4). A series of chiral oxazolines were prepared starting from the corresponding acid (Scheme 4). An Ullmann coupling was performed on a variety of oxazolines (**1.29-1.33**) to arrive at the

biaryl precursor to the mastigophorenes (**1.34-1.38**). One of the interesting aspects of this work was that the smaller the auxiliary, the greater the level of selectivity in the biaryl formation. This phenomenon had not been previously observed. As in other approaches, the oxazoline could be cleaved to the acid and reduced to the methyl group as reported earlier.²⁰ This furnished a direct synthesis of mastigophorene A (**1.22**) in an atropselective manner.

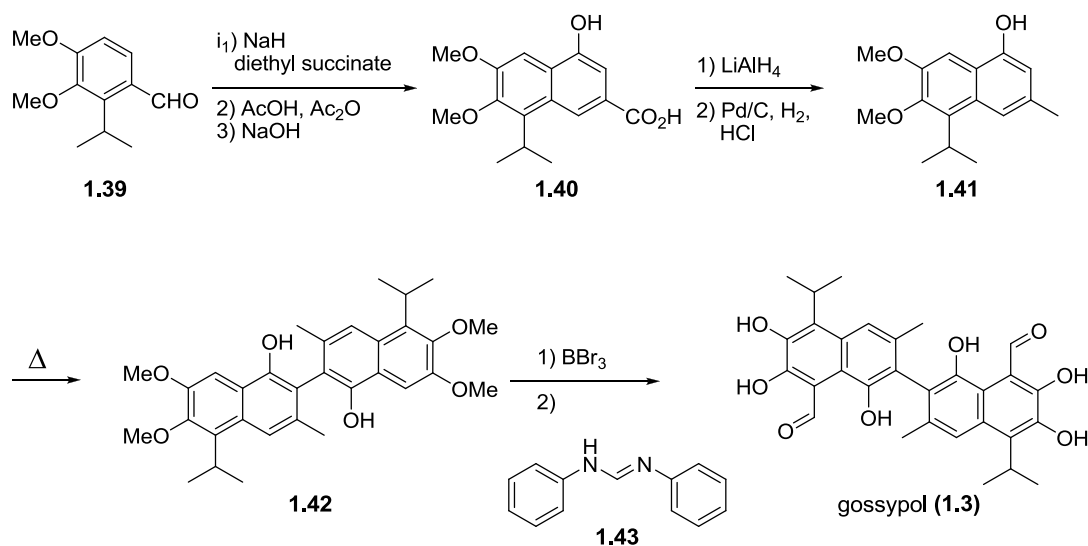


	R	%	<i>aS</i>	<i>aR</i>
1.29	<i>t</i> -Bu	85	3	1
1.30	Phenyl		4	1
1.31	<i>i</i> -Pr	85	6.4	1
1.32	Et		7.1	1
1.33	Me	75	7.2	1

Scheme 4. Meyers Oxazoline Approach to the Mastigophorenes.

Of all the biaryl natural products known, gossypol (**1.3**) has garnered much attention from the scientific community since its isolation in the late 19th century. Gossypol (**1.3**) was first isolated by Longmore and Marchlewski²¹ from cotton seed oil, but it was not identified as the toxic substance until 1915.²² The absolute configuration of gossypol was not elucidated until 1938 by Adams.²³ While both enantiomers were found in nature, each had a different biological effect. The *aR* antipode is used in China as an oral contraceptive²⁴, while theaSantipode has been used as a treatment for

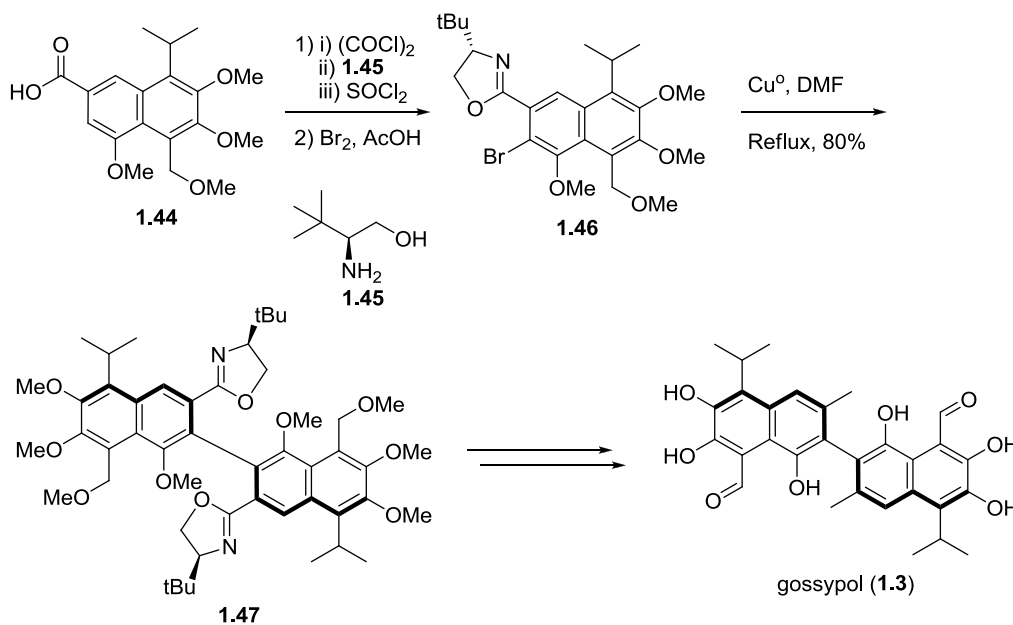
herpes,²⁵ among other activities. The structure of gossypol was not confirmed until Edwards^{26 27} completed the total synthesis in 1958 (Scheme 5). This synthesis started with the condensation of diethyl succinate and benzaldehyde **1.39**. This product was then treated with acetic anhydride and saponified to afford naphthyl derivative **1.40**. Reduction of carboxylic acid **1.40** to a methyl group was followed by a phenolic coupling to arrive at binaphthyl **1.42** as a racemate. Cleavage of the methyl ethers and installation of the aldehyde completed the first total synthesis of (±)-gossypol (**1.3**).



Scheme 5. Edward's Synthesis of Gossypol.

The first enantioselective synthesis of gossypol was accomplished by Meyers²⁸ using a chiral oxazoline auxiliary. (*S*)-(+)-*tert*-leucinol (**1.45**) was condensed with the acid chloride derived from **1.44**. The derived amide was dehydrated to form the oxazoline (**1.46**) (Scheme 6). Selective bromination was followed by an Ullmann coupling to arrive at the *aS*-**1.47** with a 11:1 atropo-diastereoselectivity.²⁹ The selectivity observed in this coupling results from the steric hindrance of the *t*-butyl group moving away from the aromatic ring in the bond forming step. The synthesis of gossypol was

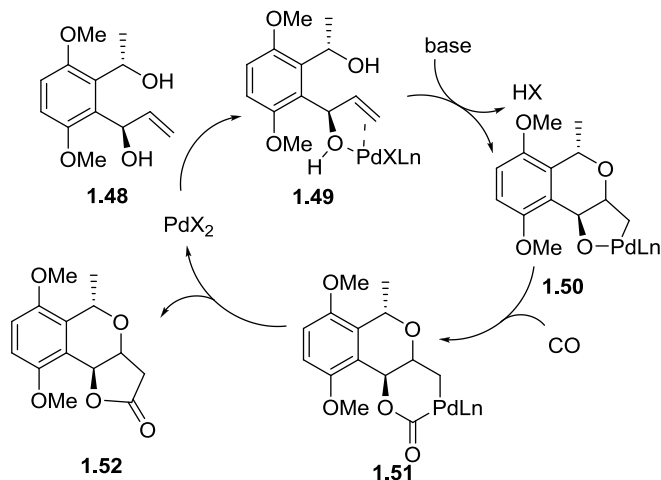
then completed by hydrolysis of the oxazoline to the carboxylic acid followed by its reduction to a methyl group. The methyl ethers were then removed, and the primary alcohol was oxidized to arrive at the *aS* antipode of gossypol (**1.3**).



Scheme 6. Meyer's Synthesis of Gossypol.

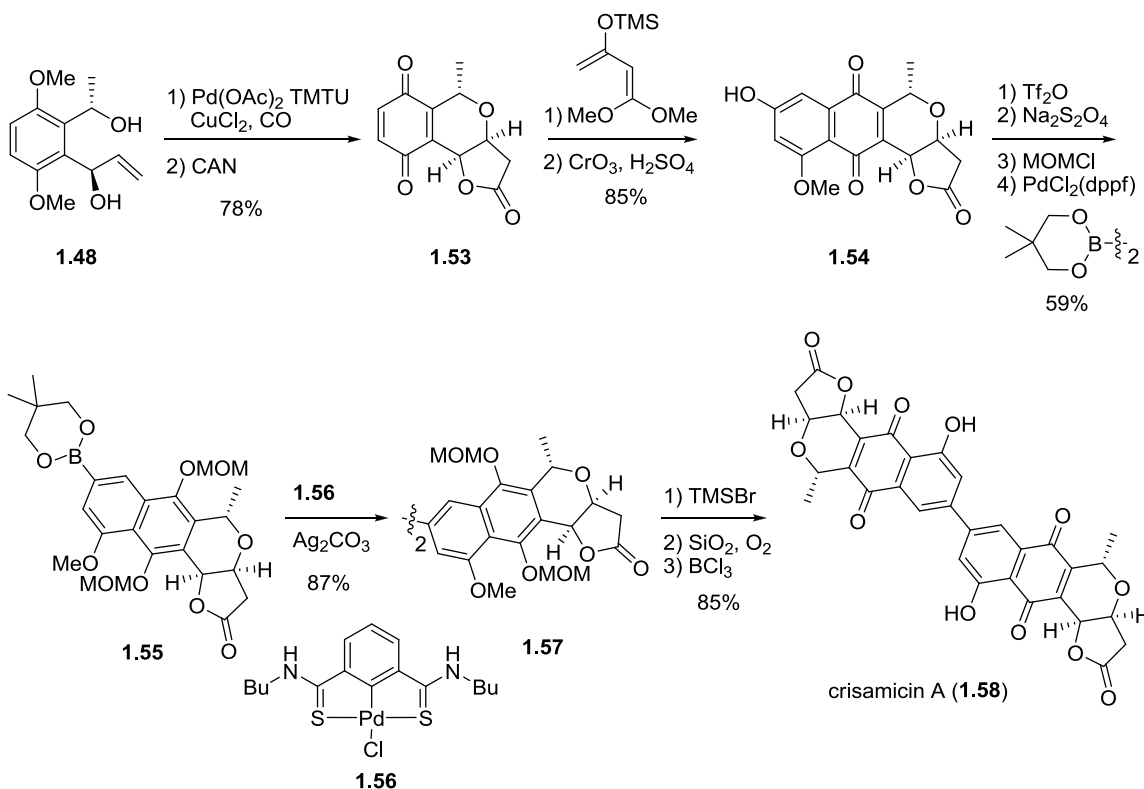
In the course of screening natural products for antibiotic activity, Schaffner³⁰ isolated a novel compound from the bacteria *Micromonospora purpureochromogenes* subsp. *halotolerans*, named crisamicin A (**1.58**), that showed minimal inhibitory concentration of 0.2 to 10. µg/mL for several strains of gram positive bacteria. Crisamicin A also showed activity against B16 Murine melanoma and herpes simplex.³¹ With only two *ortho* substituents, crisamicin does not exhibit atropisomerism. A single total synthesis has been completed by Yang³² starting with palladium catalyzed alkoxy carbonylative annulations to form the *cis*-pyran lactone **1.52** (Scheme 7). This transformation can be explained by the formation of the palladium complex **1.49** followed

by a nucleophilic attack of the free alcohol arising to the alkylpalladium **1.50**. Carbon monoxide insertion into **1.50** followed by reductive elimination forms the lactone **1.52**.



Scheme 7. Mechanism for Palladium Catalyzed Alkoxy carbonylative Annulations.

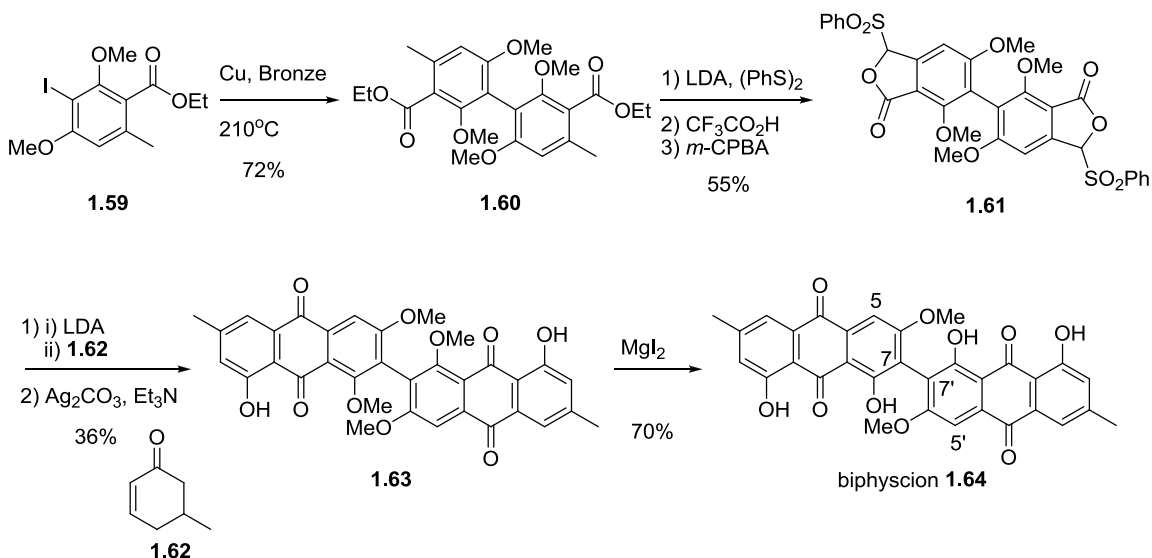
The lactone **1.52** was then oxidized to the quinone **1.53** (Scheme 8). The quinone then undergoes a Diels-Alder reaction with diene **1.54** regioselectively. After oxidation, the phenol was converted to the boronate ester **1.55**. Homocoupling of **1.55** was attempted with various palladium, nickel, and copper catalysts with no success. The robust catalyst **1.56** was found to be active enough to provide the cross coupling product **1.57**. The protected hydroquinone was then liberated and oxidized to the quinone. The total synthesis of crisamicin A (**1.58**) was completed by removal of the methyl ether.



Scheme 8. Yang's Synthesis of Crisamicin A.

Bianthraquinones have been isolated from several different sources. Biphysson is one of these anthraquinones. An interesting aspect is that both the C7,C7' and C5,C7' linkage of the anthraquinone have been isolated. The C5,C7' isomer has been isolated from the roots of *Senna lindheimeriana*.³³ A glycosylated variant of this isomer was also isolated from the plant *Cassia torosa Cav.* The C7,C7' isomer has been isolated from the extracts of a toadstool³⁴ in Europe. All three possible isomers (C7,C7', C5,C7', and C5,C5') were isolated from volcanic ash soil.³⁵ These bisanthraquinones were isolated as a single atropisomer. The only synthesis of a molecule in this family was accomplished by Hauser.³⁶ The biaryl was formed through an Ullmann coupling of iodotoluene **1.59** (Scheme 9). Utilizing a two directional approach, biaryl **1.60** was then converted to the sulfone **1.61**. The bis-anion derived from **1.61** was reacted with 5-

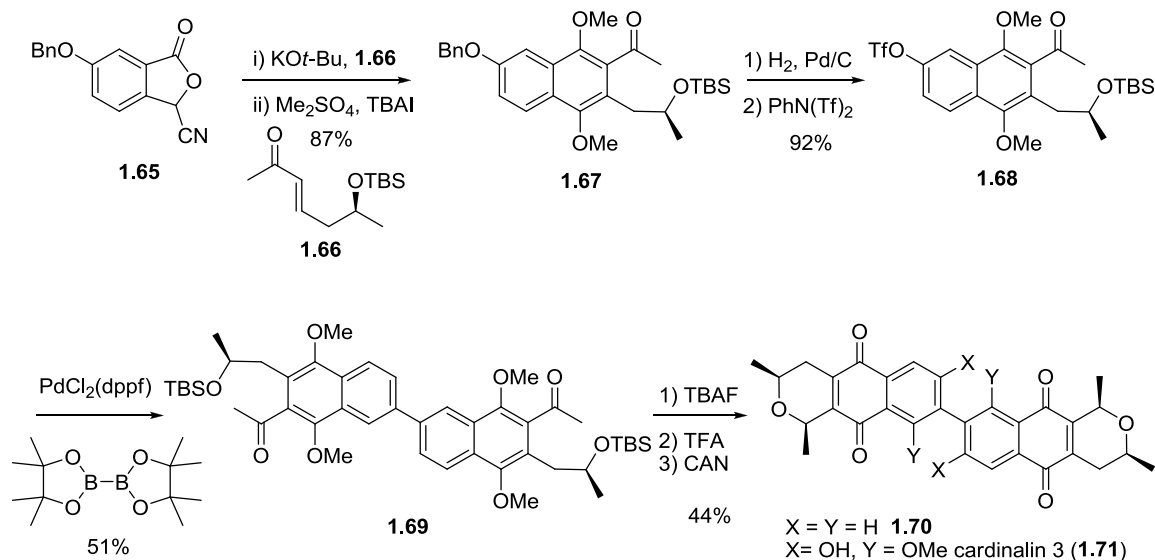
methyl cyclohexenone **1.62**. The bis-annulation product was then oxidized to bis-anthraquinone **1.63**. Finally, racemic biphyscion **1.64** was furnished by selective removal of the C8 and C8' methyl ether.



Scheme 9. Hauser's Synthesis of Biphyscion.

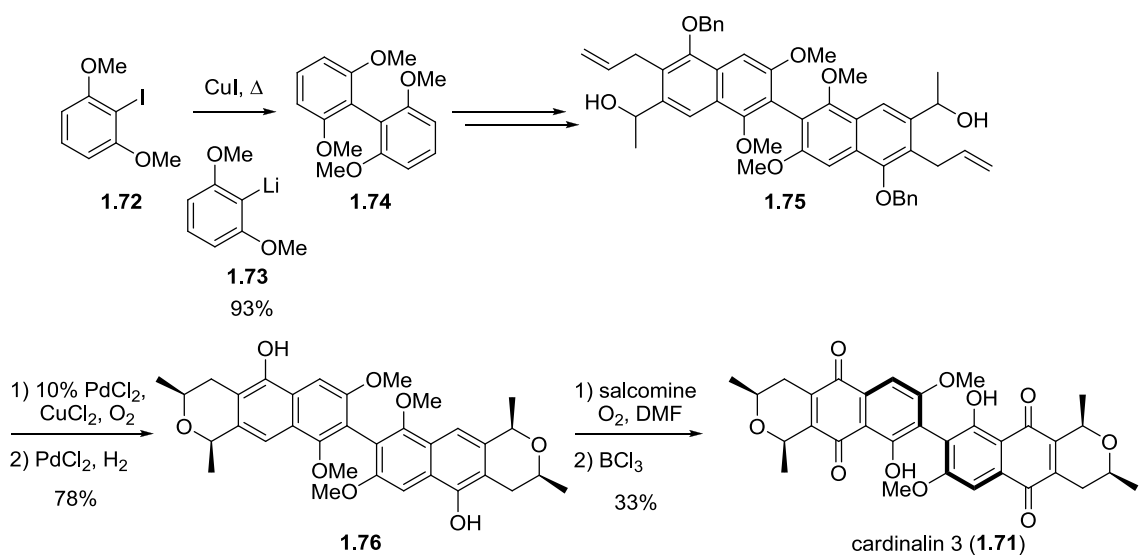
The New Zealand toadstool *Dermocybe cardinalis* was found to be the source of a family of pyranonaphthoquinones termed the cardinalins. Cardinalin 4 and 5 were shown to inhibit the growth of P388 murine leukemia cell with an IC₅₀ values of 0.28 and 0.40 µg/mL respectively.³⁷ Several approaches towards the total synthesis of the cardinalin family of natural products have been reported. Brimble's^{38, 39} approach led to the core of the cardinalins without the central phenols to encumber the dimerization (Scheme 10). This approach entailed a Hauser-Kraus annulation between the cyano-phthalide **1.65** and the Michael acceptor **1.66** to arrive at the naphthyl core **1.67**. The benzyl phenol was then converted to the activated naphthyl triflate **1.68**. A Suzuki-Miyaura cross coupling provided the binaphthyl **1.69**. Formation of the dihydropyran ring

and oxidation to the naphthylquinone completed the dimeric pyranonaphthoquinone core **1.70** of the cardinalins.



Scheme 10. Brimble's Approach to the Cardinalins.

In 2007, the total synthesis of cardinalin 3 was reported by de Koning.⁴⁰ In his first approach to cardinalin 3, de Koning reported the late stage dimerization of the monomer, ventiloquinone L. The choice was then made to form the biaryl bond early in the synthesis. The biaryl coupling was accomplished by an Ullmann type coupling to arrive at **1.74**. With the biaryl core in place, a two directional approach was used to complete the synthesis. The biaryl was elaborated in very much the same manner as Edward's synthesis of gossypol with a Stobbe condensation and Claisen rearrangement to arrive at **1.75**. The palladium mediated dihydropyran formation was followed by the reduction of the resulting alkene to arrive at **1.75** exclusively as a *cis*-1,3-dimethylpyran. Oxidation to the naphthylquinone and selective removal of the methyl ether provided an atropo-diastereoisomeric mixture of cardinalin 3 (**1.76**) plus less than 5% of leakage to the *trans*-1,3-dimethylpyran.

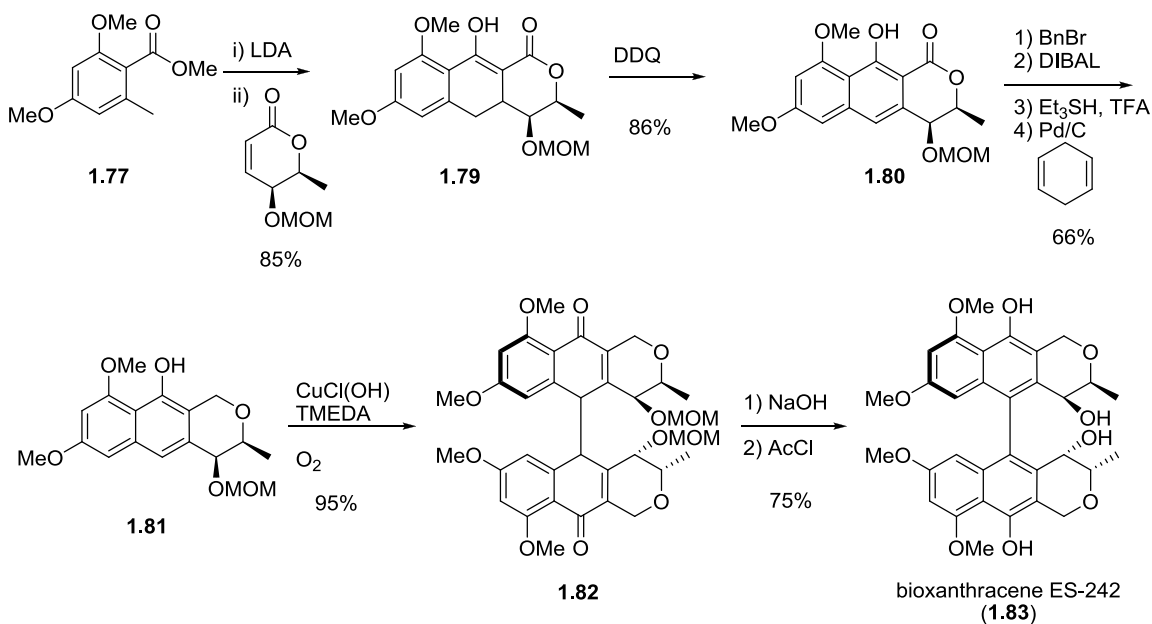


Scheme 11. De Koning's Total Synthesis of Cardinalin 3.

Eight bioanthracene ES-242 natural products were isolated in 1992 by Matsuda⁴¹ from a fungus, *Vertucillium* sp. SPC-15898. A group of eleven bioanthracenes were later isolated from the insect pathogenic fungus *Cordyceps pseudomilitaris* BCC1620.⁴² An interesting observation was that not all of the bioanthracenes had the same connectivity. Of the eleven compounds, eight were dimeric; and of the eight, six are symmetrical while the other two were unsymmetrical isomers. ES 242-1 and ES 242-2 were shown to bind to the *N*-methyl-*D*-aspartate (NMDA) receptor inhibiting [³H] TCP binding. The activity was shown to inhibit [³H] TCP binding in the μM concentration range in a competitive manner. Bioanthracene ES-242 was ineffective on binding to [3H] kainite, another subtype of the excitatory amino acid receptor. Tatsuta⁴³ accomplished the first racemic synthesis of bioanthracene (Scheme 12). The synthesis started with a Stauton-Weinreb annulation was accomplished between the toluate anion of methyl ester **1.77** and lactone **1.78** to furnish the tricycle **1.79**. Oxidation and complete reduction of the lactone produces naphthyl ether **1.81**.

The biaryl was formed through oxidative coupling using CuCl(OH) resulting in a 1:1 mixture of atropo-diastereomers. The synthesis was then completed following aromatization and hydrolysis of the MOM group.

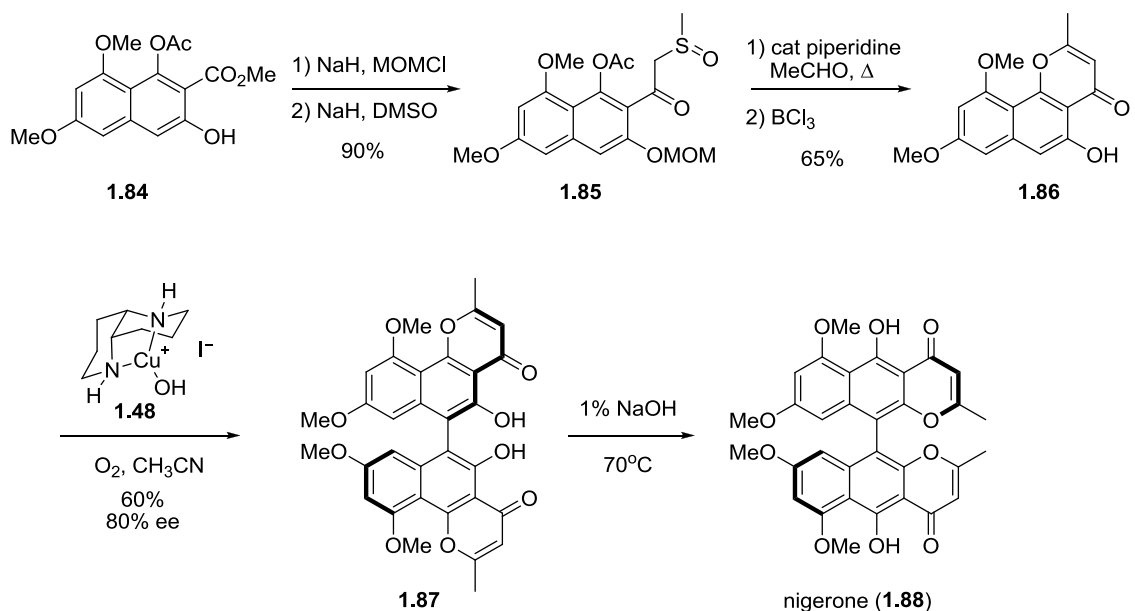
Bioxanthracene ES-242-4 was isolated as a single atropisomer but the absolute stereochemistry about the biaryl bond was unknown. Assignment of the absolute stereochemistry was later reported based on single crystal x-ray analysis of the bis-benzyl ether derived from the phenol in ES-242-4⁴⁴. From the crystal structure, the natural product ES-242-4 was assigned the aS configuration. The absolute configuration of all the bioxanthracenes⁴⁵ were determined by relating the optical rotation and the crystal structure of ES 242-4 with the known optical rotations of the other molecules in the family of bioxanthracenes.



Scheme 12. Tatsuta's Synthesis of Bioxanthracene ES-242-4.

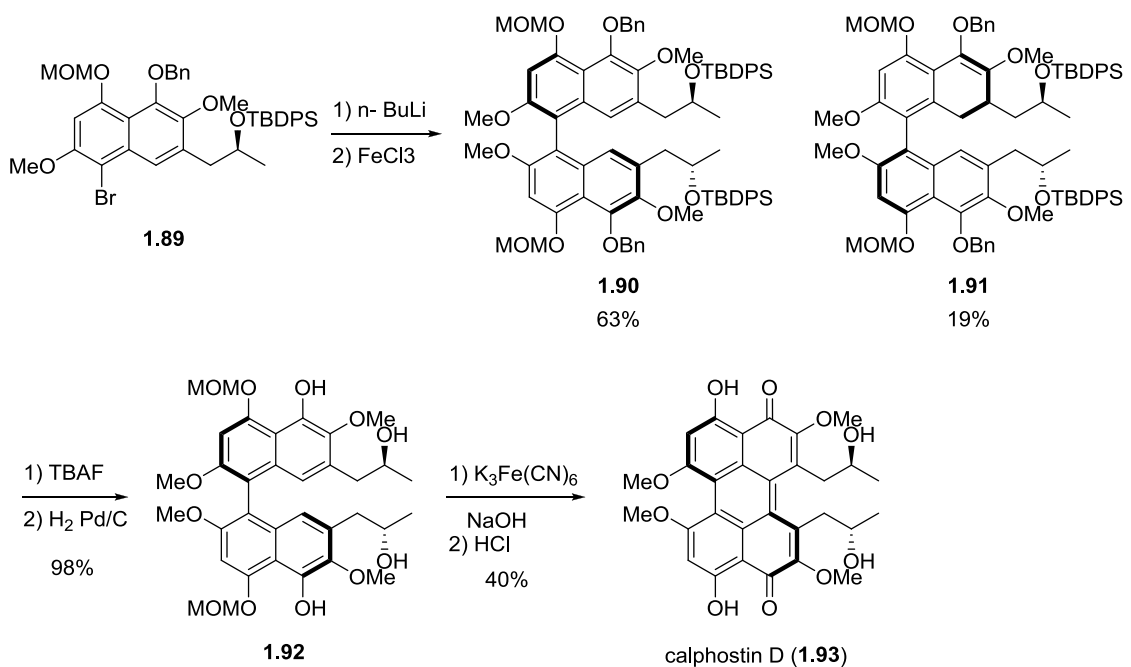
Nigerone⁴⁶ (**1.88**) was isolated as the major toxic pigment from the fungus *Aspergillus niger* V. Tiegh taken off a Mozambican ground nut. The observed optical

rotation of nigerone was attributed to atropisomerism of the central biaryl bond. The barrier of rotation was found to be high enough that heating at reflux in acetic acid for four hours only caused minor change in optical rotation. The absolute configuration of nigerone was later assigned by a total synthesis completed by Kozlowski.⁴⁷ The binaphthylpyrone moiety was prepared from the keto-sulfoxide **1.85** (Scheme 13). The sulfoxide was condensed with acetaldehyde following Kozlowski's elimination of the sulfenic acid to afford pyrone **1.86**. An oxidative coupling using 1,5 diazo-*cis*-decalin copper catalyst formed binaphthyl **1.87** in 80% ee. The ambiguity of the binaphthyl bond configuration was resolved when the calculated CD spectra of the *aR* and *aS* atropisomers were compared to the natural product.⁴⁸ This comparison allowed for the assignment of the binaphthyl bond to be of the *aR* configuration. The synthesis of nigerone was completed by a base mediated isomerization from binaphthyl **1.87**.



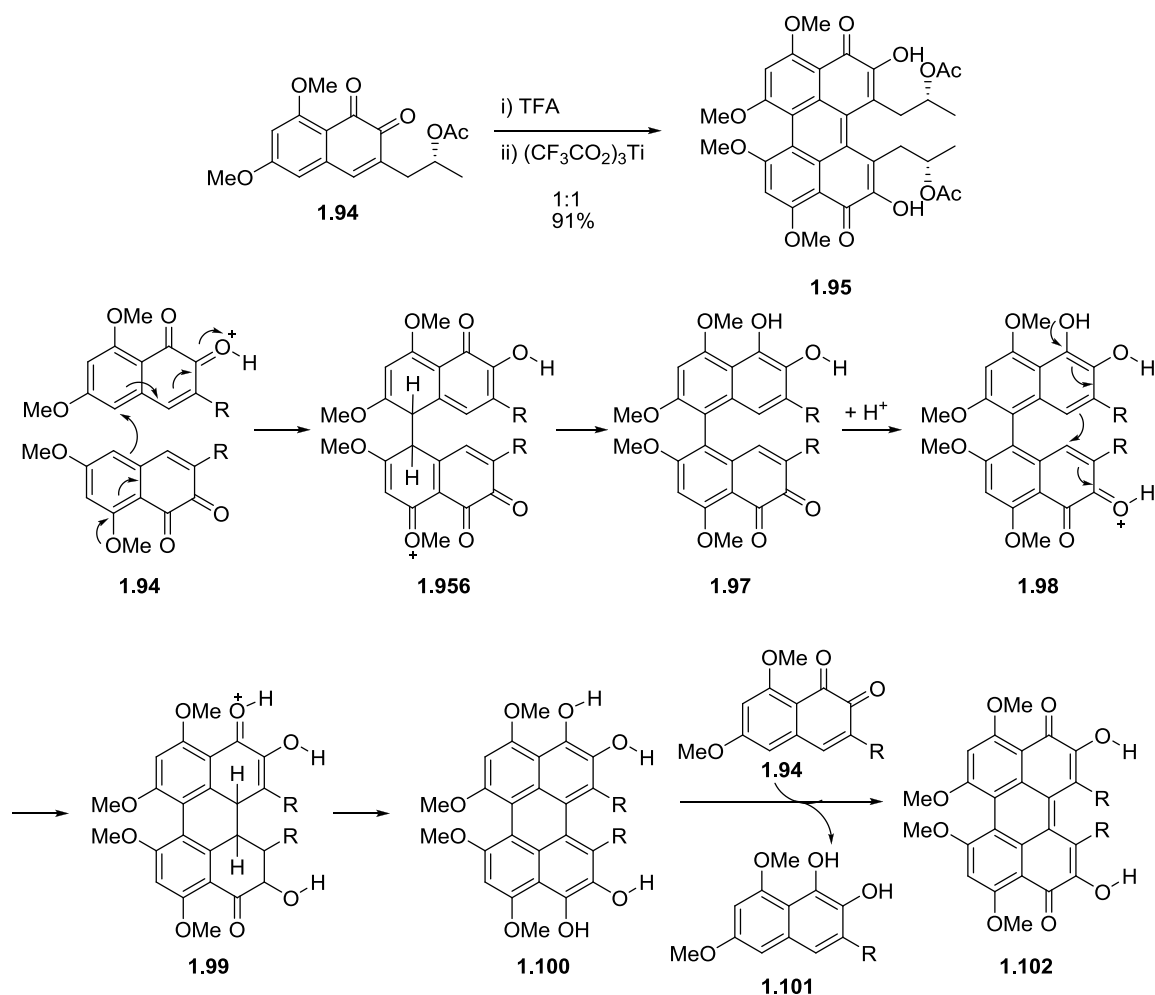
Scheme 13. Asymmetric Synthesis of Nigerone by Kozlowski.

The identification of small molecules that inhibit protein kinase C without inhibition of protein kinase A has been a goal of many groups. Protein kinase C has been considered a good molecular target for cancer therapy. The calphostins were reported to be selective PKC inhibitors. The calphostins were isolated from a fungi *Cladosporium cladosporioides*.⁴⁹ The four compounds showed IC₅₀ values ranging from 0.05-0.25 μ M without inhibition of the protein kinase A at two hundred times concentration. This family was also found to act as a photosensitizer and produce singlet oxygen. The chiral axis was assigned as aS based on the comparison of the CD spectra with that of the known cercosporin.⁵⁰ The first total synthesis was performed by Broka's group at Syntex.⁵¹ The naphthyl quinone was formed by the iron oxidation of the lithium naphthyl **1.89** (Scheme 14), arriving at both atropisomers **1.90** and **1.91**, that were separable. After removal of the TBDPS and benzyl groups, the core of the calphostins was completed by a second iron oxidation to arrive at calphostin D (**1.93**).



Scheme 14. Broka's Approach to Calphostin D.

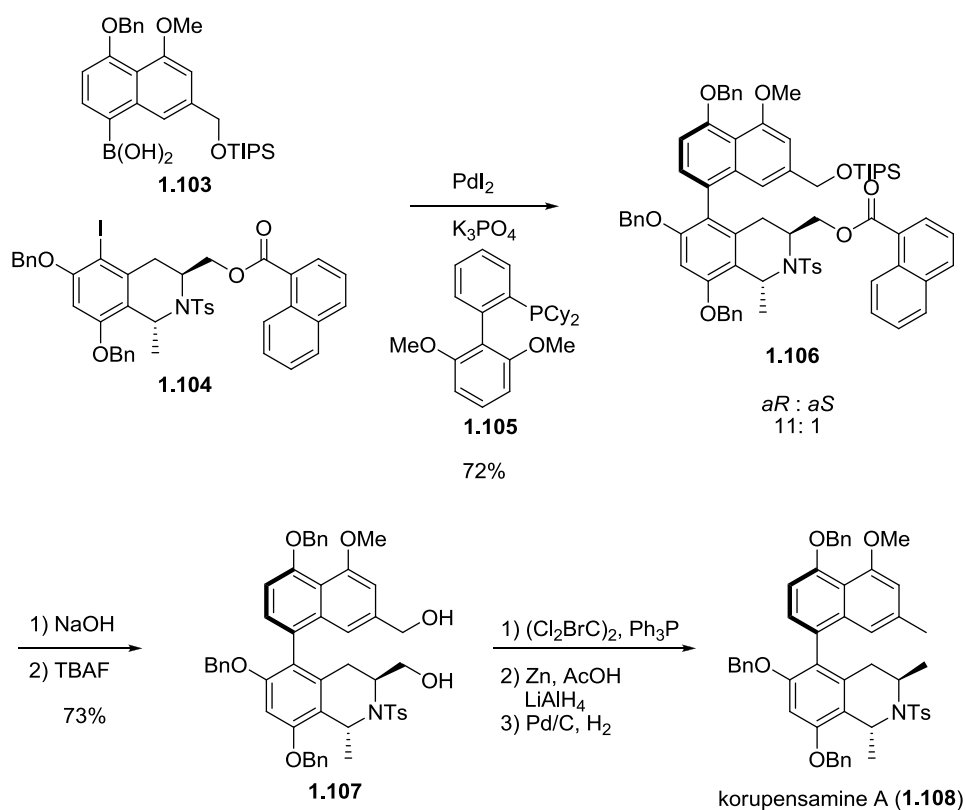
A second approach to calphostion D was reported by Hauser⁵². The key step of this approach was dimerization of *o*-naphthoquinone **1.94** with TFA followed by the slow addition of the titanium reagent to re-oxidize the hydroquinone resulting from the *o*-naphthoquinone (Scheme 15). The ability to couple without an oxidizing agent shows that this coupling proceeds through an ionic mechanism and not a one electron transfer mechanism. An ionic mechanism was supported by the observation that *o*-naphthoquinone **1.94** in the absence of oxidant gave a 1:1 mixture of the coupled product **1.102** and the hydroquinone **1.101**. With a Lewis acid coordination to an *o*-naphthoquinone, a conjugate addition from a second *o*-naphthoquinone followed by aromatization will afford the first binaphthyl linkage. This process is then repeated to give the bis-fused binaphthyl ring system. Oxidation of the hydroquinone can then be envisioned by the reduction of a third molecule of *o*-naphthoquinone **1.94** to provide the hydroquinone **1.101**.



Scheme 15. Proposed Lewis Acid Catalysed Dimerization.

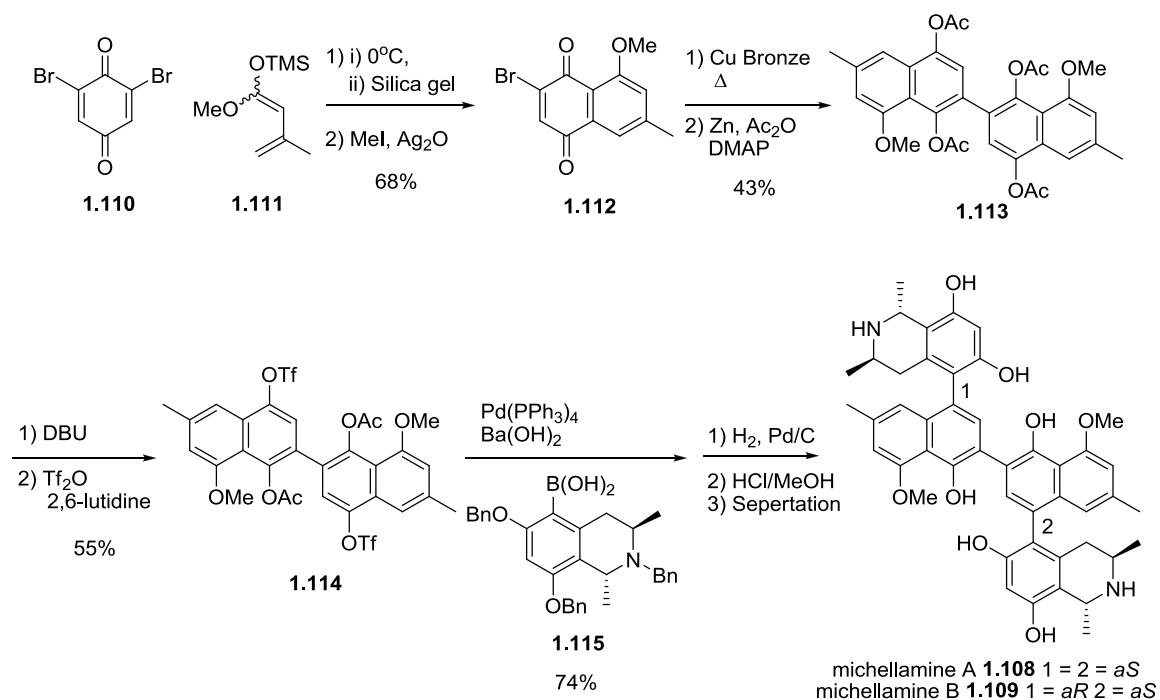
During the course of screening for novel HIV drugs, the National Cancer institute isolated a novel pair of atropisomers termed the michellamines⁵³ from the tropical vine *Ancistrocladus abbreviatus* collected in Cameroon. Both michellamines showed anti-HIV activity against several HIV cell lines. One novel observation was that both type I and type II HIV cell lines were affected by the michellamines while most compounds to date only affect one. Michellamine B showed greater effectiveness with EC_{50} values ranging from 1 to 88 μM .⁵⁴ During structure elucidation, the michellamines revealed three biaryl bonds with two points of axial chirality with no hindered rotation about the

central binaphthyl bond. Proven to be a dimer of korupensamine, michellamine A was shown to have both atropisomers of the *aS* configuration while michellamine B was shown to have one *aR* antipode and one *aS* antipode. Lipshutz⁵⁵ synthesized the monomeric unit korupensamine in an stereoselective manner (Scheme 16). The key coupling proceeded through Suzuki coupling of **1.103** and **1.104**. The coupling proceeded in a very stereoselective manner due to proposed pi stacking of the naphthyl ring effectively blocking one face of the biaryl bond. The biaryl was then converted to korupensamine A (**1.108**) by liberation of the two primary alcohols and reduction to the methyl group.



Scheme 16. Lipshutz Synthesis of Korupensamine A.

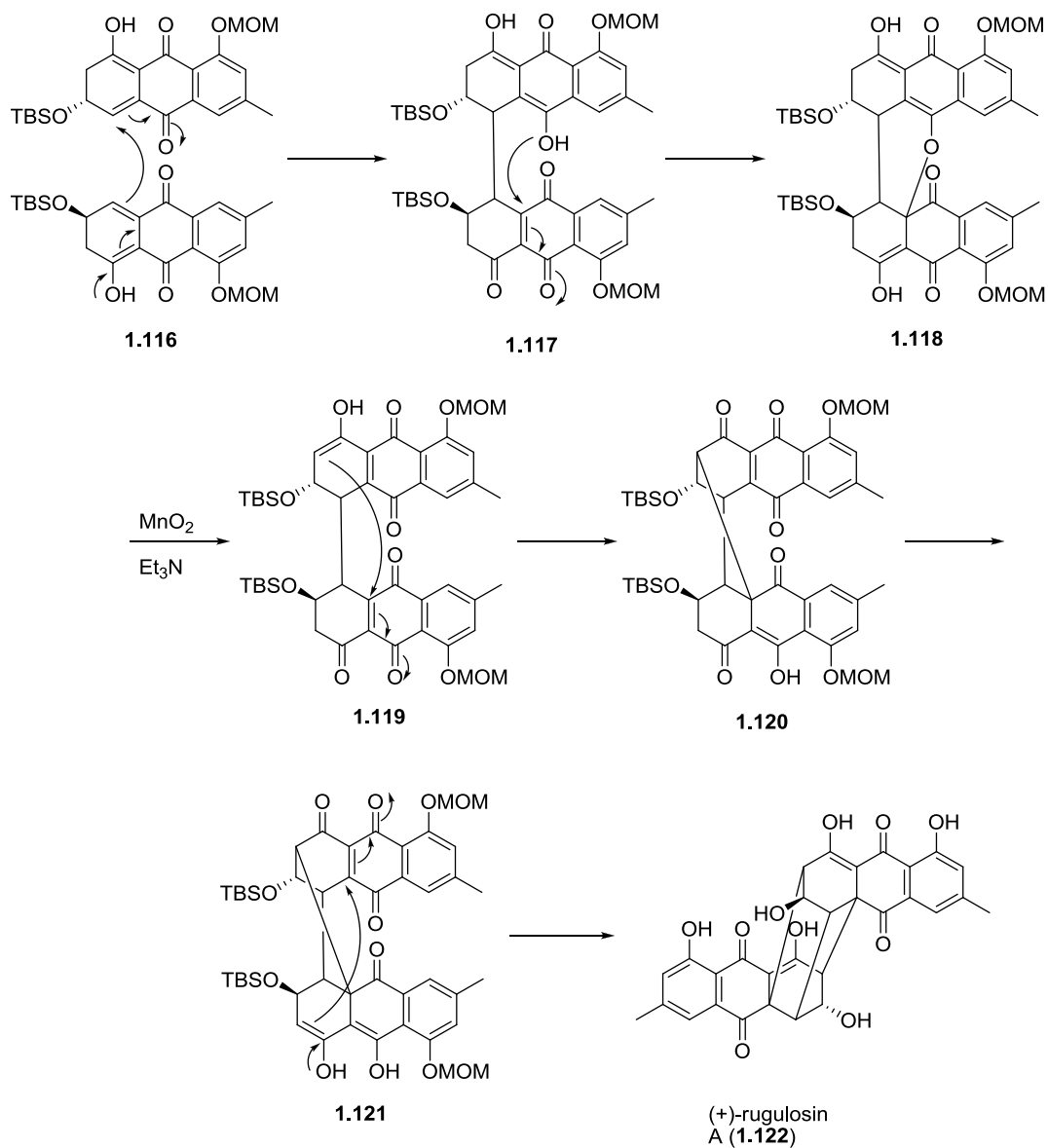
In a convergent total synthesis of the michellamines, Bringmann began with a Diels-Alder reaction between bromoquinone **1.110** and diene **1.111** (Scheme 17). Aromatization and methyl ether formation led to naphthoquinone **1.112**. The naphthoquinone was then homocoupled by means of an Ullmann coupling and reductive acetylation afforded **1.113**. Selective acetate removal and activation of the phenol as a triflate led to the bis-triflate **1.114**. Suzuki coupling of **1.114** and **1.115**, global deprotection and chiral separation of the three possible pairs of atropisomers completed the total synthesis of natural michellamine A (**1.108**) and B (**1.109**), plus the unnatural michellamine C.



Scheme 17. Convergent Total Synthesis of the Michellamines.

Rugulosin A is an interesting dimeric natural product, isolated from the fungus *P. rugulosum* Thom⁵⁶ and has been found to have anti-influenza and anti-HIV properties.

The cage like core, termed skyrin, made the determination of the structure difficult until the X-ray structure of a heavy atom derivative was solved.⁵⁷ The structure was then confirmed by total synthesis concurrently by the Nicolaou group and the Snider group. The Nicolaou⁵⁸ approach was based on a novel multistep “cytoskryin cascade” reaction to form the skyrin core (Scheme 18). The monomer unit was dimerized through a double Michael type addition. This reaction in most cases stalled at the ether **1.118**. Further oxidation to the bis-quinone followed by treatment with triethyl amine provided a further two Michael type additions arriving at the skyrin core. Removal of the protecting groups led to the natural product (+)-rugulosin. This procedure was later optimized to arrive at a one pot procedure with subsequent addition of oxidant and triethyl amine.⁵⁹

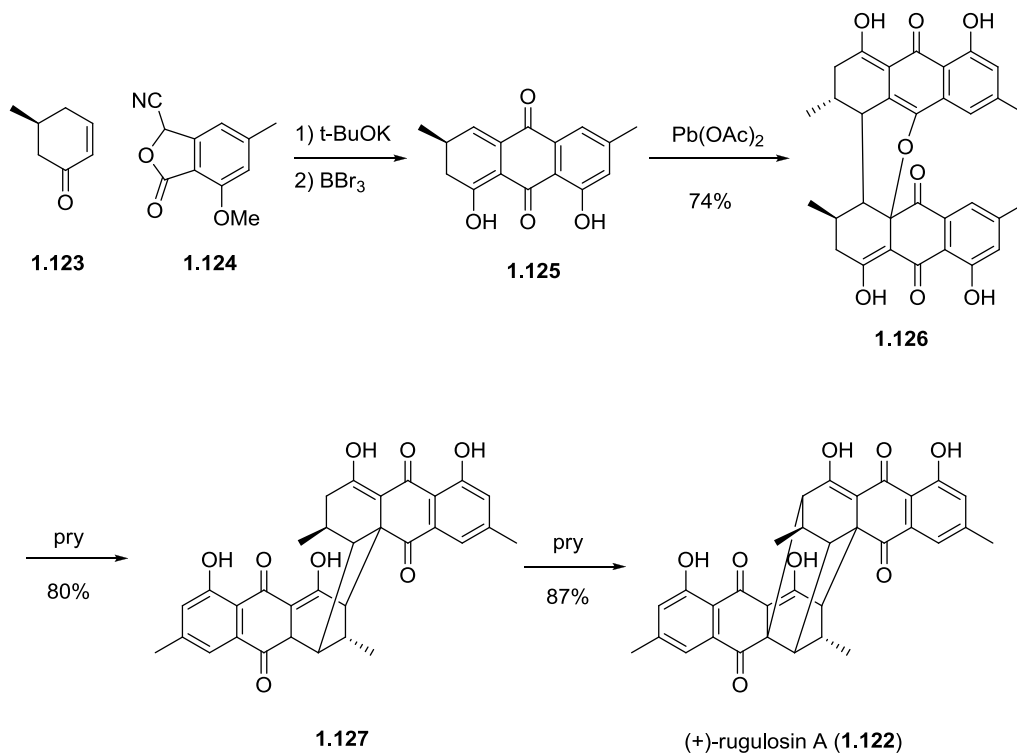


Scheme 18. The Multistep "Cytoskryin Cascade."

An explanation offered for the observed diastereoselectivity of the dimerization suggests spatial arrangements the monomer could orientate itself in the dimerization. The two endo arrangements are equivalent but unfavorable due to the sterics of a hydroxyl group positioned between the two ring systems. Of the two exo approaches the syn arrangement would be more sterically congested with two hydroxyl groups

positioned between the two rings where the anti arrangement would position these two hydroxyl groups far away from each other.

Snider's⁶⁰ approach to a rugulosin analog was much along the same strategic vein but more of a stepwise approach (Scheme 19). A Hauser annulation with cyclohexenone **1.123** and the anion of **1.124** provided the tricycle **1.125**. The dimerization and ether formation in **1.126** was accomplished with the use of lead acetate as an oxidant. The double Michael addition was then accomplished by heating in pyridine.



Scheme 19. Snider's Approach to Rugulosin Analogs.

Isolation, Structure and Biological Activity of Hibarimicins

Angelmicin B

In 1993, Uehara and coworkers reported the isolation of two novel inhibitors of oncogenic signal transduction.⁶¹ These compounds, termed the angelmicins, were isolated from a rare actinomycete *Microbispora* sp. AA9966 collected at Mt. Tennyō, Japan. Angelmicin B showed selective growth inhibition against *abl* as well as *src* transformed cells in the range of 0.3 μM to 3.0 μM . The inhibitory effects on *ras* transformed cells were not significant, while doxorubicin treated cells displayed no shift in IC_{50} . This information suggests that angelmicin B selectively inhibits tyrosine kinase activity. Honma⁶² later reported that angelmicin B inhibited 50% cell growth (IC_{50}) at 0.06 μM in leukemia HL-60 cells. Angelmicin B was also shown to promote the differentiation of HL-60 cells into mature cells. The differentiation was demonstrated by the induction of NBT reduction and morphological changes in the cells. The concentration needed to induce this maturation by most other anticancer drugs is near the level of cytotoxicity for the cell. In the case of the angelmicins, the main observation in the treated cells was differentiation without apoptosis. This study also showed that the growth inhibition and the tyrosine kinase inhibition do not correlate with each other.

Isolation and Biological Activity of the Hibarimicins

In 1998, Hori and coworkers⁶³ described another novel tyrosine-kinase inhibitor, isolated from a soil sample collected at Hibari, Toyama Prefecture, Japan. This sample contained 10 different compounds collectively called the hibarimicins (Figure 5). The bacteria strain that produced these compounds was identified as *Microbispora rosea* subspecies *Hibaria* TP A0121. Biological activity of the hibarimicins was evaluated in an assay that allowed detection of the inhibition of four different protein kinases during a

single assay. Hibarimicin A (**1.128**), B (**1.129**), C (**1.130**) and D (**1.131**) inhibited the activity of protein tyrosine kinase (PTK) without significant effect on protein kinase A (PTA) or C (PTC). Hibarimicin A (**1.128**) showed the most potent inhibition of PTK. All four hibarmicins displayed some inhibition of calmodulin-dependant protein kinase III (CAMKIII) as is seen in other PTK inhibitors. The *in vitro* studies showed modest activity against gram positive bacteria, and cytotoxicity towards cell lines B16-F10 (Murine melanoma) and HCT-116 (Human colon carcinoma) showed IC₅₀ of 0.7 to 2.0 µg/mL and 1.9 to 3.6 µg/mL, respectively. This study also demonstrated the inhibition of several different leukemia cell lines with IC₅₀ values between 1.79 µg/mL and 0.5 µg/mL.

Structure Elucidation

The hibarimicins were shown to have identical UV-visible spectra and similar IR spectra.⁶⁴ The similar spectra suggested that all the hibarimicins share a common chromophore and, thus, a common aglycone. In neutral or acidic conditions, the solutions were red in color with an absorption band at 511 nm. In basic conditions, the solution turned green and the absorption band at 511 nm disappeared while bands at 614 and 647 nm appeared. The structure of hibarimicin B (**1.129**) was elucidated first and structural assignment of other hibarimicins were based on comparison to hibarimicin B (**1.129**). Through extensive spectroscopic analysis, the structure of hibarimicin B (**1.129**) was determined to be the structure in Figure 5. Due to the complexity of the NMR spectra, several ambiguities were left unresolved. Coupling constants combined with NOE correlations confirmed the relative stereochemistry of the A and H rings but the absolute configuration remains unsolved. The absolute and relative stereochemistry of C13 on the A ring was left unassigned, but if we assume that the hibarimicins are made through a dimerization, the stereochemistry should match C13

of the H ring. The absolute configuration of the sugars has also been left unassigned. A topic that was not addressed was whether the hibarimicins exist as a single atropisomer or if there is free rotation about the central aryl-quinone bond. Once the structure was elucidated, hibarimicin B (**1.129**) was shown to be the same compound as angelmicin B.⁶⁵

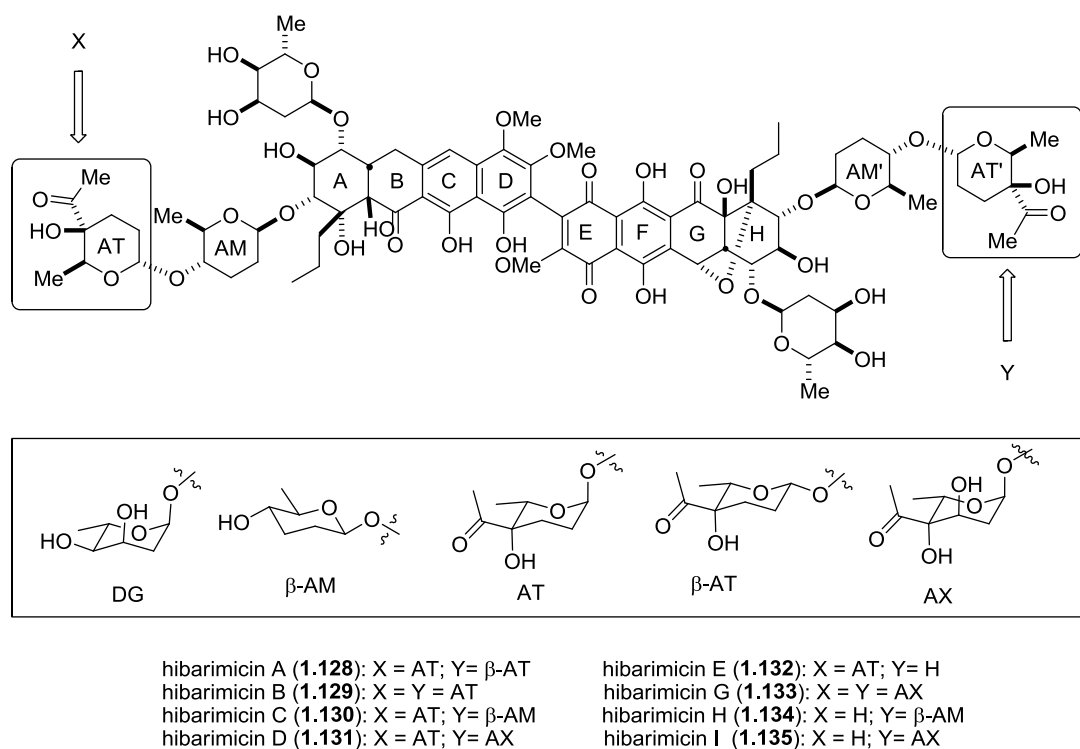
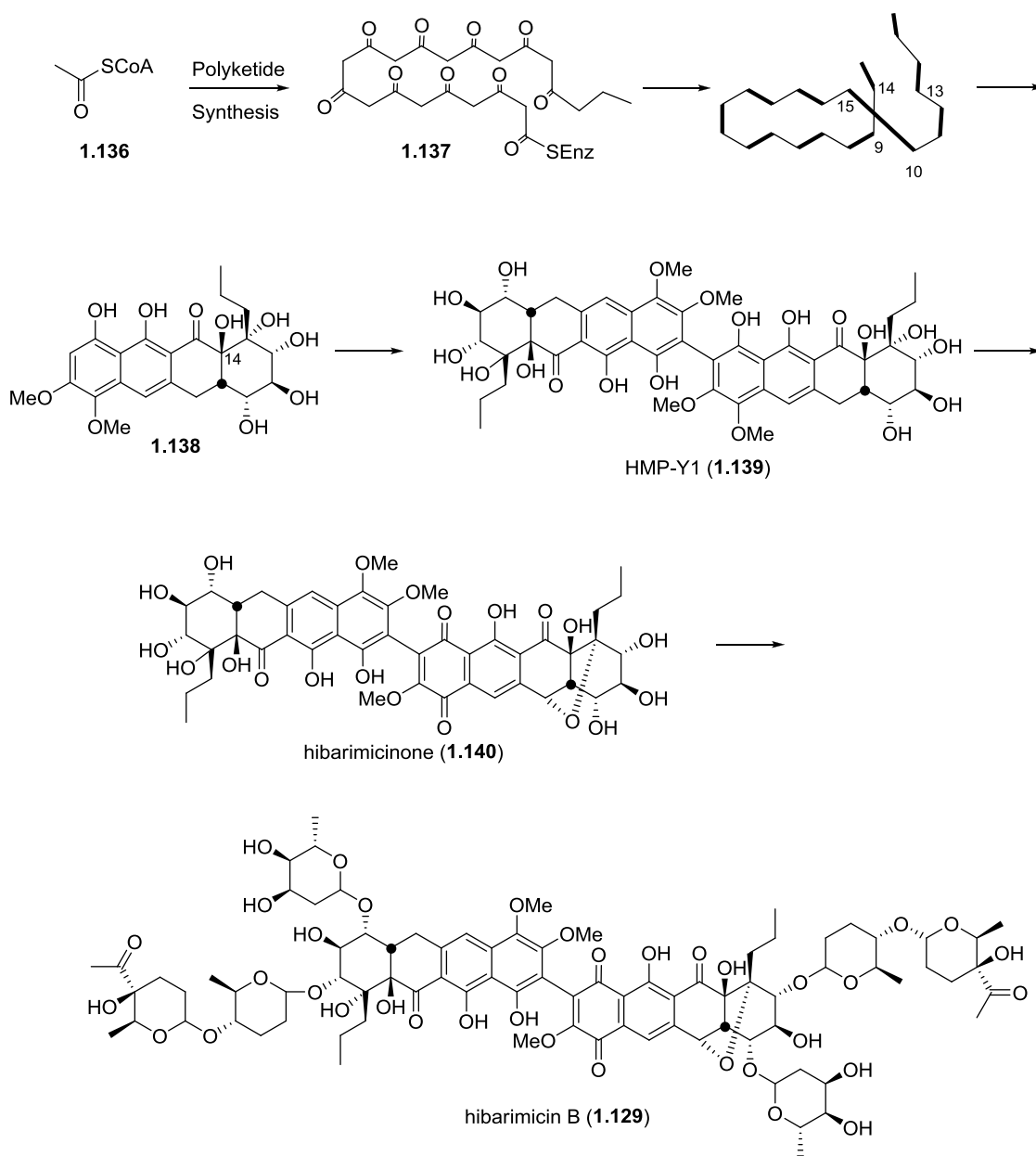


Figure 5: Structures of the Hibarimicins.

Biosynthesis

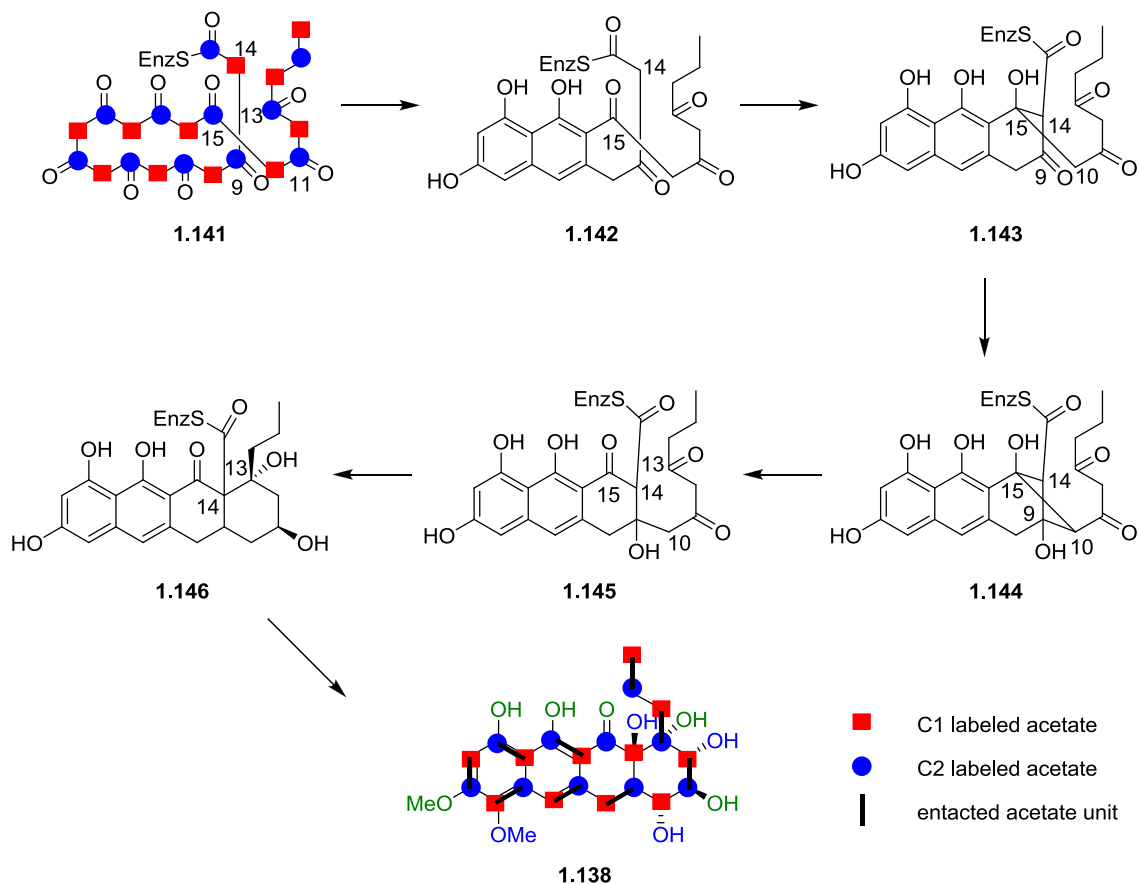
In an attempt to determine the biosynthesis of the hibarimicins, *Microbispora rosea* was fed with 1-¹³C, 2-¹³C, and 1,2-¹³C labeled acetates.⁶⁶ All carbons in the hibarimicins were shown to be derived from these acetates except the methoxy carbon suggesting that the hibarimicins are arrived at through a polyketide pathway. The ¹³C incorporation of the different feeding experiments suggested that the aglycone is

produced by a decarboxylation (at C-14) and skeletal rearrangement of an undecaketide chain (Scheme 20). Following the rearrangement, an oxidative dimerization of the two subunits **1.138** arrives at the symmetric core of the hibarimicins. The hibarimicins are then completed by post-polyketide glycosylation of the aglycone.



Scheme 20: The Proposed Biosynthesis of the Hibarimicins.

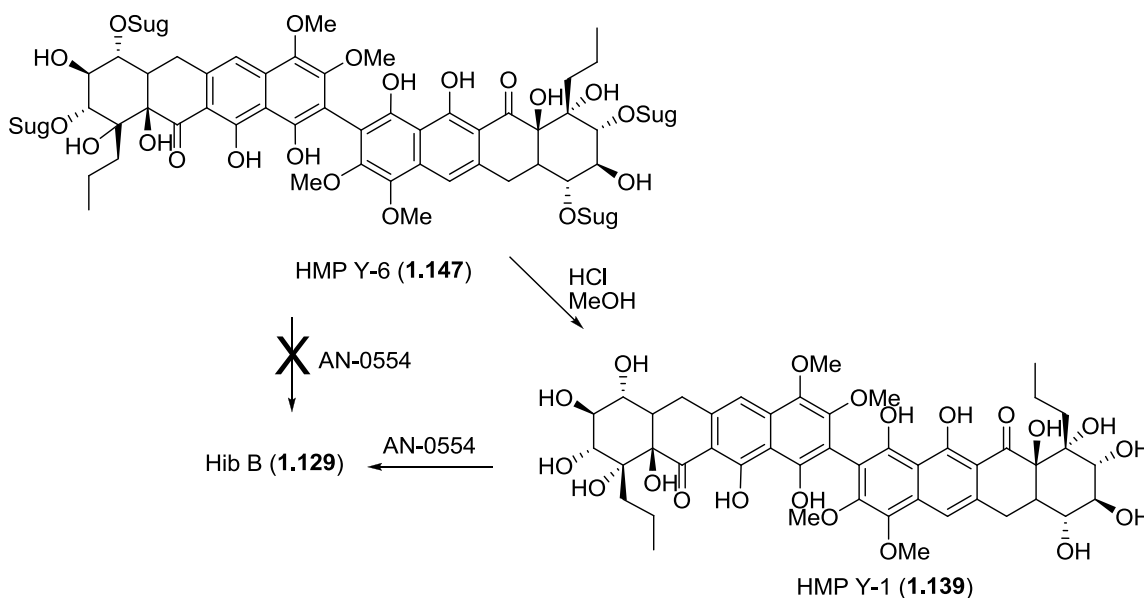
The proposed biosynthesis of the hibarimicins incorporates a unique skeletal rearrangement. Very little is understood about the actual rearrangement, except for the ^{13}C labeled acetate incorporation pattern. The ^{13}C labeling pattern shows an intact acetate unit is incorporated for all the carbons in the aglycone except that of C-10, C-14, and C-15. A plausible explanation for this incorporation pattern could involve two successive aldol condensations from the undecaketide chain (Scheme 21) which would provide a naphthalene core (**1.142**). An aldol reaction would form the C-14-C-15 bond to afford compound **1.143**, while a second aldol reaction forms the carbon-carbon bond between carbon 9 and 10. The second aldol creates a [3.1.1] bicyclic system (**1.144**) with a highly strained four-member ring that may undergo a retro-aldol, cleaving the C-11-C-15 bond. The tetracycle can then be completed with a final aldol reaction, forming the C-13-C-14 bond. That is followed by a decarboxylation at the C-14 position to form the core of the tetracycle. This proposed pathway would correlate to the correct incorporation pattern of ^{13}C acetates shown in Hori's work.



Scheme 21. Plausible Pathway for Skeletal Rearrangement in the Hibarimicins.

This proposed biosynthesis was supported by mutating TP-A0121 with *N*-Methyl-*N'*-nitro-*N*-nitrosoguanidine (NTG).⁶⁷ This random mutation method allowed for isolation of biosynthetic precursors, providing an insight into the details of the biosynthesis of the hibarimicins. From this study, formation of the tetracyclic core as the first step was confirmed by the isolation of a tetracycle that did not incorporate the skeletal rearrangement. The next important compound that was isolated was a glycosylated symmetric dimer of the tetracyclic core, HMP-Y6 (**1.147**) (Scheme 22). This dimer was then fed to a mutant strain that was a non-producer of hibarimicin and was not converted to hibarimicin B (**1.129**). HMP-Y6 (**1.147**) was deglycosylated to arrive at the symmetric dimer HMP-Y1 (**1.139**). A knockout strain of the bacteria that could not produce the

hibarimicins was then fed HMP-Y1 (**1.139**), which was converted to the fully glycosylated hibarimicins. The conversion of HMP-Y1 (**1.139**) was confirmed by repeating the feeding study with ^{13}C labeled HMP-Y1 (**1.139**) through acidic methanolysis of the labeled HMP-Y6 (**1.147**). These block mutants provide a timeline for the biosynthesis of the hibarimicins. The oxidative dimerization to a symmetric dimer is followed by selective oxidation and ether formation to arrive at the core of the hibarimicins. This core is glycosylated in a final step to arrive at the individual hibarimicins.

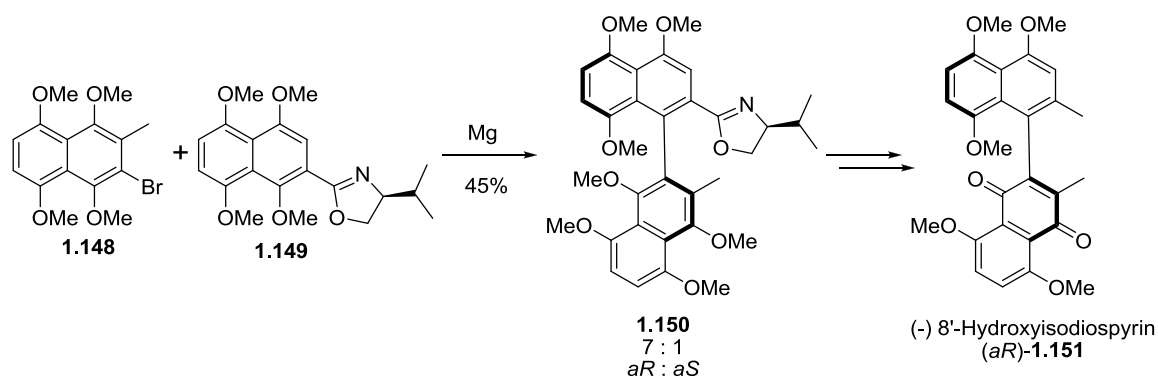


Scheme 22. Block Mutants that Describe the Biosynthetic Timeline of Hibarimicins.

Models that demonstrate Hibiramicin Atropisomers

Hibarimicins present a seemingly unique aryl-quinone linkage at the biaryl bond. Only one other natural product has been shown to have this motif. 8'-Hydroxyisodiospyrin (**1.151**) has shown to be stable atropisomers as shown by the isolation of both racemic⁶⁸ and enantiomerically⁶⁹ pure forms from different natural sources. Synthesis of the (+) isomer was provided by the H_2O_2 oxidation of (+)-

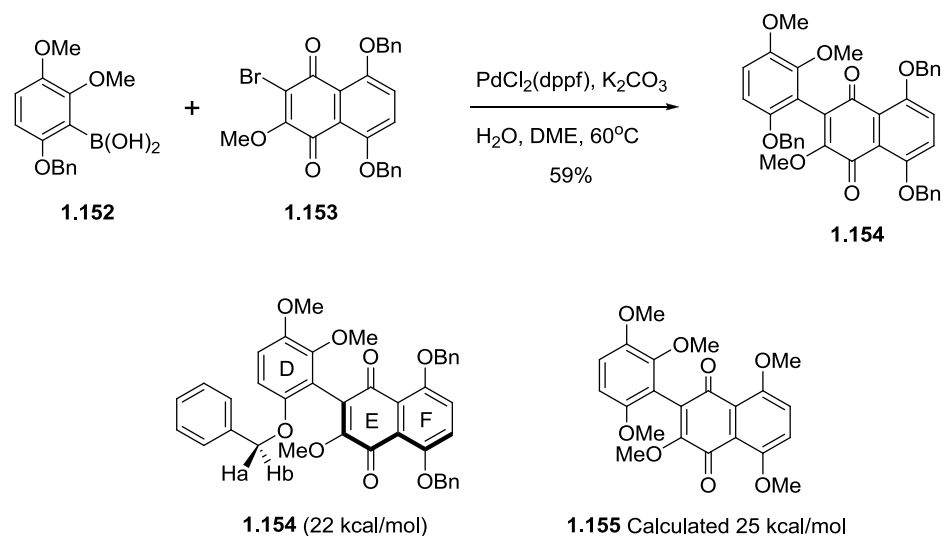
isodiospyrin in poor yields.⁶⁹ Sargent⁷⁰ determined the absolute stereochemistry by means of Meyers oxazoline **1.149** (Scheme 23). This coupling proceeded in a 7:1 selectivity for the *aR* atropisomer. The 7:1 ratio of atropisomers remained consistent until the final product showing no rotation about the biaryl axis.



Scheme 23. Sargent's Synthesis of Aryl Quinone by a Meyers Oxazoline.

Roush's Model of the Angelmicin Core

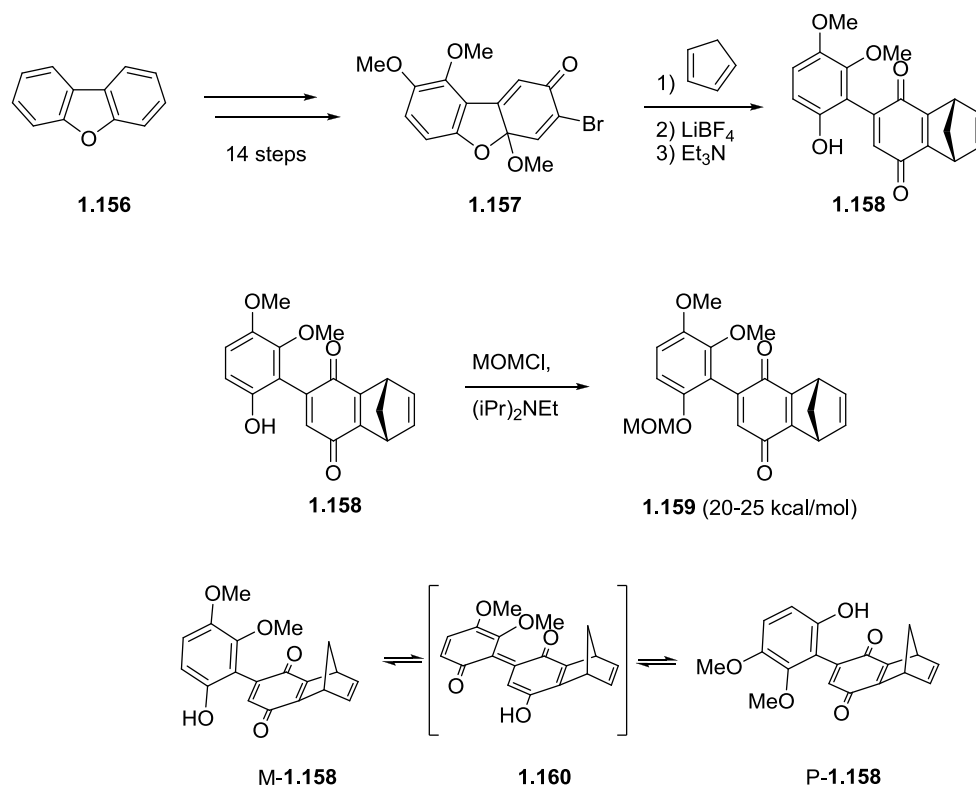
One topic that was left uninvestigated in the structural elucidation of the hibarimicins is the possibility of atropisomers. Roush's group⁷¹ synthesized a model system to examine if there is a chiral axis (Scheme 24). Roush attempted the formation of the naphthyl-naphthylquinone core through both cross coupling and an Ullmann coupling with no success. Suzuki coupling of the arylboronic acid (**1.152**) and the bromonaphthylquinone (**1.153**) eventually provided the desired biaryl (**1.154**). The methylene protons on the benzyl ether appeared as an AB quartet in ¹H NMR indicating the presence of chirality, thus atropisomers. In an effort to determine the barrier of rotation, variable temperature NMR experiments were performed. The rotational barrier of this model was determined to be greater than 22 kcal/mol. With this barrier, calculation for the trimethoxy biaryl (**1.155**) was then estimated to be 25 kcal/mol.



Scheme 24. Roush's Model of Atropisomerism in Angelmicin.

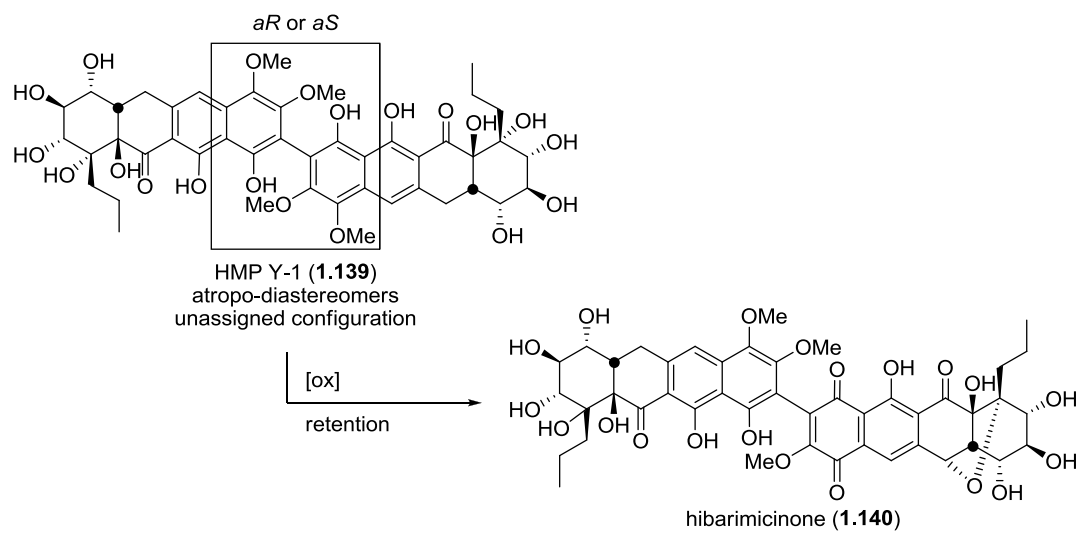
Sulikowski Model of the Hibarimicin Core

Another model was provided by our group.⁷² This model was initiated with the biaryl bond already in place with dibenzofuran. This furan was elaborated to the monoketal quinone **1.157** (Scheme 25). The quinone was a very reactive dienophile in a Diels-Alder reaction with cyclopentadiene. Hydrolysis and dehydrobromination lead to the biaryl phenol **1.158**. The rotational barrier was so small for the free hydroxyl at room temperature that **1.158** appeared as a single isomer. The free hydroxyl was protected as a methoxymethyl ether **1.159**, and the methylene protons appeared as an AB quartet indicating the presence of approximately 1:1 mixture of atropisomers. The rotation barrier was again probed by variable temperature NMR and found not to coalesce at 148°C. This failure to coalesce at 148°C would correspond to a minimum barrier of rotation being between 20 and 25 kcal/mol. The low barrier to rotation for the free hydroxyl **1.158** was speculated to be a result of the lower energy state produced by tautomerization of the phenol through the quinone **1.160**.



Scheme 25. Sulikowski Model of Atropisomerism in Hibarimicins.

Comparison of HMP-Y1 (**1.139**) to other natural products suggests that HMP-Y1 (**1.139**) exists as a stable atropo-diastereomer, with unassigned configuration. Oxidation of HMP-Y1 (**1.139**) to hibarimicinone (**1.140**) would be expected to occur with retention of configuration of the biaryl bond (Scheme 26). One of the major goals of this research is the assignment of absolute configuration about the biaryl bond in this family of natural products. This goal will be addressed in Chapter II.



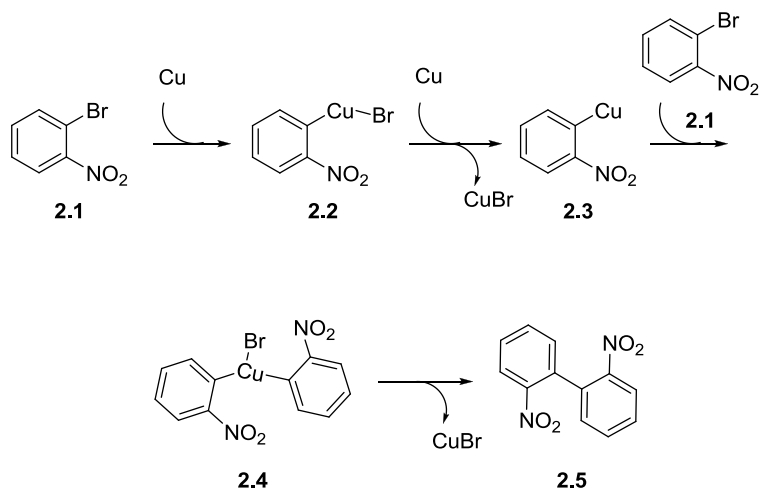
Scheme 26. Absolute Configuration of HMP-Y1 is Retained in Hibarimicinone.

CHAPTER II

SYNTHETIC METHODS DIRECTED TOWARD DIMERIC BIARYL NATURAL PRODUCTS

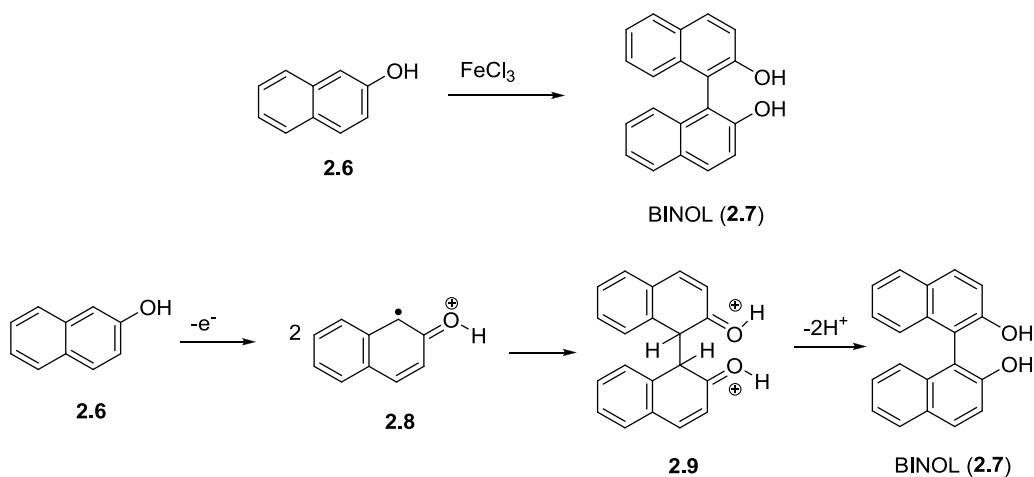
Synthetic Methods for Formation of Biaryl Carbon-Carbon Bonds

The formation of biaryl bonds has long been a challenge in synthetic chemistry. At the turn of the century, Ullmann discovered a synthetically useful transformation in the coupling of bromo-benzene (**2.1**).⁷³ The mechanism of this reaction begins with oxidative insertion of copper into the carbon-bromine bond. This copper(II) intermediate **2.2** is then reduced by a second equivalent of copper to arrive at the aryl copper **2.3** (Scheme 27). This copper(I) species then undergoes a second oxidative insertion leading to **2.4**. Once at the copper(III) intermediate (**2.4**), the copper reductively eliminates to arrive at the biaryl product and a second equivalent of copper(I) bromide. The Ullmann coupling has shown to be effective with a wide scope of substrates especially sterically encumbered biaryls.⁷⁴



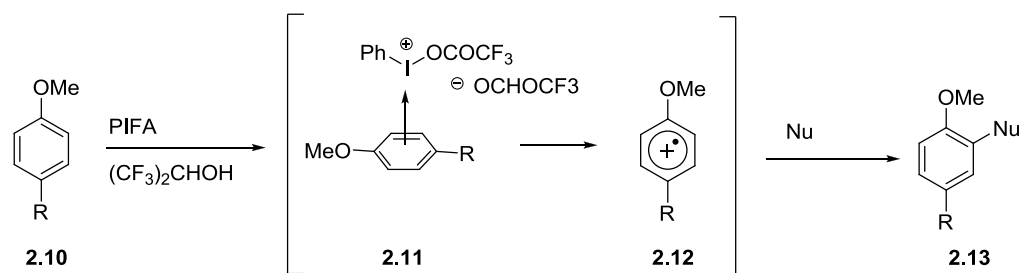
Scheme 27. A Mechanistic View of the Ullmann Coupling

An early method to form a biaryl carbon-carbon bond is oxidative phenol coupling. This coupling reaction is promoted using molecular oxygen⁷⁵ or iron trichloride⁷⁶ as an oxidant. Mechanistically, the removal of one electron from naphthol **2.6** by an oxidant provides radical cation **2.8** (Scheme 28). Dimerization of **2.8** followed by loss of a proton and tautomerization provides BINOL (**2.7**). Interest in biaryl atropisomers was modest until the development of BINAP⁷⁷ (derived from BINOL) as a ligand in asymmetric synthesis. Since that time, several metals including gold⁷⁸, manganese⁷⁹, ruthenium⁸⁰ and vanadium⁸¹ have been shown to facilitate oxidative dimerization of β -naphthol (**2.6**).



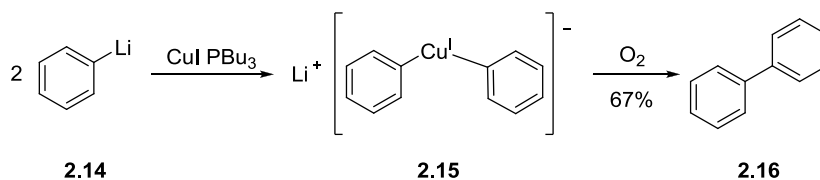
Scheme 28. Proposed Mechanism for the One Electron Oxidation of β -Naphthol (**2.6**).

Hypervalent iodine reagents such as bis(trifluoroacetate)iido-benzene (PIFA)⁸² have the ability to oxidize electron rich aromatic rings leading to radical cation intermediates **2.12** (Scheme 29). The latter can then be trapped by a variety of nucleophiles including a second benzene ring to form a biaryl carbon-carbon bond.



Scheme 29. Mechanism of PIFA Oxidative Coupling.

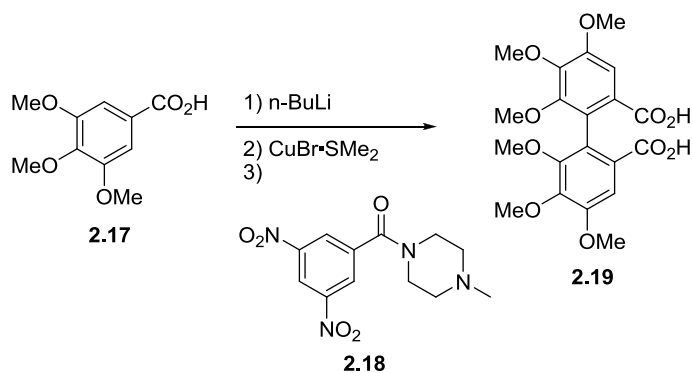
Oxidative coupling of copper complexes (cuprates) was described by Whitesides⁸³ in the late 1960's. In this coupling, two equivalents of the aryl lithium **2.14** are added to a copper(I) salt to form the copper ate species **2.15** (Scheme 30). This copper species is then oxidized by molecular oxygen to arrive at biaryl **2.16**. Typically the required aryl lithium is produced from an aryl halide through a lithium halogen exchange. Lipshutz⁸⁴ expanded on this chemistry by employing higher order cuprates to form unsymmetrical biaryls⁸⁵ and demonstrating intramolecular biaryl couplings.⁸⁶



Scheme 30. Oxidative Coupling of Cuprates.

One drawback to the oxidation of organocuprates with molecular oxygen is frequently observed oxidative by-products resulting in low yields. To solve this problem other organic oxidants have been examined. For example, benzoquinone⁸⁷ has been used as the oxidant leading to hydroquinone as a by-product. In 2005, Spring⁸⁸ reported dinitrobenzamide **2.18** as an oxidant that produced by-products easily removed by filtration and only required sub-stoichiometric amounts of **2.18**. (Scheme 31). Spring

later showed that the initial use of an aryl halide was not necessary as a starting material, but demonstrated directed ortho lithiation of an aromatic ring could lead to the copper ate complex.



Scheme 31. Spring's Direct Lithiation and Cuprate Oxidation.

Finally, the widely utilized Suzuki and Stille couplings are limited to the preparation of sterically less encumbered biaryls.⁸⁹

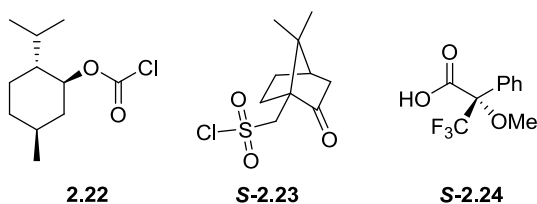
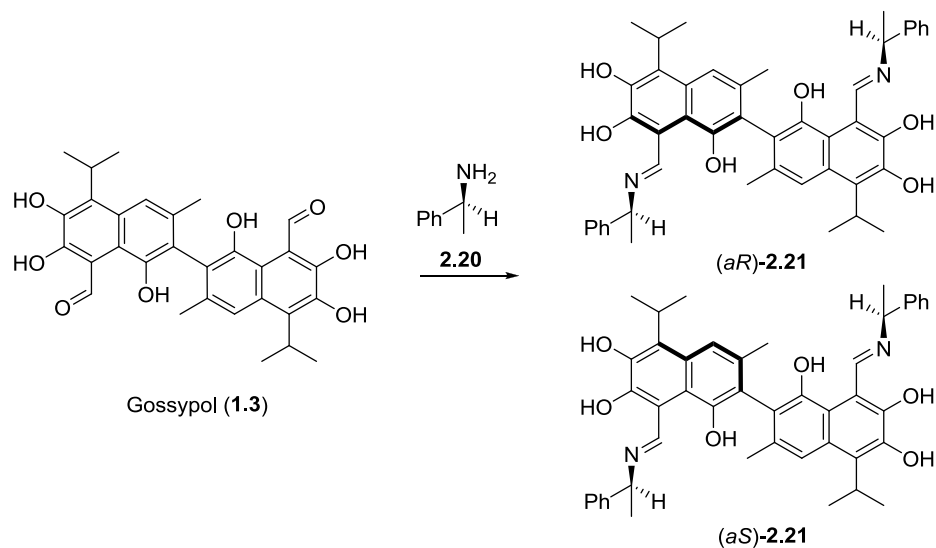
Methods to Arrive at a Single Atropisomer

The ability to derive a single atropisomer has become important since the utility of BINAP in asymmetric synthesis has been demonstrated. Further, many complex natural products incorporate atropisomers within their structure. There are three general methods to produce a single atropisomer. First, resolution has been employed, typically requiring the formation of the biaryl as a racemate followed by classical formation of diastereomeric salts or esters. A more efficient method is to employ a dynamic kinetic resolution. Dynamic resolution is accomplished by changing the nature of the biaryl bond so that the barrier of rotation is lowered and the atropisomer easily interconverts at room temperature. Once an equilibrium is established a single atropisomer can be

derived from the interconverting pair of atropisomers by a chemical reaction under kinetic control. The third and most effective method is direct asymmetric coupling.

Resolution of atropisomers has a high dependence on structure and/or functional group requirements. Advances in chromatography occasionally allow direct separation of atropo-diastereomers or atropo-enantiomers. Direct separation by chromatography was employed in the isolation of atropo-diastereomeric natural products mastigophorene A (**1.22**) and B (**1.23**). Atropo-enantiomers have been separated by chiral chromatography. A classical method for resolution of BINOL (**2.7**) atropisomers is crystallization of diastereomeric salts. For example, BINOL (**2.7**) have been separated by selective crystallization of copper(I) salts of cinchonine alkaloid complexes.^{90, 91}

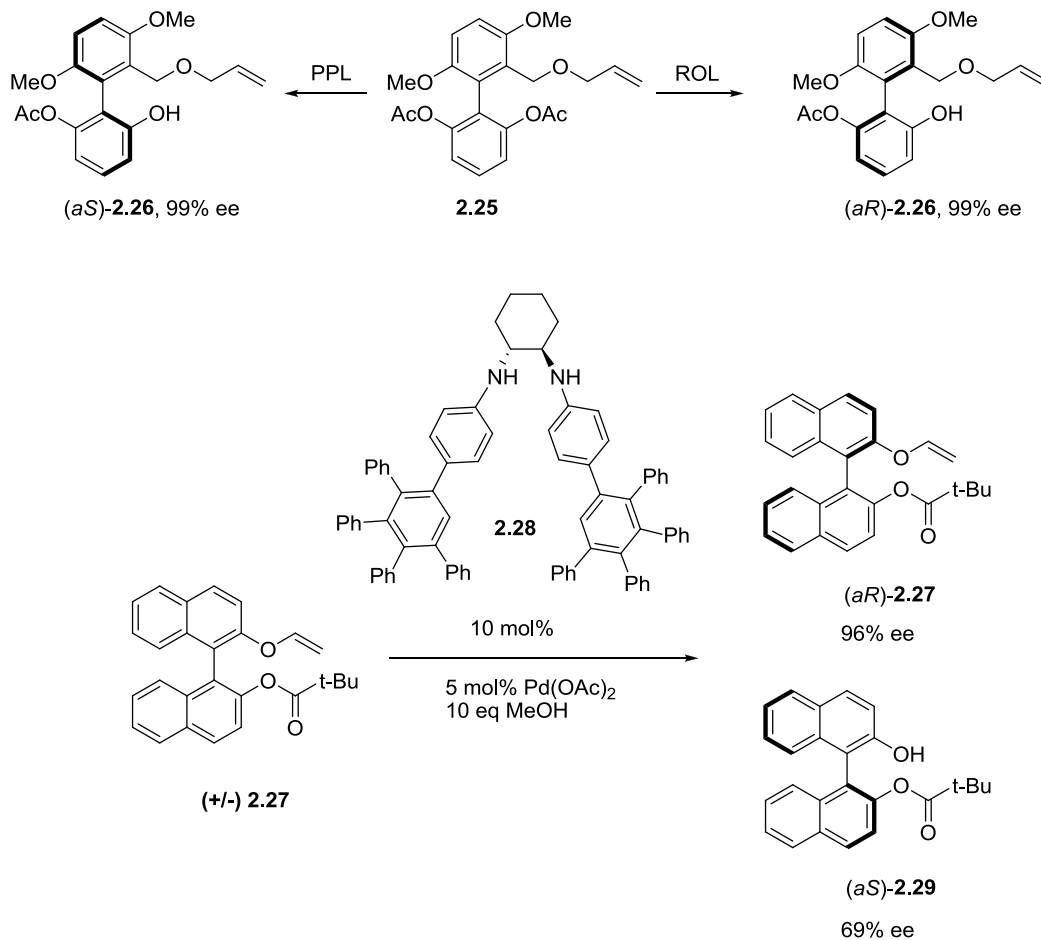
Other methods of resolution use temporary covalent modification of a chiral atropisomer using a chiral auxiliary resulting in atropo-diastereomers separable by chromatography. This requires a method for reversal of the covalent bond and recovery of single atropo-enantiomers. An early example of this approach is the resolution of gossypol (**1.3**) by formation of diastereomeric Schiff bases (**2.21**)⁹² (Scheme 32). Other biaryls have used free phenols or amines to create diastereomeric esters and amides, respectively. Three chiral auxiliaries that are most often used are: menthol chloroformate (**2.22**),⁹³ camphorsulfonyl chloride (**2.23**),⁹⁴ and Mosher's acid (**2.24**).⁹⁵ All of these compounds allow for the resolution of atropisomers through chromatography of diastereomeric ethers/amides.



Scheme 32. Example of Auxiliaries used in the Resolution of Atropisomers.

Enzymes have been used in the desymmetrization of meso isomers and kinetic resolution of racemic mixtures. Typically lipases are employed in these transformations.⁹⁶ For example, the hydrolysis of a single enantiotopic acetate of meso biaryl **2.25** allowed for the desymmetrization of the molecule and production of a single atropisomer (Scheme 33).⁹⁷ If porcine pancreatic lipase (PPL) is used as the enzyme then phenol **2.26** with the aS configuration predominates. If rhizopus *oryzae* lipase (ROL) is used in the hydrolysis of **2.25** then phenol aR-**2.26** predominates. The chiral recognition of the active site of an enzyme has been mimicked using a chiral diamine in the kinetic resolution of BINOL (**2.7**). In this kinetic resolution, the vinyl ether derivative of BINOL (**2.27**) was subjected to palladium mediated methanolysis with bulky diamine

2.28. The (*aR*)-**2.27** was then recovered in 96% ee while the *aS* isomer was converted to the naphthol (*aS*)-**2.29** in a modest 69% ee.

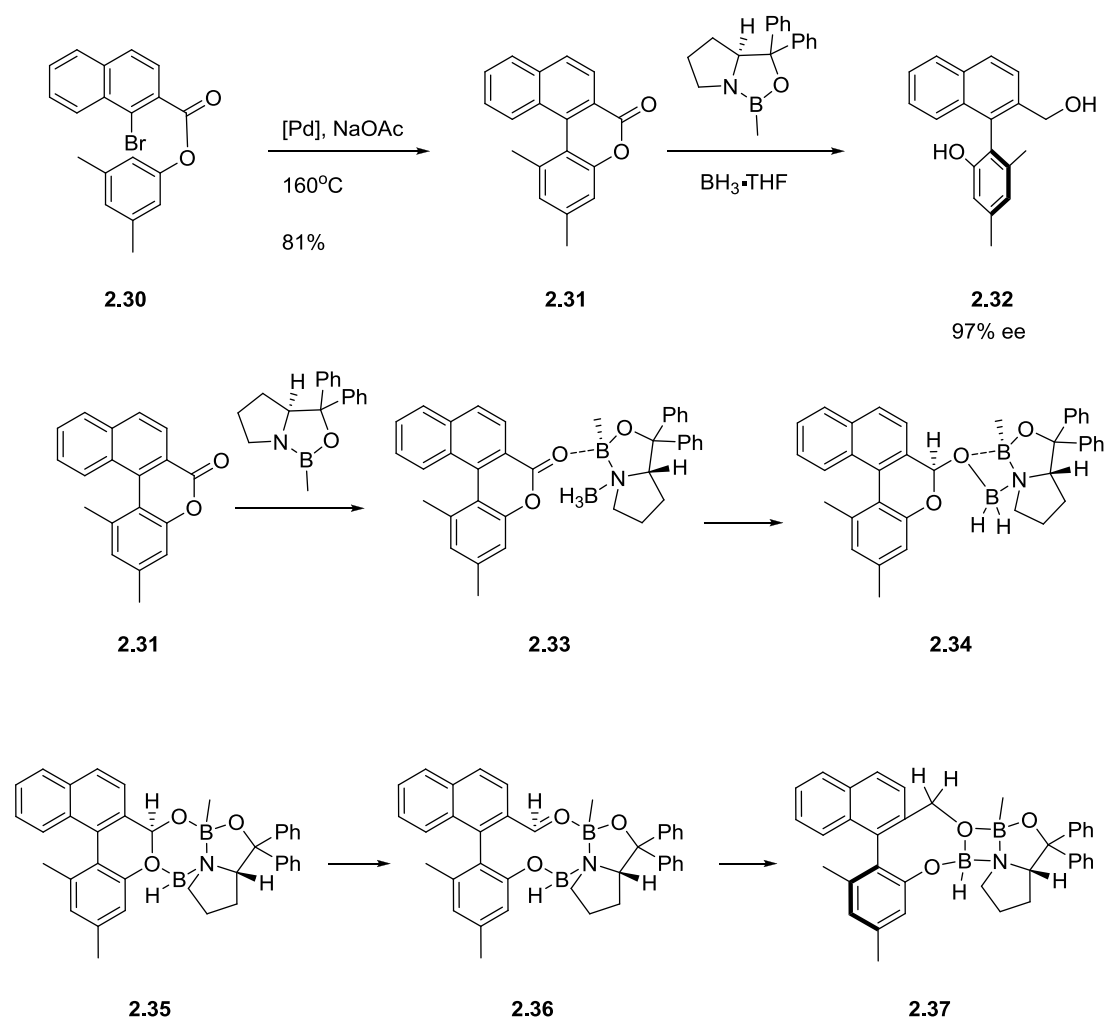


Scheme 33. Desymmetrization and Kinetic Resolution Using Enzymatic and Non-Enzymatic methods.

Resolution can provide optically pure atropisomers but a disadvantage is half of the material is lost as the undesired atropisomer. Dynamic resolution addresses this problem as all the material is converted to a single atropisomer. Dynamic kinetic resolution in biaryl systems has been championed by Bringmann. A common molecular structure for the identification of dynamic kinetic resolution is the formation of a biaryl

lactone such as **2.31**. The biaryl lactone **2.31** was shown to be configurationally labile (Scheme 34). The lactone bridge lowers the barrier of rotation such that the atropisomers interconvert readily at room temperature. This interconversion allows for an enantioselective ring opening with many different chiral nucleophiles. The use of oxygen⁹⁹ and nitrogen¹⁰⁰ nucleophiles have been shown. While Bringmann first demonstrated a hydride addition with a chiral aluminum hydride,¹⁰¹ the use of chiral borane reductions has been more effective⁹⁸.

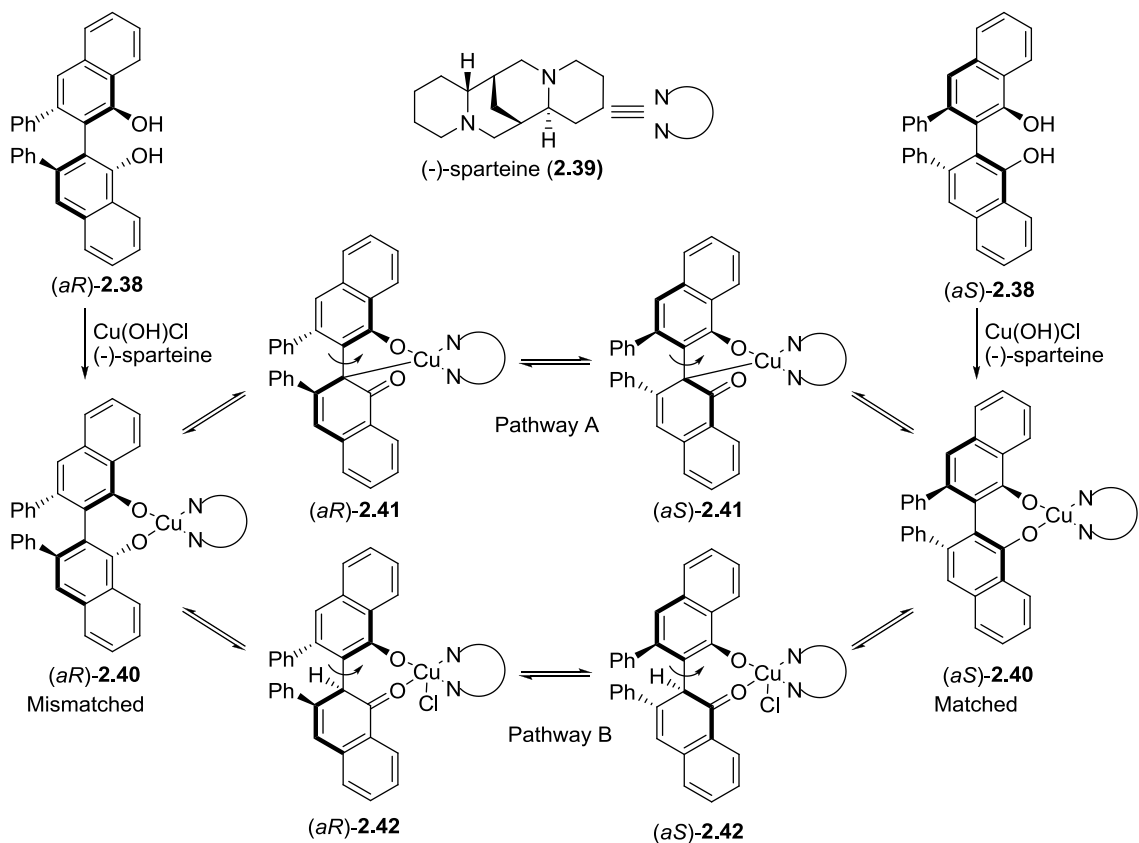
Molecular modeling¹⁰² of the chiral borane reduction reaction showed that the initial hydride attack was not the critical stereochemical step as was shown earlier with chiral nucleophiles. The coordination of the oxaborolidine to the lactone is followed by the first addition of hydride. The axial addition of hydride was shown to add preferentially to the Re face of the lactone carbonyl. The resulting diboroheterocycle **2.34**, although energetically more stable, expanded to the six-membered **2.35** and then ring opening to aldehyde **2.36**. Interconversion of atropisomers is still possible at this point because of the relative low difference in barrier of rotation when compared to the energy barrier of the second hydride addition. Although in the second hydride delivery the energy difference between Re and Si faces is very low (0.3 kcal/mol) the difference in the *aR* vs. *aS* interconversion was significant at 3.5 kcal/mol. The difference in calculated energy predicted a mixture of isomers in a 99.8:0.2 ratio with a predominance of the *aR* isomer. When **2.31** was reduced, there was a high correlation with this calculated energy difference as the selectivity gave a 98.5:1.5 ratio of the *aR* isomer **2.32**. This selective reduction has been demonstrated with the *R* or *S* oxaborolidine to afford the *aS* or *aR* isomer.¹⁰³



Scheme 34. Mechanistic Analysis of Dynamic Kinetic Resolution

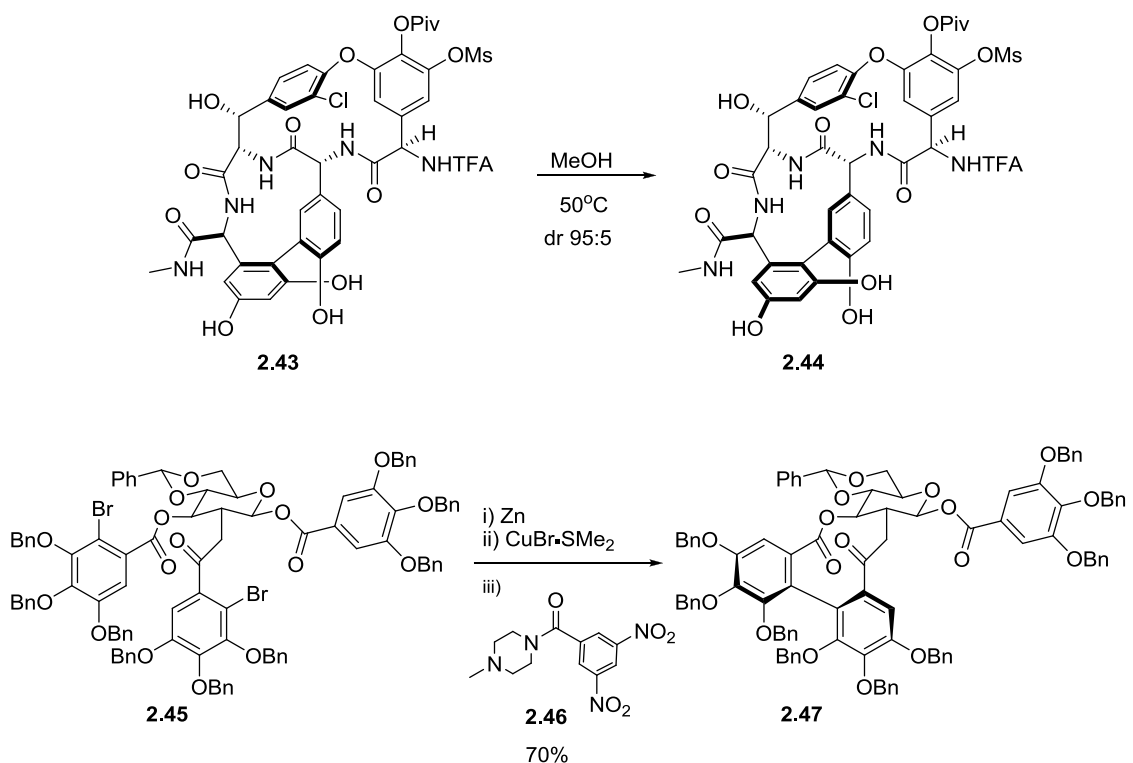
Very few examples of dynamic thermodynamic resolution (DTR) of atropisomers have been reported in the literature.¹⁰⁴ The use of biaryls in DTR began with Kocovsky's¹⁰⁵ discovery that a secondary asymmetric transformation controlled the enantioselection of self coupled 2-naphthols in Cu(II) diamine coupling. This secondary asymmetric transformation was found to be one of three possible processes for directing the stereochemistry shown.¹⁰⁶ The other two processes described were a diastereoselective crystallization and direct enantioselective coupling. It was found that the substrate dictated which mechanism was followed. Expanding on this methodology,

oligonaphthalenes¹⁰⁷ were later synthesized and asymmetricized through this secondary transformation. Wulff then used this methodology to deracemize vaulted biaryl **2.38** (Scheme 35).¹⁰⁸ With little mechanistic details known, Wulff¹⁰⁹ proposed two pathways for this deracemization. The first pathway follows an unusual copper C,O binding that was supported by some biaryl platinum complexes.¹¹⁰ The matched mode displays the O-Cu-O binding dominant while the mismatched mode breaks aromaticity to provide the copper bonding to oxygen and carbon of the biaryl bond in (*aR*)-**2.41**. This mismatched binding motif allows for rotation about the biaryl bond, then relax to the matched pair in (*aS*)-**2.41**. The matched (*aS*)-**2.41** will then prefer the O-Cu-O bonding in (*aS*)-**2.40**. The second plausible path would include a tautomerism to the ketone, providing a SP₃ hybridized center in **2.42** allowing for the free rotation about the biaryl core. This rotation allows for the matching for the diamine with the axis of symmetry. The matched pair will then be rearomatized and cleavage of the copper complex provides the atropo-enantiomer enriched biaryl.



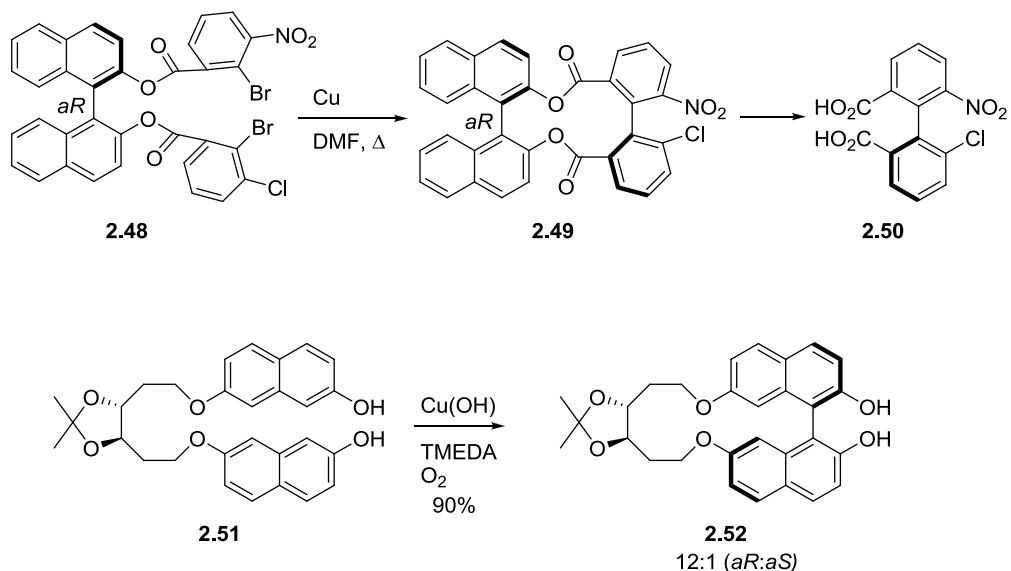
Scheme 35. Proposal for the Mechanism of Dynamic Thermodynamic Resolution.

The last method to arrive at a single atropisomer is that of direct asymmetric coupling reactions. Coupling in this manner has been demonstrated using substrate and reagent control. In the former method, substrate stereochemistry influences the biaryl bond stereoselectivity either under kinetic or thermodynamic control. An example of undesired kinetic product converting to the thermodynamic, Evans^{111, 112} showed that the AB ring of vancomycin (**1.1**) could be formed initially in the undesired atropisomer (**2.43**) but when more of the global structure was in place, gentle heating resulted in adapting the correct biaryl stereochemistry (**2.44**) (Scheme 36). Spring¹¹³ showed that the structural restraints in sanguin H-5 (**1.4**) imparted complete selectivity in formation of the *aS* atropisomer.



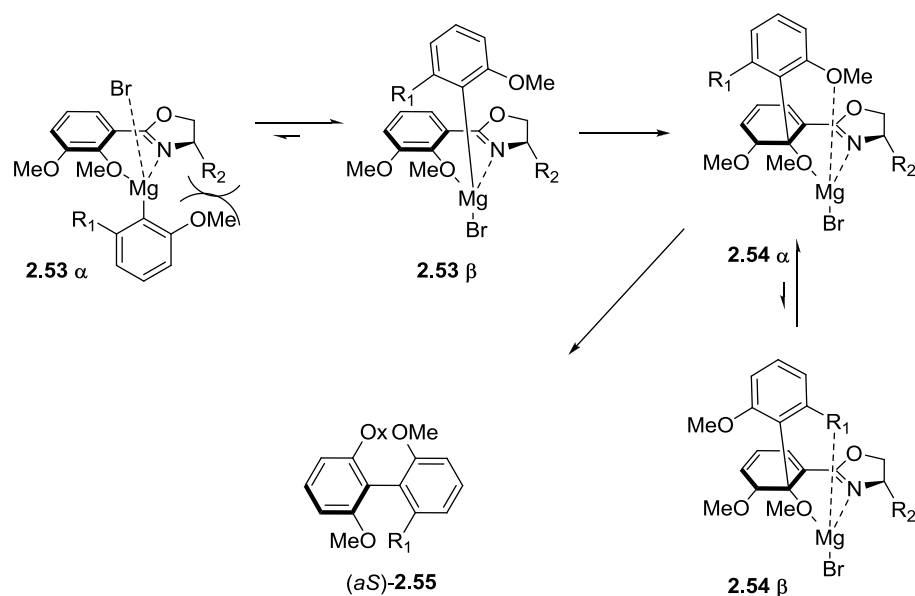
Scheme 36. Atropo-diastereoselectivity under substrate control

In 1988 Miyano¹¹⁴ demonstrated BINOL as a chiral auxiliary in biaryl asymmetric synthesis. Following esterification of BINOL, bis-benzoate **2.48** was subjected to an Ullmann coupling to provide **2.49** in good yield and greater than 99% de (Scheme 37). The ester was then cleaved to provide **2.50** as a single atropisomer.¹¹⁵ Lipshutz⁸⁶ later elaborated on this method of asymmetric biaryl synthesis by using a C-2 symmetric diol auxiliary. Mitsunobo reaction of β -naphthol BINOL with *trans*-hex-3-ene-1,6-diol, followed by a Sharpless asymmetric dihydroxylation, and protection led to acetonide **2.51**. Copper coupling then provided a 12:1 mixture of bi-naphthol **2.52** favoring the *aR* isomer.



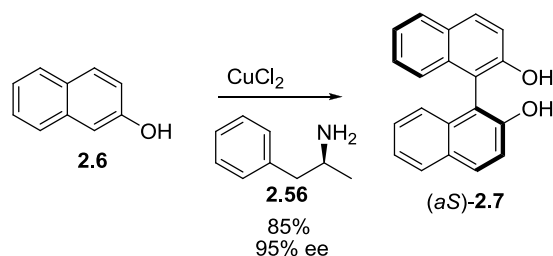
Scheme 37. Chiral Tethers of Miyano and Lipshutz.

Meyers¹¹⁶ used a chiral oxazoline auxiliary to effect an asymmetric aromatic substitution resulting in biaryl bond formation. Meyers proposed the formation of complex **2.53** (Scheme 38). The aryl prefers complexation on the beta face of **2.53** β based on minimized steric interaction. The addition of the aryl group follows the complexation where the aryl group may turn, providing room for loss of stereochemistry. This explains the loss of selectivity when the R_1 group is an electron donating group, as it will compete with the methoxy in coordination to the magnesium. The loss of BrMgOMe then completes the formation of the biaryl (*aS*)-**2.55**. This provides stereoselectivity for the *aR* atropisomer in a ratio of 9:1. The first stereoselective total synthesis of gossypol (**1.3**)¹¹⁷ and a diastereoselective total synthesis of mastigophorene A (**1.22**) and B (**1.23**)¹¹⁸ was later reported by Meyers using this methodology. The synthesis of mastigophorene A (**1.22**) and B (**1.23**) proved to be interesting as each atropisomer was prepared by uses of the *aR* and *aS* chiral oxazolidines.



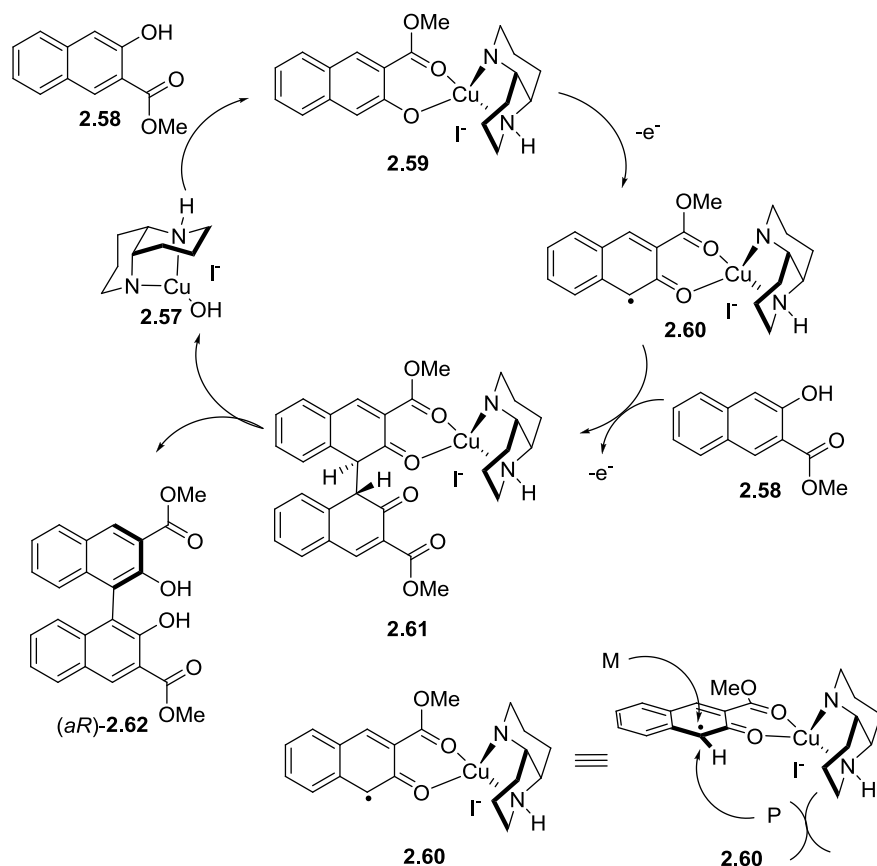
Scheme 38. Mechanism of Selectivity in the Meyers Chiral Oxazolidine Coupling.

Direct (catalytic) coupling of biaryls to arrive at a single atropisomer without use of a chiral auxiliary has been studied with minimal success. Brussee¹¹⁹ first coupled 2-naphthol in the presence of CuCl_2 and four equivalents of amphetamine (**2.56**) to provide (*aS*)-BINOL in 95% ee (Scheme 39). The mechanism was later investigated and proposed to involve a square planar copper complex.¹²⁰ Also shown in this study was the observed enantioselectivity resulted from dynamic thermodynamic resolution of the coupled products.



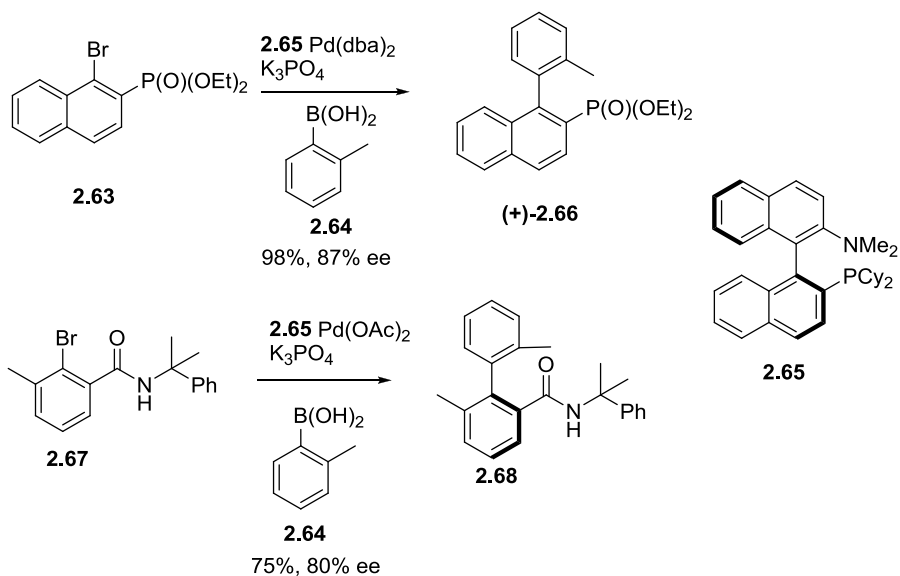
Scheme 39. Brussee's First Observed Enantioenriched Coupling of BINOL.

The first to have success in kinetic biaryl carbon-carbon bond formation using a copper diamine complex was Kozlowski.¹²¹ Although several metals worked in this system, copper was the only metal to turn over in the catalytic cycle. The proposed catalytic cycle starts with copper diamine **2.57** complexation to methyl 3-hydroxy-2-naphthoate (**2.58**) (Scheme 40). Oxidation then leads to the radical **2.60**. Differing from Brussee's, the copper species was shown in this mechanism to be tetrahedral and not square planar and the atropisomeric products were a result of kinetic coupling.¹²² The selectivity is proposed to be derived from the coupling of radical **2.60** to naphthol **2.58**. The diamine blocks the α face from attack so the coupling proceeds from the β face. The sp^3 hybridized carbon relays the stereochemistry to the biaryl through tautomerization and the chiral catalyst turns over during the catalytic cycle to arrive at the (*aR*)-**2.62**. Unfortunately, the scope of this coupling is limited to binaphthyl atropisomers.



Scheme 40. Proposed Catalytic Cycle of Kozlowski Coupling.

Suzuki couplings have been demonstrated to provide an asymmetric biaryl. An early report of this type of coupling was demonstrated by Buchwald.¹²³ Initial reports coupled naphthyl halide **2.63** to boronic acid **2.64** in good to excellent enantiomeric excess with binaphthyl phosphine **2.65** as the chiral ligand (Scheme 41). This methodology has only recently been expanded to coupling of functionalized biaryls.¹²⁴ Aryl bromide **2.67** was coupled with boronic acid **2.64** to provide the biaryl **2.68** with an 80% ee. Unfortunately, this method is doomed for failure when using electron rich biaryls common to many natural products due to the required oxidative insertion of Pd(0) into the aryl-halide bond.

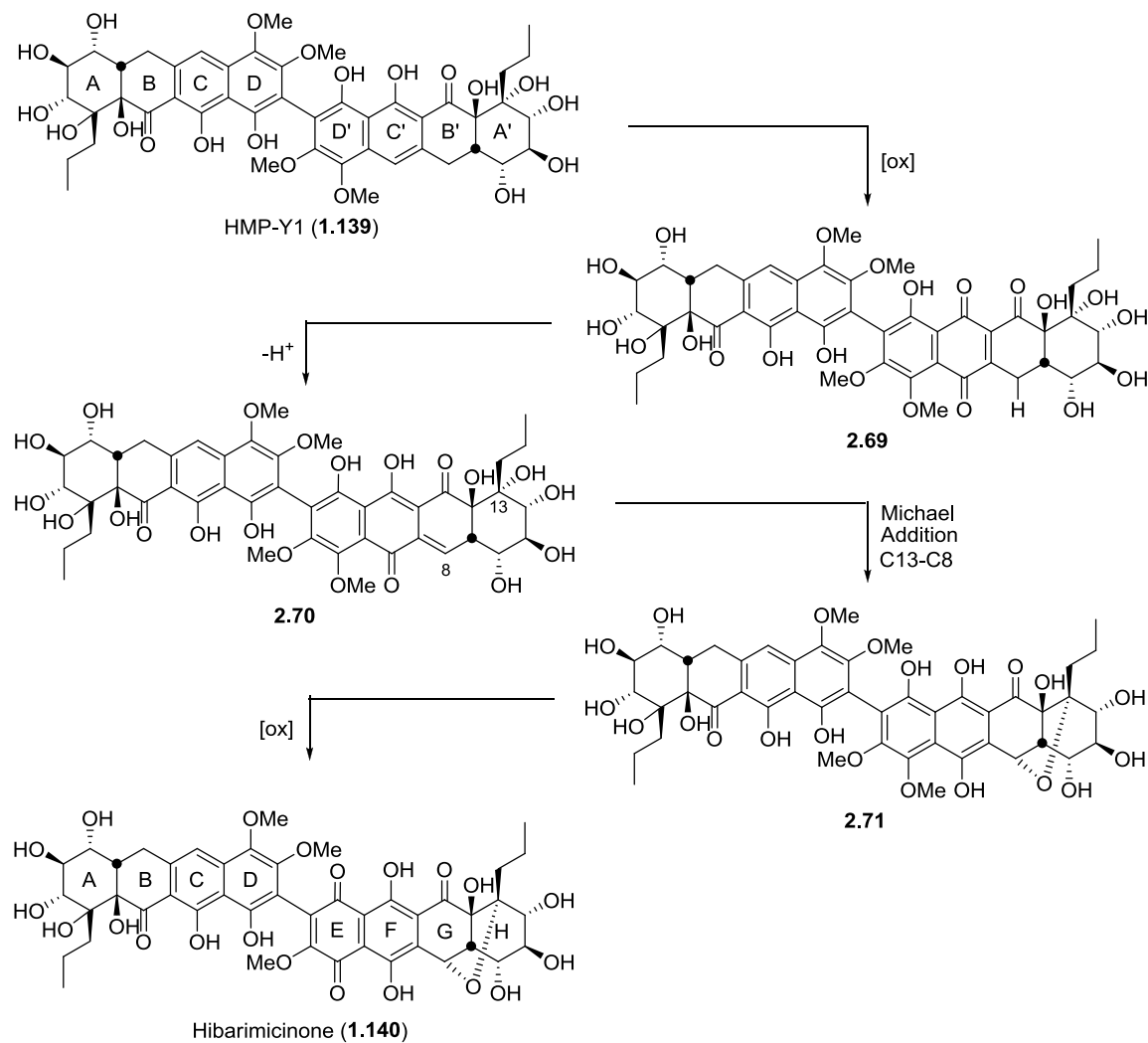


Scheme 41. Buchwald's Asymmetric Suzuki Coupling.

Synthetic Analysis of HMP-Y1 / Hibarimicins and Preliminary Studies

During the course of biosynthetic studies on the hibarimicins Kajjura^{125, 126} showed ¹³C Labeled HMP-Y1 fed to a mutated strain of the hibarimicin producer provided ¹³C labeled hibarimicin B, while HMP-Y6 fed to the same mutated strain produced no hibarimicin B. This result supports the biosynthetic pathway leading to the hibarimicins proceeds by oxidation of HMP-Y1 (**1.139**) to hibarimicinone followed by glycosylation to afford hibarimicin B (**1.140**). We propose to employ a biomimetic oxidation of HMP-Y1 (**1.139**) to quinone **2.69** as a key step in the total synthesis of hibarimicinone (Scheme 42). We anticipate tautomerization of quinone **2.69** to o-quinomethide **2.70** will set the stage for the addition of C13 tertiary alcohol to C8 to give furan **2.71**. Oxidation of hydroquinone **2.71** will then deliver hibarimicinone (**1.140**). Our immediate objective is to develop a synthesis of HMP-Y1 (**1.139**), a C-2 symmetric natural product. Significantly, HMP-Y1 and hibarimicinone exist as atropo-diastereomers of unassigned configuration, a structural feature not discussed in the

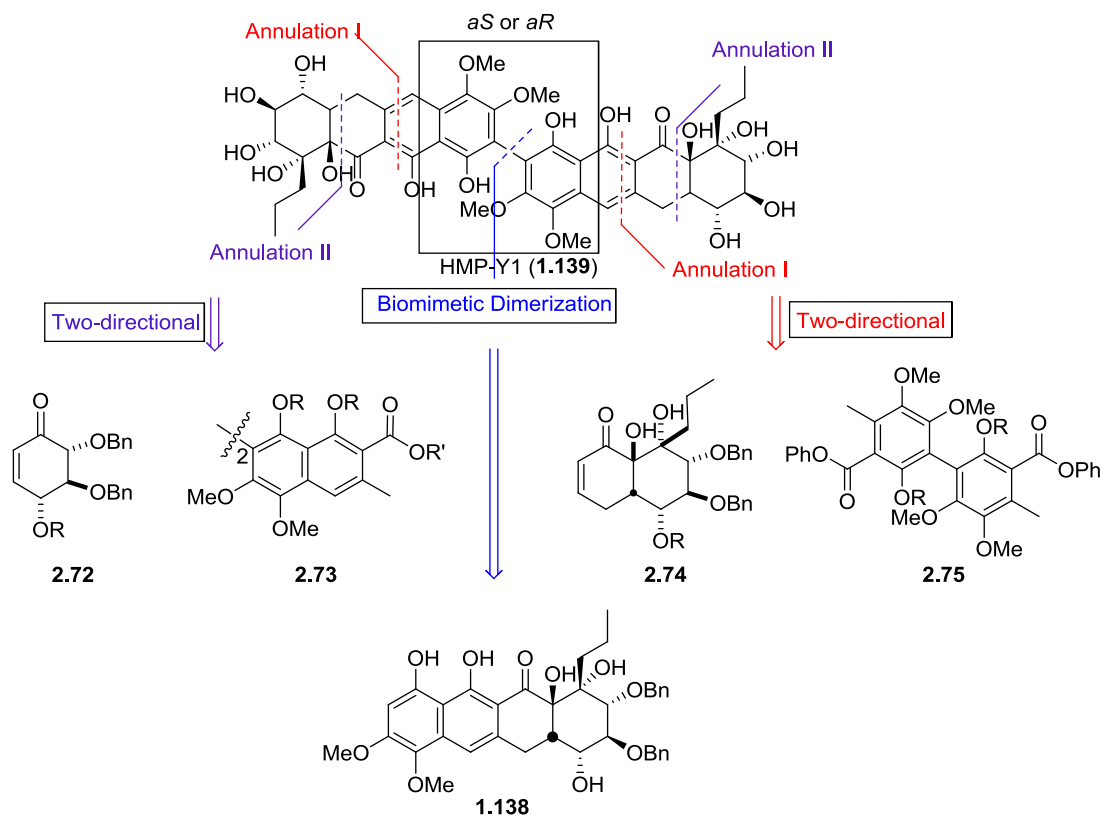
original isolation or subsequent biosynthesis studies. One objective of our synthetic program is the assignment of configuration about the biaryl bond of HMP-Y1 (**1.139**) and hibarimicinone (**1.140**).



Scheme 42. Proposed Oxidative Conversion of HMP-Y1 to Hibarimicinone B.

As symmetrical dimers occur frequently in nature and several have been the subject of total synthesis. In general, two approaches to dimeric natural products such as HMP-Y1 have been employed, biomimetic dimerization and two-directional assembly.¹²⁷ Biomimetic dimerizations are perhaps most effective, in the case of HMP-

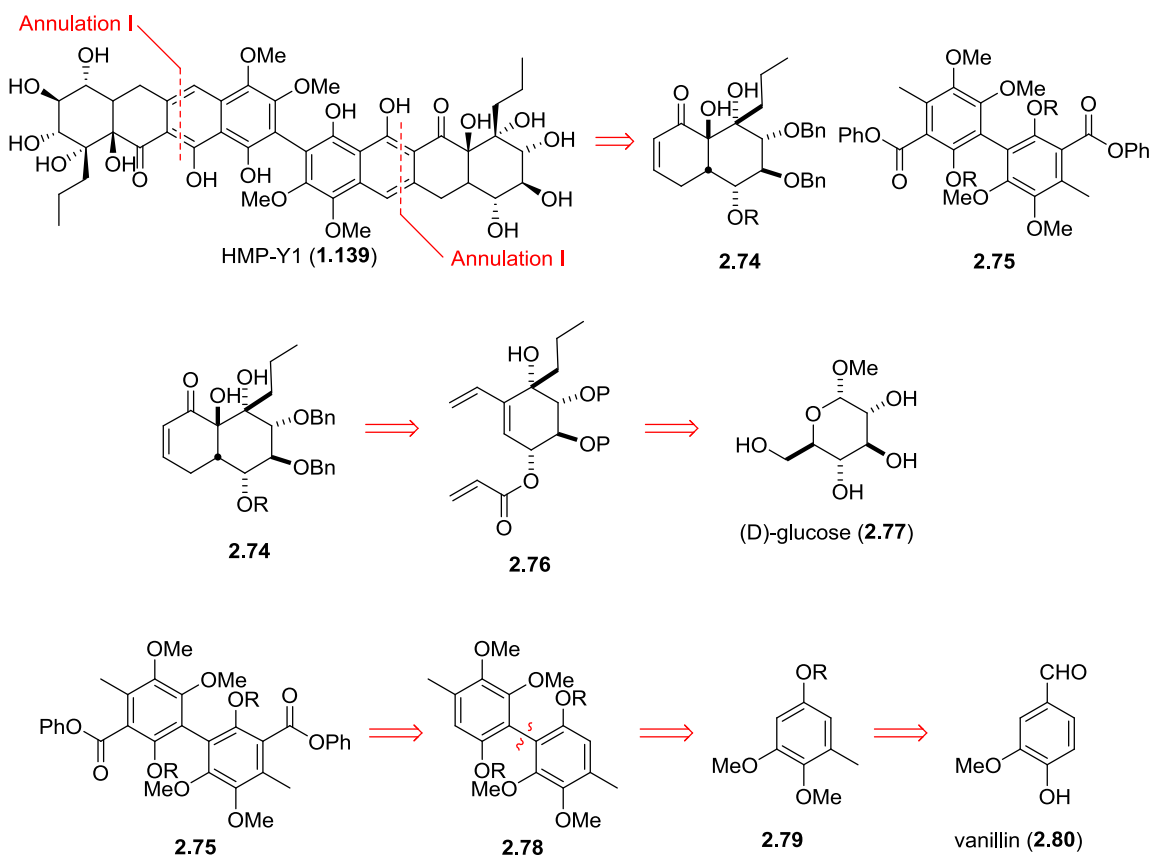
Y1, this requires synthesis of aromatic polyketide **1.138** (Scheme 43). A second approach starts from formation of biaryl **2.75** early in the synthesis and elaborate in a two directional manner. For HMP-Y1 (**1.139**), we considered two bi-directional strategies. The first entailed two consecutive annulations with the second annulation involving binaphthyl **2.73** and cyclohexenone **2.72**. The second two-directional approach involved annulation between *cis*-decalin **2.74** and biaryl **2.75**. *In either synthetic approach establishment of a single atropisomer of known configuration is a key issue to be addressed.*



Scheme 43. Strategic Analysis of HMP-Y1.

Our initial strategy directed toward HMP-Y1 was to effect a double Staunton-Weinreb annulation using two equivalents of *cis*-decalin **2.74** and bis-toluate anion

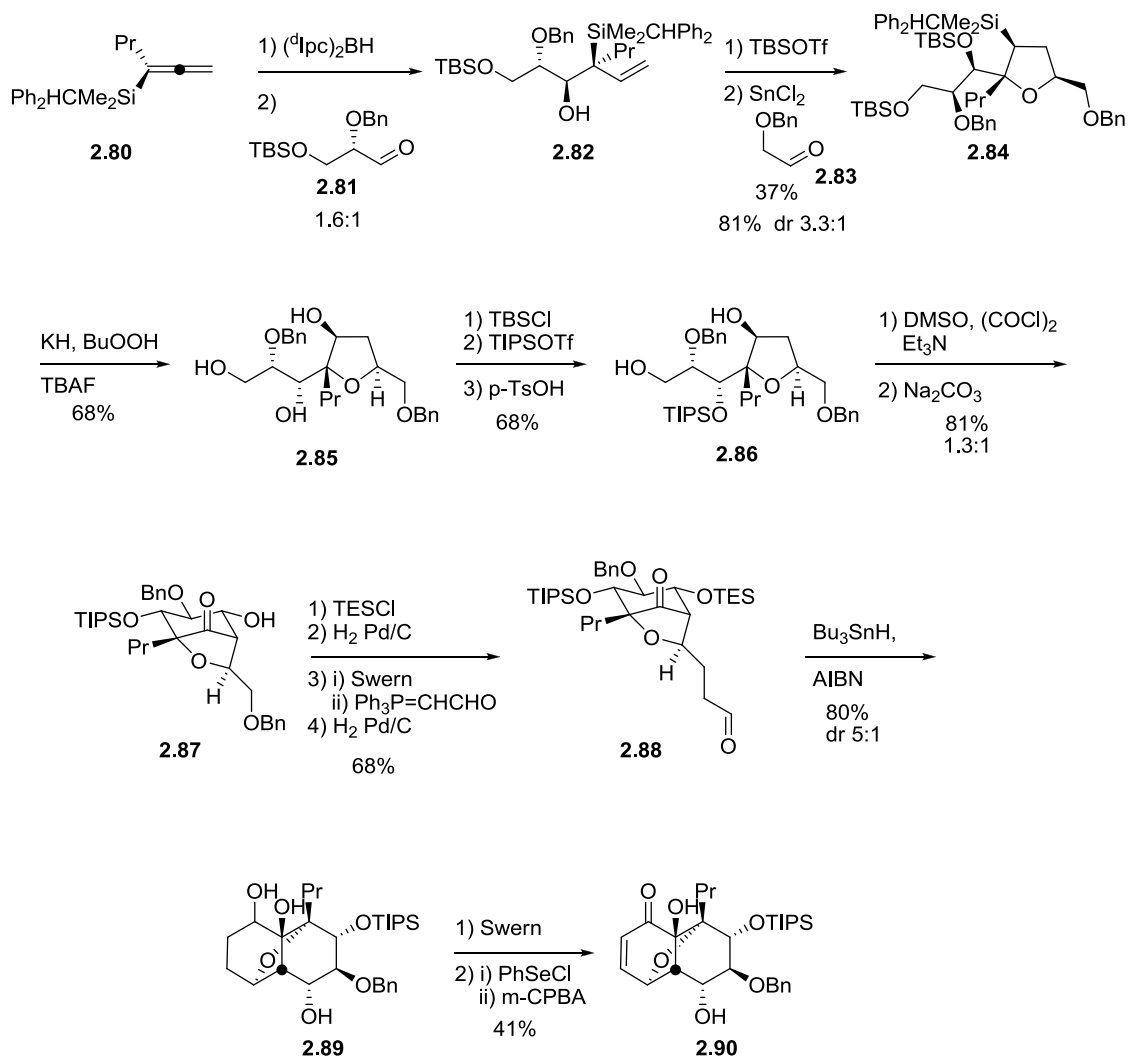
derived from biaryl ester **2.75** (Scheme 44). We initially planned to assemble *cis*-decalin **2.75** by way of an intramolecular Diels-Alder using triene **2.76** as a substrate. Triene **2.76** was proposed to be derived from D-methyl glucose (**2.77**). We required biaryl ester **2.75** to be prepared as a single atropisomer of known configuration by way of biaryl **2.78**, The latter ultimately derived from the oxidative coupling of toluene **2.79** available from inexpensive vanillin (**2.80**).^{128, 129}



Scheme 44. Single Bis-Annulation Approach to HMP-Y1.

Three synthetic approaches to the hibarimicin *cis*-decalin have been described in the literature by the research groups of Roush, Mootoo and Sulikowski. Roush and Mootoo prepared the *cis*-decalin common to hibarimicinone that incorporates a bridging

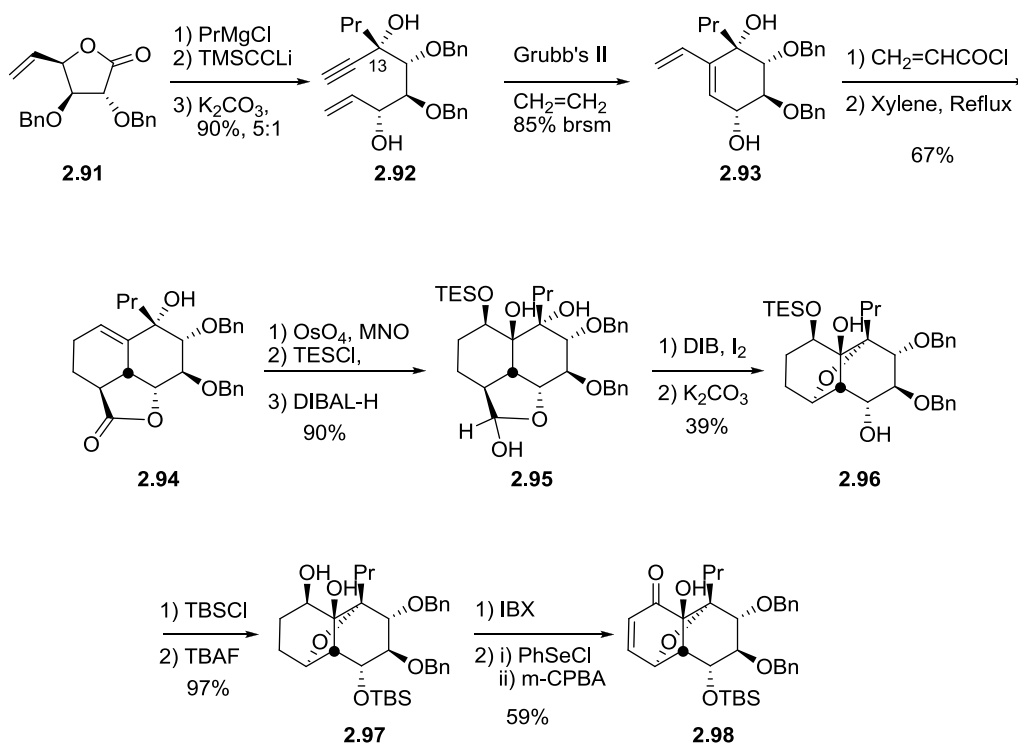
furan heterocycle in the G/H ring system. Roush's¹³⁰ route began with the hydroboration of allene **2.80** and addition of the derived allyl borane to aldehyde **2.81** to provide β -hydroxysilane **2.82** (Scheme 45). Following silylation of the secondary alcohol, a tin (II) mediated [3+2] annulations proceeded with modest stereoselectivity to provide furan **2.84**. A Tamao-Fleming oxidation of **2.84** led to triol **2.85**. A series of protecting group manipulations then provided diol **2.86**. A double Swern oxidation provided an intermediate keto-aldehyde that was subjected to an intramolecular aldol reaction to provide beta-hydroxy ketone **2.81** as a nearly 1:1 mixture of alcohols **2.87** (equatorial alcohol). The axial alcohol could be re-equilibrated to a 1.3:1 mixture of alcohols resulting in recycling of the axial alcohol. The equatorial alcohol was then protected and the primary benzyl group removed. A one-carbon homologation and reduction provided the new keto-aldehyde **2.88**. Pinacol cyclization afforded a 5:1 mixture of diastereomers in favor of the *cis*-decalin **2.89**. Swern oxidation was followed by installation of unsaturation to complete *cis*-decalin **2.90**.



Scheme 45. Roush's Route to the *cis*-Decalin of the Hibarimicins.

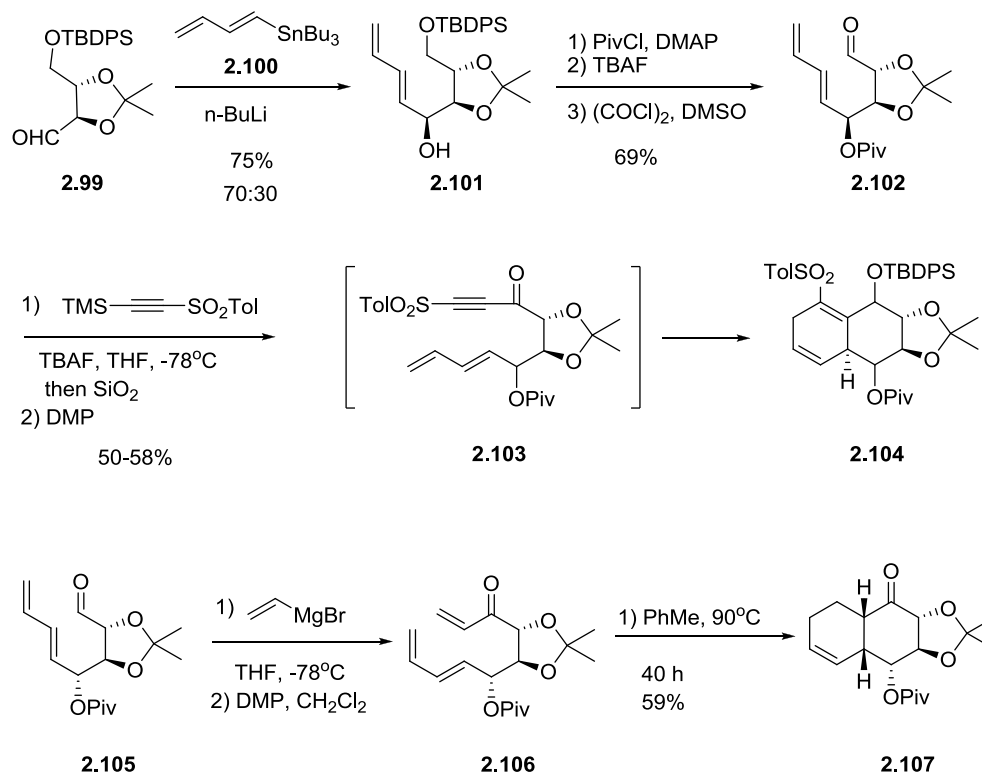
The Mootoo¹³¹ synthesis of the hibarimicinone GH *cis*-decalin began from known lactone **2.91** available from D-glucose (**2.76**) (Scheme 46). Propyl Grignard addition to **2.91** provided an intermediate hemiketal which on treatment with lithium trimethylsilylacetylide provided tertiary alcohol **2.92** (5:1 mixture of C13 epimers). The major product was subjected to a ring closing enyne metathesis under an atmosphere of ethylene to provide diene **2.93**. Esterification of the secondary alcohol with acryloyl chloride provided a triene that on heating in xylene led to the desired Diels-Alder adduct

2.94. Diels Alder adduct **2.94** was then subjected to a dihydroxylation which occurred from the convex face of the decalin ring system. The secondary alcohol was protected and the lactone reduced to provide lactol **2.95**. Iodination of lactol **2.95** proceeded with 3:1 selectivity although none of the β -iodide was isolated as this isomeric iodide was intercepted by a displacement reaction of the C13 hydroxyl leading to formation of the bridging furan ring. Hydrolysis of the formate group, protection of the secondary alcohol and removal of the TES group provided diol **2.97**. The synthesis was then completed by oxidation and installation of the unsaturation. Notably the Roush and Mootoo approaches provide access to only the GH and not the AB ring system of the hibarimicins.



Scheme 46. Mootoo's Route to the *cis*-Decalin of the Hibarimicins.

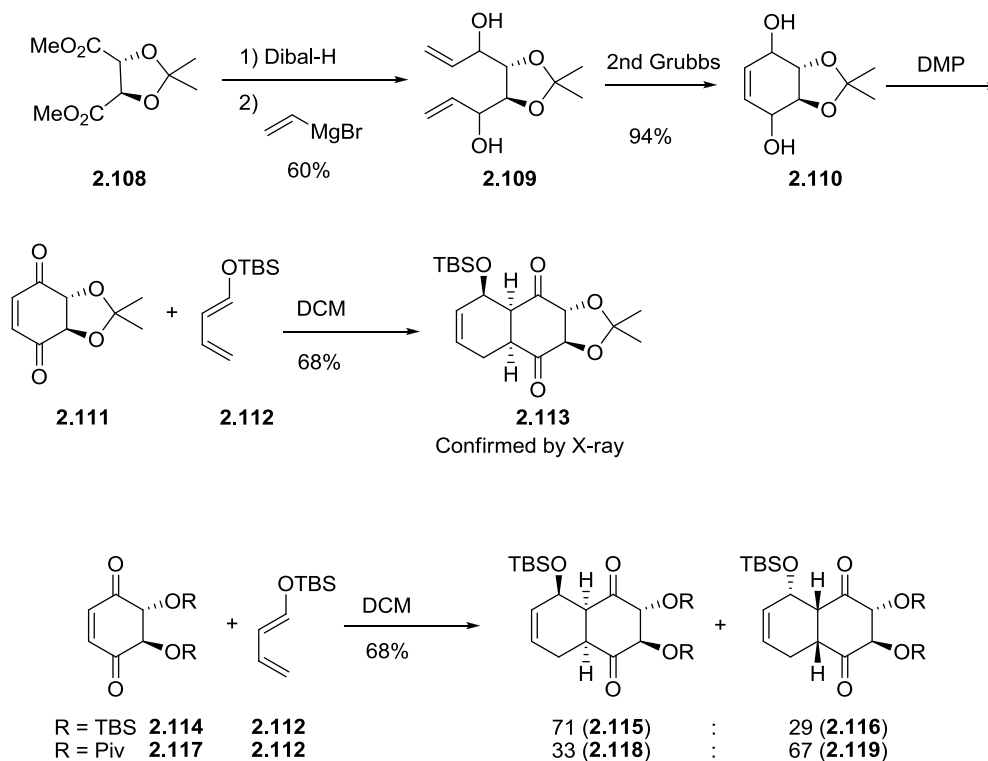
The Sulikowski group has published on three approaches to *cis*-decalin ring system, each employing a Diels-Alder reaction. Two of the three approaches used tartaric acid as starting material, which can be converted to known aldehyde **2.99** in four steps. Addition of butadienyllithium to aldehyde **2.99** led to a 70:30 mixture of separable epimers of the allylic alcohol with **2.101** as the major¹³² (Scheme 47) (note: incorrect C10 configuration for hibarimicins). Protection of the secondary alcohol, removal of the silyl protecting group and oxidation provided aldehyde **2.102**. In an attempt to obtain asymmetric induction from the Diels-Alder reaction and set the *cis*-decalin stereochemistry, trimethylsilylethynyl *p*-tolylsulfone was added to the aldehyde **2.102**. The alkyne produced was oxidized to ketone **2.103** and spontaneously underwent a Diels-Alder cycloaddition to afford decalin **2.104**. Unfortunately, the incorrect configuration at C9 (ring fusion) was confirmed by a single X-ray crystal analysis. The reaction sequence was repeated with the C10 epimer but unfortunately the same incorrect C9 configuration was observed. A second Diels-Alder adduct **2.106** was prepared starting from the Grignard addition of vinyl magnesium bromide to the aldehyde **2.105** and oxidation. This adduct was then heated to form the Diels-Alder product **2.107**. When the α -epimer of the allylic alcohol was the starting material, the correct *cis*-decalin **2.107** was produced and confirmed again by an X-ray crystal structure. The *cis*-decalin **2.107** was judged to be under functionalized and not a good intermediate to proceed with a synthesis of the hibarimicins



Scheme 47. First Attempt of an Intramolecular Diels-Alder Reaction to Form the *cis*-Decalin.

In an effort to achieve better stereocontrol, an intermolecular Diels Alder was examined. In this approach demonstrated the importance of the diol protecting group in controlling stereochemistry (Scheme 48). Diethyl tartrate **2.108** was reduced to the dialdehyde then alkylated with vinyl Grignard to provide the diene **2.109**. Ring closing metathesis with Grubbs' second generation catalyst afforded cyclohexene **2.110**. Oxidation with the Dess-Martin periodinane provided a dienophile to be employed in the proposed intermolecular Diels-Alder reaction. The acetonide **2.111** was allowed to react with diene **2.112** to form a single cycloadduct **2.113** that was assigned by X-ray crystal analysis. The incorrect facial selectivity led to the examination of different diol protecting groups. Protecting the diol as a bis-TBS in **2.114** led to a mixture of diastereomers in a 71:29 ratio of the undesired stereochemistry. The diol was then protected as a pivaloate

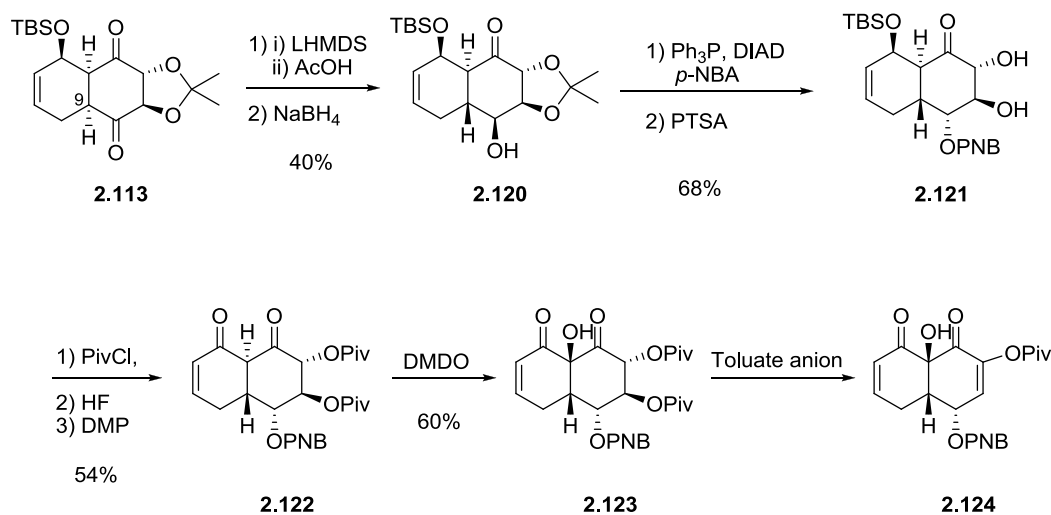
in **2.117** and subjected to the Diels-Alder reaction to provide a 33:67 mixture of the desired stereochemistry at the ring fusion.



Scheme 48. Intermolecular Diels-Alder Route to *cis*-Decalin.

In unpublished results from our lab, acetonide **2.113** was subjected to inversion of the stereochemistry at the C9 position through a kinetic deprotonation followed by an acid quench (Scheme 49). The product was immediately reduced to provide alcohol **2.120**, which was also confirmed by a single X-ray crystal analysis. The stereochemistry of the free alcohol was then inverted through a Mitsunobu esterification with *p*-nitrobenzoate¹³³ to set four of the six required stereocenters. The strain imposed by the acetonide on the system was the thought to be the reason that attempts to remove the TBS led to β -elimination. The acetonide was then removed to provide diol **2.121**. With the diol protected as the bis-pivolate, the TBS was cleanly removed and oxidized to

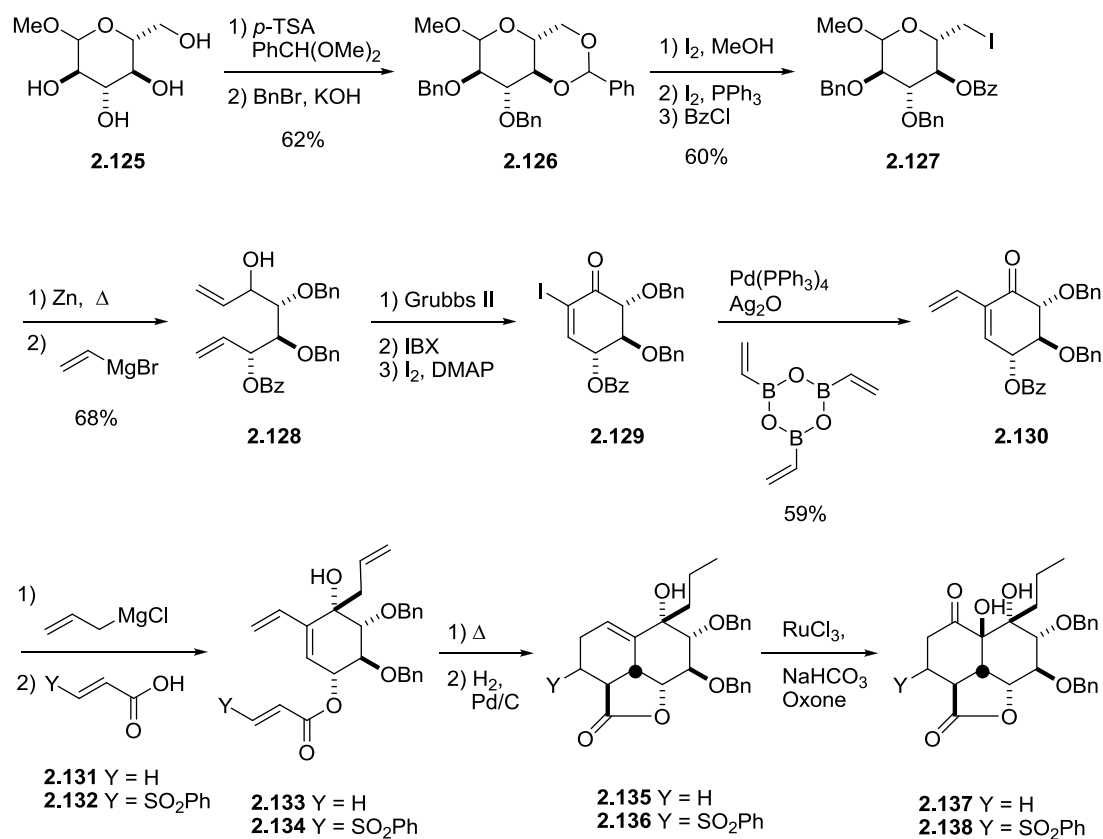
provide the bis ketone **2.122**. As shown in previous work by our lab¹³⁴ the tertiary alcohol could be installed by DMDO oxidation of the bis ketone **2.122** to arrive at the *cis*-decalin **2.123** with five of the six stereocenters in place. The stereochemistry was assigned based on NOE correlation of the tertiary alcohol and the C9 proton. Further elaboration of this route was unsuccessful as treatment of **2.123** with mild base or the toluate anion directly led to β -elimination product **2.124**. As both approaches failed to control the C9 stereochemistry with acceptable selectivity we chose to examine an intramolecular Diels-Alder approach that would assure control of the C9 stereochemistry.



Scheme 49. Kim's Progress Toward the *cis*-Decalin Ring System.

The third route to the hibarimicin *cis*-decalin common to hibarimicinone began with the formation benzylidene acetal from methyl glucose **2.125** and protection of the remaining alcohols as benzyl ethers to provide **2.126** (Scheme 50). A Hannesian¹³⁵ ring opening was initially performed but optimization showed that removal of the acetal with I_2 and iodination of the primary alcohol followed by benzoylation produced **2.127** better results. A Vasella fragmentation^{136, 137} followed in a second step with vinyl Grignard

addition yielded an inconsequential mixture of diastereomeric alcohols **2.128**. Diene **2.128** was then subjected to ring closing metathesis with Grubbs' second generation catalyst. Oxidation and iodination produces iodo-enone **2.129**. Suzuki cross coupling with vinyl boronate anhydride provided diene **2.130**. Allyl Grignard addition provided the desired asymmetric induction with the allyl group adding to C13 from the equatorial face with an 2:1 selectivity. Excess Grignard simultaneously removes the benzoate. Esterification of the secondary alcohol with a variety of acrylates led to the ability to separate the previous mixture diastereomers. Heating of the desired diastereomer provided the Diels-Alder adducts, while selective hydrogenation with Pd/C for five minutes yielded decalin ring systems **2.135** - **2.136**. In-situ generation of ruthenium tetroxide¹³⁸ provided the hydroxyl-ketone **2.137** – **2.138**. Setting all six of the contiguous stereocenters left only the installation of the α,β -unsaturation to complete the AB ring of the hibarimicins. Unfortunately, all attempts to install the C7-C16 double bond were unsuccessful.

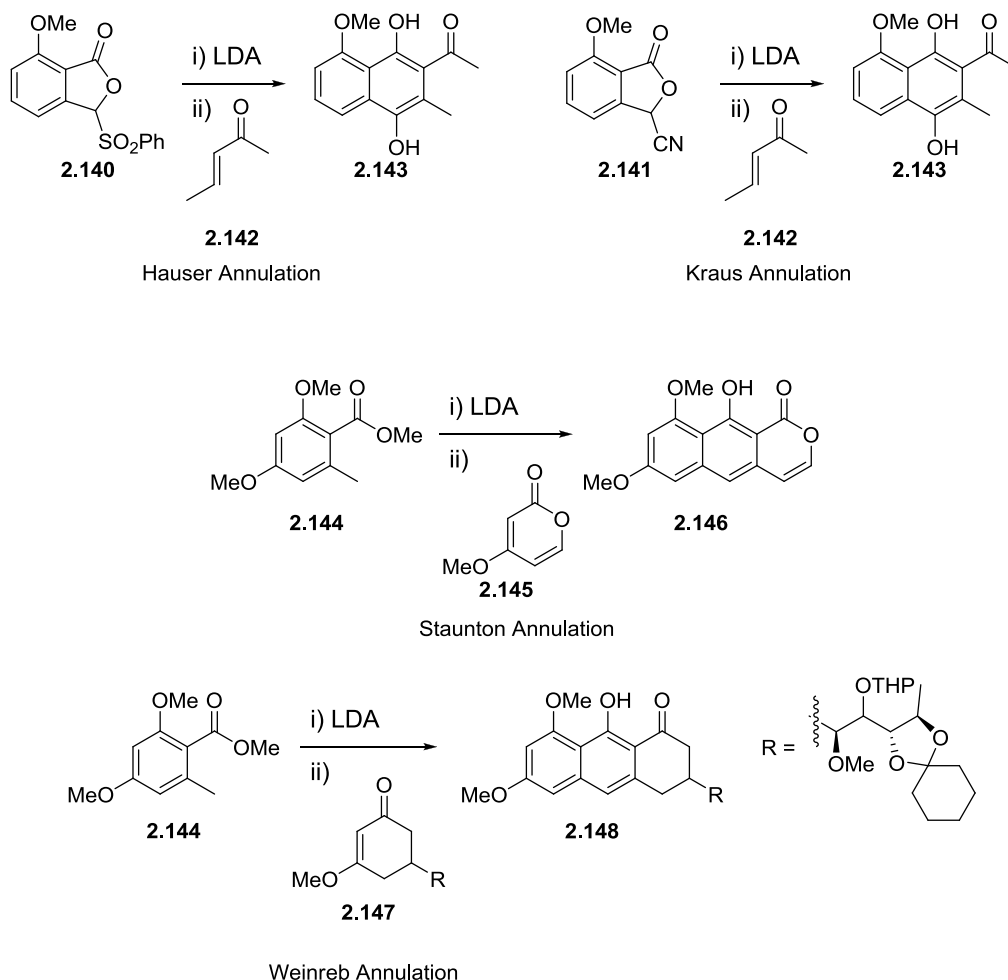


Scheme 50. Engers/Hempel Approach to the *cis*-Decalin.

Two Directional Approach

A two-directional or biomimetic coupling synthetic strategy toward HMP-Y1 (**1.139**) require an efficient annulation method to access the common tetracyclic structure. The synthesis of linear aromatic polyketide related to HMP-Y1 was addressed in 1978 by Hauser and Kraus by development of anion-based annulation reactions. Hauser¹³⁹ initially used the phenyl sulfone phthalide **2.140** and Kraus¹⁴⁰ cyano-phthalide **2.141** that on deprotonation and reaction with unsaturated carbonyls afforded naphthylene **2.143** in the hydroquinone oxidation state (Scheme 51). This methodology was later expanded to access lower oxidation states of the annulation product. For example, Staunton¹⁴¹ and Weinreb¹⁴² developed methods to generate toluate anion of

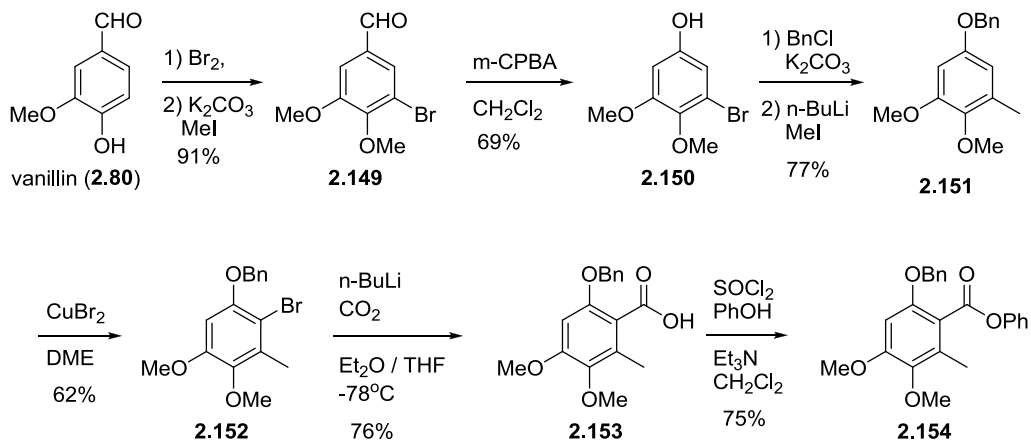
2.144 that on reaction with an α,β -unsaturated ketone afforded naphthylene **2.146** and **2.148** respectively.



Scheme 51. Original Annulations Performed by Hauser, Kraus, Staunton, and Weinreb.

In 2005, Andy Myers¹⁴³ conducted a study to optimize the Staunton Weinreb annulation in connection with his work on the tetracycline antibiotics and determined phenyl benzoates to be optimal annulation reagents. With this in mind, we undertook the synthesis of ester **2.154** (Scheme 52). This work began with the known regioselective bromination of vanillin¹⁴⁴ (**2.80**) followed by phenol methylation¹²⁸ to provide aldehyde **2.149**. Aldehyde **2.149** was then converted to phenol **2.150** by a

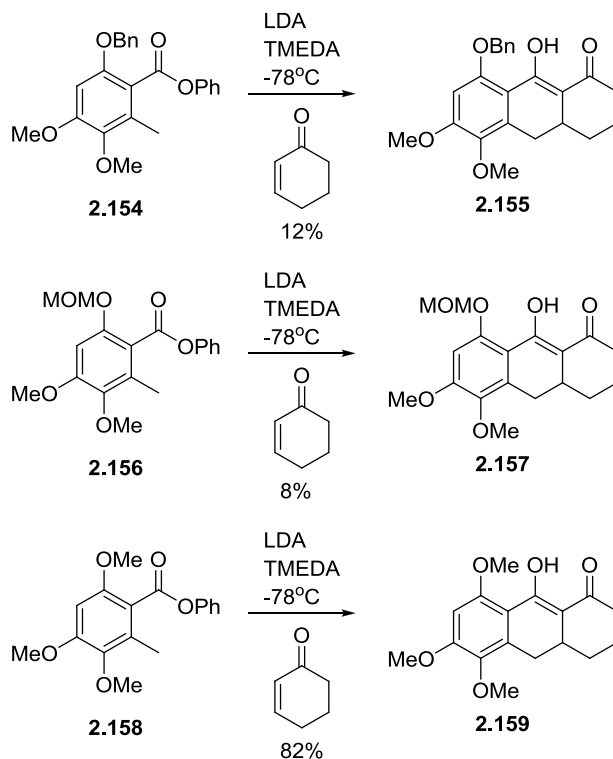
Baeyer-Villiger¹⁴⁵ oxidation. In an attempt to differentially protect the C1 phenol common to HMP-Y1 (**1.139**), phenol **2.150** was protected as a benzyl ether and the aryl bromide was converted to toluene **2.151** by way of a lithium halogen exchange followed by a methyl iodide quench. The regioselective bromination¹⁴⁶ was achieved by treatment with copper(II) bromide to provide bromide **2.152**. The latter was subjected to a second lithium-halogen exchange this time followed by a carbon dioxide quench and the resulting carboxylic acid **2.153** was converted to phenyl ester **2.154** using a standard two-step process.



Scheme 52. Synthesis of Staunton-Weinreb Annulation Precursor

We next evaluated phenyl ester **2.154** as an annulating reagent using cyclohexenone as the coupling partner (Scheme 53). Initial annulation attempts using benzyl ether **2.154** provided **2.155** in poor yield with the major product recovered phenol, as a result of loss of benzyl group. To identify a superior annulation partner other protecting groups were examined. The benzyl protecting group was removed by hydrogenolysis, and the phenol protected using a variety of alkyl, silyl and Boc groups. Each of these protected phenols was then subjected to the annulation conditions (Scheme 51). MOM ether **2.156** provided negligible product **2.157** and the optimal

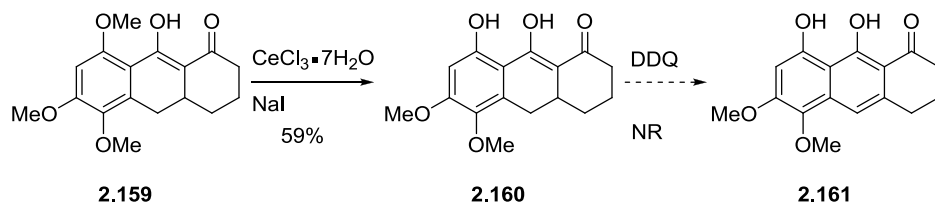
protecting group proved to be methyl ether **2.158**, providing the annulation product **2.159** in 82% yield. The BOC and TBS protected benzoates provided poor results.



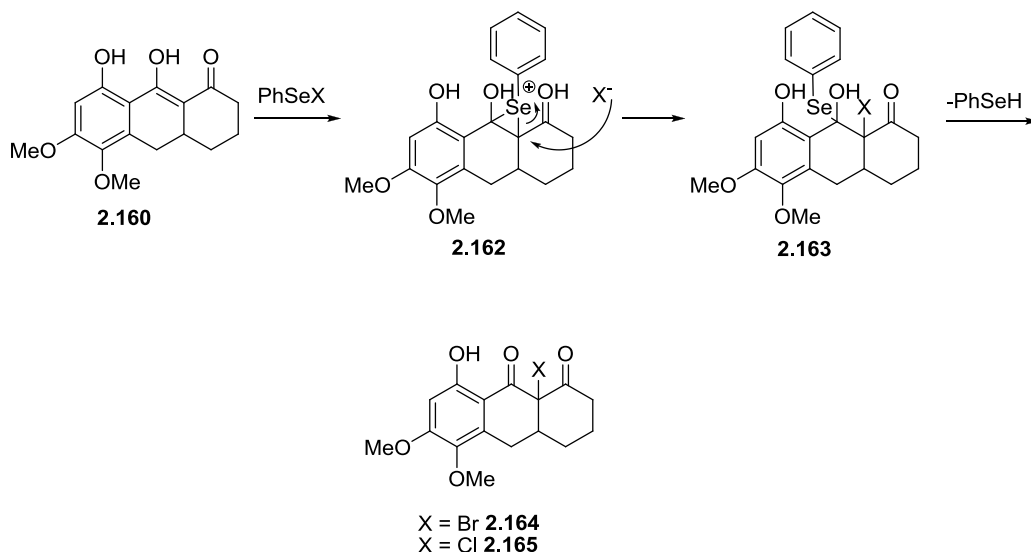
Scheme 53. Effect of Protecting Group on the Staunton-Weinreb Annulation.

The cleavage of a methyl ether located in a peri position relative to an oxygen is predated in the literature^{147, 148}. The use of BBr_3 provided decomposition, while the use of cerium trichloride heptahydrate¹⁴⁹ and sodium iodide provided the desired deprotection (Scheme 54). This selectivity is likely the result of formation of cerium(III) chelate to the peri carbonyl. The selective removal of the C1 methyl ether was supported by NOE experiments. However, oxidation of **2.160** to naphthylene **2.161** proved problematic. Attempts to provide a phenyl selenide in order to effect a selenoxide elimination provided interesting results. Instead of formation of the selenide, all attempts resulted in α -halogenation. The halogen incorporation was confirmed by low

resolution mass spectrometry analysis. This was possibly due to the formation of the selenonium ion **2.162** (Scheme 55), followed by opening by halogen at the tertiary carbon to provide **2.163**. Loss of phenyl selenide provides **2.164** or **2.165**.



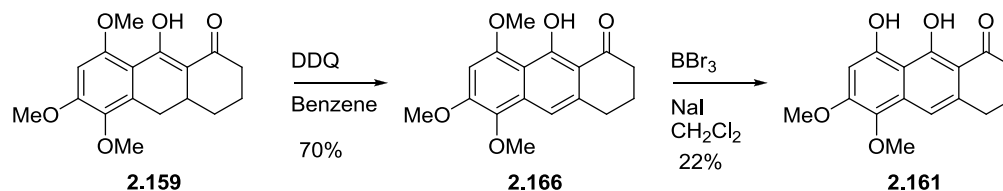
Scheme 54. Selective Demethylation Followed by Oxidation to Naphthyl Ring System.



Scheme 55. Possible Mechanism for the Alpha Halogenations of Phenol **2.157**.

In contrast to the failed oxidation of phenol **2.160**, oxidation of methyl ether **2.159** proceeded smoothly with DDQ¹⁵⁰ to afford naphthyl **2.166** in 70% yield (Scheme 56). Unfortunately attempted removal of the C1 methyl ether using previously successful CeCl₃-NaI combination now failed. Based on literature precedent we returned to BBr₃ as a demethylating reagent.¹⁴⁸ Optimal conditions were observed a combination of NaI and

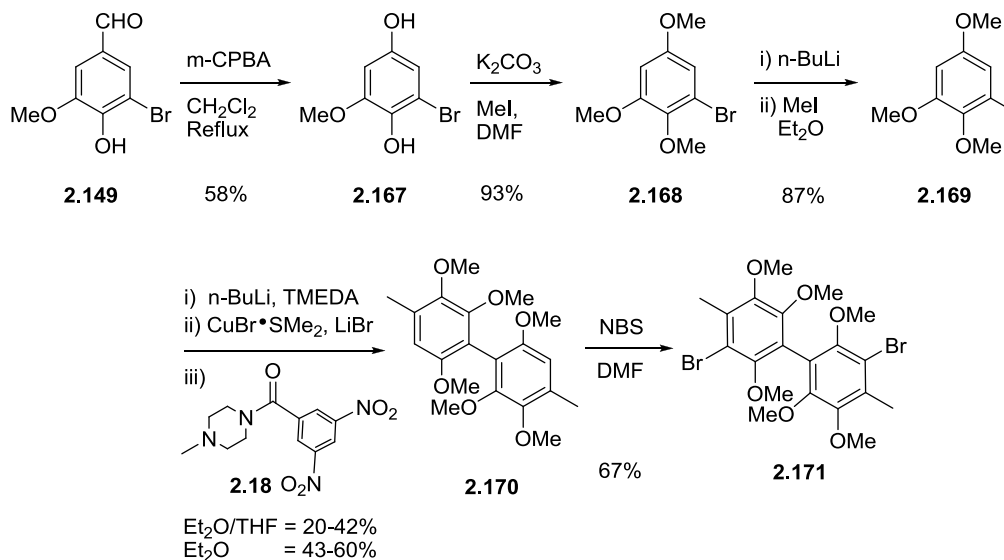
BBr_3 was added to afford demethylated **2.161** with minimal formation of the hydroquinone.



Scheme 56. Oxidation and Demethylation to Naphthol Ring system **2.164**.

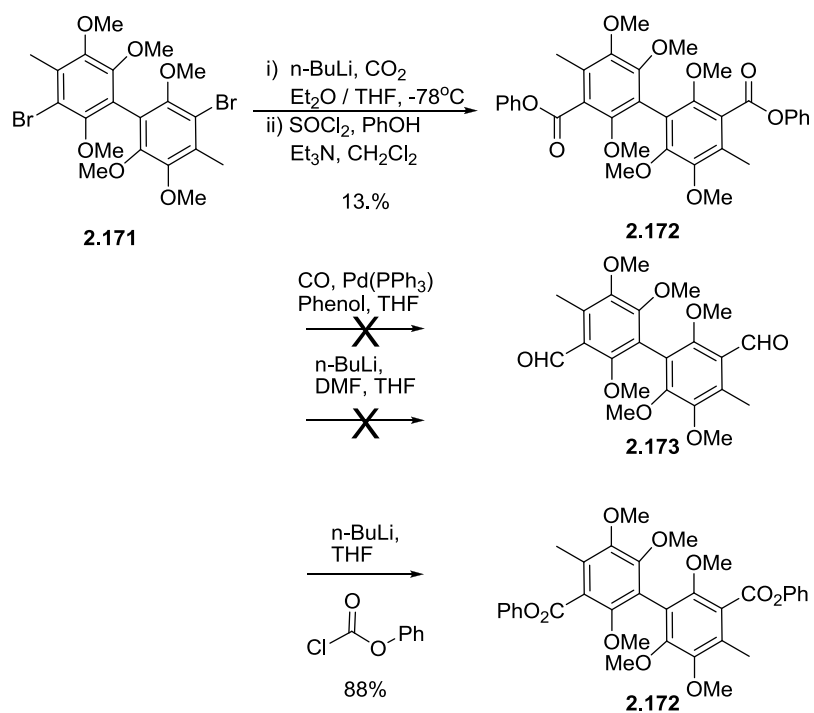
Having developed a viable annulation, oxidation and demethylation sequence in the context of a monomeric tricycle, we next turned our attention to applying this approach in the context of a two-directional strategy starting from bis-phenyl benzoate (**2.75**, Scheme 43). As presented in Chapter 1 a variety of biaryl couplings are available but highly substrate dependant. In the case of electron rich bis-phenyl ester (**2.75**) an oxidative coupling seemed most appropriate. Unfortunately no asymmetric oxidative couplings are available and we would need to later address how to generate **2.75** as a single atropo-enantiomer. The oxidative coupling recently described by Spring and co-workers¹⁵¹ drew our attention as it employed a direct resorcinol lithiation and oxidation. Trimethoxytoluene (**2.169**) was selected as the substrate for the oxidative homocoupling and was prepared from aldehyde **2.149** starting with a Baeyer-Villiger oxidation to afford hydroquinone **2.167** (Scheme 57). Not surprisingly, this hydroquinone was found to be very susceptible to air oxidation to provide the corresponding quinone. Immediate methylation of **2.167** followed by a lithium halogen exchange and methyl iodide quench provided trimethoxy toluene **2.169**. The Spring homodimerization proceeded smoothly on deprotonation of **2.169** with *n*-BuLi-TMEDA complex, cuprate formation and oxidation

to give biaryl **2.170** in yields ranging from 40 to 60%. Finally, bromination with NBS¹⁵² afforded dibromide **2.171**.



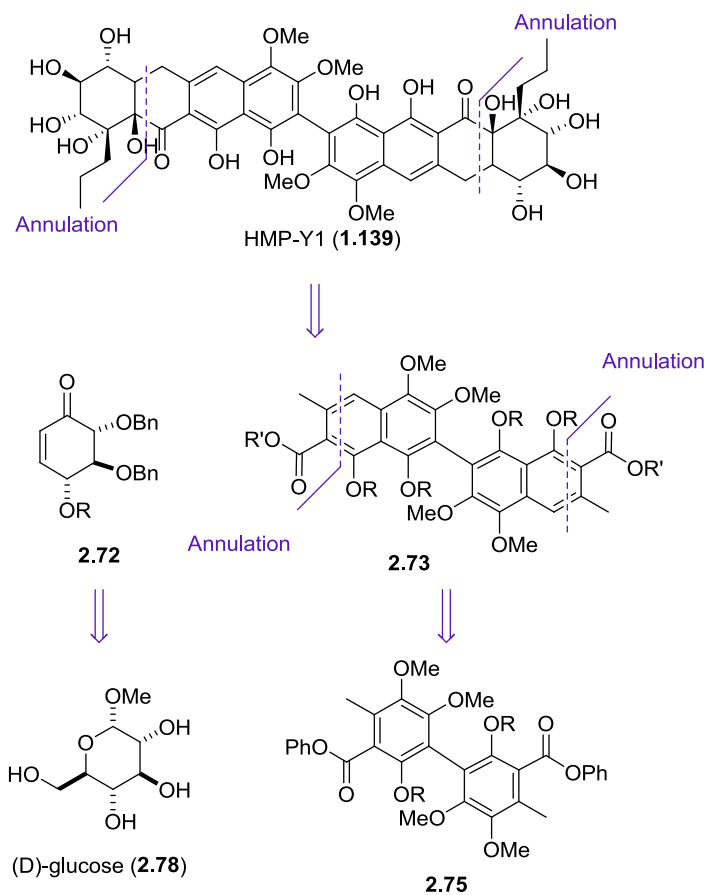
Scheme 57. Biaryl Formation

Initial attempts at converting the dibromide **2.171** to the bis-phenyl ester **2.172** employing the previously described three step reaction proceeded in poor yields (Scheme 58). A variety of methods to convert dibromide **2.171** to **2.172** were examined including DMF quench of the derived dianion and palladium mediated carbophenoxylation, all failed to yield positive results. Gratifyingly and somewhat surprising phenyl chloroformate reacted with the dianion derived from **2.171** to afford bis-phenyl ester **2.172** in 88% yield.



Scheme 58. Methods to Form the bis-Phenyl Ester **2.170**.

As an alternative two-directional annulation we considered was a sequential two annulation process to form HMP-Y1 (**1.139**, Scheme 59). We envisioned a primary annulation of bis phenyl ester **2.75** with a crotonate followed by aromatization to provide intermediate bi-naphthyl **2.73**. A second and final annulation of bis-naphthyl **2.73** with enone **2.72** would then lead to HMP-Y1 (**1.139**). As we had prepared enone **2.72** from D-glucose (**2.77**) our attention turned to the examination of bis-phenyl ester **2.75** as an annulation partner.

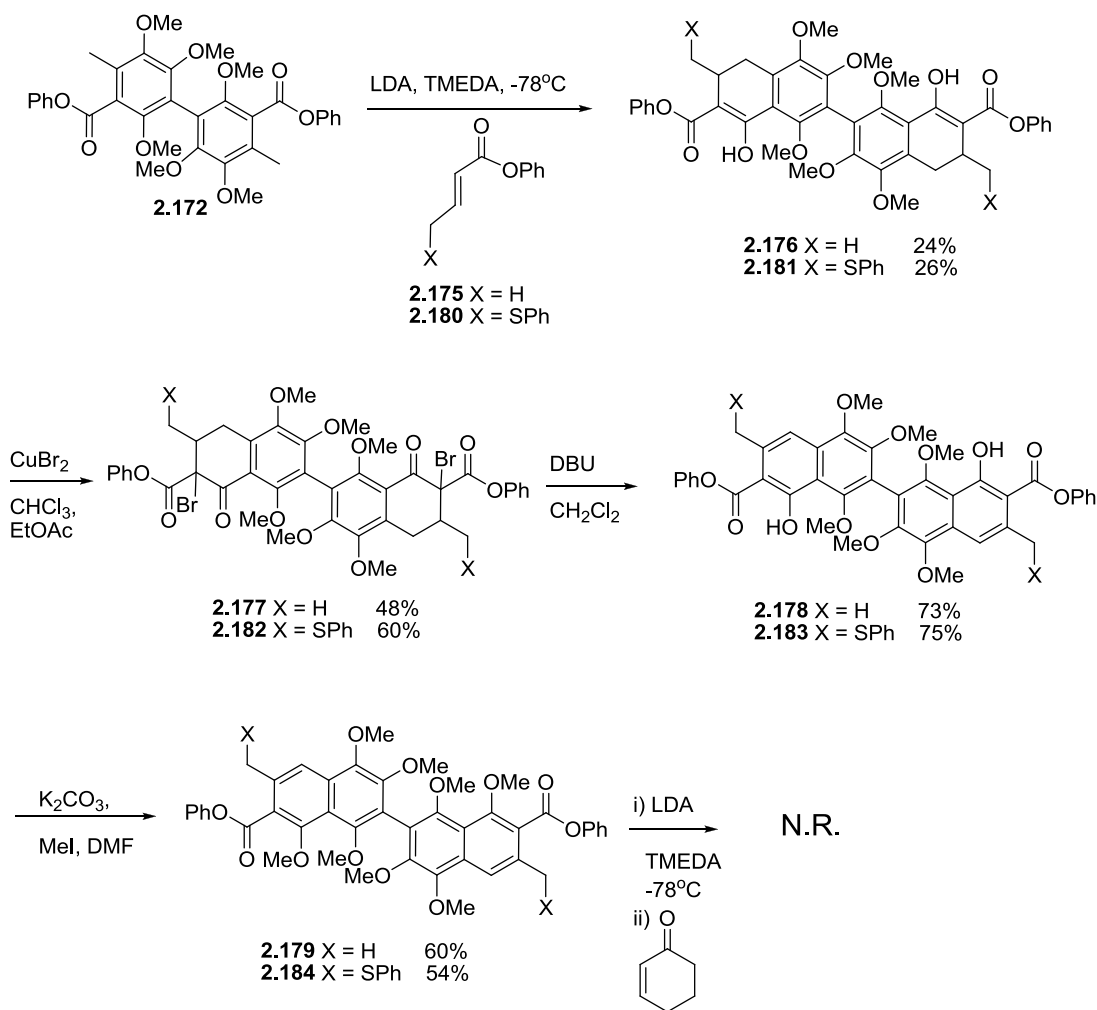


Scheme 59. Two bis-Annulation Approaches to HMP-Y1

Key to a successful double annulation leading to bi-naphthyl **2.73** was efficient double deprotonation of **2.172** which was optimized using a deuterium incorporation study. An interesting result from this study was that no deprotonation was observed when one or two equivalents of LDA-TMEDA complex were added. Double deprotonation was not observed until four equivalents of base were added. There was also no improvement in the deprotonation between four and six equivalents.

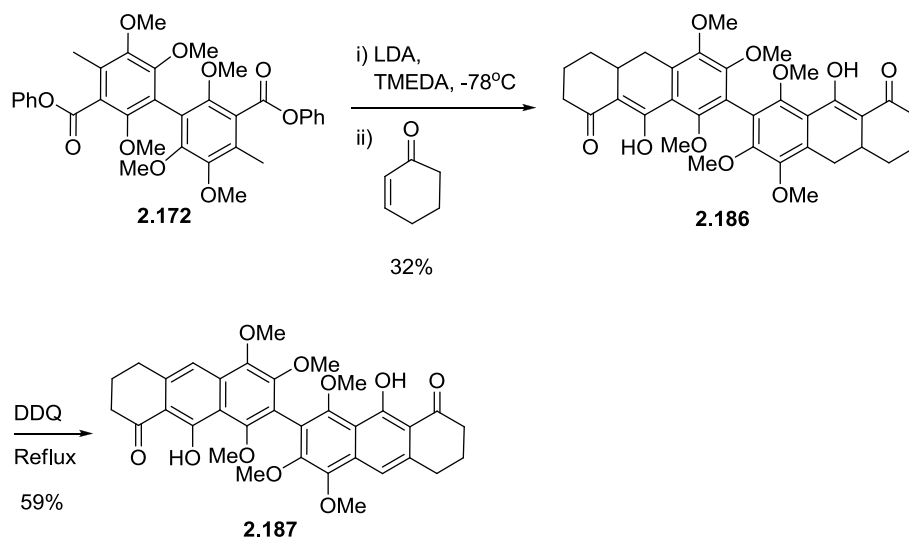
Once we optimized conditions for the formation of the bis-toluato anion we turned our attention to effecting a two-directional annulation. A two-directional synthetic strategy had earlier been applied by Hauser¹⁵³ in the synthesis (+)- biphyscion, We first examined phenyl crotonate **2.175** as the annulation substrate. In the event, we obtained

a modest yield of the bis-annulation product **2.176** and a small amount of the mono-annulation product (Scheme 60). Attempts to directly oxidize **2.176** with DDQ failed, but a two-step bromination-dehydrobromination sequence provided naphthylene **2.178**. Naphthylene **2.178** was then methylated to give **2.179** in preparation for a second annulation. Unfortunately a second bis annulation failed due to difficulty in generating the required toluate anion. The reaction sequence was repeated to give the thiophenyl dimer **2.184** but this did not improve the efficiency of the second annulation



Scheme 60. Attempts at a Two-Annulation Approach.

A second model system was examined based on a two directional annulation with the anticipated completion of the required *cis*-decalin leading to HMP-Y1 (Scheme 60). In this case, the bis-phenyl ester **2.174** was condensed with cyclohexenone to provide a modest yield of the bis-annulated product **2.186** (Scheme 61). Oxidation of **2.186** with DDQ in refluxing benzene gave **2.187** in 59% yield.¹⁵⁴

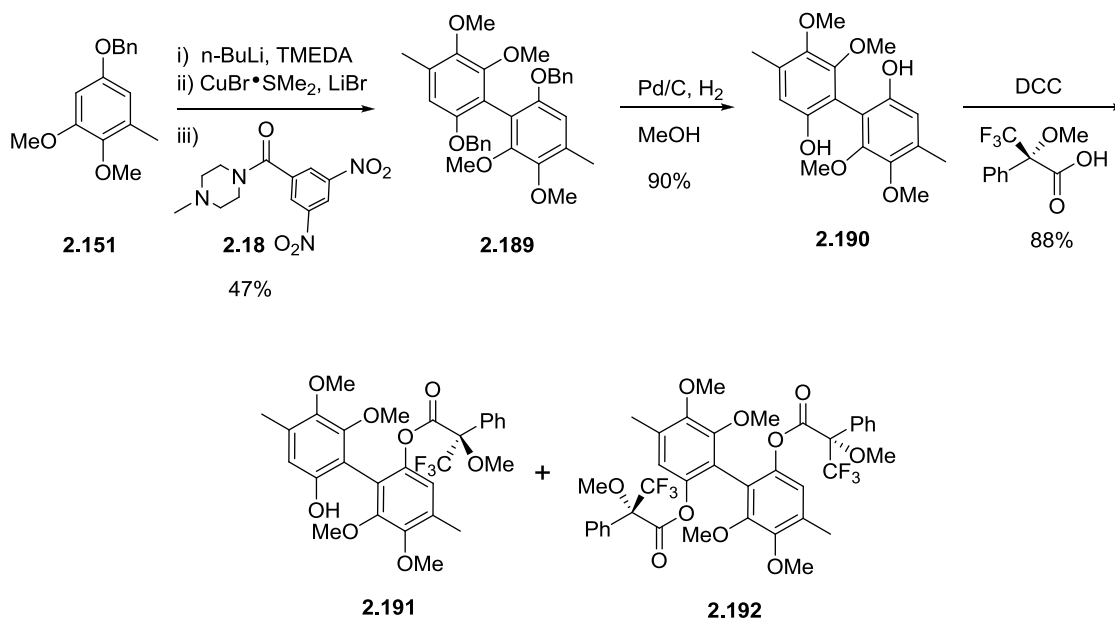


Scheme 61. Synthesis of BCD-EFG Rings Model of HMP-Y1.

Resolution of Atropisomers and Assignment of Absolute Stereochemistry

We next turned our attention to the synthesis of a single atropo-enantiomer and determination of the absolute stereochemistry about the biaryl bond. With this goal in mind, we returned to the benzyl ether **2.151** as a homocoupling substrate. Spring coupling of **2.151** proceeded in 47% yield to give (Scheme 62). The benzyl protons of biaryl **2.189** appeared in ¹H NMR in chloroform as an AB quartet with $\Delta\nu = 22$ Hz and $J_{AB} = 12.6$ Hz, suggesting inhibited rotation about the central carbon-carbon bond. When the solvent was changed to DMSO the diastereotopic benzyl methylene group appeared as a singlet (Figure 6). Resolution of related bis-phenols have been reported by Bringmann¹⁵⁵ by formation of atropo-diastereomeric Mosher esters. With this form of

resolution in mind, the benzyl groups were removed by hydrogenolysis and the resulting bis-phenol condensed with Mosher's acid to initially provide a mixture of diastereomeric mono-Mosher esters **2.191**. The bis-Mosher ester was obtained when an excess of Mosher acid was used. The diastereomeric bis-Mosher esters were readily separated by semi-preparative HPLC. The faster eluting diastereomer proved to be crystalline and submitted to a single X-ray crystal analysis allowing assignment of the chiral axis as (*aS*)-**2.192** (Figure 7).



Scheme 62. Synthesis of the Mono-Mosher's Ester.

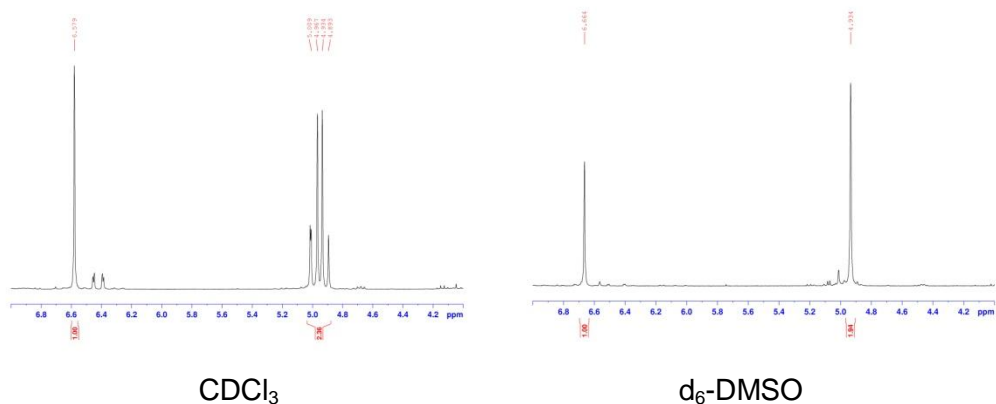


Figure 6. Benzyl Protons of **2.189** in CDCl_3 and $\text{D}_6\text{-DMSO}$.

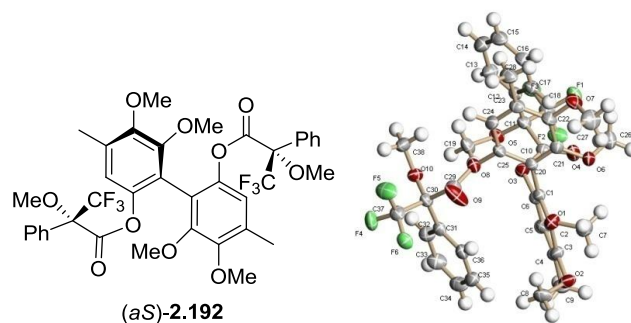
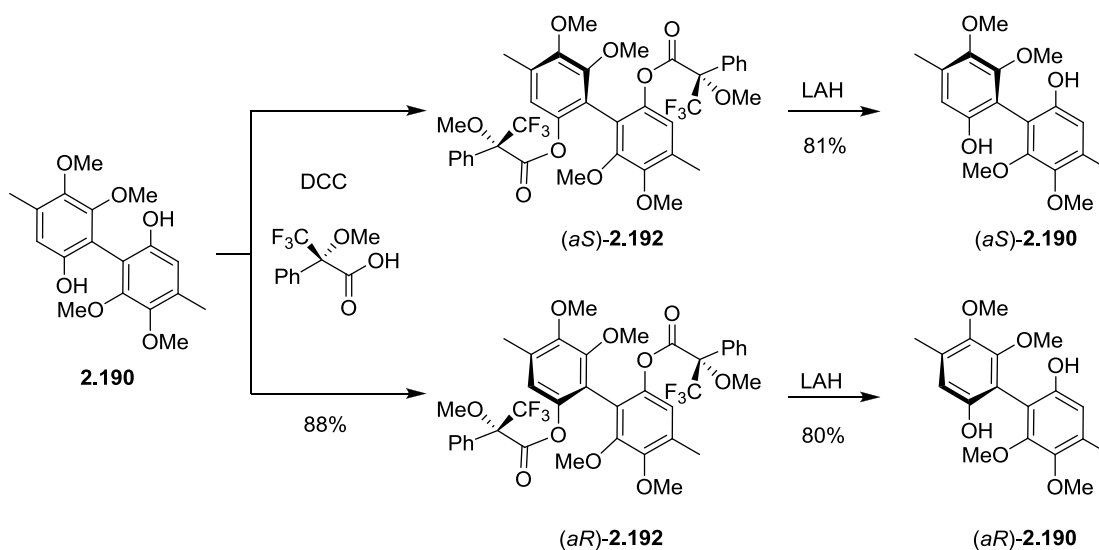


Figure 7. X-ray Crystal Structure of the Faster Eluting bis-Mosher Ester.

(*aR*)- and (*aS*)- bis-Mosher esters were then converted to (*aR*)- and (*aS*)- phenyl ester **2.170**. Reduction of Mosher esters using LiAlH_4 provided (*aS*)-**2.184** and (*aR*)-**2.184** (Scheme 63). The bis-ester is configurationally stable but the removal of the steric bulk does not ensure that the bis-phenol will still be configurationally stable. The phenols were proven to be configurationally stable by the examination of their CD spectra (Figure 8).



Scheme 63. Separation of Bis-Mosher Ester and Retention of Optical Activity

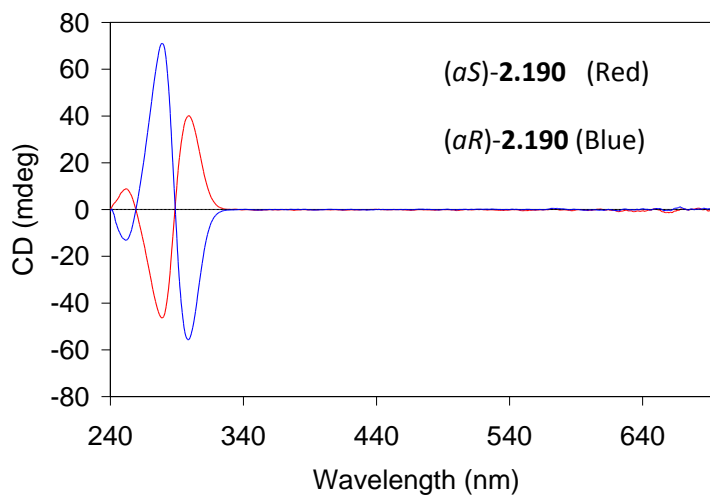
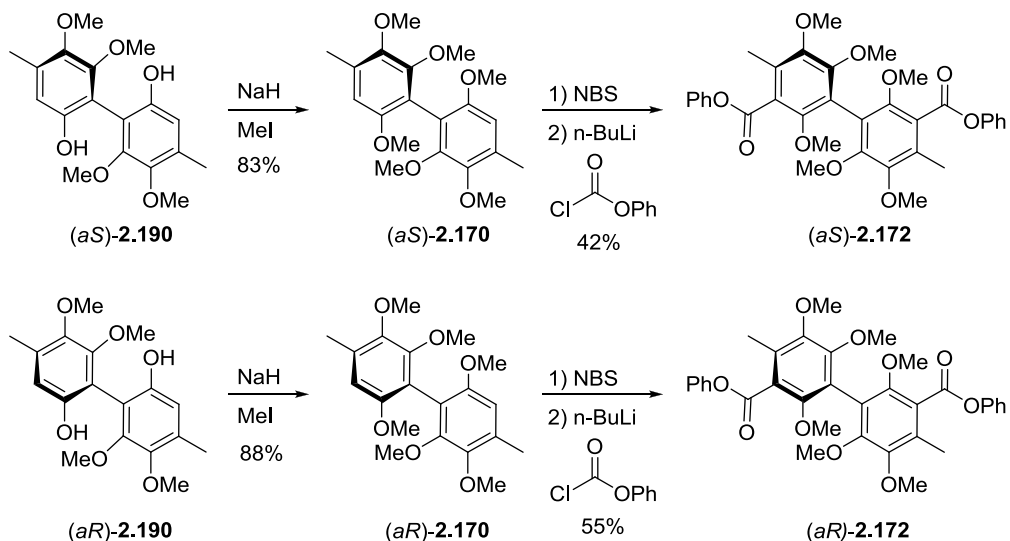


Figure 8. ECD Spectra of Phenol **(aS)-2.190** and **(aR)-2.190**.

The *aS* and *aR* atropisomers were individually converted to the corresponding *aS*-(+)-**2.170** and *aR* -(-)-**2.170** phenyl esters following the same reaction sequence used in the racemic synthesis of **2.170** (Scheme 64). With preparative chiral LC available we examined the separation of atropisomers **(±)-2.190**, **(±)-2.168** and **(±)-2.170** in order to find a more practical resolution method to replace the cumbersome Mosher ester

resolution method. Of the three biaryls examined only the bis-phenyl ester **2.164** provided sufficient separation. Separation of the atropisomers was accomplished with the chiral AD stationary phase, but better resolution was observed with the chiral OD stationary phase. A representative chiral HPLC trace is presented in Figure 9. The separation of the bis-phenyl ester **2.168** allows for material to be brought through a racemic synthesis and then be purified into atropisomer of now known configuration.



Scheme 64. Synthesis of Enantiopure bis-Phenyl Ester.

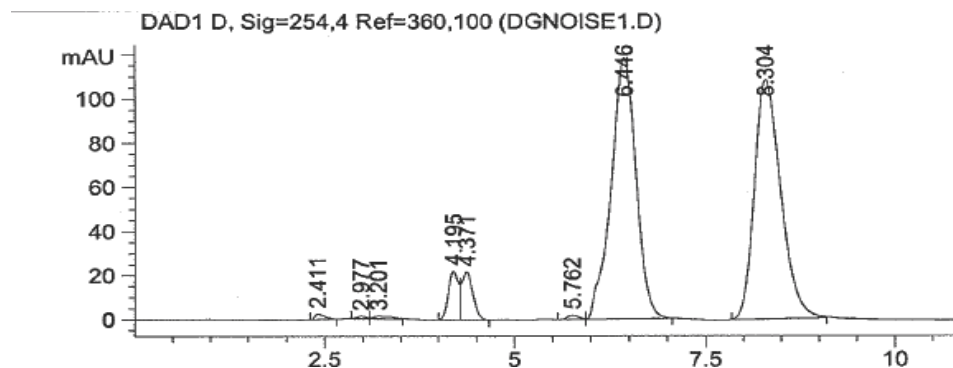
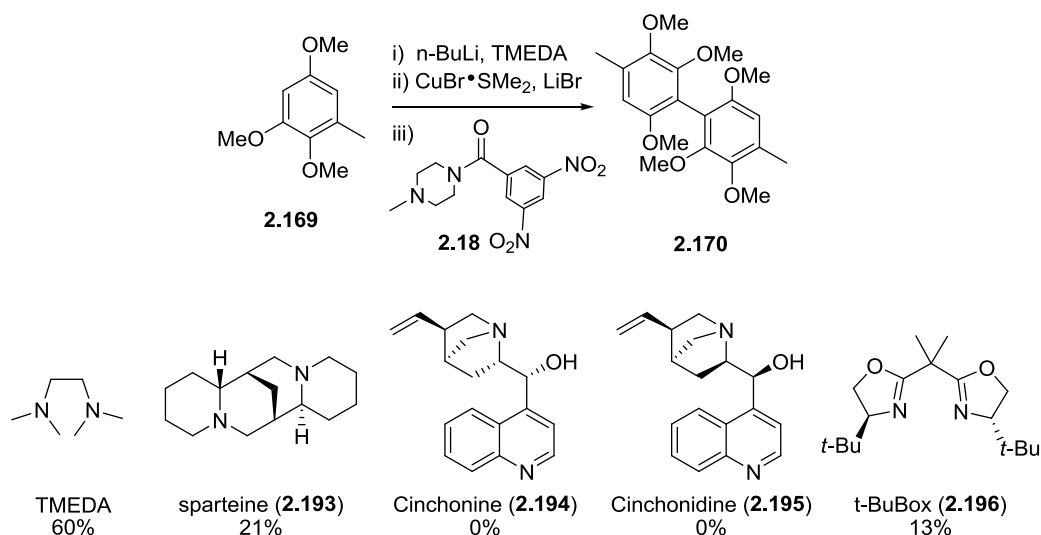


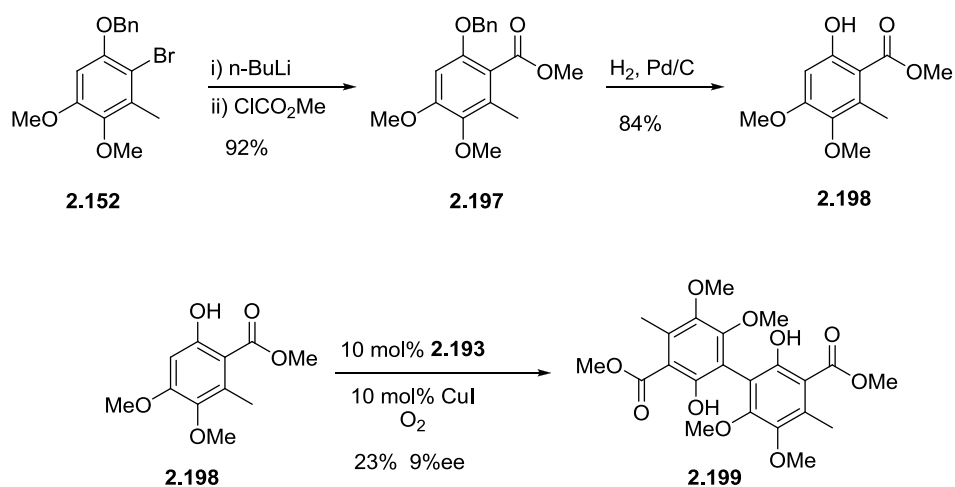
Figure 9. Trace of Chiral Separation of bis-Phenyl Ester **2.172** on OD Chiral Column

Since the central biaryl axis of hibarimicin B was of unknown configuration, we deemed it important to initially have access to both atropisomers. With a viable route to enantiopure bis-phenyl ester, our attention turned to the formation of a single atropisomer selectively. One of the advantages of the Spring coupling was the ability to substitute a chiral diamine in the place of TMEDA to achieve a chiral biaryl bond formation. Use of (-)-sparteine **2.193** in place of TMEDA did provide biaryl coupling but in a much lower yield (Scheme 65). The diamine cinchonine **2.194** and its pseudo-enantiomer cinchonidine **2.195** were also attempted with no resulting biaryl coupling. This pair of pseudo-enantiomers is best known for the selective crystallization of BINOL atropisomers. If the amine was changed to a Box ligand like *t*-BuBox **2.196** a small amount of biaryl was formed. The lower efficiency of the reaction is probably due to the increase of sterics of the copper-diamine complex in formation of the cuprate complex. The enantiomeric excess (% ee) was not measured in any of the biaryl products as yields were lower and no method for the rapid determination of ee was available.



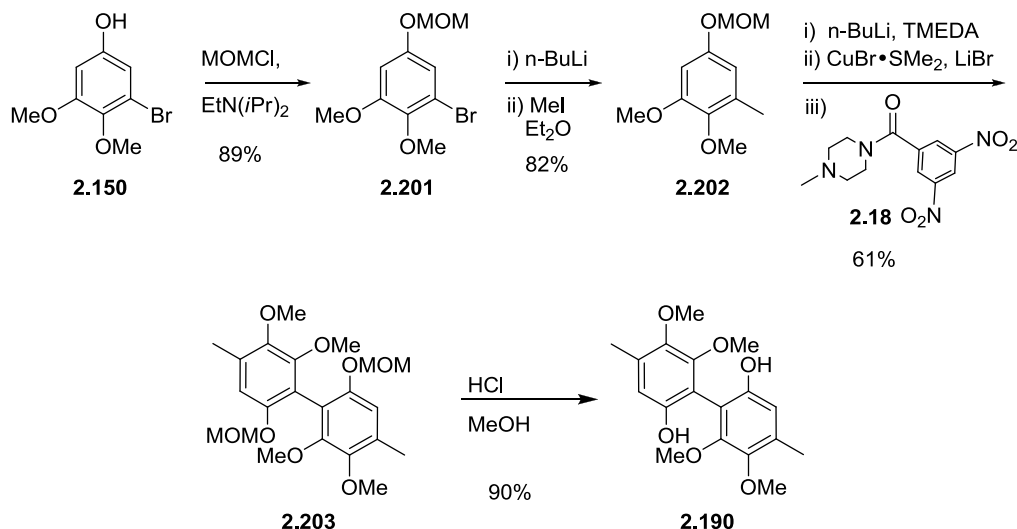
Scheme 65. Spring Coupling with Chiral Diamines

With limited success using a chiral diamine in the Spring coupling, the next approach was the catalytic biaryl coupling described by Kozlowski.¹²¹ The first substrate screened in this reaction was the phenol **2.150**. It was determined that the phenyl ester was too labile for the reaction conditions. Once the ester was unintentionally converted to the acid, the reaction halted. In examining Kozlowski's¹⁵⁶ work, the typical ester is the methyl ester. To arrive at the methyl ester, benzyl bromide **2.146** was converted to the methyl ester by a lithium-halogen exchange and quench with methyl chloroformate to provide methyl ester **2.197** (Scheme 66). The benzyl was then removed by hydrogenolysis and the phenol **2.198** was subjected to the Kozlowski coupling conditions with (-)-sparteine **2.193** in place of the synthetic (+)-sparteine equivalent Kozlowski¹⁵⁷ synthesizes. Phenol methyl ester **2.198** coupled in low yields with catalytic amounts of a copper-sparteine complex. An interesting aspect of this reaction was the lack of stereoselectivity. To date, no report of an enantioselective biphenyl coupling using Kozlowski method has appeared.



Scheme 66. Biaryl Kozlowski Coupling.

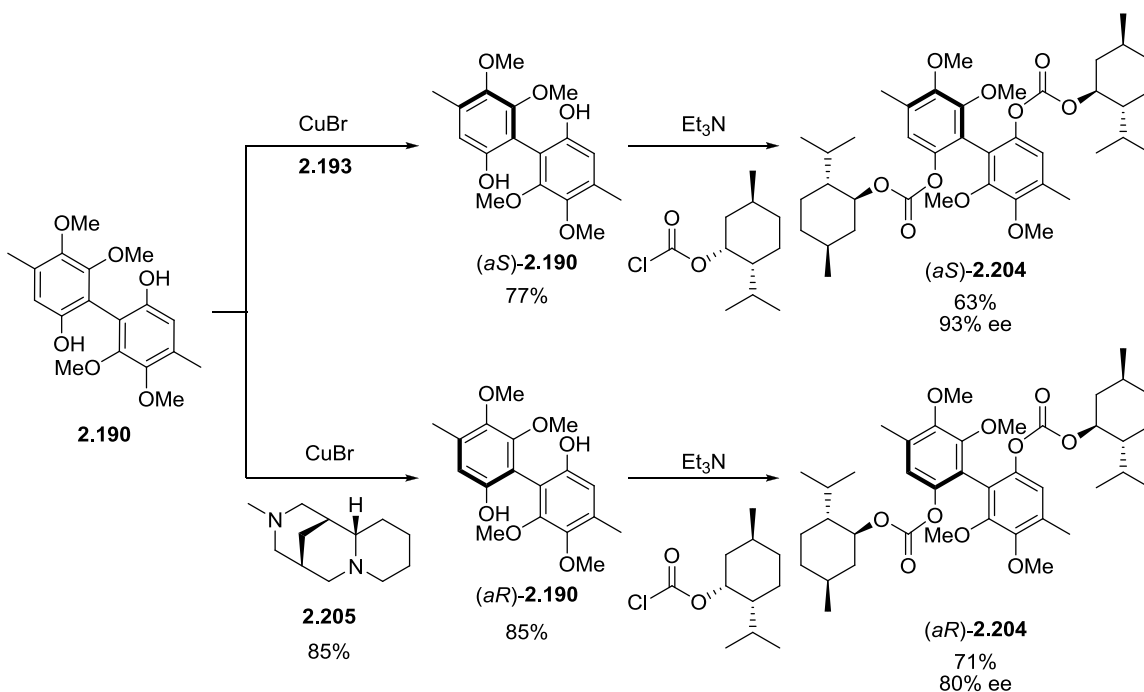
Without a viable route to produce a single atropisomer, we then turned to the work of Wulff in dynamic kinetic resolution. The biaryl phenol became important. The biaryl coupling was shown to proceed with a better yield with the MOM toluene **2.202** (Scheme 67). Toluene **2.202** was synthesized in the same manner as before by protecting the phenol **2.143** with MOMCl. Biaryl phenol **2.190** was synthesized from the biaryl MOM **2.203** by simple acid hydrolysis.



Scheme 67. Improved Route to Biaryl Phenol.

The phenol **2.190** was then subjected to dynamic thermodynamic resolution. A complex of copper and (-)-sparteine **2.193** was added to racemic phenol **2.190** and allowed to stir for a variable amount of time. It was found that with the sparteine complex at room temperature, the racemic phenol was converted to (*a*S)-**2.190** (Scheme 68). Without a method for determination of the %ee, the phenol was then converted to the menthol carbonate **2.204**. The atropo-diastereomeric ratio was then easily determined by proton NMR (Figure 10). The best induction was seen with the sparteine complex stirring at room temperature for forty-eight hours. It is also important to notice

that when the reaction was heated to reflux that no asymmetric induction was seen. To support the validity of this method and provide access to both enantiomers, an enantiomer of (-)-sparteine **2.193** is needed to provide (*aR*)-**2.190**. To this end, O'Brien's (+)-sparteine surrogate diamine **2.205** was utilized with copper bromide and the racemic phenol **2.190** to provide (*aR*)-**2.190** with 80% de.



Scheme 68. Dynamic Thermodynamic Resolution Conditions

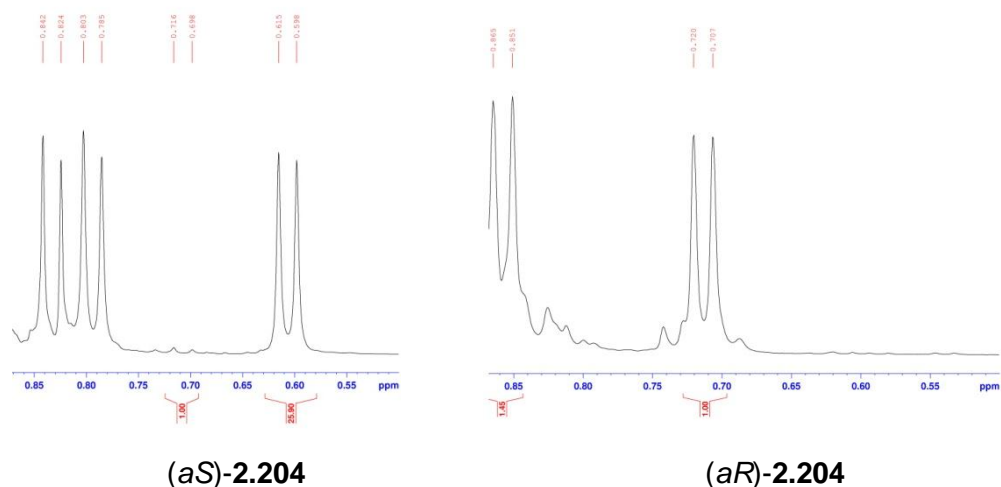
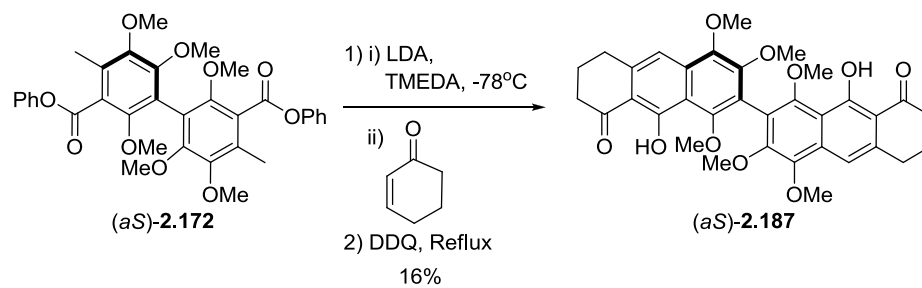


Figure 10. ^1H NMR Analysis of an Isomeric Mixture of (aS)-**2.204** and (aR)-**2.204**.

Having access to either enantiomer of the biaryl core, our attention turned to the assignment of absolute stereochemistry of HMP-Y6. In 1963, Mislow¹⁵⁸ demonstrated that circular dichroism (CD) curves of biaryl and binaphthyls correspond to the configuration of the biaryl axis. The absolute stereochemistry of several biaryl natural products like biphyscion,¹⁵⁹ have been assigned based on comparison of CD spectra to that of a similar known natural product. Correlation of the stereochemistry about the biaryl axis can be accomplished by comparing HMP-Y6 to naphthyl **2.187**. Atropisomers of naphthyl **2.187** are separable by chiral chromatography. To arrive at the known configuration about the biaryl **2.187** the aS isomer of **2.174** was subjected to the annulation and oxidation conditions to provide (aS)-**2.187** (Scheme 69) to arrive at the faster eluting atropo-enantiomer. Overlaying the CD of (aS)-**2.187** and HMP-Y6 (**1.147**), provided by Professor Igarashi, allows for assigning the absolute stereochemistry about the biaryl core in to be tentatively assigned as aS in the natural products



Scheme 69. Synthesis of (aS)-2.187 with Known Configuration about the Biaryl Axis.

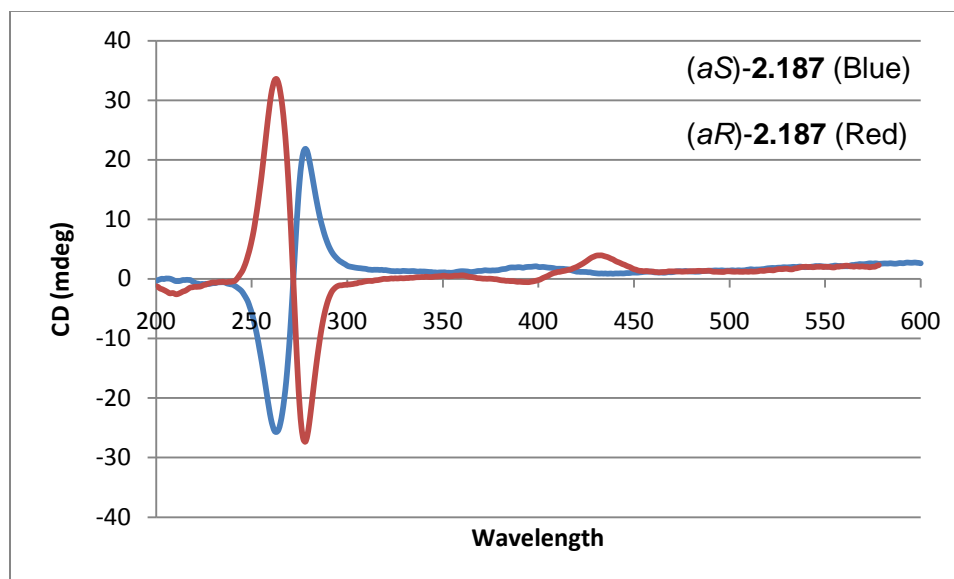


Figure 11. CD Spectra of (aR)-2.187 (aS)-2.187 .

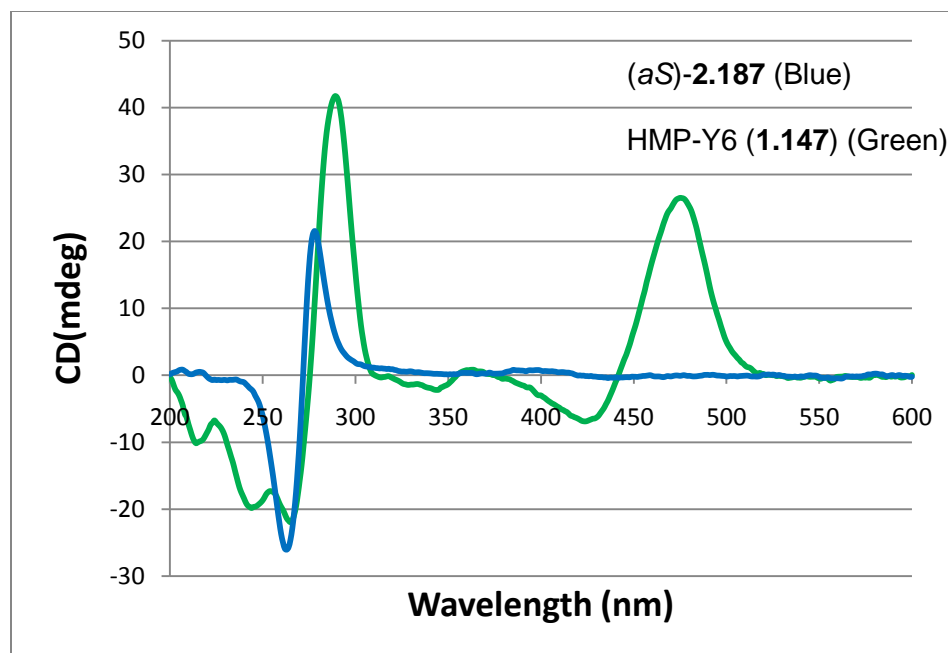
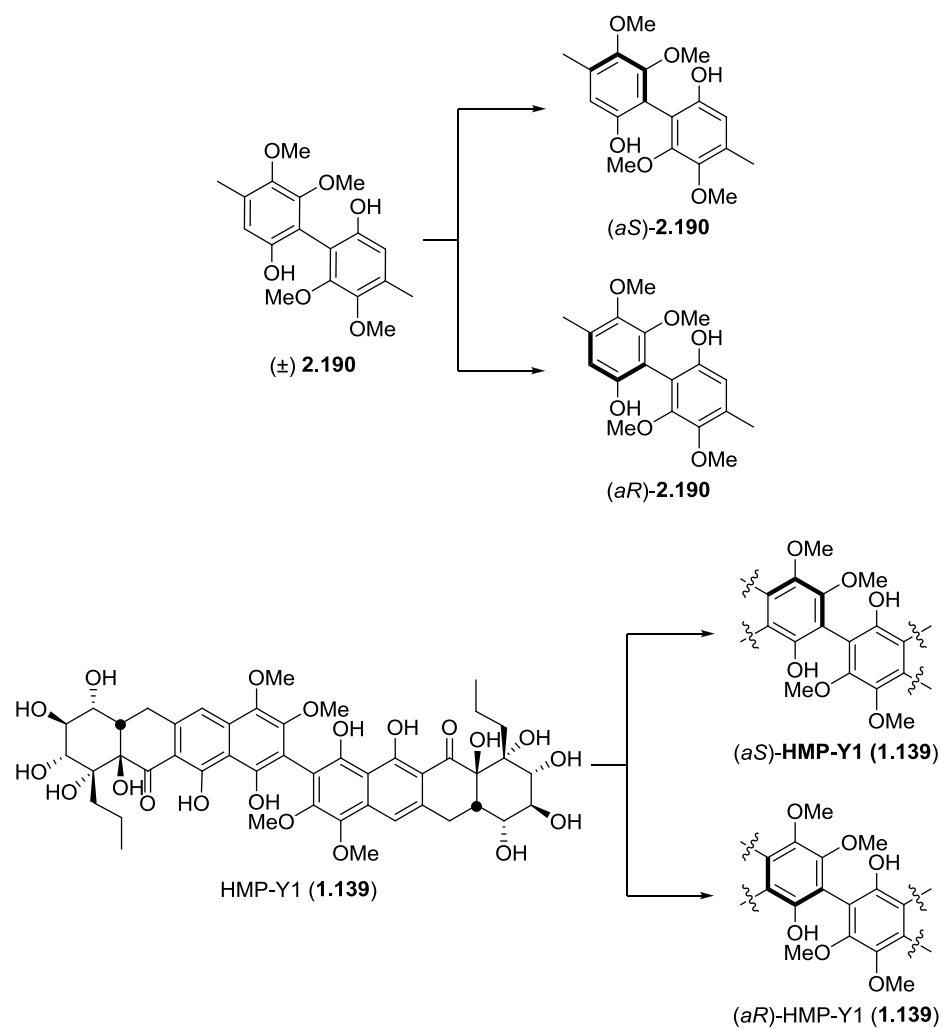


Figure 12. CD Spectra of (aS)-**2.187** and Crude HMP-Y6 (**1.147**) in MeOH

The binaphthyl **2.187** provides a method to tentatively assign absolute configuration about the biaryl bond of HMP-Y6 as *aS*. This completes one of the major goals in assigning absolute stereochemistry of the hibarimicin family of natural products. Experimentation has shown that a racemic biaryl coupling can be converted to a single atropo-diastereomer of known configuration through dynamic kinetic resolution.

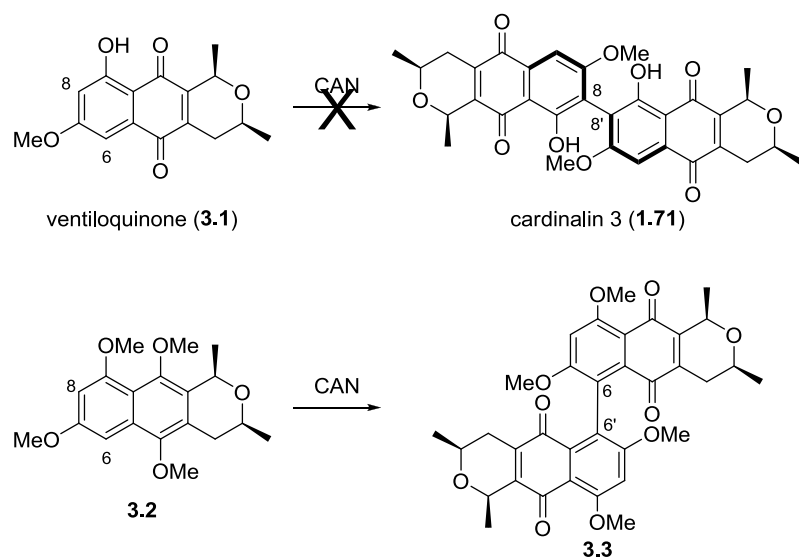


Scheme 70. Conversion of HMP-Y1 to a Single Atropo-diastereomer through Dynamic Thermodynamic Resolution

CHAPTER III

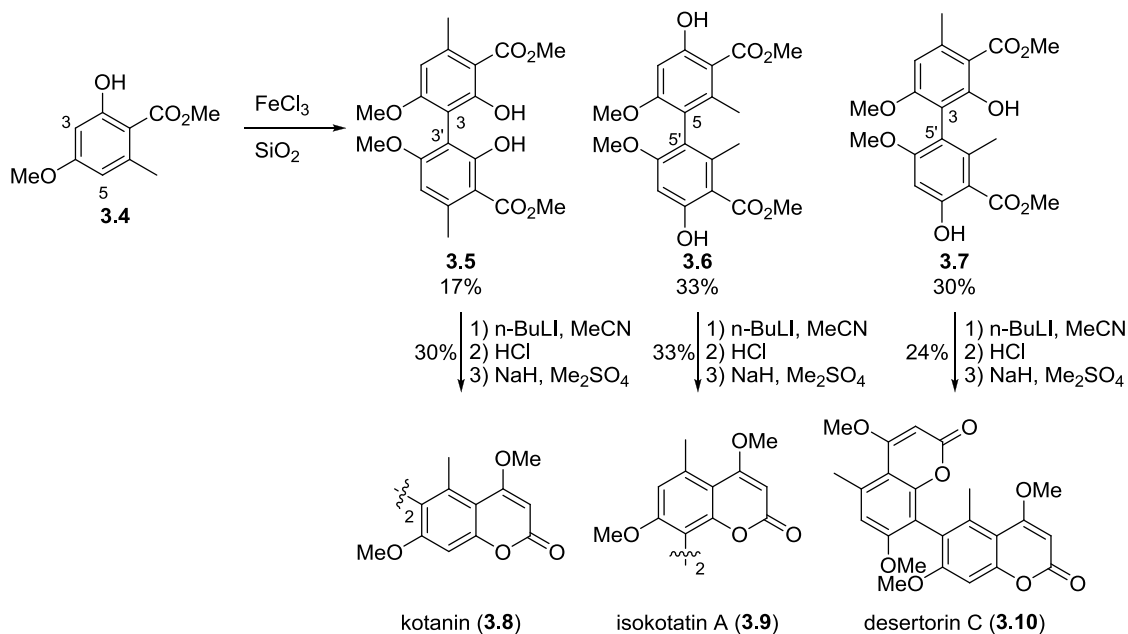
A BIOMIMETIC APPROACH TO HMP-Y1

In considering a biomimetic oxidative homodimerization strategy toward HMP-Y1 we identified three major issues to be addressed. First, and perhaps foremost, we required an atropo-diastereoselective formation of the aryl-aryl carbon-carbon bond in a configurationally defined manner as the configuration of HMP-Y1 is unknown. Based on the studies described in Chapter II we anticipated the dynamic thermodynamic resolution described in Chapter II would fulfill this requirement. The second issue to be addressed is regioselectivity. This problem is illustrated by examination of Brimble's¹⁶⁰ approach toward a biomimetic synthesis of cardinalin 3 (**1.71**) shown in Scheme 71. The Brimble group determined oxidative dimerization of ventiloquinone (**3.1**) did not afford any dimeric products. However dimerization of the protected hydroquinone **3.2** did yield the C6/C6' dimer **3.3**, none of the desired C8/C8' coupling was observed illustrating the problem of regiocontrol.



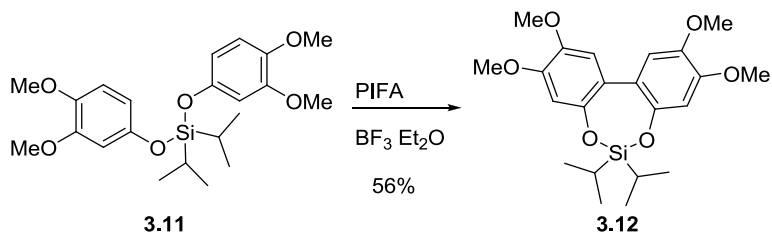
Scheme 71. Brimble's Studies Directed Toward Cardinalin 3

An example of an advantageous nonselective phenolic oxidative coupling was reported by Müller¹⁶¹ that led to the synthesis of kotanin (**3.8**), isokatanin A (**3.9**), and desertorin C (**3.10**), three isomeric natural dimers (Scheme 72). Coupling phenol **3.4** with iron trichloride absorbed on silica gel, provided all three isomeric dimers (**3.5-3.7**) when separated by flash chromatography. Each isomer was advanced to a natural product by the addition of the anion of acetonitrile to the carbonyl, hydrolysis of the cyano, and methylation of the free hydroxyl. Notably, racemic biaryl phenol **3.5** was resolved by chromatographic separation of diastereomeric esters derived from (-)-camphanic acid.



Scheme 72. Müller's Advantageous Unselective Phenolic Coupling

One approach to solve the regioselectivity issue reported by Kita¹⁶² is the use of a temporary silicon tether. In this approach condensation of a phenol with either dialkyl silyldichloride or triflate afforded silylketal **3.11** (Scheme 73). Oxidative coupling of **3.11** then selectively proceeds at the position ortho to the silylated phenol due to restrictions enforced by the silicon tether. We anticipated taking advantage of the C1 phenol HMP-Y1 we could incorporate a silicon tether at this position leading to a regiocontrolled dimerization and ultimately HMP-Y1 (**1.139**) (Figure 13).



Scheme 73. Silicon Tether to Direct Regioselectivity in Oxidative Coupling. \

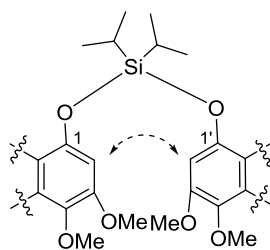
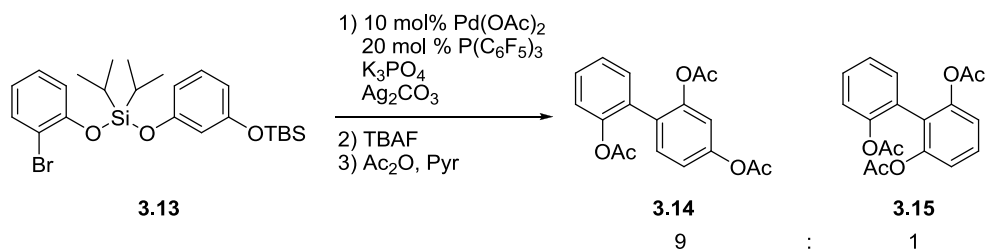


Figure 13. Proposed Silicon Tether to Direct Coupling in HMP-Y1

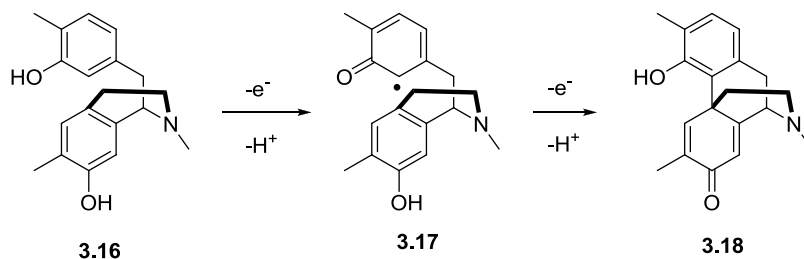
With a silicon tether strategy in mind we considered options to effect an oxidative coupling. Sequential substitution of chloride by a different phenol groups can be employed in hetero couplings leading to unsymmetrical biaryls. Gevorgyan¹⁶³ developed a semi-one-pot procedure using different phenols leading to, for example, unsymmetrical silylketal **3.13** (Scheme 74). A palladium mediated coupling was then used to provide a 9:1 mixture of **3.14** and **3.15**. The scope of the coupling was shown to be good allowing electron donating or releasing in the para position. However, electron rich and sterically hindered (ortho/ortho') couplings as needed for HMP-Y1 were not shown and would likely fail due to limitations associated with the required palladium(0) oxidative insertion step.



Scheme 74. Unsymmetrical Biaryl Coupling Through a Silicon Tether.

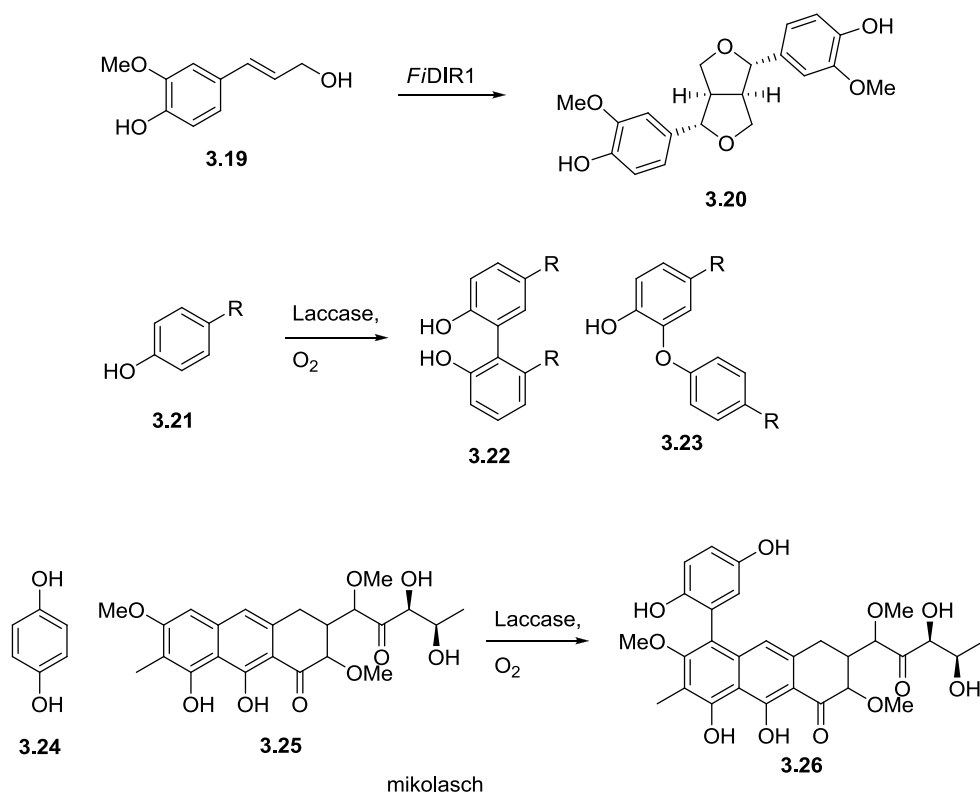
The most direct method to address regio- and stereoselectivity of biomimetic couplings is to employ an enzymatic oxidation. Several examples of selective enzymatic

oxidative aryl couplings have been described following enzyme expression, purification and characterization. Plant derived cytochrome P-450s¹⁶⁴ have been identified that effect the oxidative coupling leading to the alkaloid salutaridine (**3.18**). In this enzyme mediated transformation phenol **3.16** is oxidized to radical **3.17** leading to carbon-carbon bond formation and salutaridine following loss of a second proton and electron (Scheme 75).



Scheme 75. Cytochrome p-450 Oxidation to Provide Salutaridine **3.18**

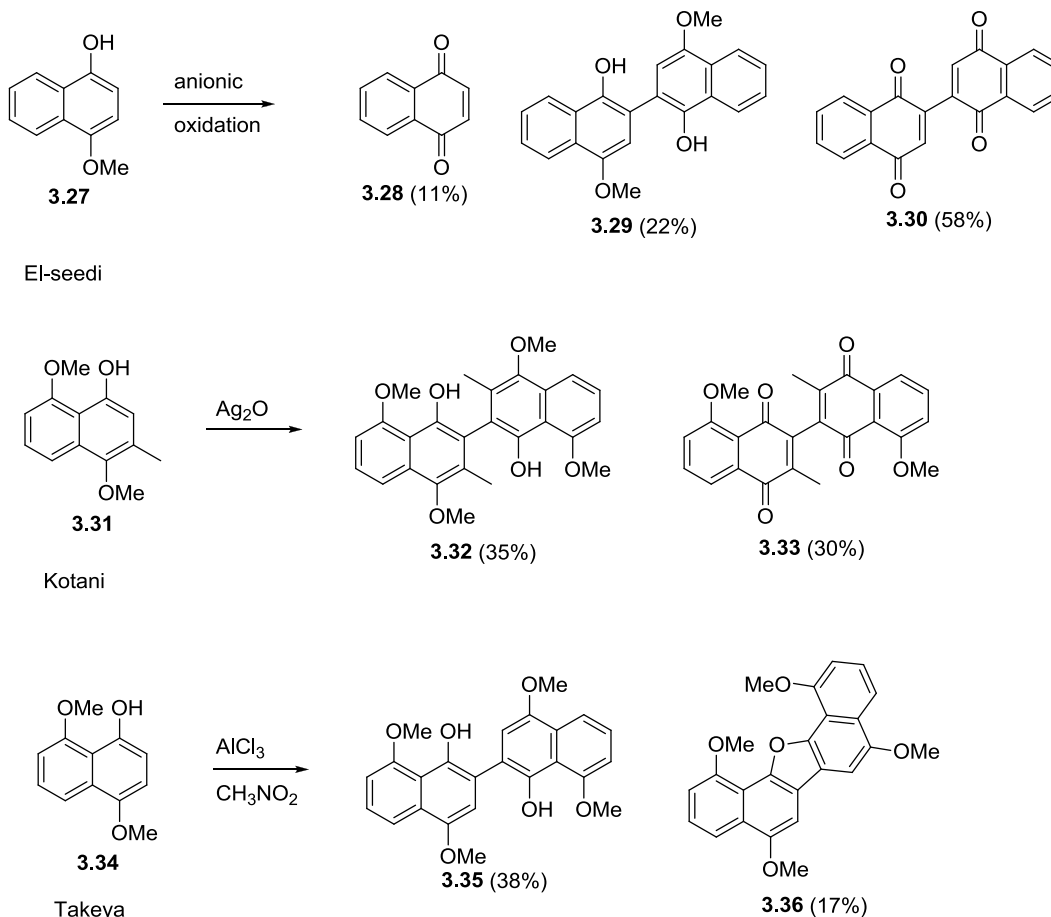
A well studied oxidative dimerization is the phenolic oxidative coupling cinnamyl alcohols mediated by laccase¹⁶⁵. For example, oxidation of substituted cinnamyl alcohol **3.19** occurred in with high enantioselectivity to give (+)-pinoresinol **3.20** (Scheme 76). This enzyme has shown to be one of the few enzymes that demonstrates high substrate scope leading to a variety of phenolic coupling. Mikolasch¹⁶⁶ determined that laccase is a copper(I) and oxygen dependent enzyme. The promiscuity of this enzyme leads to a loss of selectivity, for example oxidation of phenol **3.21** produced both C-arylation **3.22** and O-arylation **3.23** products. The enzyme was also shown to couple hydroquinone **3.24** to the naphthylene ring system **3.25**.



Scheme 76. Laccase Enzymatic Dimerization of Phenols.

A third problem encountered in oxidative biomimetic couplings of electron rich phenols is over oxidation. The issue of over oxidation is illustrated by several examples from the literature (Scheme 77). Nishiyama¹⁶⁷ showed that the anodic oxidative coupling of naphthol **3.27** yielded a mixture of three products, quinone **3.28**, desired binaphthyl **3.29** and bis-quinone **3.30**. Takeya¹⁶⁸ showed that silver oxide oxidation of phenol **3.31** provided a 1:1 mixture of bi-naphthyl **3.32** and bis-quinone **3.33**. Over oxidation could be avoided by using tin(II) chloride as an oxidant that provided only bi-naphthyl **3.32**. Takeya¹⁶⁹ also showed that in the absence of over-oxidation, side reactions were observed leading to undesired by-products depending on the reactivity of the intermediate coupling partners. In the oxidation of phenol **3.34**, the coupling product **3.35** in addition to dinaphthofuran **3.36** were isolated. The ability to overcome the

production of this side product is dependent upon adjusting the oxidant to the nature of the specific substrate.

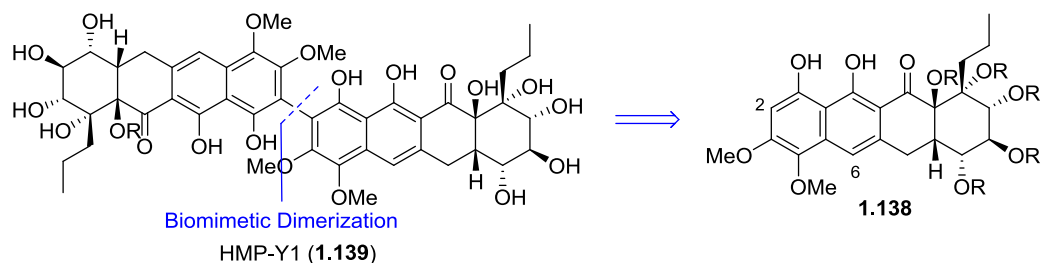


Scheme 77. Over Oxidation and Side Products in Oxidative Coupling.

Preliminary Studies Directed Toward HMP-YI

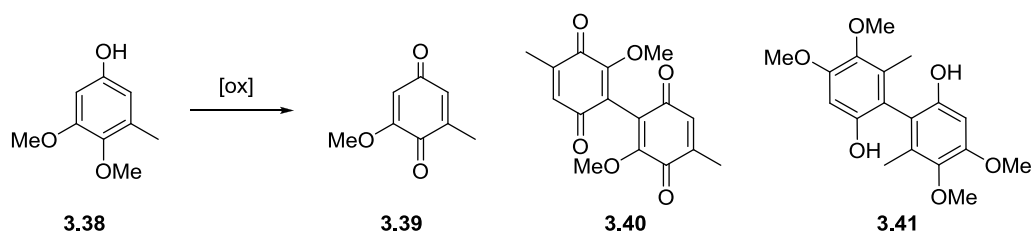
The biomimetic approach to HMP-Y1 (**1.139**) requires a late stage oxidative homo coupling of tetracycle **1.138**. As discussed earlier, oxidative coupling of **1.138** would likely lead to mixture of atropo-diastereomers which hypothetically could be resolved to a single either atropo-diastereomer employing dynamic thermodynamic resolution (Scheme 78). In regard to the regioselectivity of the homocoupling, three

isomeric products could be produced (C2-C2', C6-C6' and C2-C6'). In preparation of the proposed dimerization of **1.138** we examined model substrates to address the issues of choice of oxidant and regioselectivity of the coupling.



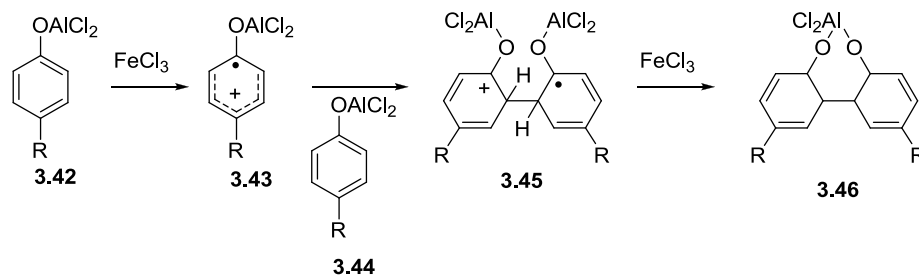
Scheme 78. Biomimetic Approach to HMP-Y1

Readily available phenol **3.38** was subjected to a variety of oxidizing agents in an effort to identify optimal reaction conditions. First, vanadium oxychloride¹⁷⁰ provided a unproductive mixture of quinone **3.39** (44%) and bis-quinone **3.40** (11%) (Scheme 79). Oxidative coupling by the use of copper(II) chloride-TMEDA¹⁷¹ complex or hypervalent iodine¹⁶², provided primarily the over oxidized product bis-quinone **3.40**. The Sartori¹⁷² method uses a mixture of aluminum trichloride and ferric chloride, the latter Lewis acid is added to the pre-complexed aluminum bis-phenolate contributing to regiocontrolled coupling. Oxidation of phenol **3.38** under these conditions led to biaryl **3.41** in 61% yield. The latter results were considered optimal as no over oxidation was observed and regioselectivity would not be problematic in the tetracyclic phenol **1.138**.



Scheme 79. Oxidative Coupling of the Phenol **3.19**.

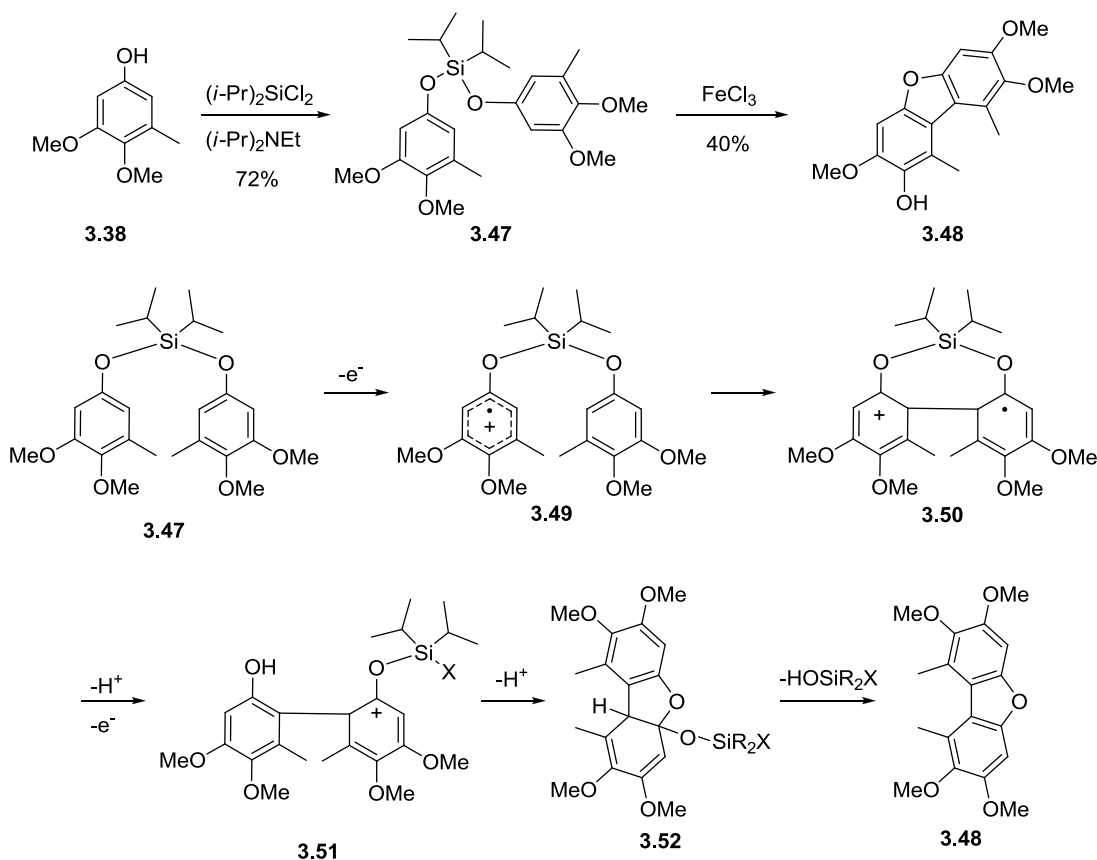
Sartori¹⁷³ has proposed the following mechanism of the oxidative coupling using the $\text{AlCl}_3\text{-FeCl}_3$ complex, starting from aluminum phenolate **3.42**. One electron oxidation of **3.42** then affords aryloxy radical cation **3.43** (Scheme 80) that couples with phenolate **3.42** to provide the radical cation radical **3.45**. Loss of an electron and two protons from **3.45** then provides the biaryl product **3.46**. This two-step oxidation was supported by cyclic voltammetry, with the observation of two irreversible oxidation steps. Sartori's reaction was shown to be under kinetic control, and larger substituents hindered the reaction progress. The regioselectivity observed in the coupling of **3.46** would then be explained as a kinetic coupling at the least hindered site.



Scheme 80. Mechanistic Understanding of the Aluminum Phenolate Coupling

As a second approach we examined the effect of a silicon tether on the oxidation process (Scheme 81). To this end, phenol **3.38** was reacted with diisopropyldichlorosilane to provide the silylketal **3.47**. Oxidation of **3.47** using ferric

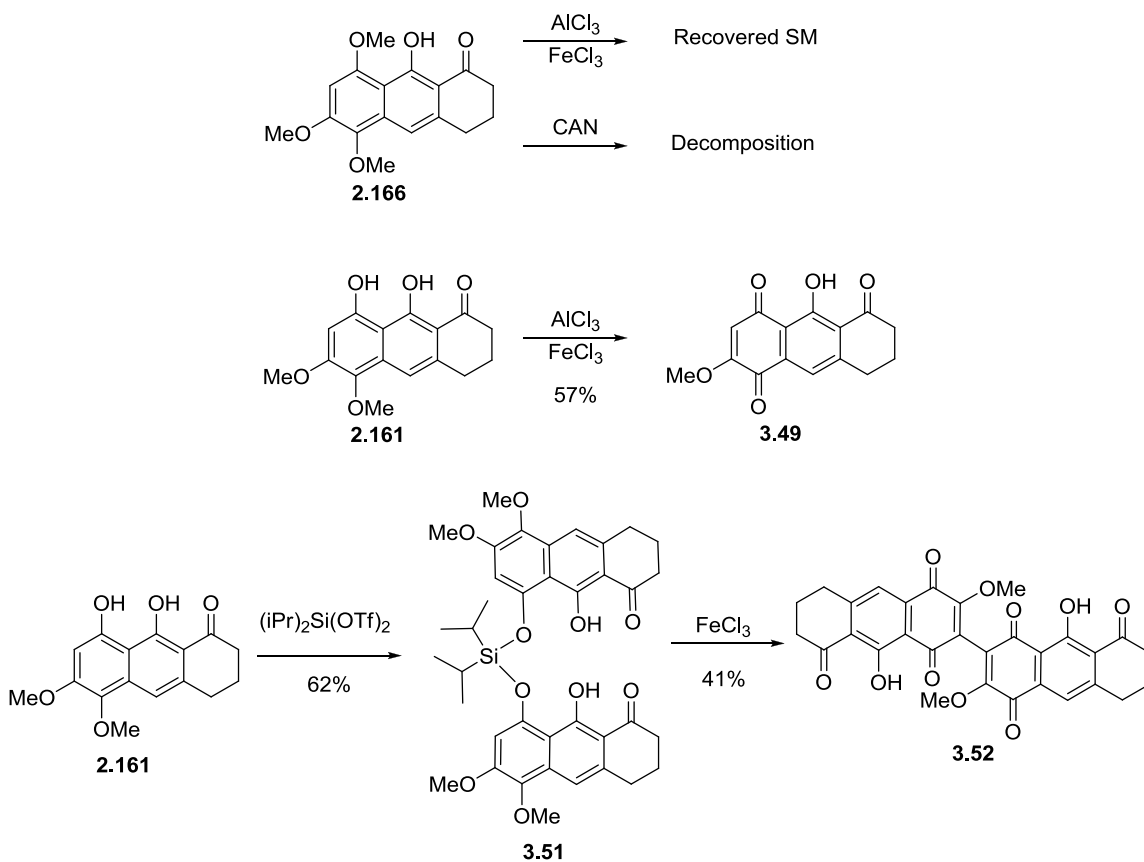
chloride unexpectedly provided furan **3.48**. This result can be explained by the removal of an electron from silylketal **3.47** to give aryl radical cation **3.49**. Following coupling, aromatization and loss of a second electron, radical **3.49** is converted to form cation **3.51**. Capture of the intermediate cation by the free phenol followed by loss of a proton leads to **3.52**. Iron trichloride can also act as a Lewis acid, catalyzing demethylation to furnish the observed furan **3.48**.



Scheme 81. Unexpected Furan Formation and Possible Mechanism

Having collected sufficient information on the proposed biaryl coupling we turned our attention to tricyclic ketone **2.158** as a model substrate for HMP-Y1. Attempts to directly oxidize trimethoxy naphthyl **2.158** using Satori's or Brimble's¹⁶⁰ coupling

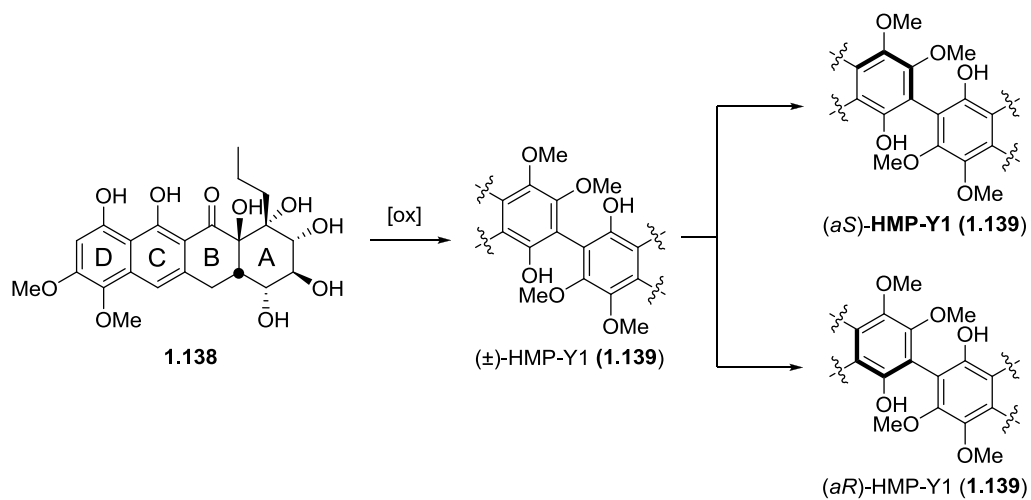
conditions afforded no identifiable products. Coupling of the free naphthol **2.157** with Sartori's conditions lead to oxidation to the naphthylquinone **3.49** (Scheme 82). Phenol **2.157** was then reacted with diisopropylsilyl ditriflate to give silylene **3.51**. A single attempt was made at the oxidation of the silylketal **3.51** using four equivalents of ferric chloride to provide the red bisnaphthylquinone **3.52**, an over oxidation product. This preliminary result provides promising precedent for a biomimetic coupling route to HMP-Y1 with the issue of over oxidation requiring further refinement.



Scheme 82. Oxidative Coupling of Naphthyl Ring Systems

The biomimetic route to HMP-Y1 requires a homodimerization to form the biaryl linkage (Scheme 83). Phenolic biaryl coupling will provide the racemic HMP-Y1 (**1.139**)

when the proper oxidant is found to provide coupling and not oxidation. With the racemic coupling, either atropo-diastereomer can be obtained from the dynamic thermodynamic resolution described in chapter II.



Scheme 83. Biomimetic Oxidative Coupling Followed by Deracemization.

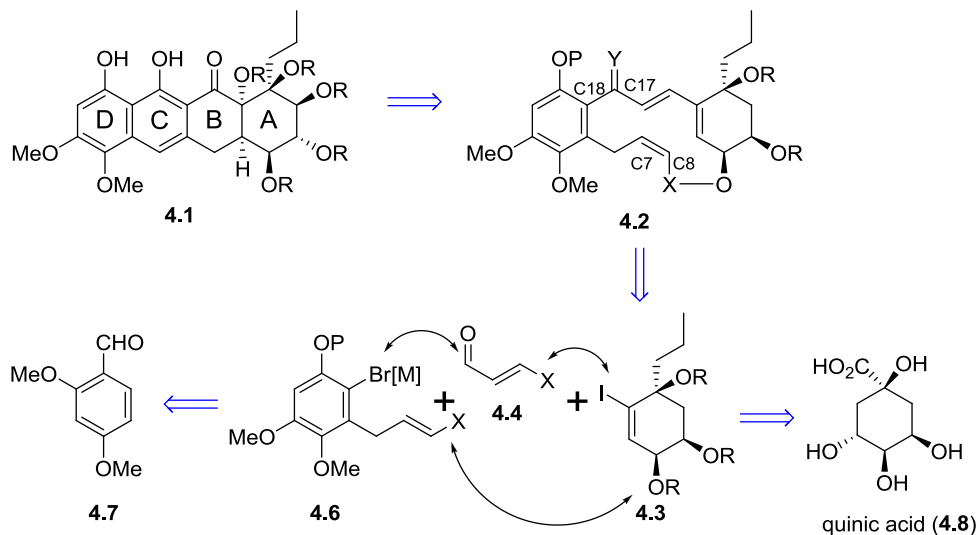
CHAPTER IV

ANALYSIS AND PROGRESS TOWARD ABCD RING SYSTEM

Our long-term goal is to prepare hibarimicin B by total synthesis. We plan to approach this by first preparing HMP-Y1 and by a biomimetic oxidation convert HMP-Y1 to hirbarimicinone. In order to proceed with a total synthesis of HMP-Y1 we required a method to address control of atropo diastereomers and assign the configuration of the chiral axis. Based on the work presented in this thesis we have tentatively assigned the configuration of the natural HMP-Y1 atropisomer and presumably hibarimicin assuming HMP-Y1 to hibarimicinone oxidation proceed with retention of configuration. Comparison of the two-directional and biomimetic coupling strategy investigated in chapters III and IV favor the latter approach as the efficiency of the two-directional approach is poor. In addition our groups experience, as well as the Mootoo and Roush groups suggests a synthesis of the AB/GH cis-decalin rings followed by annulation is a less than optimal approach to ring construction either using the two-directional or monomeric annulation. Briefly described in this chapter is progress toward the synthesis of the HMP-Y1 monomer (a.k.a. ABCD ring of hibarimicinone).

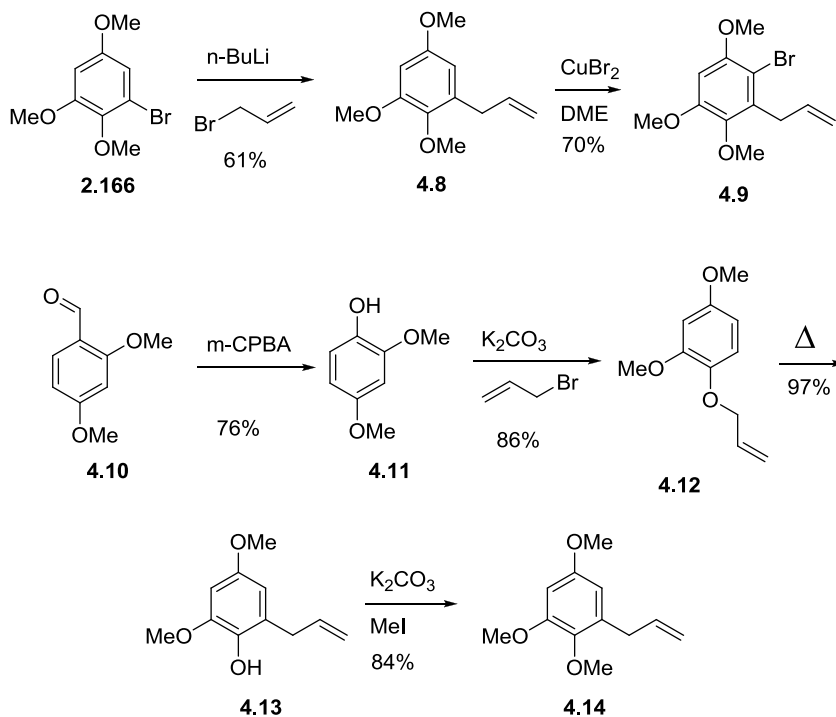
In considering a synthetic strategy toward the HMP-Y1 monomer **4.1** we note low yields observed in the Hauser-Staunton annulation using cyclohexenone and difficulty in controlling the C9 ring fusion stereochemistry. With these considerations in mind we conceived a transannular Diels-Alder reaction employing macrocycle **4.2** (Scheme 84). The Diels-Alder precursor **4.2** can be formed by closing the C17 / C18 bond first then formation of the macrocycle. This analysis identifies iodide **4.3**, aryl bromide **4.6** and a three carbon linker **4.4** as three components to form the Diels Alder Precursor. Iodide **4.3** can be produced in six steps from quinic acid (**4.8**). Aryl bromide **4.6** can be

generated in five steps from the aldehyde **4.7**. Note, the absolute stereochemistry of the Hibarimicins is unknown and the choice of (-)-quinic acid as starting material.



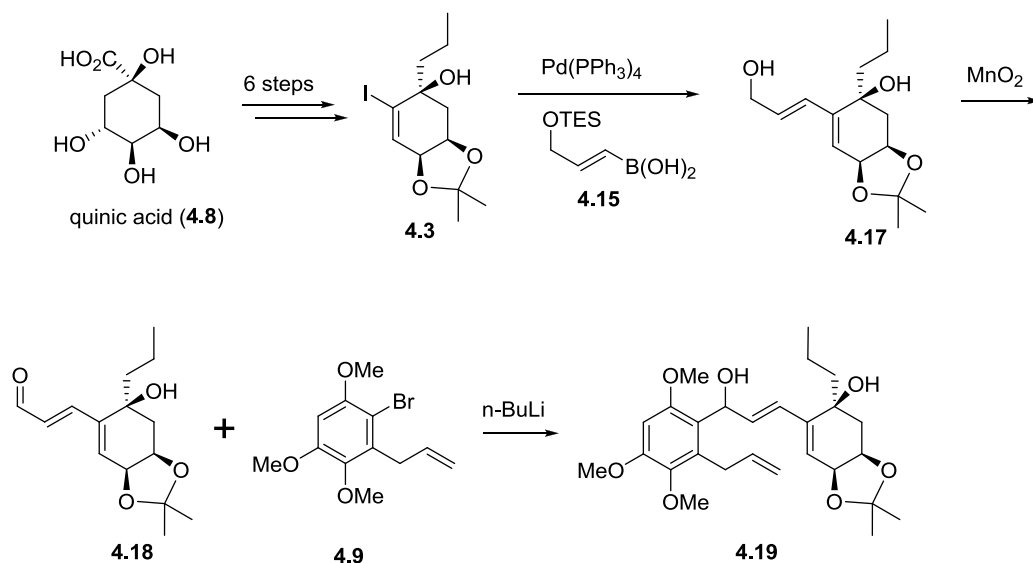
Scheme 84. Biomimetic Approach to HMP-Y1

The synthesis of bromide **4.6** started with alkylation of trimethoxy bromide **2.166** with allyl bromide to form the allyl benzene **4.8** (Scheme 85). The allyl **4.8** was selectively brominated with copper(II) bromide¹⁷⁰ to provide the aryl bromide **4.9**. The selectivity was confirmed by NOE correlation of the aromatic proton to the two methoxy groups. A second approach to the aryl bromide was accomplished by a known Baeyer-Villiger oxidation of dimethoxy benzaldehyde **4.10** to give phenol **4.11**, which was alkylated with allyl bromide to yield allyl **4.12**.¹⁷¹ Optimization of the Claisen rearrangement produced phenol **4.13** in near quantitative yield. The phenol **4.13** was then alkylated with methyl iodide to afford the allyl benzaldehyde **4.14**.



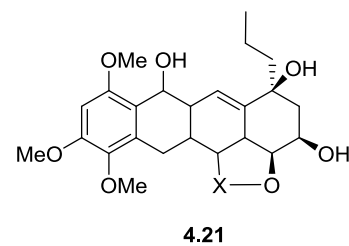
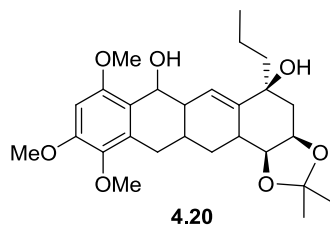
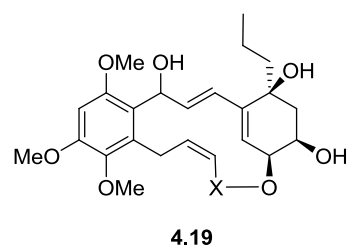
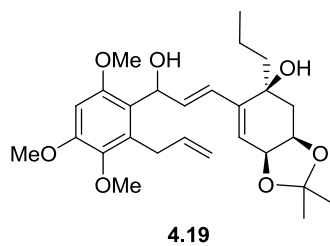
Scheme 85. Two Routes to the Allyl Bromide **4.18**

Jonathan Hempel, a graduate student in our lab, has shown an effective route to the formation of the C17 / C18 bond. Iodide **4.3** can be arrived at in six steps from quinic acid (**4.8**). A Suzuki coupling with boronic acid **4.18** afforded the diol **4.19** (Scheme 86). Oxidation of the primary alcohol yields aldehyde **4.20**. Aryl bromide **4.6** was converted to the aryl lithium and addition of the lithium produced the C17/ C18 bond in **4.21**.



Scheme 86. Hempel's Work Toward the Formation of the C17/C18 Bond

An important outcome is to set the stereochemistry of the C9 bridge head. We have demonstrated that this stereochemistry can be set by an intramolecular type II Diels Alder. The stereocontrol of the intramolecular Diels Alder of **4.19** might provide the syn stereochemistry to the alcohol (Scheme 87). If this does not occur, a tethered approach as in **4.21** to provide a trans annular Diels Alder should provide the desired stereochemistry.



Scheme 87. Future approaches to the Diels Alder.

CHAPTER V

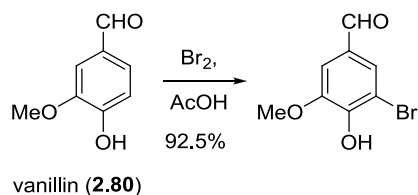
EXPERIMENTAL

General procedure: All non-aqueous reactions were performed in flame-dried or oven dried round-bottomed flasks under an atmosphere of argon. Stainless steel syringes or cannulae were used to transfer air- and moisture-sensitive liquids. Reaction temperatures were controlled using a thermocouple thermometer and analog hotplate stirrer. Reactions were conducted at room temperature (rt, approximately 23 °C) unless otherwise noted. Flash column chromatography was conducted as described Still et. al. using silica gel 230-400 mesh.¹⁷⁴ Where necessary, silica gel was neutralized by treatment of the silica gel prior to chromatography with the eluent containing 1% triethylamine. Analytical thin-layer chromatography (TLC) was performed on E. Merck silica gel 60 F254 plates and visualized using UV, ceric ammonium molybdate, potassium permanganate, and anisaldehyde stains. Yields were reported as isolated, spectroscopically pure compounds.

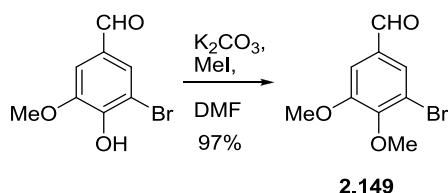
Materials. Solvents were obtained from either an MBraun MB-SPS solvent system or freshly distilled (tetrahydrofuran was distilled from sodium-benzophenone; Diethyl Ether was distilled from sodium-benzophenone and used immediately; Commercial reagents were used as received. The molarity of *n*-butyllithium solutions was determined by titration using diphenylacetic acid as an indicator (average of three determinations).

Instrumentation. HPLC was conducted on a Varian ProStar 210 HPLC system using a Dynamax 21.4 x 250 mm column. Infrared spectra were obtained as thin films on NaCl plates using a Thermo Electron IR100 series instrument and are reported in terms of

frequency of absorption (cm^{-1}). ^1H NMR spectra were recorded on Bruker 300, 400, 500, or 600 MHz spectrometers and are reported relative to deuterated solvent signals. Data for ^1H NMR spectra are reported as follows: chemical shift (δ ppm), multiplicity (s = singlet, d = doublet, t = triplet, dt = doublet of triplets, q = quartet, m = multiplet, br = broad, app = apparent), coupling constants (Hz), and integration. ^{13}C NMR spectra were recorded on Bruker 75, 100, 125, or 150 MHz spectrometers and are reported relative to deuterated solvent signals or ^{40}F is relative to trifluoroacetic acid. LC/MS was conducted and recorded on an Agilent Technologies 6130 Quadrupole instrument. High-resolution mass spectra were obtained from the Department of Chemistry and Biochemistry, University of Notre Dame using either a JEOL AX505HA or JEOL LMS-GCmate mass spectrometer or from Vanderbilt Institute of Chemical Biology Drug Discovery Program laboratory using a Waters Acquity UPLC and Micromass Q-ToF Ultima API. The structure of bis mosher ester 11 was obtained by Dr. Joseph Reibenspies at the X-ray diffraction facility of Department of Chemistry, Texas A&M University. Optical rotations were measured with and are reported as follows $[\alpha]_{\lambda}^T$ (c g/100 mL, solvent). ECD were obtained by a Jasco 720 polarimeter.

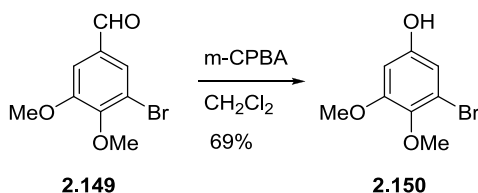


3-Bromo-4-hydroxy-5-methoxybenzaldehyde. - To a solution of vanillin (16.0 g, 105 mmol) in glacial acetic acid (175 mL) was added Br₂ reagent (11.0 mL, 210 mmol). After 2 h, the solution was diluted with a water/ice mixture (200 mL) to produce a white precipitate. The solid was filtered off and dissolved in CH₂Cl₂: acetone mixture (1:4, 400 mL). The combined organic extracts were dried (MgSO₄) and concentrated to give 22.5 g (93%) of bromide as a white solid. IR (neat) 3345, 1673, 1425, 1290, 1156, 1047, 793 ¹H NMR (CDCl₃) δ 9.76 (s, 1H), 7.62 (d, *J* = 1.8 Hz, 1H), 7.34 (d, *J* = 1.5 Hz, 1H), 6.52 (s, 1H), 3.96 (s, 3H). ¹³C NMR (CDCl₃) δ 221.8, 189.7, 148.8, 147.6, 130.1, 129.9, 108.1, 107.9, 56.6. LRMS calculated for C₈H₈BrO₃ (M+H)⁺ *m/z*: 231.0 Measured 231.0 *m/z*.

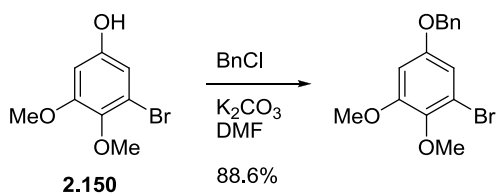


3-Bromo-4,5-dimethoxybenzaldehyde (2.149). - To a suspension of bromide 3-Bromo-4-hydroxy-5-methoxybenzaldehyde (22.5 g, 97.4 mmol) and K₂CO₃ (40.0 g, 292 mmol) in DMF (150 mL) was added MeI (18 mL, 292 mmol). After 16 h, the reaction was diluted with H₂O (200 mL), and extracted with EtOAc (3 x 75 mL). The combined organic extracts were washed with brine (200 mL), dried (MgSO₄) and concentrated to afford an oil. The residue was purified by column chromatography with EtOAc/Hexane (1:2) to afford 21.4 g (90%) of methyl ether **2.149**. IR (neat) 2945, 2851, 2360, 1586,

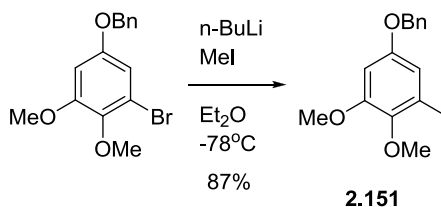
1566, 1486, 1393, 1281, 1132, 1047, 991 ^1H NMR (CDCl_3) δ 9.85 (s, 1H), 7.65 (d, J = 1.5Hz, 1H), 7.39 (d, J = 1.5Hz, 1H), 3.95 (s, 3H), 3.94 (s, 3H); ^{13}C NMR (CDCl_3) δ 189.8, 154.0, 151.6, 132.9, 128.5, 117.8, 110.0, 60.69, 56.1. LRMS calculated for $\text{C}_9\text{H}_{10}\text{BrO}_3$ ($\text{M}+\text{H}$) $^+$ m/z : 244.97 Measured 245.0 m/z .



3-Bromo-4,5-dimethoxyphenol (2.150). – To a solution of methyl ether **2.149** (19.0 g, 77.5 mmol) in CH_2Cl_2 (250 mL) was added *m*-CPBA (27.0 g, 155 mmol). After 4.5 h of heating at reflux, saturated NaHCO_3 (250 mL) was added and the resulting solution stirred for 45 min. The aqueous layer was extracted with CH_2Cl_2 (2 x 150 mL). The combined organic layers were dried (MgSO_4), and concentrated to yield an orange residue. This residue was dissolved in $\text{MeOH}/\text{conc HCl}/\text{H}_2\text{O}$ (2:1:1, 150mL) and the resulting solution was allowed to stir for 45 min. MeOH was removed and extracted with EtOAc (3 x 75 mL). The combined organic extracts were dried (MgSO_4), and concentrated. The residue was purified by column chromatography with $\text{EtOAc}/\text{Hexane}$ (1:4) to afford 10.7 g (59%) of phenol **2.150**. ^1H NMR (CDCl_3) δ 6.60 (d, J = 2.7 Hz, 1H), 6.40 (d, J = 3.0 Hz, 1H), 3.83 (s, 3H), 3.79 (s, 3H); ^{13}C NMR (CDCl_3) δ 154.0, 152.6, 117.4, 110.6, 100.1, 60.7, 56.0; LRMS calculated for $\text{C}_8\text{H}_{10}\text{BrO}_3$ ($\text{M}+\text{H}$) $^+$ m/z : 232.97 Measured 233.0 m/z .

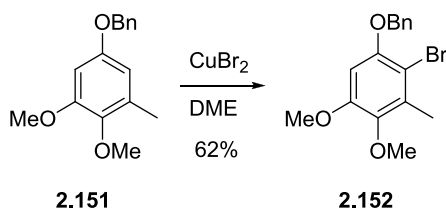


5-(Benzyloxy)-1-bromo-2,3-dimethoxybenzene. - To a suspension of phenol **2.150** (4.6 g, 20 mmol) and K_2CO_3 (8.2 g, 59 mmol) in DMF (60 mL) was added benzyl bromide (4.5 mL, 59 mmol). After 20 h, the reaction mixture was diluted by H_2O (100 mL) and extracted with EtOAc (3 x 100 mL). The combined organic extracts were washed with brine (100 mL), dried (MgSO_4) and concentrated. The residue was purified by column chromatography with EtOAc/Hexane (1:6) to afford 5.6 g (89%) of benzyl ether. IR (neat) 1598, 1570, 1452, 1427, 1232, 1207, 1177, 1144, 1047, 1025, 1003, 819, 697; ^1H NMR (CDCl_3) δ 7.36 (m, 5H), 6.75 (d, $J = 2.7$ Hz, 1H), 6.53 (d, $J = 2.7$ Hz, 1H), 4.94 (s, 2H), 3.82 (s, 3H), 3.77 (s, 3H); ^{13}C NMR (CDCl_3) δ 155.5, 154.0, 140.8, 136.3, 128.5, 128.1, 127.5, 117.3, 108.7, 100.6, 70.5, 60.6, 55.9; LRMS calculated for $\text{C}_{15}\text{H}_{16}\text{BrO}_3$ ($\text{M}+\text{H}$) $^+$ m/z : 323.02 Measured 323.0 m/z .

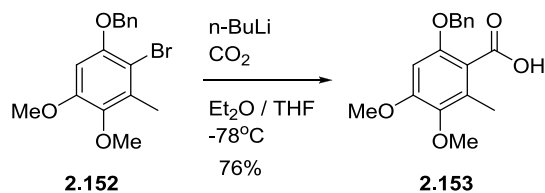


5-(Benzyloxy)-1,2-dimethoxy-3-methylbenzene (2.151). To a solution of 5-(benzyloxy)-1-bromo-2,3-dimethoxybenzene (2.8 g, 8.5 mmol) in diethyl ether (30 mL) at -78°C was added 2.2 M n-BuLi (6.8 mL, 17 mmol). After 1 h at -78°C , neat methyl iodide (1.6 mL, 26 mmol) was added. After 16 h, the reaction mixture was diluted with H_2O (50 mL) and extracted with ethyl acetate (3 x 30 mL). The combined organic

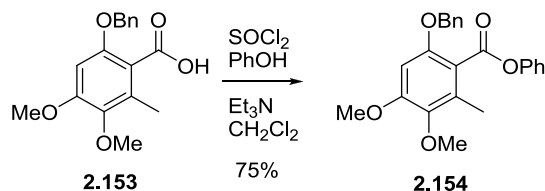
extracts were dried (MgSO_4) and concentrated to afford a yellow oil. The residue was purified by column chromatography with EtOAc/Hexane (1:4) to afford 1.7 g (79%) of toluene **2.151**. IR (neat) 1599, 1498, 1464, 1454, 1224, 1191, 1176, 1096, 1046, 1010, 735, 698; ^1H NMR (CDCl_3) δ 7.35 (m, 5H), 6.46 (d, $J = 3.0$ Hz, 1H), 6.39 (d, $J = 2.7$ Hz, 1H), 5.02 (s, 2H), 3.83 (s, 3H), 3.76 (s, 3H), 2.28 (s, 3H); ^{13}C NMR (CDCl_3) δ 155.0, 153.2, 141.5, 137.0, 132.0, 128.5, 127.9, 127.5, 106.8, 98.6, 70.3, 60.2, 55.6, 16.1; LRMS calculated for $\text{C}_{16}\text{H}_{19}\text{O}_3$ ($\text{M}+\text{H}$) $^+$ m/z : 259.13 Measured 259.2 m/z .



1-(Benzyloxy)-2-bromo-4,5-dimethoxy-3-methylbenzene (2.152). To a solution of toluene **2.151** (1.7 g, 6.5 mmol) in dimethoxy ethane (22 mL) was added CuBr_2 (2.2 g, 9.9 mmol). After 4 h, the reaction mixture was filtered, washed with EtOAc (3 x 30 mL) and concentrated. The residue was purified by column chromatography with EtOAc/Hexane (1:4) to afford 1.4 g (62%) of bromo **2.152**. Mp 72-74°C IR (neat) 1579, 1484, 1448, 1390, 1337, 1241, 1203, 1074, 1011, 800, 751, 700 ^1H NMR (CDCl_3) δ 7.39 (m, 5H), 6.48 (s, 1H), 5.12 (s, 2H), 3.82 (s, 3H), 3.75 (s, 3H), 2.40 (s, 3H); ^{13}C NMR (CDCl_3) δ 152.0, 151.5, 142.1, 136.7, 133.1, 128.5, 127.9, 127.1, 106.2, 98.0, 71.7, 60.6, 55.9, 16.3; LRMS calculated for $\text{C}_{16}\text{H}_{18}\text{BrO}_3$ ($\text{M}+\text{H}$) $^+$ m/z : 337.0. Measured 337.1 m/z

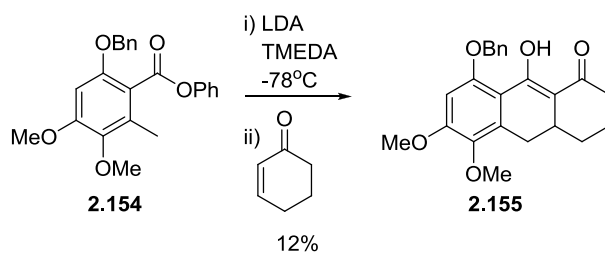


6-(Benzyloxy)-3,4-dimethoxy-2-methylbenzoic acid (2.153). To a solution of bromide **2.152** (2.7 g, 8.0 mmol) in $\text{Et}_2\text{O}/\text{THF}$ (7:1, 40 mL) at -78°C was added $n\text{-BuLi}$ (6.4 mL, 16 mmol) turning the solution an orange color. After 1 h at -78°C , CO_2 was bubbled through the solution for 10 minutes, followed by the addition of crushed dry ice (50 mL). The reaction was then diluted with H_2O (50 mL). The organic layer was washed with H_2O , and the combined aqueous layers were treated with conc. HCl , to produce a white precipitate. The reaction mixture was filtered, to afford 1.70 g (70%) of acid **2.153**. ^1H NMR (CDCl_3) δ 7.35 (m, 5H), 6.42 (s, 1H), 5.14 (s, 2H), 3.81 (s, 3H), 3.71 (s, 3H), 2.40 (s, 3H).



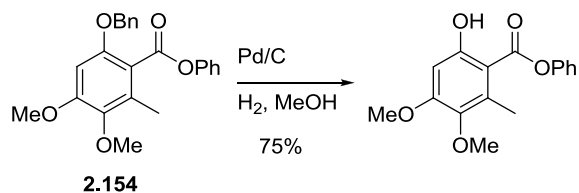
Phenyl 6-(benzyloxy)-3,4-dimethoxy-2-methylbenzoate (2.154). To a solution of acid **2.153** (1.7 g, 5.6 mmol) in CH_2Cl_2 (30 mL) was added SOCl_2 (1.3 mL, 17 mmol). After 5 h of heating at reflux, the excess SOCl_2 , along with the solvent, was removed. The residue was dissolved in CH_2Cl_2 (30 mL) and phenol (1.1 g, 11 mmol) was added. At 0°C , Et_3N (2.0 mL, 14 mmol) was added, producing HCl gas. After 16 h, the reaction mixture was washed with 1N HCl (2 x 25 mL) and brine (1 x 25 mL). The organic layer was dried (MgSO_4), and concentrated to provide a yellow solid. The residue was

purified by column chromatography with EtOAc/Hexane (1:4) to afford 1.6 g (75%) of ester **2.154**. ^1H NMR (CDCl_3) δ 7.64 (m, 10H), 6.47 (s, 1H), 5.12 (s, 2H), 3.84 (s, 3H), 3.75 (s, 3H), 2.38 (s, 3H); ^{13}C NMR (CDCl_3) δ 166.4, 154.5, 12.8, 150.9, 141.4, 136.5, 130.9, 129.4, 128.5, 128.0, 127.5, 125.8, 121.8, 96.5, 71.3, 60.5, 55.8, 12.9; LRMS calculated for $\text{C}_{23}\text{H}_{23}\text{O}_5$ ($\text{M}+\text{H}$) $^+$ m/z : 379.2 Measured 379.2 m/z .

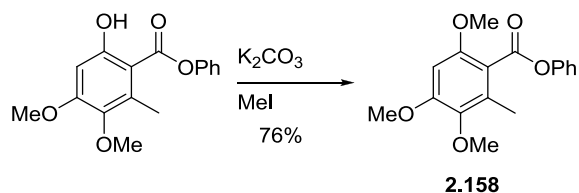


8-(benzyloxy)-9-hydroxy-5,6-dimethoxy-3,4,4a,10-tetrahydroanthracen-1(2H)-one

(2.155). To a solution of diisopropyl amine (0.15 mL, 1.0 mmol) in THF (3 mL) at 0°C was added 2.0 M *n*-BuLi (0.53 mL). After 30 min, TMEDA (0.10 mL, 0.14 mmol) was added and then cooled to -78°C . Then a solution of **2.154** (0.18 g, 0.51 mmol) in THF (2 mL) was added, forming a blood red color. After 1 h at -78°C a solution of cyclohexenone (0.60 g, 1.9 mmol) in THF was added resulting in a yellow color. This solution was then allowed to warm up to 0°C , over the next 2 h. The reaction mixture was diluted with 0.2M KH_2PO_4 (5 mL) and extracted with EtOAc (3 x 10 mL). The combined organic layers were dried (MgSO_4), and concentrated. The residue was purified by column chromatography with EtOAc/Hexane (1:2) to afford 17 mg (12%) of annulation product **2.155**. ^1H NMR (CDCl_3) δ 16.51 (s, 1H), 7.38 (m, 2H), 7.19 (m, 3H) 6.43 (s, 1H), 5.11 (s, 2H), 3.92 (s, 3H), 3.87 (s, 3H), 3.20 (dd, $J = 15.2, 4.0$ Hz, 1H), 2.51 (m, 1H), 2.40 (m, 2H), 2.14 (m, 2H), 1.89 (m, 1H), 1.59 (m, 2H)

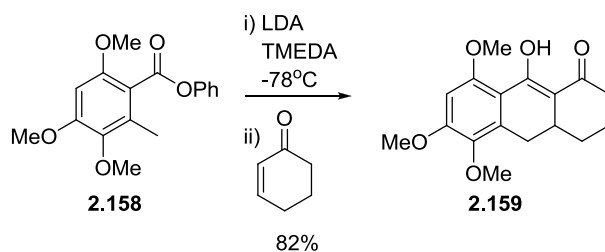


Phenyl 6-hydroxy-3,4-dimethoxy-2-methylbenzoate. To a solution of ester **2.154** (1.6 g, 4.6 mmol) in MeOH (20 mL) was added 5% Pd/C (0.3 g). This solution was placed in a hydrogen atmosphere, and allowed to stir for 16 h. The reaction was filtered over a celite 454 / silica plug (1:1) and washed with MeOH (3 x 20 mL). The combined organic extracts were dried (MgSO₄) and concentrated to afford 1.0 g (85%) of phenyl 6-hydroxy-3,4-dimethoxy-2-methylbenzoate. IR (neat) 2932, 1650, 1614, 1589, 1490, 1444, 1324, 11251, 1219, 1161, 1054, 1034, 1004, 956, 847, 829, 788, 733, 686 ¹H NMR (CDCl₃) δ 7.31 (m, 5H), 6.41 (s, 1H), 3.89 (s, 3H), 3.71 (s, 3H), 2.61 (s, 3H); ¹³C NMR (CDCl₃) δ 170.2, 161.8, 158.8, 149.7, 140.6, 133.9, 129.5, 126.0, 121.7, 103.6, 98.3, 60.4, 55.5, 30.8, 14.7.



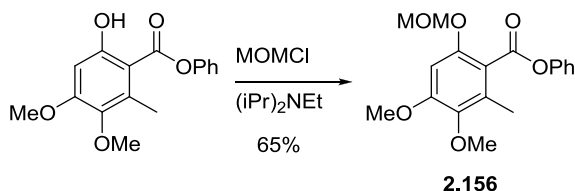
Phenyl 3,4,6-trimethoxy-2-methylbenzoate (2.158). To a suspension of phenyl 6-hydroxy-3,4-dimethoxy-2-methylbenzoate (0.50 g, 1.7 mmol) and K₂CO₃ (0.73 g, 5.2 mmol) in DMF (5.8 mL) was added MeI (0.32 mL, 5.2 mmol). After 16 h, the reaction was diluted H₂O (10 mL) and extracted with EtOAc (3 x 10 mL). The combined organic layers were washed with Brine (20 mL), dried (MgSO₄), and concentrated. The residue

was purified by column chromatography with EtOAc/Hexane (1:2) to afford 0.42 g (77%) of ester **2.158** as a white solid. mp 74-77 °C; IR (neat) 2926, 1731, 1593, 1492, 1462, 1338, 1257, 1191, 1085, 1037, 750; ¹H NMR (CDCl₃) δ 7.4 (m, 5H), 6.71 (s, 1H), 4.19 (s, 3H), 4.16 (s, 3H), 4.04 (s, 3H), 2.65 (s, 3H); ¹³C NMR (CDCl₃) δ 166.0, 154.4, 153.5, 150.7, 140.8, 130.3, 129.2, 125.6, 121.4, 115.1, 94.7, 60.1, 56.1, 55.5, 12.6; LRMS calculated for C₁₇H₁₈O₅ (M+H)⁺ 303.1 *m/z*. Measured 303.2 *m/z*

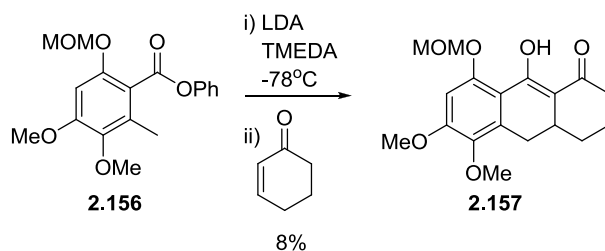


9-hydroxy-5,6,8-trimethoxy-3,4,4a,10-tetrahydroanthracen-1(2H)-one (2.159). To a solution of diisopropyl amine (0.070 mL, 0.50 mmol) in THF (1 mL) at 0°C was added 2.1 M *n*-BuLi (0.2 mL). After 30 min, TMEDA (0.085 mL, 0.56 mmol) was added, then cooled to -78°C. A solution of ester **2.158** (0.10 g, 0.33 mmol) in THF (2 mL) was added, forming a blood red color. After 1 h at -78°C a solution of cyclohexenone (0.10 g, 0.33 mmol) in THF was added resulting in a yellow color. This solution was then allowed to warm up to 0°C, over the next 2 h. The reaction mixture was diluted with 0.2M KH₂PO₄ (5 mL). The aqueous layers were extracted with EtOAc (3 x 10 mL). The combined organic layers were dried (MgSO₄), and concentrated. The crude product was purified by flash chromatography with EtOAc/Hexane (1:2) to afford 57 mg (56%) of the annulation product **2.159**. IR (neat) 2939, 1702, 1593, 1460, 1335, 1257, 1088, 1068, 1043, 812; ¹H NMR (CDCl₃) δ 16.51 (s, 1H) 6.43 (s, 1H), 4.77 (s, 1H) 3.90 (s, 3H), 3.89 (s, 3H), 3.21 (dd, *J* = 15.2, 4.0 Hz, 1H), 2.50 (m, 1H), 2.40 (m, 2H), 2.12 (m, 2H), 1.90

(m, 1H), 1.61 (m, 2H); ^{13}C NMR (CDCl_3) δ 186.9, 181.5, 158.1, 156.8, 138.6, 137.7, 113.9, 108.7, 95.2, 60.7, 56.4, 55.7, 32.6, 31.2, 30.2, 29.9, 20.9; LRMS calculated for $\text{C}_{17}\text{H}_{20}\text{O}_5$ ($\text{M}+\text{H}$) $^+$ m/z : 305.1, Measured 305.1 m/z

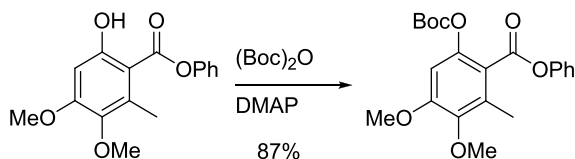


Phenyl 3,4-dimethoxy-6-(methoxymethoxy)-2-methylbenzoate (2.156). To a solution of phenyl 6-hydroxy-3,4-dimethoxy-2-methylbenzoate (0.10 g, 0.35 mmol) in CH_2Cl_2 (1.2 mL) was added diisopropyl ethyl amine (0.13 mL, 0.70 mmol) followed by MOMCl (0.040 mL, 0.52 mmol). After 16 h., the solution was then diluted with CH_2Cl_2 (2 mL), and washed with H_2O (5 mL), 1N HCl (5 mL), NaHCO_3 (saturated, 5 mL), and Brine (5 mL). Each aqueous layer was washed with CH_2Cl_2 (10 mL). The combined organic layers were dried (MgSO_4) and concentrated. The residue was purified by column chromatography with EtOAc/Hexane (1:4) to afford 74.6 mg (65%) of **2.156**. ^1H NMR (CDCl_3) δ 7.32 (m, 5H), 6.66 (s, 1H), 5.19 (s, 2H), 3.87 (s, 3H), 3.75 (s, 3H), 3.50 (s, 3H), 2.36 (s, 3H).



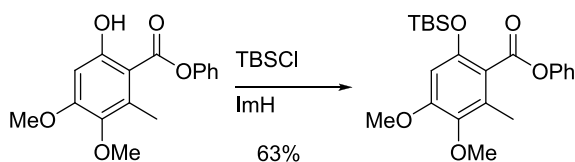
5,6-Dimethoxy-8-(methoxymethoxy)-3,4,4a,10-tetrahydroanthracene-1,9(2H,9aH)-

dione (2.157). To a solution of diisopropyl amine (0.032 mL, 0.23 mmol) in THF (0.5 mL) at 0°C was added 2.5 M *n*-BuLi (0.1 mL). After 30 min, TMEDA (0.038 mL, 0.28 mmol) and the solution was then cooled to -78°C . To this was added a solution of MOM ether **2.156** (50 mg, 0.15 mmol) in THF (2 mL), forming a blood red color. After 1 h at -78°C a solution of 0.5 M cyclohexenone (0.30 mL, 0.15 mmol) in THF was added resulting in a yellow color. This solution was then allowed to warm up to 0°C , over the next 2 h. The reaction mixture was diluted with 0.2M KH_2PO_4 (5 mL) and extracted with EtOAc (3 x 10 mL). The combined organic layers were dried (MgSO_4), and concentrated. The residue was purified by column chromatography with EtOAc/Hexane (1:2) to afford 1.2 mg (9%) of **2.157** a yellow oil. ^1H NMR (CDCl_3) δ 6.72 (s, 1H), 5.26 (dd, $J = 18.5, 7.0$ Hz, 2H), 3.92 (s, 3H), 3.75 (s, 3H), 3.57 (s, 3H), 3.25 (dd, $J = 15.2, 4.1$ Hz, 1H), 2.54 (m, 1H), 2.44 (m, 2H), 2.15 (m, 2H), 2.07 (m, 2H), 1.94 (m, 1H).

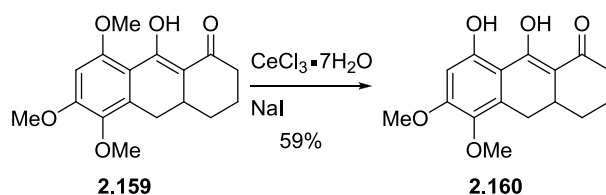


Phenyl 6-(tert-butoxycarbonyloxy)-3,4-dimethoxy-2-methylbenzoate. To a solution of phenyl 6-hydroxy-3,4-dimethoxy-2-methylbenzoate (50 mg, 0.17 mmol) in CH_2Cl_2 (0.6 mL) was added BOC anhydride (45 mg, 0.21 mmol), and DMAP (1 mg, 0.008 mmol).

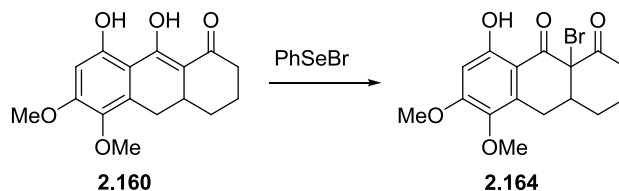
After 1 h, the reaction mixture was washed with brine (2 mL), 1N HCl (2 mL), and NaHCO₃ (2 mL). The organic layer was dried (MgSO₄), and concentrated. The residue was purified by column chromatography with EtOAc/Hexane (1:4) to afford 57 mg (85%) of phenyl 6-(tert-butoxycarbonyloxy)-3,4-dimethoxy-2-methylbenzoate. ¹H NMR (CDCl₃) δ 7.31 (m, 5H), 6.66 (s, 1H), 3.86 (s, 3H), 3.76 (s, 3H), 2.42 (s, 3H), 1.41 (s, 9H).



Phenyl 6-(tert-butyldimethylsilyloxy)-3,4-dimethoxy-2-methylbenzoate (2.155). To a solution of phenyl 6-hydroxy-3,4-dimethoxy-2-methylbenzoate (0.15 g, 0.52 mmol) in DMF (1 mL) was added imidazole (0.090 g, 1.3 mmol) and TBSCl (0.095 g, 0.62 mmol). After 16 h, the reaction mixture was diluted with NaHCO₃ (3 mL) and extracted with EtOAc (3 x 10 mL). The combined organic layers were dried (MgSO₄), and concentrated. The residue was purified by column chromatography with EtOAc/Hexane (1:10) to afford 0.097 g (63%) of phenyl 6-(tert-butyldimethylsilyloxy)-3,4-dimethoxy-2-methylbenzoate. ¹H NMR (CDCl₃) δ 7.32 (m, 5H), 6.32 (s, 1H), 3.82 (s, 3H), 3.74 (s, 3H), 2.36 (s, 3H), 0.98 (s, 9H), 0.25 (s, 6H).

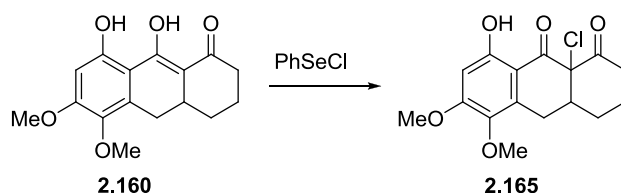


8,9-dihydroxy-5,6-dimethoxy-3,4,4a,10-tetrahydroanthracen-1(2H)-one (2.160). To a solution of **2.159** (40 mg, 0.13 mmol) in acetonitrile (1.4 mL) was added $\text{CeCl}_3 \cdot 7\text{H}_2\text{O}$ (73 mg, 0.20 mmol) and sodium iodide (0.29 g, 0.20 mmol). After 3.5 h of heating to reflux, the reaction was diluted with H_2O (5 mL) and extracted with EtOAc (3 x 10 mL). The combined organic layers were dried (MgSO_4), and concentrated to a yellow solid. The crude product was purified by flash chromatography with EtOAc/Hexane (1:4) to afford 19.6 mg (59%) of phenol **2.160**. ^1H NMR (CDCl_3) δ 14.58, (s, 1H), 12.22(s, 1H), 6.32 (s, 1H), 3.88 (s, 3H), 3.71 (s, 3H), 3.23 (dd, $J = 11.6, 4.6$ Hz, 1H), 2.62-.5 (m, 1H), 2.48-2.43 (m, 1H), 2.37-2.35 (m, 1H), 2.25-2.15 (m, 1H), 2.06-2.01 (m, 1H), 1.98-1.93 (m, 1H), 1.71-1.60 (m, 1H), 1.45-1.32 (m, 1H); ^{13}C NMR (CDCl_3) δ 191.9, 177.3, 160.9, 159.3, 138.0, 134.9, 109.2, 107.3, 98.5, 60.8, 55.8, 32.7, 30.3, 30.0, 29.0, 20.8; Selected NOSEY 14.58, 6.32, 3.88; LRMS calculated for $\text{C}_{16}\text{H}_{18}\text{O}_5$ ($\text{M}+\text{H}$) $^+$ m/z : 291.1, Measured 291.1 m/z .

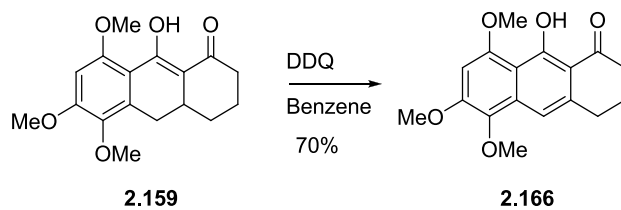


9a-bromo-8-hydroxy-5,6-dimethoxy-3,4,4a,10-tetrahydroanthracene-1,9(2H,9aH)-dione (2.164). To a solution of diphenyl diselenide (163 mg, 0.517 mmol) in THF at 0°C was added two drops of bromine and the resulting solution was allowed to stir for 30 min

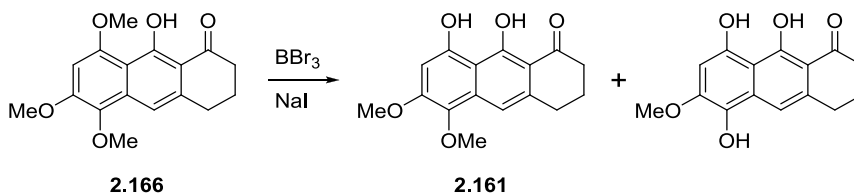
at 0°C. A solution of phenol **2.160** (20 mg, 0.069 mmol) in 1 ml of THF was added. After 1 h, the solution was diluted with sat. NH₄Cl and extracted with EtOAc (3 x 5 mL). The combined organic extracts dried (MgSO₄), and concentrated to afford an oil. The residue was purified by column chromatography with EtOAc/Hexane (1:4) to afford 8 mg (37%) of bromide **2.164** and 7 mg (41%) of phenol **2.160**. ¹H NMR (CDCl₃) δ, 6.45 (s, 1H), 3.96 (s, 3H), 3.79 (s, 3H), 3.23 (dd, *J* = 18, 4.5 Hz, 1H), 2.83 (m, 1H), 2.67 (m, 1H), 1.27 (d, *J* = 6.0 Hz, 3H) LRMS calculated for C₁₆H₁₉BrO₅ (M+H)⁺ *m/z*: 369.0, Measured 369.0 *m/z*.



9a-chloro-8-hydroxy-5,6-dimethoxy-3,4,4a,10-tetrahydroanthracene-1,9(2H,9aH)-dione (2.165) To a solution of phenol **2.160** (24 mg, 0.086 mmol) in 2 mL of EtOAc was added phenyl selenium chloride (28 mg, 0.14 mmol). After 16 h, the reaction was concentrated to an oil. The residue was purified by column chromatography with EtOAc/Hexane (1:4) to afford 16 mg (58 %) of chloride **2.165**. ¹H NMR (CDCl₃) δ, 6.45 (s, 1H), 3.96 (s, 3H), 3.79 (s, 3H), 3.23 (dd, *J* = 18, 4.5 Hz, 1H), 2.83 (m, 1H), 2.67 (m, 1H), 1.27 (d, *J* = 6.0 Hz, 3H) ¹³C NMR (CDCl₃) δ 202.0, 191.1, 163.7, 160.6, 138.2, 133.6, 108.3, 98.9, 70.4, 60.7, 56.0, 45.8, 37.4, 27.1, 27.0, 24.3 ; LRMS calculated for C₁₆H₁₈ClO₅ (M+H)⁺ *m/z*: 325.1, Measured 325.2 *m/z*.



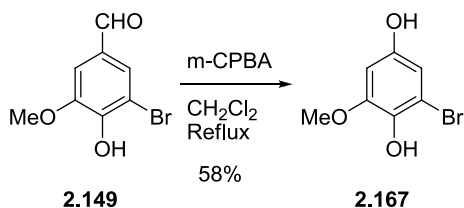
9-hydroxy-5,6,8-trimethoxy-3,4-dihydroanthracen-1(2H)-one (2.166). To a solution of **2.159** (0.45 g, 1.5 mmol) in benzene (15.0 mL) was added DDQ (0.42 mg, 1.77mmol). After 1 h at R.T. the reaction mixture was concentrated. The residue was purified by column chromatography with EtOAc/Hexane (1:1) to afford 306 mg (70%) of the naphthyl **2.163**. IR (neat) 3246, 2935, 1621, 1595, 143, 1344, 1326, 1187, 1114; ^1H NMR (CDCl_3) δ 15.35 (s, 1H) 7.19 (s, 1H), 6.52 (s, 1H), 3.99 (s, 1H) 3.98 (s, 3H), 3.83 (s, 3H), 2.96 (t, $J = 6.0$ Hz, 2H), 2.70 (t, $J = 6.4$ Hz, 2H), 2.06 (m, 2H), ^{13}C NMR (CDCl_3) δ 204.0, 166.4, 157.5, ,152.8, 139.4, 135.6, 134.5, 110.4, 109.9, 109.1, 94.4, 60.9, 56.5, 56.2, 38.7, 30.4, 22.7; LRMS calculated for $\text{C}_{17}\text{H}_{19}\text{O}_5$ ($\text{M}+\text{H}$) $^+$ m/z : 303.1, Measured 303.1 m/z .



8,9-dihydroxy-5,6-dimethoxy-3,4-dihydroanthracen-1(2H)-one (2.161). To solution of **2.166** (0.10 g, 0.33 mmol) in DCM (3.5 mL) was added sodium iodide (74 mg , 0.50 mmol). This solution was cooled to 0°C , where 1.0 M BBr_3 in DCM (0.40 ml) was added. The resulting solution was then allowed to warm to R.T. and stir for 16 h. At this time the solution was diluted w/ sat NaHCO_3 and extracted with DCM (3x). The combined organics were then concentrated. The residue was purified by Gilson chromatography

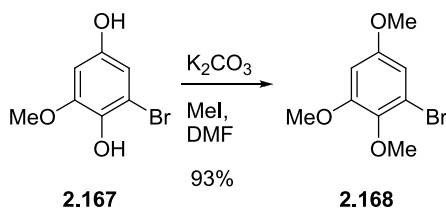
with CH₃CN/H₂O 1% TFA to afford 17 mg (18%, BRSM 40%) of the demethylated **2.161** and 33 mg (39%) of 5,8,9-trihydroxy-6-methoxy-3,4-dihydroanthracen-1(2H)-one. ¹H NMR (CDCl₃) δ 15.25 (s, 1H) 7.29 (s, 1H), 6.60 (s, 1H), 5.50 (s, 1H), 4.02 (s, 3H), 3.99 (s, 3H), 3.00 (t, *J* = 6.0 Hz, 2H), 2.73 (t, *J* = 6.4 Hz, 2H), 2.09 (m, 2H), ¹³C NMR (CDCl₃) δ 204.5, 166.5, 154.7, 145.7, 139.0, 138.3, 133.1, 128.8, 109.2, 109.9, 94.3, 57.2, 56.5, 38.9, 30.4, 22.8; LRMS calculated for C₁₆H₁₇O₅ (M+H)⁺ *m/z*: 289.1, Measured 289.2 *m/z*.

5,8,9-trihydroxy-6-methoxy-3,4-dihydroanthracen-1(2H)-one. ¹H NMR (CDCl₃) δ 13.74 (s, 1H) 7.56 (s, 1H), 6.17 (s, 1H), 3.92 (s, 3H), 3.09 (t, *J* = 6.1 Hz, 2H), 2.78 (t, *J* = 6.45 Hz, 2H), 2.18 (m, 2H), LRMS calculated for C₁₆H₁₇O₅ (M+H)⁺ *m/z*: 273.2, Measured 273.2 *m/z*.

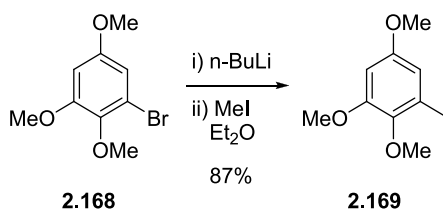


2-Bromo-6-methoxybenzene-1,4-diol (2.167). To a solution of aldehyde **2.149** (14.8 g, 64.0 mmol) in CH₂Cl₂ (160 mL) was added *m*-CPBA (22.1 g, 128 mmol). After 3.5 h of heating at reflux, saturated NaHCO₃ (200 mL) was added and allowed to stir for 45 min. The aqueous layer was extracted with CH₂Cl₂ (3 x 100 mL). The combined organic layers were dried (MgSO₄), and concentrated. This residue was dissolved in MeOH / conc HCl / H₂O (2:1:1, 200 mL). After 30 min, the MeOH was removed and extracted with EtOAc (3 x 100 mL). The combined organic layers were dried (MgSO₄), and concentrated. The residue was purified by column chromatography with EtOAc/Hexane

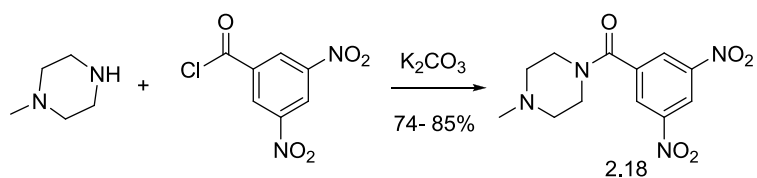
(1:4) to afford 10.7 g (77%) of the bis-phenol **2.167**. $^1\text{H NMR}$ (CDCl_3) δ 6.58 (d, $J = 2.7$ Hz, 1H), 6.42 (d, $J = 2.7$ Hz, 1H), 5.49 (bs, 1H), 3.87 (s, 3H). LRMS calculated for $\text{C}_7\text{H}_8\text{BrO}_3$ ($\text{M}+\text{H}$) $^+$ m/z : 219.0 Measured 219.0 m/z .



1-Bromo-2,3,5-trimethoxybenzene (2.168). To a solution of hydroquinone **2.167** (10.3 g, 49.0 mmol) in DMF (200 mL) was added K_2CO_3 (20.3 g, 147 mmol) and MeI (9.15 mL, 147 mmol). After 16 h, the reaction was diluted with H_2O (200 mL) and extracted with EtOAc (3 x 75 mL). The combined organic layers were washed with brine (100 mL), dried (MgSO_4), and concentrated. The residue was purified by column chromatography with EtOAc/Hexane (1:3) to afford 11.2 g (92%) of the trimethoxy bromide **2.168**. IR (neat) 1599, 1571, 1489, 1464, 1425, 1235, 1212, 1174, 1147, 1053, 1037, 1002 cm^{-1} $^1\text{H NMR}$ (CDCl_3) δ 6.59 (d, $J = 2.8$ Hz, 1H), 6.40 (d, $J = 2.8$ Hz, 1H), 3.79 (s, 3H), 3.76 (s, 3H), 3.71 (s, 3H); $^{13}\text{C NMR}$ (CDCl_3) δ 156.3, 153.9, 140.5, 117.3, 107.7, 99.7, 60.4, 55.8, 55.5; LRMS calculated for $\text{C}_9\text{H}_{12}\text{BrO}_3$ ($\text{M}+\text{H}$) $^+$ m/z : 247.0, Measured 247.0 m/z .

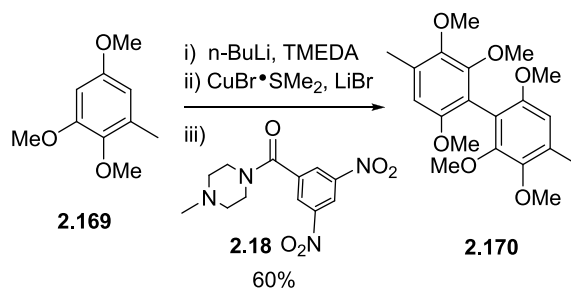


1,2,5-Trimethoxy-3-methylbenzene (2.169). To a solution of bromide **2.168** (1.0 g, 4.2 mmol) in Et₂O (150 mL) at -78°C was added *n*-BuLi (3.4 mL, 8.2 mmol). After 1 h, MeI (0.80 mL, 13 mmol) was added, and the solution was allowed to warm to room over the next 4 h.. The reaction mixture was diluted by H₂O (100 mL), and extracted with EtOAc (3 x 75 mL). The residue was purified by column chromatography with EtOAc/Hexane (1:3) to afford 560 mg (73%) of toluene **2.169** as a yellow oil. ¹H NMR (CDCl₃) δ 6.34 (d, *J* = 2.7 Hz, 1H), 6.27 (d, *J* = 2.7 Hz, 1H), 3.81 (s, 3H), 3.74 (s, 3H), 3.73 (s, 3H) 2.25 (s, 3H). ¹³C NMR (CDCl₃) δ 153.1, 151.7, 145.7, 131.3, 115.3, 107.9, 60.2, 60.1, 56.9, 15.7. LRMS calculated for C₁₀H₁₄O₃ (M+H)⁺ *m/z*: 183.2, Measured 183.2 *m/z*.

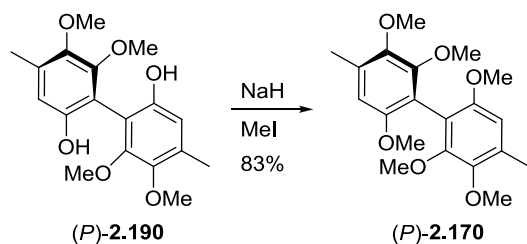


(3,5-dinitrophenyl)(4-methylpiperazin-1-yl)methanone (2.18). A solution of 3,5-dinitrobenzoyl chloride (10.0 g, 43 mmol) in CHCl₃ (80 mL) was slowly added to a solution of 1-methylpiperazine (6.0 mL, 52 mmol) and K₂CO₃ (6.0 g, 43 mmol) in CHCl₃ (80 mL) at 0°C. After 1.5 h, the reaction mixture was then washed with H₂O (3 x 40 mL). The organic layer was dried (MgSO₄) and concentrated. The product was then re-crystallized from Hexane and CH₂Cl₂ to afford a tan solid (8.6 g, 68%). Yields range (85%) ¹H NMR

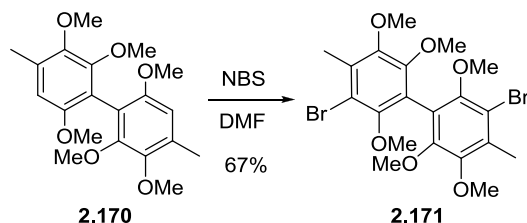
(CDCl₃) δ 8.96 (d, *J* = 1.3 Hz, 1H), 8.50 (t, *J* = 1.0 Hz, 2H), 3.74 (bs, 2H), 3.38 (bs, 2H), 2.46 (bs, 2H), 2.35 (bs, 2H), 2.27 (s, 3H)



2,2',3,3',6,6'-hexamethoxy-4,4'-dimethylbiphenyl (2.170). To a solution of toluene **2.169** (1.4 g, 7.6 mmol) in diethyl ether (38 mL) at 0 °C was added 2.2 M *n*-BuLi (4.2 mL, 9.2 mmol) and the resulting solution stirred for 5 h at 0 °C. To the reaction mixture was added a solution of CuBr·SMe₂ (0.79 g, 3.8 mmol) and LiBr (0.67 g, 7.6 mmol) in THF (3 mL) via canula. After the mixture was stirred for 30 min, (3,5-dinitrophenyl)(4-methylpiperazin-1-yl)methanone (3.4 g, 11.5 mmol) was added by a solid addition adaptor. After 1.5 h, the reaction mixture was passed over a silica plug and the filtrate concentrated *in vacuo*. The residue was purified by column chromatography with EtOAc/Hexane (1:4) to afford 0.79 g (57%) biaryl **2.170** as a white solid: mp 114-117 °C; IR (neat) 2937, 1464, 1393, 1232, 1101, 1033 cm⁻¹; ¹H NMR (CDCl₃) δ 6.54 (s, 1H), 3.80 (s, 3H), 3.69 (s, 3H), 3.67 (s, 3H), 2.33 (s, 3H)¹⁷⁵; ¹³C NMR (CDCl₃) δ 153.4, 151.8, 145.3, 131.1, 115.8, 108.2, 60.2, 60.2, 56.0, 16.4; HRMS calculated for C₂₀H₂₆O₆Li (M+Li)⁺ *m/z*: 369.1889, Measured 369.1907 *m/z*.

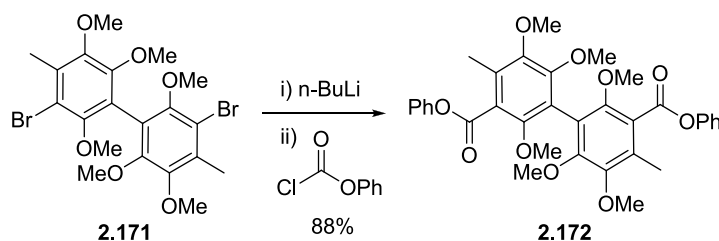


Method 2. To a solution of (+)-(P)-**2.190** (23 mg, 0.069 mmol) in THF (2.0 mL) was added NaH (21 mg, 0.46 mmol) followed by MeI (0.20 mL, 0.27 mmol). After 16 h the solution was diluted with H₂O (5 mL), extracted with CH₂Cl₂ (3 x 5 mL) and the combined organic extracts were dried (MgSO₄) and concentrated. The residue was purified by column chromatography with EtOAc/Hexane (1:4) to afford 17 mg (68%) of (-)-(P)-**2.170** as a white solid: $[\alpha]_{589}^{22}$ -4.7 (c 0.41, CHCl₃). Bis-phenol (-)-(M)-**2.190** was methylated using the same procedure to afford (+)-(M)-**2.170** isomer as a colorless oil: $[\alpha]_{589}^{22}$ +6.8 (c 0.30, CHCl₃).



3,3'-dibromo-2,2',5,5',6,6'-hexamethoxy-4,4'-dimethylbiphenyl (2.171). To a solution of biaryl **2.170** (1.2 g, 3.2 mmol) in DMF (160 mL) at room temperature was added N-bromosuccinimide (2.9 g, 13 mmol). After 16 h, the solution was diluted with 0.2 M sodium bisulfite (200 mL). The mixture was then extracted with EtOAc (3 x 100 mL). The combined organic extracts were washed with brine (150 mL), dried (MgSO₄), and concentrated to afford a yellow oil. The residue was purified by column chromatography on silica gel with EtOAc/Hexane (1:4) to afford 1.3 g (78%) of bis-bromide **2.171** as a

white solid: mp 139-142 °C; IR (neat) 2941, 1458, 1391, 1084, 1009, 939; ¹H NMR (CDCl₃) δ 3.80 (s, 3H), 3.70 (s, 3H), 3.58 (s, 3H), 2.43 (s, 3H); ¹³C NMR (CDCl₃) δ 151.3, 150.6, 148.2, 132.9, 121.7, 114.7, 60.5, 60.4, 16.6; LRMS calculated for C₂₀H₂₅Br₂O₆ (M+H)⁺ *m/z*: 521.2, Measured 521.0 *m/z*.

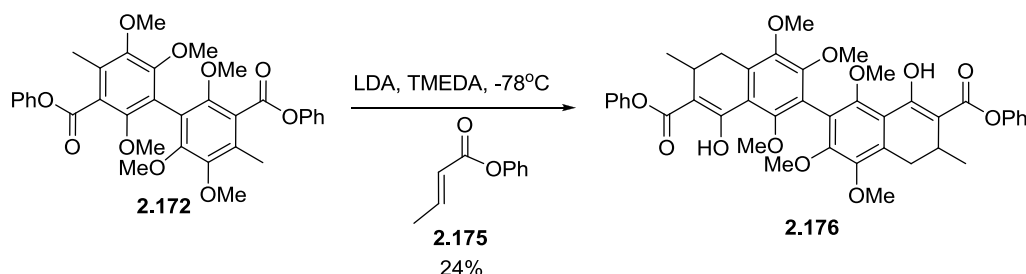


Diphenyl 2,2',5,5',6,6'-hexamethoxy-4,4'-dimethylbiphenyl-3,3'-dicarboxylate

(2.172). To a solution of bromide **2.170** (250 mg, 0.48 mmol) in diethyl ether (50 mL) at -78 °C was added 2.5 M n-BuLi (0.85 mL, 1.9 mmol). After 1 h at -78 °C, neat phenyl chloroformate (0.14 mL, 1.9 mmol) was added. The reaction mixture was allowed to warm to room temperature and after 16 h, diluted with H₂O (15 mL) and extracted with ethyl acetate (3 x 15 mL). The combined organic extracts were dried (MgSO₄) and concentrated to afford a red/orange oil. The residue was purified by column chromatography with EtOAc/Hexane (1:4) to afford 230 mg (80%) of bis-phenyl ester **2.170** as a white solid and 34 mg (9%) of **2.172**: mp 102-105 °C; IR (neat) 1747, 1460, 1397, 1303, 1259, 1187, 1090, 1039, 1010, 953; ¹H NMR (CDCl₃) δ 7.35 (m, 5H), 3.84 (s, 3H), 3.81 (s, 3H), 3.66 (s, 3H), 2.42 (s, 3H); ¹³C NMR (CDCl₃) δ 166.2, 155.5, 152.9, 151.7, 150.5, 147.3, 130.4, 129.3, 125.8, 123.7, 121.3, 120.2, 115.0, 61.7, 60.2, 59.9, 12.8; LRMS calculated for C₃₄H₃₄O₁₀ (M+Na)⁺ *m/z*: 625.2, Measured 626.2 *m/z*.

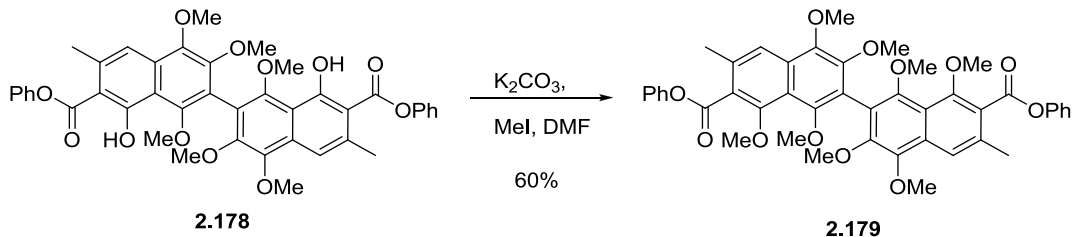
Resolution of bis-phenyl ester 2.170 by Preparative HPLC. A Varian Prostar system was used for HPLC separation of bis-phenyl ester **2.172**. The HPLC column used was a

Chiralpak OD column (5 × 50 cm, 20 μm). The LC flow rate was 75 mL/min. The mobile phase consisted of an isocratic mixture of 1% isopropanol/hexane. (+)-(*M*)-**2.172**, t_r = 13 min; $[\alpha]_{589}^{22}$ +6.8 (c 0.30, CHCl₃); (-)-(*P*)-**2.172**, t_r = 16 min; $[\alpha]_{589}^{22}$ -4.7 (c 0.41, CHCl₃). Analytical (Chiralpak OD, (4.6 × 250 mm) 1.0 mL/min, 1% isopropanol/hexane) (+)-(*M*)-**2.172**, t_r = 6.4 min, (-)-(*P*)-**2.172**, t_r = 8.3 min.]

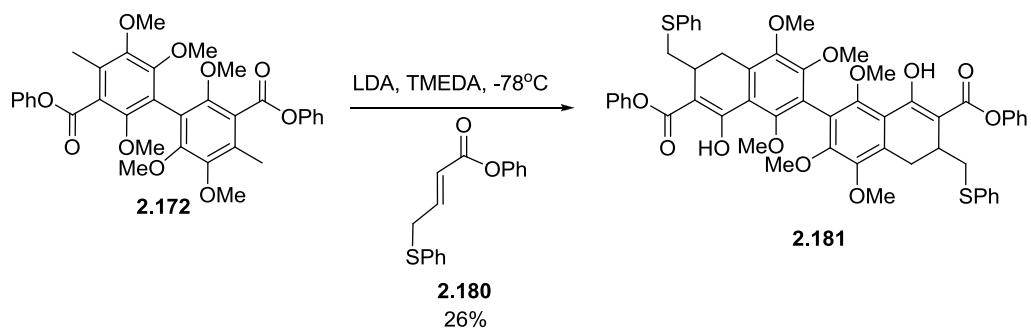


Diphenyl 1,1', 3,3', 4,4'- hexamethoxy- 6,6' -dimethyl- 8,8' -dioxo -5,5', 6,6', 7,7', 8,8'-octahydro-2,2'-binaphthyl-7,7'-dicarboxylate (2.176). To a solution of diisopropyl amine (0.30 mL, 2.0 mmol) in THF (1 mL) was added 2.5 M *n*-BuLi (0.80 mL, 2.0 mmol) at 0°C. After 30 min, TMEDA (0.35 mL, 2.1 mmol) was added. At -78°C, a solution of ester **2.172** (0.20 g, 0.34 mmol) in THF (1.0 mL) was added, forming a blood red color. After 1 h at -78°C a solution of crotonate **2.175** (0.20 g, 1.3 mmol) in THF (1.0 mL) was added resulting in a yellow color. After 16 h, reaction mixture was diluted with saturated NH₄Cl (5 mL). The aqueous layers were extracted with EtOAc (3 × 10 mL). The combined organic layers were dried (MgSO₄), and concentrated. The residue was purified by column chromatography with EtOAc/Hexane (1:2) to afford 59 mg (24%) of bis annulation product **2.176** and 54 mg (16%) of the mono annulation product. ¹H NMR (CDCl₃) δ 7.41 (m, 2H), 7.26 (m, 3H), 3.86 (s, 3H), 3.82 (d, *J* = 2.8 Hz, 3H), 3.63 (bs, 3H), 3.43 (m, 1H), 2.82 (m, 1H), 2.62 (m, 1H), 1.36 (d, *J* = 6.4 Hz, 3H).

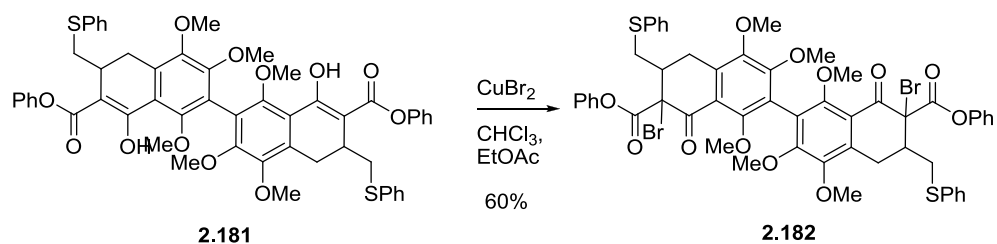
2.178. $^1\text{H NMR}$ (CDCl_3) δ 11.21 (s, 1H), 7.54 (s, 1H), 7.46 (m, 2H), 7.30 (m, 3H), 3.96 (s, 3H), 3.90 (s, 3H), 3.66 (s, 3H), 2.72 (s, 3H).



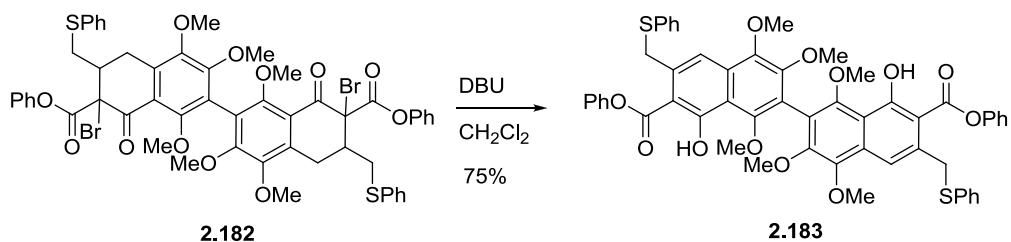
Diphenyl 1,1',3,3',4,4',8,8'-octamethoxy-6,6'-dimethyl-2,2'-binaphthyl-7,7'-dicarboxylate (2.179). To a suspension of **2.178** (6.3 mg, 0.0086 mmol) and K_2CO_3 (7 mg, 0.050 mmol) in DMF (0.9 mL) was added MeI (40 μL , 0.050 mmol). After 16 h, the reaction was diluted with H_2O (2 mL) and extracted with EtOAc (3 x 2 mL). The combined organic layers were dried (MgSO_4), and concentrated. The residue was purified by column chromatography with EtOAc/Hexane (1:2) to afford 3.9 mg (60%) of methyl ether **2.179**. $^1\text{H NMR}$ (CDCl_3) δ 7.90 (s, 1H), 7.47 (m, 2H), 7.31 (m, 3H), 4.01 (s, 3H), 3.98 (s, 3H), 3.82 (s, 3H), 3.69 (s, 3H), 2.64 (s, 3H); $^{13}\text{C NMR}$ (CDCl_3) δ 167.0, 153.7, 150.8, 149.0, 132.7, 132.4, 129.5, 126.0, 125.7, 122.9, 121.6, 118.3, 117.7, 64.0, 62.0, 60.9, 60.4, 19.8.



Diphenyl 1,1',3,3',4,4'- hexamethoxy-8,8'-dioxo- 6,6'- bis(phenylthiomethyl)- 5,5',6,6',7,7', 8,8' -octahydro-2,2'-binaphthyl-7,7'-dicarboxylate (2.181). To a solution of diisopropyl amine (0.15 mL, 1.0 mmol) in THF (0.5 mL) was added 2.5 M *n*-BuLi (0.40 mL, 1.0 mmol) at 0°C. After 30 min, TMEDA (0.18 mL, 1.5 mmol) was added. At -78°C, a solution of ester **2.172** (0.2 g, 0.336 mmol) in THF (1.0 mL) was added, forming a blood red color. After 1 h at -78°C a solution of thiophenyl crotonate **2.180** (0.16 g, 1.33 mmol) in THF (0.5 mL) was added resulting in a yellow color. After 16 h, reaction mixture was diluted with saturated NH₄Cl (5 mL). The aqueous layers were extracted with EtOAc (3 x 10 mL). The combined organic layers were dried (MgSO₄), and concentrated. The residue was purified by column chromatography with EtOAc/Hexane (1:2) to afford 44 mg (26%) of **2.181** and 21 mg (13%) of the mono annulation product. ¹H NMR (CDCl₃) δ 7.33 (m, 5H), 3.80 (m, 9H), 3.54 (s, 3H), 3.47 (s, 0.5H), 3.28 (m, 0.5H), 3.10 (m, 1H), 2.96 (m, 0.5H), 2.65 (m, 1.5H), 2.33 (d, *J* = 5.2 Hz, 0.5H).

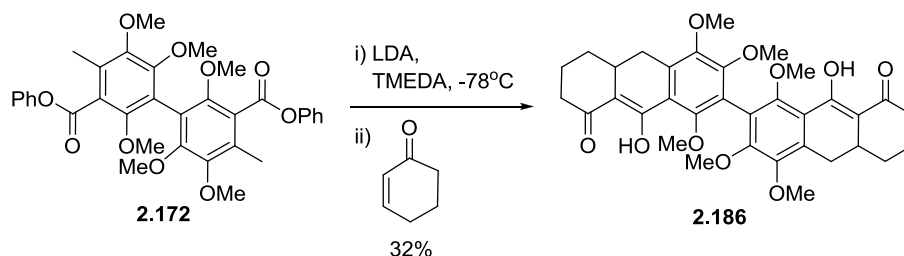


Diphenyl 7,7'- dibromo- 1,1', 3,3', 4,4' -hexamethoxy- 8,8' -dioxo- 6,6'- bis(phenylthiomethyl)- 5,5', 6,6', 7,7', 8,8' -octahydro- 2,2' -binaphthyl-7,7'- dicarboxylate (2.182). To a solution of bis annulation product **2.181** (36 mg, 0.044 mmol) in CHCl_3 (0.75 mL) and EtOAc (0.75 mL) was added CuBr_2 (42 mg, 0.15 mmol). After 16 h, the reaction was concentrated to a solid. The residue was purified by column chromatography with EtOAc/Hexane (1:2) to afford 26 mg (60%) of bromide **2.182**. ^1H NMR (CDCl_3) δ 7.21 (d, $J = 7.6$ Hz, 2H), 7.33 (t, $J = 7.6$ Hz, 2H), 7.24 (d, $J = 7.2$ Hz, 1H), 3.80 (m, 9H), 3.73 (m, 1H), 3.51 (d, $J = 2.4$ Hz, 3H), 3.13 (d, $J = 13.6$ Hz, 1H), 2.98 (m, 1H), 2.85 (m, 1H), 2.65 (m, 1H).



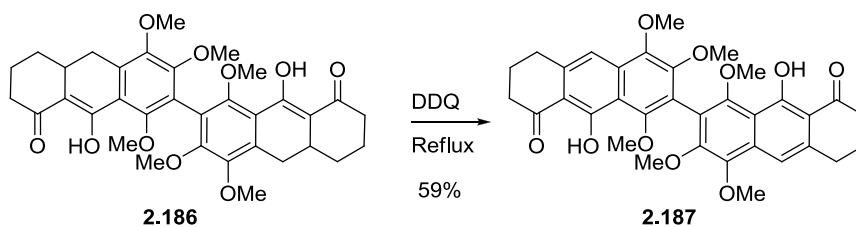
Diphenyl 8,8'-dihydroxy-1,1',3,3',4,4'-hexamethoxy-6,6'-bis(phenylthiomethyl)-2,2'- binaphthyl-7,7'-dicarboxylate (2.183). A solution of bromide **2.182** (26 mg, 0.026 mmol) in CH_2Cl_2 (0.3 mL) at 0°C was added DBU (20 μL , 0.11 mmol). After 16 h, the reaction was diluted with saturated NH_4Cl (8 mL) and extracted with EtOAc (3 x 10 mL). The combined organic layers were dried (MgSO_4) and concentrated. The residue was purified by column chromatography with EtOAc/Hexane (1:2) to afford 15 mg (70%) of

bi-naphthyl **2.183**. $^1\text{H NMR}$ (CDCl_3) δ 7.39 (m, 4H), 7.24 (s, 1H), 7.19 (m, 1H), 4.46 (s, 2H), 3.98 (s, 3H), 3.84 (s, 3H), 3.76 (s, 3H), 3.62 (s, 3H),



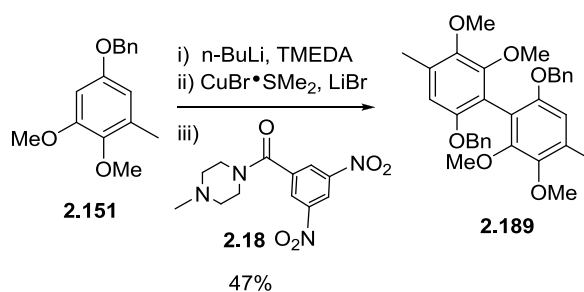
9,9'-dihydroxy-1,1',3,3',4,4'-hexamethoxy-6,6',7,7',10,10a,10',10'a-octahydro-2,2'-

bianthracene-8,8'(5H,5'H)-dione (2.186). A solution of diisopropyl amine (50 mL, 0.33 mmol) in THF (1 mL) was cooled to 0 °C and a solution of 2.1 M *n*-BuLi (0.15 mL, 0.33 mmol) was added. After 30 min, TMEDA (50 mL, 0.33 mmol) was added (neat) and the LDA solution was added via canula to a pre-cooled solution of **2.172** (50 mg, 0.083 mmol) in THF (1 mL) at -78 °C resulting in a deep-red colored solution. After 30 min at -78 °C, cyclohexenone (62 mg, 0.66 mmol) was added resulting in a yellow color solution. The reaction mixture was allowed to warm up to 0 °C and stir for two hours. The reaction was diluted with saturated NH_4Cl (5 mL) and extracted with EtOAc (3 x 5 mL). The combined organic layers were dried (MgSO_4), and concentrated. The residue was purified by column chromatography with EtOAc/Hexane (1:4) to afford 15 mg (32%) of bis-annulated product **2.186**: $^1\text{H NMR}$ (CDCl_3) 16.57 (s, 1H), 3.80 (s, 3H), 3.27 (dd, $J = 7.8, 2.8$ Hz, 1H), 2.72-2.68 (m, 1H), 2.48-2.43 (m, 2H) 2.27-2.20 (m, 1H), 2.10-2.08 (m, 1H), 1.95-1.93 (m, 1H), 1.72-1.66 (m, 1H), 1.56 (bs, 2H), 1.41-1.35 (m, 1H), 1.27-1.25 (m, 1H); $^{13}\text{C NMR}$ (CDCl_3) δ 185.4, 184.2, 155.9, 155.3, 145.1, 137.4, 122.3, 120.8, 109.1, 61.9, 60.5, 32.5, 31.8, 30.3, 30.1, 21.0. LRMS calculated for $\text{C}_{16}\text{H}_{15}\text{O}_6$ ($\text{M}+\text{H}$) $^+$ 303.1 *m/z*. Measured 303.1 *m/z*



9,9'-dihydroxy-1,1',3,3',4,4'-hexamethoxy-6,6',7,7'-tetrahydro-2,2'-bianthracene-

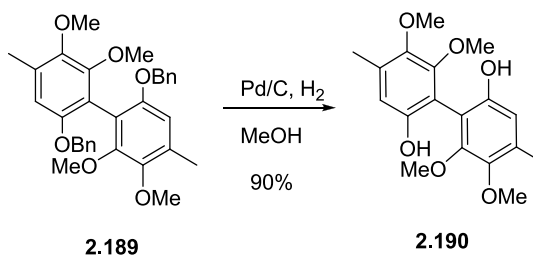
8,8'(5H,5'H)-dione (2.187). To a solution of **2.186** (31 mg, 0.051 mmol) in benzene (0.5 mL) was added DDQ (26 mg, 0.12 mmol). After refluxing for 5 h, the reaction mixture was concentrated and purified by column chromatography with EtOAc/Hexane (1:2) to afford 19 mg (62%) of the **2.187**. ^1H NMR (CDCl_3) δ 15.09 (s, 1H), 7.41 (s, 1H), 3.95 (s, 3H), 3.83 (s, 3H), 3.70 (s, 3H), 3.07 (t, $J = 5.6$ Hz, 2H), 2.78 (t, $J = 6.4$ Hz, 2H), 2.19-2.14 (m, 2H); ^{13}C NMR (CDCl_3) δ 204.3, 165.7, 156.7, 152.8, 139.4, 135.6, 134.7, 111.3, 110.7, 110.0, 94.7, 60.2, 56.4, 56.2, 39.0, 30.4, 23.6 LRMS calculated for $\text{C}_{34}\text{H}_{34}\text{O}_{10}$ ($\text{M}+\text{H}$) $^+$ m/z : 603.2, Measured 603.2 m/z .



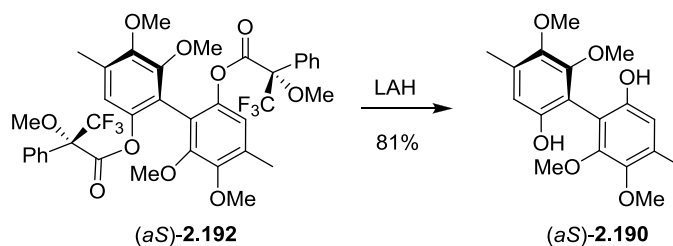
6,6'-Bis(benzyloxy)-2,2',3,3'-tetramethoxy-4,4'-dimethylbiphenyl (2.189).

To a solution of benzyl toluene **2.151** (0.10 g, 0.39 mmol) in diethyl ether (2.0 mL) at 0 °C was added 2.5 M $n\text{-BuLi}$ (0.20 mL, 0.47 mmol). After 5 h at 0 °C, a solution of $\text{CuBr}\cdot\text{SMe}_2$ (40 mg, 0.19 mmol) and LiBr (34 mg, 0.39 mmol) in THF (1 mL) was added via canula. After the mixture was stirred for 30 min, (3,5-dinitrophenyl)(4-methylpiperazin-1-yl)methanone

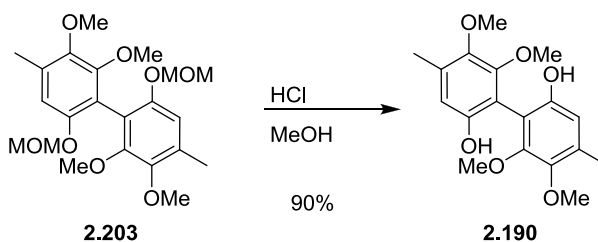
(**2.18**) (0.19 g, 0.58 mmol) was added by a solid addition adaptor. After 1 h, the reaction mixture was passed over a silica plug and the filtrate concentrated *in vacuo*. The residue was purified by column chromatography with EtOAc/Hexane (1:4) to afford 47 mg (47%) of biaryl **2.189** as a solid: mp 126-128 °C; ¹H NMR (CDCl₃) δ 7.17 (m, 5H), 6.58 (s, 1H), 4.95 (dd, *J* = 9.9, 12.6 Hz, 2H), 3.81 (s, 3H), 3.71 (s, 3H), 2.28 (s, 3H); ¹³C NMR (CDCl₃) δ 152.4, 151.6, 145.2, 137.5, 130.8, 128.3, 127.8, 127.3, 126.9, 126.2, 116.7, 110.1, 70.4, 60.1, 60.0, 16.1; LRMS calculated for C₃₂H₃₅O₆ (M+H)⁺ *m/z*: 515.24, Measured 515.2 *m/z*.



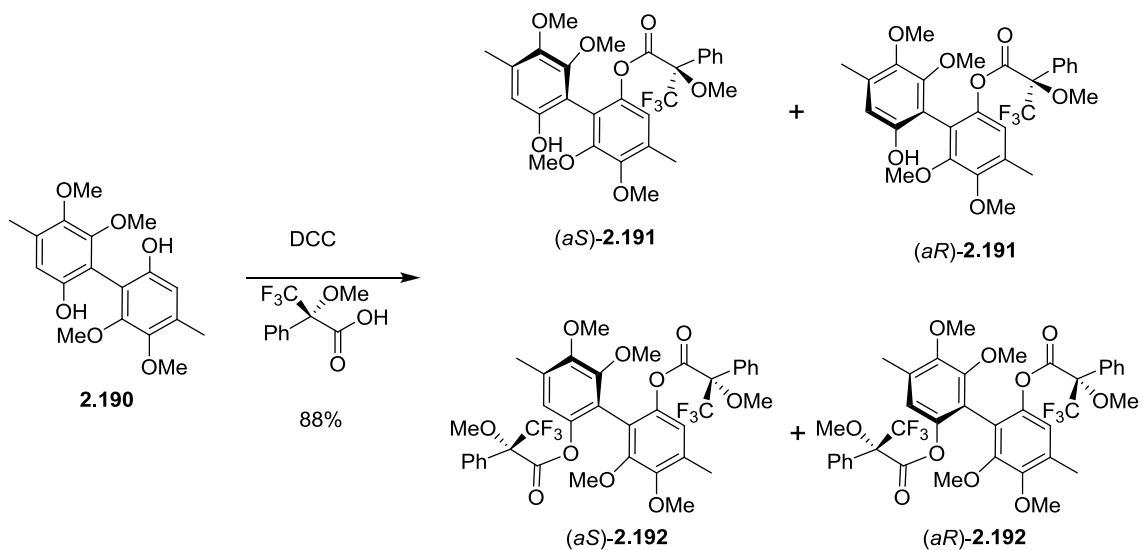
5,5',6,6'-tetramethoxy-4,4'-dimethylbiphenyl-2,2'-diol (2.190) - To a solution of bis-benzyl ether **2.189** (80 mg, 0.16 mmol) in anhydrous MeOH (3.0 mL) was added 5% Pd/C (30 mg). This solution was placed under one atmosphere of hydrogen and allowed to stir at room temperature for 16 h. The reaction was filtered through a plug of Celite 454 and silica gel (1:1). The filtrate was concentrated and the residue was purified by column chromatography with EtOAc/Hexane (1:4) to afford 47 mg (90%) of bis-phenol **2.190**. ¹H NMR (CDCl₃) δ 6.67 (s, 1H), 5.41 (s, 1H), 3.81 (s, 3H), 3.69 (s, 3H), 2.29 (s, 3H); ¹³C NMR (CDCl₃) δ 150.5, 149.5, 145.1, 133.4, 114.0, 111.7, 60.7, 60.3, 15.7. LRMS calculated for C₁₈H₂₂O₆ (M+H)⁺ *m/z*: 334.9, Measured 334.9 *m/z*.



Method 2 - A solution of (aS)-**2.192** (17 mg, 0.022 mmol) in CH_2Cl_2 (0.5 mL) and Et_2O (1.8 mL) was cooled to 0 °C and LiAlH_4 (6.2 mg, 0.16 mmol) was added. The reaction mixture was allowed to warm to room temperature over 2.5 h and carefully quenched with saturated NH_4Cl (3 mL), extracted with CH_2Cl_2 (3 x 3 mL) and the combined organic extracts dried (MgSO_4) and concentrated. The residue was purified by column chromatography with EtOAc/Hexane (1:4) to afford 6 mg (82%) of (-)-(aS)-**2.190** identical to (\pm)-**9** except optical rotation: $[\alpha]_{589}^{22} -8.3$ (c 0.14, CHCl_3). Mosher ester (aR)-**2.192** was reduced under identical conditions to afford (+)-(aR)-**2.190**: $[\alpha]_{589}^{22} +3.6$ (c 0.22, CHCl_3) using an identical procedure.



Method 3 - To a solution of bis-MOM ether **2.203** (0.41 g, 0.97 mmole) in MeOH (10 mL) was added 12 drops of conc. HCl . This solution was allowed to stir at room temperature for 2.5 h, MeOH was removed *in vacuo* and the residue was purified by column chromatography with EtOAc/Hexane (1:4) to afford 0.24 g (74%) of bis-phenol **2.190** as a colorless oil:



(2R,2'R)-(5,5',6,6'-tetramethoxy-4,4'-dimethylbiphenyl-2,2'-diyl) bis(3,3,3-trifluoro-2-methoxy-2-phenylpropanoate) ((aR)-2.192 / (aS)-2.192) - To a solution of bis-phenol **2.190** (47 mg, 0.14 mmol) in CH₂Cl₂ (5.5 mL) at 0 °C was added Mosher's acid (87 mg, 0.35 mmol), DCC (82 mg, 0.36 mmol), and several crystals of DMAP. After 16 h, additional Mosher's acid (67 mg, 0.28 mmol) and DCC (58 mg, 0.28 mmol) were added along with several crystals of DMAP. After 24 h, the reaction was judged complete by TLC and concentrated. The residue was purified by flash chromatography on silica gel with EtOAc/Hexane (1:4) to afford a mixture of diastereomers **(aR)-2.192** and **(aS)-2.192** (65 mg, 84%). The diastereomers were separated by HPLC using a Dynamax column (21.4 × 250 mm, 60 Å). The mobile phase consisted of a gradient mixture of EtOAc/hexane (10%-60%) over 45 min.

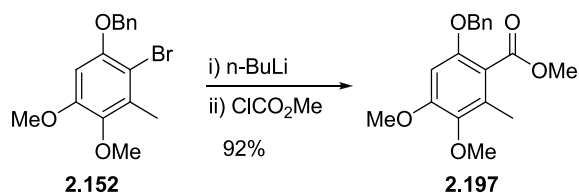
(aS)-2.191 - IR (neat) 3351, 2921, 1759, 1457, 1401, 1269, 1238, 1218, 1182, 1167, 1122, 1080, 1015, 1002, 733, 699. ¹H NMR (CDCl₃) δ 7.26 (m, 5H), 6.71 (s, 1H), 6.58 (s, 1H), 4.83 (s, 1H), 3.87 (s, 3H), 3.71 (s, 6H), 3.57 (s, 3H), 3.27 (s, 3H), 2.33 (s, 3H),

2.30 (s, 3H); ^{19}F NMR (CDCl_3) δ -69.7 LRMS calculated for $\text{C}_{28}\text{H}_{30}\text{F}_3\text{O}_8$ ($\text{M}+\text{H}$) $^+$ 551.2 m/z . Measured 551.0 m/z

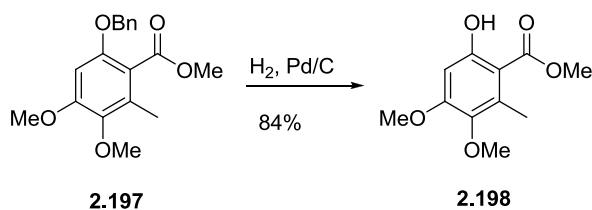
(*aR*)-**2.191** - ^1H NMR (CDCl_3) δ 7.25 (m, 5H), 6.80 (s, 1H), 6.61 (s, 1H), 4.81 (s, 1H), 3.88 (s, 3H), 3.71 (s, 3H), 3.61 (s, 3H), 3.49 (s, 3H), 3.48 (s, 3H), 2.36 (s, 3H), 2.29 (s, 3H); ^{19}F NMR (CDCl_3) δ -70.2 LRMS calculated for $\text{C}_{28}\text{H}_{30}\text{F}_3\text{O}_8$ ($\text{M}+\text{H}$) $^+$ 551.2 m/z . Measured 551.0 m/z

(*aS*)-**2.192**: t_r = 29 min; $[\alpha]_{589}^{22^\circ\text{C}}$ -44 (c 0.56, CHCl_3); mp 126-128 $^\circ\text{C}$; IR (neat) 1762, 1455, 1400, 1240, 1221, 1191, 1170, 1070, 1011 cm^{-1} ; ^1H NMR (CDCl_3) δ 7.31 (m, 6H), 6.65 (s, 1H), 3.71 (s, 3H), 3.56 (s, 3H), 3.28 (s, 3H); 2.32 (s, 3H), ^{13}C NMR (CDCl_3) δ 165.2, 151.8, 149.5, 143.5, 133.0, 131.3, 129.3, 129.2, 128.3, 128.2, 127.4, 127.1, 124.6, 121.7, 118.4, 118.2, 60.3, 58.8, 55.0, 16.1; ^{40}F NMR (CDCl_3) δ -71.6; LRMS calculated for $\text{C}_{38}\text{H}_{36}\text{F}_6\text{NaO}_{10}$ ($\text{M}+\text{Na}$) $^+$ 789.2 m/z . Measured 788.9 m/z

(*aR*)-**2.192**: t_r = 31 min; $[\alpha]_{589}^{22^\circ\text{C}}$ +0.65 (c 0.40, CHCl_3); IR (neat) 2930, 1761, 1467, 1225, 1174, 1073, 1006 cm^{-1} ; ^1H NMR (CDCl_3) δ 7.28 (m, 6H), 6.69 (s, 1H), 3.68 (s, 3H), 3.59 (s, 3H), 3.39 (s, 3H); 2.30 (s, 3H), ^{13}C NMR (CDCl_3) δ 164.9, 151.8, 149.4, 143.4, 132.9, 131.7, 129.5, 129.1, 128.2, 127.1, 126.0, 124.4, 121.6, 118.3, 118.2, 60.3, 59.8, 55.3, 16.1 ^{40}F NMR (CDCl_3) δ -72.0; LRMS calculated for $\text{C}_{38}\text{H}_{36}\text{F}_6\text{NaO}_{10}$ ($\text{M}+\text{Na}$) $^+$ 789.2 m/z . Measured 788.9 m/z

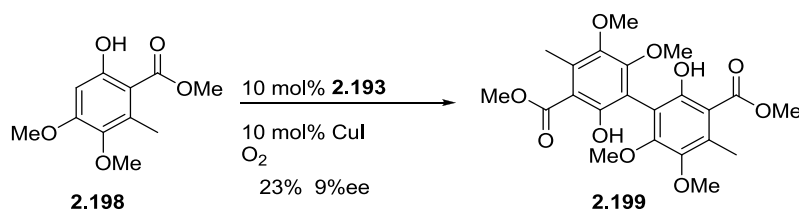


Methyl 6-(benzyloxy)-3,4-dimethoxy-2-methylbenzoate (2.197) - To a solution of **2.152** (478 mg, 1.42 mmol) in THF (15 mL) at -78 °C was added 2.5 M n-BuLi (1.1 mL, 2.8 mmol). After 1 h at -78 °C, neat methyl chloroformate (0.20 mL, 2.8 mmol) was added. The reaction mixture was allowed to warm to room temperature. After 16 h, H₂O (15 mL) was added and extracted with ethyl acetate (3 x 15 mL). The combined organic extracts were dried (MgSO₄) and concentrated to afford a red/orange oil. The residue was purified by column chromatography with EtOAc/Hexane (1:4) to afford 392 mg (85%) of **2.197**. ¹H NMR (CDCl₃) δ 7.39 – 7.37 (m, 5H), 6.40 (s, 1H), 5.08 (s, 2H), 3.87 (s, 3H), 3.81 (s, 3H), 3.72 (s, 3H), 2.23 (s, 3H) ¹³C NMR (CDCl₃) δ 168.3, 154.1, 152.4, 141.5, 136.9, 130.5, 128.5, 127.8, 127.0, 117.2, 97.0, 71.4, 60.4, 55.8, 52.1, 12.9.

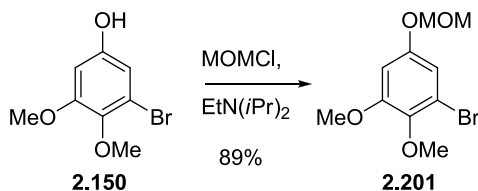


Methyl 6-hydroxy-3,4-dimethoxy-2-methylbenzoate (2.198) - To a solution of **2.197** (270 mg, 0.86 mmol) in anhydrous MeOH (4.5 mL) was added 5% Pd/C (20 mg). This solution was placed under one atmosphere of hydrogen and allowed to stir at room temperature for 16 h. The reaction was filtered through a plug of Celite 454 and silica gel (1:1). The filtrate was concentrated and the residue was purified by column chromatography with EtOAc/Hexane (1:4) to afford 80 mg (84%) of **2.198**. IR (neat)

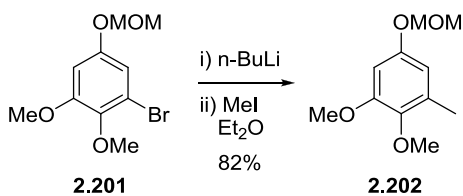
2955, 1648, 1606, 1443, 1325, 1243, 1216, 1199, 1161, 1063, 1040, 1008 cm^{-1} ; ^1H NMR (CDCl_3) δ 6.30 (s, 1H), 3.85 (s, 3H), 3.80 (s, 3H), 3.62 (s, 3H), 2.38 (s, 3H); ^{13}C NMR (CDCl_3) δ 171.9, 161.0, 158.0, 140.3, 133.6, 104.3, 98.1, 60.2, 55.4, 51.6, 14.4; LRMS calculated for $\text{C}_{10}\text{H}_{15}\text{O}_5$ ($\text{M}+\text{H}$) $^+$ 227.2 m/z . Measured 227.2 m/z



Dimethyl 2,2' -dihydroxy- 5,5', 6,6' -tetramethoxy- 4,4' -dimethylbiphenyl- 3,3'-dicarboxylate (2.199) – To a solution of copper(I) bromide (19 mg, 0.13mmol) in CH_3CN (1 mL) was added sparteine (25 μL , 0.013 mmol). After 15 min of sonication open to the air, 30 mg (0.13 mmol) of phenol **2.198** in CH_3CN (0.5 mL) was added. This solution was placed under one atmosphere of oxygen and allowed to stir at room temperature for 4 d. At this time the reaction mixture was diluted with 10% NaOH (2 mL) and extracted with CH_2Cl_2 (3 x 5 mL). The combined organic extracts were dried (MgSO_4) and concentrated to afford an oil. The residue was purified by column chromatography with EtOAc/Hexane (1:4) to afford 11 mg (23%) of **2.199**. IR (neat) 2928, 1655, 1957, 1444, 1399, 1320, 1240, 1211, 1165, 1097, 1059, 1009, 809; ^1H NMR (CDCl_3) δ 11.48 (s, 1H), 3.94 (s, 3H), 3.78 (s, 3H), 3.75 (s, 3H), 2.52 (s, 3H); ^{13}C NMR (CDCl_3) δ 172.1, 157.7, 157.0, 144.3, 134.5, 114.0, 108.1, 60.5, 52.0, 29.6, 14.8; LRMS calculated for $\text{C}_{22}\text{H}_{26}\text{NaO}_{10}$ ($\text{M}+\text{H}$) $^+$ m/z : 473.1, Measured 473.2 m/z

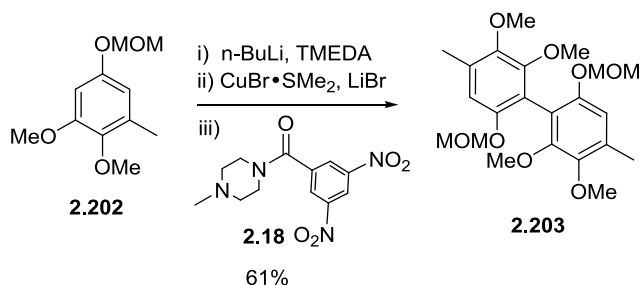


1-bromo-2,3-dimethoxy-5-(methoxymethoxy)benzene (2.201) - To a solution of **2.150** (0.12 g, 0.72 mmol) in 2.5 mL of CH₂Cl₂ was added diisopropyl ethyl amine (0.26 mL, 1.4 mmol) and MOMCl (0.081 mL, 1.1 mmol). After 16 h., the solution was diluted with CH₂Cl₂ (4 mL), and successively washed with H₂O (5 mL), 1N HCl (5 mL), NaHCO₃ (saturated, 5 mL), and Brine (5 mL). Each aqueous layer was washed with CH₂Cl₂ (10 mL). The combined organic layers were dried (MgSO₄) and concentrated. The residue was purified by column chromatography with EtOAc/Hexane (1:4) to afford 135 mg (89%) of **2.201**. ¹H NMR (CDCl₃) δ 6.72 (d, J = 2.4 Hz, 1H), 6.48 (d, J = 2.4 Hz, 1H), 5.00 (s, 2H), 3.71 (s, 3H), 3.67 (s, 3H), 3.34 (s, 3H); ¹³C NMR (CDCl₃) δ 151.6, 150.0, 144.2, 111.7, 106.7, 101.9, 95.2, 56.3, 55.8, 55.8.



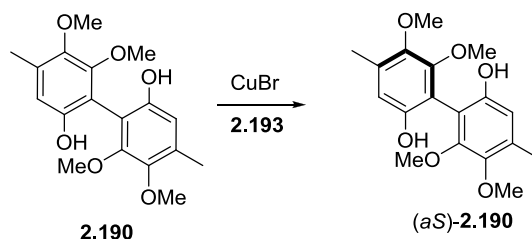
1,2-dimethoxy-5-(methoxymethoxy)-3-methylbenzene (2.202) - To a solution of **2.201** (2.2 g, 8.0 mmol) in diethyl ether (30 mL) at -78 °C was added 2.2 M *n*-BuLi (7.5 mL, 16 mmol). After 1 h at -78 °C, neat methyl iodide (1.5 mL, 24 mmol) was added. After 16 h, the reaction was diluted with H₂O (45 mL) and extracted with ethyl acetate (3 x 15 mL). The combined organic extracts were dried (MgSO₄) and concentrated to afford a red/orange oil. The residue was purified by column chromatography with EtOAc/Hexane

(1:4) to afford 1.1 g (65%) of **2.202** as a yellow oil. IR (neat) 1600, 1494, 1224, 1146, 1096, 1029, 754 cm^{-1} ; ^1H NMR (CDCl_3) δ 6.47 (d, $J = 2.8$ Hz, 1H), 6.45 (d, $J = 2.8$ Hz, 1H), 5.11 (s, 2H), 3.82 (s, 3H), 3.74 (s, 3H), 3.48 (s, 3H), 2.24 (s, 3H); ^{13}C NMR (CDCl_3) δ 151.6, 151.2, 146.3, 131.4, 117.3, 112.4, 95.3, 60.1, 60.0, 55.6, 16.2 LRMS calculated for $\text{C}_{11}\text{H}_{17}\text{O}_4$ ($\text{M}+\text{H}$) $^+$ m/z : 213.1, Measured 213.2 m/z

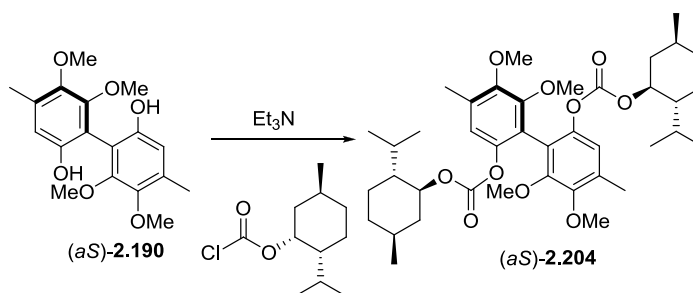


2,2',3,3'-tetramethoxy-6,6'-bis(methoxymethoxy)-4,4'-dimethylbiphenyl (2.203). –

To a solution of MOM **2.202** (0.50 g, 2.4 mmol) in diethyl ether (12.0 mL) at 0 °C was added 2.0 M $n\text{-BuLi}$ (1.7 mL, 3.4 mmol). After 5 h at 0 °C, a solution of $\text{CuBr}\cdot\text{SMe}_2$ (24 mg, 0.192 mmol) and LiBr (20 mg, 2.4 mmol) in THF (2 mL) was added via canula. After the mixture was stirred for 30 min, (3,5-dinitrophenyl)(4-methylpiperazin-1-yl)methanone (**2.18**) (1.0 g, 3.5 mmol) was added by a solid addition adaptor. After 1 h, the reaction mixture was passed over a silica plug and the filtrate concentrated *in vacuo*. The residue was purified by column chromatography with EtOAc/Hexane (1:4) to afford 200 mg (39%) of biaryl **2.203** as a white solid: mp 134-137 °C; IR (neat) 1475, 1393, 1235, 1150, 1091, 1068 cm^{-1} ; ^1H NMR (CDCl_3) δ 6.77 (s, 1H), 4.98 (s, 2H), 3.80 (s, 3H), 3.68 (s, 3H), 3.33 (s, 3H), 2.30 (s, 3H); ^{13}C NMR (CDCl_3) δ 151.6, 151.2, 146.3, 131.4, 117.3, 112.4, 65.2, 60.1, 60.0, 55.6, 16.2; HRMS calculated for $\text{C}_{22}\text{H}_{31}\text{O}_8$ ($\text{M}+\text{H}$) $^+$ m/z : 423.2019, Measured 423.2025 m/z .



Deracemization of Bis-Phenol (\pm)-2.190. A mixture of CuCl (15 mg, 0.14 mmol) and (-) sparteine (**2.193**) (50 μL , 0.27 mmol) in MeOH (2.0 mL) was sonicated open to the air for ca. 30 min. The resulting green solution was then transferred via cannula to a solution of (\pm)-**2.190** (24 mg, 0.072 mmol) in CH_2Cl_2 (5 mL). This solution was allowed to stir for 48 h at room temperature and a concentrated solution of HCl (2 mL) was added. After stirring for 15 min, the mixture was extracted with CH_2Cl_2 (3 x 10 mL). The combined organic extracts were then dried (MgSO_4) and concentrated to give 19 mg (77%) of (-)-**2.190** as determined by optical rotation: $[\alpha]_{589}^{22} -18$ (c 0.354, CHCl_3). (+)-**2.190** is arrived at in a like manner except the use of (+)-O'Brian's Diamine (**2.205**) in place of sparteine (**2.193**)

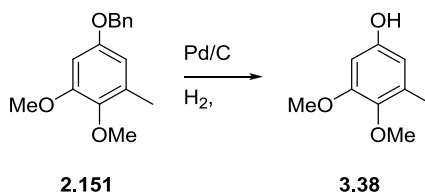


Bis ((1S,2R,5S) -2-isopropyl -5- methylcyclohexyl) 5,5', 6,6' -tetramethoxy- 4,4'-dimethylbiphenyl-2,2'-diyl dicarbonate - *Determination of Enantiomeric Excess.* To a solution of resolved (-)-**2.190** in THF (1.0 mL) was added Et_3N (0.10 mL, 0.72 mmol)

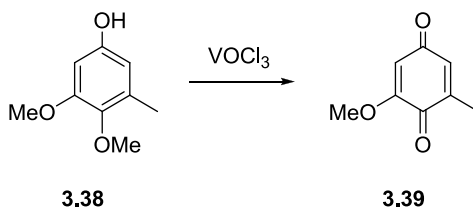
followed by (S)-menthyl chloroformate (0.15 mL, 0.72 mmol). After 2 h, the reaction mixture was diluted with H₂O (3 mL) and extracted with CH₂Cl₂ (3 x 5 mL). The combined organics were then dried (MgSO₄) and concentrated. The residue was purified by column chromatography with EtOAc/Hexane (1:10) to afford a mixture of diastereomeric bis-menthylcarbonates (*aS*)-**2.204** and (*aR*)-**2.204** (26 mg, 67%). The mixture was analyzed by ¹H NMR (400 MHz, CDCl₃) to determine the ratio of diastereomers (dr) by integration of the well differentiated doublets due to C5' methyl groups: ¹H NMR (CDCl₃) δ (*aS*)-**2.204** = 0.58 (d, *J* = 6.8 Hz, 1H), (*aR*)-**2.204** = 0.68 (d, *J* = 7.2 Hz, 1H) giving 93% de by ¹H NMR. The ratio of diastereomers (dr) when the use of (+)-O'Brian's Diamine (**2.205**) provides a 80% de by ¹H NMR.

(*aS*)-**2.204** - IR (neat) 2954, 2932, 2870, 1698, 1474, 1457, 1423, 1282, 1248, 1223, 1172, 993; ¹H NMR (CDCl₃) δ 6.82 (s, 1H), 4.36 (dt, *J* = 10.8, 4.4 Hz, 1H), 3.83 (s, 3H), 3.68 (s, 3H), 2.30 (s, 3H). 1.90 (d, *J* = 11.6, 1H), 1.66-1.59 (m, 3H), 1.57 (s, 2H), 1.28 (d, *J* = 11.6 Hz, 1H), 0.96 (s, 1H), 0.93 (s, 1H), 0.88 (d, *J* = 6.4 Hz, 3H), 0.77 (d, *J* = 7.2 Hz, 3H), 0.58 (d, *J* = 6.8 Hz, 3H); ¹³C NMR (CDCl₃) δ 153.0, 151.6, 149.1, 144.4, 132.3, 118.6, 118.5, 78.6, 60.4, 60.0, 46.6, 40.4, 33.9, 31.2, 25.8, 23.2, 22.0, 20.5, 16.1 ; HRMS calculated for C₄₀H₅₈NaO₁₀ (M+H)⁺ *m/z*: 721.3922, Measured 721.3952 *m/z*.

(*aR*)-**2.204** - IR (neat) 2954, 2932, 2870, 1698, 1474, 1457, 1423, 1282, 1248, 1223, 1172, 993; ¹H NMR (CDCl₃) δ 6.82 (s, 1H), 4.38 (dt, *J* = 10.8, 4.4 Hz, 1H), 3.83 (s, 3H), 3.70 (s, 3H), 2.30 (s, 3H). 1.84 (m, 1H), 1.64-1.60 (m, 3H), 1.56 (s, 2H), 1.28 (d, *J* = 11.6 Hz, 1H), 0.96 (s, 1H), 0.93 (s, 1H), 0.87 (d, *J* = 6.5 Hz, 3H), 0.83 (d, *J* = 7.0 Hz, 3H), 0.69 (d, *J* = 7.0 Hz, 3H); ¹³C NMR (CDCl₃) δ 152.9, 151.5, 149.0, 144.5, 118.8, 118.2, 78.7, 60.4, 60.1, 46.7, 40.4, 34.1, 31.2, 25.9, 23.2, 22.0, 20.7, 16.1, HRMS calculated for C₄₀H₅₈NaO₁₀ (M+H)⁺ *m/z*: 721.3922, Measured 721.3952 *m/z*.

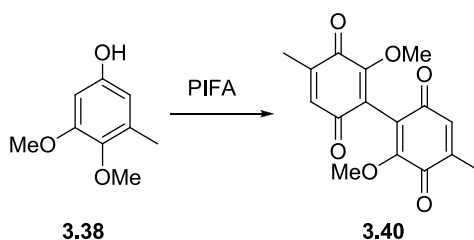


3,4-Dimethoxy-5-methylphenol (3.38) - To a solution of **2.151** (0.5 g, 1.9 mmol) in anhydrous MeOH (65 mL) was added 5% Pd/C (160 mg). This solution was placed under one atmosphere of hydrogen and allowed to stir at room temperature for 16 h. The reaction was filtered through a plug of Celite 454 and silica gel (1:1). The filtrate was concentrated and the residue was purified by column chromatography with EtOAc/Hexane (1:4) to afford 232 mg (72%) of **3.38**. $^1\text{H NMR}$ (CDCl_3) δ 6.32 (d, $J = 2.7$ Hz, 1H), 6.23 (d, $J = 2.7$ Hz, 1H), 4.85 (s, 1H), 3.82 (s, 3H), 3.76 (s, 3H), 2.24 (s, 3H). $^{13}\text{C NMR}$ (CDCl_3) δ 154.2, 150.7, 141.6, 132.6, 110.7, 97.7, 60.5, 55.7, 12.8. LRMS calculated for $\text{C}_9\text{H}_{13}\text{O}_3$ ($\text{M}+\text{H}$) $^+$ m/z : 169.1, Measured 169.1 m/z



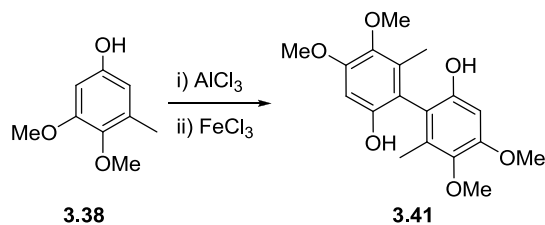
2-methoxy-6-methylcyclohexa-2,5-diene-1,4-dione (3.39). A solution of **3.38** (40 mg, 0.24 mmol) in CH_2Cl_2 (5.0 mL) was cooled to -78 $^\circ\text{C}$. At this temperature VOCl_3 (30 μL , 0.25 mmol) was added. After 1 h at -78 $^\circ\text{C}$, the solution was diluted with 5% aq NH_4OH (5 ml), then extracted with CH_2Cl_2 (3 x 5 ml). The combined organics were then dried (MgSO_4) and concentrated. The residue was purified by column chromatography with EtOAc/Hexane (1:2) to afford 16 mg (44%) of benzoquinone **3.39** and 8 mg (11%) of bis-

quinone **3.40**. $^1\text{H NMR}$ (CDCl_3) δ 6.53 (d, $J = 2.4$ Hz, 1H), 5.88 (d, $J = 2.4$ Hz, 1H), 3.81 (s, 3H), 2.07 (d, $J = 1.6$ Hz, 3H). $^{13}\text{C NMR}$ (CDCl_3) δ 187.4, 182.4, 158.8, 143.6, 133.8, 107.3, 56.3, 15.5. LRMS calculated for $\text{C}_8\text{H}_8\text{O}_3$ ($\text{M}+\text{H}$) $^+$ m/z : 153.1, Measured 153.1 m/z

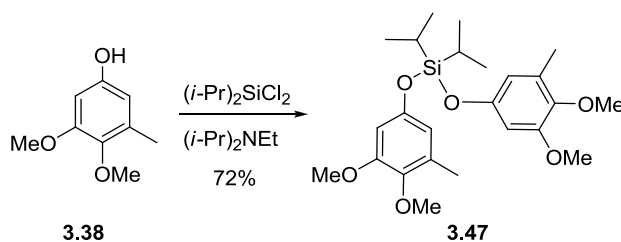


6,6'-dimethoxy-4,4'-dimethyl-1,1'-bi(cyclohexa-3,6-diene)-2,2',5,5'-tetraone (3.40).

To a solution of **3.38** (74 mg, 0.45 mmol) in CH_2Cl_2 (7.0 mL) cooled to -20 °C was added a solution of PIFA (227 mg, 0.54 mmol) and $\text{BF}_3 \cdot \text{OEt}_2$ (130 μL , 1.1 mmol) in CH_2Cl_2 (4.0 mL). After 30 min at -20 °C, the reaction mixture was concentrated *in vacuo*. The residue was purified by flash chromatography with EtOAc/Hexane (1:2) to afford 42 mg, (62%) of bis-quinone **3.40** and 6 mg (9%) of benzoquinone **3.39**. $^1\text{H NMR}$ (CDCl_3) δ 5.96 (s, 1H), 3.84 (s, 3H), 1.89 (s, 3H). $^{13}\text{C NMR}$ (CDCl_3) δ 184.7, 181.4, 158.7, 141.4, 137.9, 107.3, 56.3, 13.4. LRMS calculated for $\text{C}_{16}\text{H}_{15}\text{O}_6$ ($\text{M}+\text{H}$) $^+$ m/z : 303.1, Measured 303.0 m/z

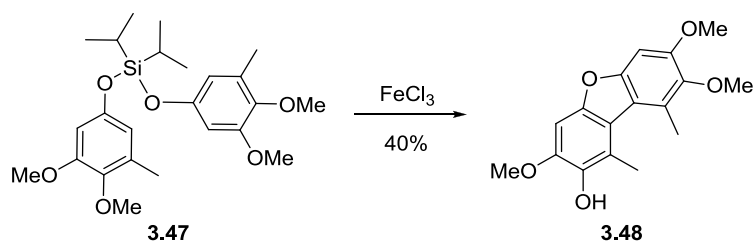


4,4',5,5'-tetramethoxy-6,6'-dimethylbiphenyl-2,2'-diol (3.41) - To a solution of **3.38** (31 mg, 0.18 mmol) in CH_3NO_2 (1.0 mL) was added AlCl_3 (28 mg, 0.18 mmol). After 1 h, a solution of FeCl_3 (54 mg, 0.36 mmol) in CH_3NO_2 (2.0 mL) was added. This was allowed to stir for 3 h when 1N HCl (5 mL) was added and extracted with CH_2Cl_2 (3 x 10 mL). The combined organic extracts were dried (MgSO_4) and concentrated. The residue was purified by column chromatography with EtOAc/Hexane (1:2) to afford 18 mg (60%) of **3.41**. ^1H NMR (CDCl_3) δ 6.52 (s, 1H), 4.64 (s, 1H), 3.88 (s, 3H), 3.77 (s, 3H), 1.92 (s, 3H). ^{13}C NMR (CDCl_3) δ 154.2, 150.7, 141.6, 132.6, 11.8, 97.7, 60.5, 55.7, 12.8. LRMS calculated for $\text{C}_{18}\text{H}_{22}\text{O}_6$ ($\text{M}+\text{H}$) $^+$ m/z : 335.1, Measured 335.1 m/z

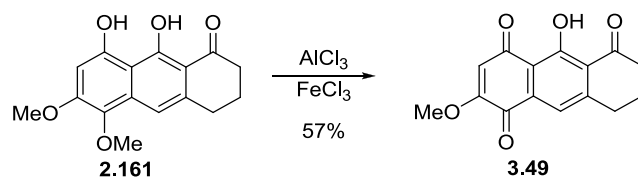


bis(3,4-dimethoxy-5-methylphenoxy)diisopropylsilane (3.47) – To a solution of phenol **3.38** in CH_2Cl_2 (8.0 mL) was added Et_3N (0.35 mL, 0.26 mmol) and a few crystals of DMAP. At -78°C , diisopropyl silyl dichloride (0.1 mL, 0.54 mmol) was added. The reaction mixture was allowed to warm to room temperature and after 3 h, diluted with sat NH_4Cl (10 mL) and extracted with CH_2Cl_2 (3 x 10 mL). The combined organic extracts were dried (MgSO_4) and concentrated. The residue was purified by column

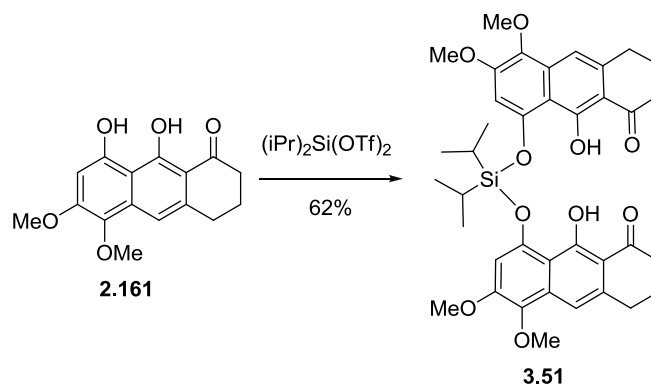
chromatography with EtOAc/Hexane (1:4) to afford 204 mg (76%) of **3.47**. IR (neat) 2948, 2869, 1594, 1493, 1464, 1421, 1341, 1224, 1192, 1157, 1097, 1029, 859, 827, 758; ^1H NMR (CDCl_3) δ 6.34 (s, 2H), 3.72 (s, 6H), 3.71 (s, 6H), 2.19 (s, 6H), 1.12 (s, 6H), 1.10 (s, 6H) 1.07 (s, 2H); ^{13}C NMR (CDCl_3) δ 152.9, 150.5, 141.9, 132.0, 113.0, 102.3, 60.1, 55.5, 17.1, 15.8, 12.5. LRMS calculated for $\text{C}_{24}\text{H}_{37}\text{O}_6\text{Si}$ ($\text{M}+\text{H}$) $^+$ m/z : 449.2 Measured 449.3 m/z



3,7,8-trimethoxy-1,9-dimethyldibenzo[b,d]furan-2-ol (3.48) - To a solution of **3.47** (48 mg, 0.11 mmol) in CH_3NO_2 (2.0 mL) was added FeCl_3 (63 mg, 0.44 mmol) in CH_3NO_2 (2.0 mL) was added. After 3 h, 1N HCl (5 mL) was added and extracted with CH_2Cl_2 (3 x 10 mL). The combined organic extracts were dried (MgSO_4) and concentrated. The residue was purified by column chromatography with EtOAc/Hexane (1:4) to afford 18 mg (53%) of **3.48**. ^1H NMR (CDCl_3) δ 6.93 (s, 1H), 6.92 (s, 1H), 5.64 (s, 1H), 3.97 (s, 3H), 3.93 (s, 3H), 3.81 (s, 3H), 2.82 (s, 3H), 2.79 (s, 3H); ^{13}C NMR (CDCl_3) δ 152.9, 151.6, 150.2, 145.2, 143.5, 139.9, 124.8, 117.7, 117.5, 115.9, 93.2, 92.0, 60.7, 56.2, 55.9, 31.5, 16.6, 16.0 LRMS calculated for $\text{C}_{17}\text{H}_{19}\text{O}_5$ ($\text{M}+\text{H}$) $^+$ m/z : 303.1 Measured 303.1 m/z

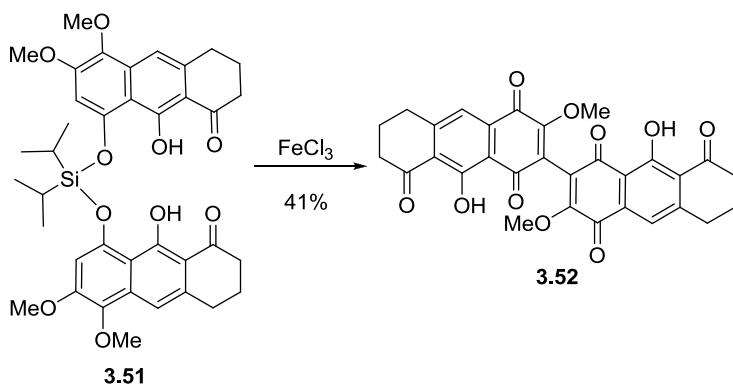


10-hydroxy-2-methoxy-7,8-dihydroanthracene-1,4,5(6H)-trione (3.49) - To a solution of **2.161** (24 mg, 0.08 mmol) in CH_3NO_2 (0.5 mL) was added AlCl_3 (11 mg, 0.08 mmol). After 1 h, a solution of FeCl_3 (23 mg, 0.17 mmol) in CH_3NO_2 (1.0 mL) was added. This was allowed to stir for 3 h when 1N HCl (5 mL) was added and extracted with CH_2Cl_2 (3 x 5 mL). The combined organic extracts were dried (MgSO_4) and concentrated. The residue was purified by column chromatography with EtOAc/Hexane (1:2) to afford 13 mg (57%) of **3.49**. ^1H NMR (CDCl_3) δ . 13.63 (s, 1H), 7.45 (s, 1H), 6.06 (s, 1H), 3.81, (s, 3H), 2.97 (t, J = 4.5 Hz, 2H), 2.67 (t, J = 4.8 Hz, 2H), 2.07 (m, 2H). ^{13}C NMR (CDCl_3) δ . 182.1, 179.7, 162.9, 159.4, 152.7, 118.1, 111.6, 56.5, 39.7, 30.91, 29.7, 22.2. LRMS calculated for $\text{C}_{18}\text{H}_{22}\text{O}_6$ ($\text{M}+\text{H}$) $^+$ m/z : 273.2, Measured 273.1 m/z .

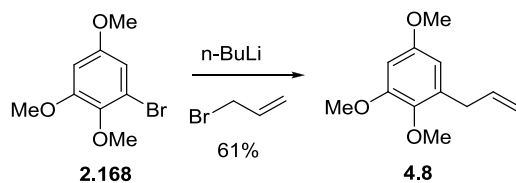


8,8'-(diisopropylsilanediyl) bis(oxy) bis (9-hydroxy-5,6-dimethoxy-3,4-dihydroanthracen-1(2H)-one) (3.51) - To a solution of phenol **2.161** (30 mg, 0.1 mmol) in CHCl_3 (0.7 mL) at 0°C was added 2,6 lutidine (24 μL , 0.21 mmol), and diisopropyl silyl ditriflate (15 μL , 0.052 mmol). The reaction mixture was allowed to warm to room

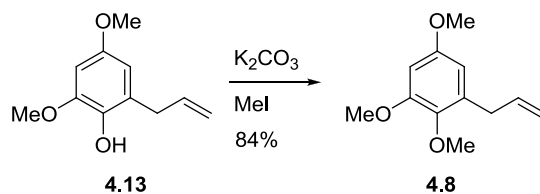
temperature and after 3 h, diluted with sat NH₄Cl (5 mL) and extracted with CH₂Cl₂ (3 x 5 mL). The combined organic extracts were dried (MgSO₄) and concentrated. The residue was purified by column chromatography with EtOAc/Hexane (1:2) to afford 24 mg (62%) of **3.51**. ¹H NMR (CDCl₃) δ. 15.23 (s, 1H), 7.22 (s, 1H), 6.49 (s, 1H), 3.92 (s, 3H), 3.91 (s, 3H), 2.90 (t, J = 4.5 Hz, 2H), 2.65 (t, J = 4.9 Hz, 2H), 2.02 (m, 2H), 1.17 (m, 1H), 0.98 (d, J = 4.8 Hz, 6H) LRMS calculated for C₁₈H₂₂O₆ (M+H)⁺ *m/z*:689.2, Measured 689.2 *m/z*.



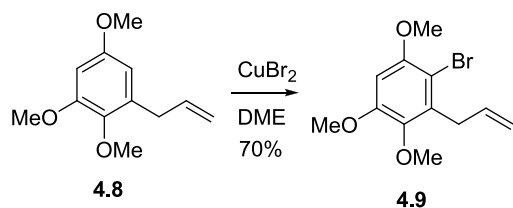
9,9'- dihydroxy- 3,3'- dimethoxy- 6,6', 7,7'- tetrahydro- 2,2'- bianthracene- 1,1',4,4',8,8'(5H,5'H)-hexaone (3.52) - To a solution of **3.51** (20 mg, 0.029 mmol) in CH₃NO₂ (3.0 mL) was added FeCl₃ (63 mg, 0.44 mmol). After 5 h, 1N HCl (5 mL) was added and extracted with CH₂Cl₂ (3 x 10 mL). The combined organic extracts were dried (MgSO₄) and concentrated. The residue was purified by column chromatography with EtOAc/Hexane (1:4) to afford 6 mg (41%) of **3.52**. ¹H NMR (CDCl₃) δ. 13.73 (s, 1H), 7.55 (s, 1H), 3.915 (s, 3H), 3.08 (t, J = 4.5 Hz, 2H), 2.77 (t, J = 4.8 Hz, 2H), 2.17 (m, 2H). ¹³C NMR (CDCl₃) δ. 199.1, 182.4, 179.7, 162.9, 159.4, 152.7, 127.5, 124.9, 118.1, 111.6, 56.5, 39.7, 29.7, 22.2. LRMS calculated for C₁₈H₂₂O₆ (M+H)⁺ *m/z*:543.2, Measured 543.1 *m/z*.



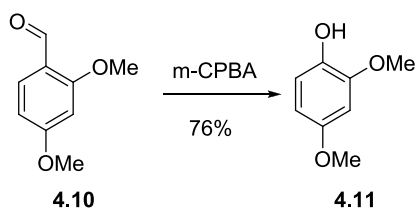
1-allyl-2,3,5-trimethoxybenzene (4.8) - To a solution of **2.168** (1.0 g, 4.0 mmol) in diethyl ether (40 mL) at -78 °C was added 2.0 M *n*-BuLi (6.0 mL, 12 mmol). After 1 h at -78 °C, allyl bromide (3.5 mL, 40 mmol) was added. After 7 h, the reaction was diluted with H₂O (45 mL) and extracted with ethyl acetate (3 x 15 mL). The combined organic extracts were dried (MgSO₄) and concentrated to afford a red/orange oil. The residue was purified by column chromatography with EtOAc/Hexane (1:4) to afford 520 mg (61%) of **4.8**. ¹H NMR (CDCl₃) δ 6.38 (d, J = 2.8 Hz, 1H), 6.29 (d, J = 2.8 Hz, 1H), 6.00-5.92 (m, 1H), 5.11-5.05 (m, 2H), 3.84 (s, 3H), 3.77 (s, 3H), 3.75 (s, 3H), 3.40 (d, J = 6.8 Hz, 1H). ¹³C NMR (CDCl₃) δ 155.9, 153.3, 141.0, 137.0, 134.0, 115.6, 105.0, 98.2, 60.8, 55.6, 55.4, 34.1



Method 2 - To a solution of **4.13** (0.94 g, 4.8 mmol) in acetone (100 mL) was added K₂CO₃ (6.8 g, 48.4 mmol) and methyl iodide (3.0 mL, 48.4 mmol). This solution was then allowed to reflux overnight. At this time the solution was cooled to R.T. The reaction mixture was filtered over a fritted filter and the filtrate concentrated *in vacuo*. The residue was purified by column chromatography with EtOAc/Hexane (1:4) to afford 0.91 g (90%) of **4.8**.

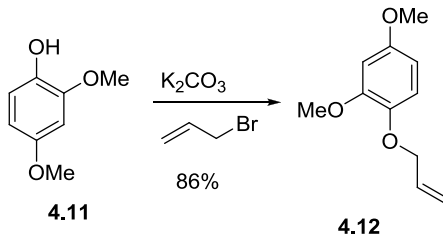


3-allyl-2-bromo-1,4,5-trimethoxybenzene (4.9) - To a solution of **4.8** (0.91 g, 4.4 mmol) in 1,2 - dimethoxyethane (15 mL) was added copper(II) bromide (1.6 g, 6.6 mmol). This was then allowed to stir at R.T. overnight. The mixture was passed over a silica plug and the filtrate concentrated *in vacuo*. The residue was purified by column chromatography with EtOAc/Hexane (1:4) to afford 0.82 g (70%) of **4.9**; ^1H NMR (CDCl_3) δ 6.47 (s, 1H), 6.00 – 5.91 (m, 1H), 5.05 (t, $J = 1.2$ Hz, 1H), 5.02 (dd, $J = 4.2, 1.6$ Hz, 1H), 3.88 (s, 3H), 3.87 (s, 3H), 3.77 (s, 3H), 3.62 (dt, $J = 6.0, 1.2$ Hz, 2H); ^{13}C NMR (CDCl_3) δ 152.6, 152.4, 141.8, 135.4, 134.5, 115.7, 104.7, 96.4, 61.1, 56.7, 56.0, 34.3. select HMBC 6.47 (152.6, 141.8, 104.7)

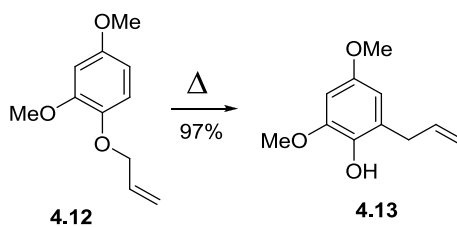


2,4-dimethoxyphenol (4.11) - To a solution of **4.10** (10 g, 60mmol) in CH_2Cl_2 (200 mL) was added *m*-CPBA (6.320 g, 120 mmol). This solution was allowed to reflux for 16 h. At this time the solution was concentrated and re-dissolved in EtOAc (100 mL). The organic layer was washed with sat NaHCO_3 (150 mL) followed by brine (150 mL), and concentrated to afford a yellow oil. To this residue was added aq KOH and MeOH (2:1)

(200 mL). After 1 h the solution was acidified with 1 N HCl and extracted with EtOAc (3 x 100 mL). The combined organic extracts were dried (MgSO₄), and concentrated to afford a yellow oil. The residue was purified by column chromatography on silica gel with EtOAc/Hexane (1:4) to afford 7.13 g (76%) of **4.11** as a solid: ¹H NMR (CDCl₃) δ 6.82 (d, *J* = 8.6 Hz, 1H), 6.49 (d, *J* = 2.6 Hz, 1H), 6.39 (dd, *J* = 8.6, 2.6 Hz, 1H), 5.22 (s, 1H), 3.87 (s, 3H), 3.76 (s, 3H) ¹³C NMR (CDCl₃) δ 153.5, 147.0, 139.8, 114.0, 104.2, 99.4, 55.9, 55.8



1-(allyloxy)-2,4-dimethoxybenzene (4.12). - To a solution of **4.11** (7.1 g, 45 mmol) in acetone (0.24 L) was added K₂CO₃ (16 g, 120 mmol) and allyl bromine (10 mL, 120 mmol). This was then allowed to reflux for 16 h. At this time the solution was filtered over a fritted filter and concentrated. The residue was purified by column chromatography on silica gel with EtOAc/Hexane (1:4) to afford 7.7 g (86%) of **4.12** as a solid: ¹H NMR (CDCl₃) δ 6.79 (d, *J* = 8.6 Hz, 1H), 6.50 (d, *J* = 2.8 Hz, 1H), 6.35 (dd, *J* = 8.6, 2.8 Hz, 1H), 6.11-6.01 (m, 1H), 5.36 (dd, *J* = 17.2, 1.6 Hz, 1H), 5.24 (dd, *J* = 10.5, 1.2 Hz, 1H), 4.52 (d, *J* = 5.5 Hz, 1H), 3.83 (s, 3H), 3.74 (s, 3H) ¹³C NMR (CDCl₃) δ 154.5, 150.4, 142.0, 133.6, 117.4, 114.8, 102.8, 100.3, 70.7, 55.6, 55.3.



2-allyl-4,6-dimethoxyphenol (4.13). To a solution of **4.12** (1.0 g, 5.14 mmol) was placed in a sealed tube and heated at 220°C for 3 days. The residue the provided 0.94 g (94%) of allyl phenol; $^1\text{H NMR}$ (CDCl_3) δ 6.38 (d, $J = 2.8$ Hz, 1H), 6.29 (d, $J = 2.8$ Hz, 1H), 6.05-5.95 (m, 1H), 5.31 (s, 1H), 5.12-5.05 (m, 2H), 3.86 (s, 3H). 3.76 (s, 3H), 3.40 (d, $J = 6.4$ Hz, 1H) $^{13}\text{C NMR}$ (CDCl_3) δ 152.8, 146.8, 137.4, 136.5, 125.7, 115.5, 105.5, 97.2, 55.9, 55.6, 34.0

REFERENCES

1. Evans, D. A.; Dinsmore, C. J.; Watson, P. S.; Wood, M. R.; Richardson, T. I.; Trotter, B. W.; Katz, J. L., Nonconventional stereochemical issues in the design of the synthesis of the vancomycin antibiotics: Challenges imposed by axial and nonplanar chiral elements in the heptapeptide aglycons. *Angewandte Chemie-International Edition* **1998**, *37*, 2704-2708.
2. Christie, G. H.; Kenner, J., LXXI.-The molecular configurations of polynuclear aromatic compounds. Part I. The resolution of γ -6 : 6'-dinitro- and 4 : 6 : 4' : 6'-tetranitro-diphenic acids into optically active components. *Journal of the Chemical Society, Transactions* **1922**, *121*, 614-620.
3. Oki, M., Topics in Stereochemistry. **1983**, *14*, 1-81.
4. Eliel, E.; Wilen, S., *Stereochemistry of organic compounds*. Wiley & Sons: New York, 1994.
5. Bringmann, G.; Mortimer, A. J.; Keller, P. A.; Gresser, M. J.; Garner, J.; Breuning, M., Atroposelective Synthesis of Axial Chiral Biaryl Compound. *Angewandte Chemie-International Edition* **2005**, *44*, 5384-5427.
6. Buchanan, M. S.; Gill, M.; Gimenez, A.; Palfreyman, A. R.; Phonh-Axa, S.; Raudies, E.; Yu, J., Pigments of fungi. LII - Anisochiral flavomannin 6,6',8-tri-O-methyl ether from an Australian Dermocybe toadstool. *Australian Journal of Chemistry* **1999**, *52*, 749-753.
7. Horak, E., New Species of Dermocybe Agaricales from New Zealand. *Sydowia* **1987**, *40*, 81-112.
8. Muller, M.; Lamottke, K.; Steglich, W.; Busemann, S.; Reichert, M.; Bringmann, G.; Spiteller, P., Biosynthesis and stereochemistry of phlegmacin-type fungal pigments. *European Journal of Organic Chemistry* **2004**, 4850-4855.
9. Takahashi, S.; Kitanaka, S.; Takido, M.; Sankawa, U.; Shibata, S., Studies of Constituents of Purgative Crude Drugs .10. Phlegmacins and Anhydrophlegmacinquinones - Dimeric Hydroanthracenes from Seedlings of Cassia-Torosa. *Phytochemistry* **1977**, *16*, 999-1002.
10. Gill, M.; Smrdel, A. F., Pigments of Fungi .16. Synthesis of Methyl (R)-(+)-Tetrahydro-2-Methyl-5-Oxo-2-Furanacetate and Its (S)-(-)-Antipode, Chiroptical References for Determination of the Absolute Stereochemistry of Fungal Pre-Anthraquinones. *Tetrahedron-Asymmetry* **1990**, *1*, 453-464.
11. Weisleder, D.; Lillehoj, E. B., Structure of Viriditoxin, a Toxic Metabolite of Aspergillus-Viridi-Nutans. *Tetrahedron Letters* **1971**, 4705-&.

12. Suzuki, K.; Nozawa, K.; Nakajima, S.; Kawai, K., Structure Revision of Mycotoxin, Viriditoxin, and Its Derivatives. *Chemical & Pharmaceutical Bulletin* **1990**, 38, 3180-3181.
13. Wang, J.; Galgoci, A.; Kodali, S.; Herath, K. B.; Jayasuriya, H.; Dorso, K.; Vicente, F.; Gonzalez, A.; Cully, D.; Bramhill, D.; Singh, S., Discovery of a small molecule that inhibits cell division by blocking FtsZ, a novel therapeutic target of antibiotics. *Journal of Biological Chemistry* **2003**, 278, 44424-44428.
14. DD Ridley, E. R. a. W. T., Chemical studies of the Proteaceae. IV. The structures of the major phenols of *Grevillea striata*; a group of novel cyclophanes *Australian Journal of Chemistry* **1970**, 23, 147-163.
15. Furstner, A.; Stelzer, F.; Rumbo, A.; Krause, H., Total synthesis of the turrianes and evaluation of their DNA-cleaving properties. *Chemistry-a European Journal* **2002**, 8, 1856-1871.
16. Fukuyama, Y.; Asakawa, Y., Novel Neurotrophic Isocuparane-Type Sesquiterpene Dimers, Mastigophorenes-a, Mastigophorene-B, Mastigophorene-C and Mastigophorene-D, Isolated from the Liverwort *Mastigophora-Dicladus*. *Journal of the Chemical Society-Perkin Transactions 1* **1991**, 2737-2741.
17. Bringmann, G.; Pabst, T.; Rycroft, D. S.; Connolly, J. D., Novel concepts in directed biaryl synthesis - Part 76 - First synthesis of mastigophorenes A and B, by biomimetic oxidative coupling of herbertenediol. *Tetrahedron Letters* **1999**, 40, 483-486.
18. Bringmann, G.; Pabst, T.; Henschel, P.; Kraus, J.; Peters, K.; Peters, E. M.; Rycroft, D. S.; Connolly, J. D., Nondynamic and dynamic kinetic resolution of lactones with stereogenic centers and axes: Stereoselective total synthesis of herbertenediol and mastigophorenes A and B. *Journal of the American Chemical Society* **2000**, 122, 9127-9133.
19. Degnan, A. P.; Meyers, A. I., Total syntheses of (-)-herbertenediol, (-)-mastigophorene A, and (-)-mastigophorene B. Combined utility of chiral bicyclic lactams and chiral aryl oxazolines. *Journal of the American Chemical Society* **1999**, 121, 2762-2769.
20. Moorlag, H.; Meyers, A. I., Oxazoline-mediated biaryl coupling reactions. Stereocontrolled synthesis of 2,2',6,6'-tetrasubstituted biphenyls. *Tetrahedron Letters* **1993**, 34, 6989-6992.
21. Marchlewski, L., Gossypol, ein Bestandtheil der Baumwollsamens. *Journal für Praktische Chemie* **1899**, 60, 84-90.
22. Withers, W. A.; Carruth, F. E., Gossypol—A Toxic Substance in Cottonseed. A Preliminary Note. *Science* **1915**, 41, 324.
23. Adams, R.; Kirkpatrick, E. C., Structure of Gossypol. XI. Absorption Spectra of Gossypol, its derivatives and of Certain Dinaphthalene Compounds. *Journal of the American Chemical Society* **1938**, 60, 2180.

24. Elsimar Metzker, C., Gossypol: a contraceptive for men. *Contraception* **2002**, 65, 259-263.
25. Radloff, R. J.; Deck, L. M.; Royer, R. E.; Vanderjagt, D. L., Antiviral Activities of Gossypol and Its Derivatives against Herpes-Simplex Virus Type-II. *Pharmacological Research Communications* **1986**, 18, 1063-1073.
26. Edwards, J. D.; Cashaw, J. L., Studies in the Naphthalene Series. III. Synthesis of Apogossypol Hexamethyl Ether¹. *Journal of the American Chemical Society* **1957**, 79, 2283-2285.
27. Edwards, J. D., TOTAL SYNTHESIS OF GOSSYPOL. *Journal of the American Chemical Society* **1958**, 80, 3798-3799.
28. Meyers, A. I.; Willemsen, J. J., The synthesis of (S)-(+)-gossypol via an asymmetric Ullmann coupling. *Chemical Communications* **1997**, 1573-1574.
29. Meyers, A. I.; Willemsen, J. J., An oxazoline based approach to (S)-Gossypol. *Tetrahedron* **1998**, 54, 10493-10511.
30. Nelson, R. A.; Pope, J. A.; Luedemann, G. M.; McDaniel, L. E.; Schaffner, C. P., Crisamicin-a, a New Antibiotic from *Micromonospora* .1. Taxonomy of the Producing Strain, Fermentation, Isolation, Physicochemical Characterization and Antimicrobial Properties. *Journal of Antibiotics* **1986**, 39, 335-344.
31. Ling, D.; Shield, L. S.; Rinehart, K. L., Isolation and Structure Determination of Crisamicin-a, a New Antibiotic from *Micromonospora-Purpureochromogenes* Subsp *Halotolerans*. *Journal of Antibiotics* **1986**, 39, 345-353.
32. Li, Z. T.; Gao, Y. X.; Tang, Y. F.; Dai, M. J.; Wang, G. X.; Wang, Z. G.; Yang, Z., Total synthesis of crisamicin A. *Organic Letters* **2008**, 10, 3017-3020.
33. Barba, B.; Diaz, J. G.; Herz, W., Anthraquinones and Other Constituents of 2 Senn a Species. *Phytochemistry* **1992**, 31, 4374-4375.
34. Gluchoff, K.; Dangycay.Mp; Arpin, N.; Pourrat, H.; Regerat, F.; Topper, E.; Steglich, W.; Deruaz, D.; Lebreton, P., Chemotaxonomic Research on Fungi - 7,7'-Biphysicon, Bianthraquinone Obtained from *Tricholoma-Equestre* L Per Fr (Basidiomycetes, Agaricales). *Comptes Rendus Hebdomadaires Des Seances De L Academie Des Sciences Serie D* **1972**, 274, 1739-&.
35. Fujitake, N.; Suzuki, T.; Fukumoto, M.; Oji, Y., Predomination of dimers over naturally occurring anthraquinones in soil. *Journal of Natural Products* **1998**, 61, 189-192.
36. Hauser, F. M.; Gauuan, P. J. F., Total synthesis of (+/-)-biphyscion. *Organic Letters* **1999**, 1, 671-672.
37. Buchanan, M. S.; Gill, M.; Yu, J., Pigments of fungi .43. Cardinalins-1-6, novel pyranonaphthoquinones from the fungus *Dermocybe cardinalis* Horak. *Journal of the Chemical Society-Perkin Transactions 1* **1997**, 919-925.

38. Brimble, M. A.; Gibson, J. S.; Sejberg, J. J. P.; Sperry, J., A facile enantioselective synthesis of the dimeric pyranonaphthoquinone core of the cardinalins. *Synlett* **2008**, 867-870.
39. Sperry, J.; Gibson, J. S.; Sejberg, J. J. P.; Brimble, M. A., Enantioselective synthesis of the dimeric pyranonaphthoquinone core of the cardinalins using a late-stage homocoupling strategy. *Organic & Biomolecular Chemistry* **2008**, 6, 4261-4270.
40. Govender, S.; Mmutlane, E. M.; van Otterlo, W. A. L.; de Koning, C. B., Bidirectional racemic synthesis of the biologically active quinone cardinalin 3. *Organic & Biomolecular Chemistry* **2007**, 5, 2433-2440.
41. Toki, S.; Ando, K.; Kawamoto, I.; Sano, H.; Yoshida, M.; Matsuda, Y., Es-242-2, Es-242-3, Es-242-4, Es-242-5, Es-242-6, Es-242-7, and Es-242-8, Novel Bioanthracenes Produced by *Verticillium* Sp, Which Act on the N-Methyl-D-Aspartate Receptor. *Journal of Antibiotics* **1992**, 45, 1047-1054.
42. Jaturapat, A.; Isaka, M.; Hywel-Jones, N. L.; Lertwerawat, Y.; Kamchonwongpaisan, S.; Kirtikara, K.; Tanticharoen, M.; Thebtaranonth, Y., Bioanthracenes from the insect pathogenic fungus *Cordyceps pseudomilitaris* BCC 1620 - I. - Taxonomy, fermentation, isolation and antimalarial activity. *Journal of Antibiotics* **2001**, 54, 29-35.
43. Tatsuta, K.; Yamazaki, T.; Mase, T.; Yoshimoto, T., The first total synthesis of a bioanthracene (-)-ES-242-4, an N-methyl-D-aspartate receptor antagonist. *Tetrahedron Letters* **1998**, 39, 1771-1772.
44. Tatsuta, K.; Nagai, T.; Mase, T.; Tamura, T.; Nakamura, H., Absolute and atropisomeric structure of ES-242s, N-methyl-D-aspartate receptor antagonists. *Journal of Antibiotics* **1999**, 52, 433-436.
45. Isaka, M.; Kongsaree, P.; Thebtaranonth, Y., Bioanthracenes from the insect pathogenic fungus *Cordyceps pseudomilitaris* BCC 1620 - II. - Structure elucidation. *Journal of Antibiotics* **2001**, 54, 36-43.
46. Gorstallman, C. P.; Steyn, P. S.; Rabie, C. J., Structural Elucidation of the Nigerones, 4 New Naphthopyrones from Cultures of *Aspergillus-Niger*. *Journal of the Chemical Society-Perkin Transactions 1* **1980**, 2474-2479.
47. DiVirgilio, E. S.; Dugan, E. C.; Mulrooney, C. A.; Kozlowski, M. C., Asymmetric total synthesis of nigerone. *Organic Letters* **2007**, 9, 385-388.
48. Kozlowski, M. C.; Dugan, E. C.; DiVirgilio, E. S.; Maksimenka, K.; Bringmann, G., Asymmetric total synthesis of nigerone and ent-nigerone: Enantioselective oxidative biaryl coupling of highly hindered Naphthols. *Advanced Synthesis & Catalysis* **2007**, 349, 583-594.
49. Kobayashi, E.; Ando, K.; Nakano, H.; Iida, T.; Ohno, H.; Morimoto, M.; Tamaoki, T., Calphostins (Ucn-1028), Novel and Specific Inhibitors of Protein Kinase-C .1.

- Fermentation, Isolation, Physicochemical Properties and Biological-Activities. *Journal of Antibiotics* **1989**, 42, 1470-1474.
50. Iida, T.; Kobayashi, E.; Yoshida, M.; Sano, H., Calphostins, Novel and Specific Inhibitors of Protein Kinase-C .2. Chemical Structures. *Journal of Antibiotics* **1989**, 42, 1475-1481.
 51. Broka, C. A., Total Syntheses of Phleichrome, Calphostin-a, and Calphostin-D - Unusual Stereoselective and Stereospecific Reactions in the Synthesis of Perylenequinones. *Tetrahedron Letters* **1991**, 32, 859-862.
 52. Hauser, F. M.; Sengupta, D.; Corlett, S. A., Optically-Active Total Synthesis of Calphostin-D. *Journal of Organic Chemistry* **1994**, 59, 1967-1969.
 53. Manfredi, K. P.; Blunt, J. W.; Cardellina, J. H.; McMahon, J. B.; Pannell, L. L.; Cragg, G. M.; Boyd, M. R., Novel alkaloids from the tropical plant *Ancistrocladus abbreviatus* inhibit cell killing by HIV-1 and HIV-2. *Journal of Medicinal Chemistry* **1991**, 34, 3402-3405.
 54. Boyd, M. R.; Hallock, Y. F.; Manfredi, K. P.; Blunt, J. W.; McMahon, J. B.; Buckheit, R. W.; Bringmann, G.; Schaffer, M.; Cragg, G. M.; Thomas, D. W.; Jato, J. G.; Cardellina, J. H., Anti-Hiv Michellamines from *Ancistrocladus-Korupensis*. *Journal of Medicinal Chemistry* **1994**, 37, 1740-1745.
 55. Huang, S. L.; Petersen, T. B.; Lipshutz, B. H., Total Synthesis of (+)-Korupensamine B via an Atropselective Intermolecular Biaryl Coupling. *Journal of the American Chemical Society* **2010**, 132, 14021-14023.
 56. Shibata, S.; Ogihara, Y.; Kobayash.N; Seo, S.; Kitagawa, I., Revises Structures of Luteoskyrin Rubroskyrin and Rugulosin. *Tetrahedron Letters* **1968**, 3179-&.
 57. Kobayash.N; Iitaka, Y.; Shibata, S., X-Ray Structure Determination of (+)-Dibromodehydrotetrahydrorugulosin, a Heavy Atom Derivative of (+)-Rugulosin. *Acta Crystallographica Section B-Structural Crystallography and Crystal Chemistry* **1970**, B 26, 188-&.
 58. Nicolaou, K. C.; Lim, Y. H.; Papageorgiou, C. D.; Piper, J. L., Total synthesis of (+)-rugulosin and (+)-2,2 '-epi-cytoskyrin A through cascade reactions. *Angewandte Chemie-International Edition* **2005**, 44, 7917-7921.
 59. Nicolaou, K. C.; Lim, Y. H.; Piper, J. L.; Papageorgiou, C. D., Total syntheses of 2,2 '-epi-cytoskyrin A, rugulosin, and the alleged structure of rugulin. *Journal of the American Chemical Society* **2007**, 129, 4001-4013.
 60. Snider, B. B.; Gao, X. L., Efficient syntheses of rugulosin analogues. *Journal of Organic Chemistry* **2005**, 70, 6863-6869.
 61. Uehara, Y.; Li, P. M.; Fukazawa, H.; Mizuno, S.; Nihei, Y.; Nishio, M.; Hanada, M.; Yamamoto, C.; Furumai, T.; Oki, T., Angelmicins, New Inhibitors of Oncogenic Src Signal-Transduction. *Journal of Antibiotics* **1993**, 46, 1306-1308.

62. Yokoyama, A.; OkabeKado, J.; Uehara, Y.; Oki, T.; Tomoyasu, S.; Tsuruoka, N.; Honma, Y., Angelmicin B, a new inhibitor of oncogenic signal transduction, inhibits growth and induces myelomonocytic differentiation of human myeloid leukemia HL-60 cells. *Leukemia Research* **1996**, 20, 491-497.
63. Kajiura, T.; Furumai, T.; Igarashi, Y.; Hori, H.; Higashi, K.; Ishiyama, T.; Uramoto, M.; Uehara, Y.; Oki, T., Signal transduction inhibitors, hibarimicins A, B, C, D and G produced by Microbispora - I. Taxonomy, fermentation, isolation and physico-chemical and biological properties. *Journal of Antibiotics* **1998**, 51, 394-401.
64. Hori, H.; Igarashi, Y.; Kajiura, T.; Furumai, T.; Higashi, K.; Ishiyama, T.; Uramoto, M.; Uehara, Y.; Oka, T., Signal transduction inhibitors, hibarimicins A, B, C, D and G produced by Microbispora - II. Structural studies. *Journal of Antibiotics* **1998**, 51, 402-417.
65. Hori, H.; Higashi, K.; Ishiyama, T.; Uramoto, M.; Uehara, Y.; Oki, T., Structure of angelmicin B, a novel src signal transduction inhibitor. *Tetrahedron Letters* **1996**, 37, 2785-2788.
66. Hori, H.; Kajiura, T.; Igarashi, Y.; Furumai, T.; Higashi, K.; Ishiyama, T.; Uramoto, M.; Uehara, Y.; Oki, T., Biosynthesis of hibarimicins - I. C-13-labeling experiments. *Journal of Antibiotics* **2002**, 55, 46-52.
67. Kajiura, T.; Furumai, T.; Igarashi, Y.; Hori, H.; Higashi, K.; Ishiyama, T.; Uramoto, M.; Uehara, Y.; Oki, T., Biosynthesis of hibarimicins - II. Elucidation of biosynthetic pathway by cosynthesis using blocked mutants. *Journal of Antibiotics* **2002**, 55, 53-60.
68. Tezuka, M.; Kuroyana, M.; Satake, M.; Yoshihir, K.; Natori, S., Naphthoquinone Derivatives from Ebenaceae .5. New Naphthoquinones from Diospyros. *Phytochemistry* **1973**, 12, 175-183.
69. Ferreira, M. A.; Aureacru, M.; Correia, A.; Lopes, M. H., Naphthoquinones from Euclea-Pseudebenus. *Phytochemistry* **1974**, 13, 1587-1589.
70. Baker, R. W.; Liu, S.; Sargent, M. V.; Skelton, B. W.; White, A. H., Absolute stereochemistry of 1,2'-linked bi(naphthoquinone)s. *Chemical Communications* **1997**, 451-452.
71. Narayan, S.; Roush, W. R., Studies toward the total synthesis of angelmicin B (hibarimicin B): Synthesis of a model CD-D' aryl naphthoquinone. *Organic Letters* **2004**, 6, 3789-3792.
72. Maharoo, U. S. M.; Sulikowski, G. A., Investigations into arylquinone atropisomers: synthesis and evaluation. *Tetrahedron Letters* **2003**, 44, 9021-9023.
73. Ullmann, F.; Bielecki, J., Ueber Synthesen in der Biphenylreihe. *Berichte der deutschen chemischen Gesellschaft* **1901**, 34, 2174-2185.

74. Hassan, J.; Sevignon, M.; Gozzi, C.; Schulz, E.; Lemaire, M., Aryl-aryl bond formation one century after the discovery of the Ullmann reaction. *Chemical Reviews* **2002**, 102, 1359-1469.
75. Clemo, G. R.; Cockburn, J. G.; Spence, R., CLXVII.-The catalytic production of polynuclear compounds. Part II. *Journal of the Chemical Society (Resumed)* **1931**, 1265-1273.
76. Toda, F.; Tanaka, K.; Iwata, S., Oxidative coupling reactions of phenols with iron(III) chloride in the solid state. *The Journal of Organic Chemistry* **1989**, 54, 3007-3009.
77. Miyashita, A.; Yasuda, A.; Takaya, H.; Toriumi, K.; Ito, T.; Souchi, T.; Noyori, R., Synthesis of 2,2'-bis(diphenylphosphino)-1,1'-binaphthyl (BINAP), an atropisomeric chiral bis(triaryl)phosphine, and its use in the rhodium(I)-catalyzed asymmetric hydrogenation of α -(acylamino)acrylic acids. *Journal of the American Chemical Society* **1980**, 102, 7932-7934.
78. Kar, A.; Mangu, N.; Kaiser, H. M.; Beller, M.; Tse, M. K., A general gold-catalyzed direct oxidative coupling of non-activated arenes. *Chemical Communications* **2008**, 386-388.
79. Demir, A. S.; Reis, O.; Emrullahoglu, M., Generation of aryl radicals from arylboronic acids by manganese(III) acetate: Synthesis of biaryls and heterobiaryls. *Journal of Organic Chemistry* **2003**, 68, 578-580.
80. Matsushita, M.; Kamata, K.; Yamaguchi, K.; Mizuno, N., Heterogeneously catalyzed aerobic oxidative biaryl coupling of 2-naphthols and substituted phenols in water. *Journal of the American Chemical Society* **2005**, 127, 6632-6640.
81. Joseph, J. K.; Jain, S. L.; Sain, B., V₂O₅-O-2 as a simple and efficient protocol for the oxidative coupling of 2-naphthols to binaphthols under mild reaction conditions. *Catalysis Communications* **2006**, 7, 184-186.
82. Takada, T.; Arisawa, M.; Gyoten, M.; Hamada, R.; Tohma, H.; Kita, Y., Oxidative biaryl coupling reaction of phenol ether derivatives using a hypervalent iodine(III) reagent. *Journal of Organic Chemistry* **1998**, 63, 7698-7706.
83. Whitesides, G.; Sanfilip, J.; Casey, C. P.; Panek, E. J., Oxidative Coupling Using Copper(I) Ate Complexes. *Journal of the American Chemical Society* **1967**, 89, 5302.
84. Lipshutz, B. H.; Siegmann, K.; Garcia, E., Kinetic Higher-Order Cyanocuprates - Applications to Biaryl Synthesis. *Journal of the American Chemical Society* **1991**, 113, 8161-8162.
85. Lipshutz, B. H.; Siegmann, K.; Garcia, E., Controlled Decomposition of Kinetic Higher-Order Cyanocuprates - a New Route to Unsymmetrical Biaryls. *Tetrahedron* **1992**, 48, 2579-2588.

86. Lipshutz, B. H.; James, B.; Vance, S.; Carrico, I., A potentially general intramolecular biaryl coupling approach to optically pure 2,2'-BINOL analogs. *Tetrahedron Letters* **1997**, 38, 753-756.
87. Miyake, Y.; Wu, M.; Rahman, M. J.; Kuwatani, Y.; Iyoda, M., Efficient construction of biaryls and macrocyclic cyclophanes via electron-transfer oxidation of Lipshutz cuprates. *Journal of Organic Chemistry* **2006**, 71, 6110-6117.
88. Surry, D. S.; Su, X. B.; Fox, D. J.; Franckevicius, V.; Macdonald, S. J. F.; Spring, D. R., Synthesis of medium-ring and iodinated biaryl compounds by organocuprate oxidation. *Angewandte Chemie-International Edition* **2005**, 44, 1870-1873.
89. Baudoin, O., The Asymmetric Suzuki Coupling Route to Axially Chiral Biaryls. *European Journal of Organic Chemistry* **2005**, 2005, 4223-4229.
90. Jacques, J.; Fouquey, C.; Viterbo, R., Enantiomeric cyclic binaphthyl phosphoric acids as resolving agents. *Tetrahedron Letters* **1971**, 12, 4617-4620.
91. Qiao-Sheng, H.; Vitharana, D.; Lin, P., An efficient and practical direct resolution of racemic 1,1'-bi-2-naphthol to both of its pure enantiomers. *Tetrahedron: Asymmetry* **1995**, 6, 2123-2126.
92. Fish, R. G.; Groundwater, P. W.; Morgan, J. J. G., The Photo-Epimerization of Gossypol Schiff's Bases. *Tetrahedron-Asymmetry* **1995**, 6, 873-876.
93. Blakemore, P. R.; Kilner, C.; Milicevic, S. D., Resolution, enantiomerization kinetics, and chiroptical properties of 7,7'-dihydroxy-8,8'-biquinolyl. *Journal of Organic Chemistry* **2006**, 71, 8212-8218.
94. Bringmann, G.; Tasler, S.; Endress, H.; Kraus, J.; Messer, K.; Wohlfarth, M.; Lobin, W., Murrastifoline-F: First total synthesis, atropo-enantiomer resolution, and stereoanalysis of an axially chiral N,C-coupled biaryl alkaloid. *Journal of the American Chemical Society* **2001**, 123, 2703-2711.
95. Puttmann, M.; Oesch, F.; Robertson, L. W., Characteristics of Polychlorinated Biphenyl (Pcb) Atropisomers. *Chemosphere* **1986**, 15, 2061-2064.
96. Blakemore, P. R.; Milicevic, S. D.; Zakharov, L. N., Enzymatic resolution of 7,7'-dihydroxy-8,8'-biquinolyl dipentanoate and its conversion to 2,2'-di-tert-butyl-7,7'-dihydroxy-8,8'-biquinolyl. *Journal of Organic Chemistry* **2007**, 72, 9368-9371.
97. Okuyama, K.; Shingubara, K.; Tsujiyama, S.; Suzuki, K.; Matsumoto, T., Enantiodivergent Synthesis of Tetra-ortho-Substituted Biphenyls by Enzymatic Desymmetrization. *Synlett* **2009**, 941-944.
98. Bringmann, G.; Hartung, T., Novel Concepts in Directed Biaryl Synthesis .12. 1st Atropo-Enantioselective Ring-Opening of Achiral Biaryls Containing Lactone Bridges with Chiral Hydride-Transfer Reagents Derived from Borane. *Angewandte Chemie-International Edition in English* **1992**, 31, 761-762.

99. Bringmann, G.; Breuning, M.; Walter, R.; Wuzik, A.; Peters, K.; Peters, E. M., Novel concepts in directed biaryl synthesis, 80 - Synthesis of axially chiral biaryls by atropo-diastereoselective cleavage of configurationally unstable biaryl lactones with menthol-derived O-nucleophiles. *European Journal of Organic Chemistry* **1999**, 3047-3055.
100. Bringmann, G.; Breuning, M.; Tasler, S.; Endress, H.; Ewers, C. L. J.; Gobel, L.; Peters, K.; Peters, E. M., Atropo-diastereoselective cleavage of configurationally unstable biaryl lactones with alkali metal activated primary 1-arylethylamines. *Chemistry-a European Journal* **1999**, 5, 3029-3038.
101. Bringmann, G.; Hartung, T., Novel Concepts in Directed Biaryl Synthesis .10. the Atropo-Enantioselective Ring-Opening of Achiral Lactone-Bridged Biaryls Using Chirally Modified Aluminum Hydrides. *Synthesis-Stuttgart* **1992**, 433-435.
102. Bringmann, G.; Vitt, D., Novel Concepts in Directed Biaryl Synthesis .55. Stereoselective Ring-Opening Reaction of Axially Prostereogenic Biaryl Lactones with Chiral Oxazaborolidines - an Am1 Study of the Complete Mechanistic Course. *Journal of Organic Chemistry* **1995**, 60, 7674-7681.
103. Bringmann, G.; Pabst, T.; Rycroft, D. S.; Connolly, J. D., Novel concepts in directed biaryl synthesis - Part 76 - First synthesis of mastigophorenes A and B, by biomimetic oxidative coupling of herbertenediol. *Tetrahedron Letters* **1999**, 40, 483-486.
104. Lee, W. K.; Park, Y. S.; Beak, P., Dynamic Thermodynamic Resolution: Advantage by Separation of Equilibration and Resolution. *Accounts of Chemical Research* **2009**, 42, 224-234.
105. Smrcina, M.; Lorenc, M.; Hanus, V.; Sedmera, P.; Kocovsky, P., Synthesis of Enantiomerically Pure 2,2'-Dihydroxy-1,1'-Binaphthyl, 2,2'-Diamino-1,1'-Binaphthyl, and 2-Amino-2'-Hydroxy-1,1'-Binaphthyl - Comparison of Processes Operating as Diastereoselective Crystallization and as 2nd-Order Asymmetric Transformation. *Journal of Organic Chemistry* **1992**, 57, 1917-1920.
106. Smrcina, M.; Polakova, J.; Vyskocil, S.; Kocovsky, P., Synthesis of Enantiomerically Pure Binaphthyl Derivatives - Mechanism of the Enantioselective, Oxidative Coupling of Naphthols and Designing a Catalytic Cycle. *Journal of Organic Chemistry* **1993**, 58, 4534-4538.
107. Tsubaki, K.; Miura, M.; Morikawa, H.; Tanaka, H.; Kawabata, T.; Furuta, T.; Tanaka, K.; Fuji, K., Synthesis of optically active oligonaphthalenes via second-order asymmetric transformation. *Journal of the American Chemical Society* **2003**, 125, 16200-16201.
108. Zhang, Y.; Yeung, S. M.; Wu, H. Q.; Heller, D. P.; Wu, C. R.; Wulff, W. D., Highly enantioselective deracemization of linear and vaulted biaryl ligands. *Organic Letters* **2003**, 5, 1813-1816.
109. Hu, G.; Holmes, D.; Gendhar, B. F.; Wulff, W. D., Optically Active (aR)- and (aS)-Linear and Vaulted Biaryl Ligands: Deracemization versus Oxidative

- Dimerization. *Journal of the American Chemical Society* **2009**, 131, 14355-14364.
110. Becker, J. J.; White, P. S.; Gagne, M. R., Synthesis and characterization of chiral diphosphine platinum(II) VANOL and VAPOL complexes. *Organometallics* **2003**, 22, 3245-3249.
 111. Evans, D. A.; Wood, M. R.; Trotter, B. W.; Richardson, T. I.; Barrow, J. C.; Katz, J. L., Total syntheses of vancomycin and eremomycin aglycons. *Angewandte Chemie-International Edition* **1998**, 37, 2700-2704.
 112. Evans, D. A.; Dinsmore, C. J.; Watson, P. S.; Wood, M. R.; Richardson, T. I.; Trotter, B. W.; Katz, J. L., Nonconventional stereochemical issues in the design of the synthesis of the vancomycin antibiotics: Challenges imposed by axial and nonplanar chiral elements in the heptapeptide aglycons. *Angewandte Chemie-International Edition* **1998**, 37, 2704-2708.
 113. Su, X. B.; Surry, D. S.; Spandl, R. J.; Spring, D. R., Total synthesis of sanguin H-5. *Organic Letters* **2008**, 10, 2593-2596.
 114. Mlyano, S.; Tobita, M.; Hashimoto, H., Asymmetric Synthesis of Axially Diasymmetric 1,1'-Binaphthyls via an Intramolecular Ullman Coupling reaction of (R)- and (S)- 2,2'- Bis(1-bromo-2-naphthylcarbonyloxy)-1,1'-binaphthyl. *Bulletin of the Chemical Society of Japan* **1981**, 54, 3522-3526.
 115. Mlyano, S.; Fukushima, H.; Handa, S.; Ito, H., Asymmetric Synthesis of Axially Chiral, Unsymmetrical Diphenic Acids via Intramolecular Ullmann Coupling Reaction. *Bulletin of the Chemical Society of Japan* **1988**, 61, 3249-3254.
 116. Moorlag, H.; Meyers, A. I., Oxazoline-mediated biaryl coupling reactions. Stereocontrolled synthesis of 2,2',6,6'-tetrasubstituted biphenyls. *Tetrahedron Letters* **1993**, 34, 6989-6992.
 117. Meyers, A. I.; Willemsen, J. J., The synthesis of (S)-(+)-gossypol via an asymmetric Ullmann coupling. *Chemical Communications* **1997**, 1573-1574.
 118. Degnan, A. P.; Meyers, A. I., Total syntheses of (-)-herbertenediol, (-)-mastigophorene A, and (-)-mastigophorene B. Combined utility of chiral bicyclic lactams and chiral aryl oxazolines. *Journal of the American Chemical Society* **1999**, 121, 2762-2769.
 119. Brussee, J.; Jansen, A. C. A., A highly stereoselective synthesis of s(-)-[1,1'-binaphthalene]-2,2'-diol. *Tetrahedron Letters* **1983**, 24, 3261-3262.
 120. Brussee, J.; Groenendijk, J. L. G.; Tekoppele, J. M.; Jansen, A. C. A., On the Mechanism of the Formation of "S(-)-(1,1'-Binaphthalene)-2,2'-Diol Via Copper(II)Amine Complexes. *Tetrahedron* **1985**, 41, 3313-3319.
 121. Li, X. L.; Yang, J.; Kozlowski, M. C., Enantioselective oxidative biaryl coupling reactions catalyzed by 1,5-diazadecalin metal complexes. *Organic Letters* **2001**, 3, 1137-1140.

122. Hewgley, J. B.; Stahl, S. S.; Kozlowski, M. C., Mechanistic study of asymmetric oxidative biaryl coupling: Evidence for self-processing of the copper catalyst to achieve control of oxidase vs oxygenase activity. *Journal of the American Chemical Society* **2008**, 130, 12232-+.
123. Yin, J. J.; Buchwald, S. L., A catalytic asymmetric Suzuki coupling for the synthesis of axially chiral biaryl compounds. *Journal of the American Chemical Society* **2000**, 122, 12051-12052.
124. Shen, X. Q.; Jones, G. O.; Watson, D. A.; Bhayana, B.; Buchwald, S. L., Enantioselective Synthesis of Axially Chiral Biaryls by the Pd-Catalyzed Suzuki Miyaura Reaction: Substrate Scope and Quantum Mechanical Investigations. *Journal of the American Chemical Society* **2010**, 132, 11278-11287.
125. Kajiura, T.; Furumai, T.; Igarashi, Y.; Hori, H.; Higashi, K.; Ishiyama, T.; Uramoto, M.; Uehara, Y.; Oki, T., Biosynthesis of hibarimicins - II. Elucidation of biosynthetic pathway by cosynthesis using blocked mutants. *Journal of Antibiotics* **2002**, 55, 53-60.
126. Kajiura, T., Elucidation of Biosynthetic Pathway of Hibarimicins, v-src Tyrosine Kinase Inhibitors. *Actinomycetologica* **2004**, 22-25.
127. Vrettou, M.; Gray, A. A.; Brewer, A. R. E.; Barrett, A. G. M., Strategies for the synthesis of C2 symmetric natural products--a review. *Tetrahedron* **2007**, 63, 1487-1536.
128. Shriner, R. L.; McCutchan, P., PREPARATION OF SOME METHYLATED GALLIC ACIDS. *Journal of the American Chemical Society* **1929**, 51, 2193-2195.
129. Sanchez, I. H.; Larraza, M. I.; Basurto, F.; Yanez, R.; Avila, S.; Tovar, R.; Josephnathan, P., Formal Total Synthesis of Beta-Pipitzol. *Tetrahedron* **1985**, 41, 2355-2359.
130. Lambert, W. T.; Roush, W. R., Synthesis of the A-B subunit of angelmicin B. *Organic Letters* **2005**, 7, 5501-5504.
131. Li, J.; Todaro, L. J.; Mootoo, D. R., Synthesis of the AB subunit of angelmicin B through a tandem alkoxy radical fragmentation-etherification sequence. *Organic Letters* **2008**, 10, 1337-1340.
132. Kim, K.; Maharoo, U. S. M.; Raushel, J.; Sulikowski, G. A., Diverging stereochemical pathways in an intramolecular Diels-Alder reaction determined by dienophile structure. *Organic Letters* **2003**, 5, 2777-2780.
133. Martin, S. F.; Dodge, J. A., Efficacious Modification of the Mitsunobu Reaction for Inversions of Sterically Hindered Secondary Alcohols. *Tetrahedron Letters* **1991**, 32, 3017-3020.
134. Lee, C. S.; Audelo, M. Q.; Reibenpies, J.; Sulikowski, G. A., Studies toward the total synthesis of hibarimicinone. Progress on the assembly of the AB- and GH-ring systems. *Tetrahedron* **2002**, 58, 4403-4409.

135. Giuliano, R. M.; Bryan, R. F.; Hartley, P.; Peckler, S.; Woode, M. K., Structure of Methyl 6-Deoxy-Alpha-D-Idopyranoside. *Carbohydrate Research* **1989**, 191, 1-11.
136. Bernet, B.; Vasella, A., Fragmentation of 6-Deoxy-6-Halo-Hexono-1,5-Ortholactones - a Concerted, Nonstereospecific Process. *Helvetica Chimica Acta* **1984**, 67, 1328-1347.
137. Coleman, R. S.; Dong, Y.; Carpenter, A. J., A Convenient Preparation of Terminally Differentiated, Selectively Protected 6-Carbon Synthons from D-Glucosamine. *Journal of Organic Chemistry* **1992**, 57, 3732-3735.
138. Plietker, B., The RuO₄-catalyzed ketohydroxylation. Part 1. Development, scope, and limitation. *Journal of Organic Chemistry* **2004**, 69, 8287-8296.
139. Hauser, F. M.; Rhee, R. P., New Synthetic Methods for Regioselective Annelation of Aromatic Rings - 1-Hydroxy-2,3-Disubstituted Naphthalenes and 1,4-Dihydroxy-2,3-Disubstituted Naphthalenes. *Journal of Organic Chemistry* **1978**, 43, 178-180.
140. Kraus, G. A.; Sugimoto, H., Annelation Route to Quinones. *Tetrahedron Letters* **1978**, 2263-2266.
141. Leeper, F. J.; Staunton, J., Biomimetic Syntheses of Polyketide Aromatics from Reaction of an Orsellinate Anion with Pyrones and a Pyrylium Salt. *Journal of the Chemical Society-Perkin Transactions 1* **1984**, 1053-1059.
142. Dodd, J. H.; Starrett, J. E.; Weinreb, S. M., Total Synthesis of Tri-O-Methyloliviv. *Journal of the American Chemical Society* **1984**, 106, 1811-1812.
143. Charest, M. G.; Lerner, C. D.; Brubaker, J. D.; Siegel, D. R.; Myers, A. G., A Convergent Enantioselective Route to Structurally Diverse 6-Deoxytetracycline Antibiotics. In *Science*, 2005; Vol. 308, pp 395-398.
144. Rao, D. V.; Stuber, F. A., An Efficient Synthesis of 3,4,5-Trimethoxybenzaldehyde from Vanillin. *Synthesis-Stuttgart* **1983**, 308-308.
145. Furstner, A.; Stelzer, F.; Rumbo, A.; Krause, H., Total synthesis of the turrianes and evaluation of their DNA-cleaving properties. *Chemistry-a European Journal* **2002**, 8, 1856-1871.
146. Evans, G. E.; Staunton, J., An Investigation of the Biosynthesis of Citromycetin in *Penicillium-Frequentans* Using C-13-Labeled and C-14-Labeled Precursors. *Journal of the Chemical Society-Perkin Transactions 1* **1988**, 755-761.
147. Bode, S. E.; Drochner, D.; Muller, M., Synthesis, biosynthesis, and absolute configuration of vioxanthin. *Angewandte Chemie-International Edition* **2007**, 46, 5916-5920.

148. Zhang, Z. J.; Yu, B., Total synthesis of the antiallergic naphtho-alpha-pyrone tetraglucoside, cassiaside C-2, isolated from cassia seeds. *Journal of Organic Chemistry* **2003**, 68, 6309-6313.
149. Yadav, J. S.; Reddy, B. V. S.; Madan, C.; Hashim, S. R., A mild and chemoselective dealkylation of alkyl aryl ethers by cerium(III) chloride-Nal. *Chemistry Letters* **2000**, 738-739.
150. Wang, L.; Meegalla, S. K.; Fang, C. L.; Taylor, N.; Rodrigo, R., Exploratory synthetic investigations related to 12a-deoxypillaromycinone. *Canadian Journal of Chemistry-Revue Canadienne De Chimie* **2002**, 80, 728-738.
151. Surry, D. S.; Fox, D. J.; Macdonald, S. J. F.; Spring, D. R., Aryl-aryl coupling via directed lithiation and oxidation. *Chemical Communications* **2005**, 2589-2590.
152. Zhu, G. D.; Chen, D. H.; Huang, J. H.; Chi, C. S.; Liu, F. K., Regioselective Bromination and Fluorination of Apogossypol Hexamethyl Ether. *Journal of Organic Chemistry* **1992**, 57, 2316-2320.
153. Hauser, F. M.; Gauvan, P. J. F., Total synthesis of (+/-)-biphyscion. *Organic Letters* **1999**, 1, 671-672.
154. Drochner, D.; Huttel, W.; Bode, S. E.; Muller, M.; Karl, U.; Nieger, M.; Steglich, W., Dimeric orsellinic acid derivatives: Valuable intermediates for natural product synthesis. *European Journal of Organic Chemistry* **2007**, 1749-1758.
155. Tasler, S.; Bringmann, G., Biaryllic bis-carbazole alkaloids: Occurrence, stereochemistry, synthesis, and bioactivity. *Chemical Record* **2002**, 2, 113-126.
156. Mulrooney, C. A.; Li, X.; DiVirgilio, E. S.; Kozlowski, M. C., General Approach for the Synthesis of Chiral Perylenequinones via Catalytic Enantioselective Oxidative Biaryl Coupling. *Journal of the American Chemical Society* **2003**, 125, 6856-6857.
157. Li, X. L.; Schenkel, L. B.; Kozlowski, M. C., Synthesis and resolution of a novel chiral diamine ligand and application to asymmetric lithiation-substitution. *Organic Letters* **2000**, 2, 875-878.
158. Mislow, K.; Bunnenberg, E.; Records, R.; Wellman, K.; Djerassi, C., Inherently Dissymmetric Chromophores and Circular Dichroism. II. *Journal of the American Chemical Society* **1963**, 85, 1342-1349.
159. Kitanaka, S.; Takido, M., (S)-5,7'-Biphyscion 8-Glucoside from Cassia-Torosa. *Phytochemistry* **1995**, 39, 717-718.
160. Sperry, J.; Sejberg, J. J. P.; Stiemke, F. M.; Brimble, M. A., Biomimetic studies towards the cardinalins: synthesis of (+)-ventiloquinone L and an unusual dimerisation. *Organic & Biomolecular Chemistry* **2009**, 7, 2599-2603.
161. Drochner, D.; Huttel, W.; Nieger, M.; Muller, M., Unselective phenolic coupling of methyl 2-hydroxy-4-methoxy-6-methylbenzoate - A valuable tool for the total

- synthesis of natural product families. *Angewandte Chemie-International Edition* **2003**, 42, 931-+.
162. Takada, T.; Arisawa, M.; Gyoten, M.; Hamada, R.; Tohma, H.; Kita, Y., Oxidative biaryl coupling reaction of phenol ether derivatives using a hypervalent iodine(III) reagent. *Journal of Organic Chemistry* **1998**, 63, 7698-7706.
 163. Huang, C.; Gevorgyan, V., Synthesis of Unsymmetrical o-Biphenols and o-Binaphthols via Silicon-Tethered Pd-Catalyzed C-H Arylation. *Organic Letters* **2010**, 12, 2442-2445.
 164. Zenk, M. H.; Gerardy, R.; Stadler, R., Phenol Oxidative Coupling of Benzyloquinoline Alkaloids Is Catalyzed by Regio-Selective and Stereo-Selective Cytochrome-P-450 Linked Plant Enzymes - Salutaridine and Berbamunine. *Journal of the Chemical Society-Chemical Communications* **1989**, 1725-1727.
 165. Pickel, B.; Constantin, M. A.; Pfannstiel, J.; Conrad, J.; Beifuss, U.; Schaller, A., An Enantiocomplementary Dirigent Protein for the Enantioselective Laccase-Catalyzed Oxidative Coupling of Phenols. *Angewandte Chemie-International Edition* **49**, 202-204.
 166. Mikolasch, A.; Schauer, F., Fungal laccases as tools for the synthesis of new hybrid molecules and biomaterials. *Applied Microbiology and Biotechnology* **2009**, 82, 605-624.
 167. El-Seedi, H. R.; Yamamura, S.; Nishiyama, S., Anodic oxidation of 4-methoxy-1-naphthol. *Tetrahedron Letters* **2002**, 43, 3301-3304.
 168. Takeya, T.; Doi, H.; Ogata, T.; Otsuka, T.; Okamoto, I.; Kotani, E., SnCl₄-mediated oxidative biaryl coupling reaction of 1-naphthol and subsequent ring closure of 2,2'-binaphthol to the dinaphthofuran framework. *Tetrahedron* **2004**, 60, 6295-6310.
 169. Ogata, T.; Okamoto, I.; Doi, H.; Kotani, E.; Takeya, T., SnCl₄-mediated oxidative reaction for formation of binaphthoquinone and dinaphthofuran frameworks and its application to natural product synthesis. *Tetrahedron Letters* **2003**, 44, 2041-2044.
 170. Schwartz, M. A.; Pham, P. T. K., Oxidative Coupling of Cis-3,N-Bis(Methoxycarbonyl)-N-Norreticuline - an Approach to the Asymmetric-Synthesis of Morphine Alkaloids. *Journal of Organic Chemistry* **1988**, 53, 2318-2322.
 171. Brussee, J.; Jansen, A. C. A., A highly stereoselective synthesis of s(-)-[1,1'-binaphthalene]-2,2'-diol. *Tetrahedron Letters* **1983**, 24, 3261-3262.
 172. Sartori, G.; Maggi, R.; Bigi, F.; Arienti, A.; Casnati, G., Regiochemical Control in the Oxidative Coupling of Metal Phenolates - Highly Selective Synthesis of Symmetrical, Hydroxylated Biaryls. *Tetrahedron Letters* **1992**, 33, 2207-2210.

173. Sartori, G.; Maggi, R.; Bigi, F.; Arienti, A.; Casnati, G., Oxidative Coupling of Dichloroaluminum Phenolates - Highly Selective Synthesis of Hydroxylated Biaryls and Tetraaryls. *Tetrahedron* **1992**, 48, 9483-9494.
174. Still, W. C.; Kahn, M.; Mitra, A., *Journal of Organic Chemistry* 1978, 43, 2923.
175. Eric Steiner, J. K., Etienne Charollais, Theodore Posternak, 259. Recherches sur la biochimie des champignons inferieurs IX. Synthese de precurseurs marques et biosynthese de la phoenicine et de l'oosporeine. *Helvetica Chimica Acta* 1974, 57, 2377-2387.

APPENDIX

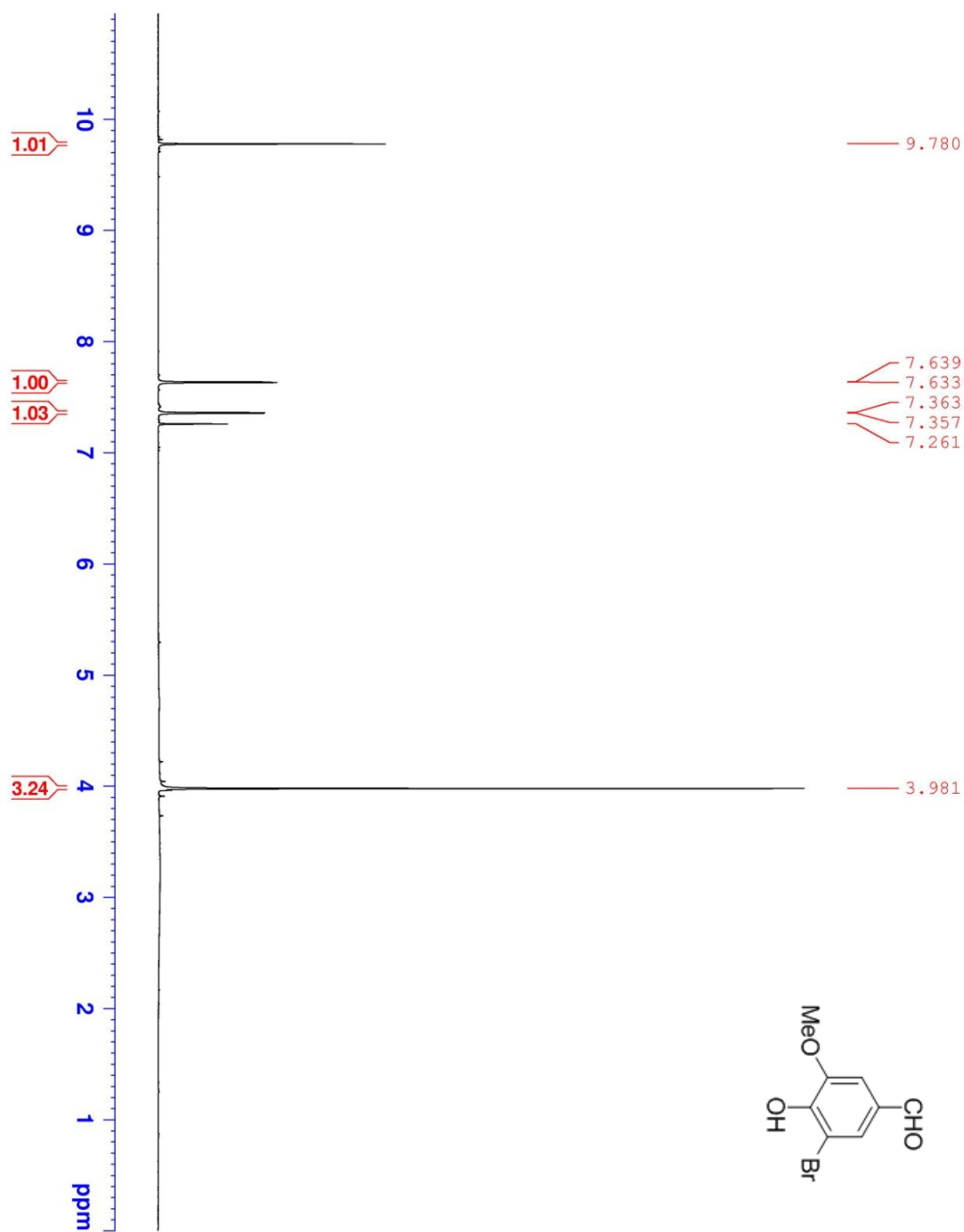


Figure A1. 300 MHz ^1H NMR of 3-Bromo-4-hydroxy-5-methoxybenzaldehyde in CDCl_3 .

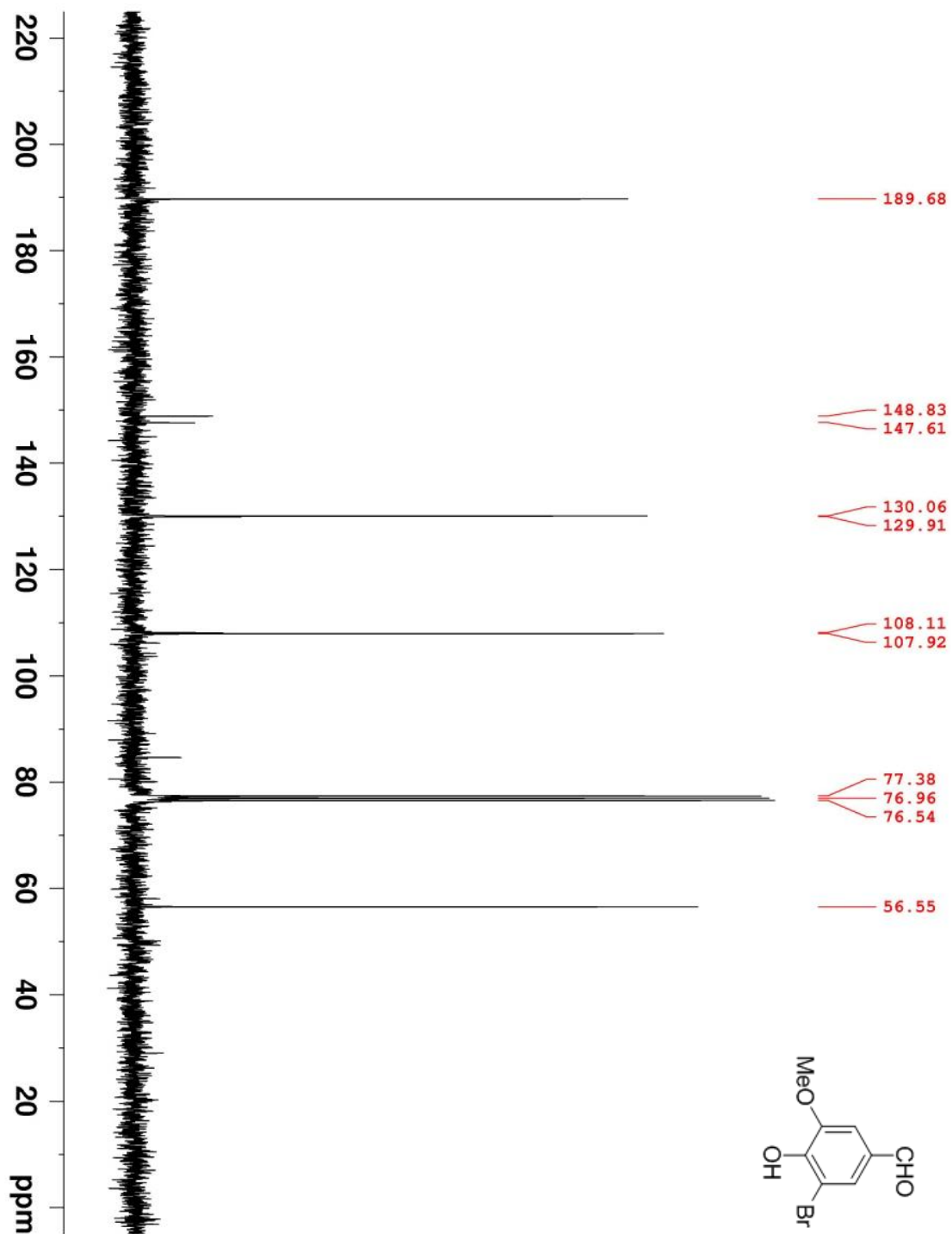
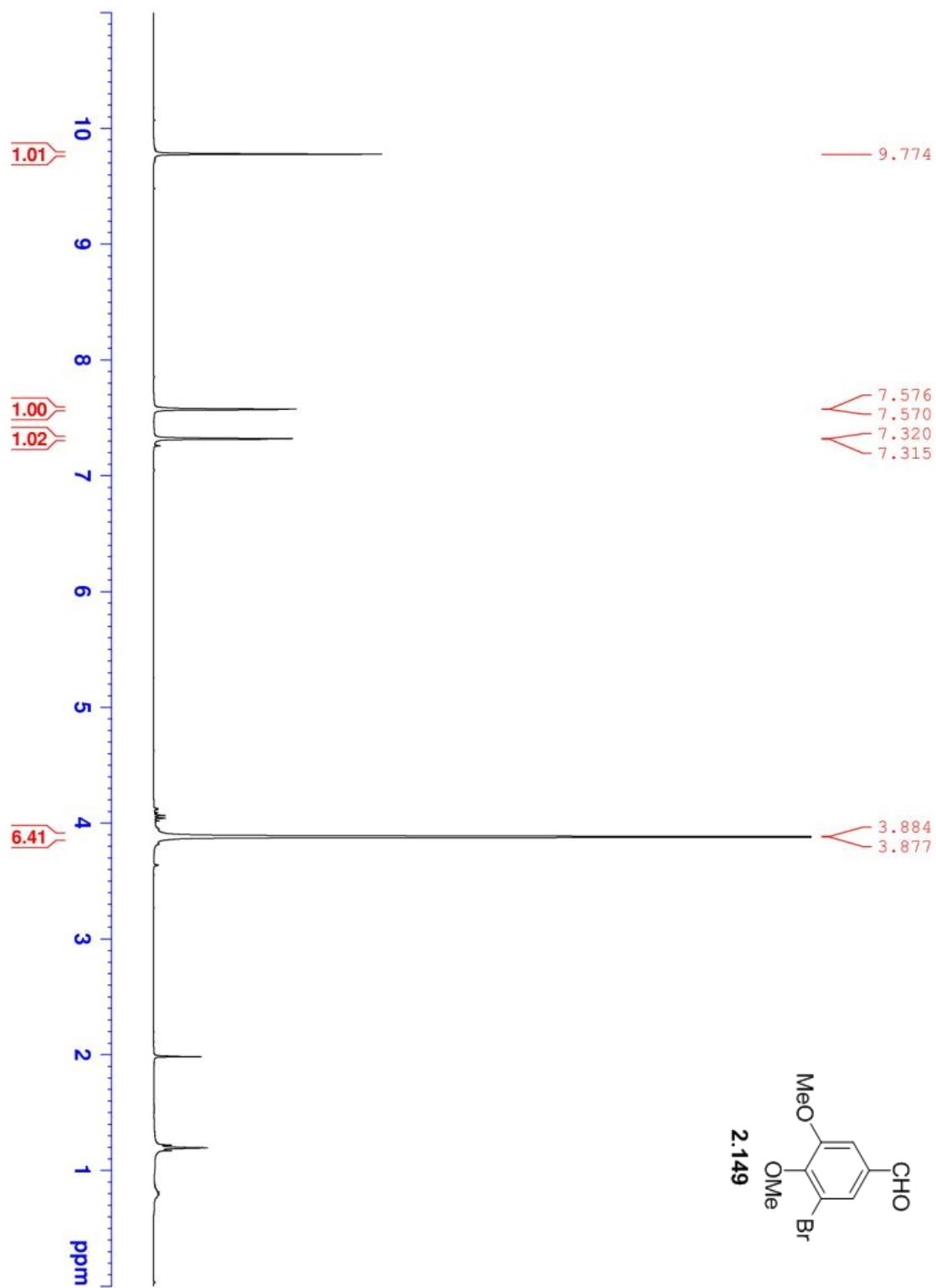


Figure A2. 75 MHz ^{13}C NMR of 3-Bromo-4-hydroxy-5-methoxybenzaldehyde in CDCl_3 .

Figure A3. 300 MHz ^1H NMR of **2.149** in CDCl_3 .

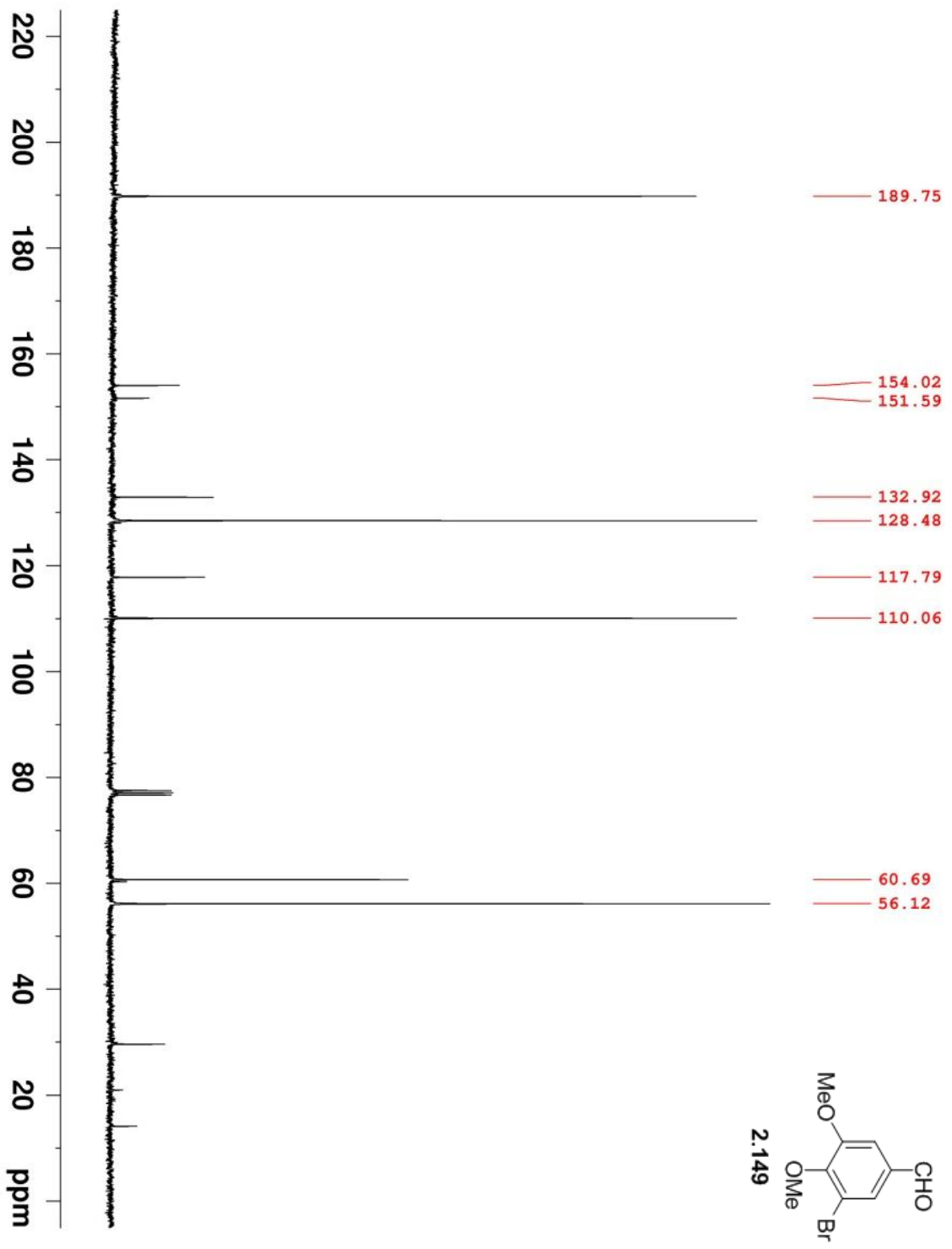


Figure A4. 75 MHz ^{13}C NMR of **2.149** in CDCl_3 .

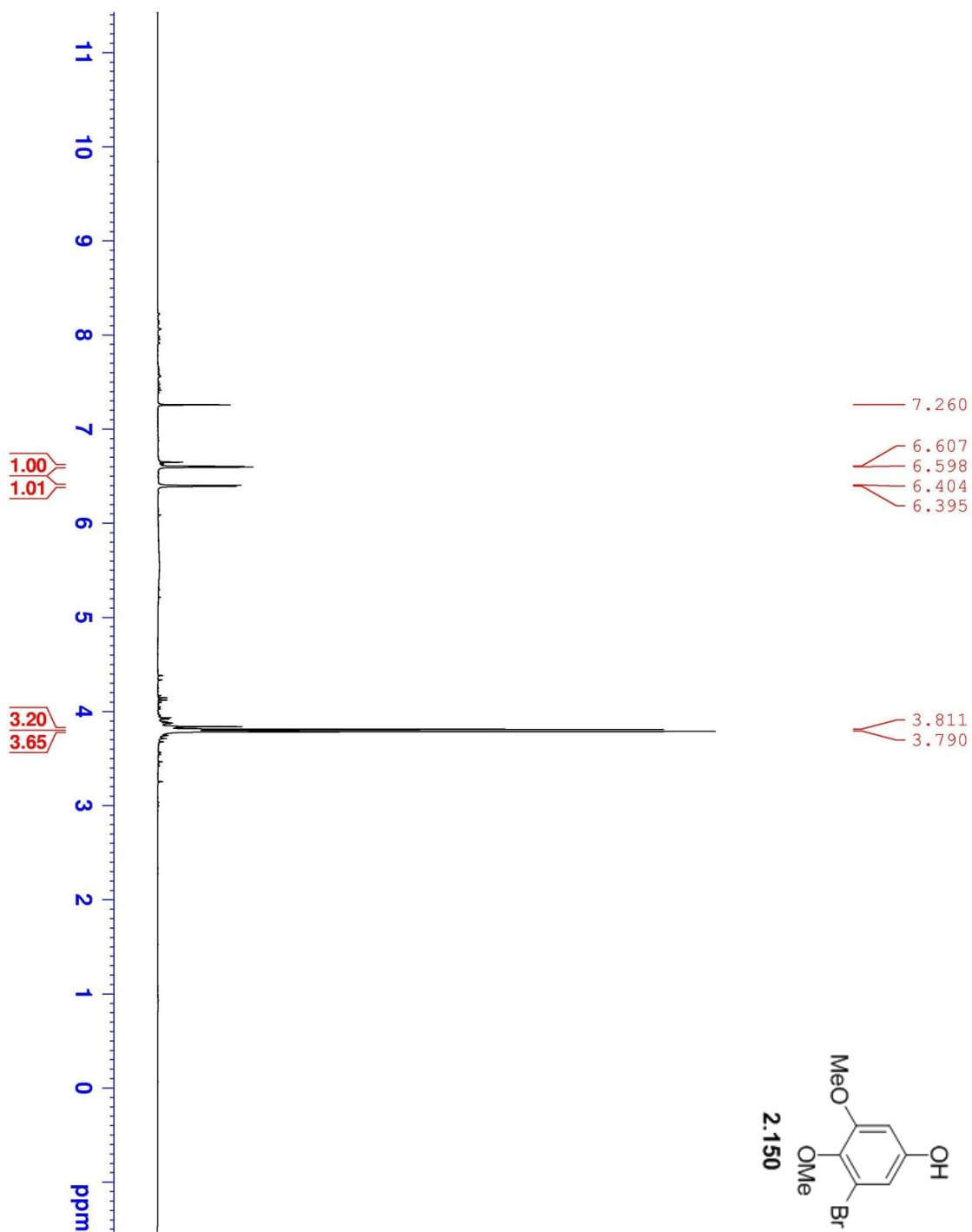


Figure A5. 300 MHz ¹H NMR of **2.150** in CDCl₃.

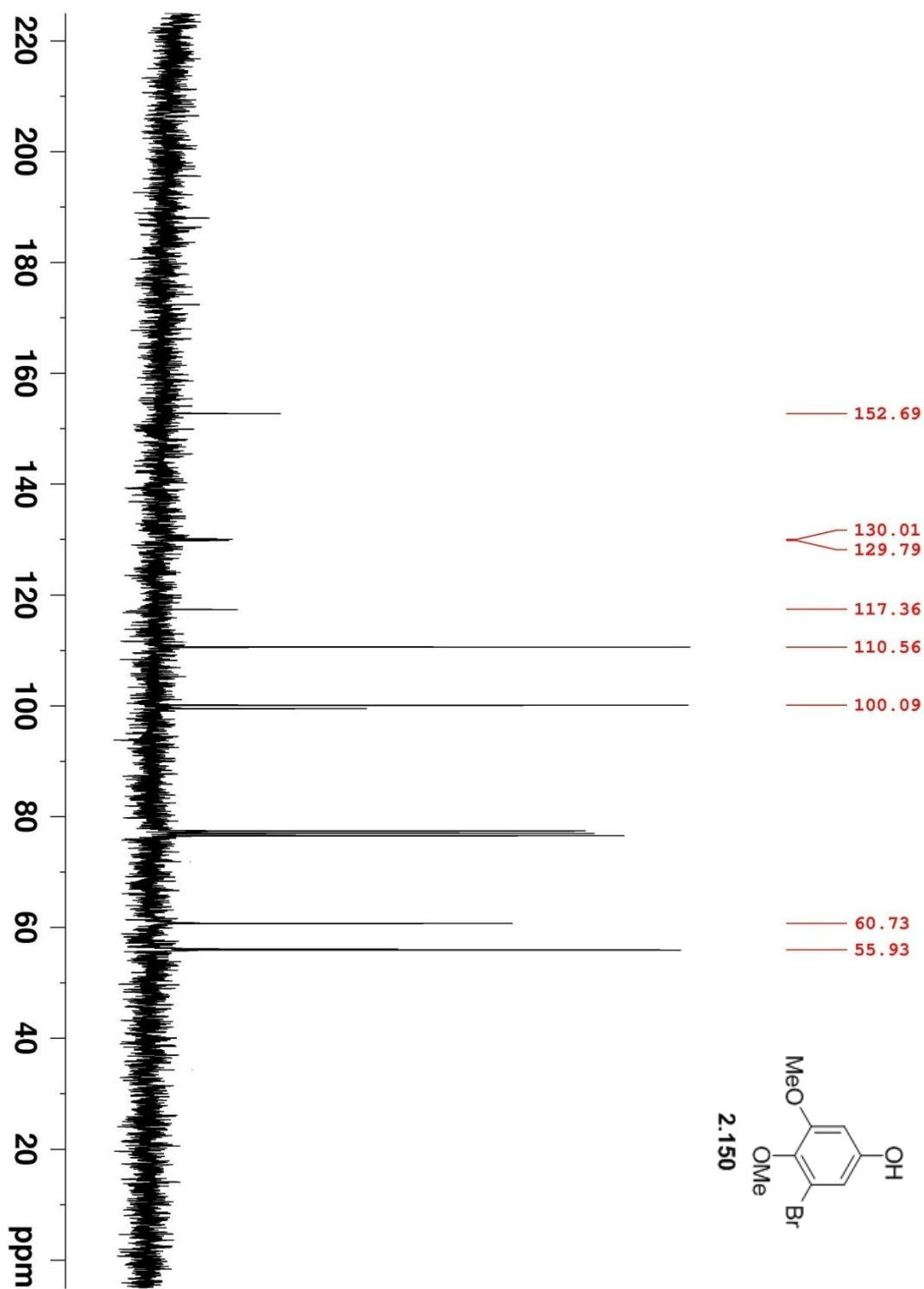


Figure A6. 75 MHz ^{13}C NMR of **2.150** in CDCl_3 .

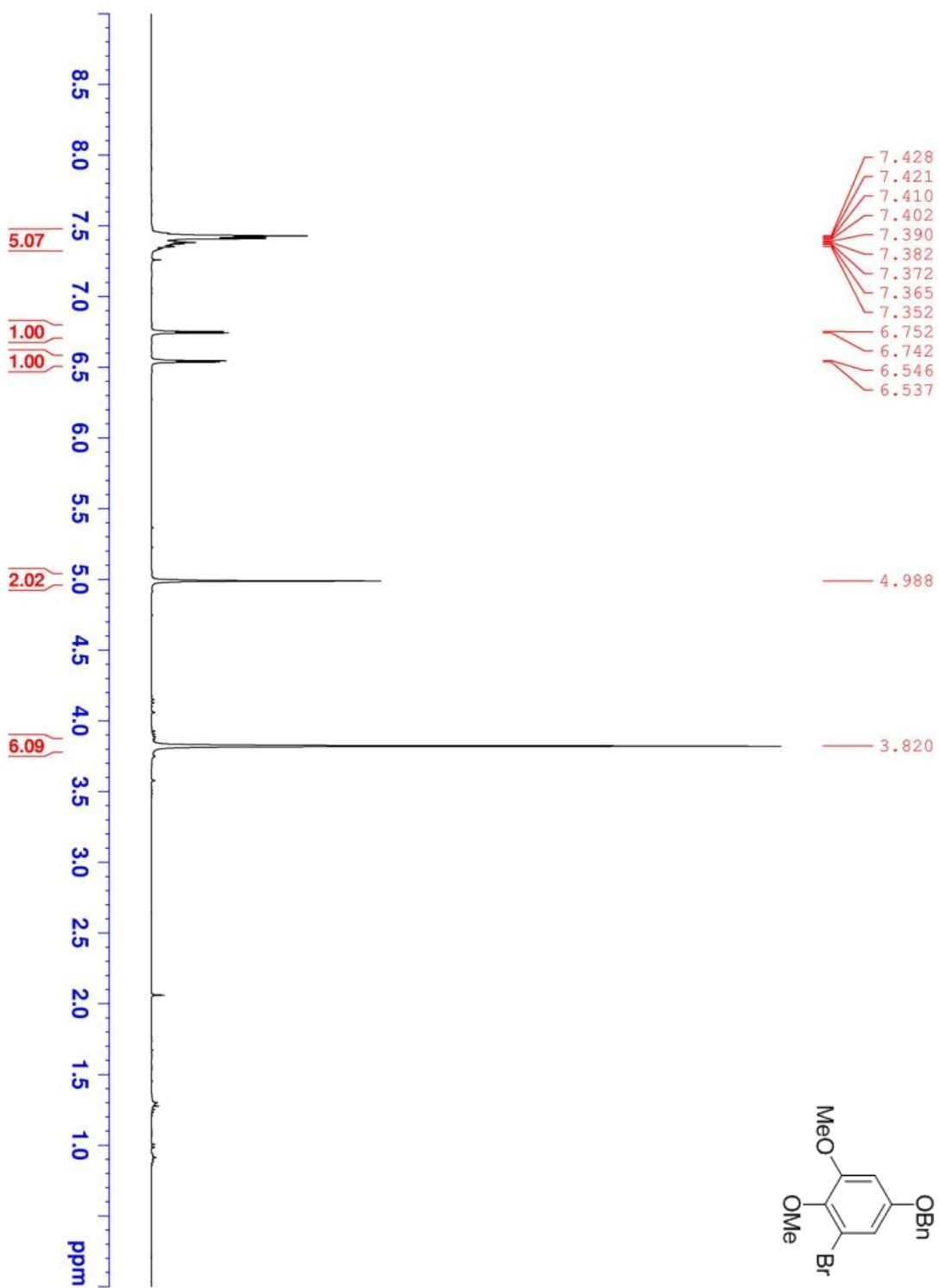


Figure A7. 300 MHz ^1H NMR of 5-(Benzyloxy)-1-bromo-2,3-dimethoxybenzene in CDCl_3 .

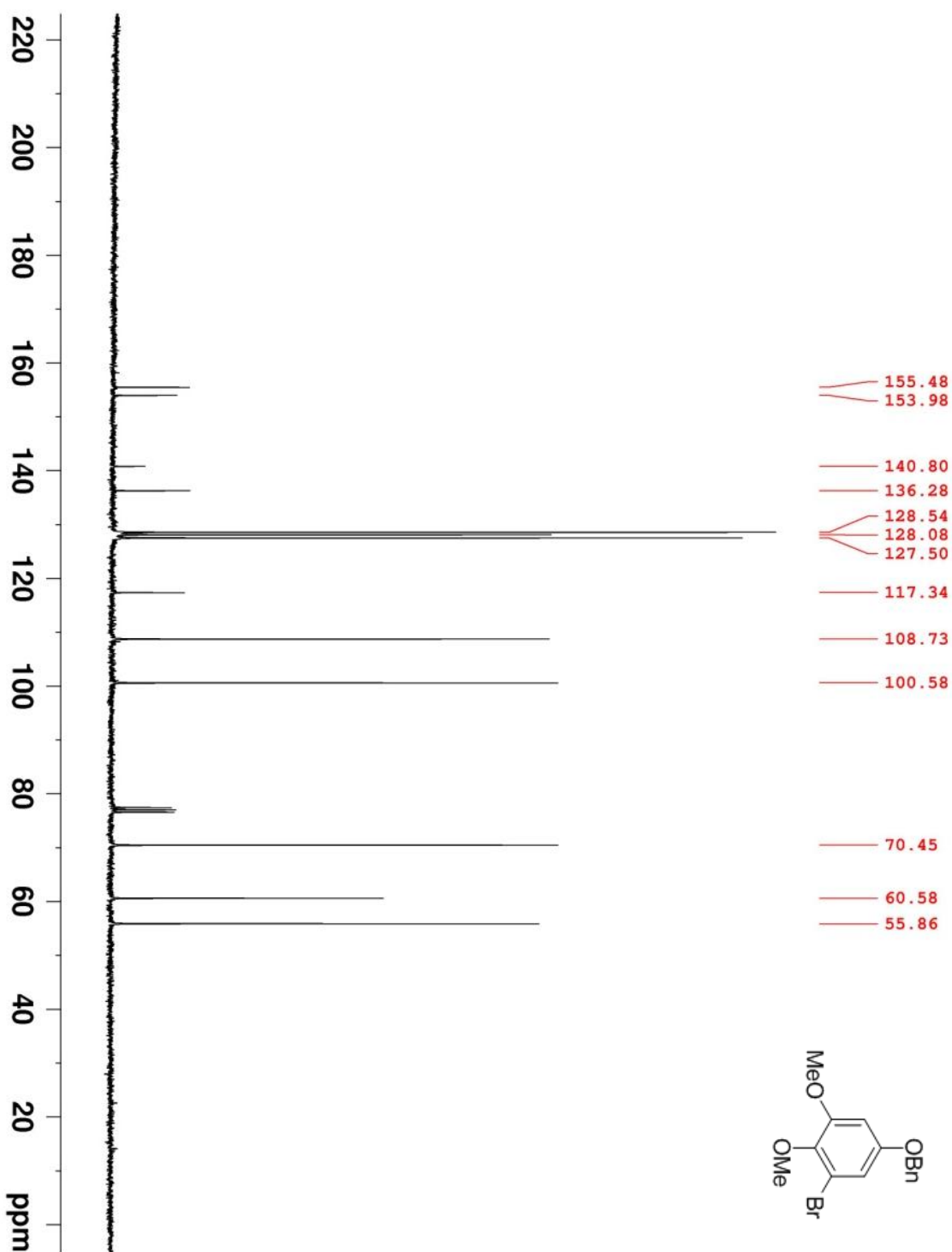


Figure A8. 75 MHz ¹³C NMR of 5-(Benzyloxy)-1-bromo-2,3-dimethoxybenzene in CDCl₃.

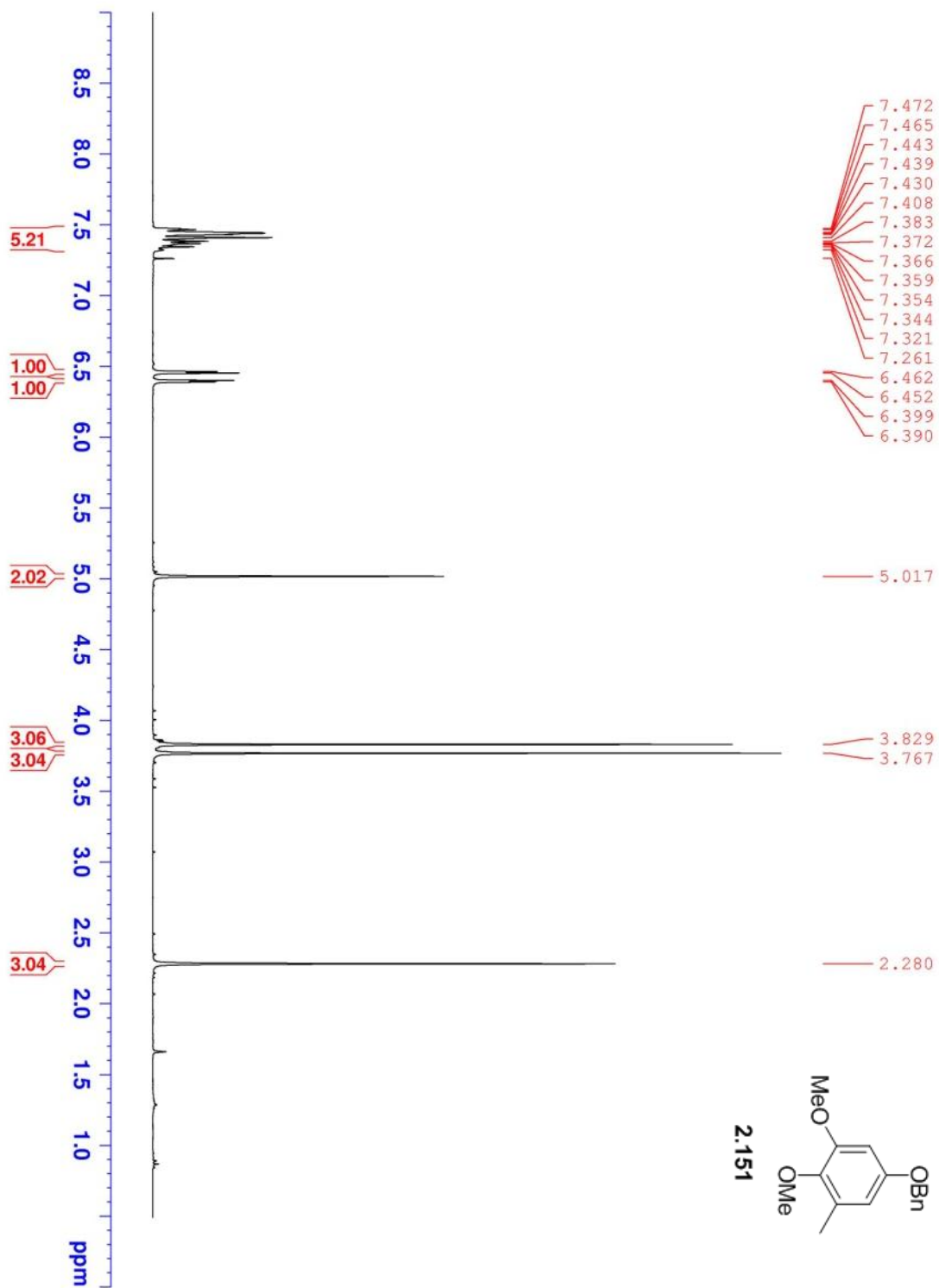


Figure A9. 300 MHz ¹H NMR of **2.151** in CDCl₃.

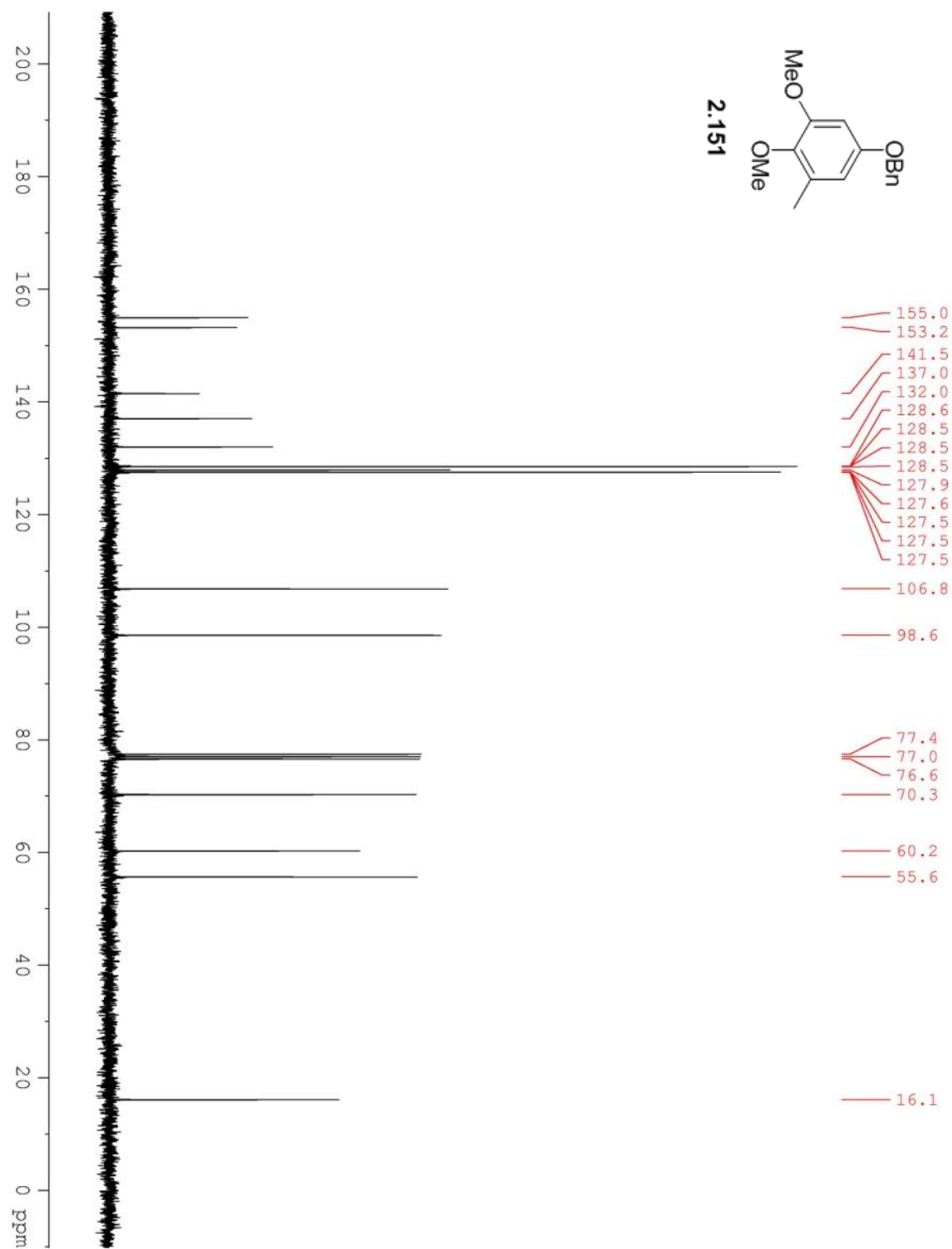


Figure A10. 75 MHz ^{13}C NMR of **2.151** in CDCl_3 .

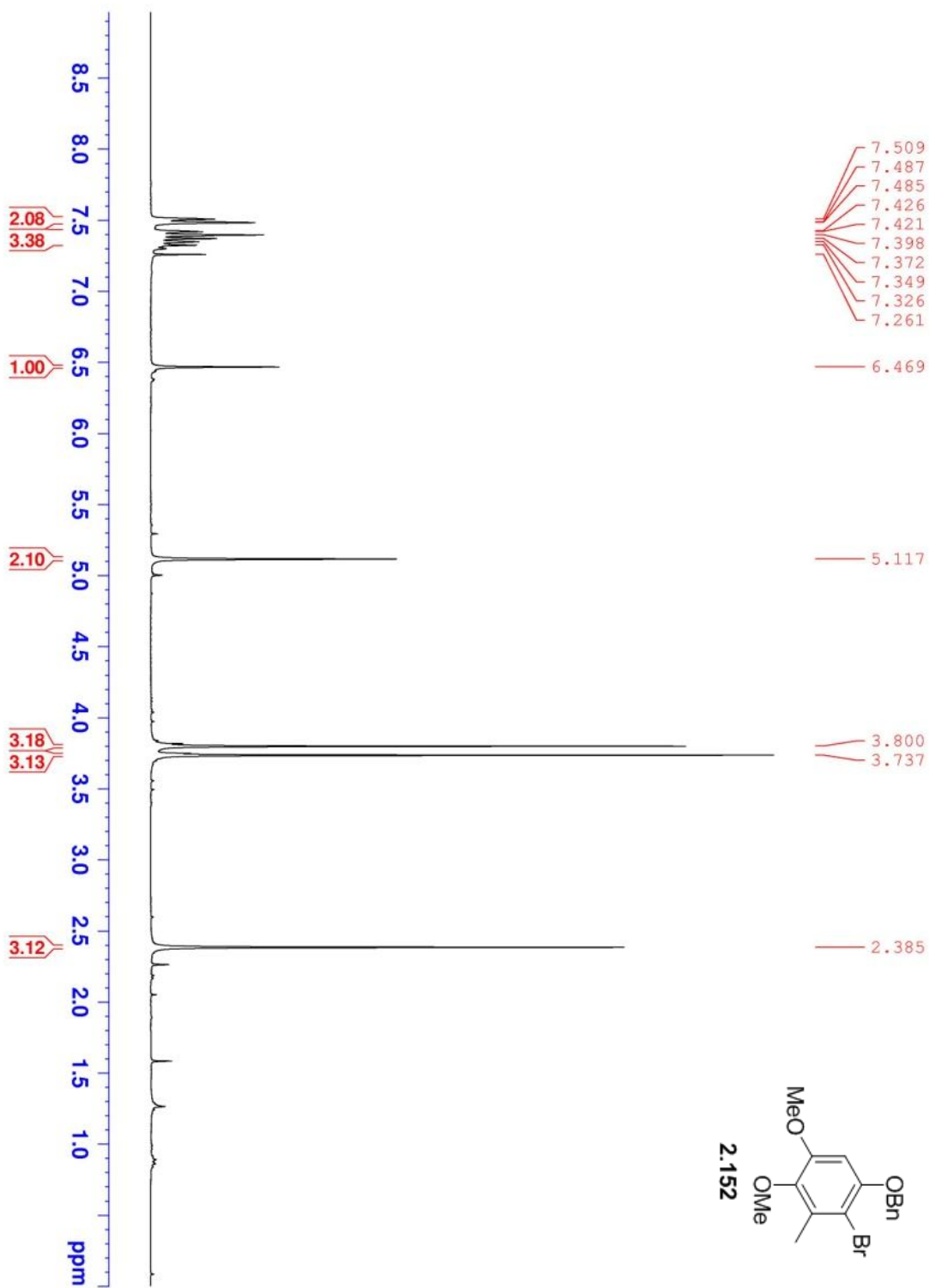


Figure A11. 300 MHz ¹H NMR of **2.152** in CDCl₃.

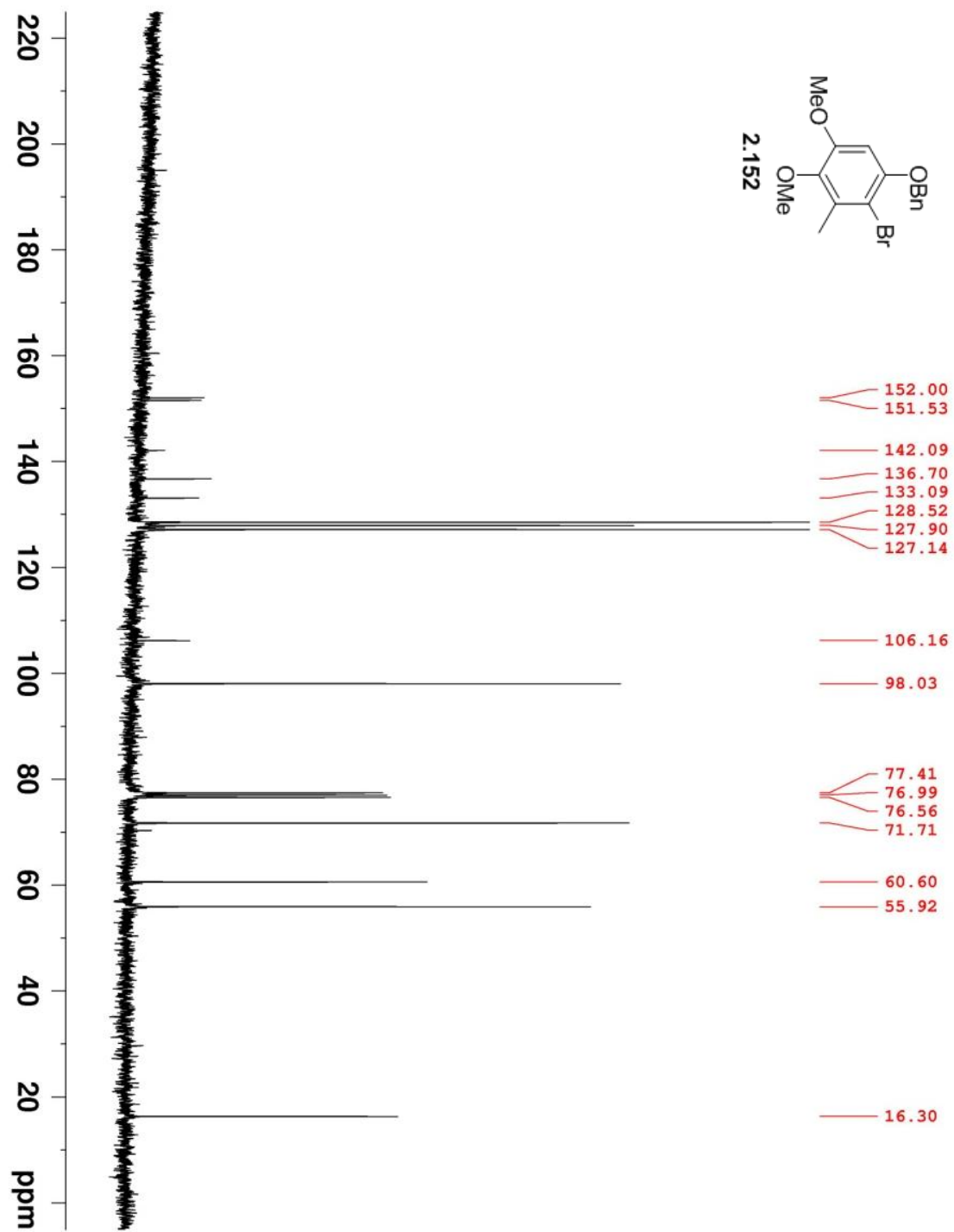


Figure A12. 75 MHz ¹³C NMR of **2.152** in CDCl₃.

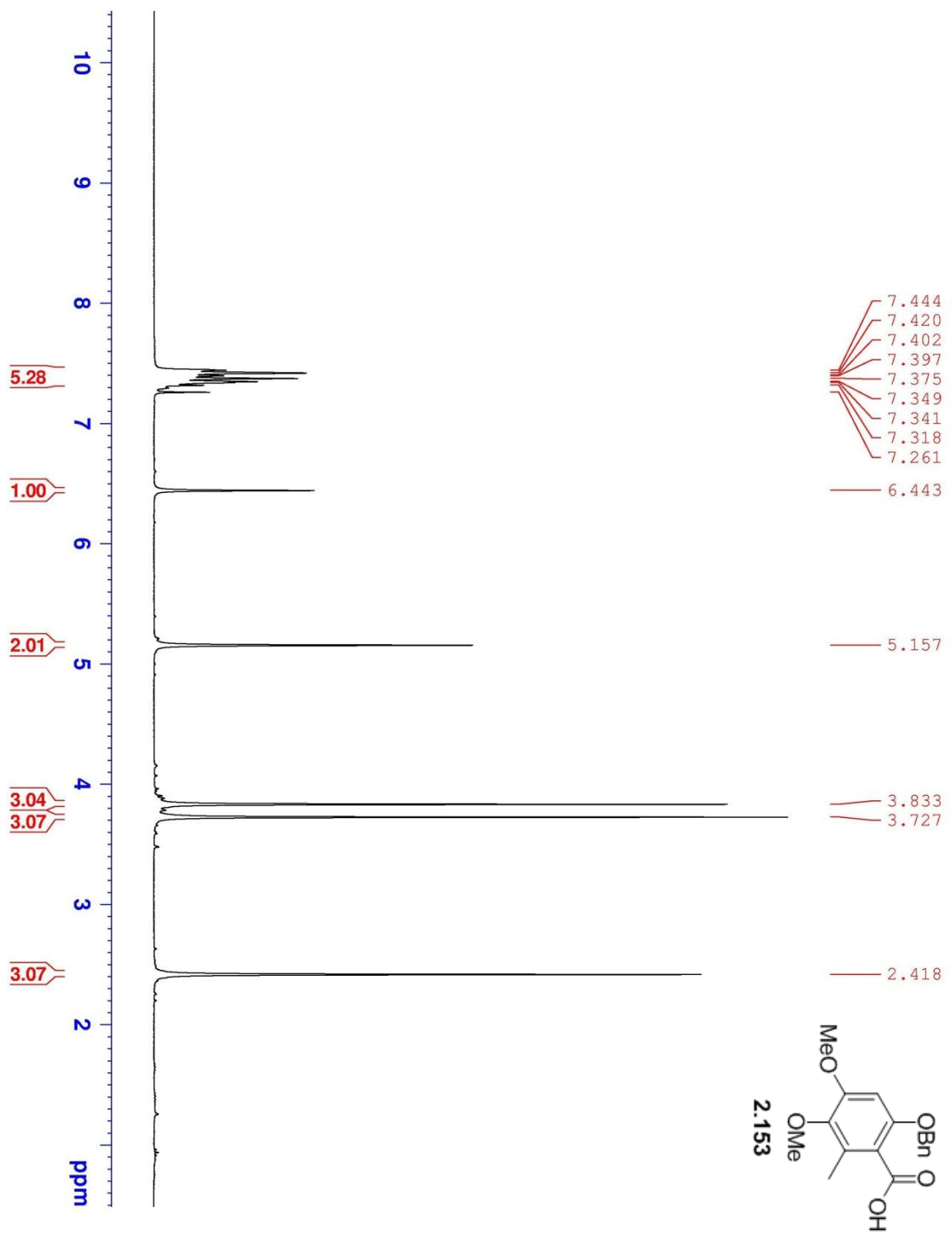


Figure A13. 300 MHz ^1H NMR of **2.153** in CDCl_3 .

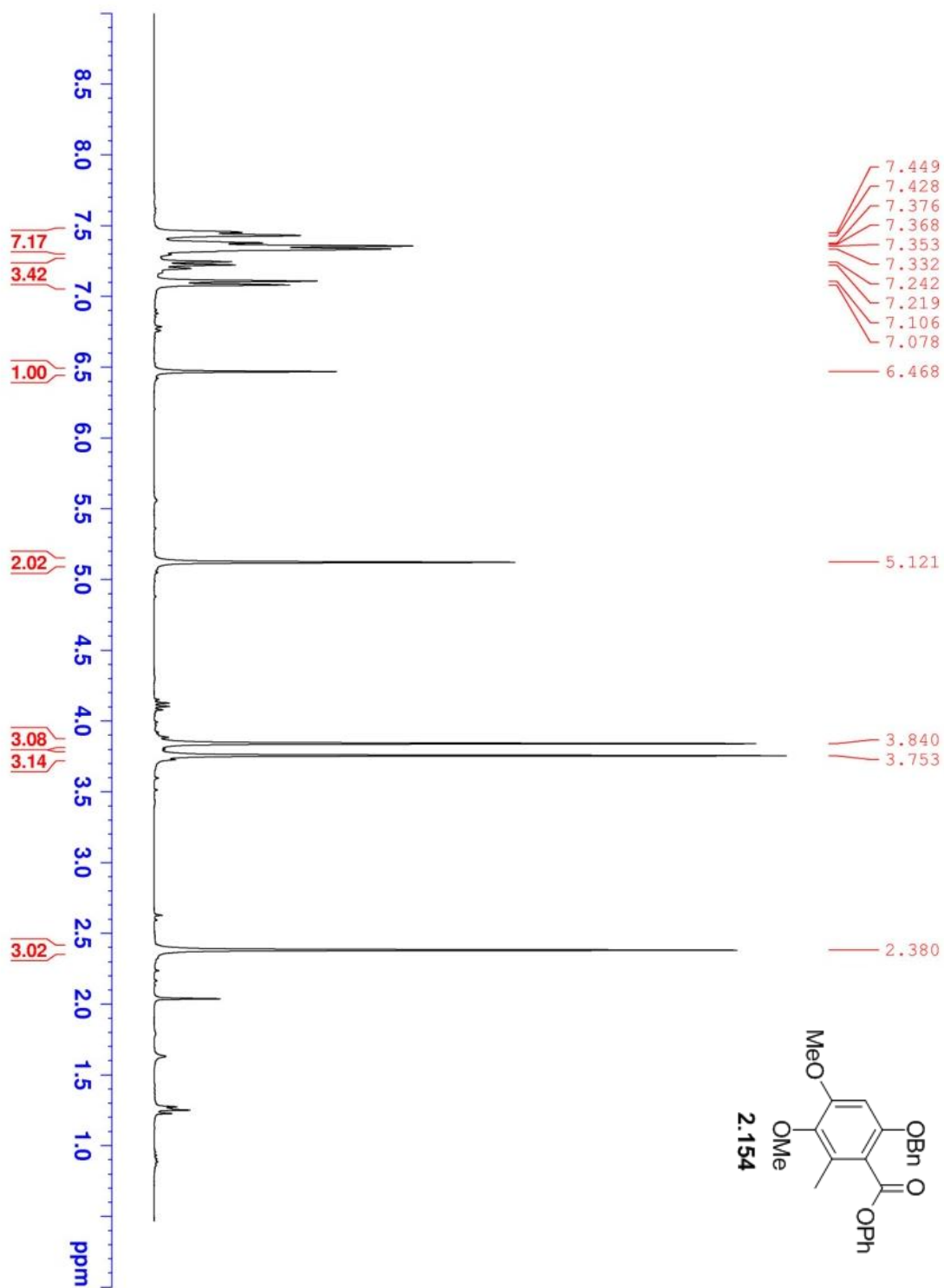


Figure A14. 300 MHz ^1H NMR of **2.154** in CDCl_3 .

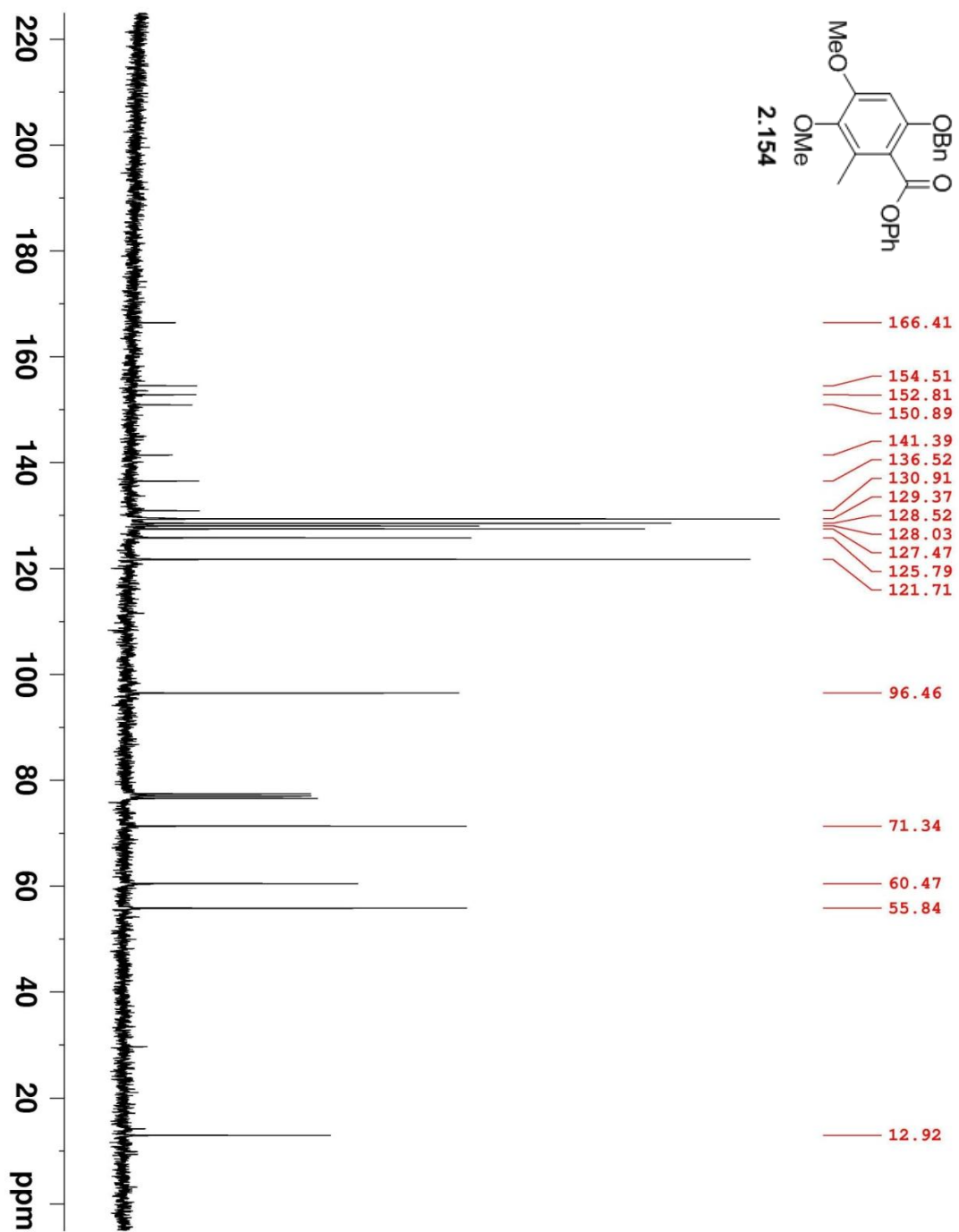


Figure A15. 75 MHz ^{13}C NMR of **2.154** in CDCl_3 .

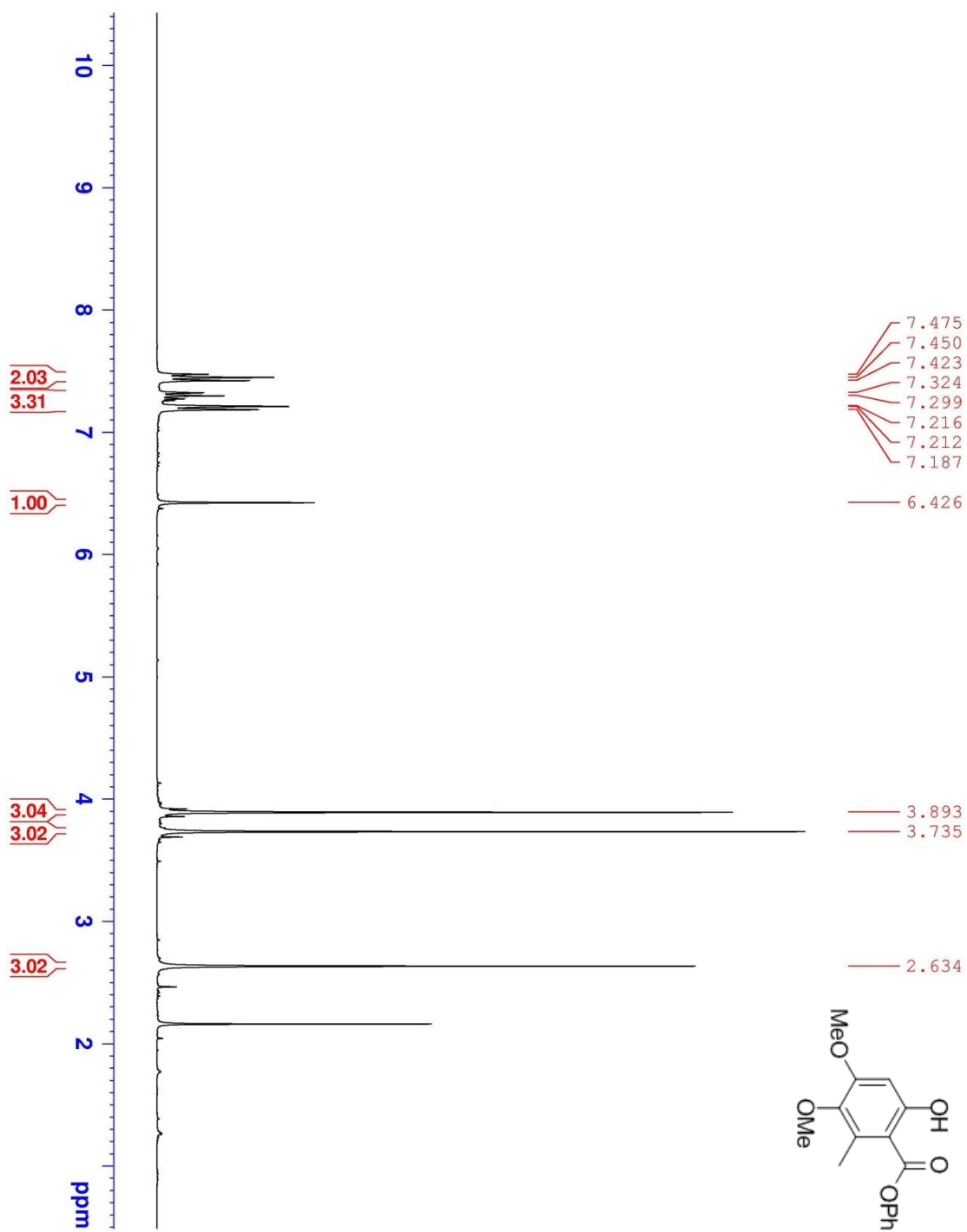


Figure A16. 300 MHz ¹H NMR of Phenyl 6-hydroxy-3,4-dimethoxy-2-methylbenzoate in CDCl₃

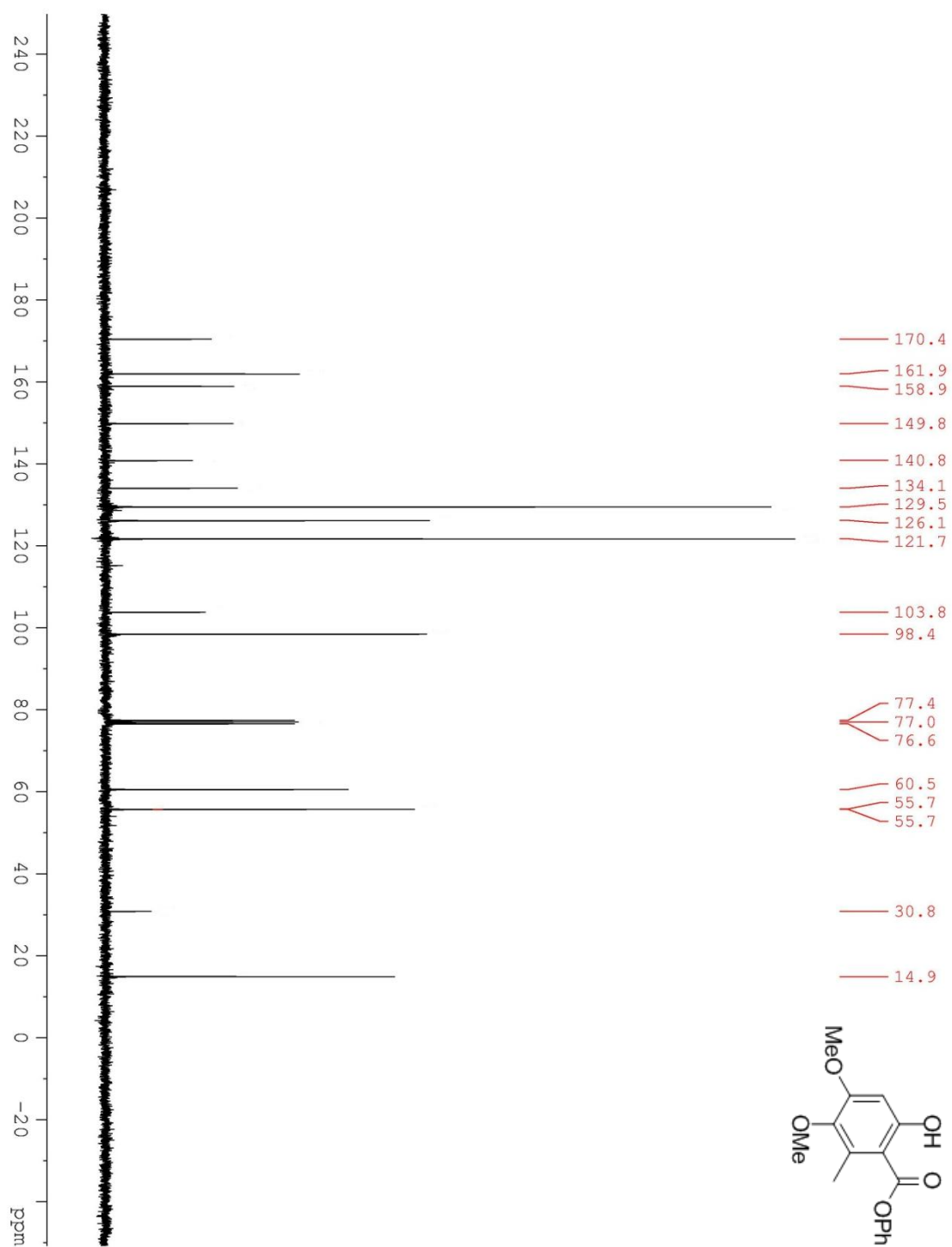


Figure A17. 75 MHz ^{13}C NMR of Phenyl 6-hydroxy-3,4-dimethoxy-2-methylbenzoate in CDCl_3

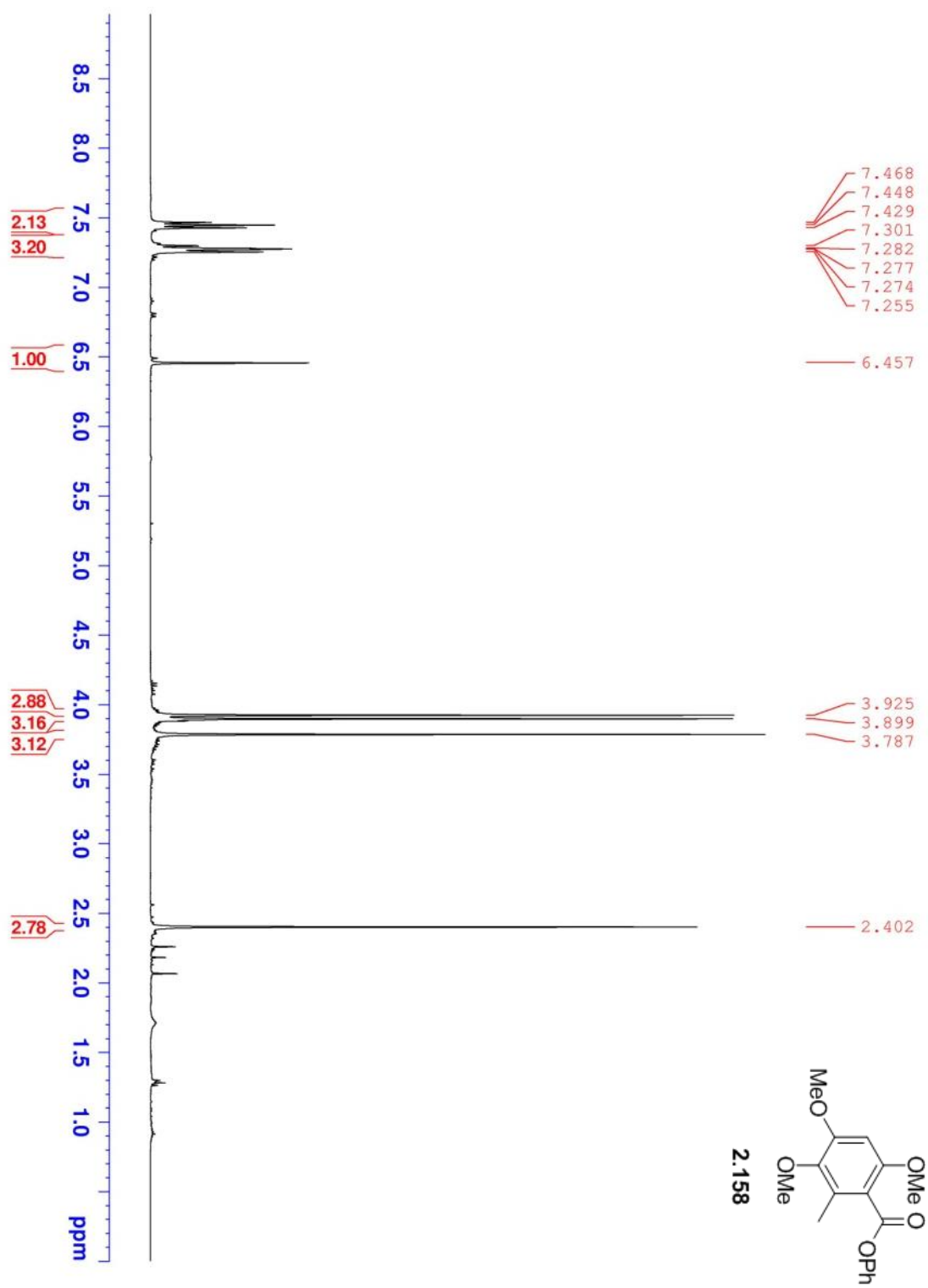


Figure A18. 300 MHz ^1H NMR of **2.158** in CDCl_3 .

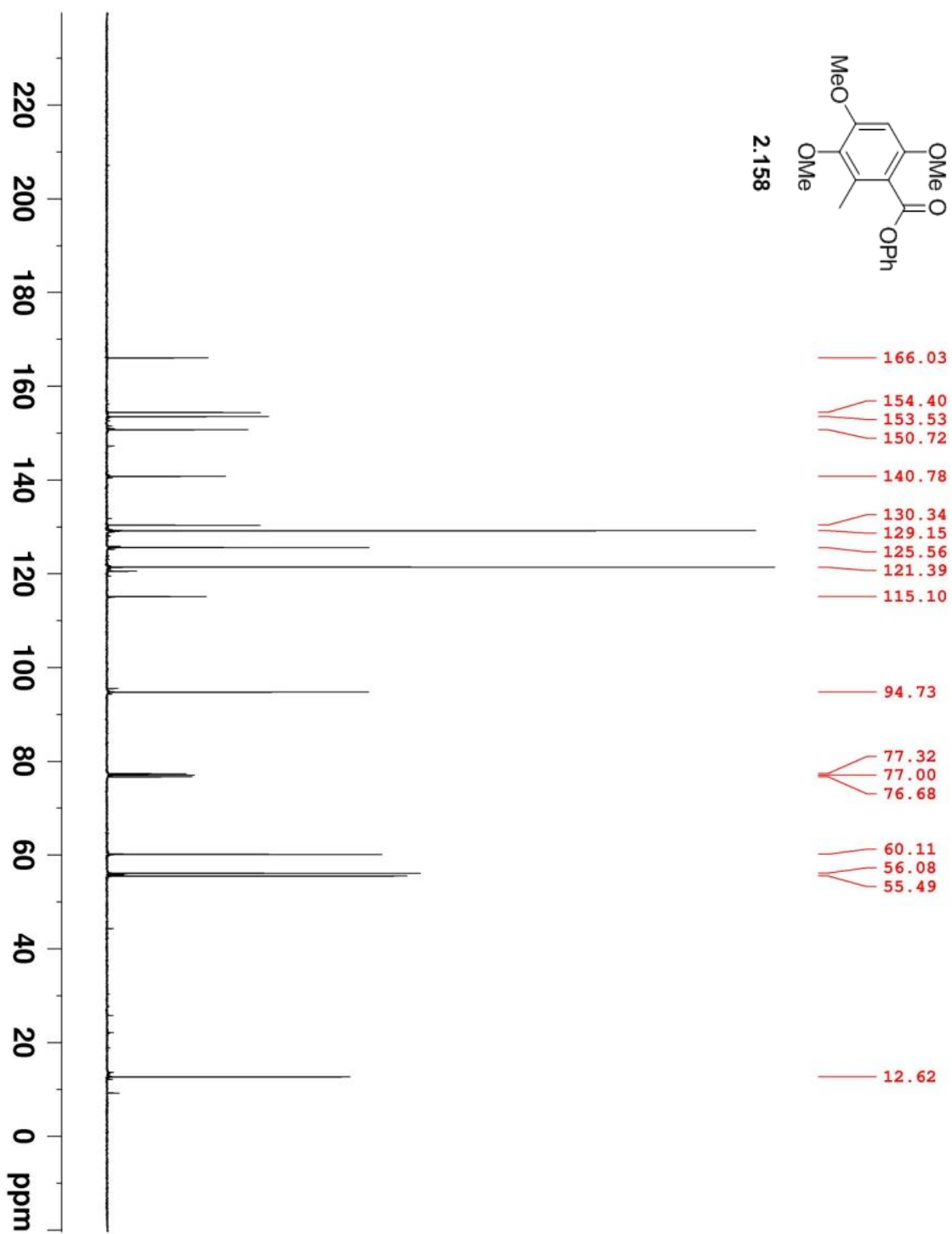


Figure A19. 75 MHz ^{13}C NMR of **2.158** in CDCl_3 .

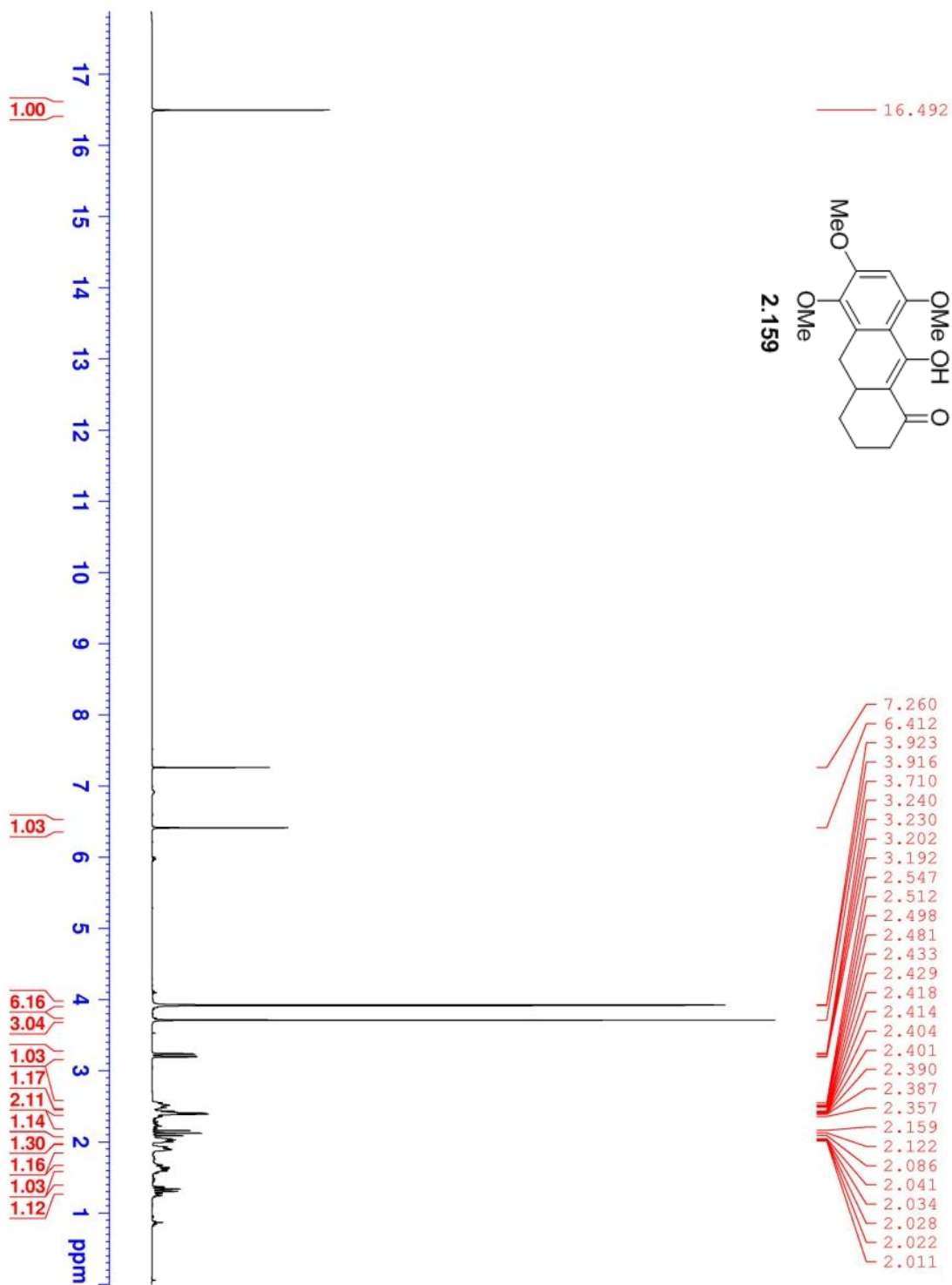


Figure A20. 300 MHz ^1H NMR of **2.159** in CDCl_3 .

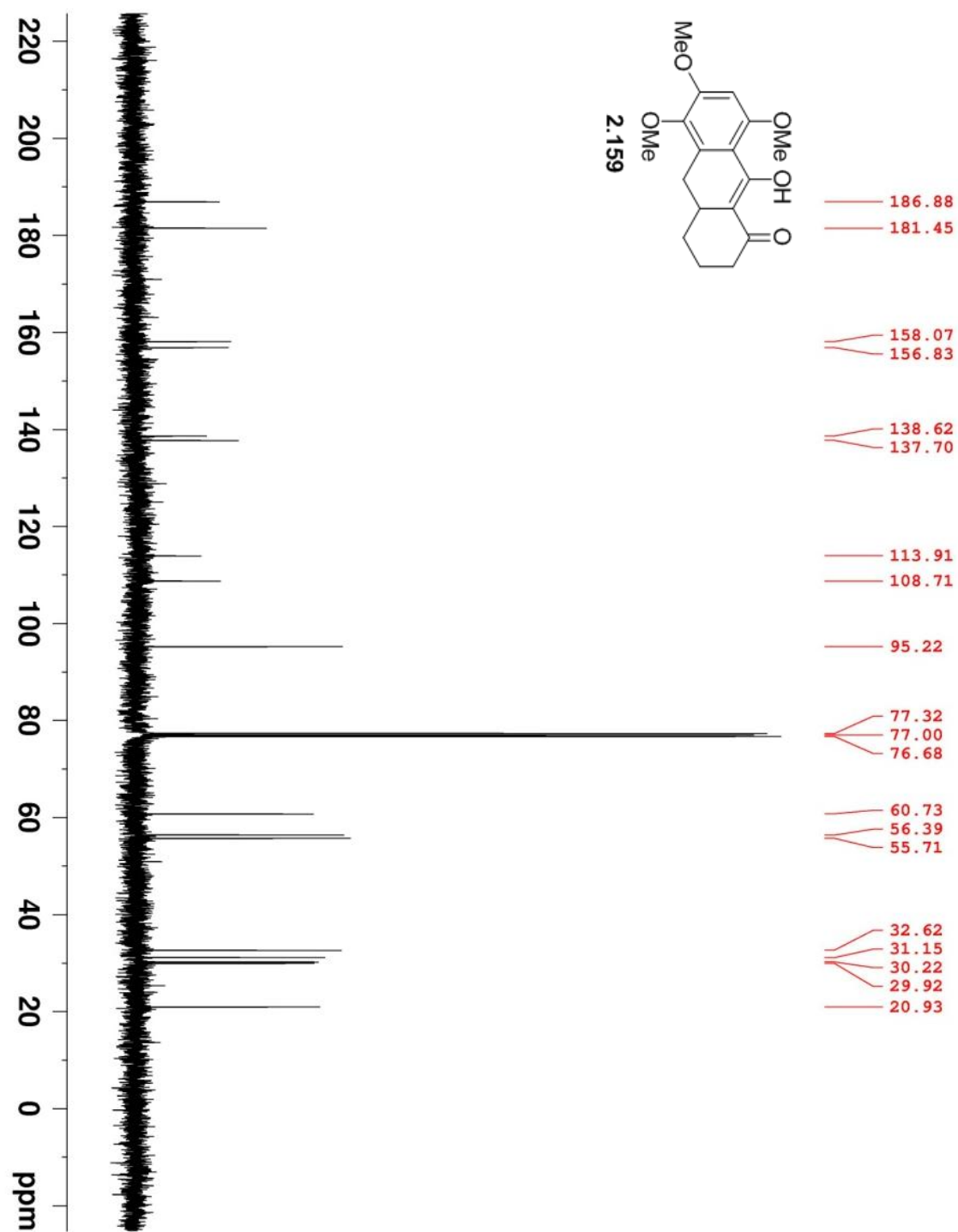


Figure A21. 75 MHz ^{13}C NMR of **2.159** in CDCl_3 .

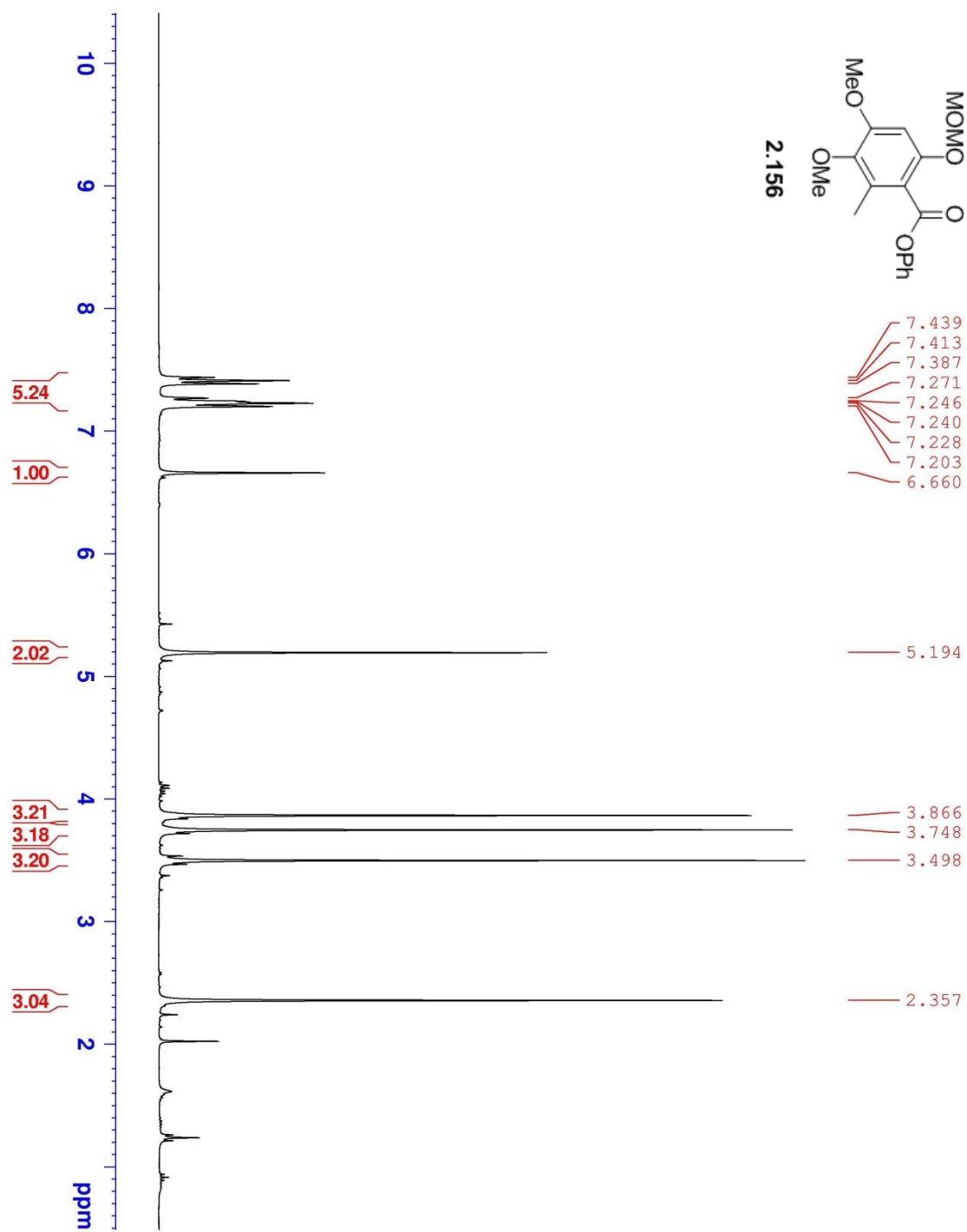


Figure A22. 300 MHz ^1H NMR of **2.156** in CDCl_3 .

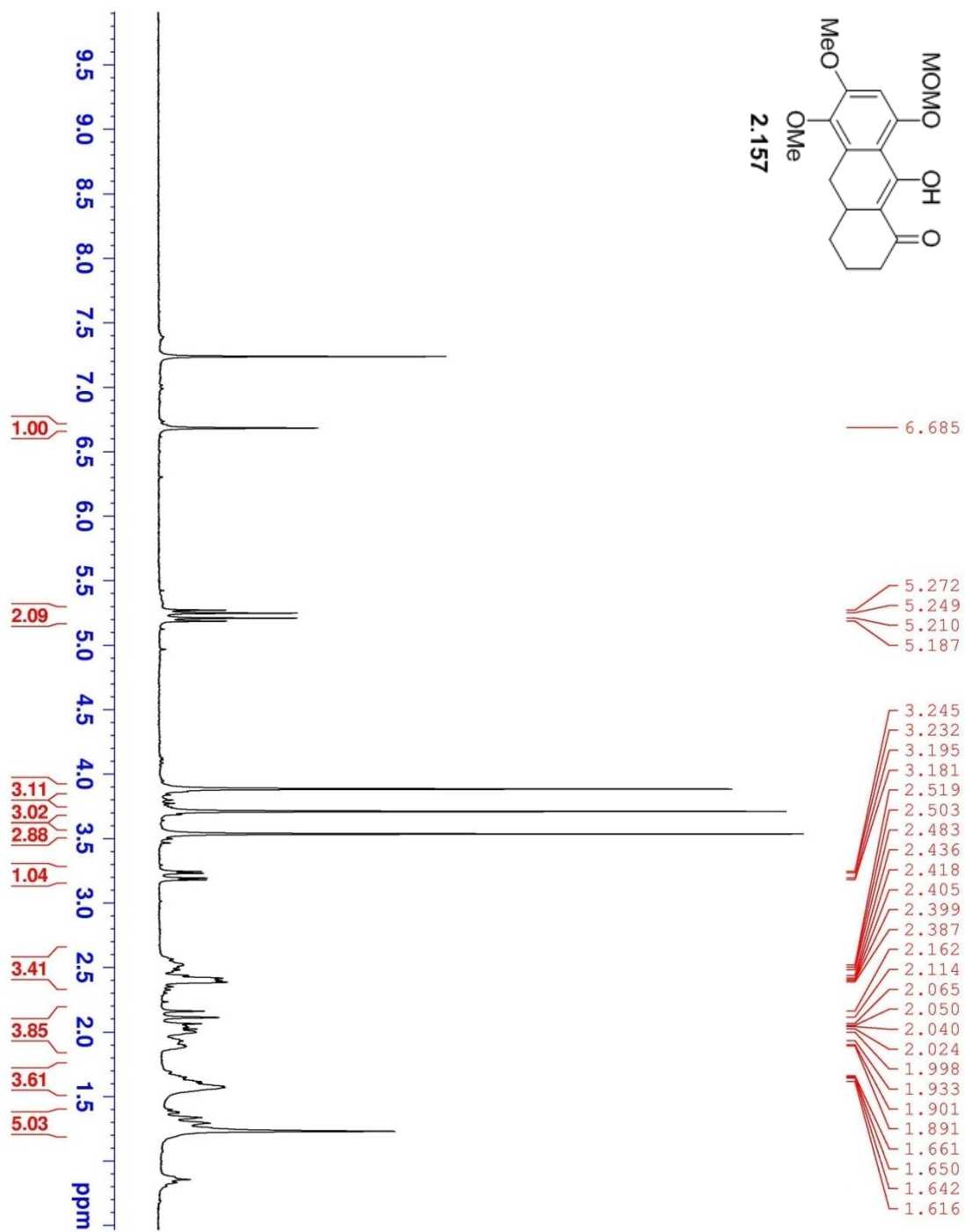


Figure A23. 300 MHz ¹H NMR of **2.157** in CDCl₃.

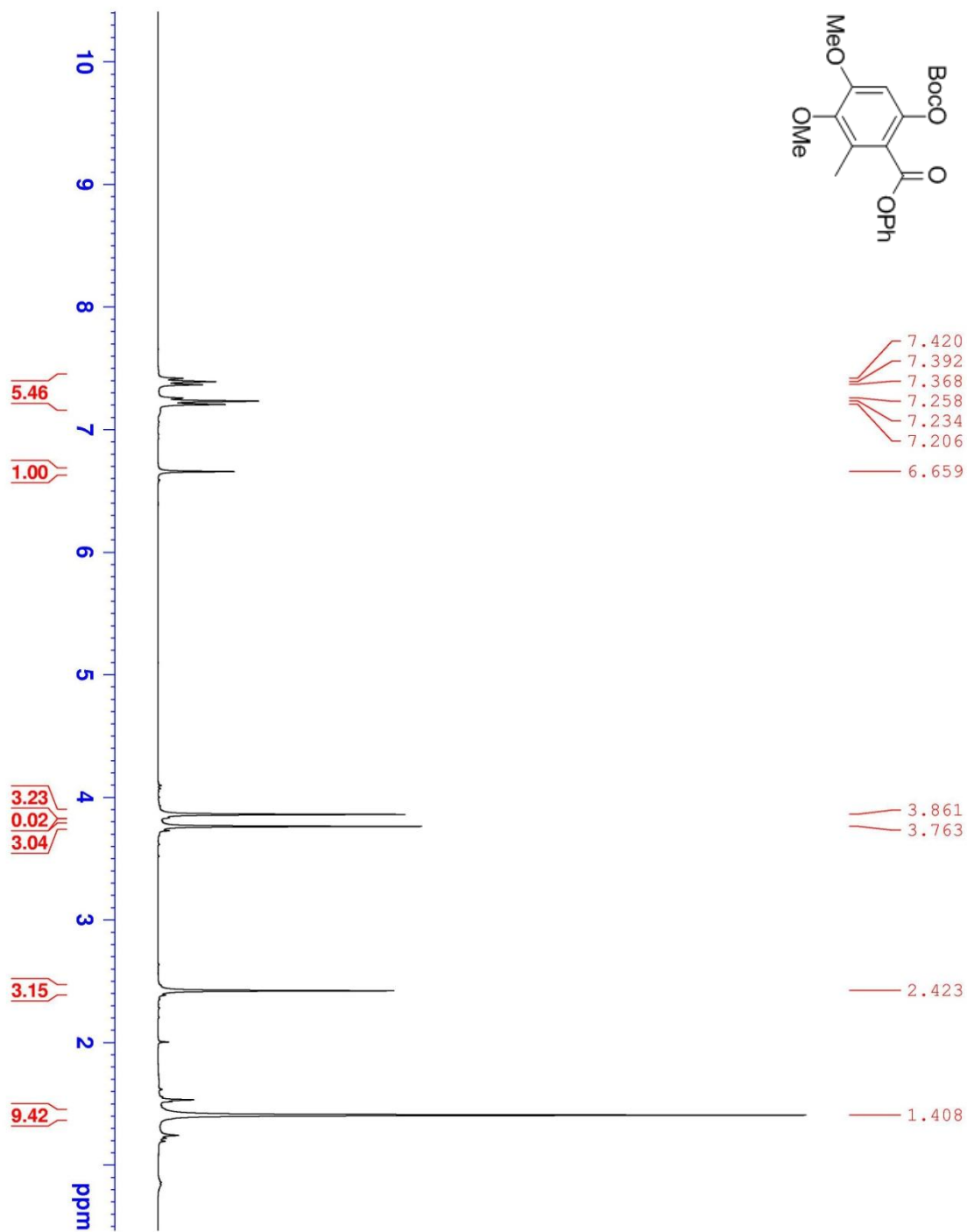


Figure A24. 300 MHz ¹H NMR of Phenyl 6-(tert-butoxycarbonyloxy)-3,4-dimethoxy-2-methylbenzoate in CDCl₃.

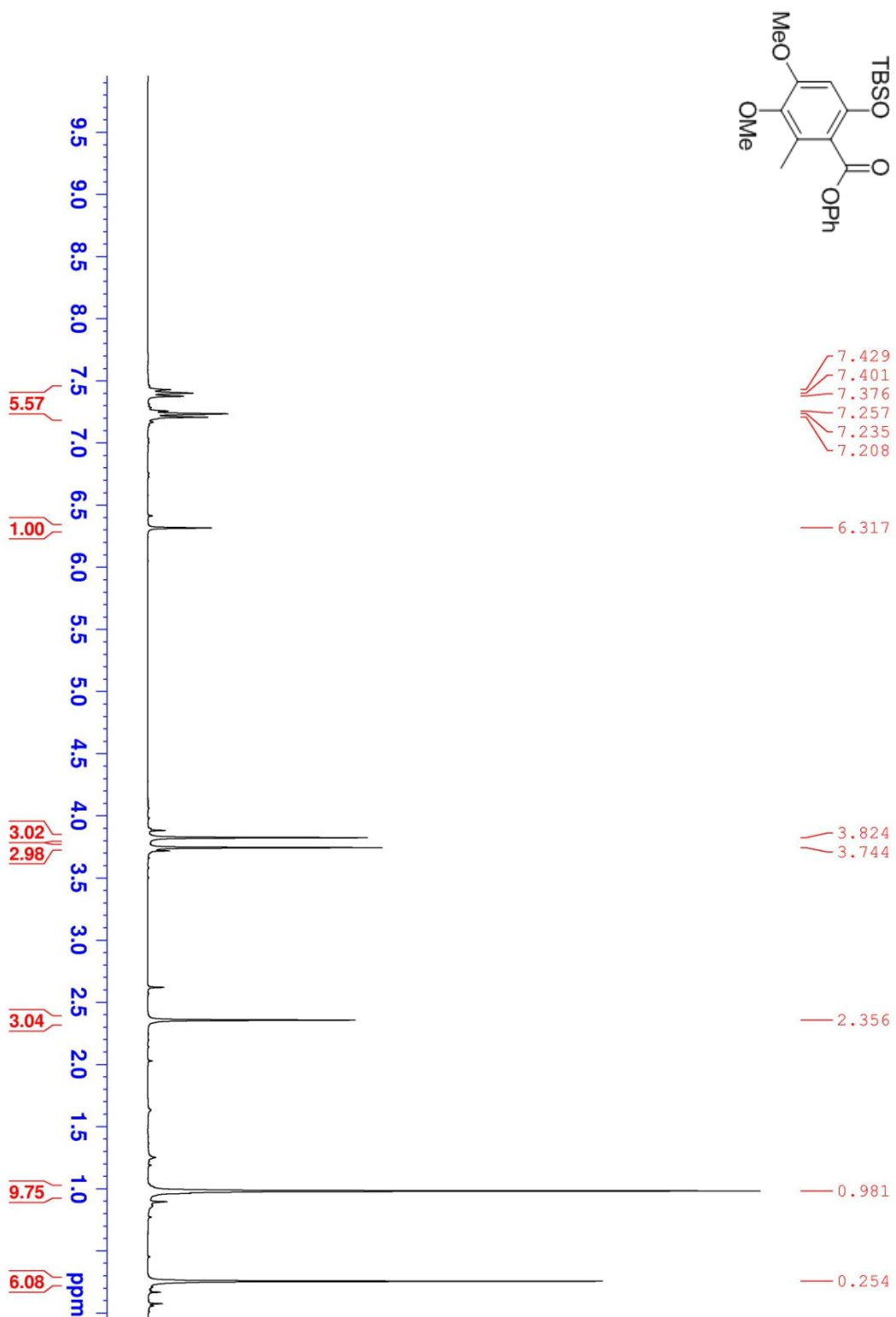


Figure A25. 300 MHz ¹H NMR of Phenyl 6-(tert-butyl dimethylsilyloxy)-3,4-dimethoxy-2-methylbenzoate in CDCl₃.

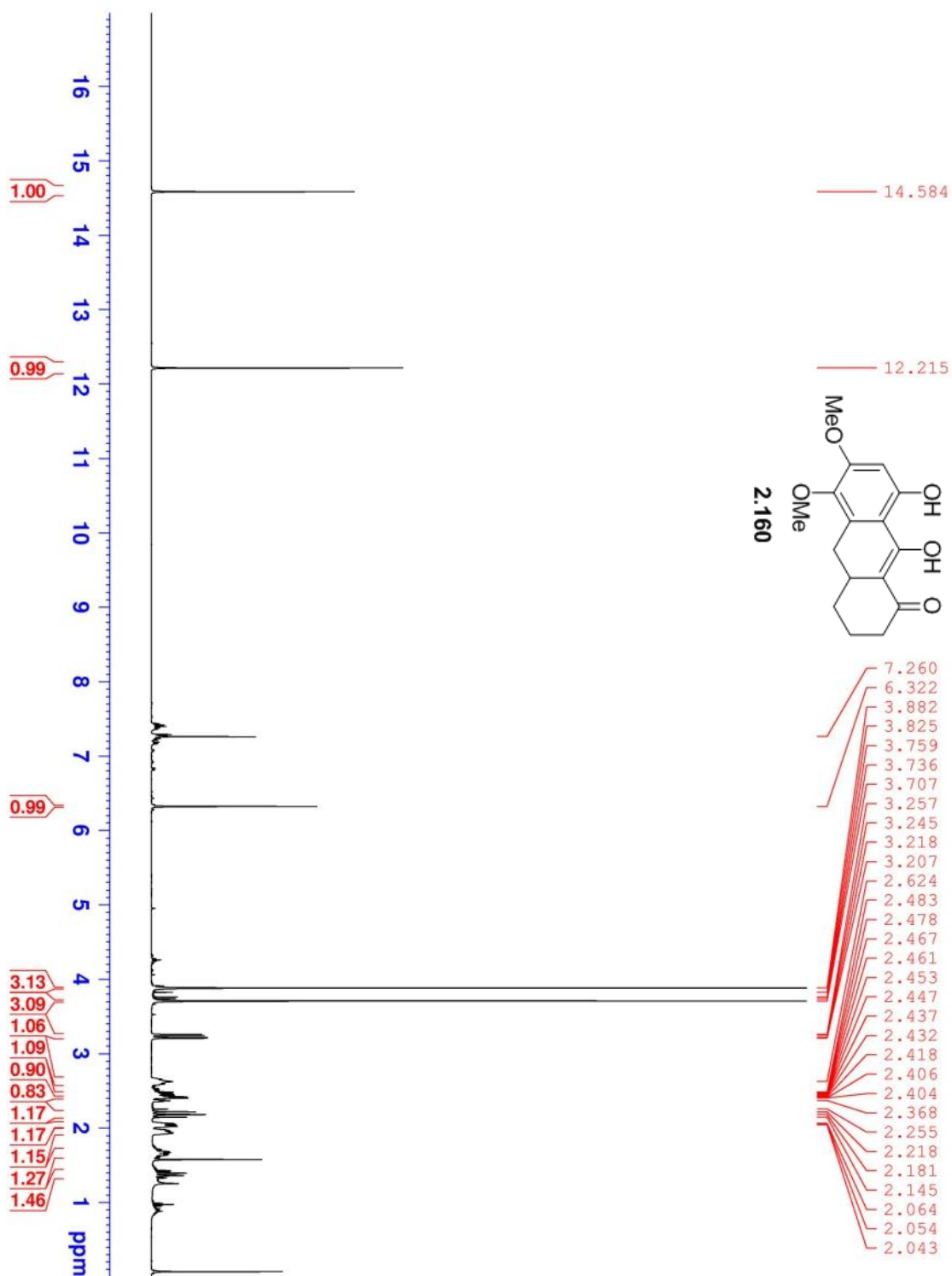


Figure A26. 400 MHz ^1H NMR of **2.160** in CDCl_3 .

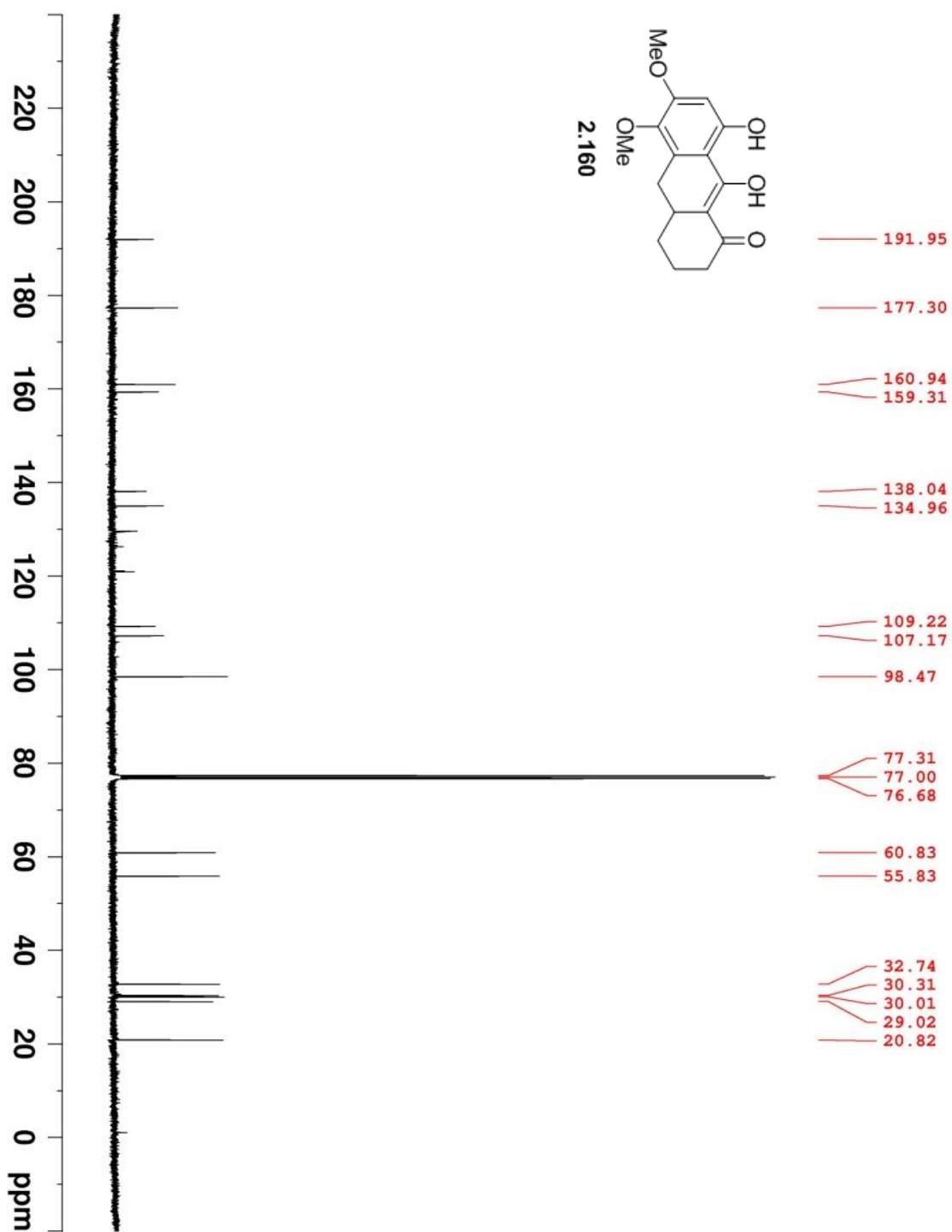


Figure A27. 100 MHz ^{13}C NMR of **2.160** in CDCl_3 .

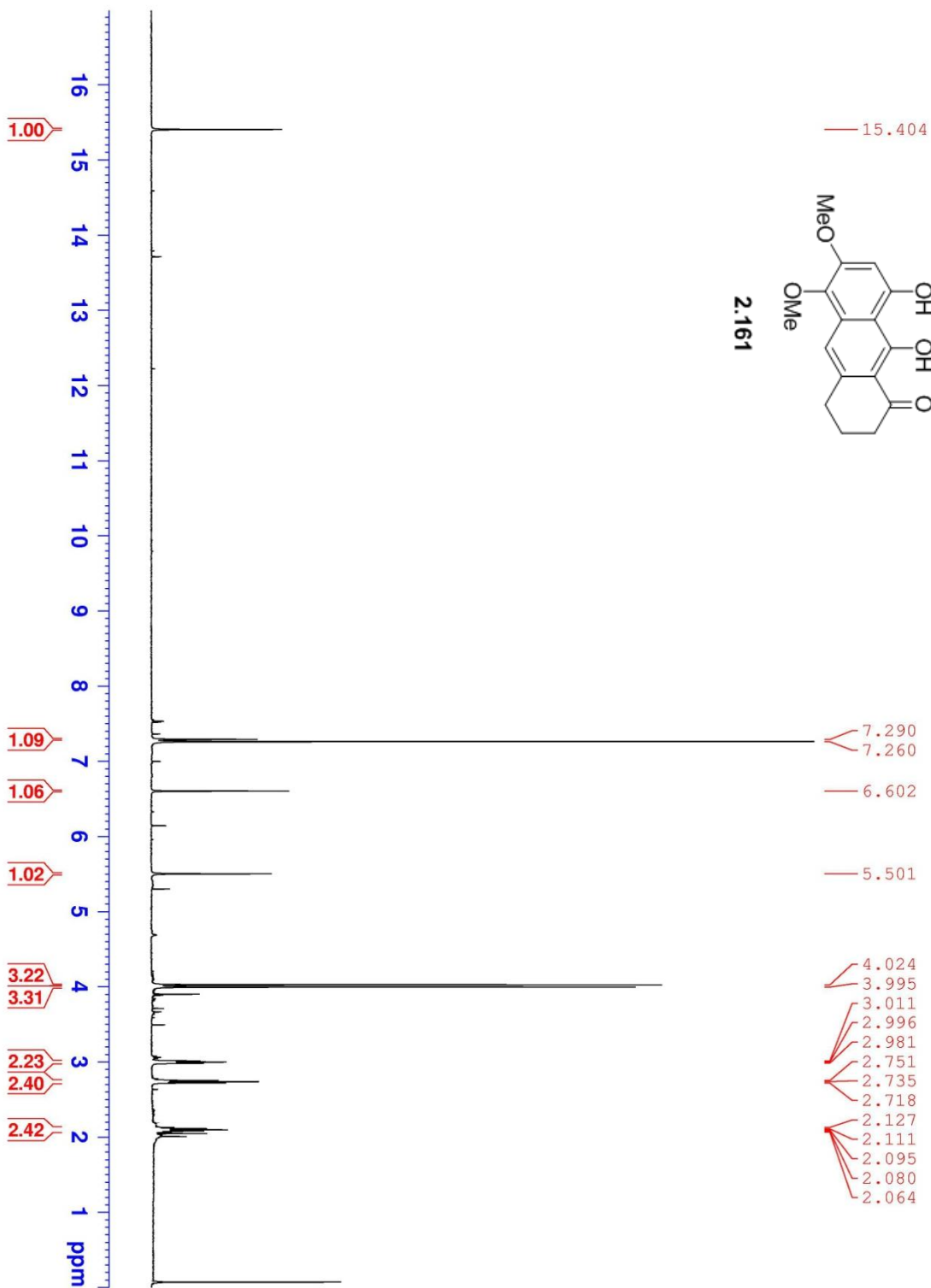


Figure A28. 400 MHz ^1H NMR of **2.161** in CDCl_3 .

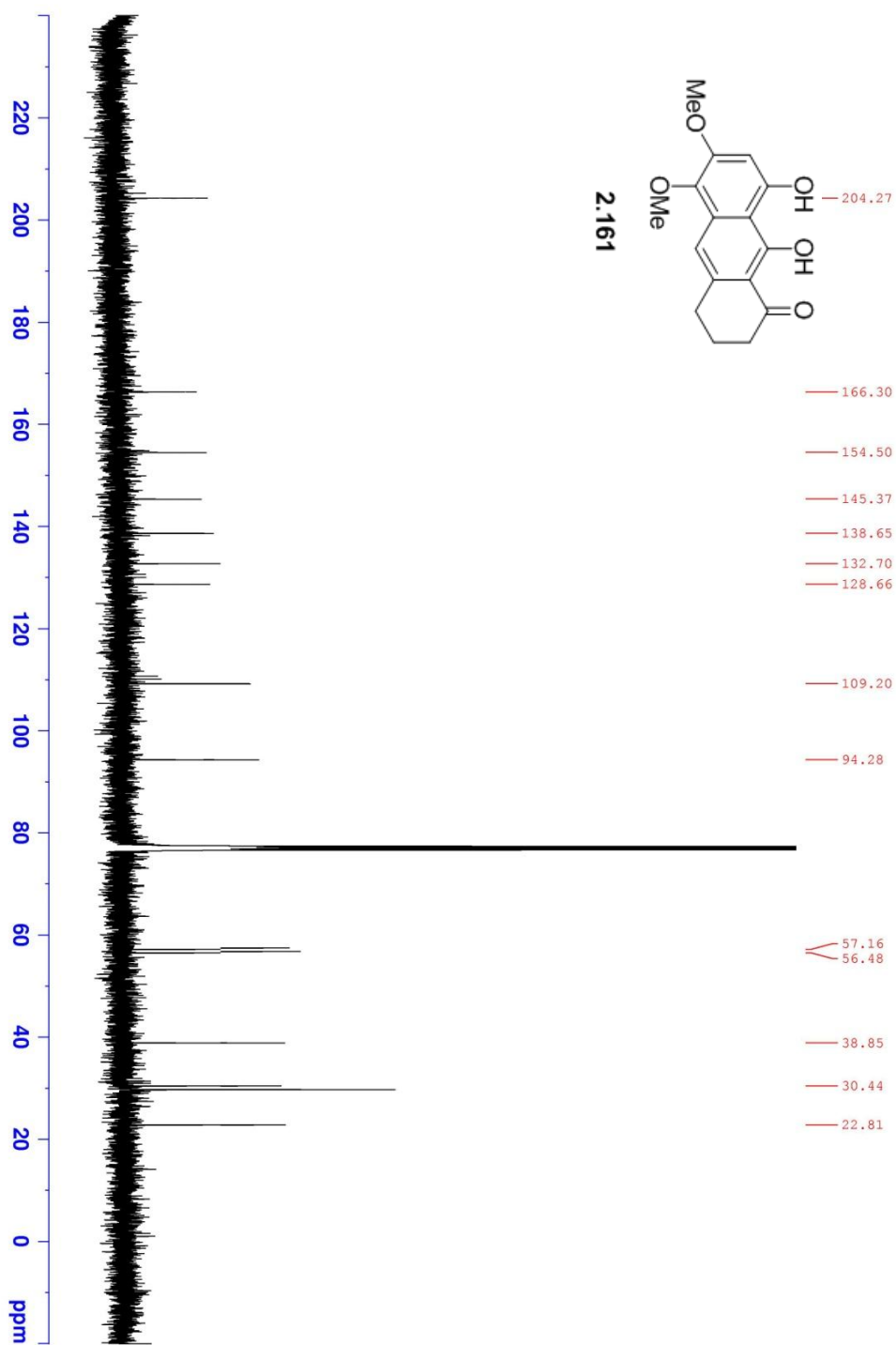


Figure A29. 100 MHz ^{13}C of **2.161** in CDCl_3 .

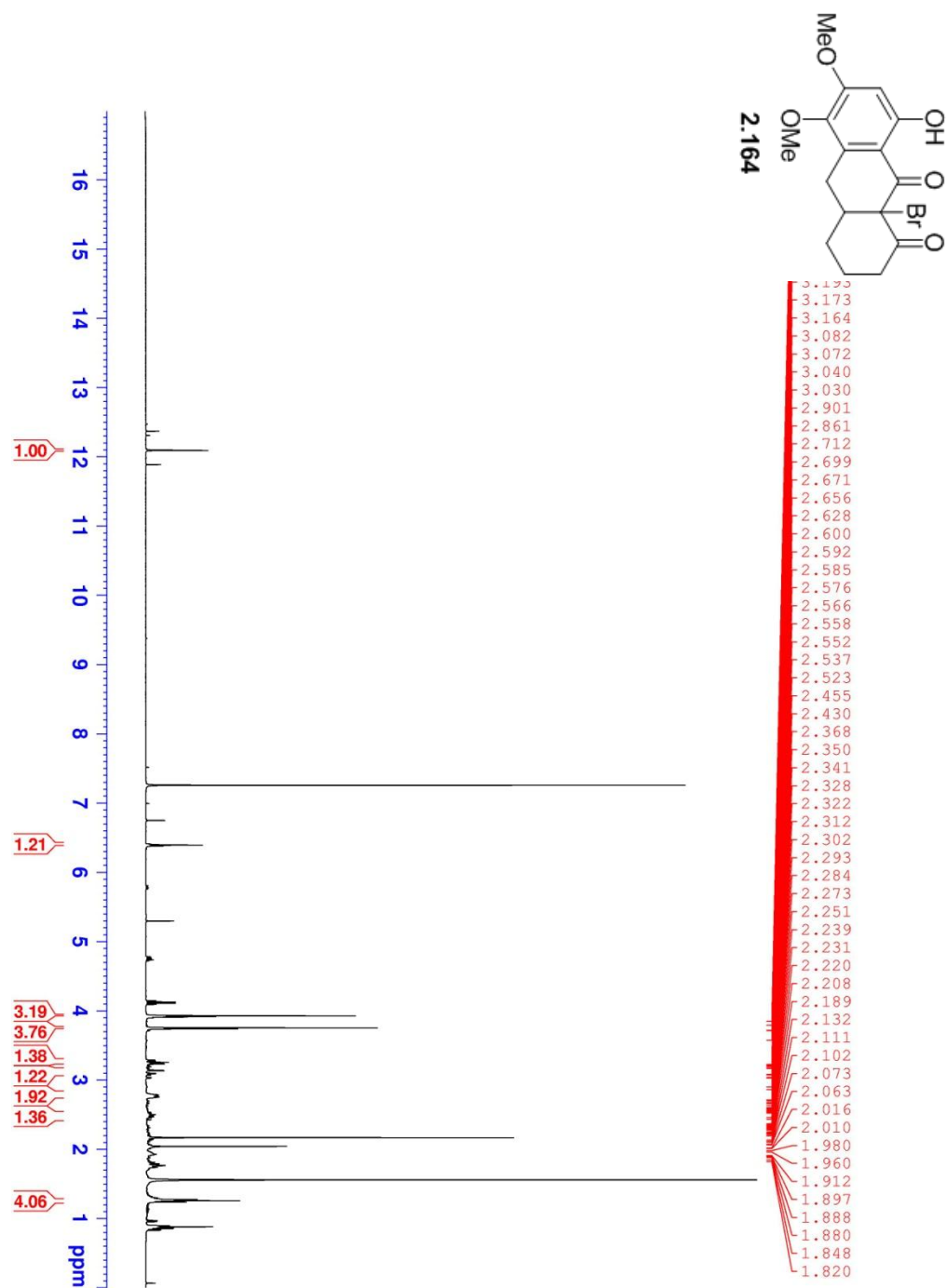


Figure A30. 400 MHz ^1H NMR of **2.164** in CDCl_3 .

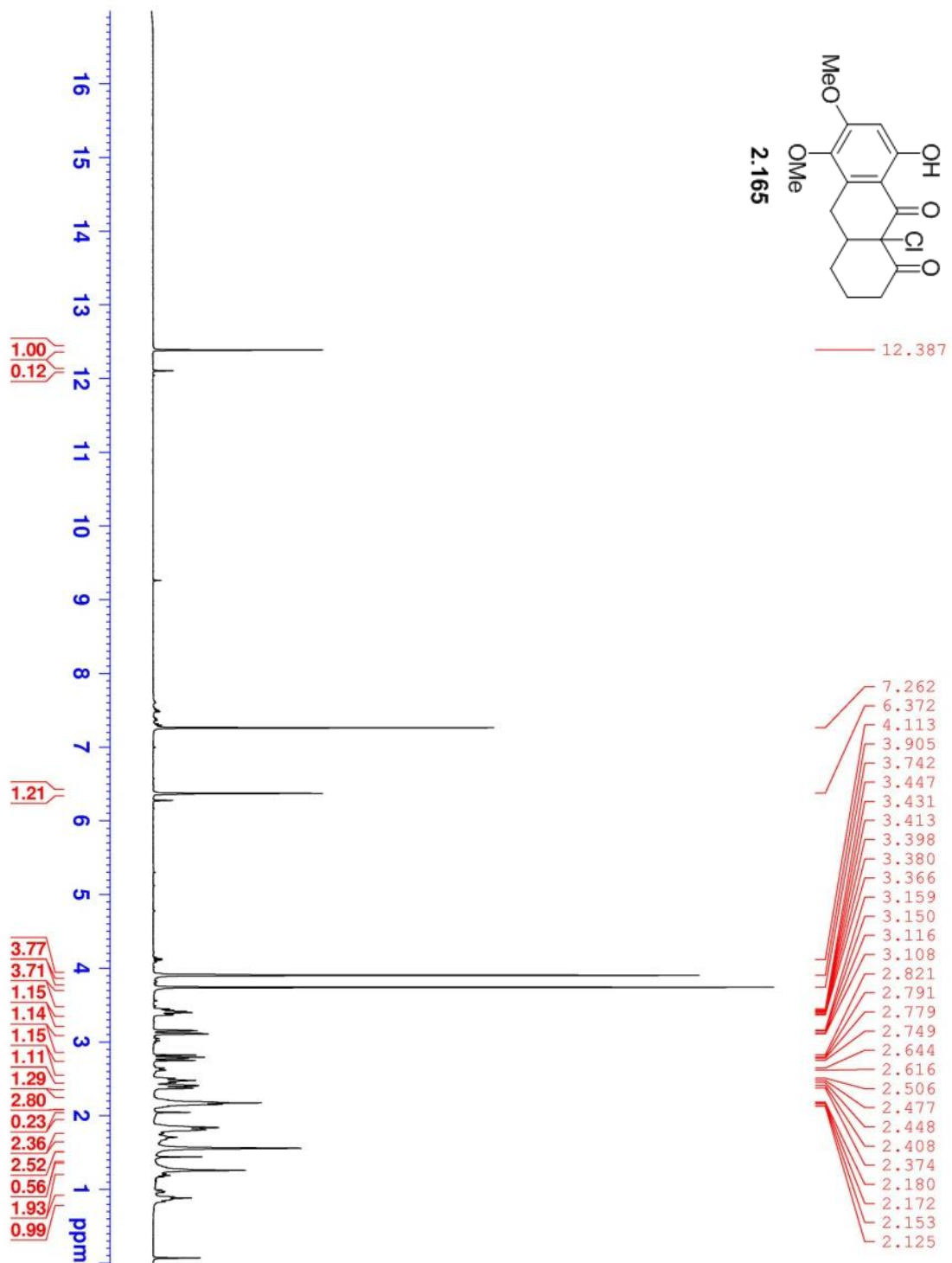


Figure A31. 400 MHz ¹H NMR of **2.160** in CDCl₃.

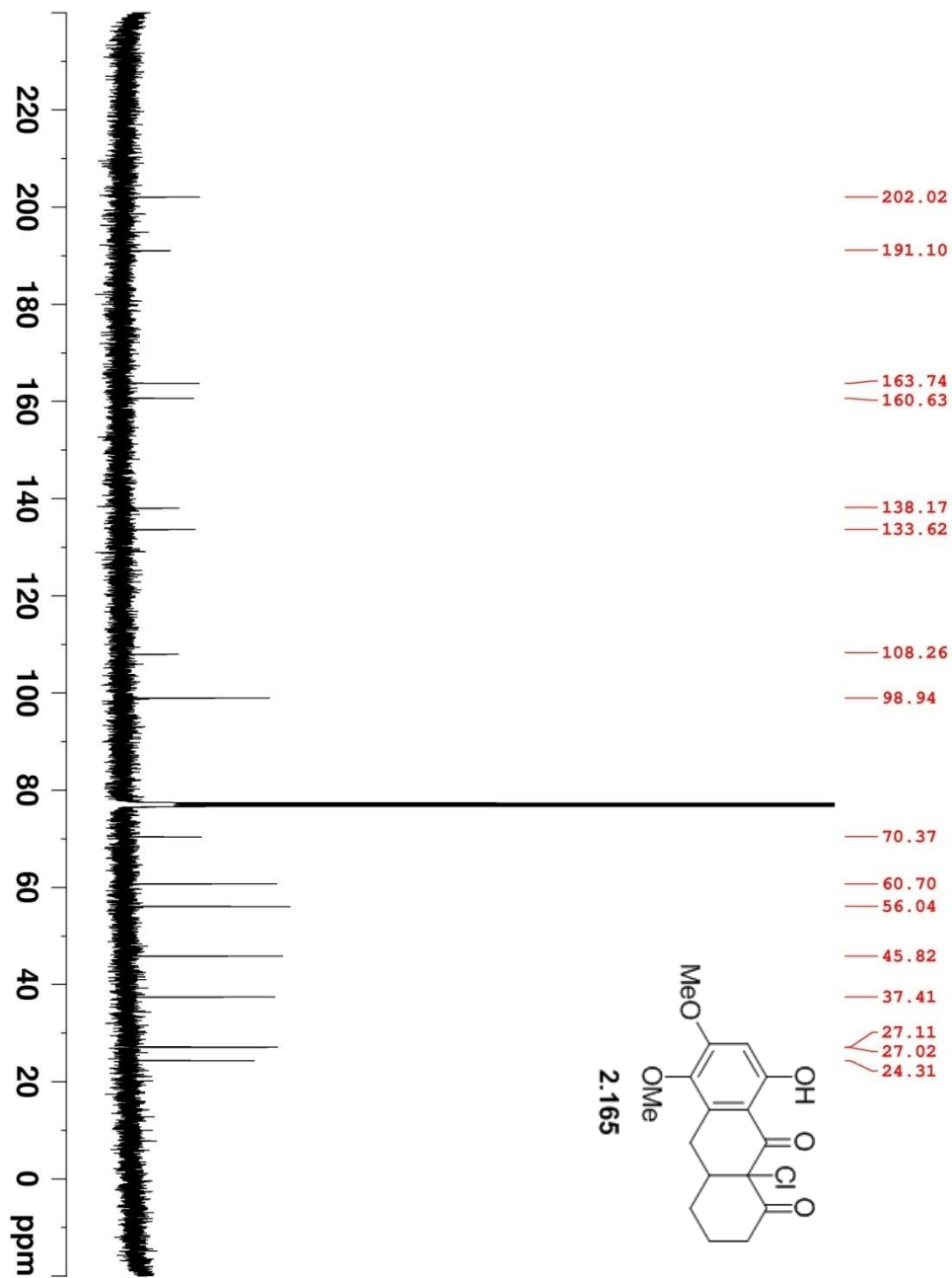


Figure A32. 100 MHz ^{13}C of **2.165** in CDCl_3 .

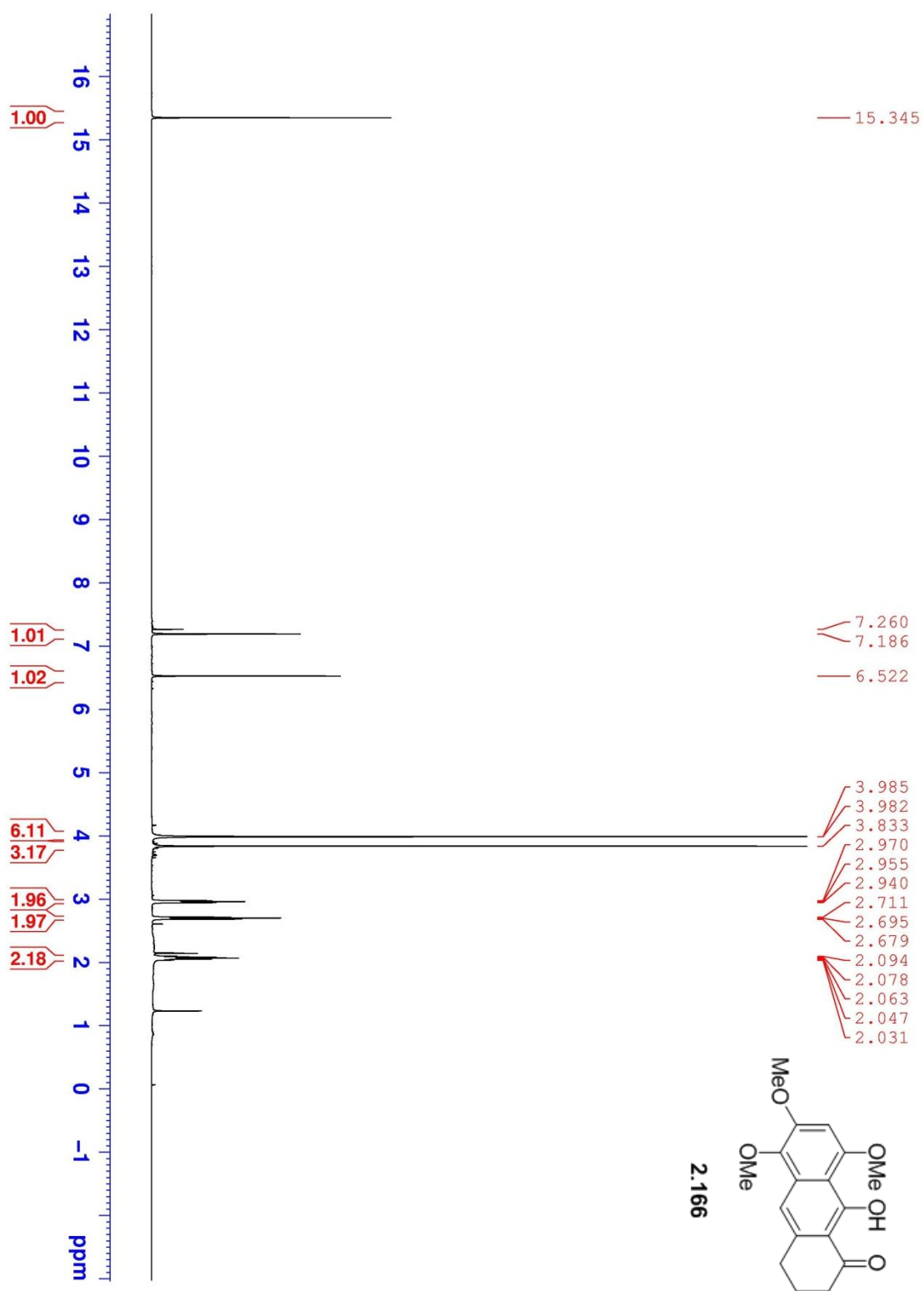


Figure A33. 400 MHz ^1H NMR of **2.166** in CDCl_3 .

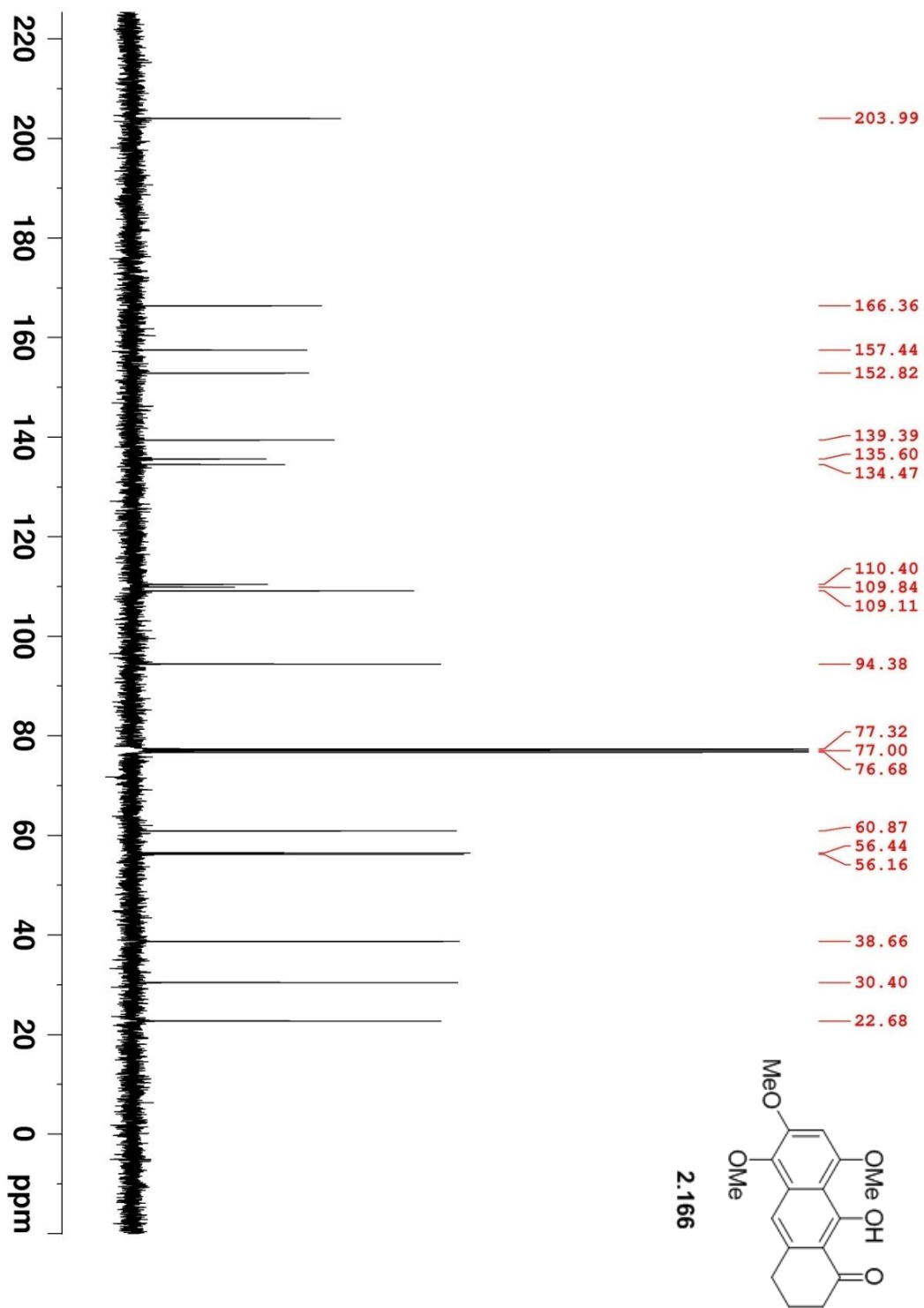


Figure A34. 100 MHz ¹³C NMR of **2.166** in CDCl₃.

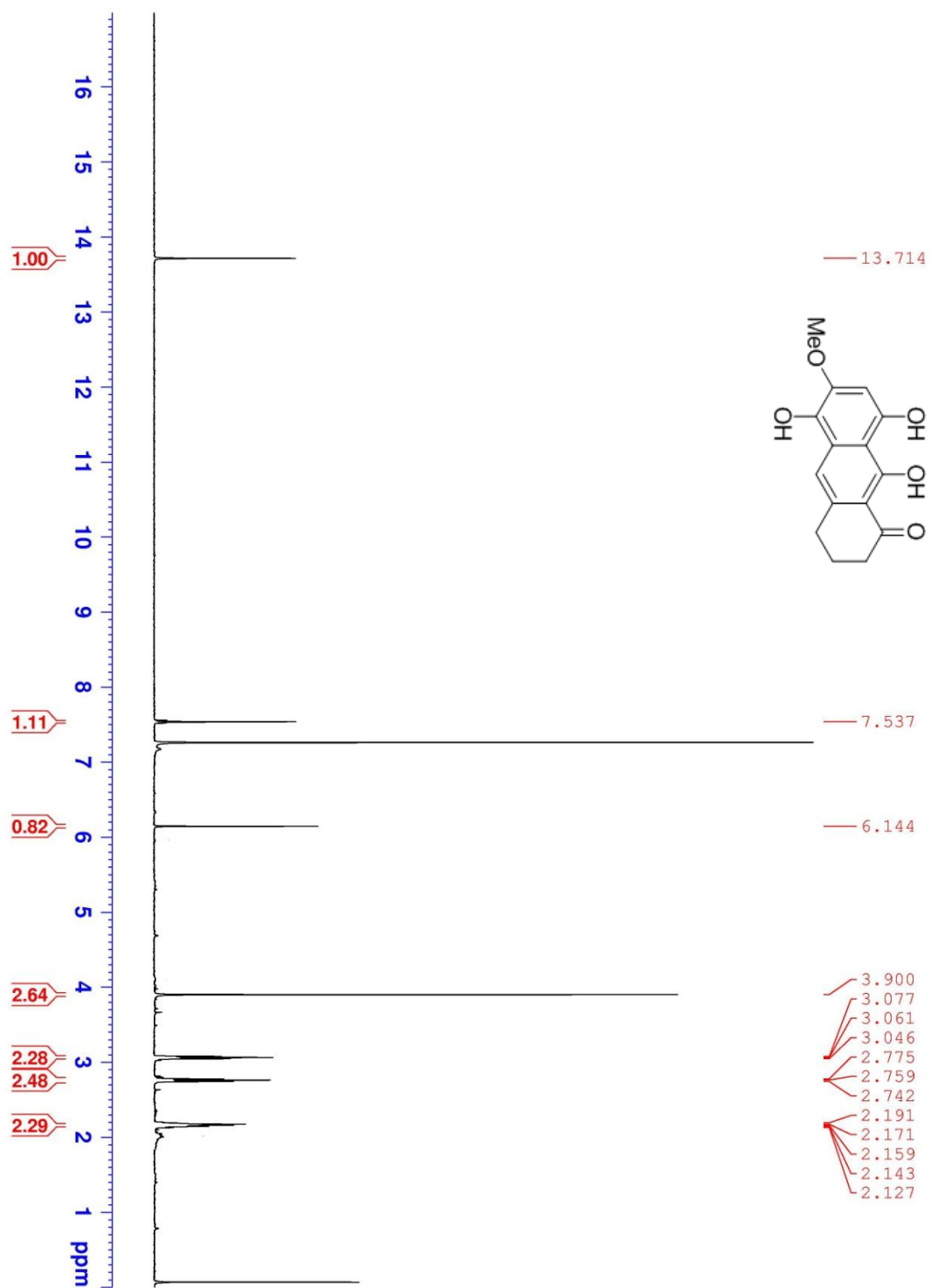


Figure A35. 400 MHz ¹H NMR of 5,8,9-trihydroxy-6-methoxy-3,4-dihydroanthracen-1(2H)-one in CDCl₃.

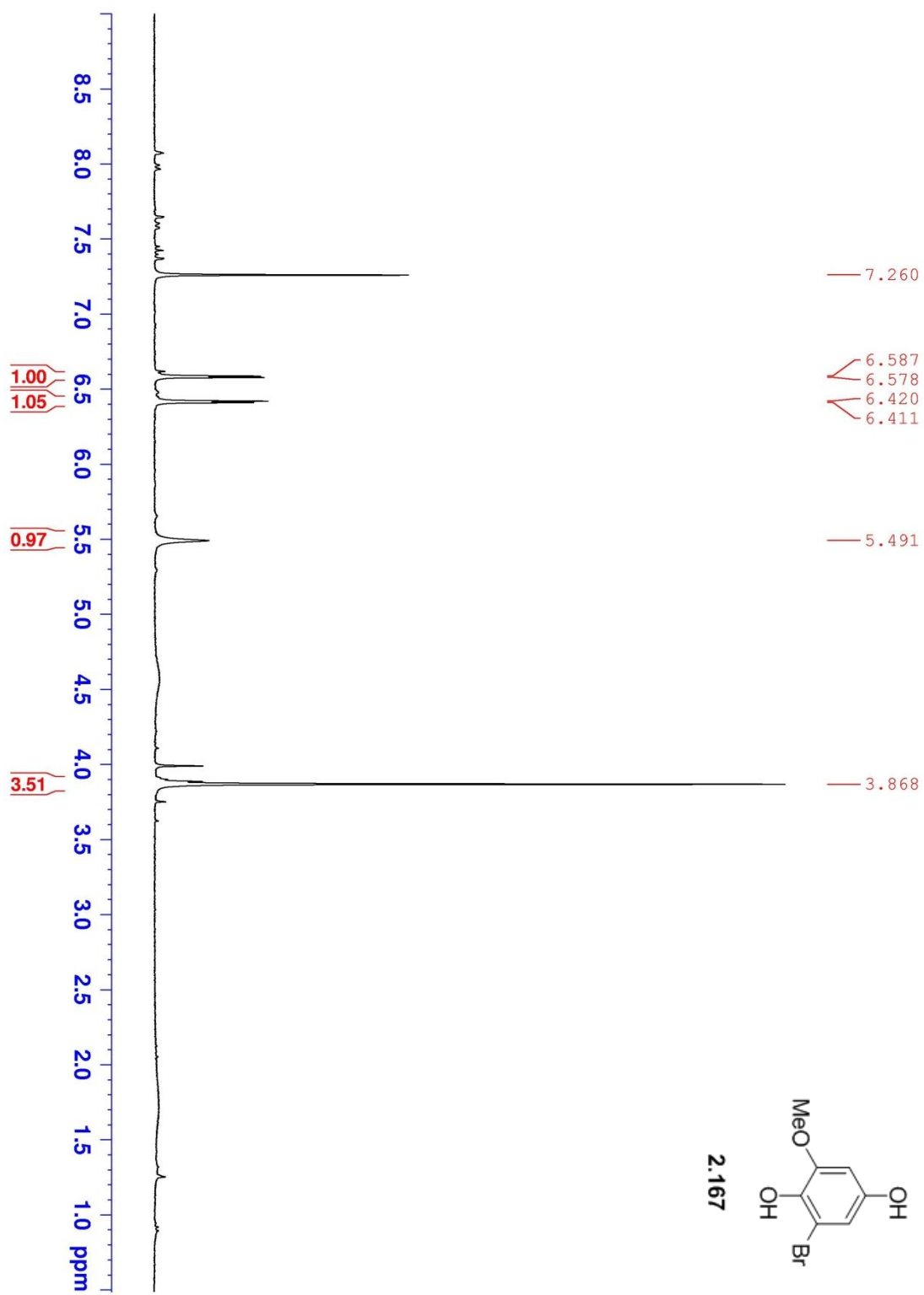


Figure A36. 400 MHz ^1H NMR of **2.167** in CDCl_3 .

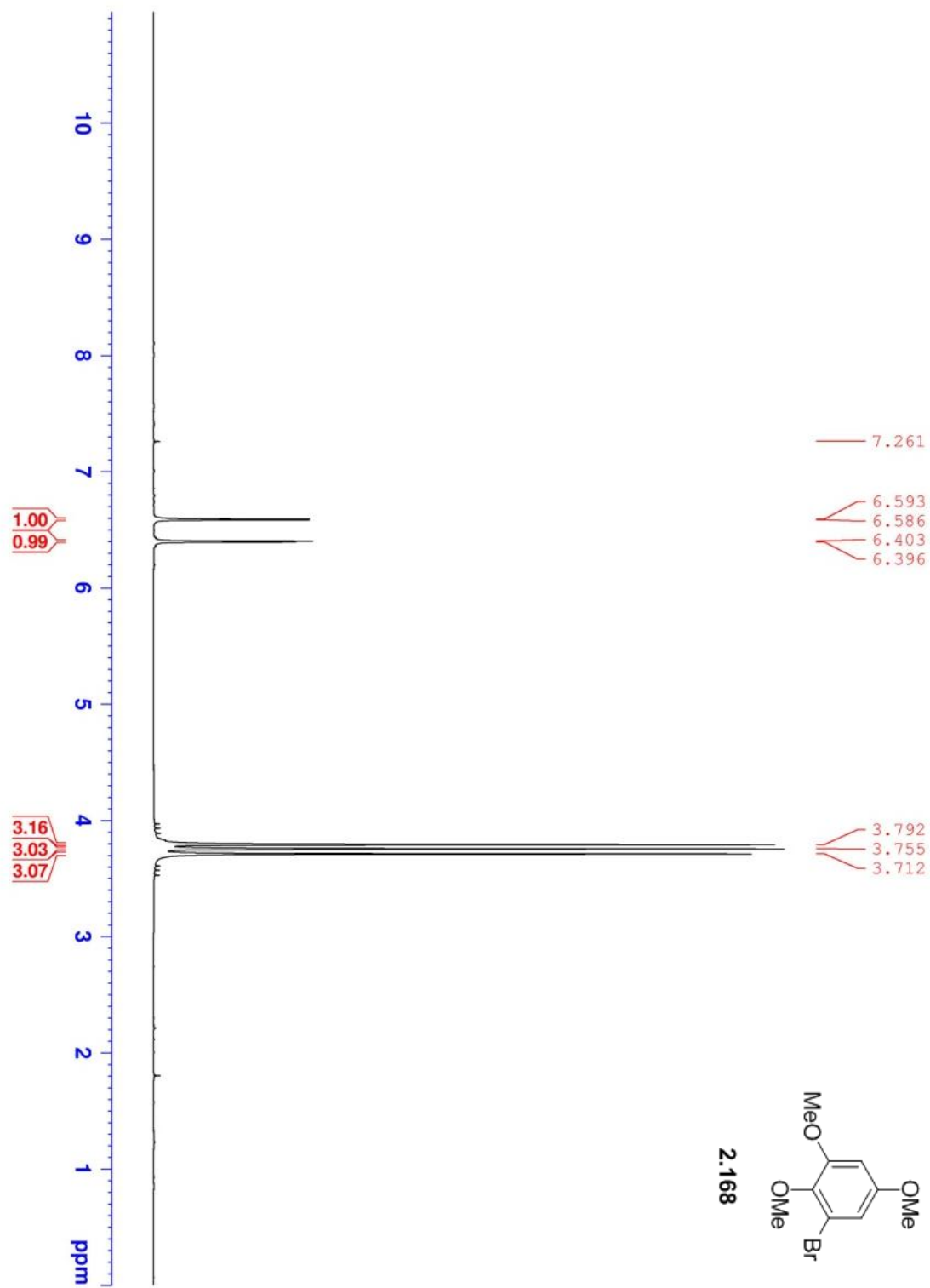


Figure A37. 400 MHz ¹H NMR of **2.168**. in CDCl₃.

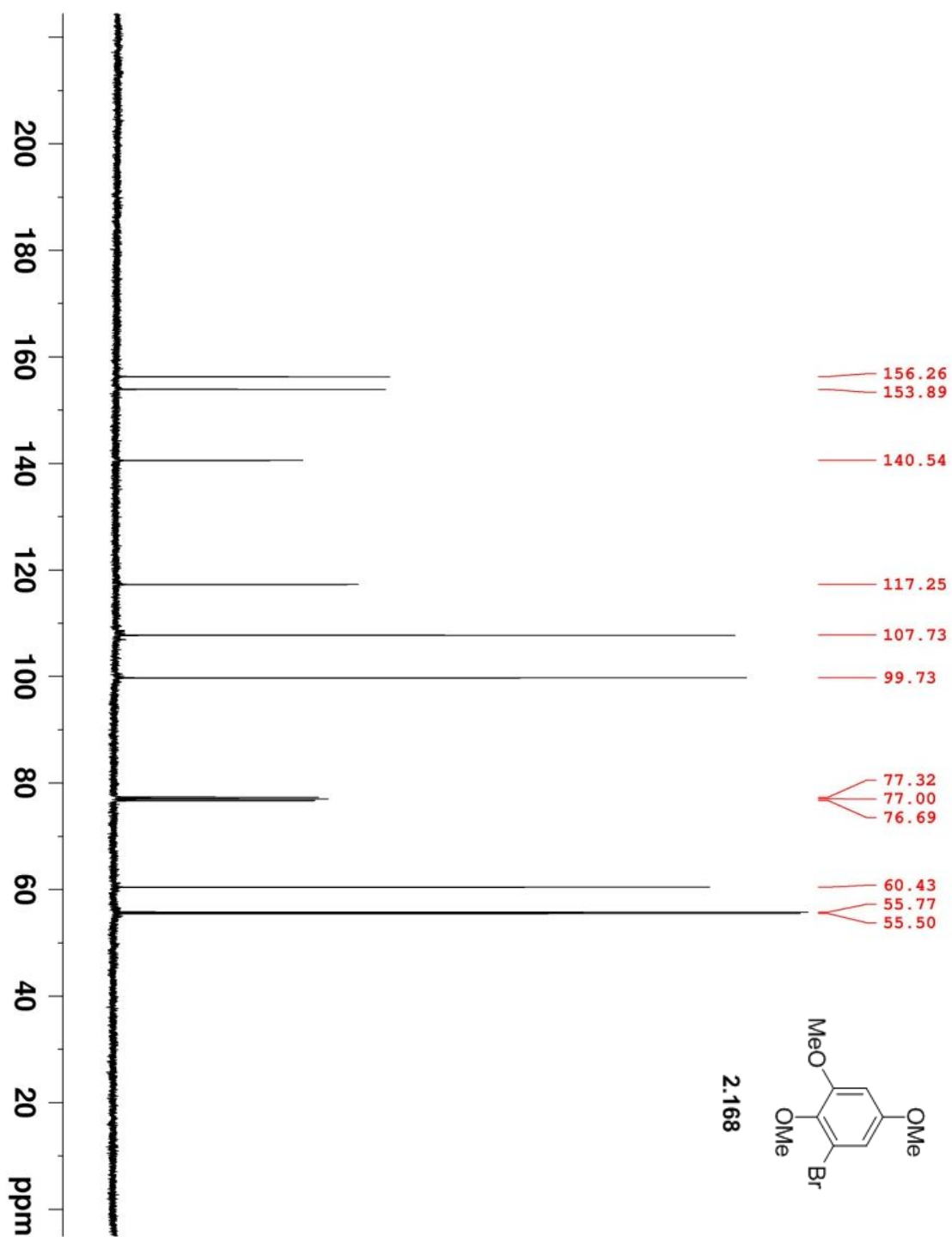


Figure A38. 100 MHz ^{13}C NMR of **2.168** in CDCl_3 .

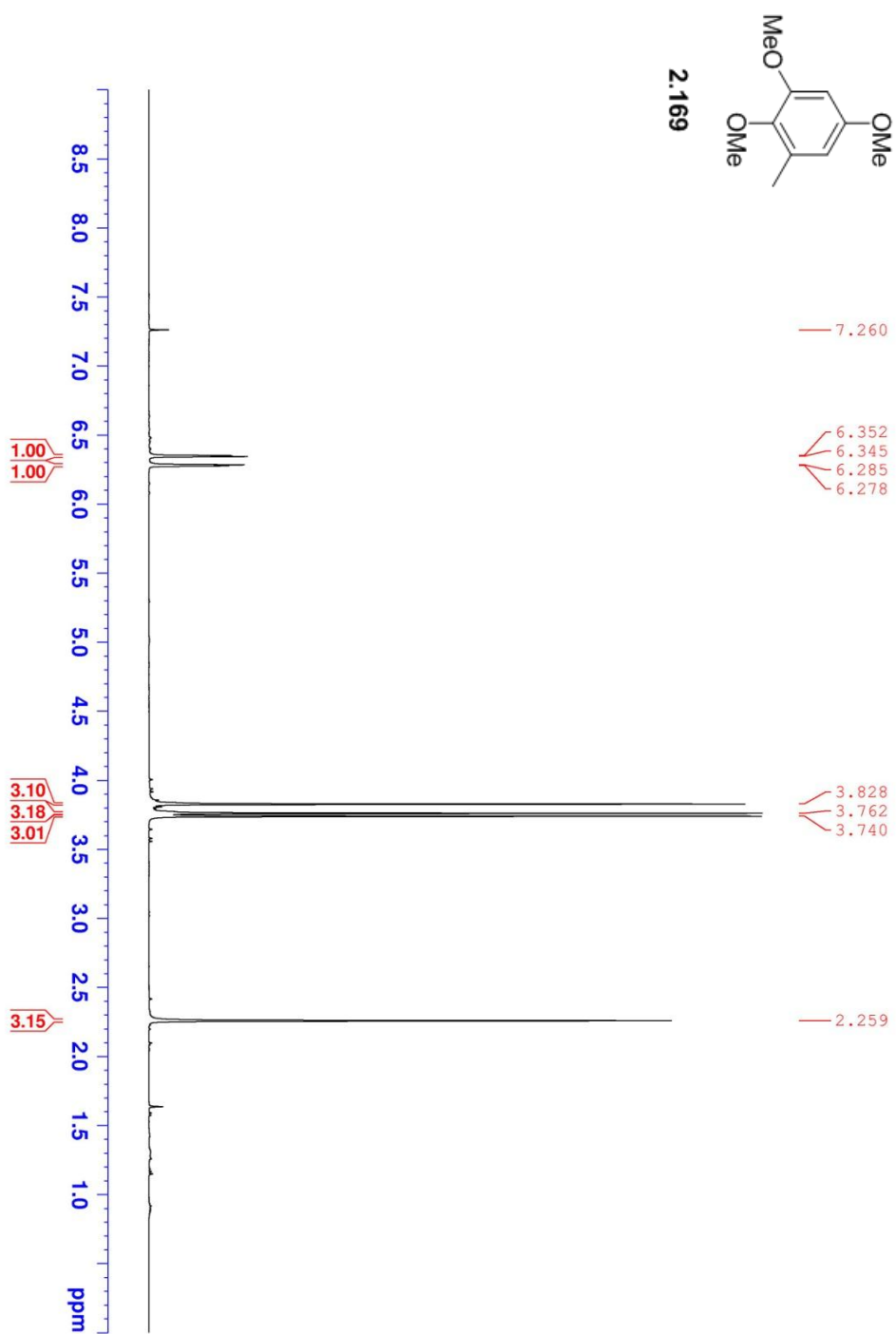


Figure A39. 400 MHz ^1H NMR of **2.169**. in CDCl_3

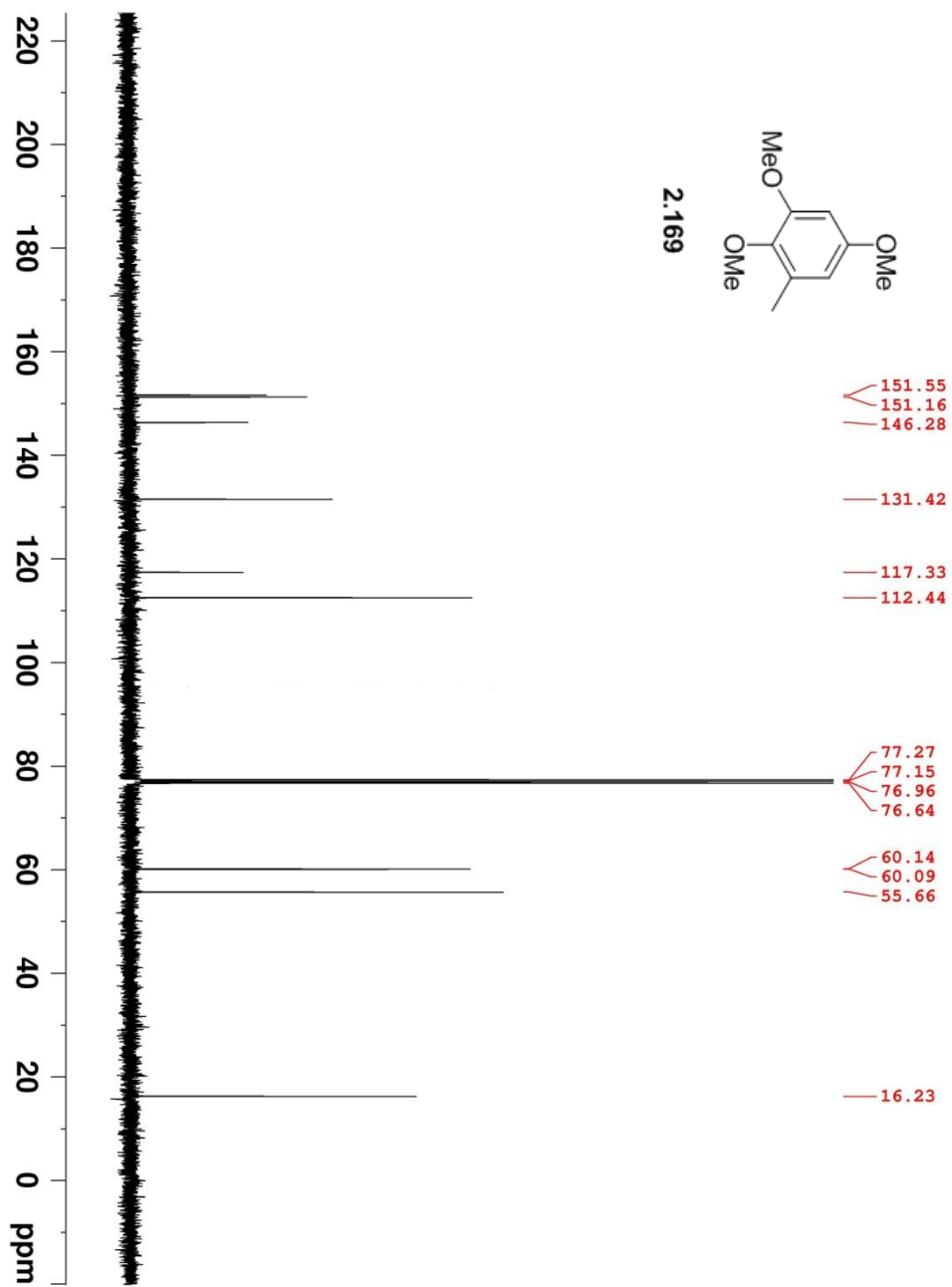


Figure A40. 100 MHz ^{13}C NMR of **2.169** in CDCl_3 .

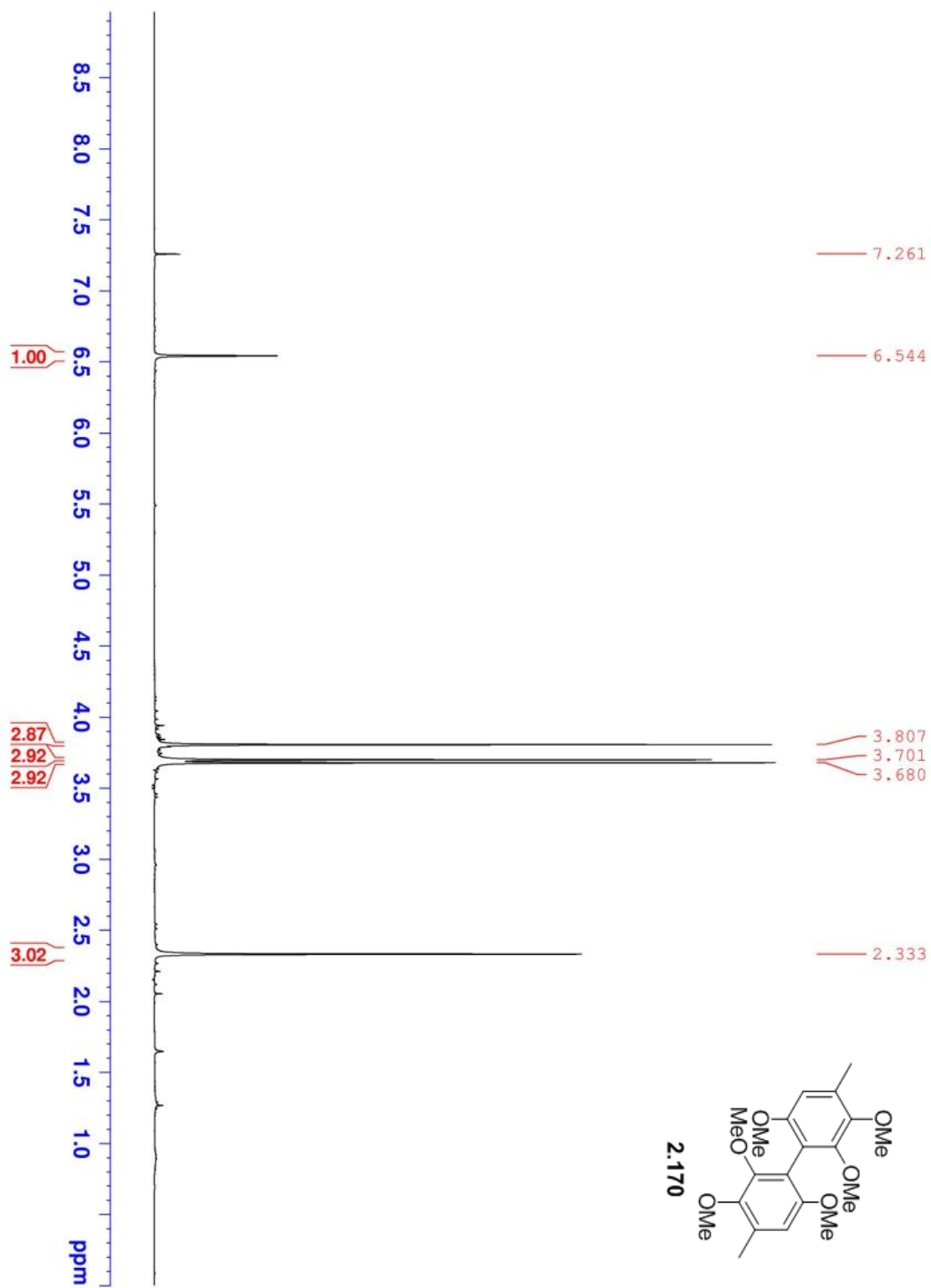


Figure A41. 400 MHz ¹H NMR of **2.170** in CDCl₃.

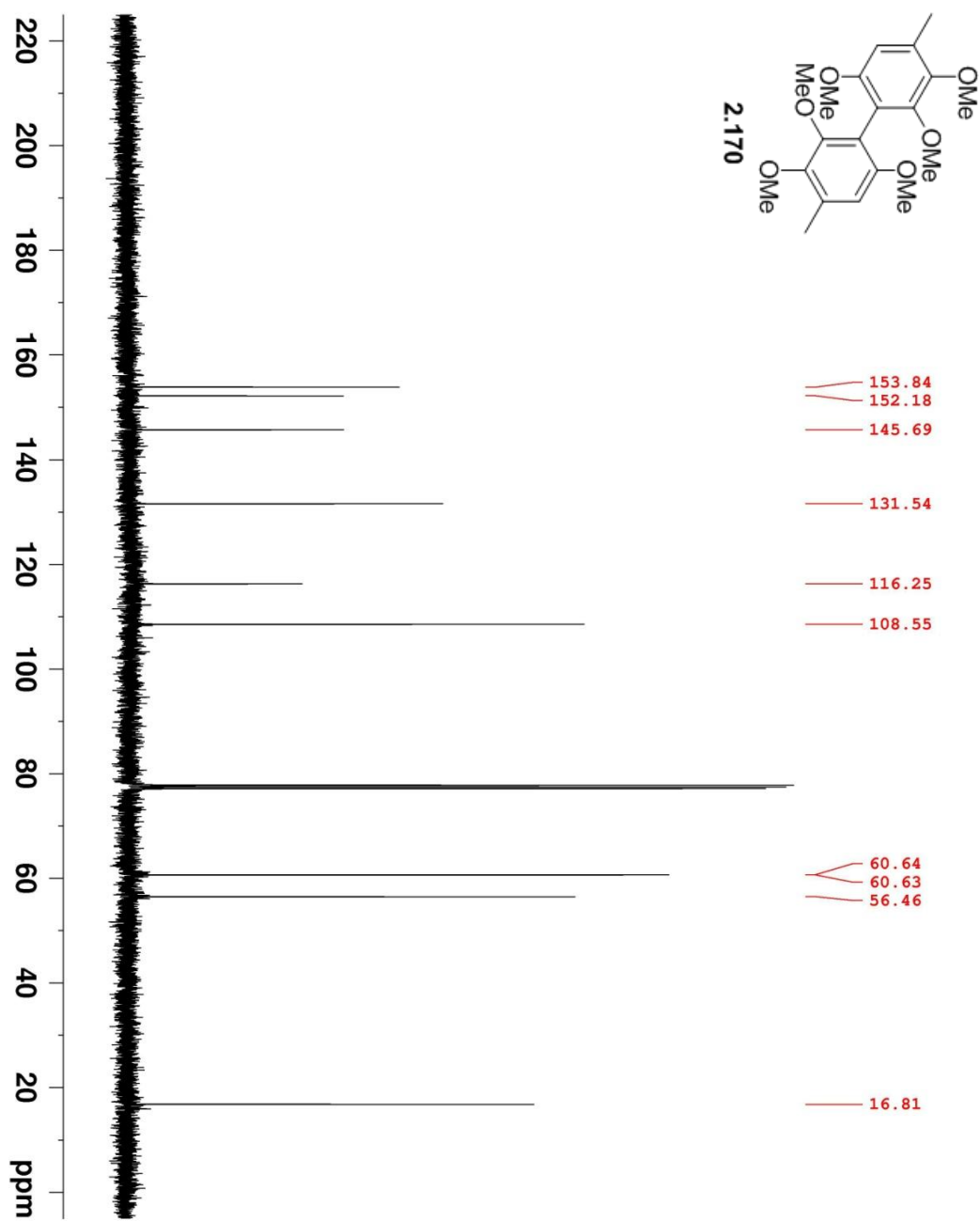


Figure A42. 100 MHz ^{13}C NMR of **2.170** in CDCl_3 .

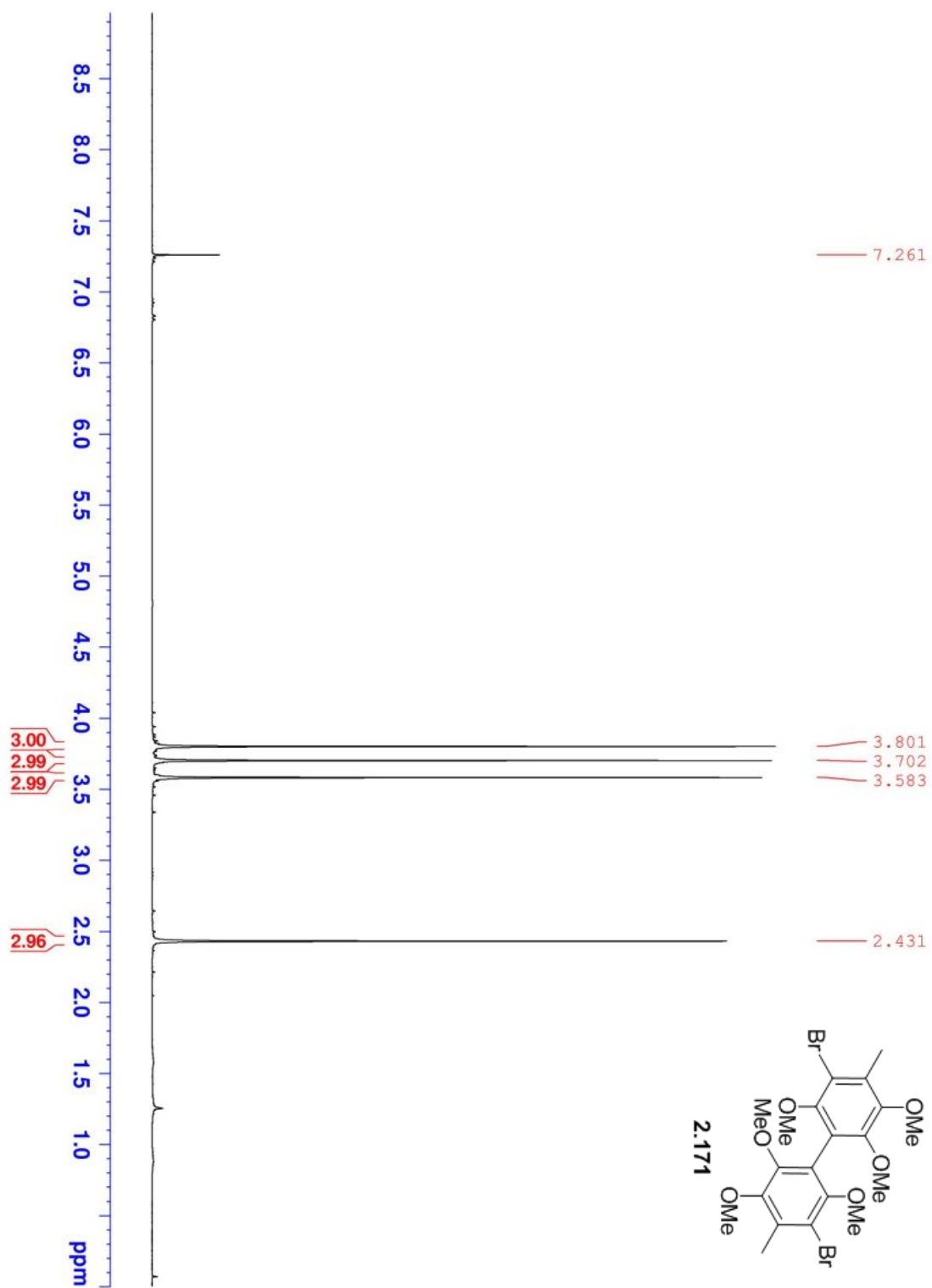


Figure A43. 400 MHz ^1H NMR of **2.171** in CDCl_3 .

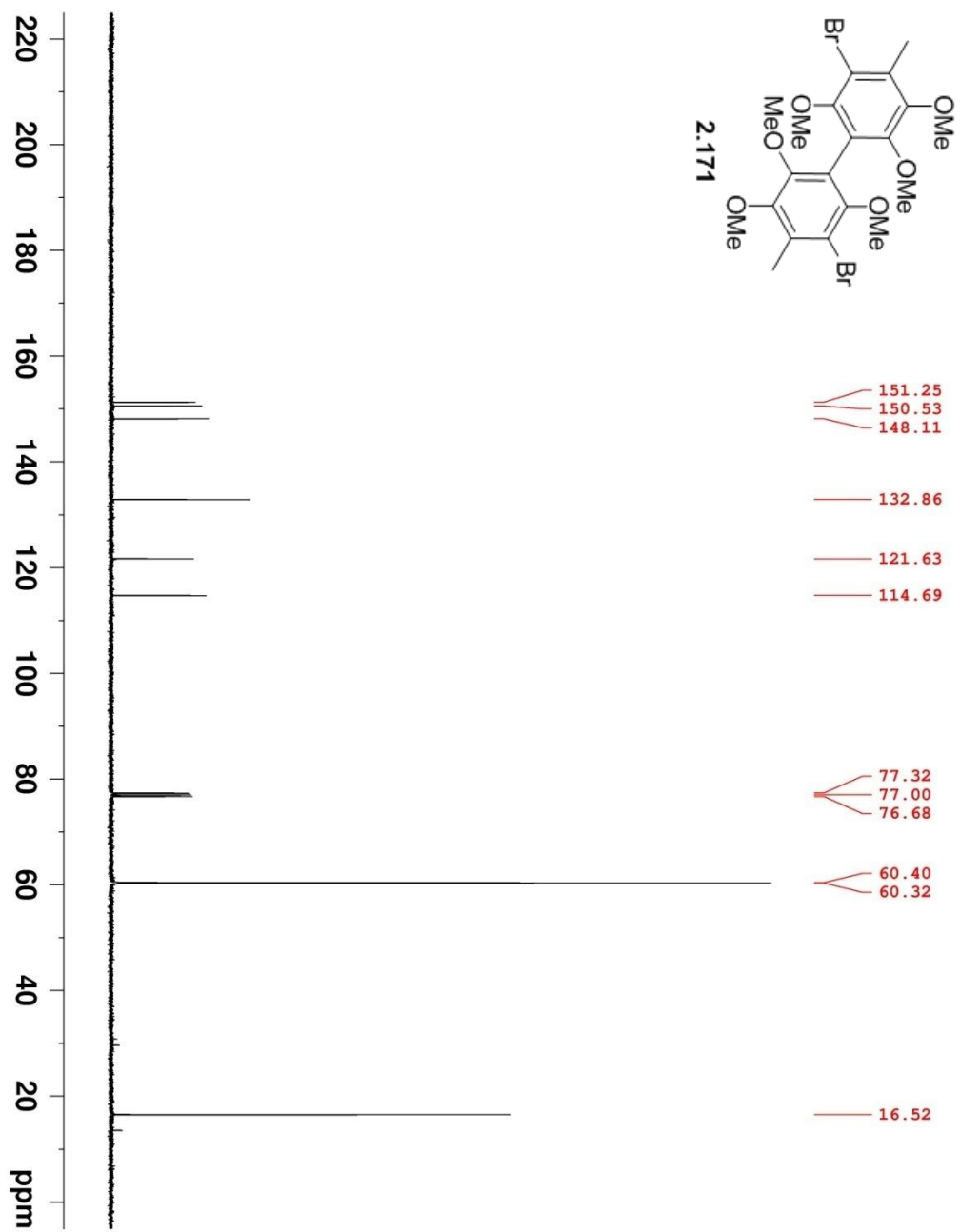


Figure A44. 100 MHz ¹³C NMR of **2.171** in CDCl₃.

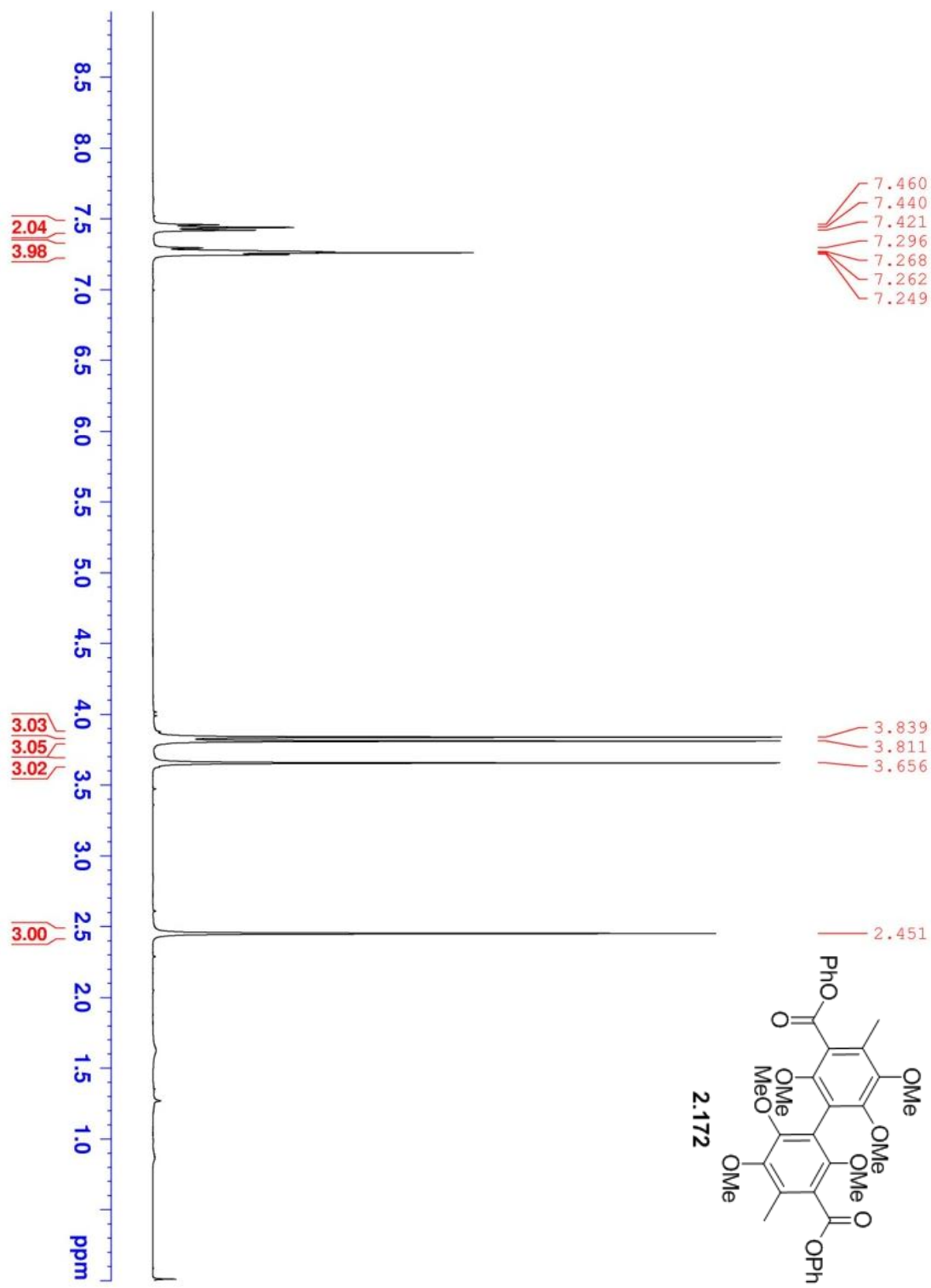


Figure A45. 400 MHz ¹H NMR of **2.172** in CDCl₃.

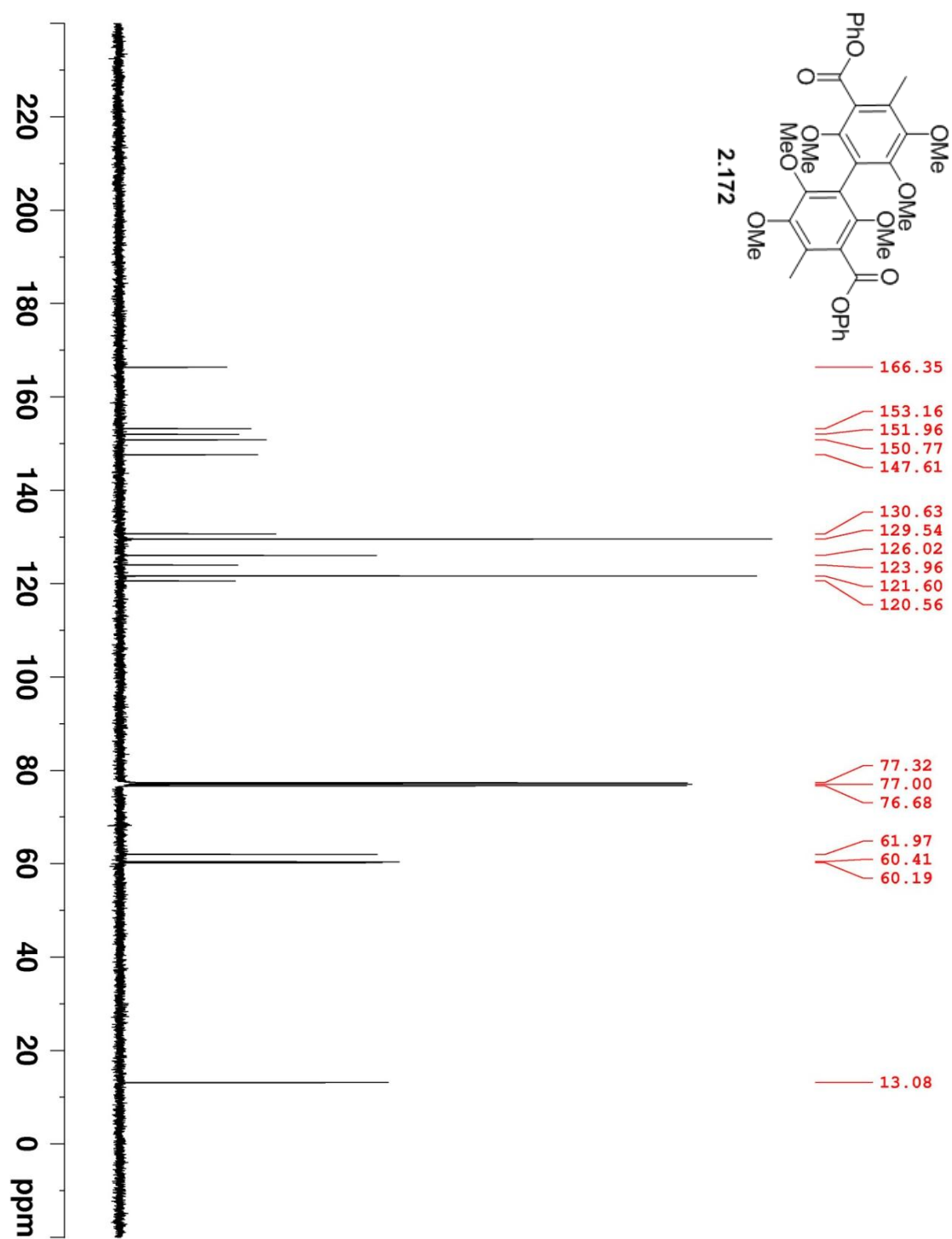


Figure A46. 100 MHz ^{13}C NMR of **2.172** in CDCl_3 .

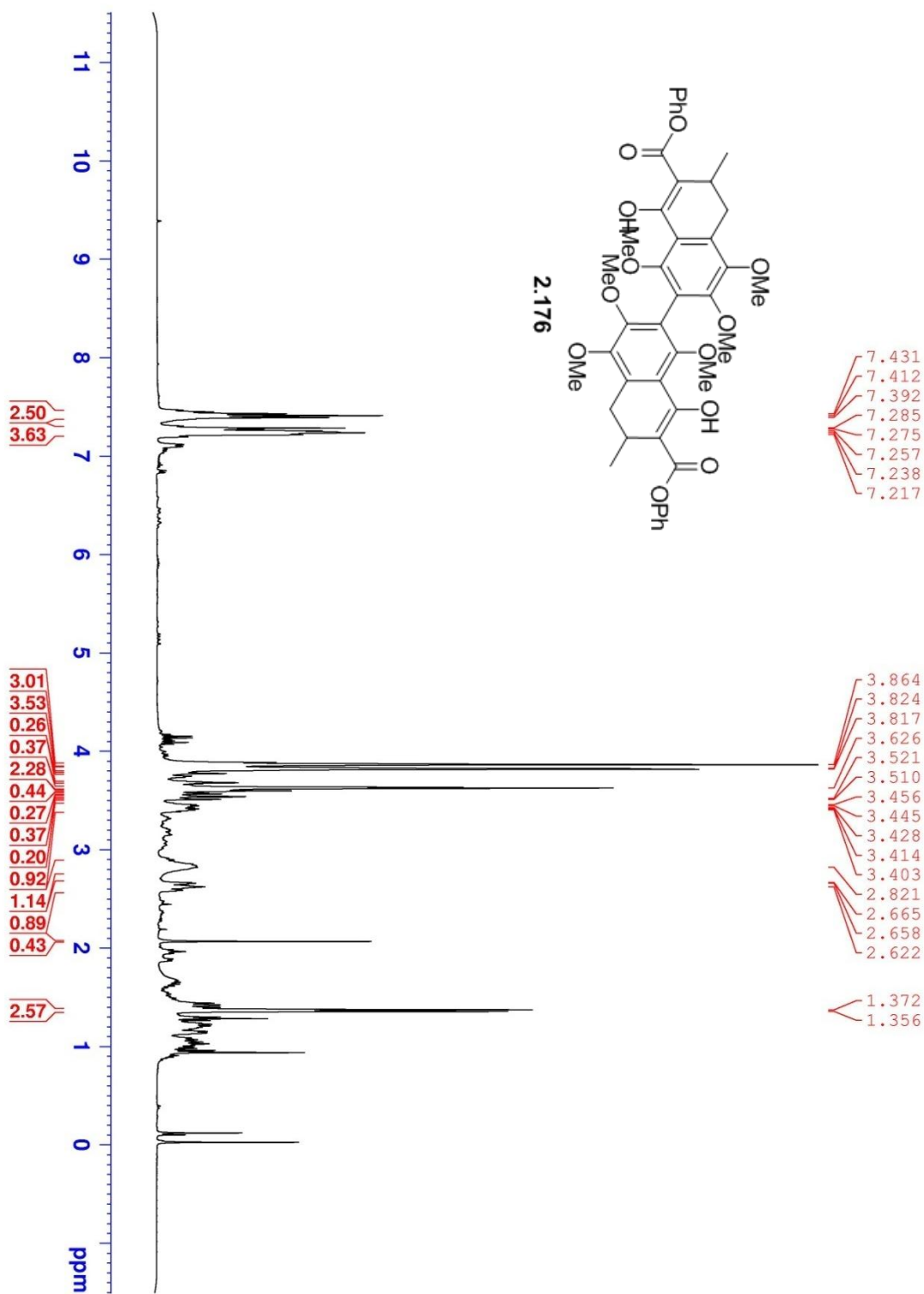


Figure A47. 400 MHz ¹H NMR of **2.176** in CDCl₃.

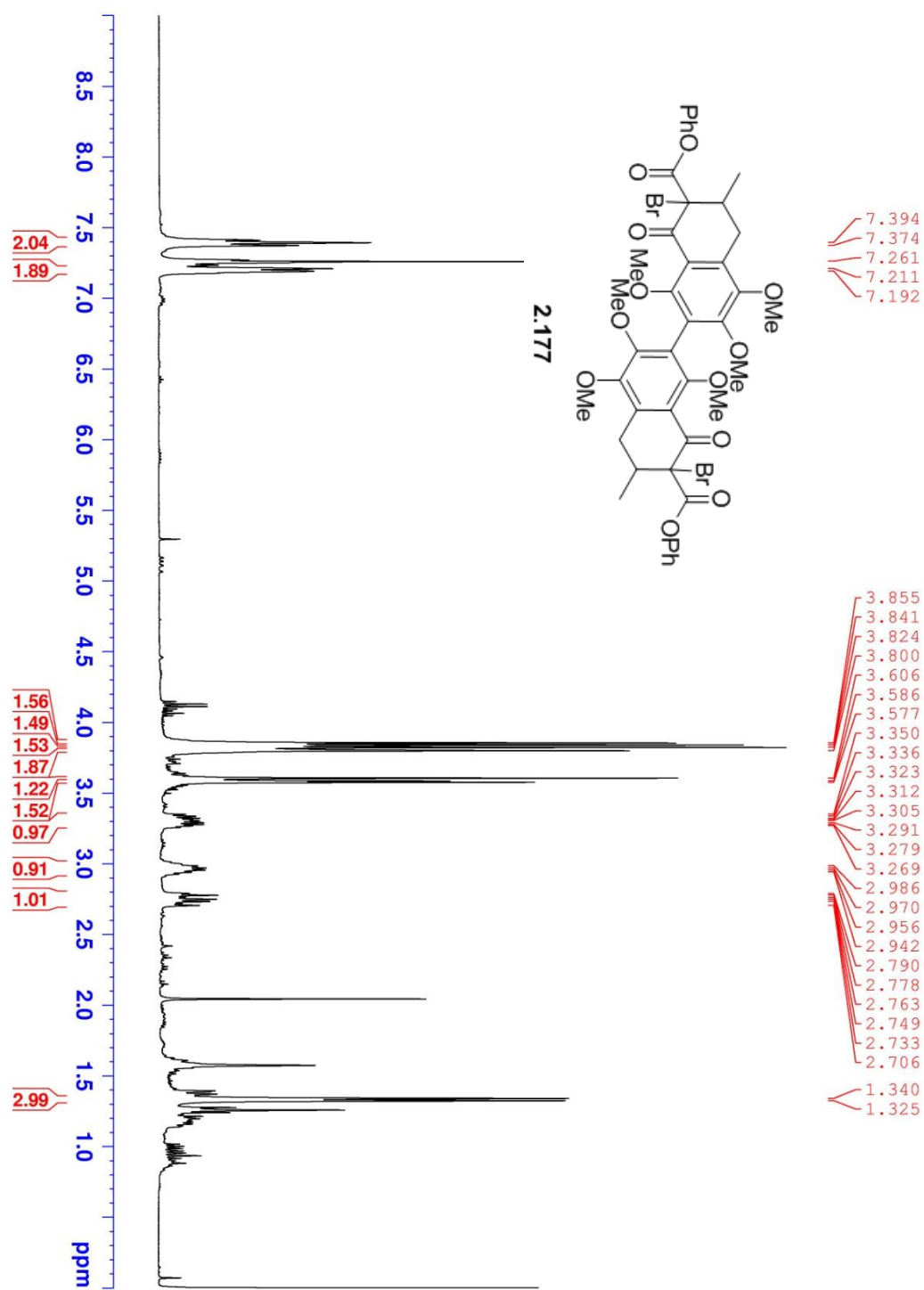


Figure A48. 400 MHz ^1H NMR of **2.177** in CDCl_3 .

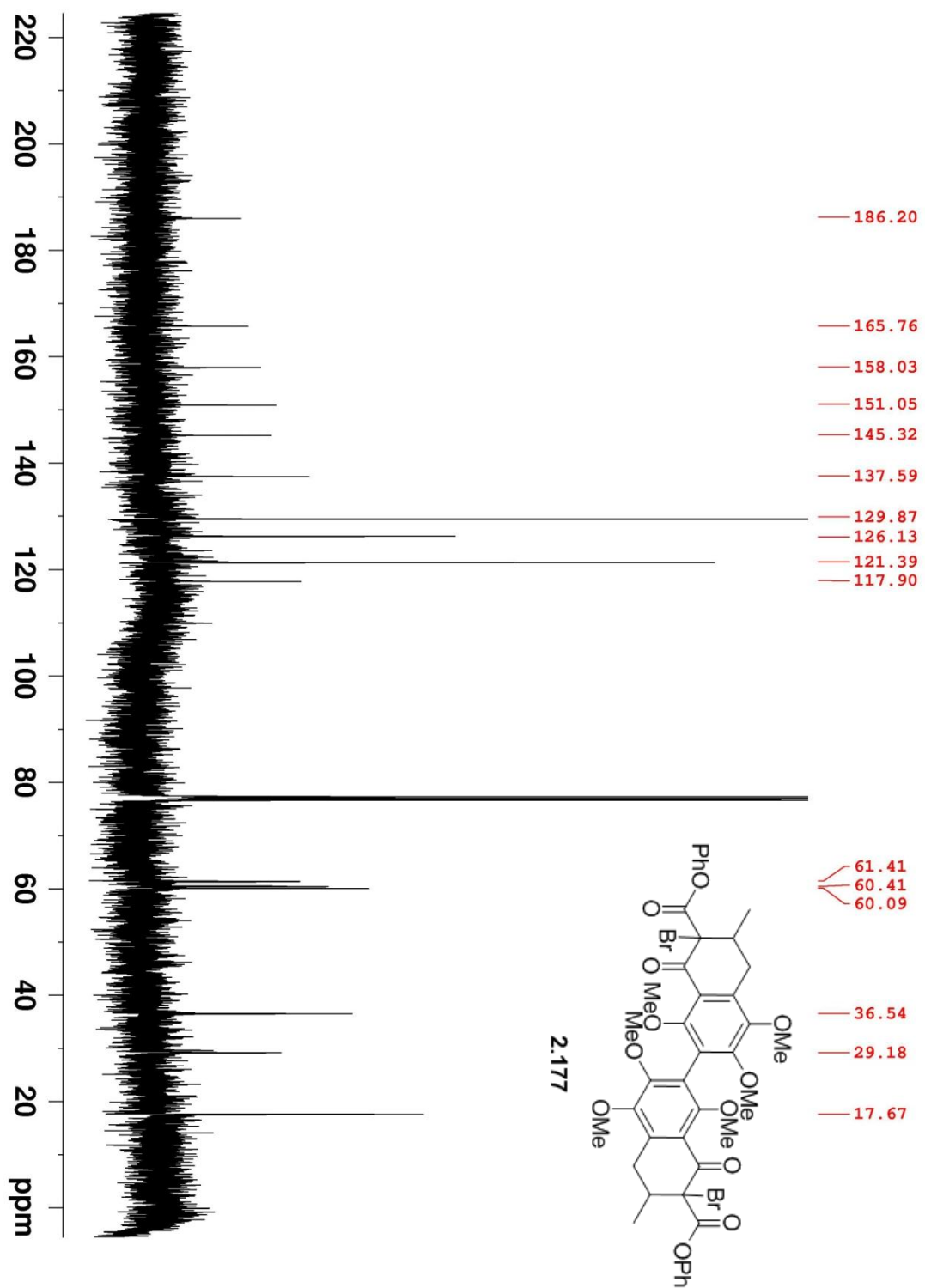


Figure A49. 75 MHz ^{13}C NMR of **2.177** in CDCl_3 .

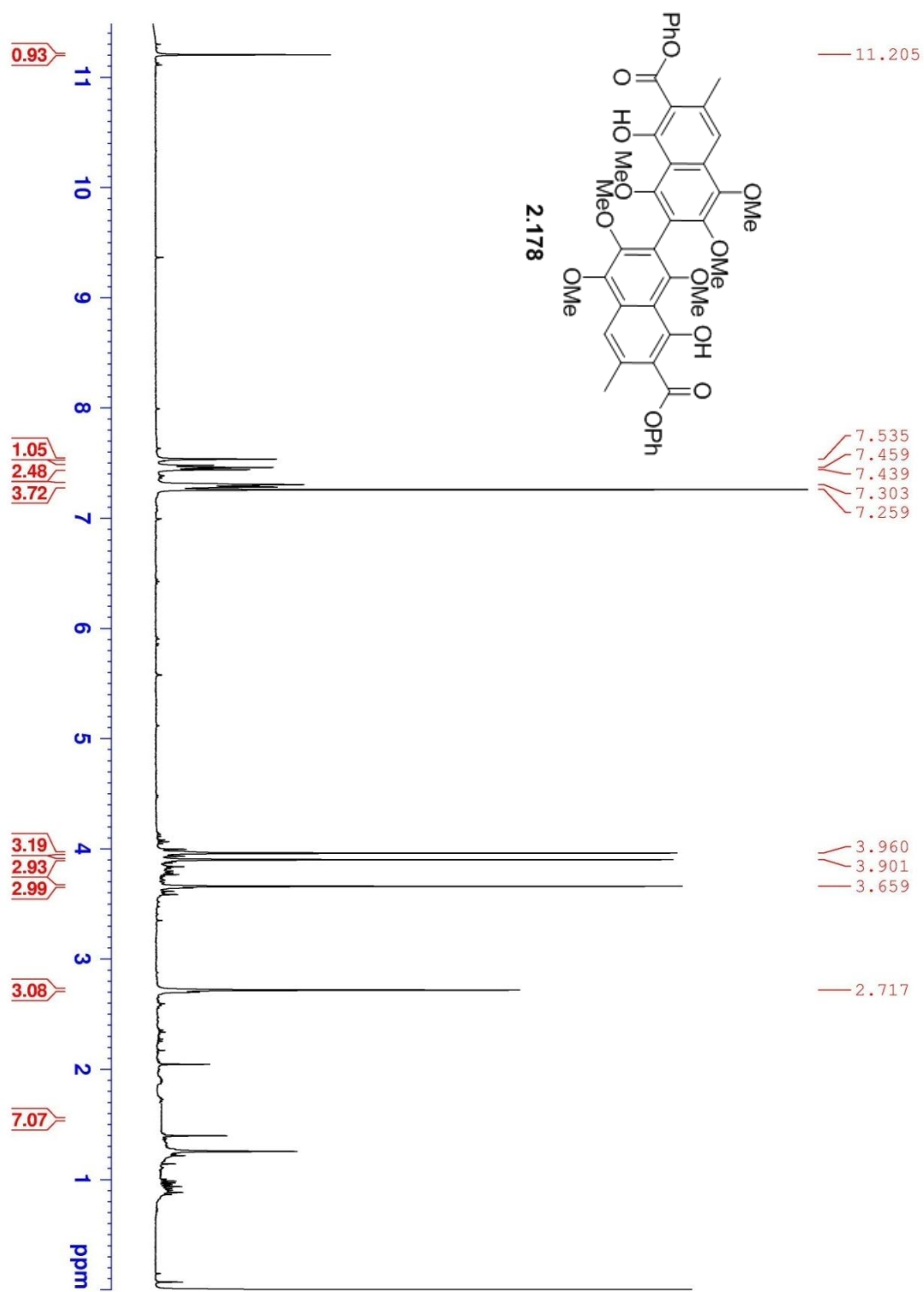


Figure A50. 400 MHz ^1H NMR of **2.178** in CDCl_3 .

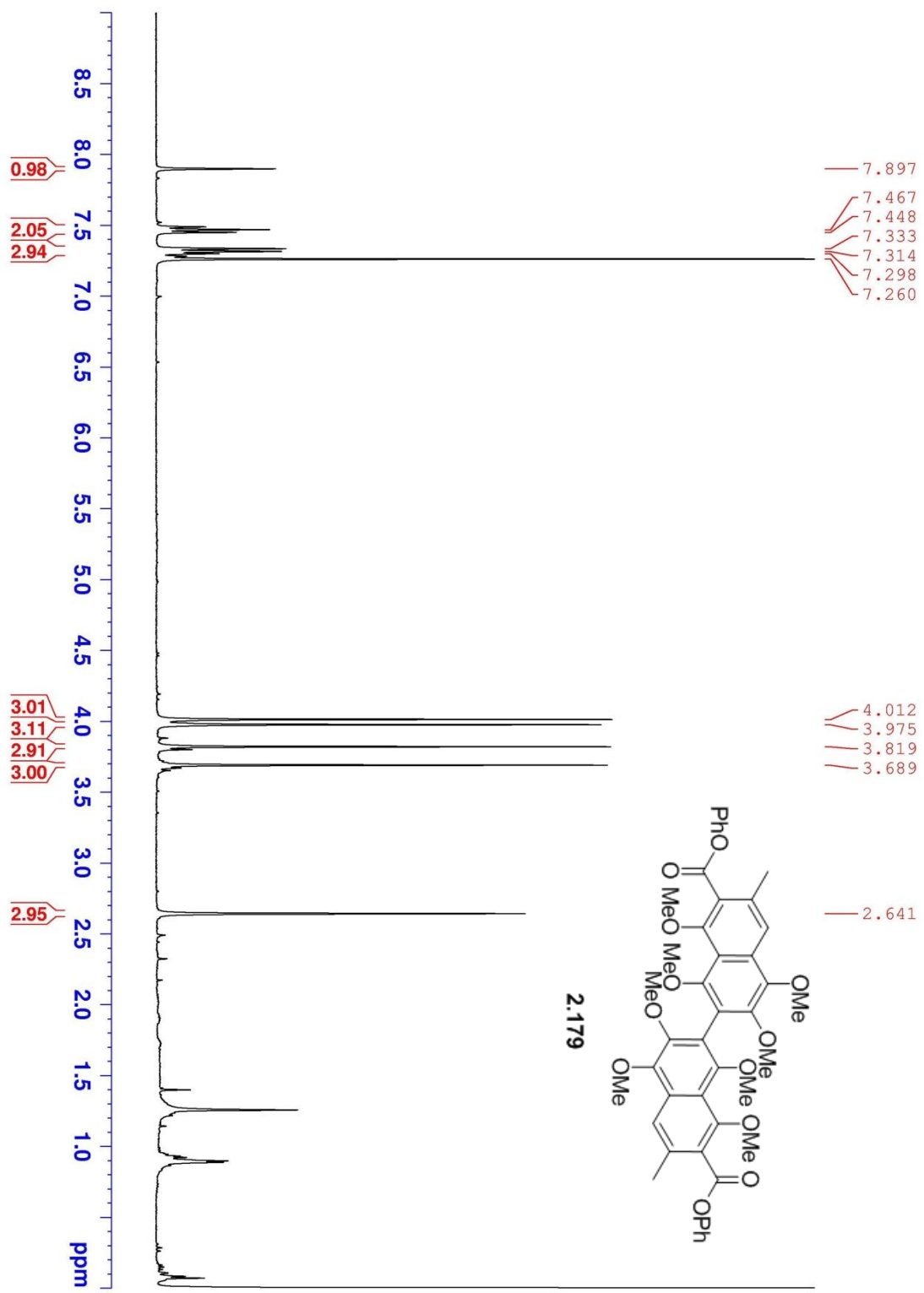


Figure A51. 400 MHz ¹H NMR of **2.179** in CDCl₃.

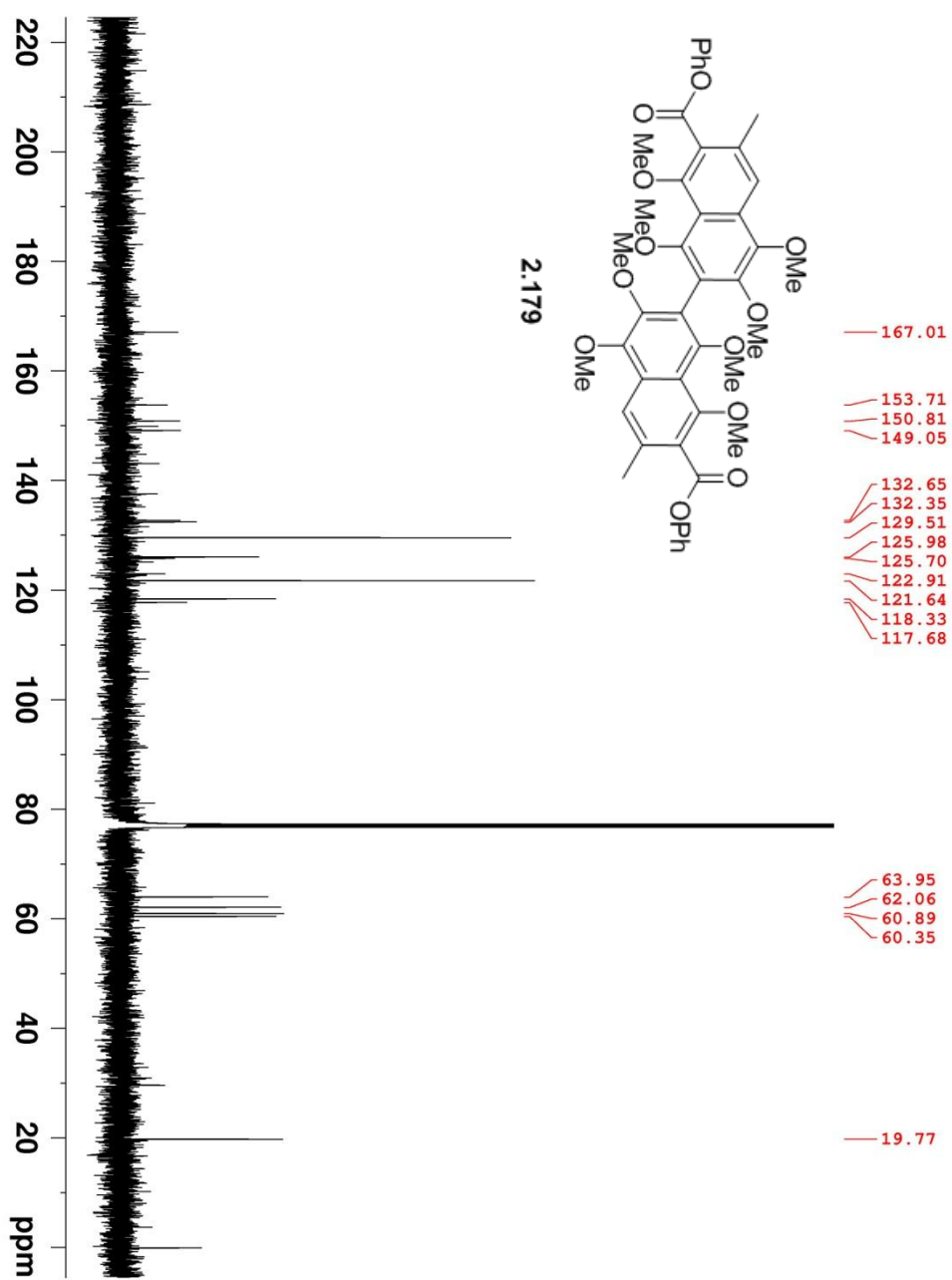


Figure A52. 75 MHz ^{13}C NMR of **2.179** in CDCl_3 .

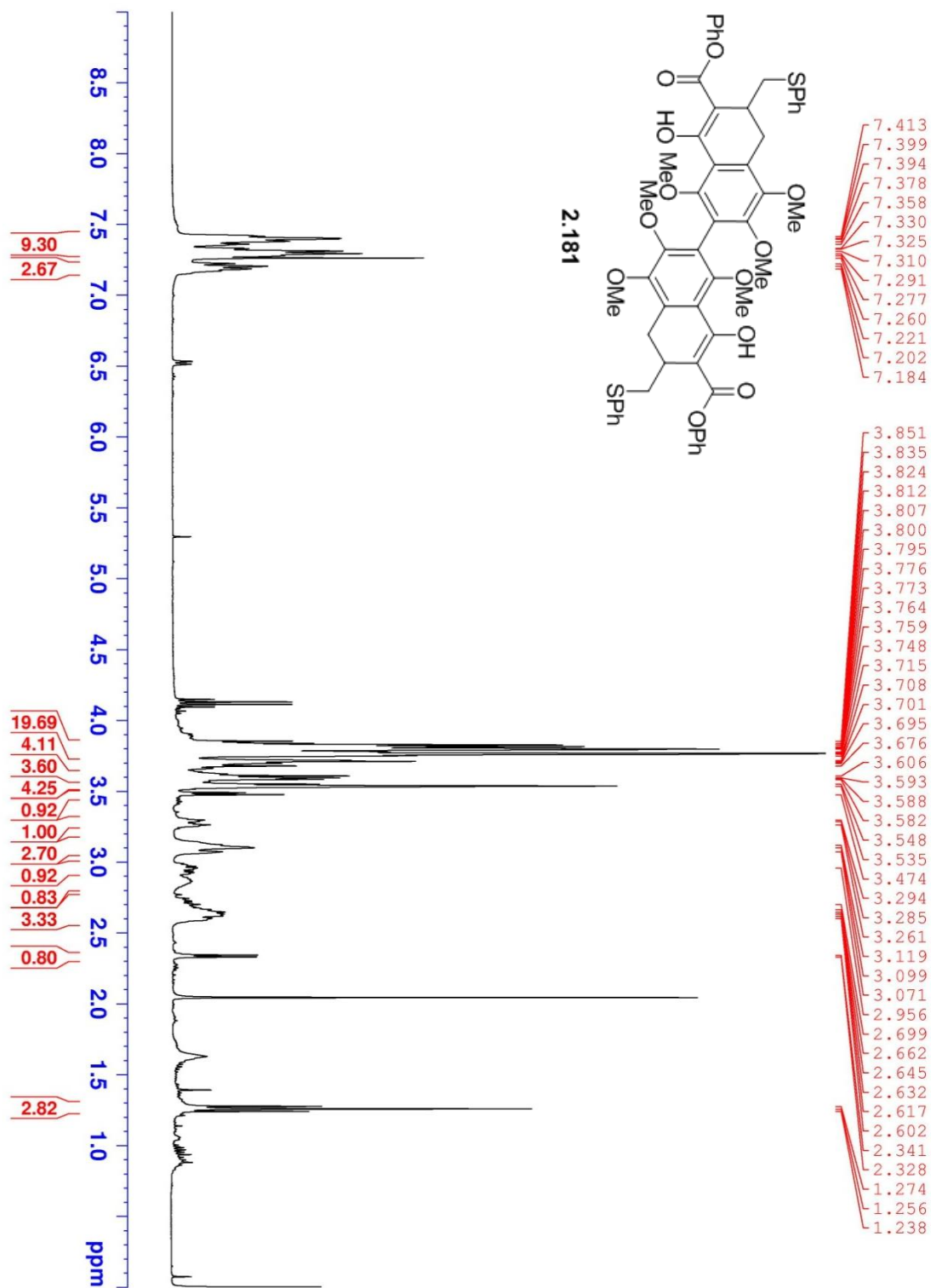


Figure A53. 400 MHz ^1H NMR of **2.181** in CDCl_3 .

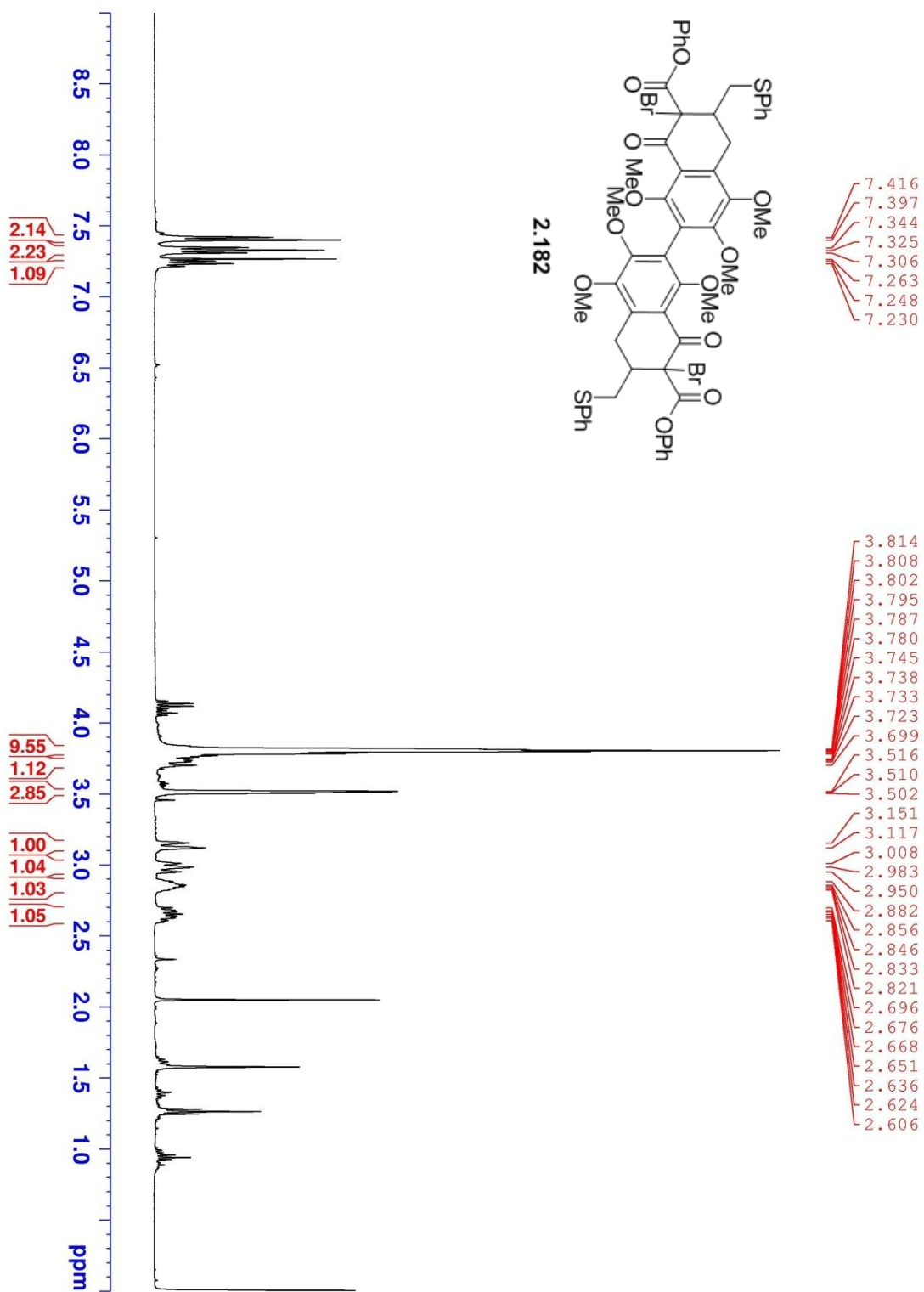


Figure A54. 400 MHz ^1H NMR of **2.182** in CDCl_3 .

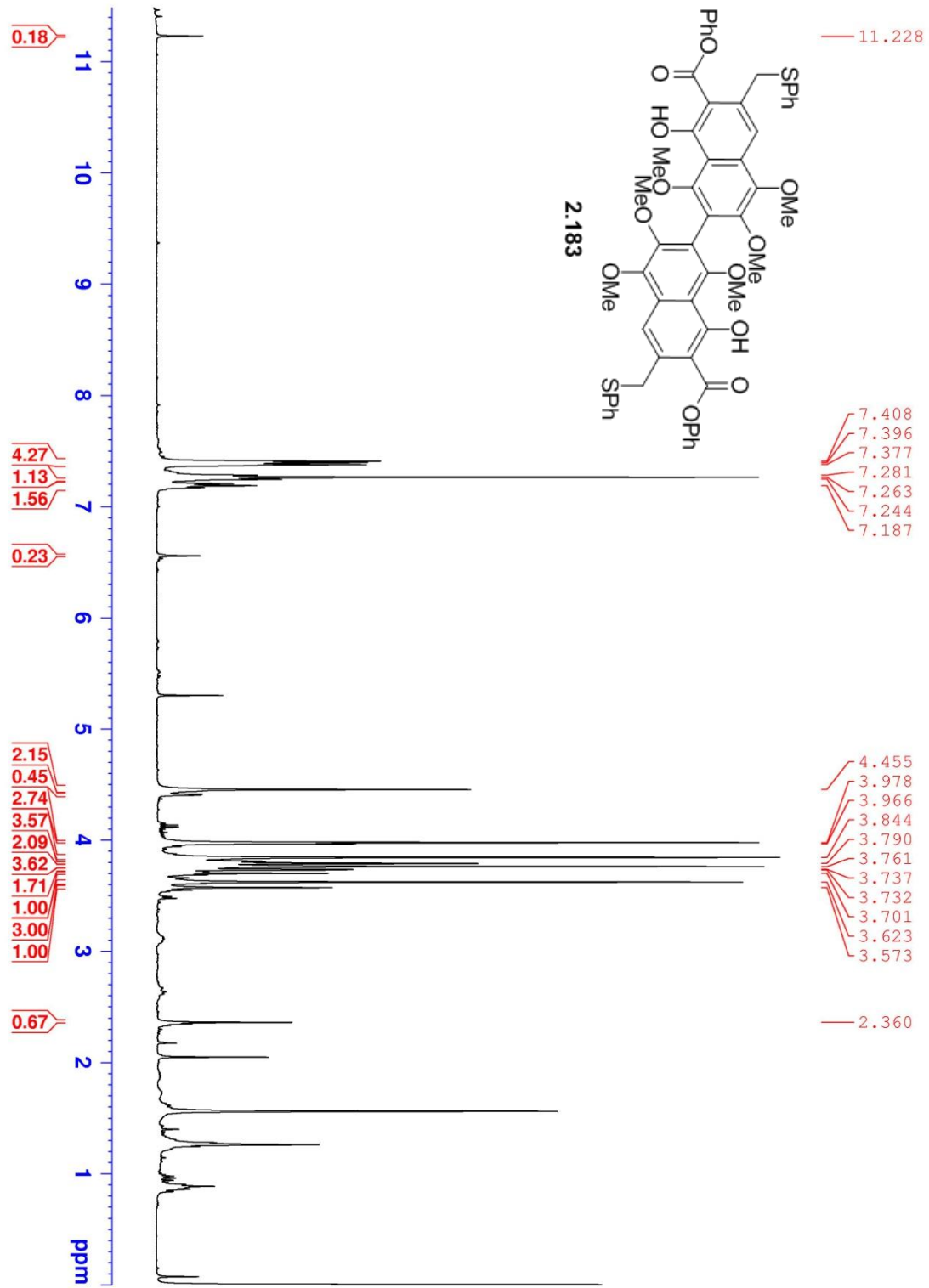


Figure A55. 400 MHz ^1H NMR of **2.183** in CDCl_3 .

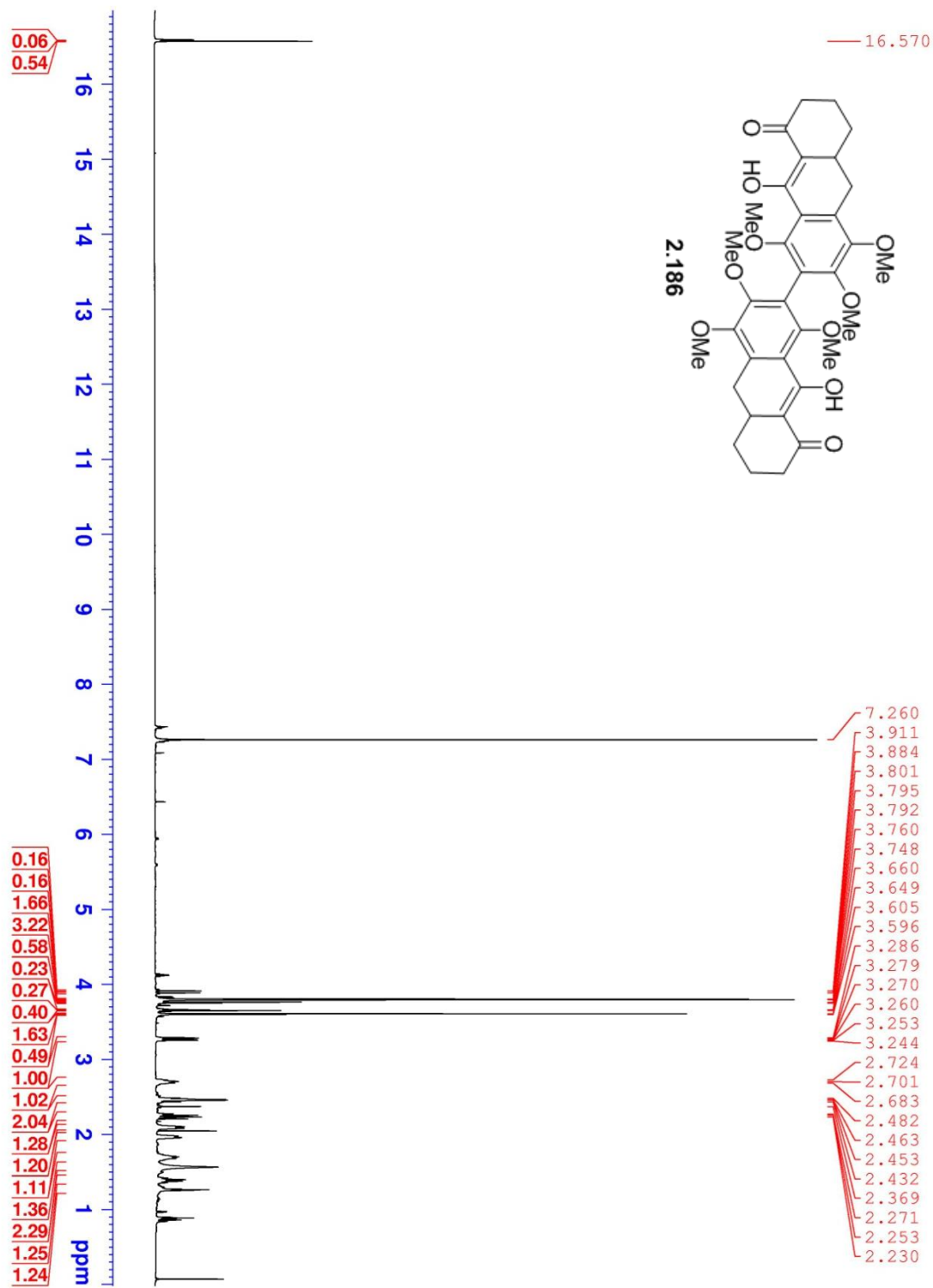


Figure A56. 600 MHz ^1H NMR of **2.186** in CDCl_3 .

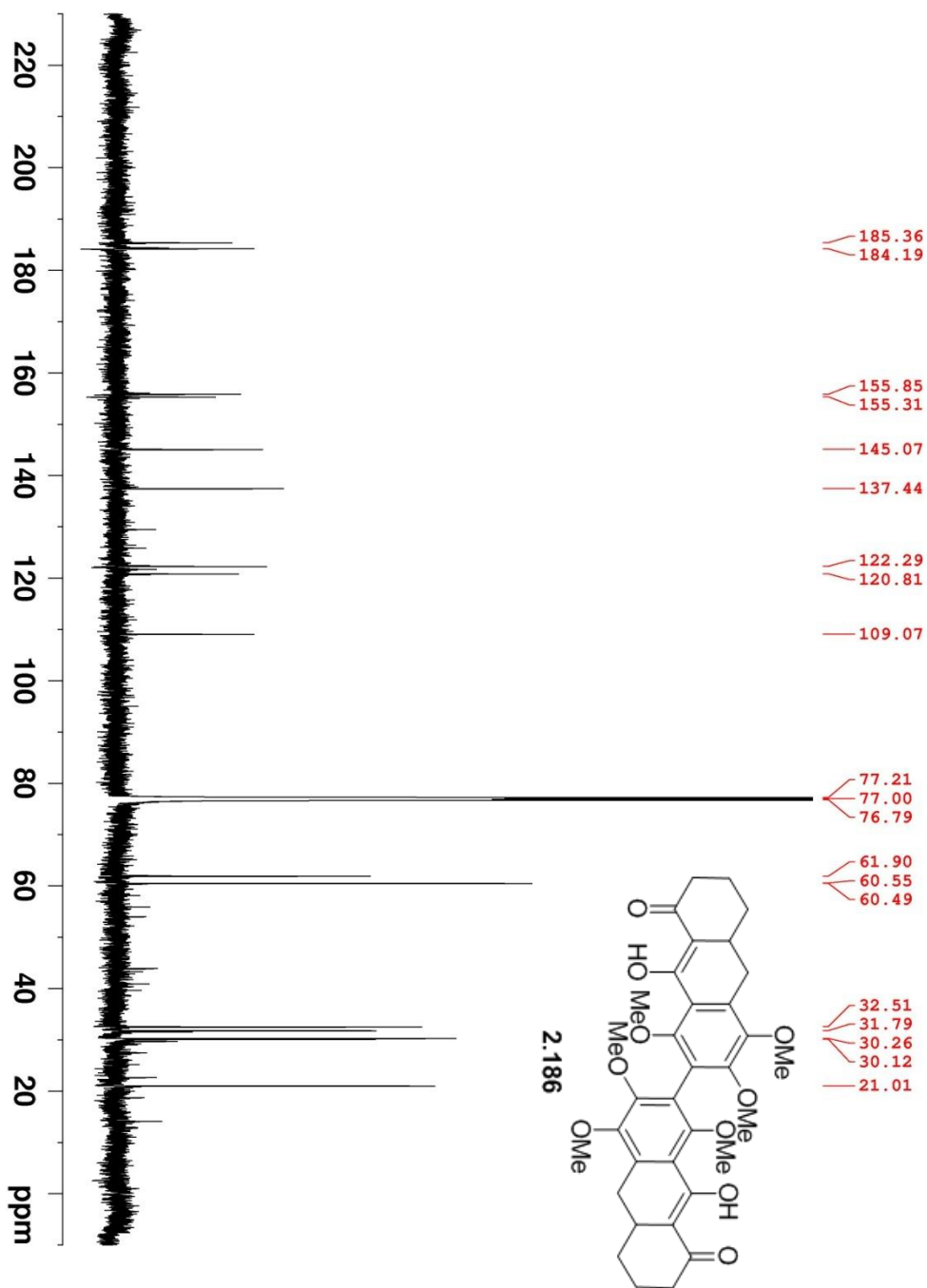


Figure A57. 150 MHz ^{13}C NMR of **2.186** in CDCl_3 .

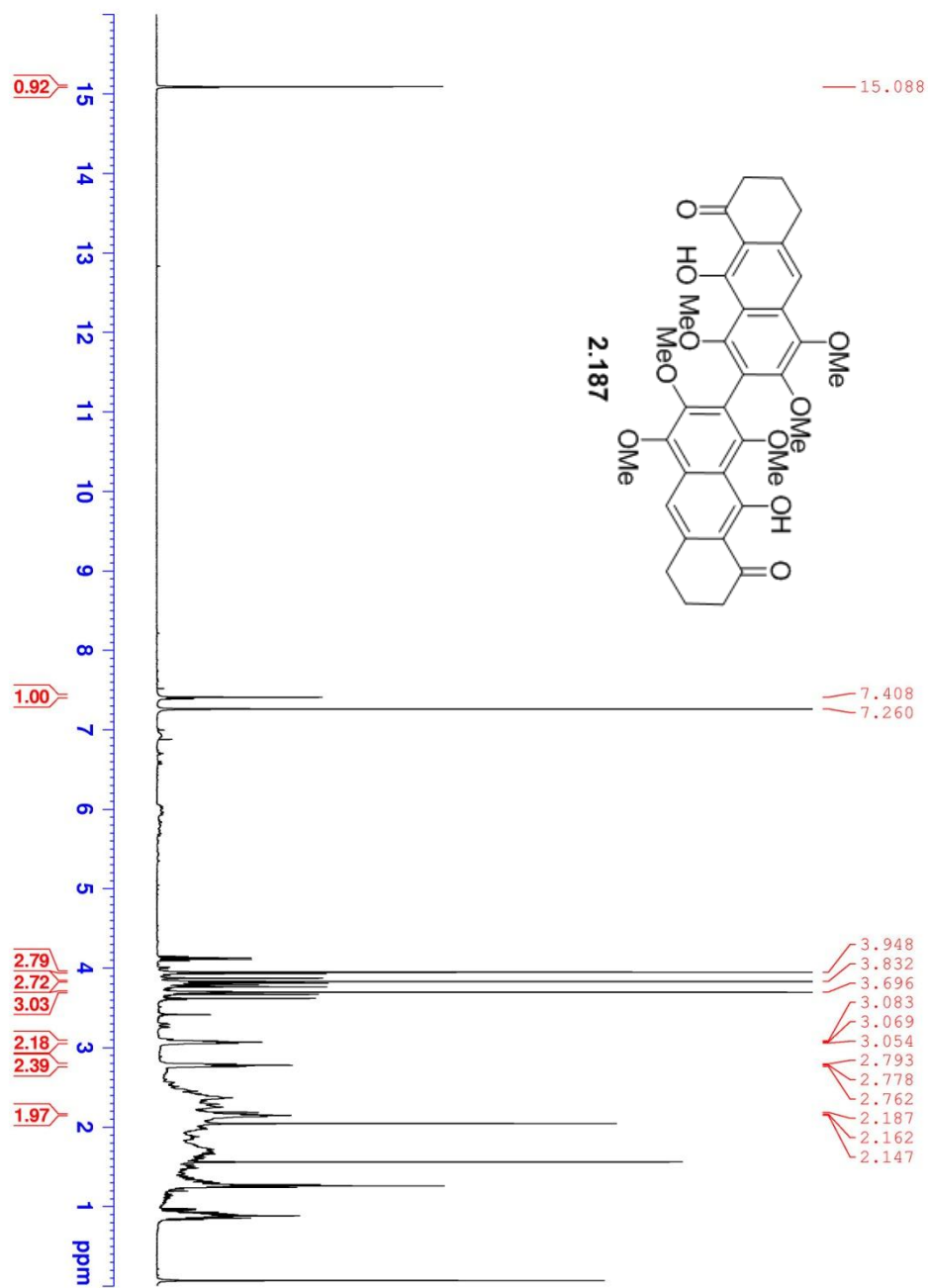


Figure A58. 400 MHz ^1H NMR of **2.187** in CDCl_3 .

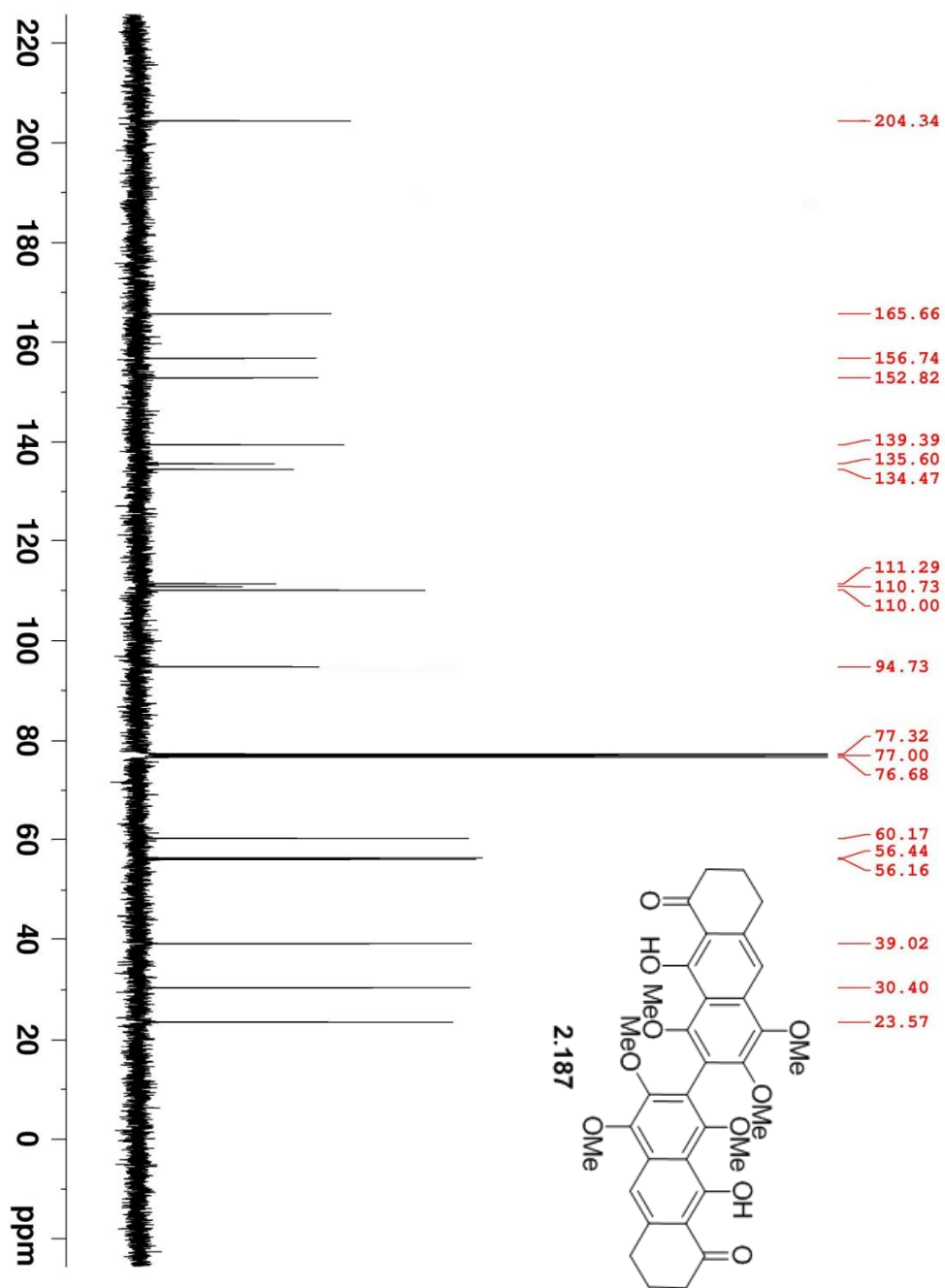


Figure A59. 100 MHz ^{13}C NMR of **2.187** in CDCl_3 .

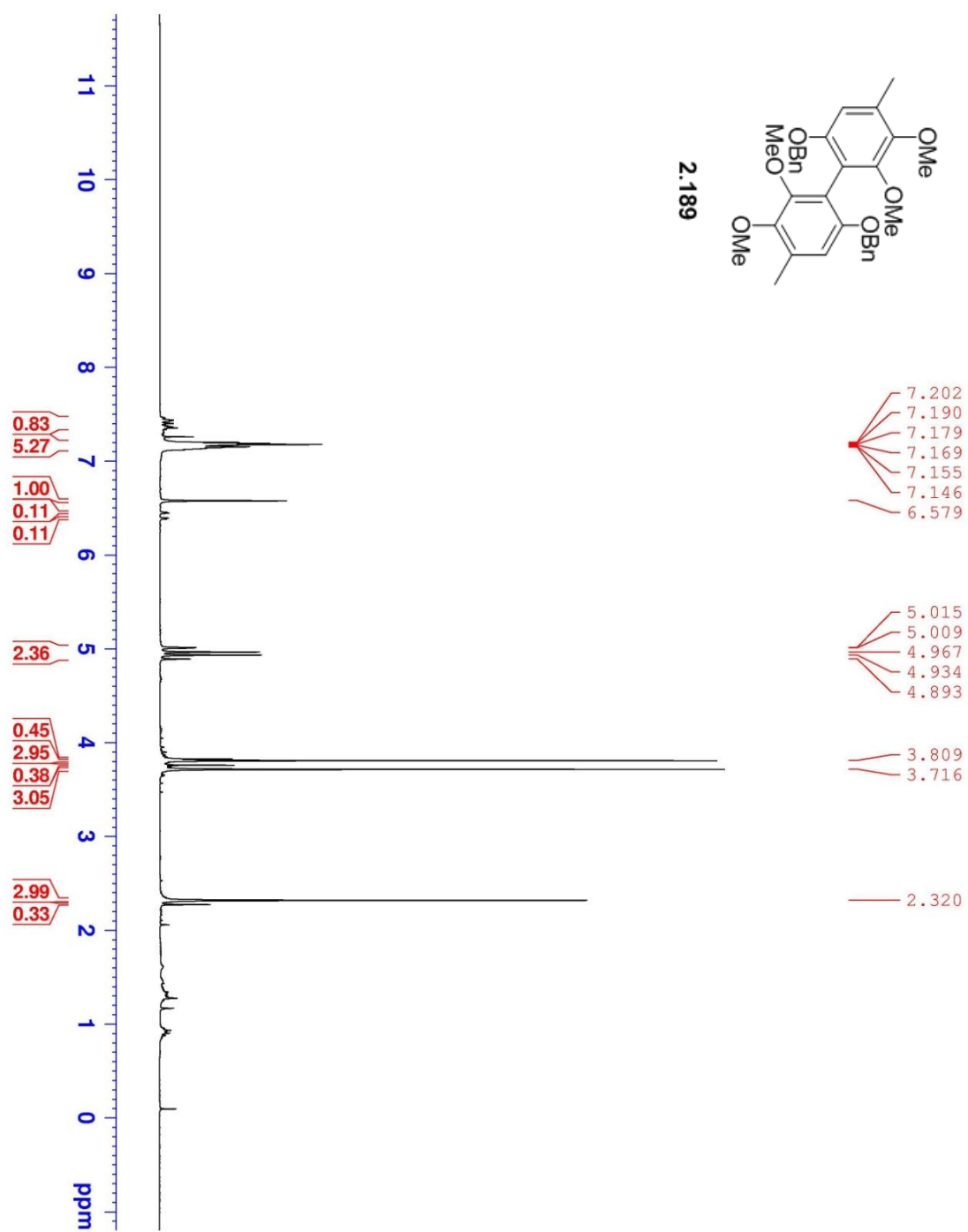


Figure A60. 400 MHz ^1H NMR of **2.189** in CDCl_3 .

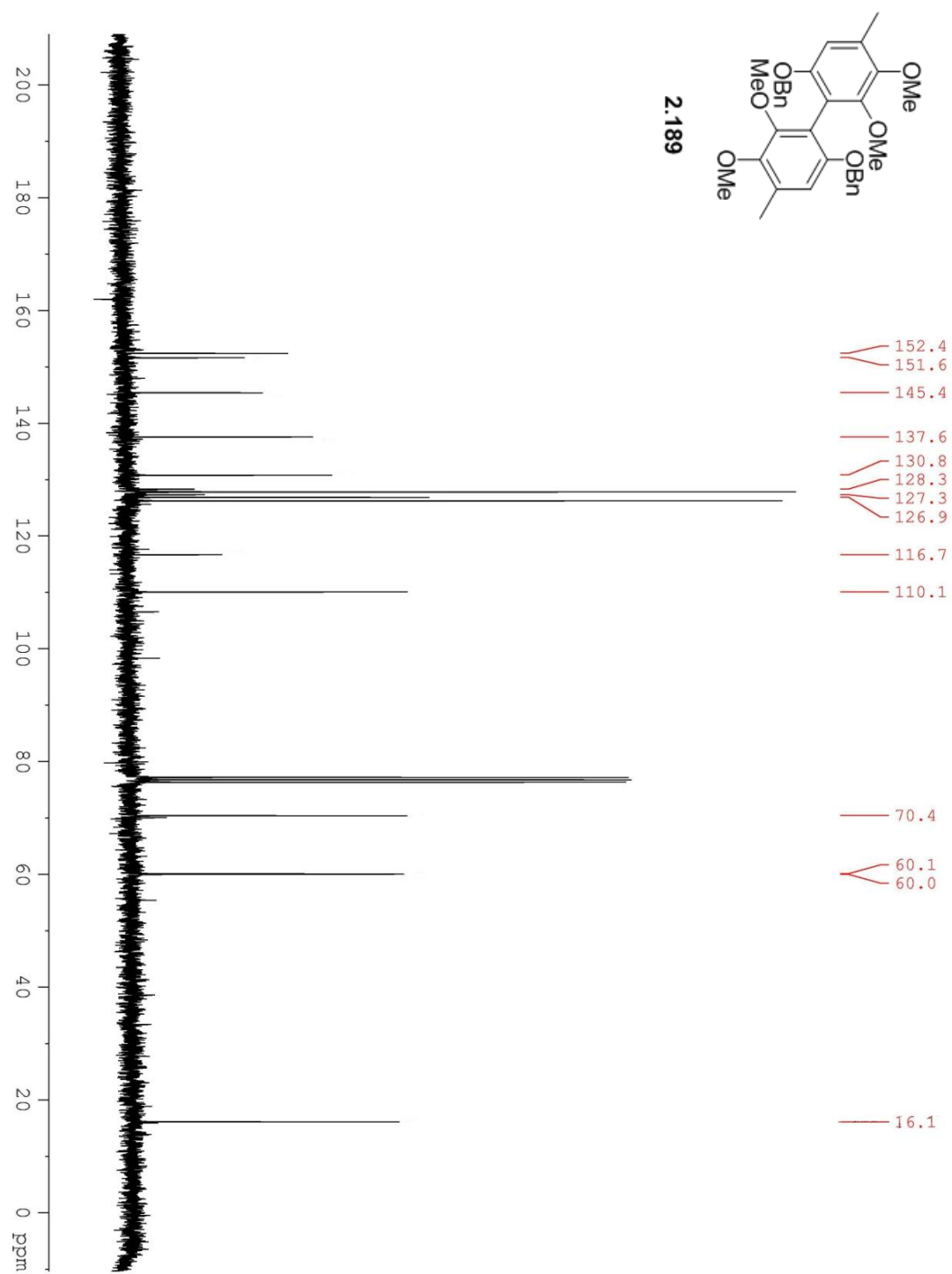


Figure A61. 100 MHz ^{13}C NMR of **2.189** in CDCl_3 .

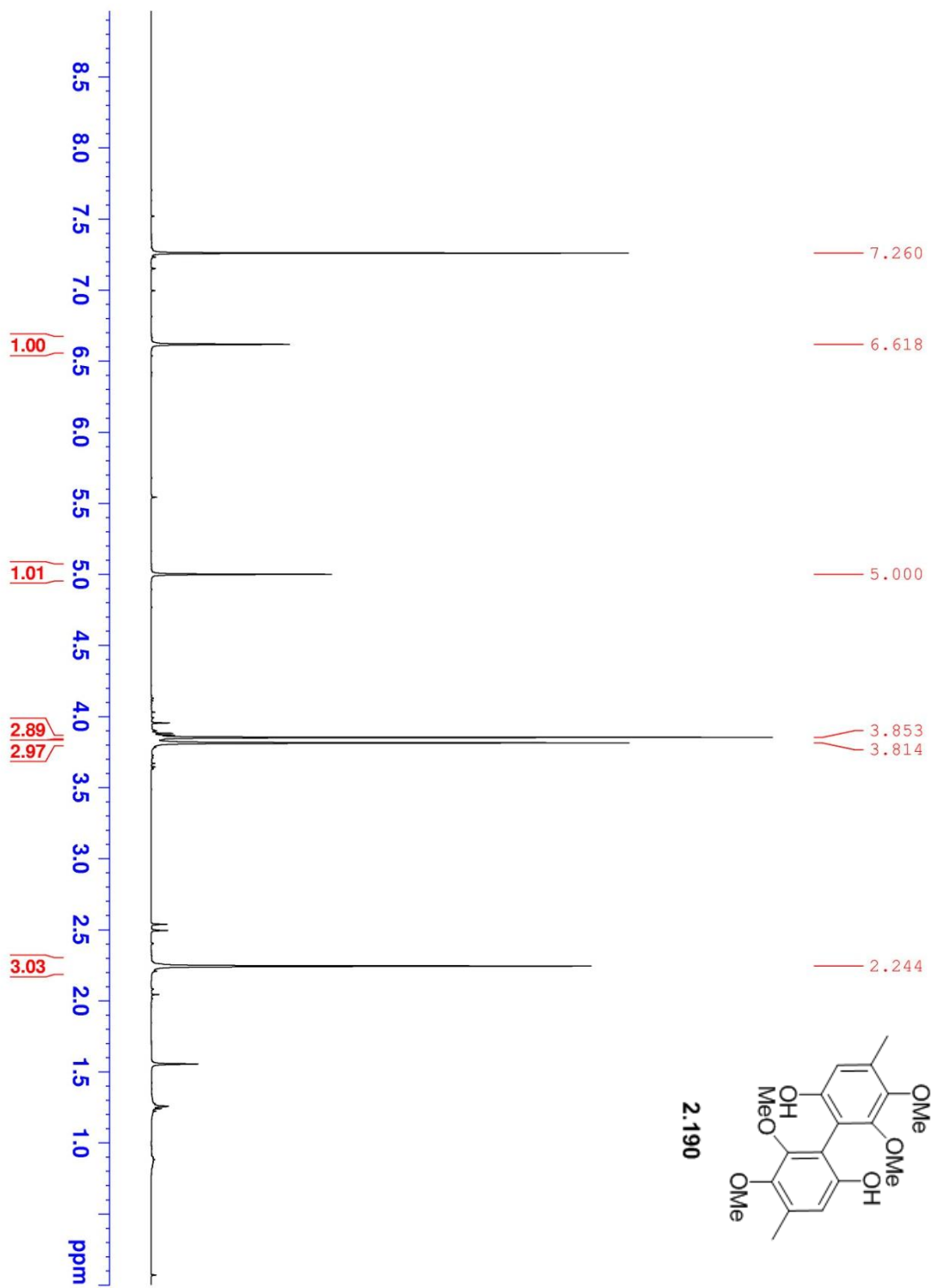


Figure A62. 400 MHz ^1H NMR of **2.190** in CDCl_3 .

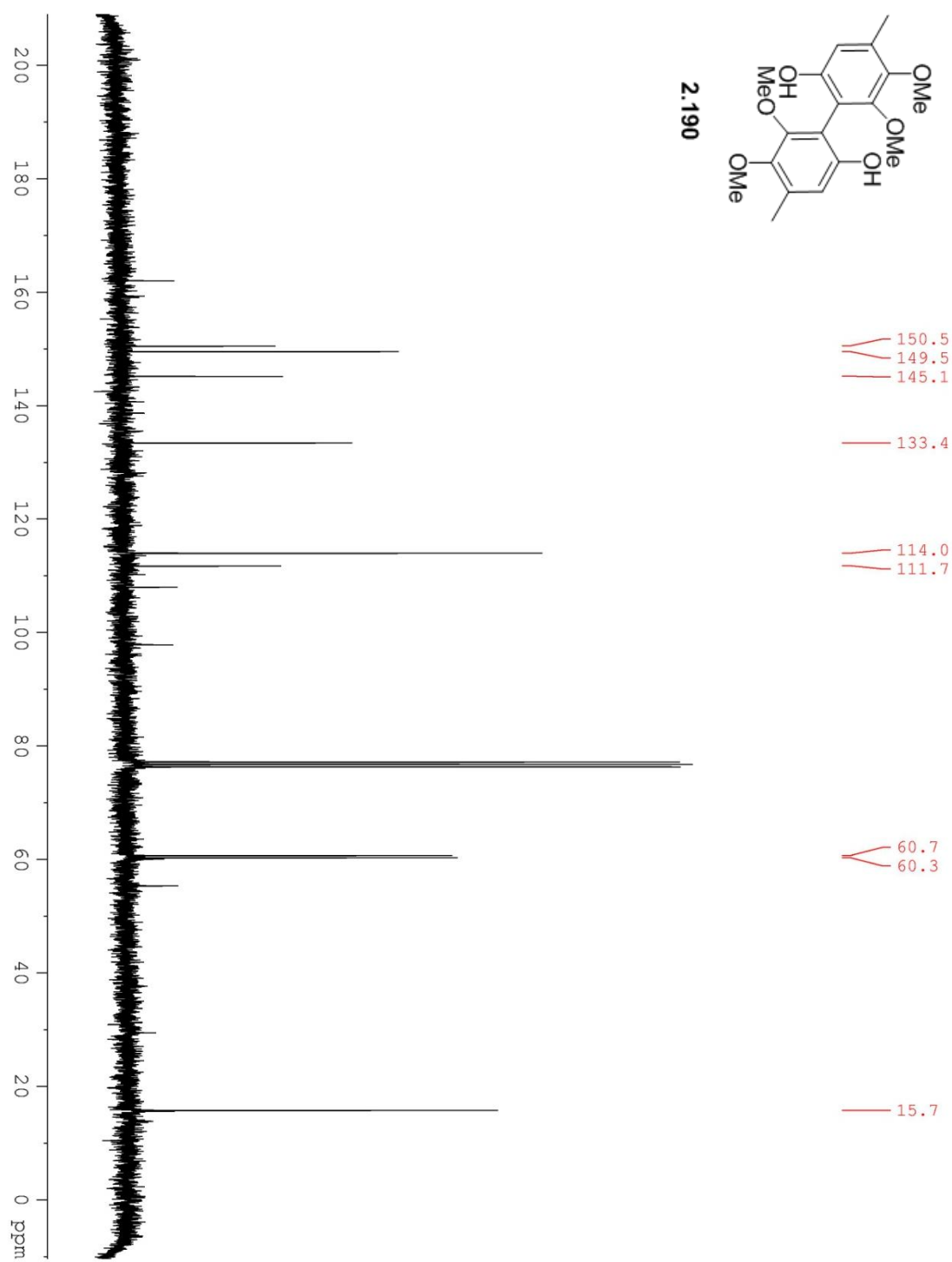


Figure A63. 100 MHz ^{13}C NMR of **2.190** in CDCl_3 .

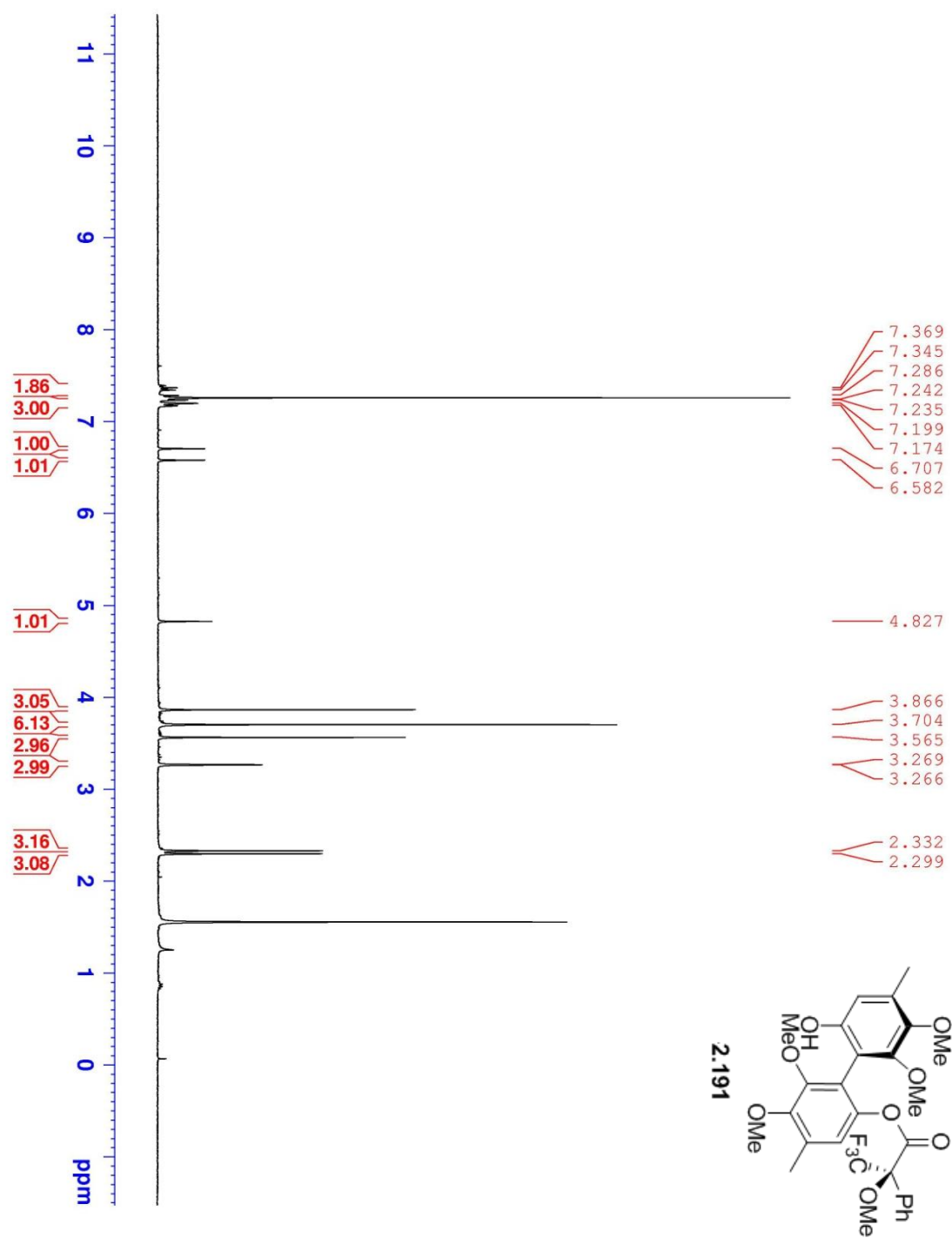


Figure A64. 400 MHz ^1H NMR of Faster Eluting **2.191** in CDCl_3 .

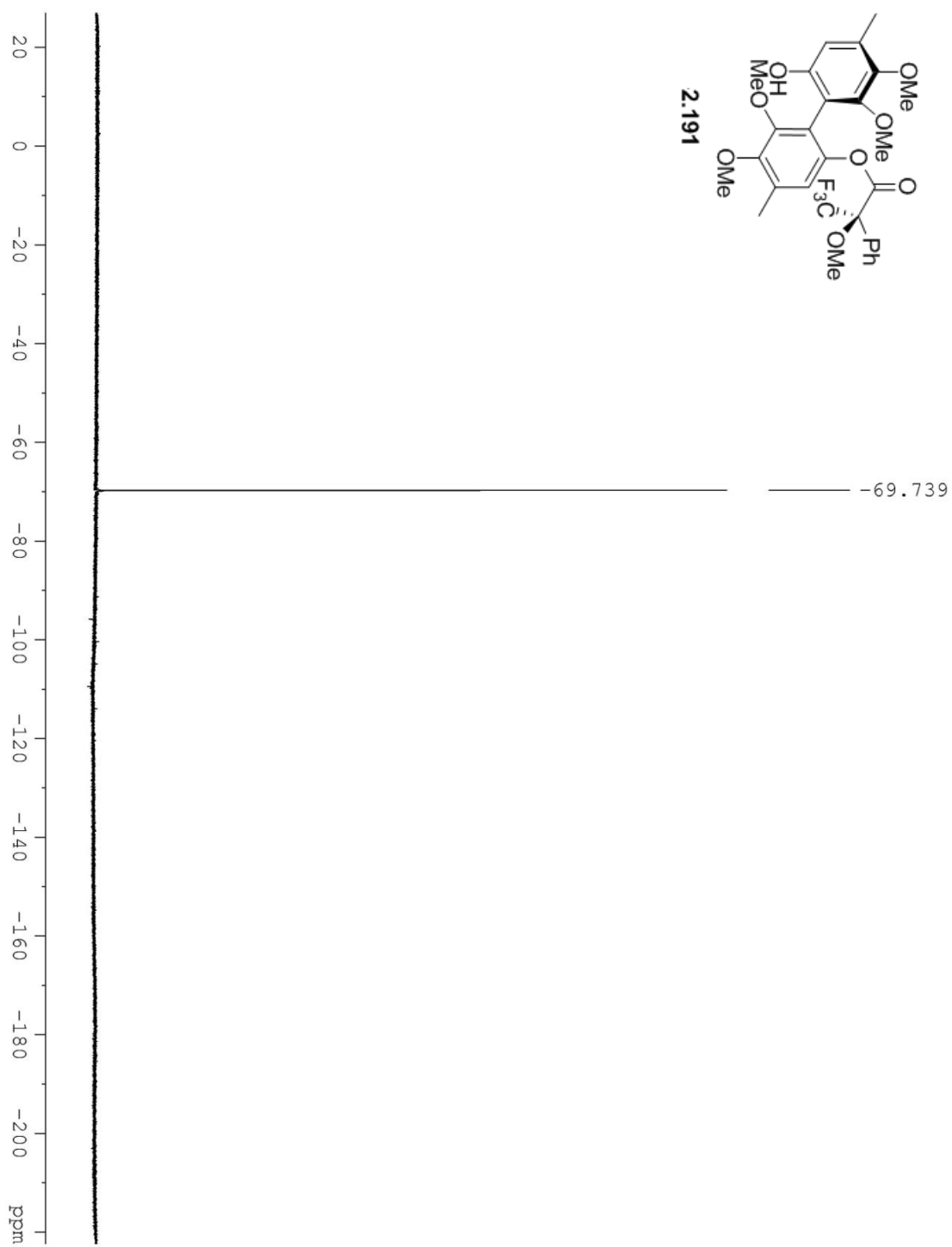


Figure A65. 282 MHz ^{19}F NMR of Faster Eluting **2.191** in CDCl_3 .

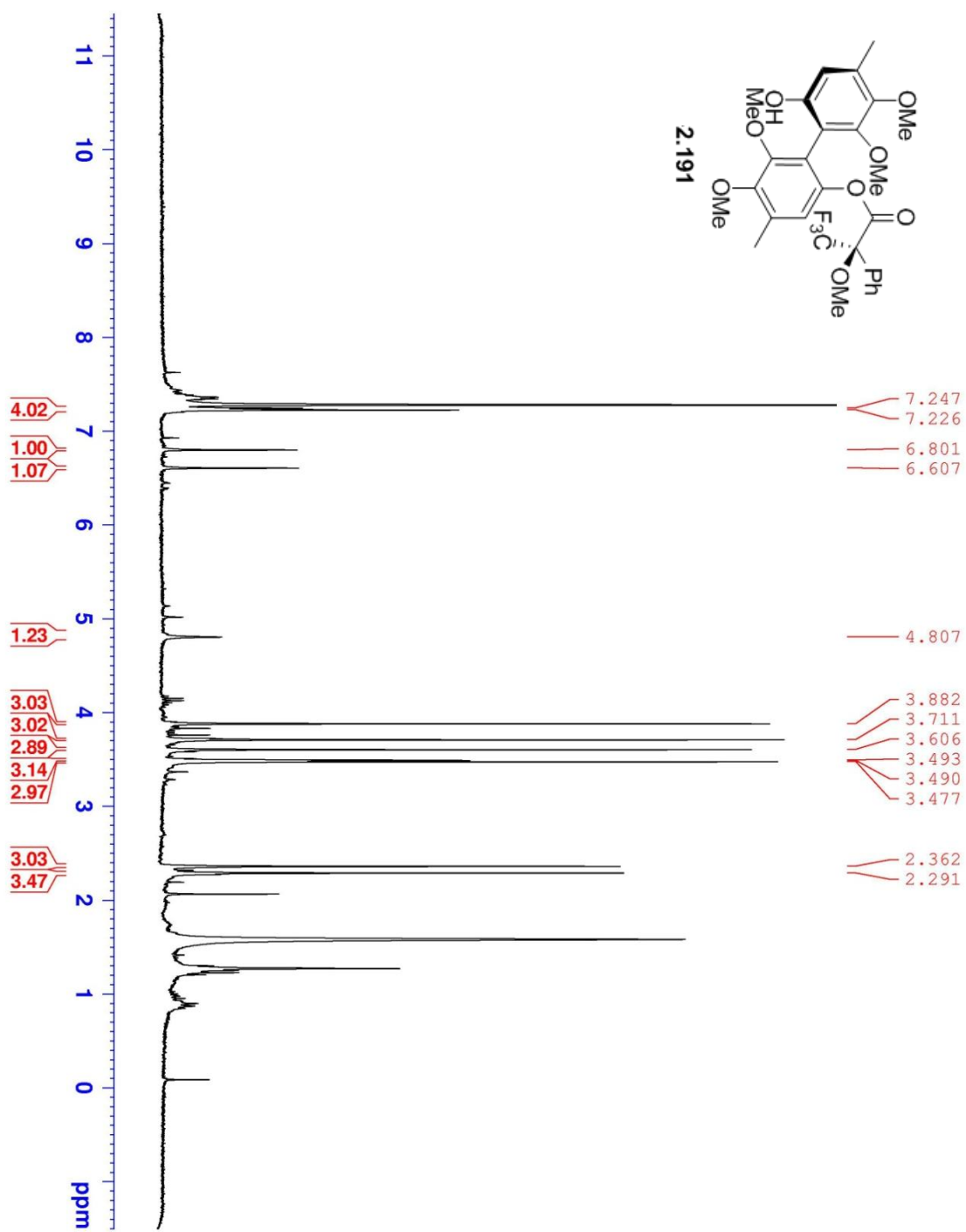


Figure A66. 300 MHz ^1H NMR of Slower Eluting **2.191** in CDCl_3 .

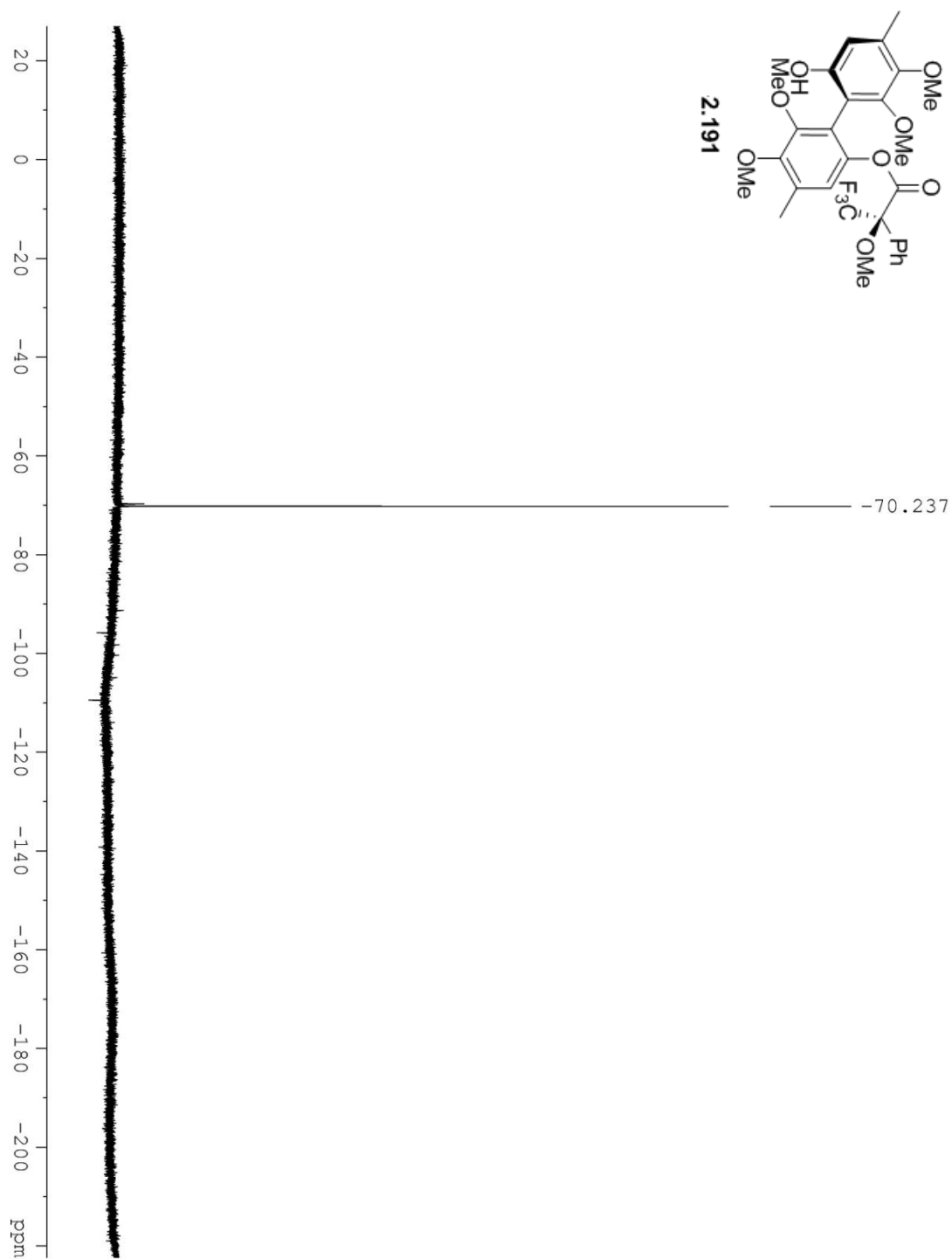


Figure A67. 282 MHz ^{19}F NMR of Slower Eluting **2.191** in CDCl_3 .

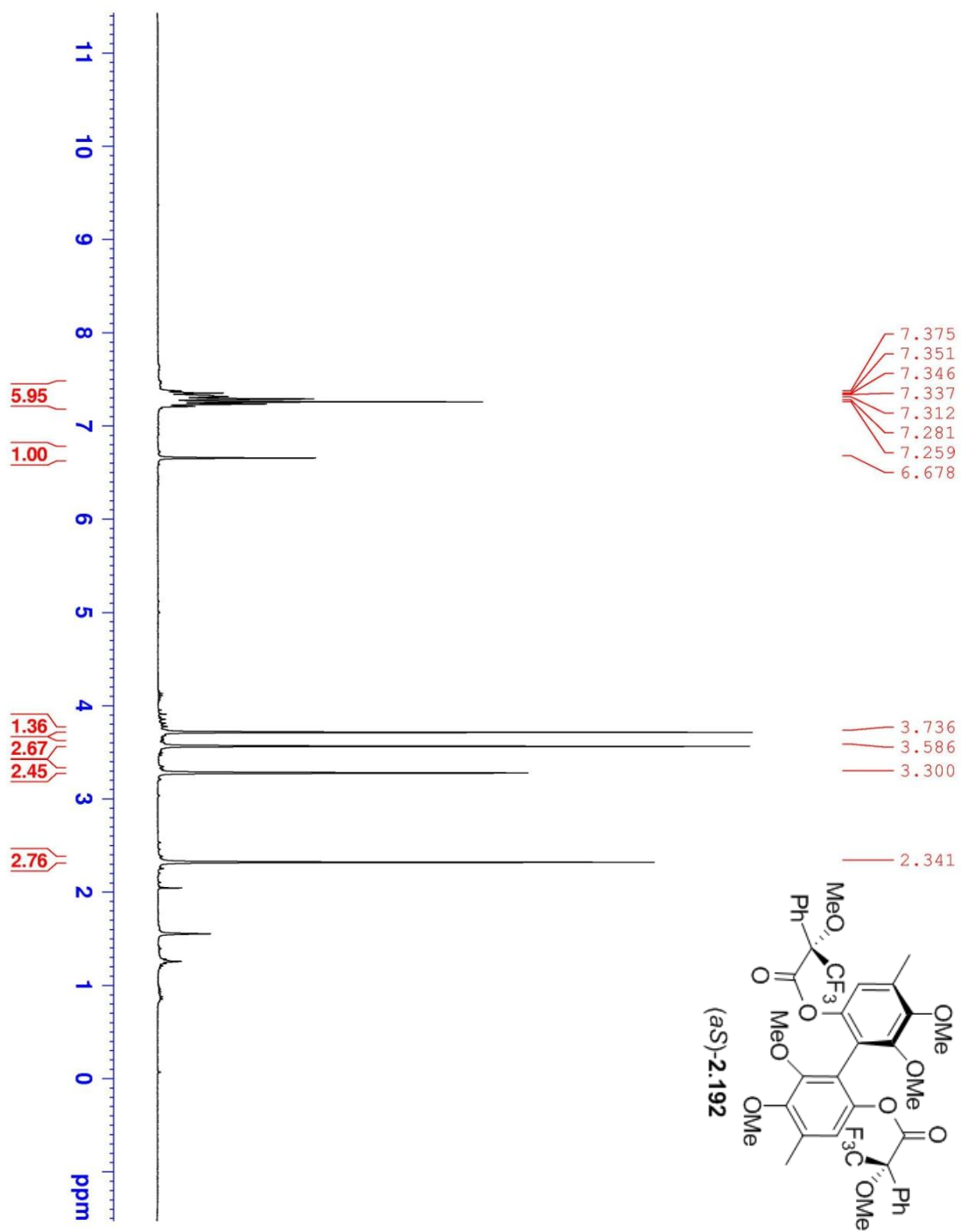


Figure A68. 300 MHz ^1H NMR of (aS)-2.192 in CDCl_3 .

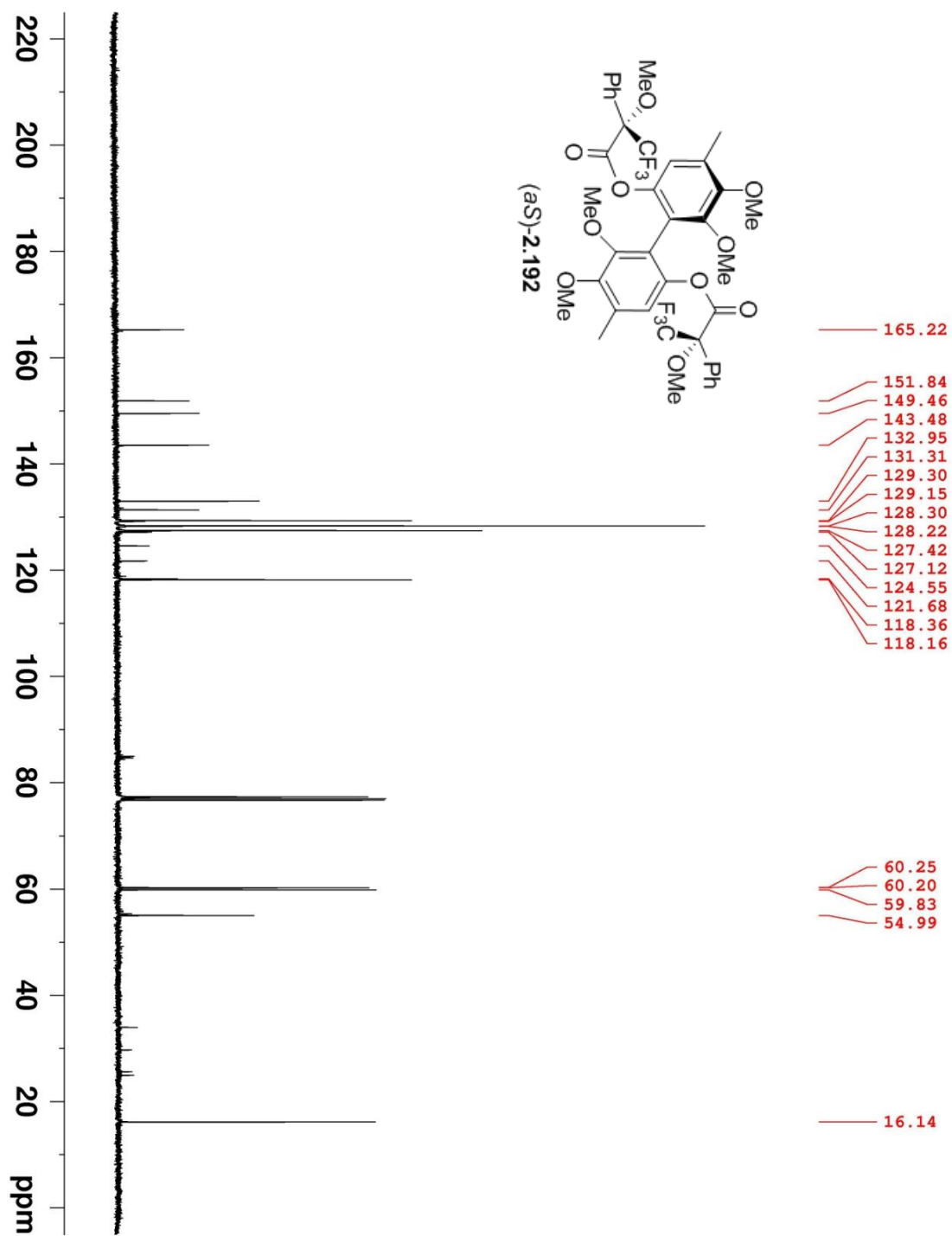


Figure A69. 100 MHz ^{13}C NMR of (aS)-2.192 in CDCl_3 .

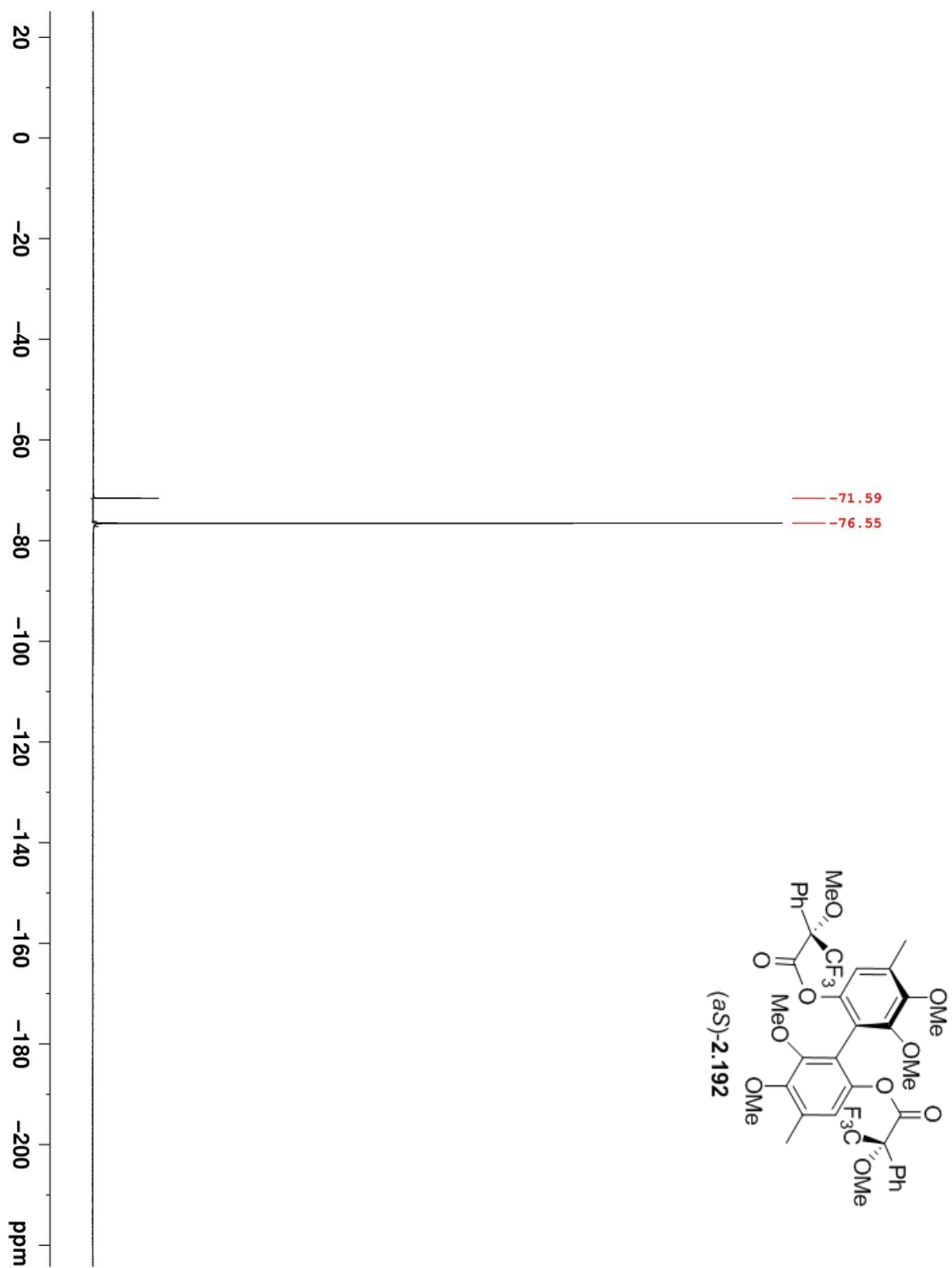


Figure A70. 282 MHz ^{19}F NMR of (aS)-2.192 in CDCl_3 .

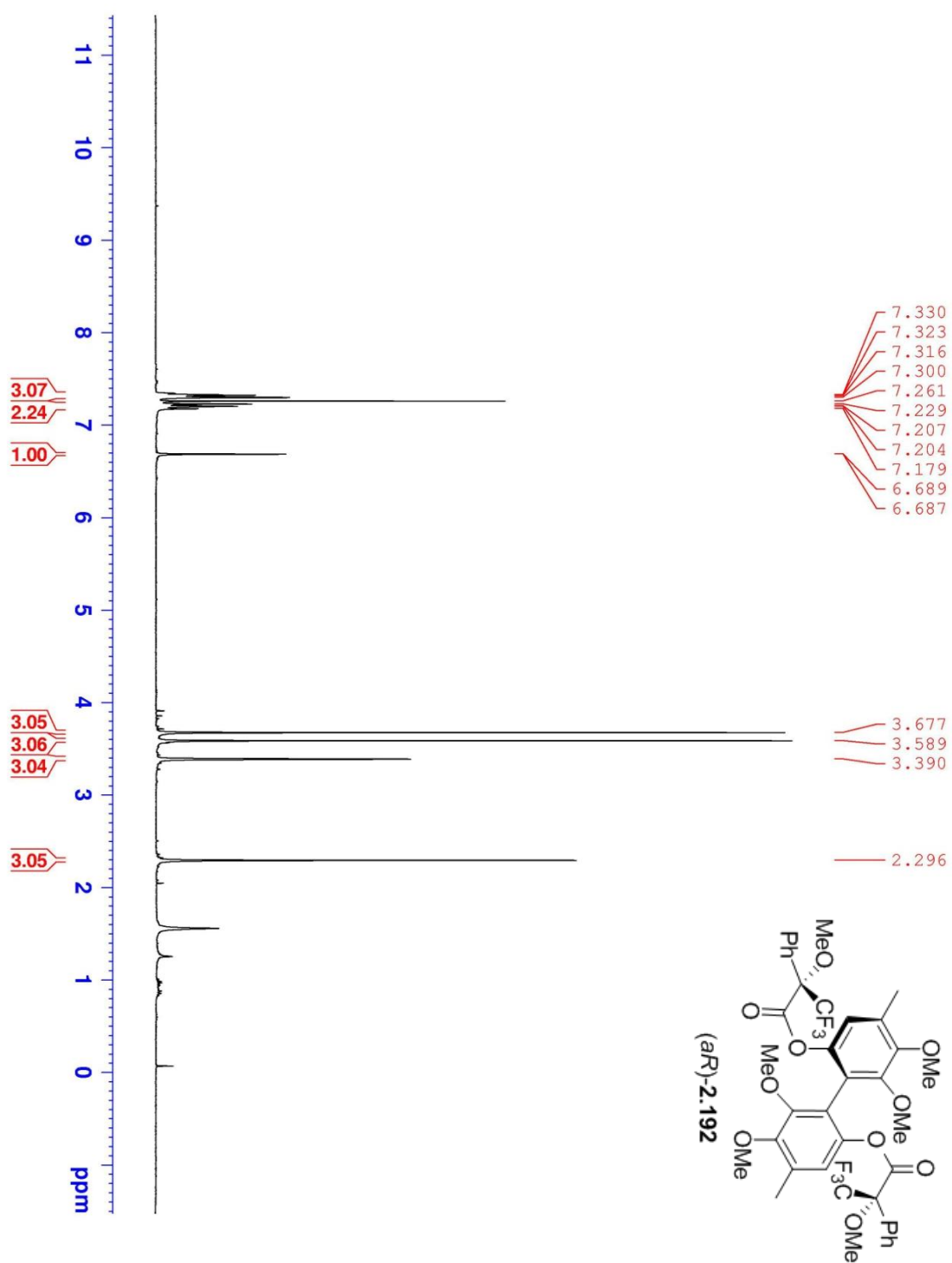


Figure A71. 400 MHz ¹H NMR of (aR)-2.192 in CDCl₃.

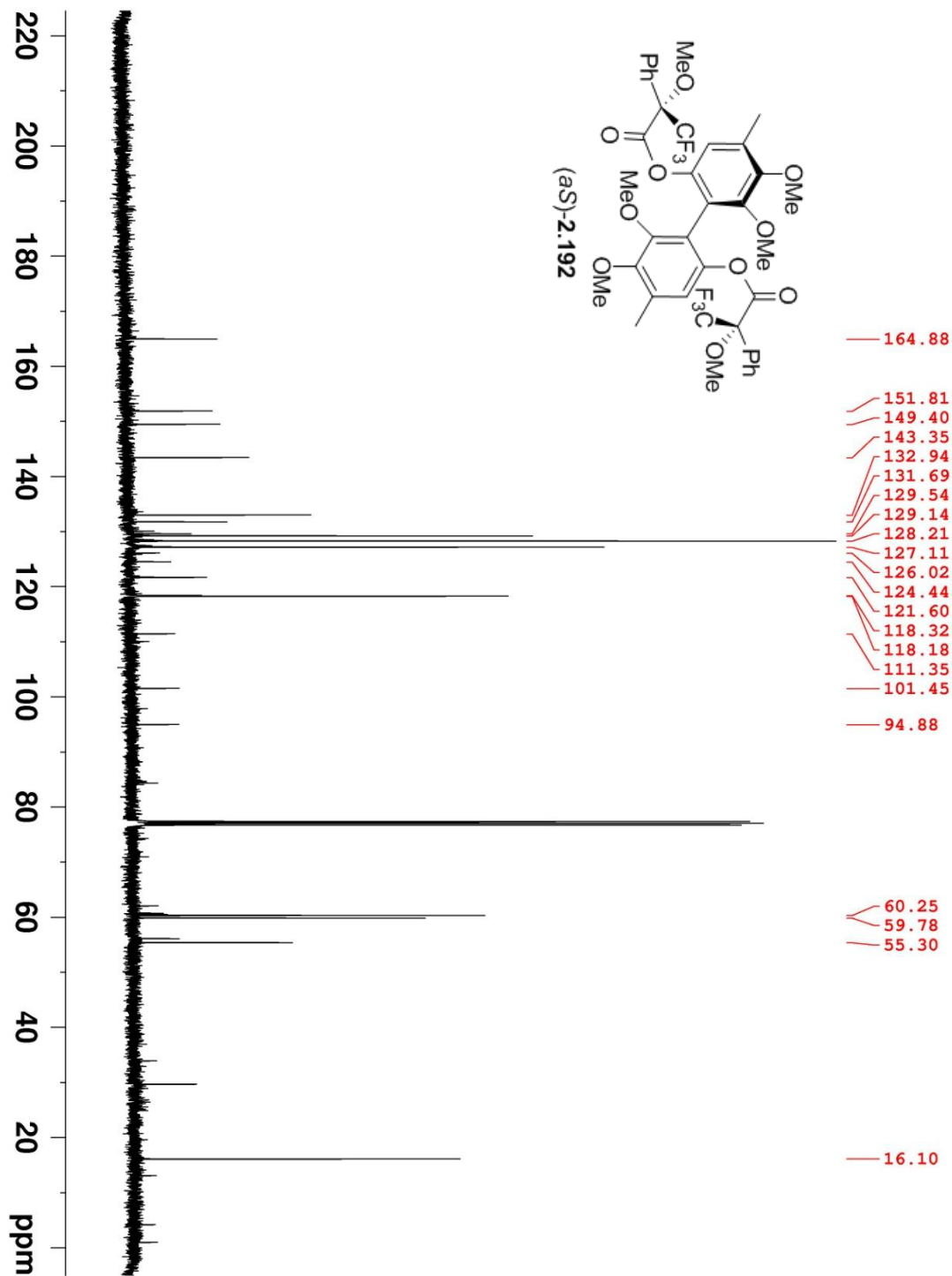


Figure A72. 100 MHz ¹³C NMR of (aS)-2.192 in CDCl₃.

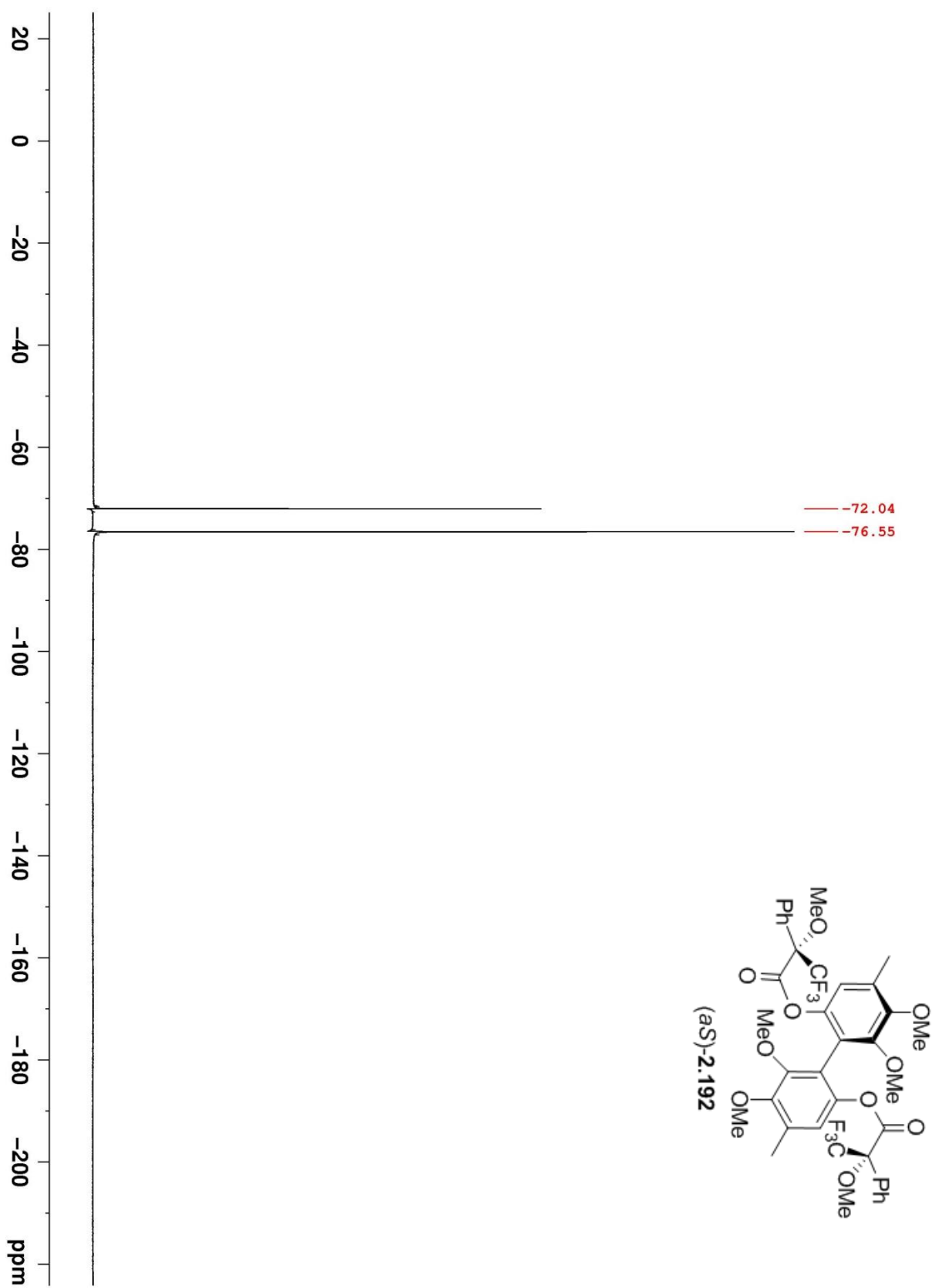


Figure A73. 282 MHz ¹⁹F NMR of (aS)-2.192 in CDCl₃.

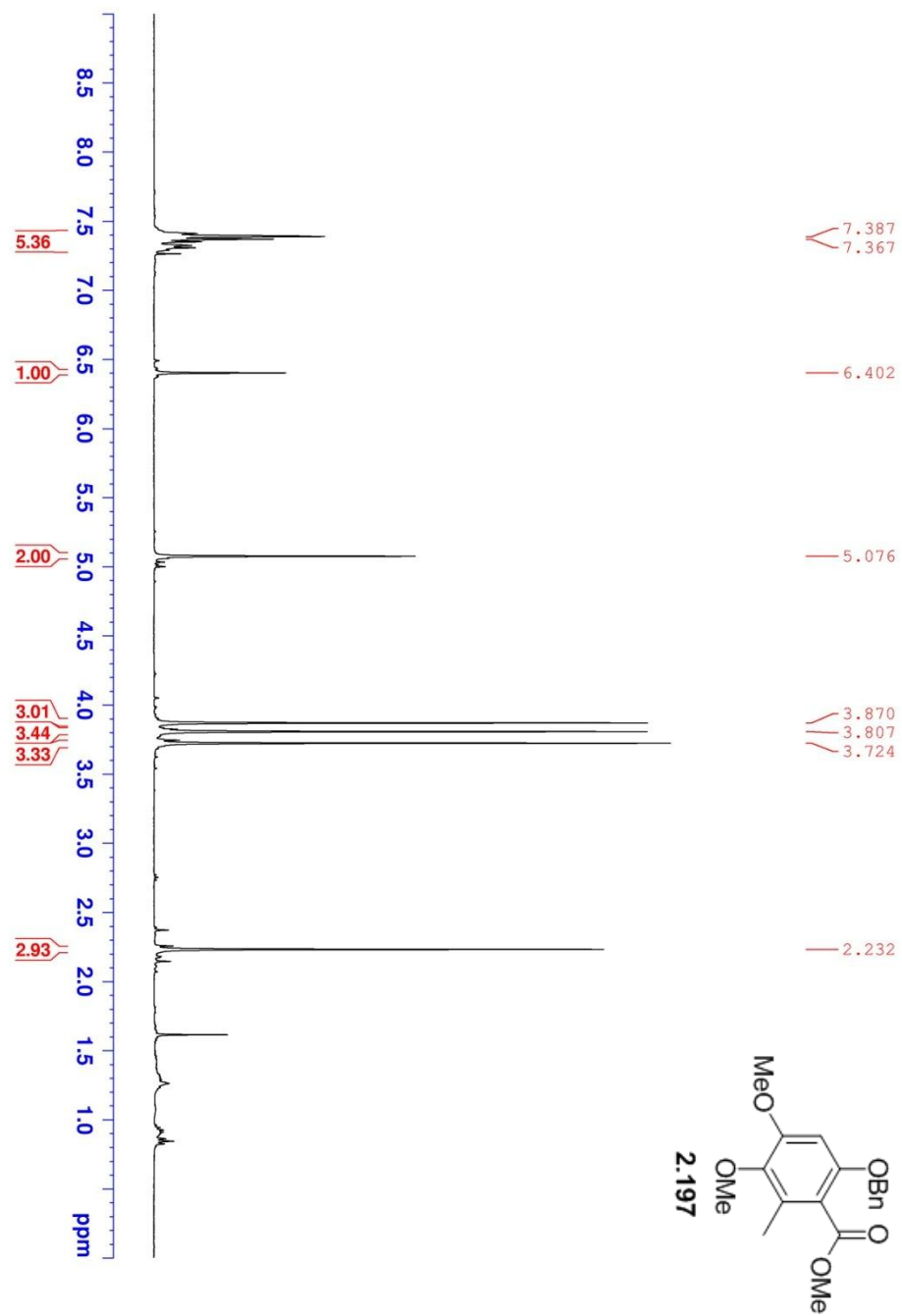


Figure A74. 400 MHz ¹H NMR of **2.197** in CDCl₃.

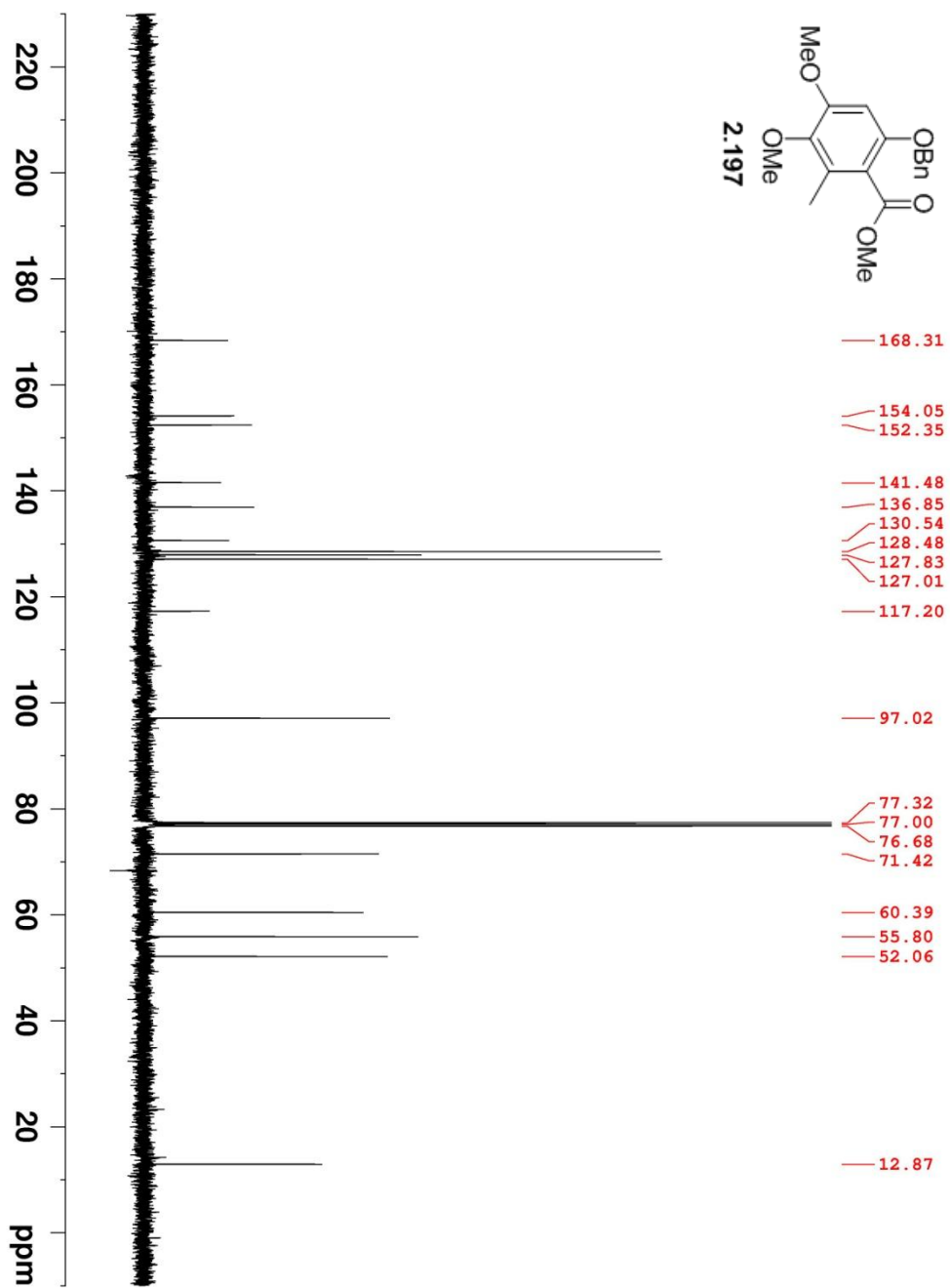


Figure A75. 100 MHz ^{13}C NMR of **2.197** in CDCl_3 .

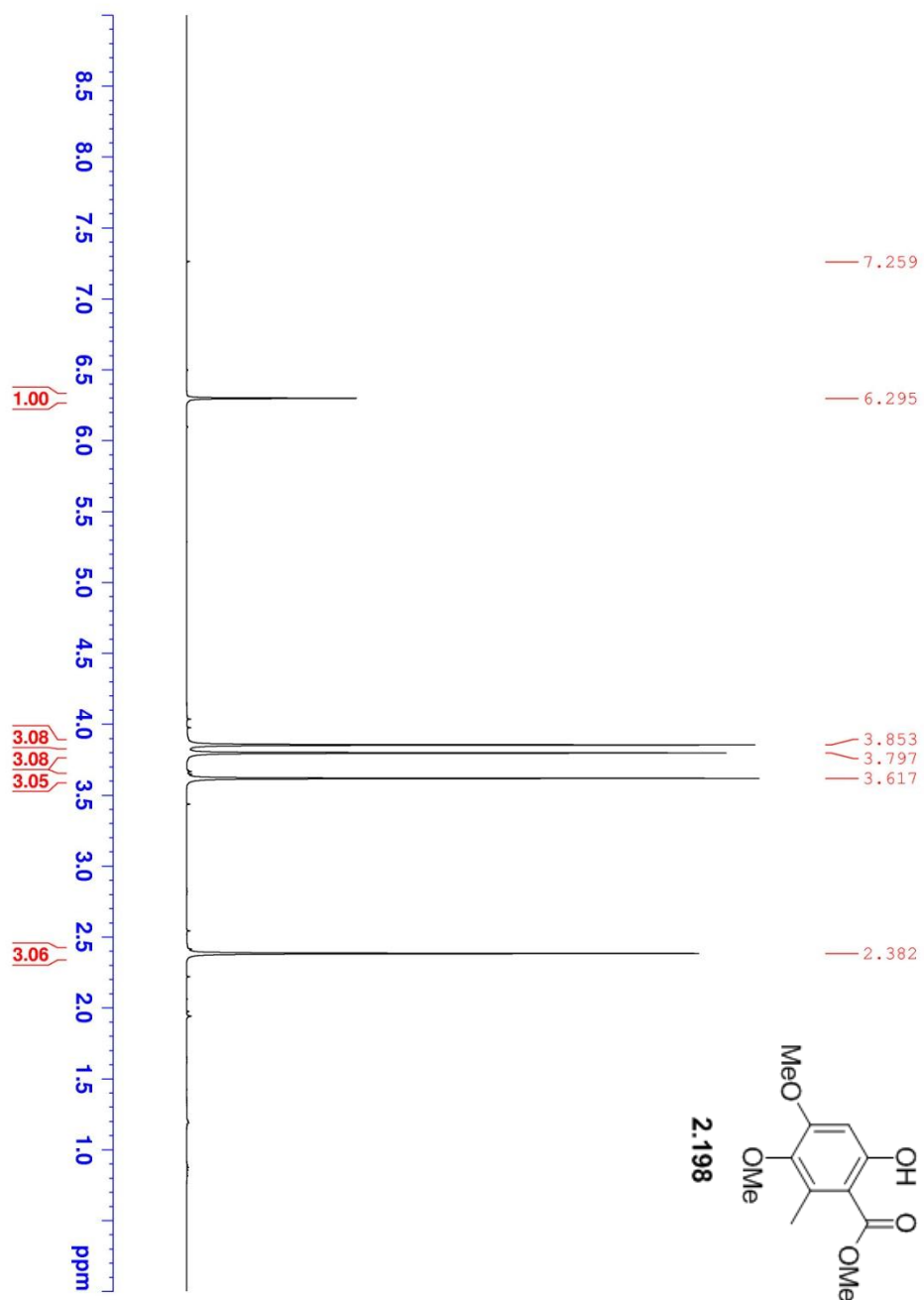


Figure A76. 400 MHz ^1H NMR of **2.198** in CDCl_3 .

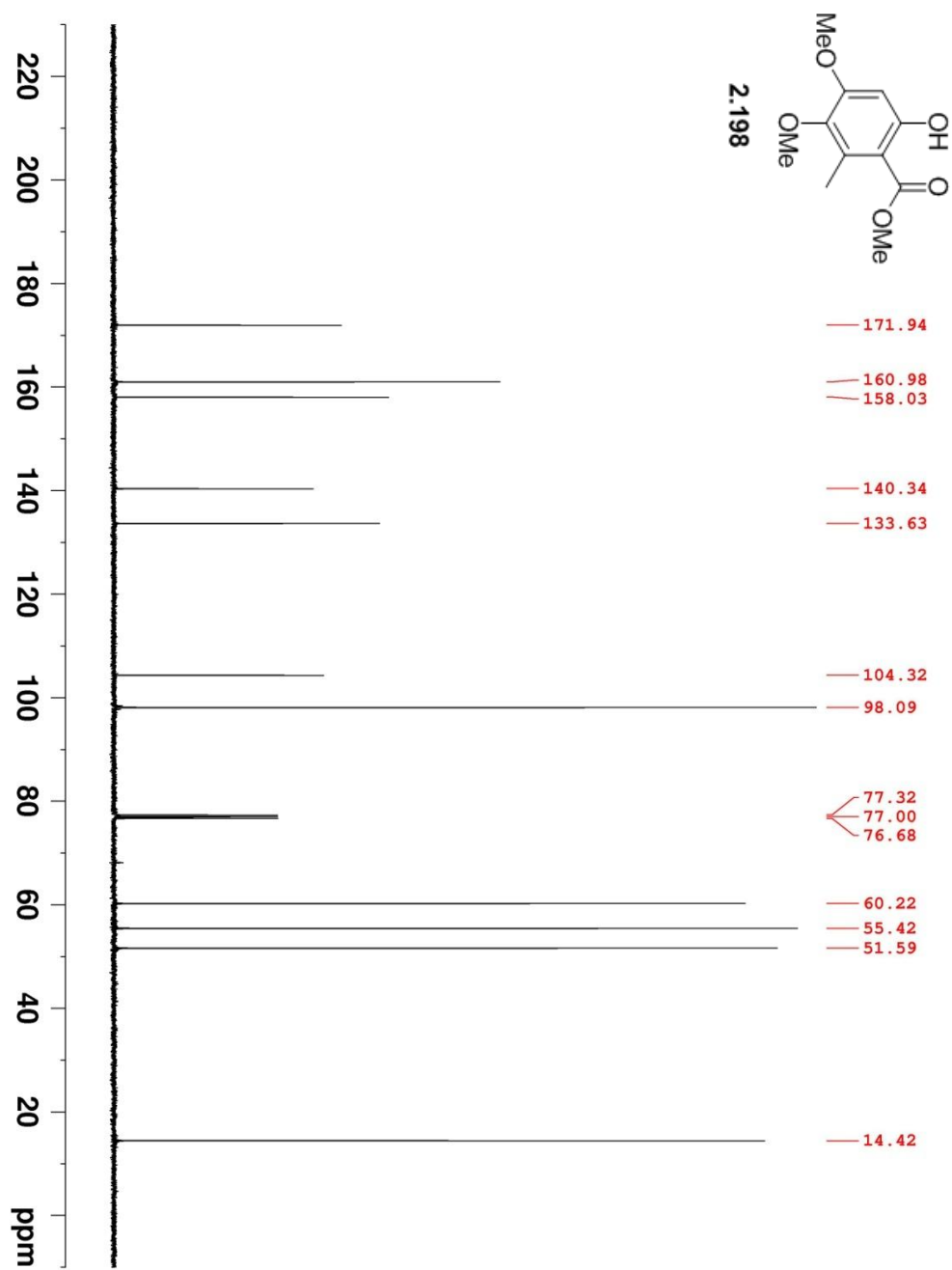


Figure A77. 100 MHz ^{13}C NMR of **2.198** in CDCl_3 .

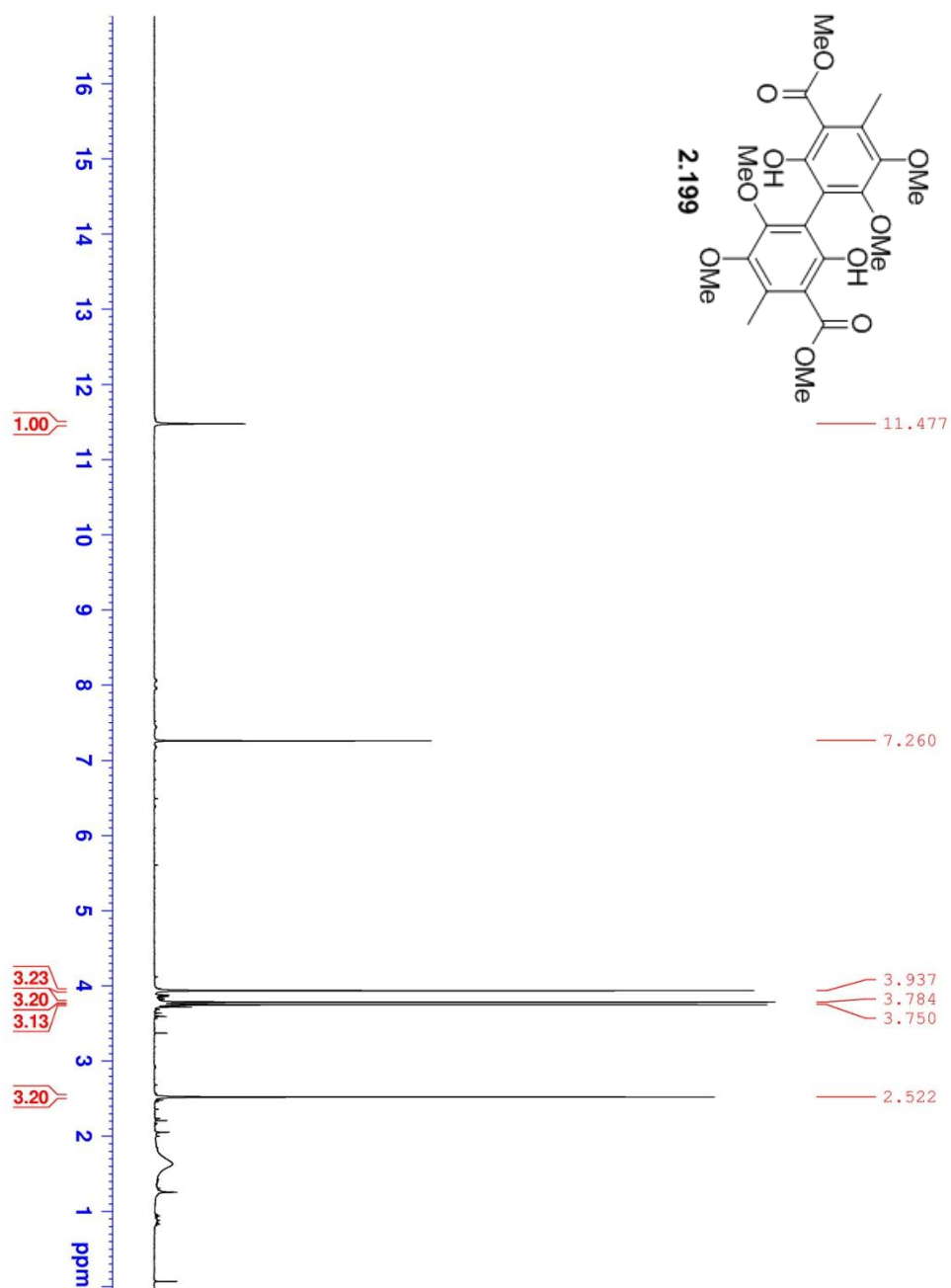


Figure A78. 400 MHz $^1\text{H NMR}$ of **2.199** in CDCl_3 .

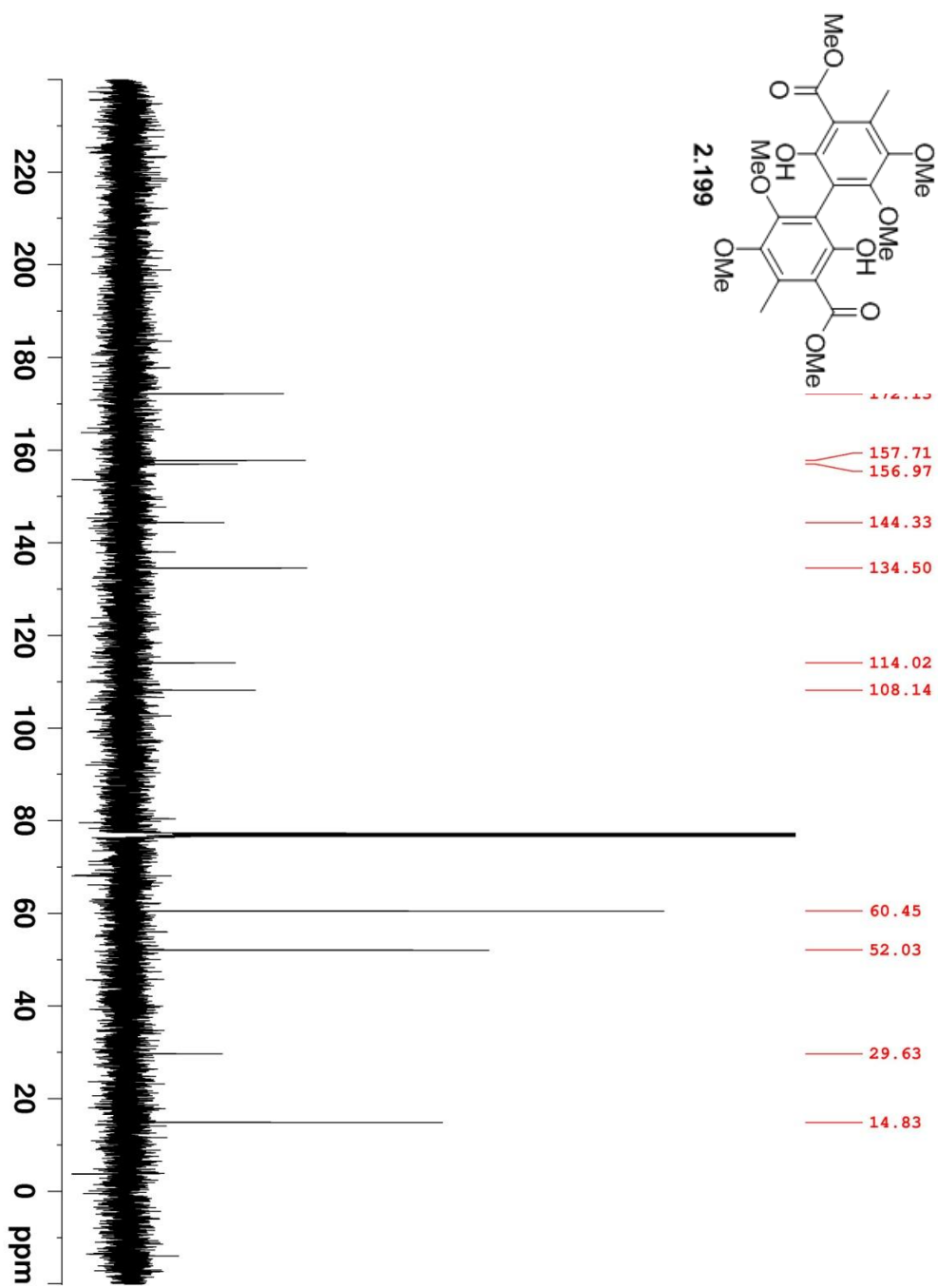


Figure A79. 100 MHz ^{13}C NMR of **2.199** in CDCl_3 .

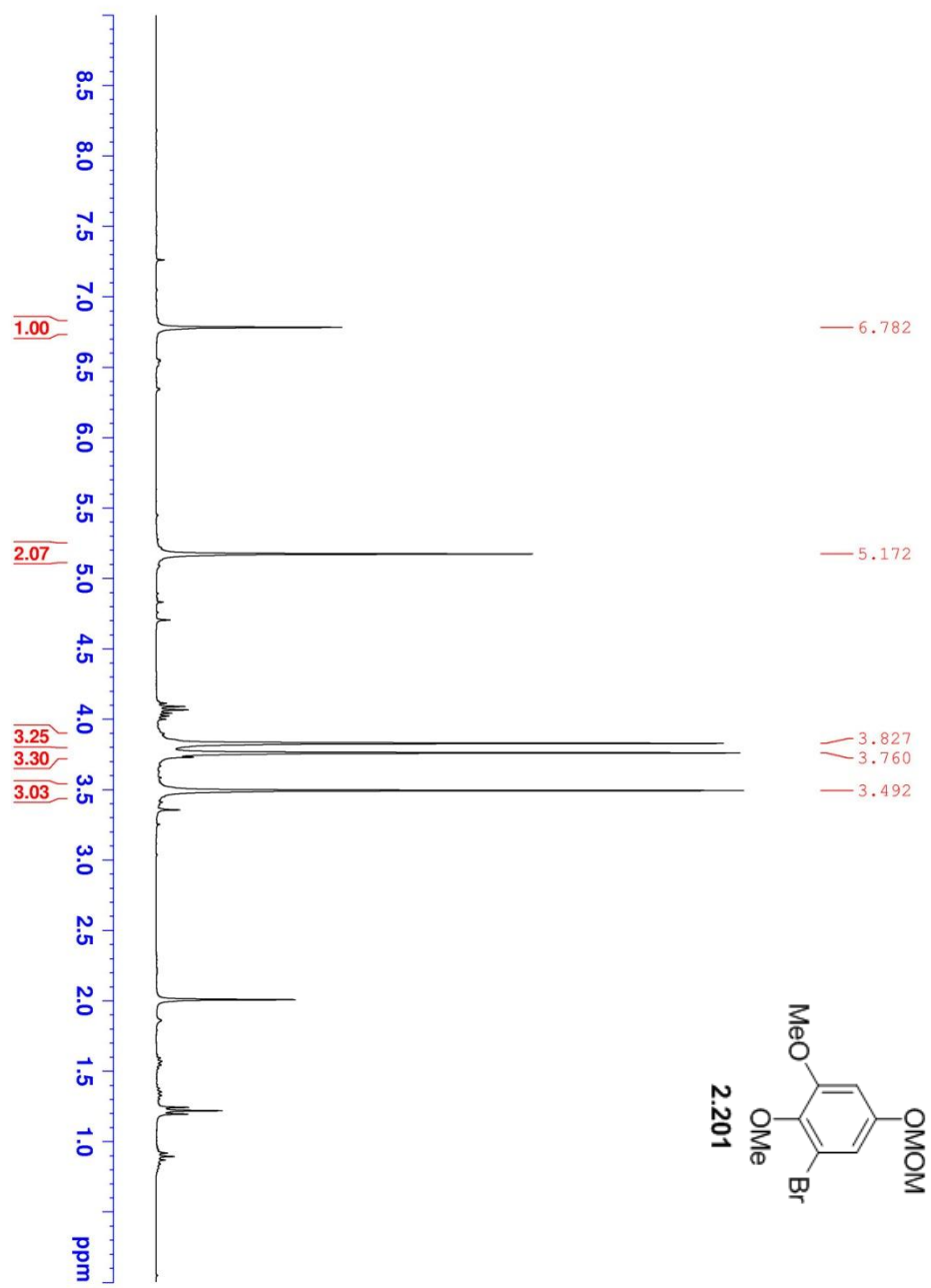


Figure A80. 300 MHz ^1H NMR of **2.201** in CDCl_3 .

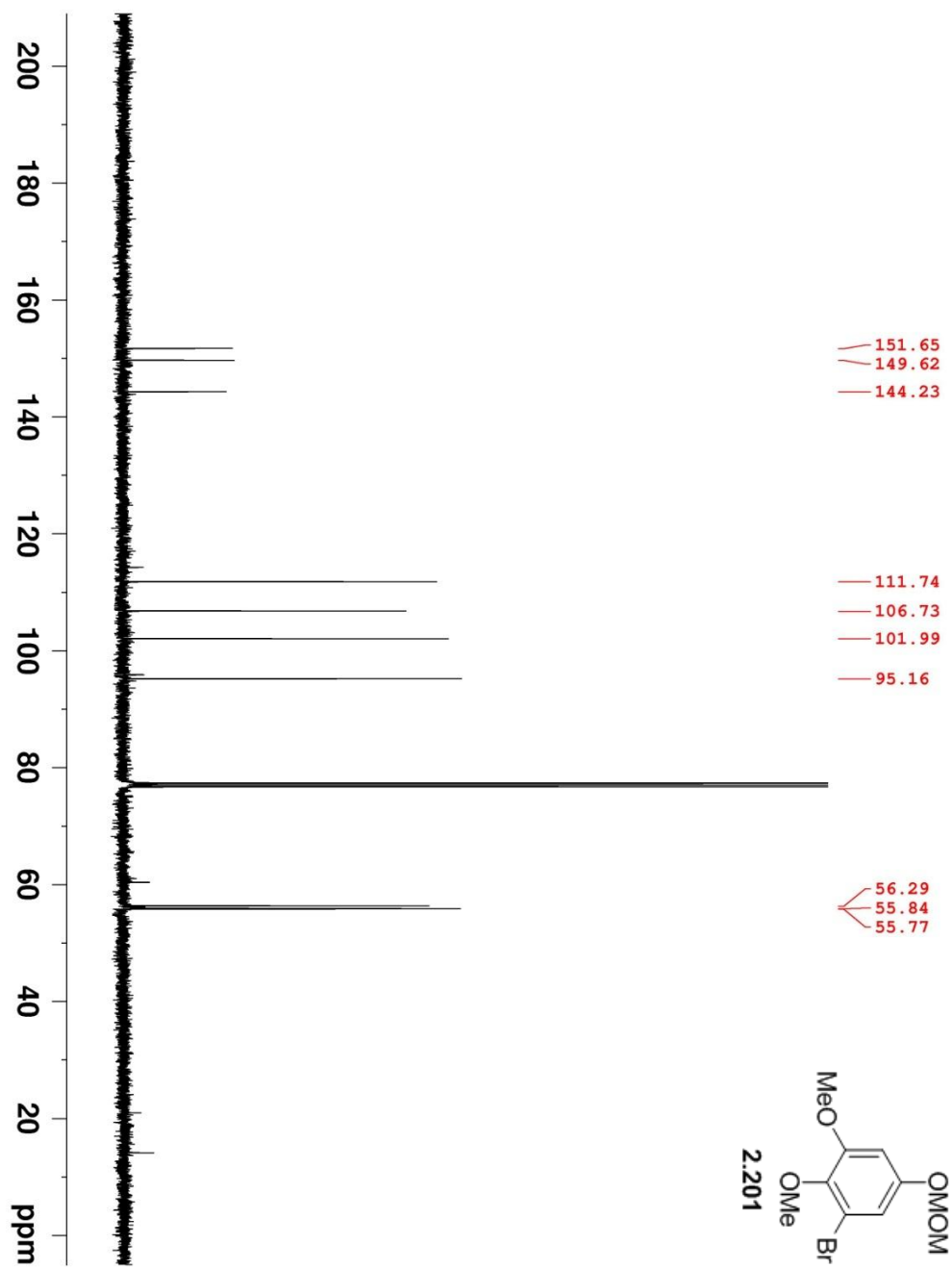


Figure A81. 100 MHz ^{13}C NMR of **2.201** in CDCl_3 .

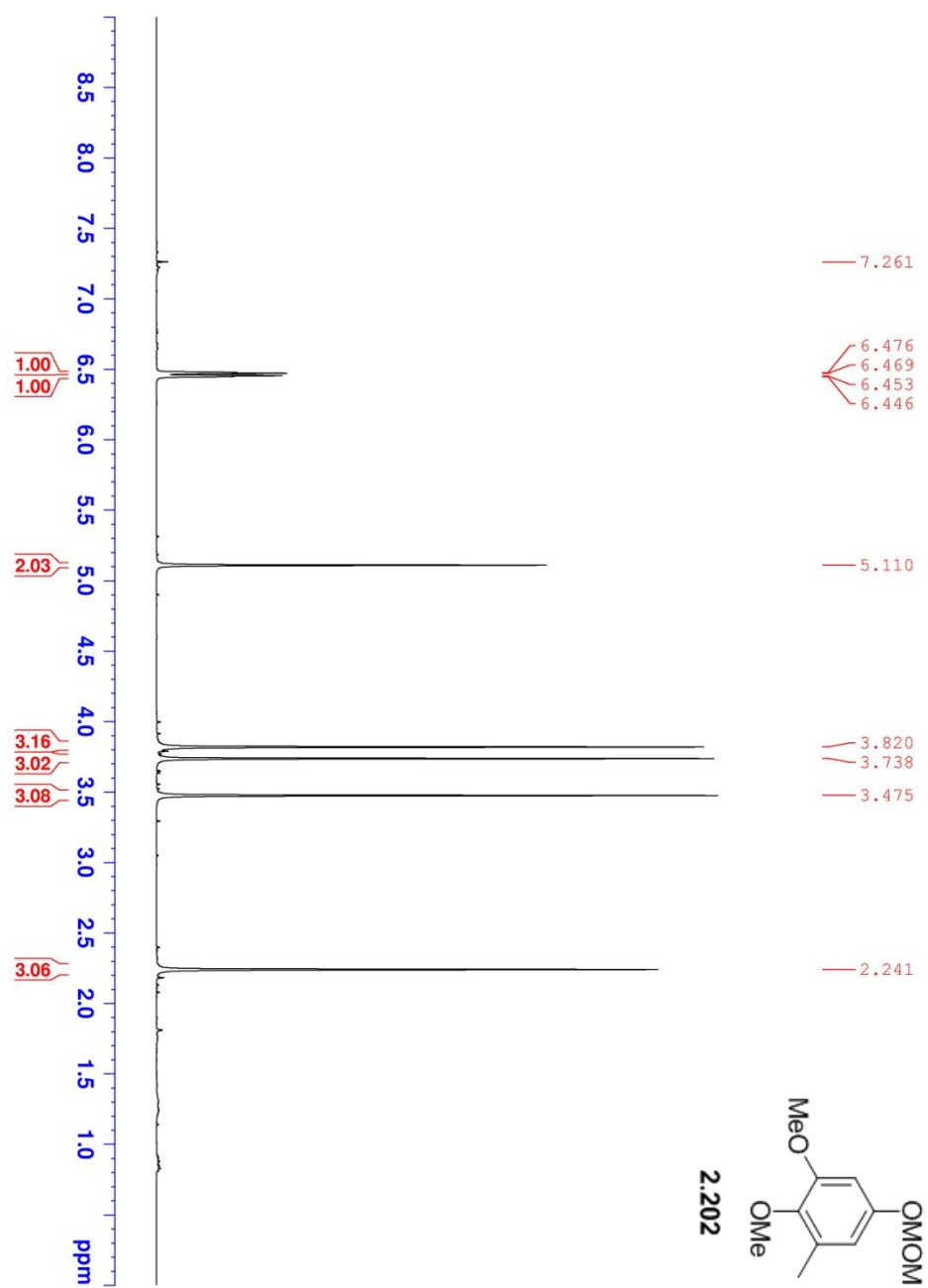


Figure A82. 400 MHz ^1H NMR of **2.202** in CDCl_3 .

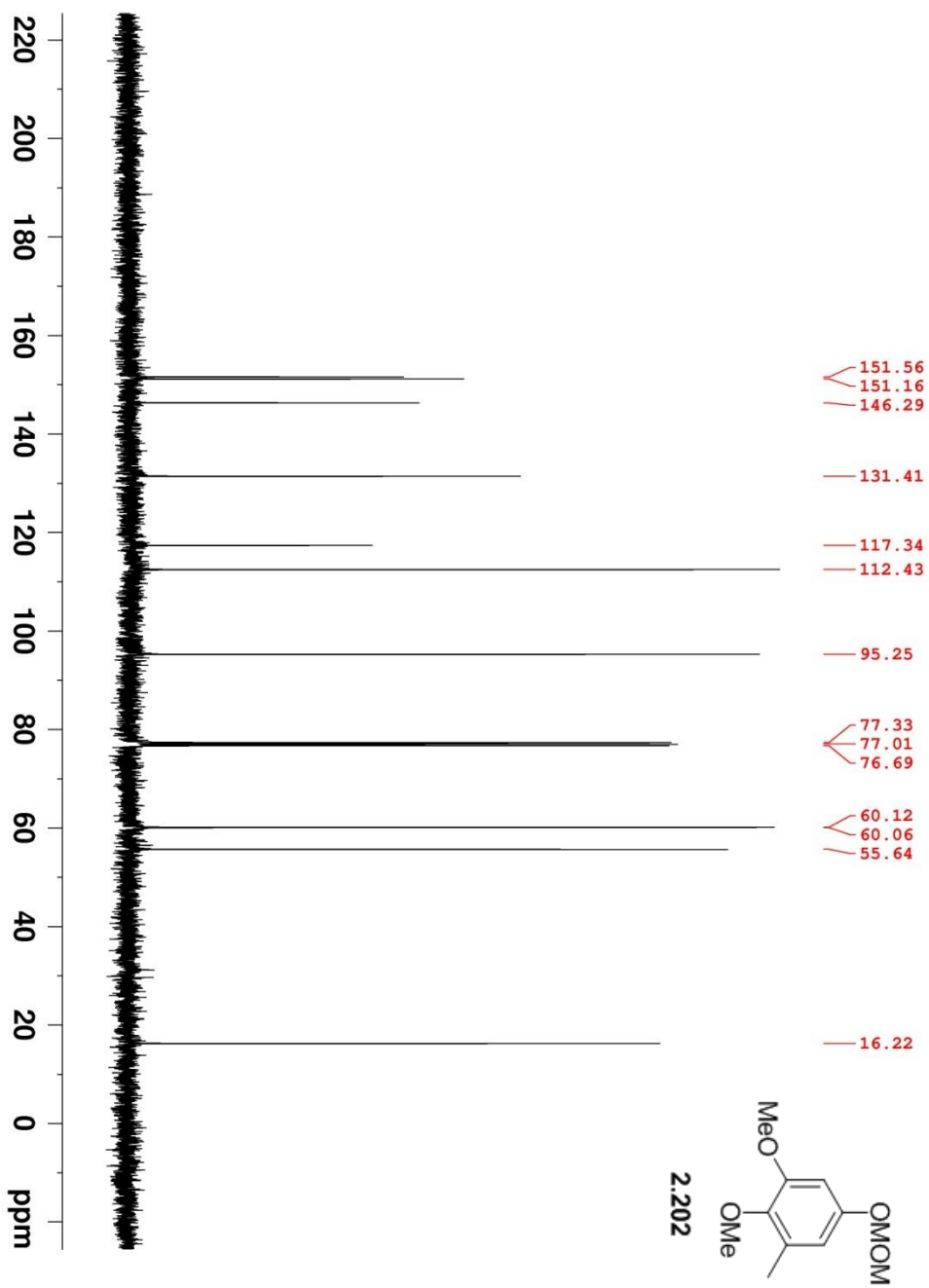


Figure A83. 100 MHz ^{13}C NMR of **2.202** in CDCl_3 .

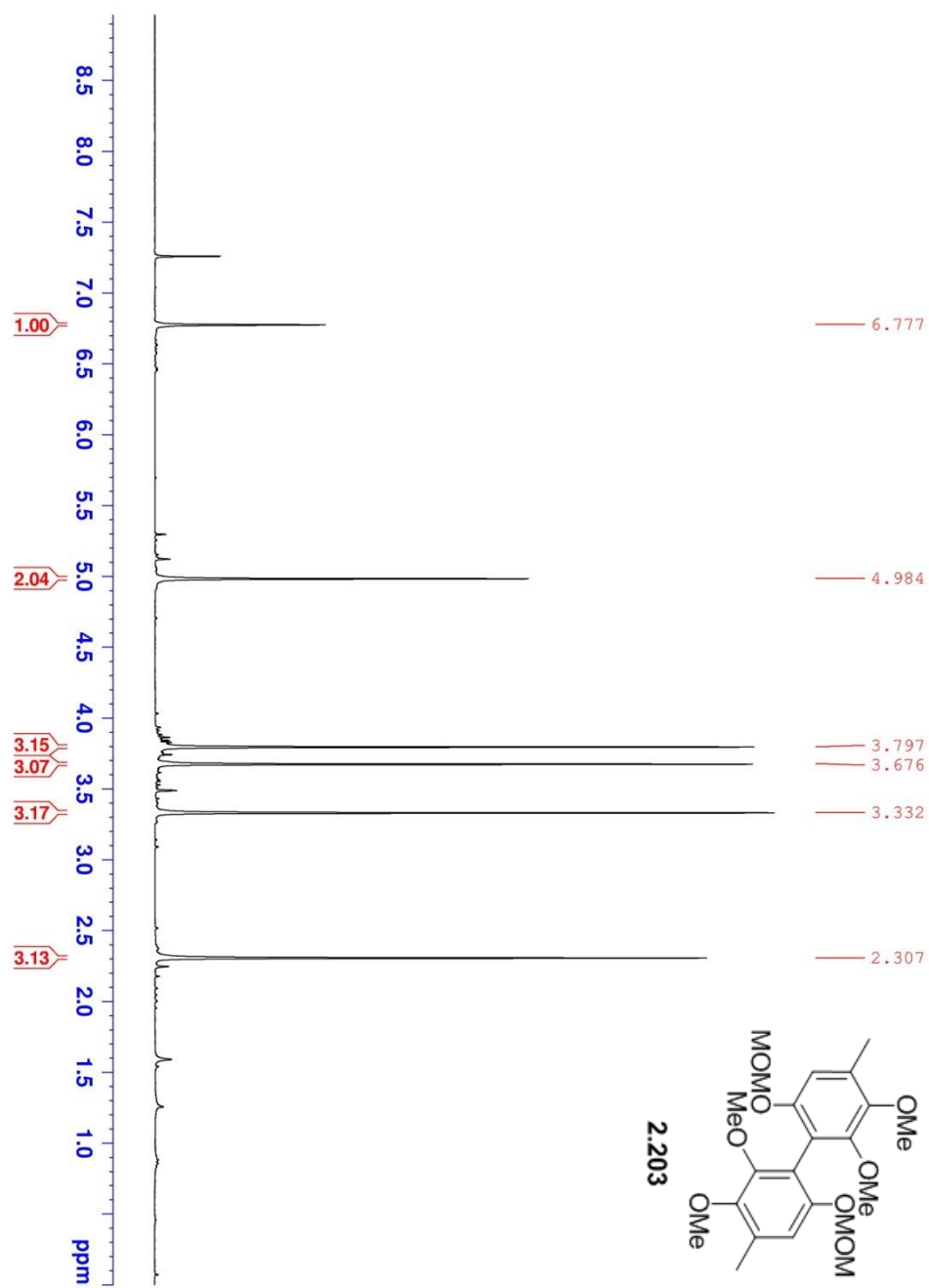


Figure A84. 400 MHz ¹H NMR of **2.203** in CDCl₃.

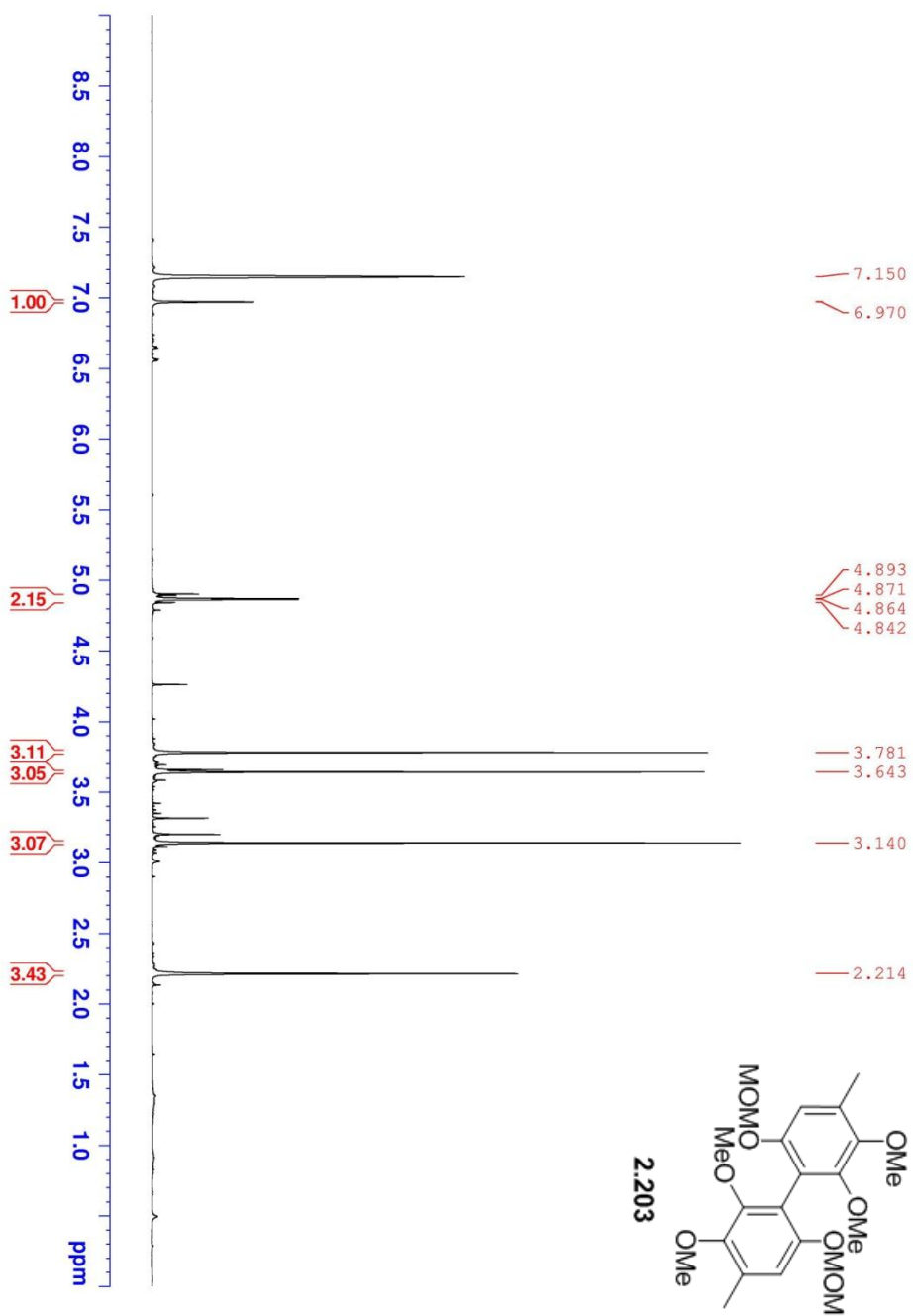


Figure A85. 400 MHz ¹H NMR of **2.203** in d₆-Benzene.

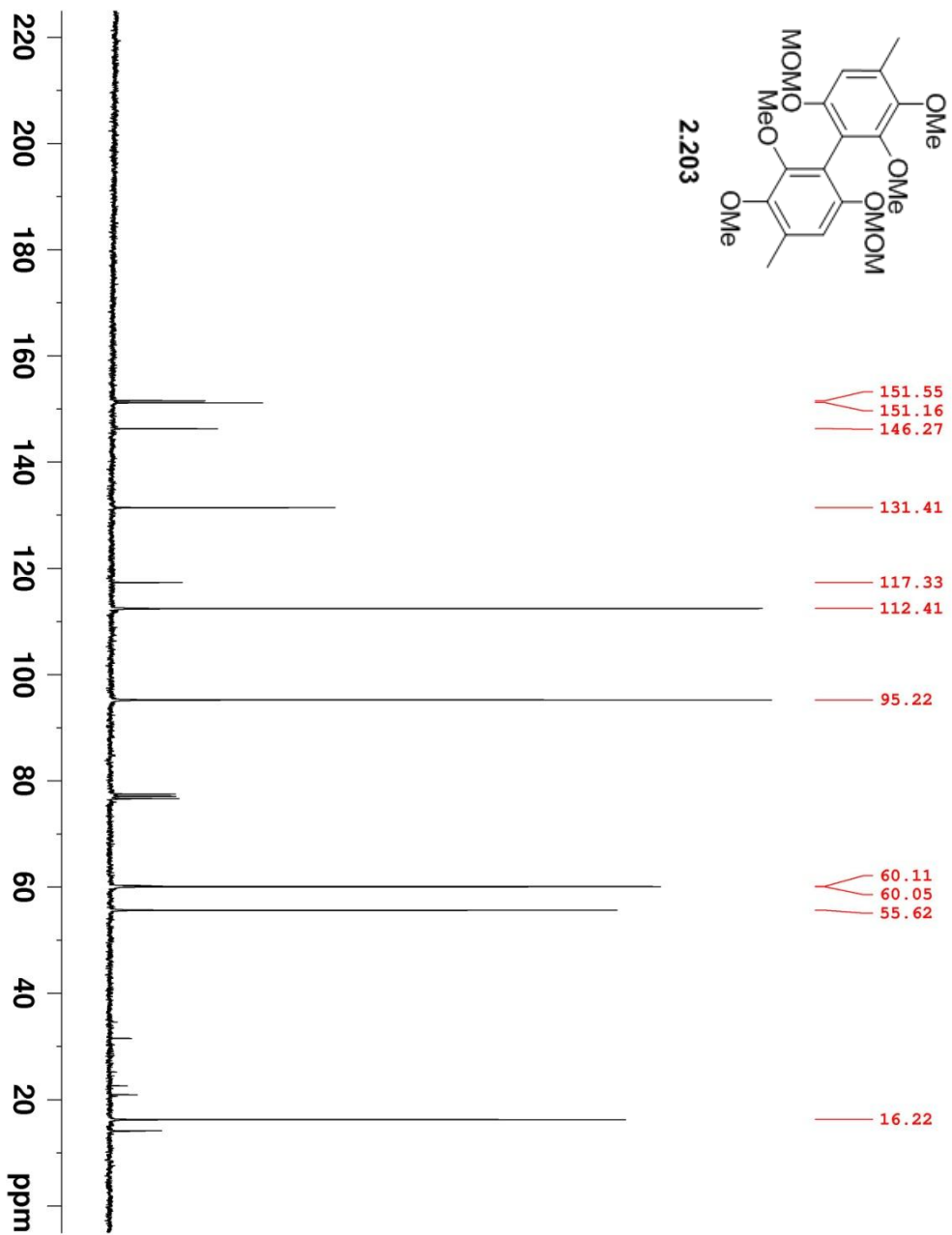


Figure A86. 100 MHz ^{13}C NMR of **2.203** in CDCl_3 .

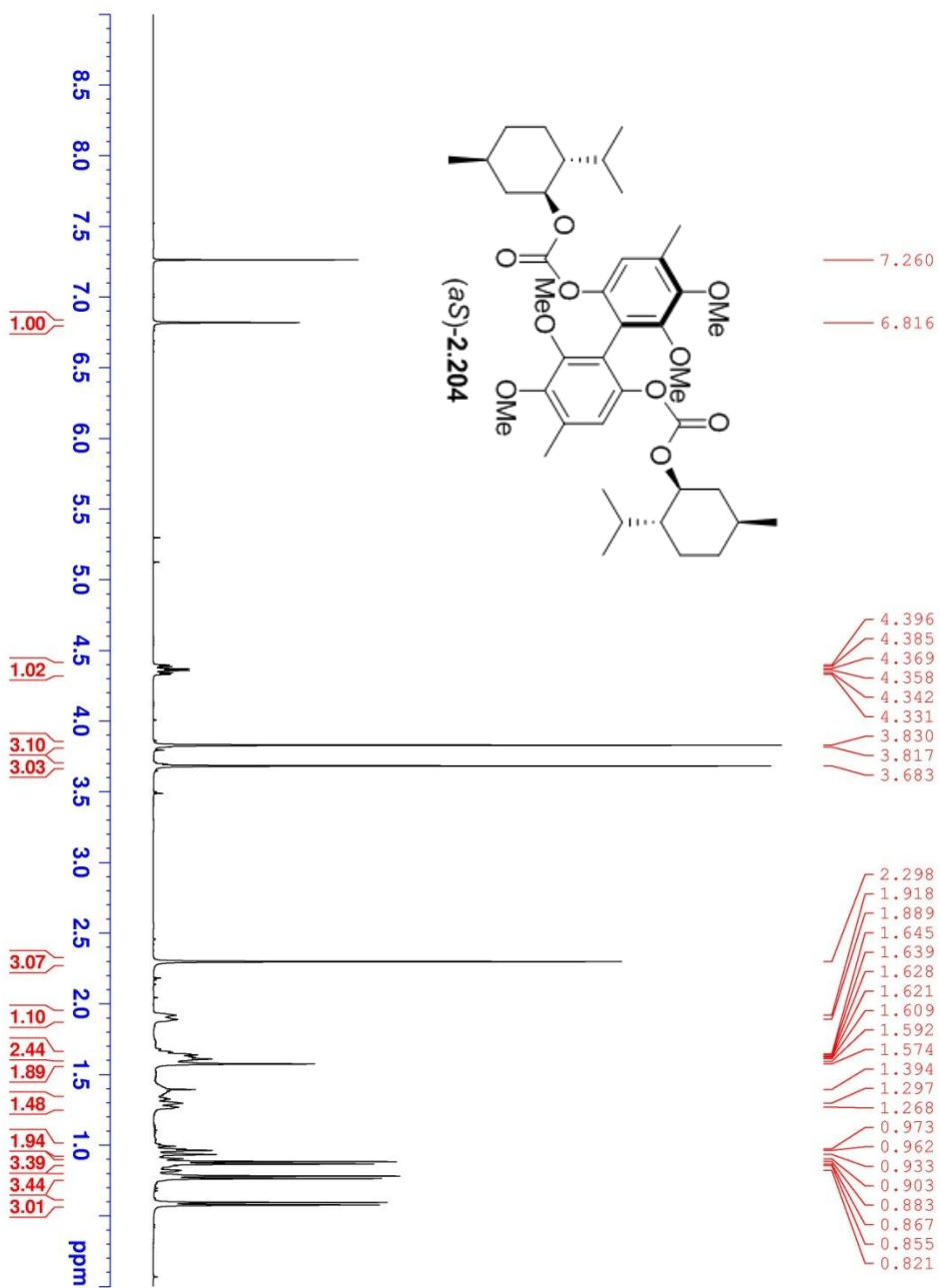


Figure A87. 400 MHz ^1H NMR of (aS)-2.204 in CDCl_3 .

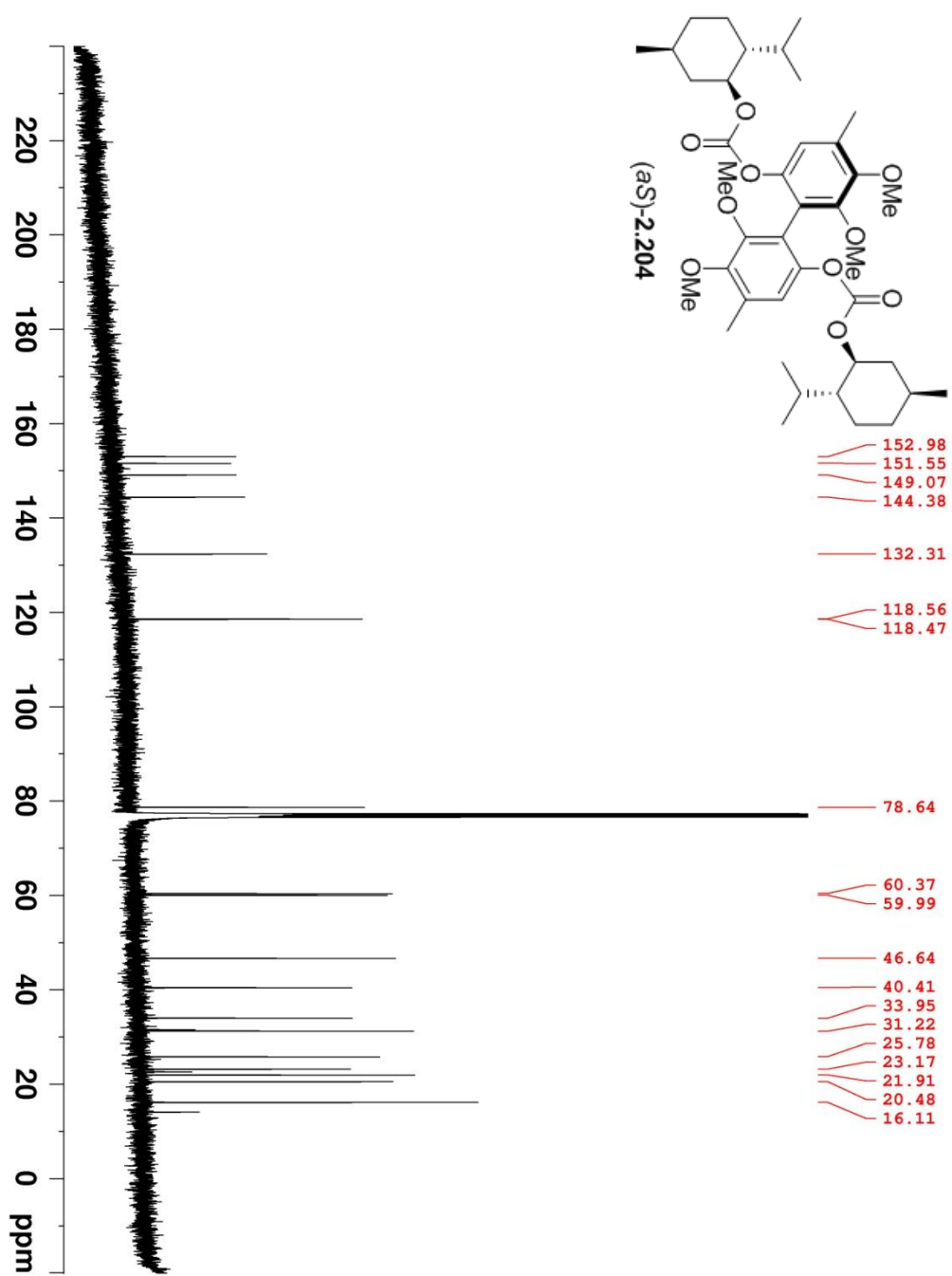


Figure A88. 100 MHz ^{13}C NMR of (aS)-2.204 in CDCl_3 .

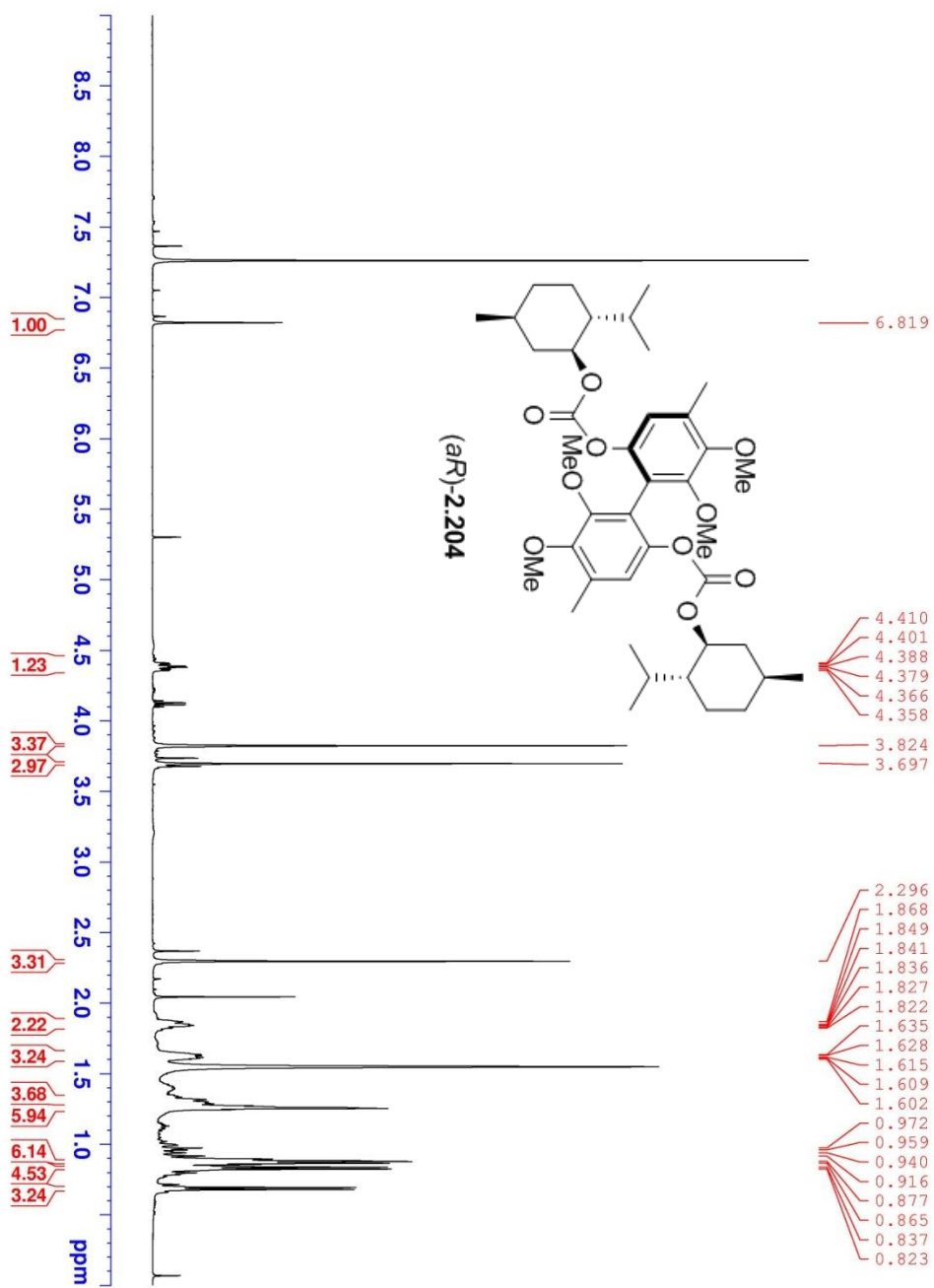


Figure A89. 400 MHz ^1H NMR of (aR)-2.204 in CDCl_3 .

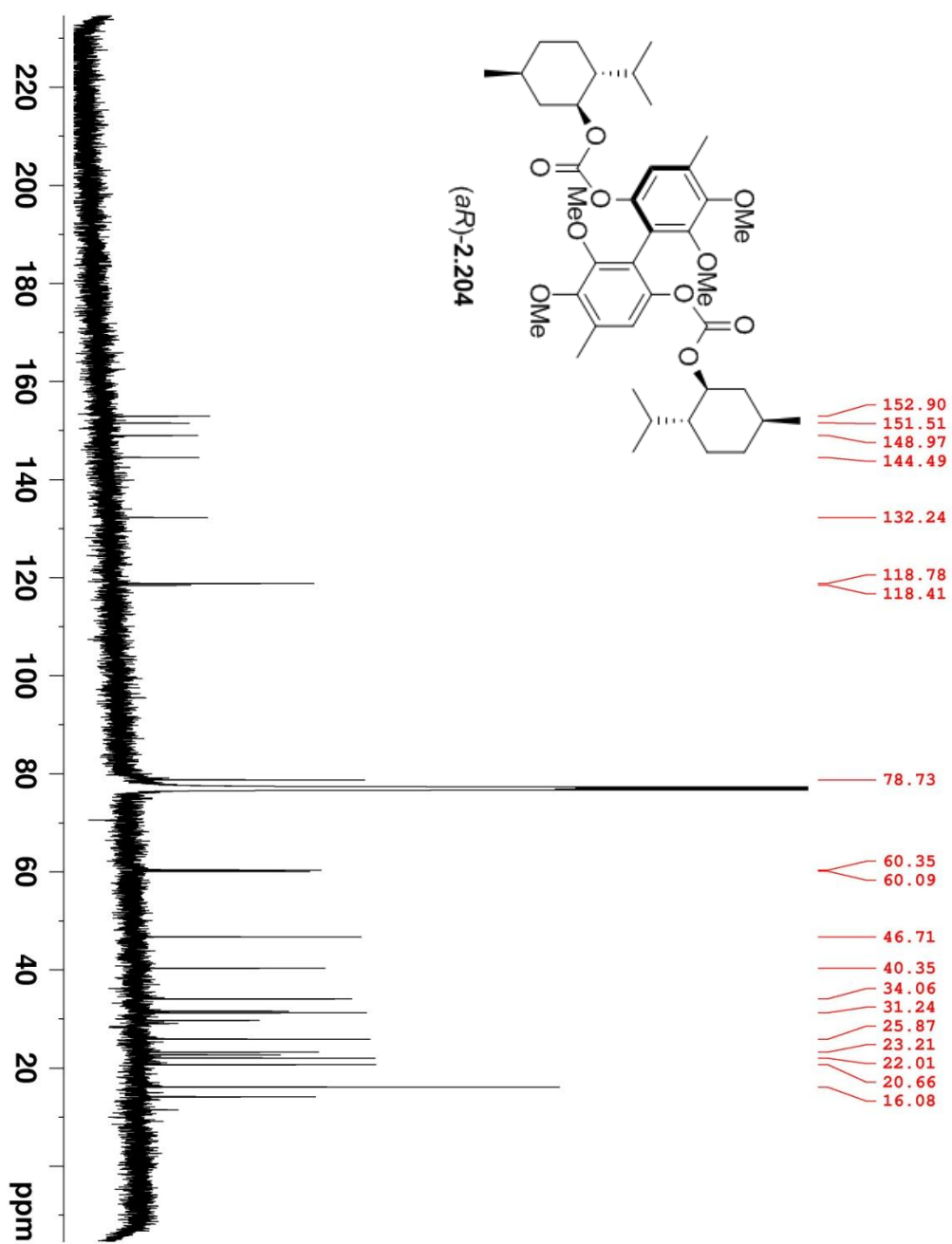


Figure A90. 100 MHz ¹³C NMR of (aR)-2.204 in CDCl₃.

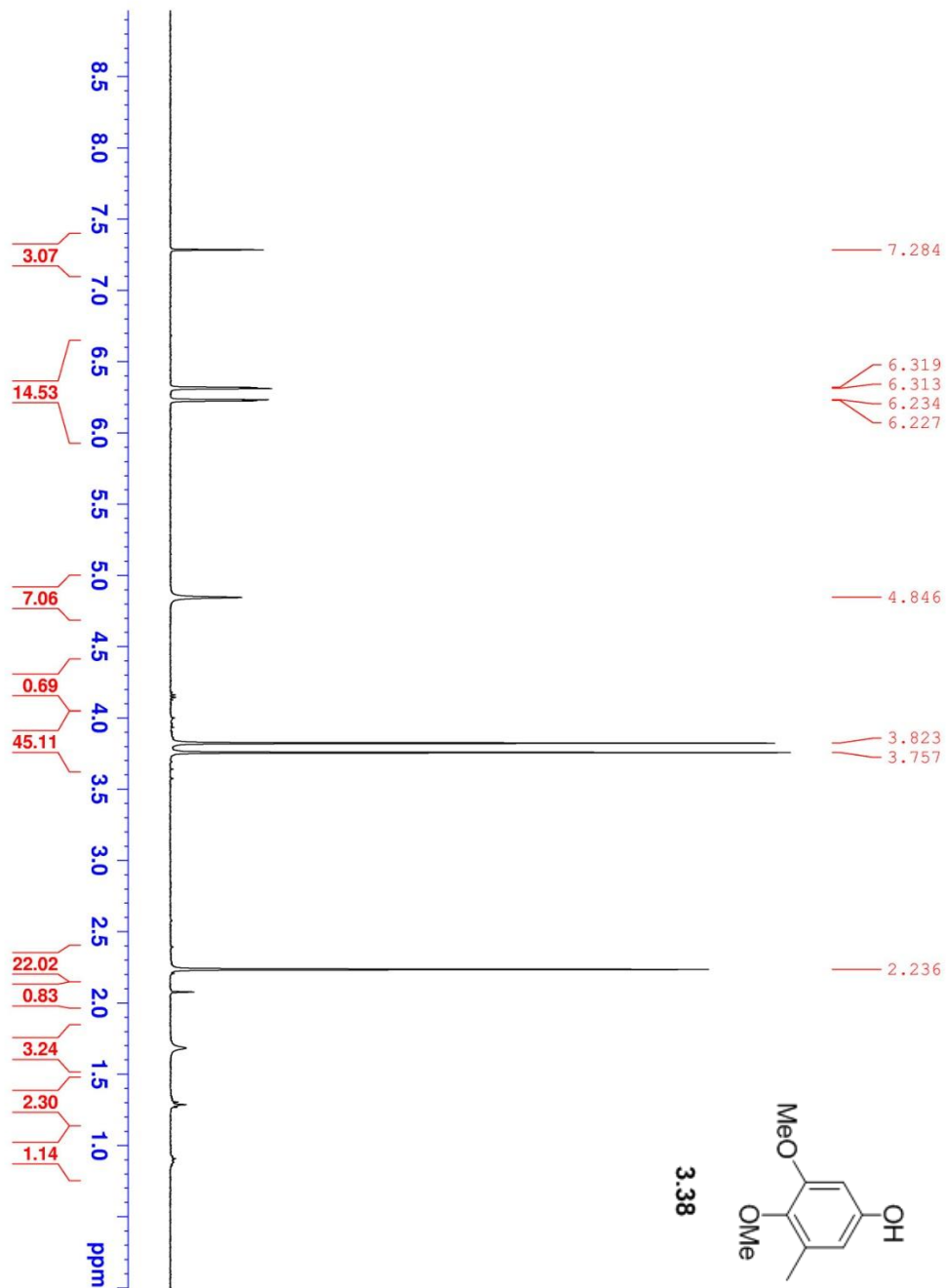


Figure A91. 400 MHz ^1H NMR of **3.38** in CDCl_3 .

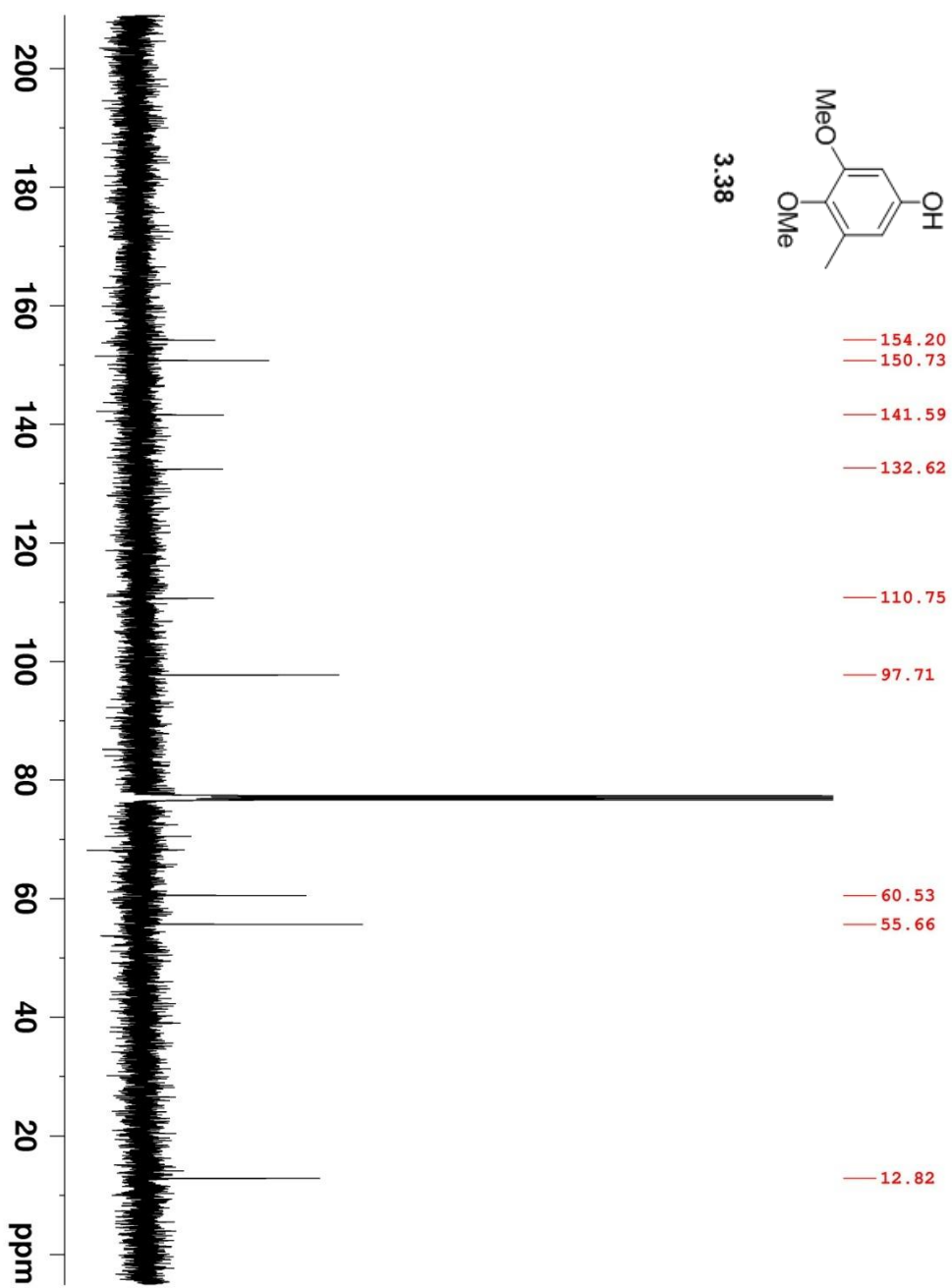


Figure A92. 100 MHz ^{13}C NMR of **3.38** in CDCl_3 .

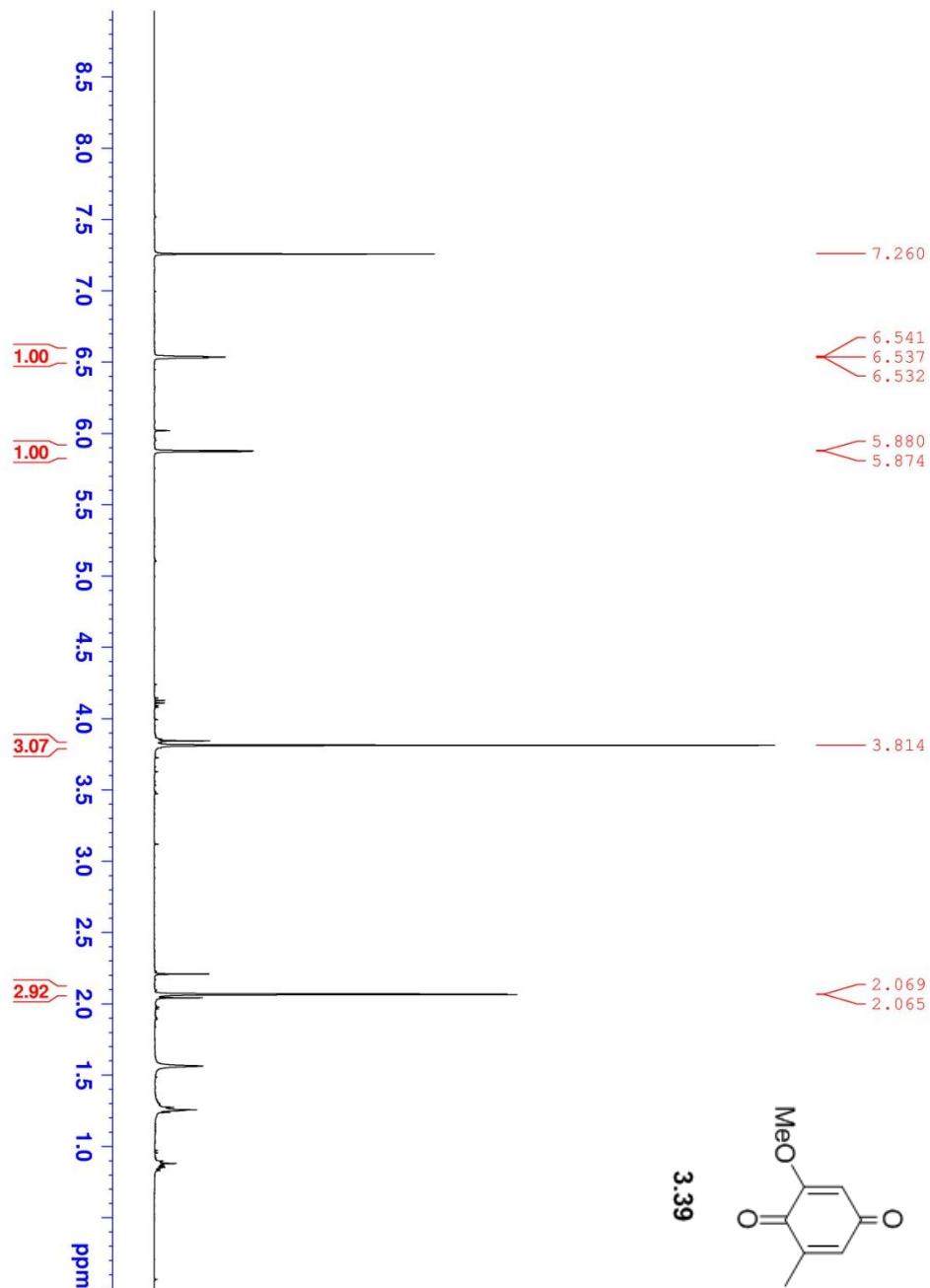


Figure A93. 400 MHz ^1H NMR of **3.39** in CDCl_3 .

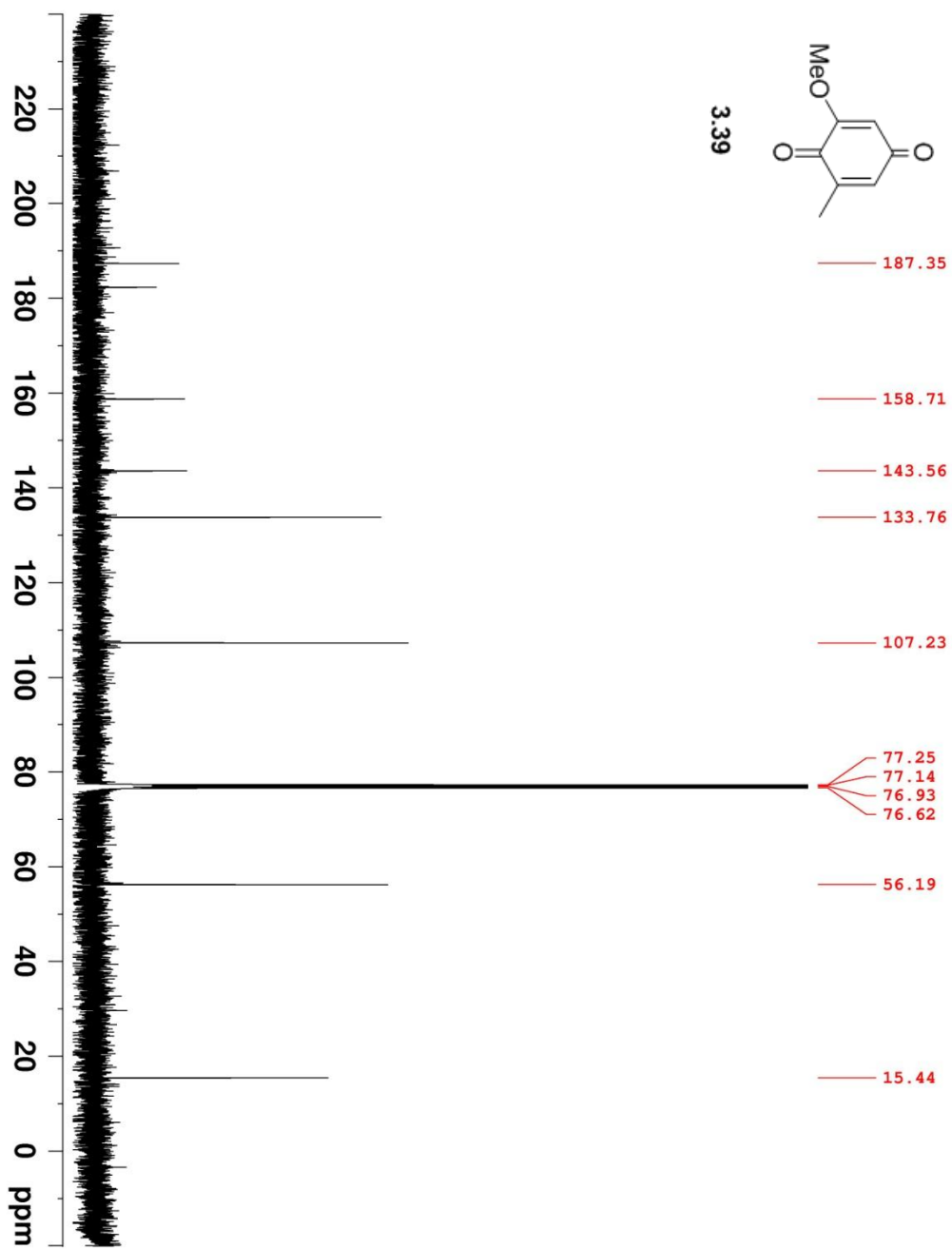


Figure A94. 100 MHz ^{13}C NMR of **3.39** in CDCl_3 .

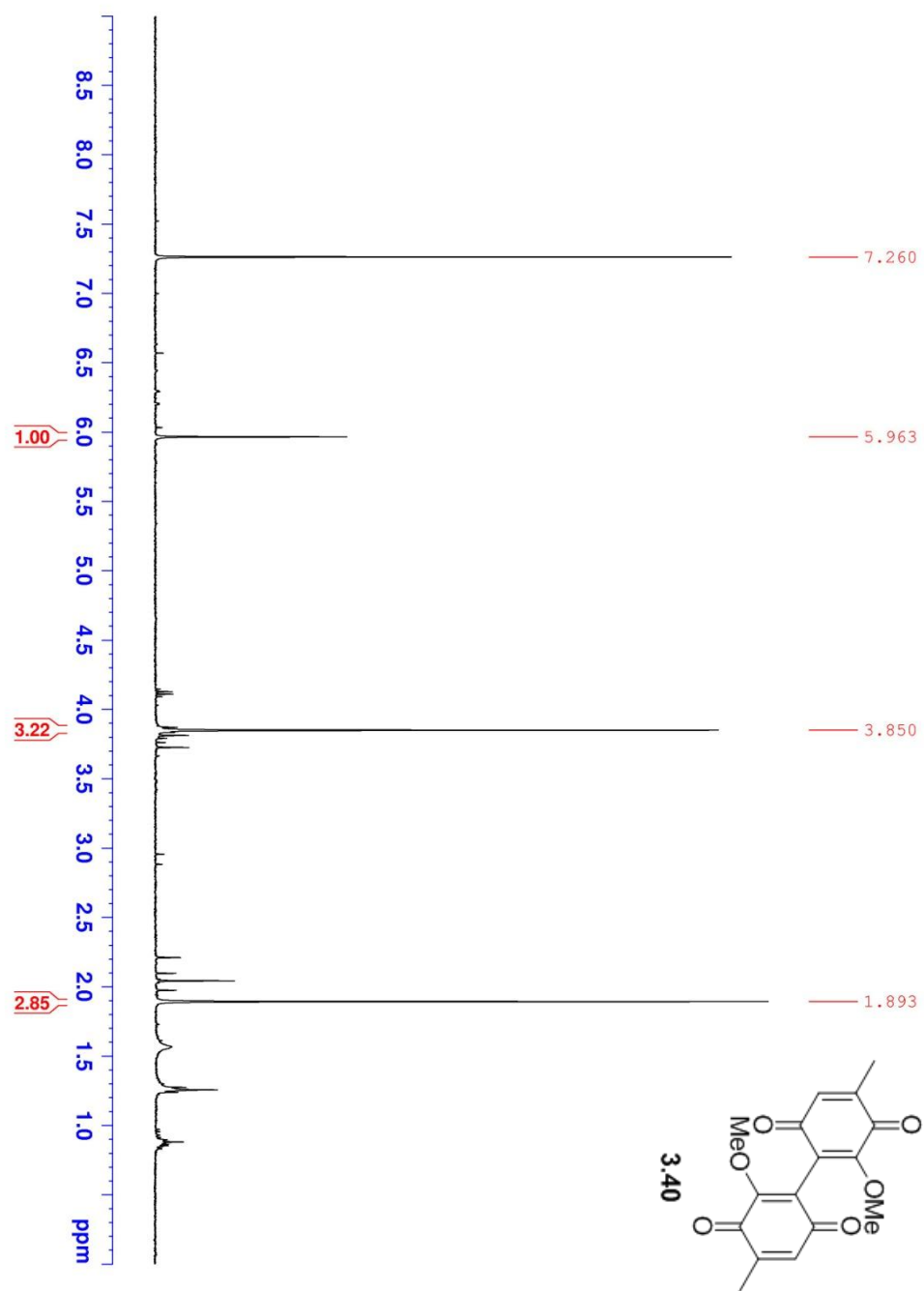


Figure A95. 400 MHz ^1H NMR of **3.40** in CDCl_3 .

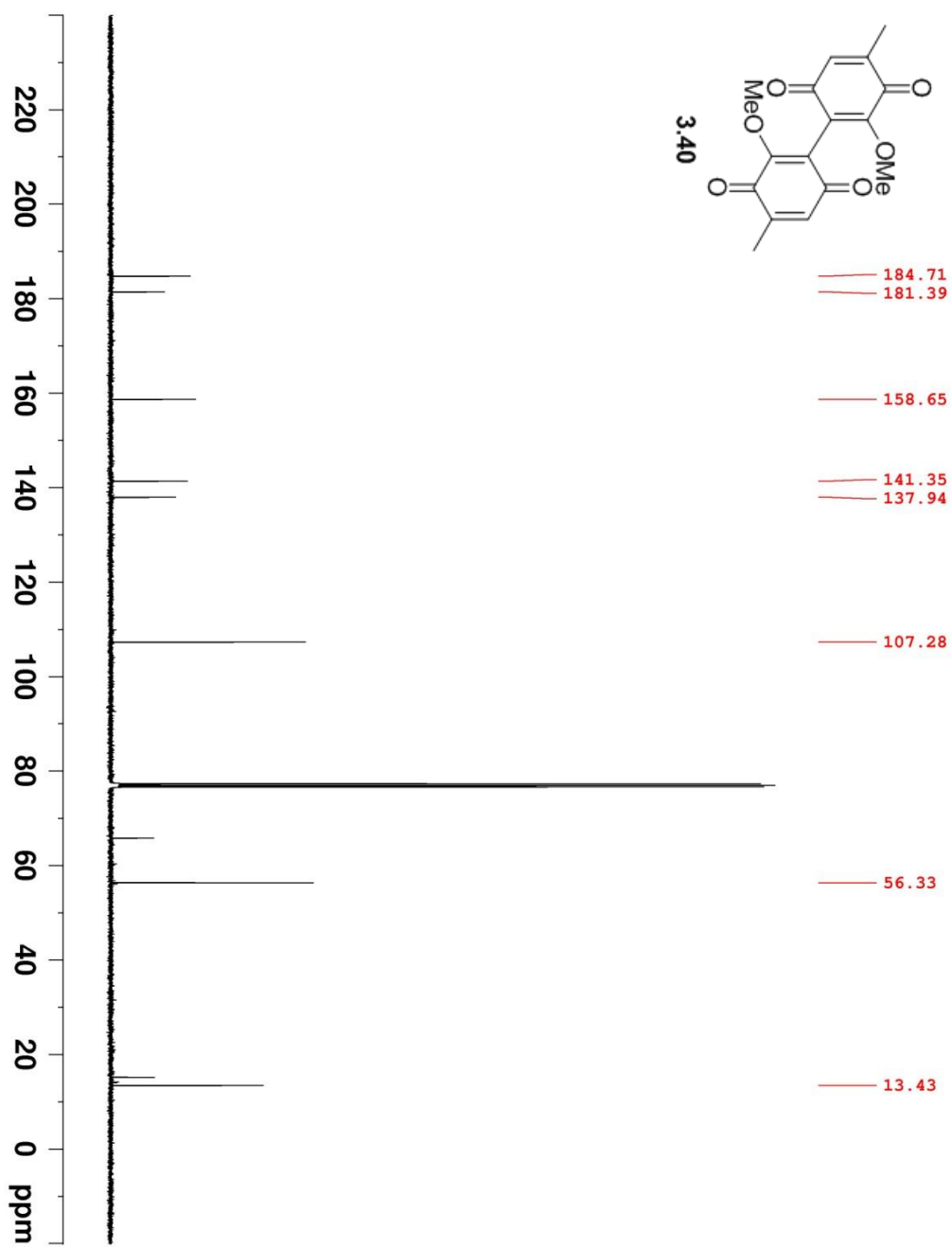


Figure A96. 100 MHz ^{13}C NMR of **3.40** in CDCl_3 .

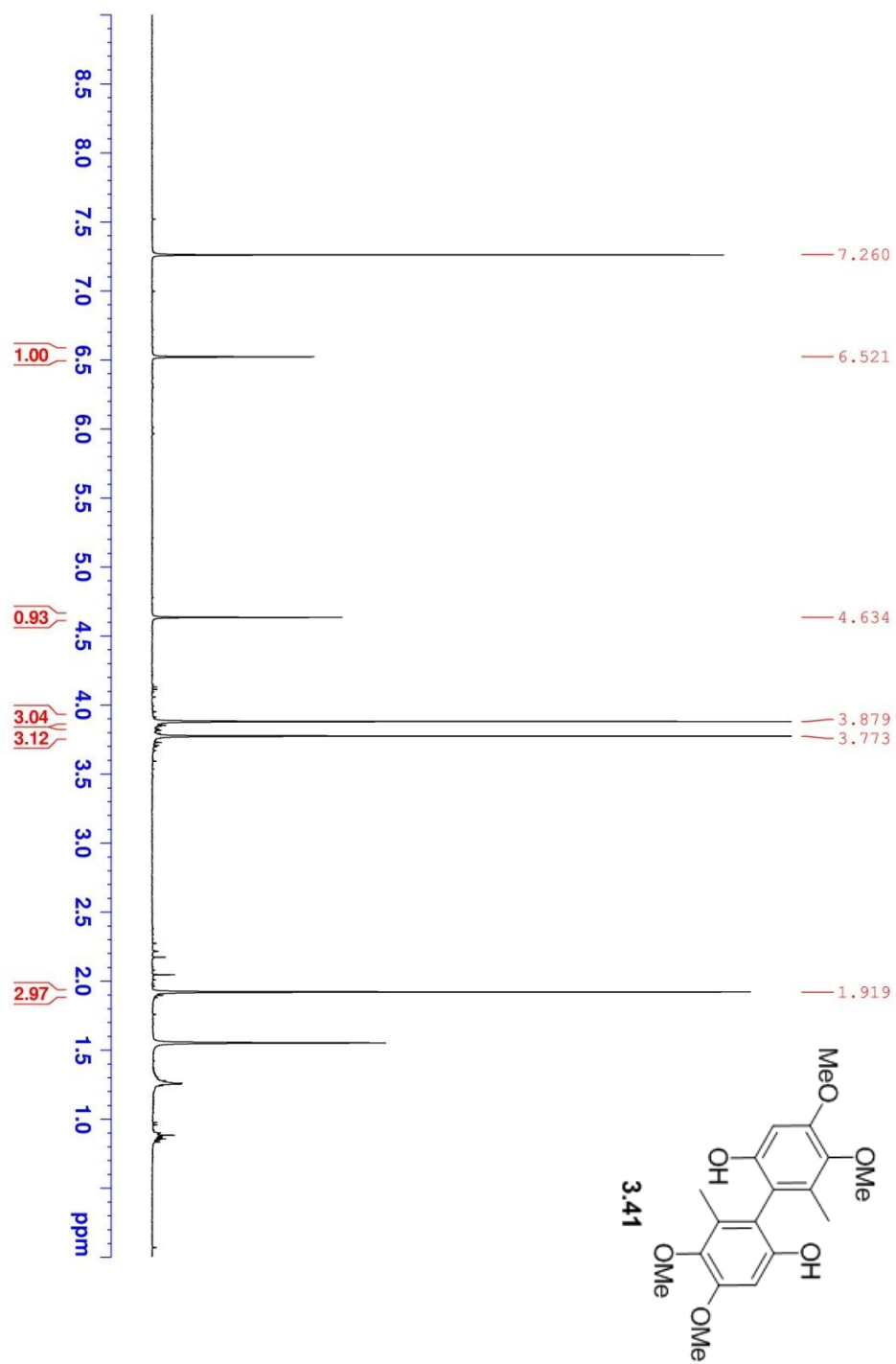


Figure A97. 400 MHz ^1H NMR of **3.41** in CDCl_3 .

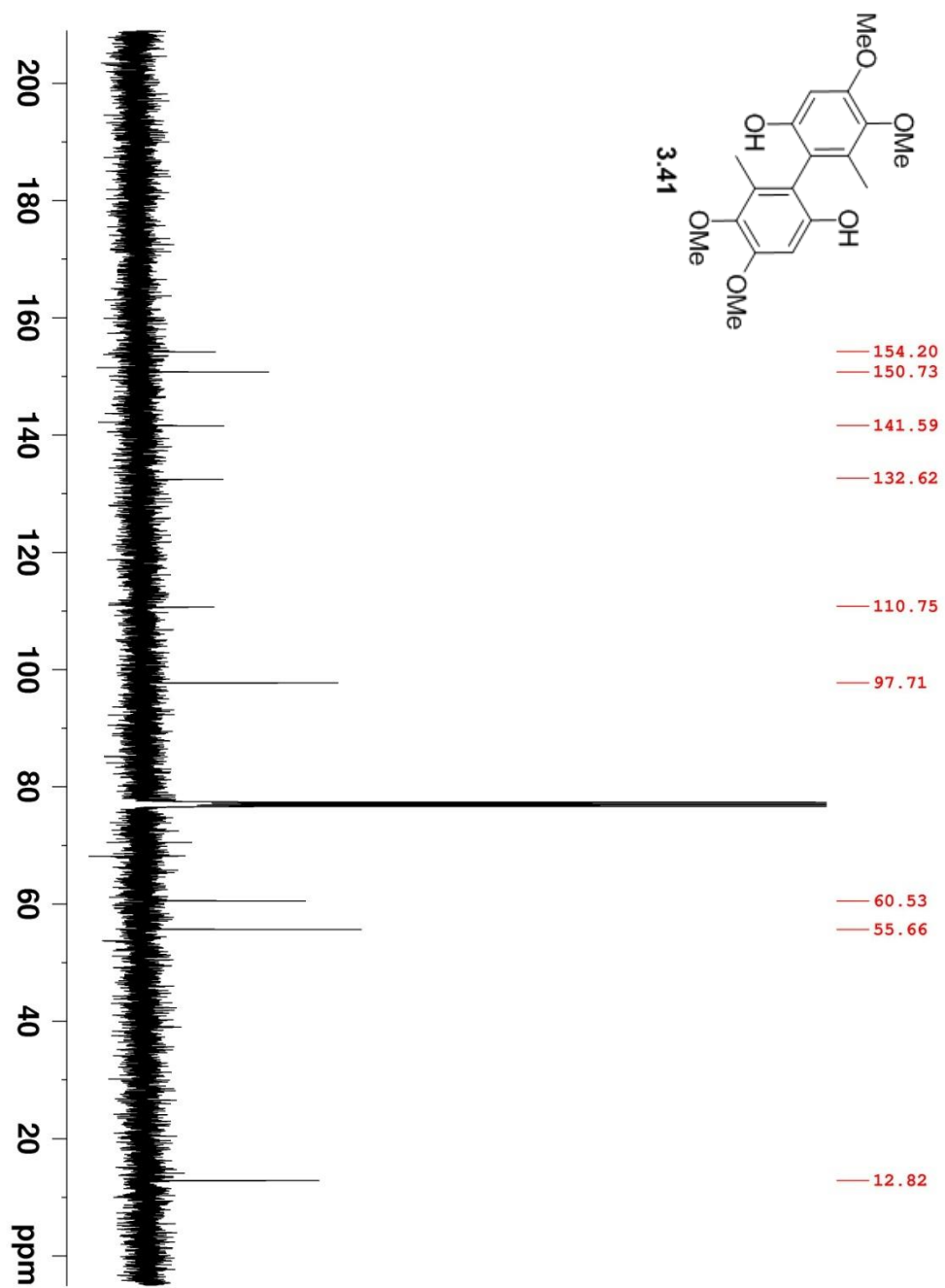


Figure A98. 100 MHz ^{13}C NMR of **3.41** in CDCl_3 .

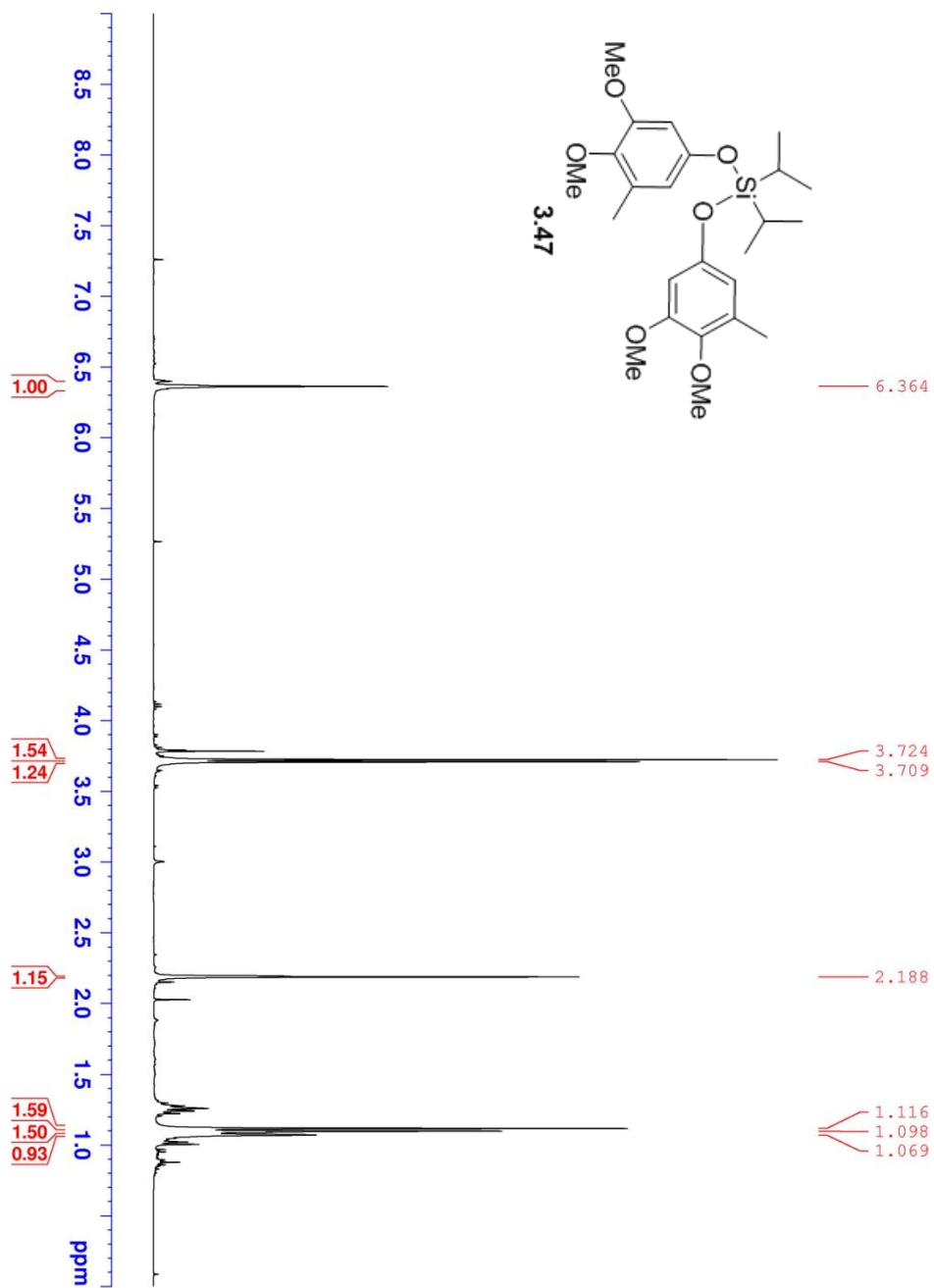


Figure A99. 400 MHz ^1H NMR of **3.47** in CDCl_3 .

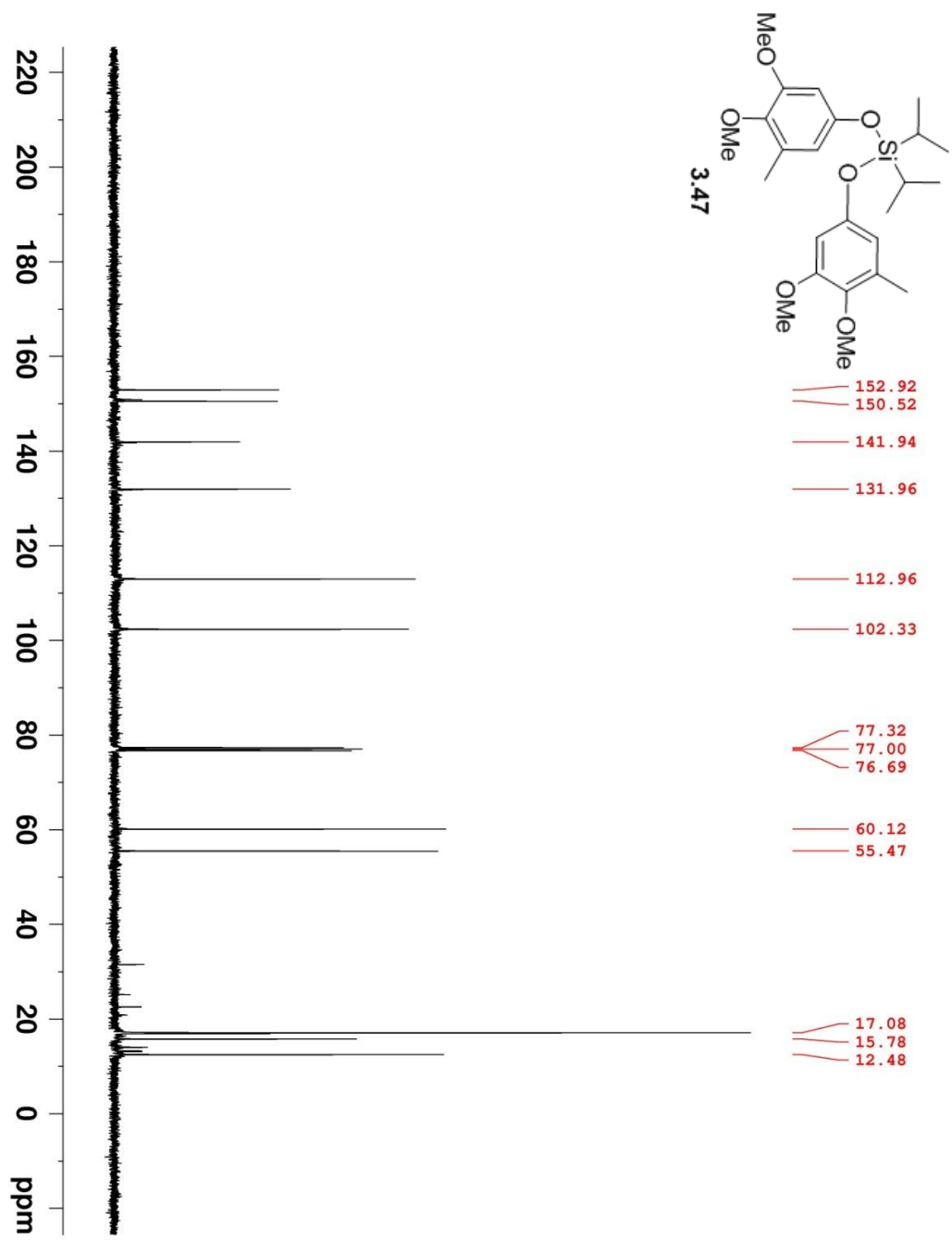


Figure A100. 100 MHz ^{13}C NMR of **3.47** in CDCl_3 .

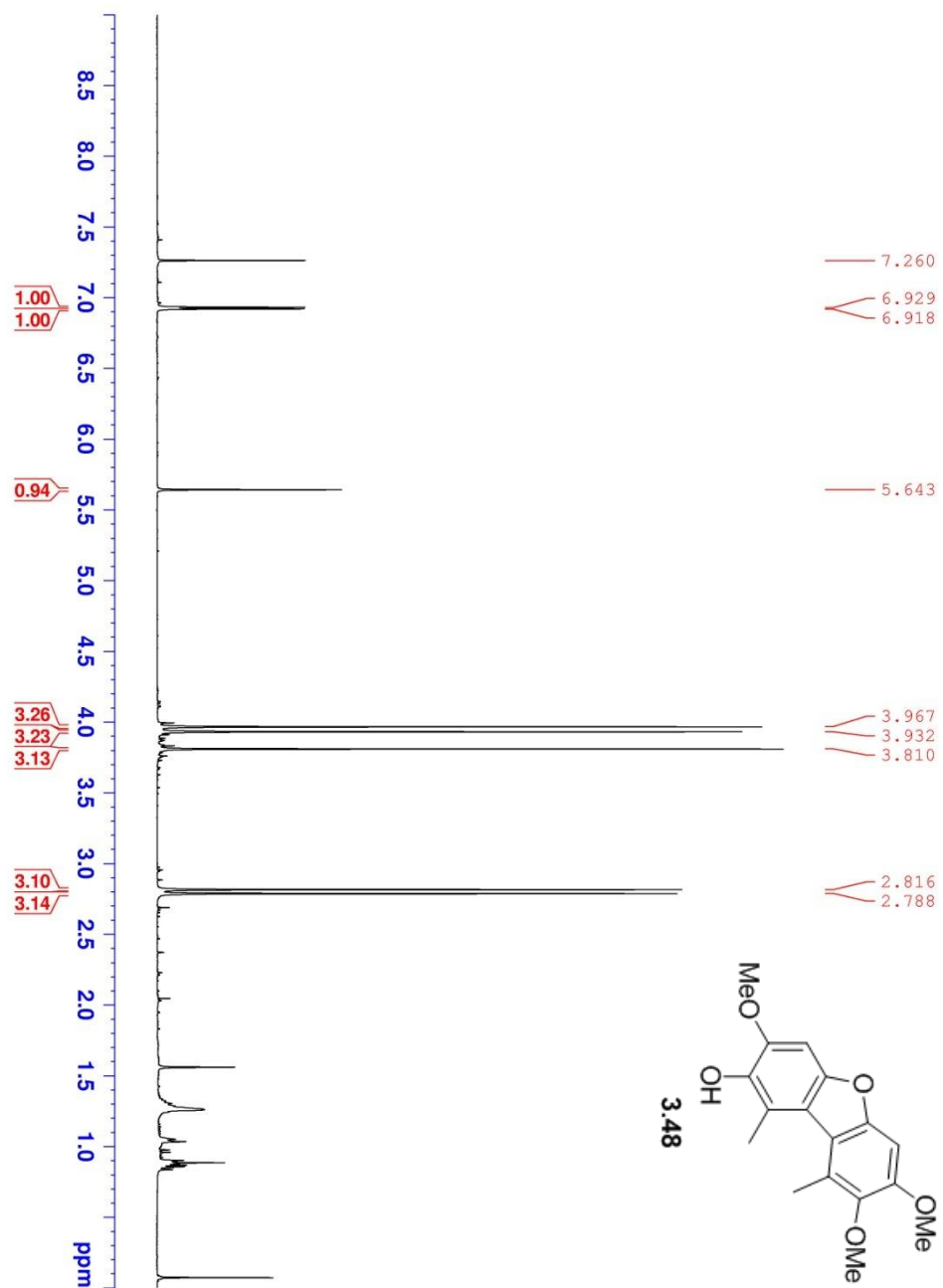


Figure A101. 400 MHz ^1H NMR of **3.48** in CDCl_3 .

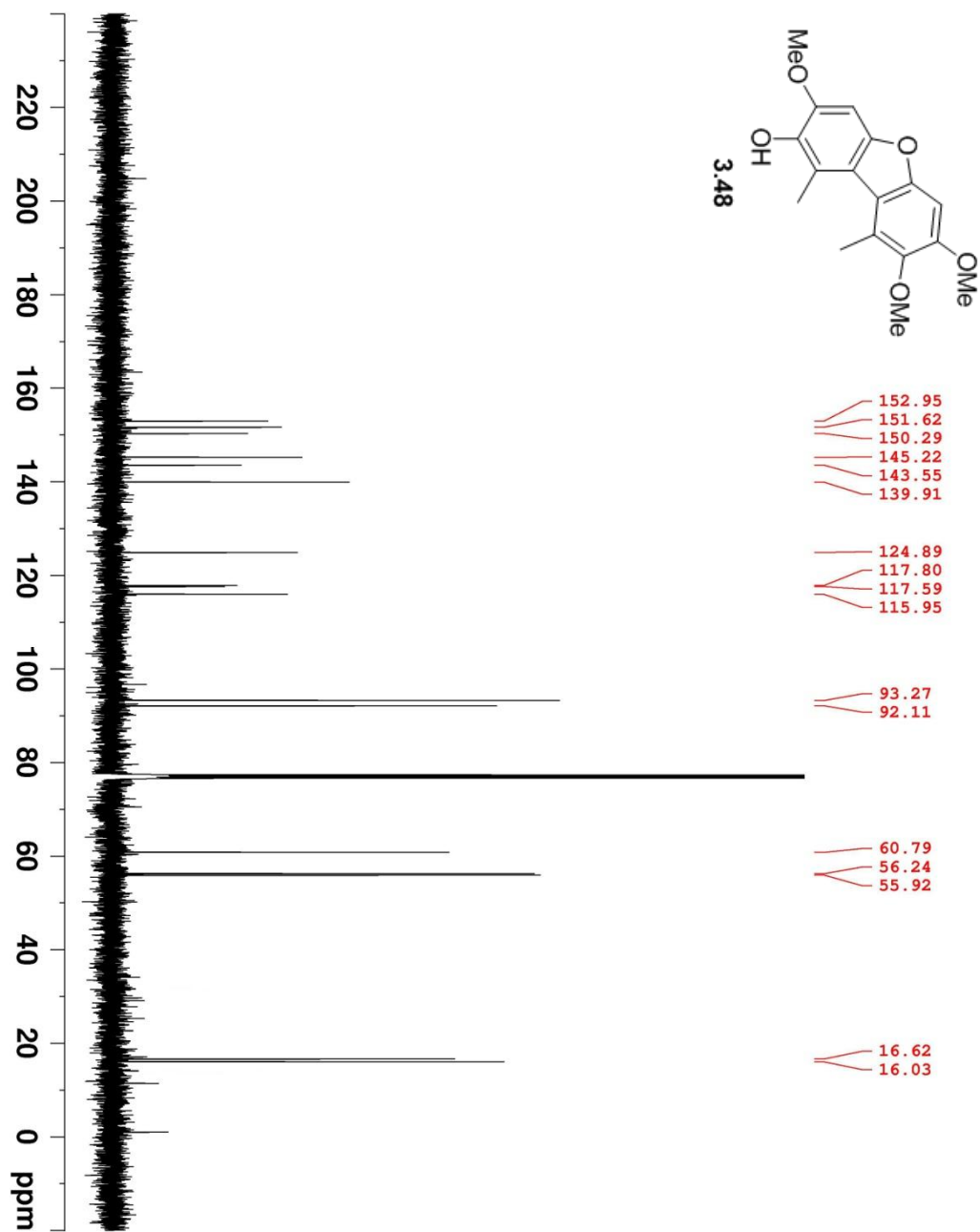


Figure A102. 100 MHz ^{13}C NMR of **3.48** in CDCl_3 .

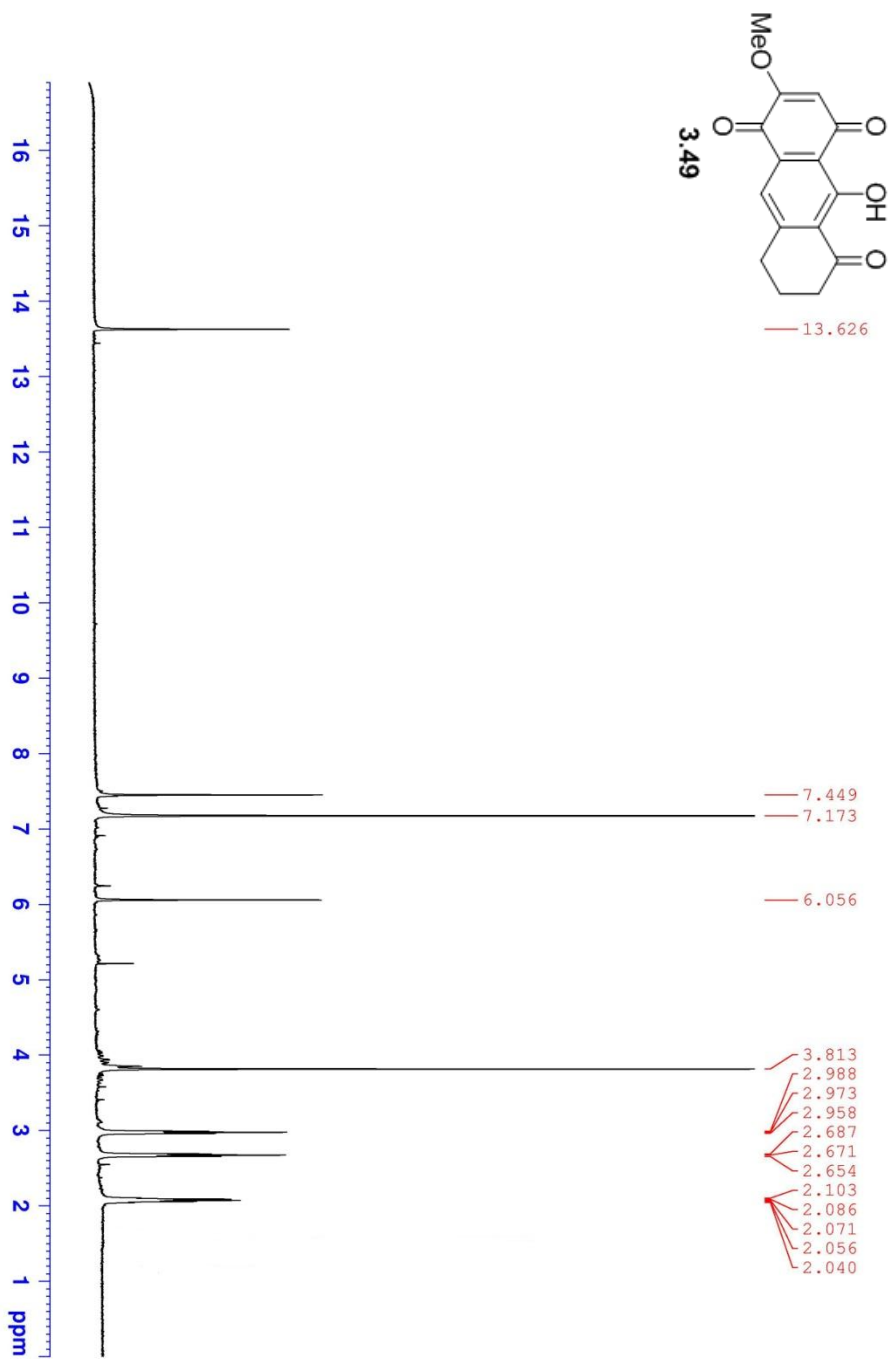


Figure A103. 400 MHz ¹H NMR of **3.49** in CDCl₃.

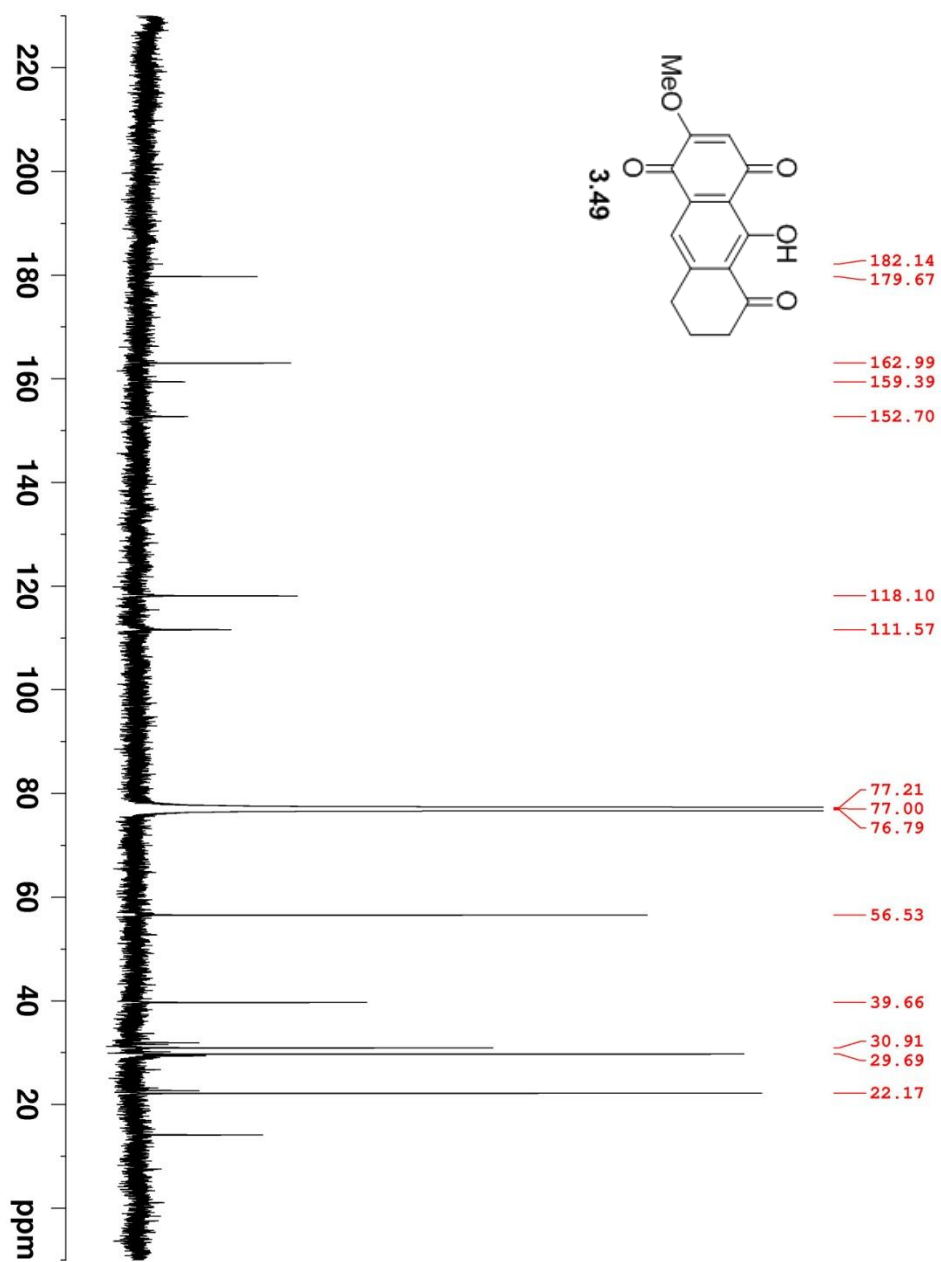


Figure A104. 100 MHz ^{13}C NMR of **3.49** in CDCl_3 .

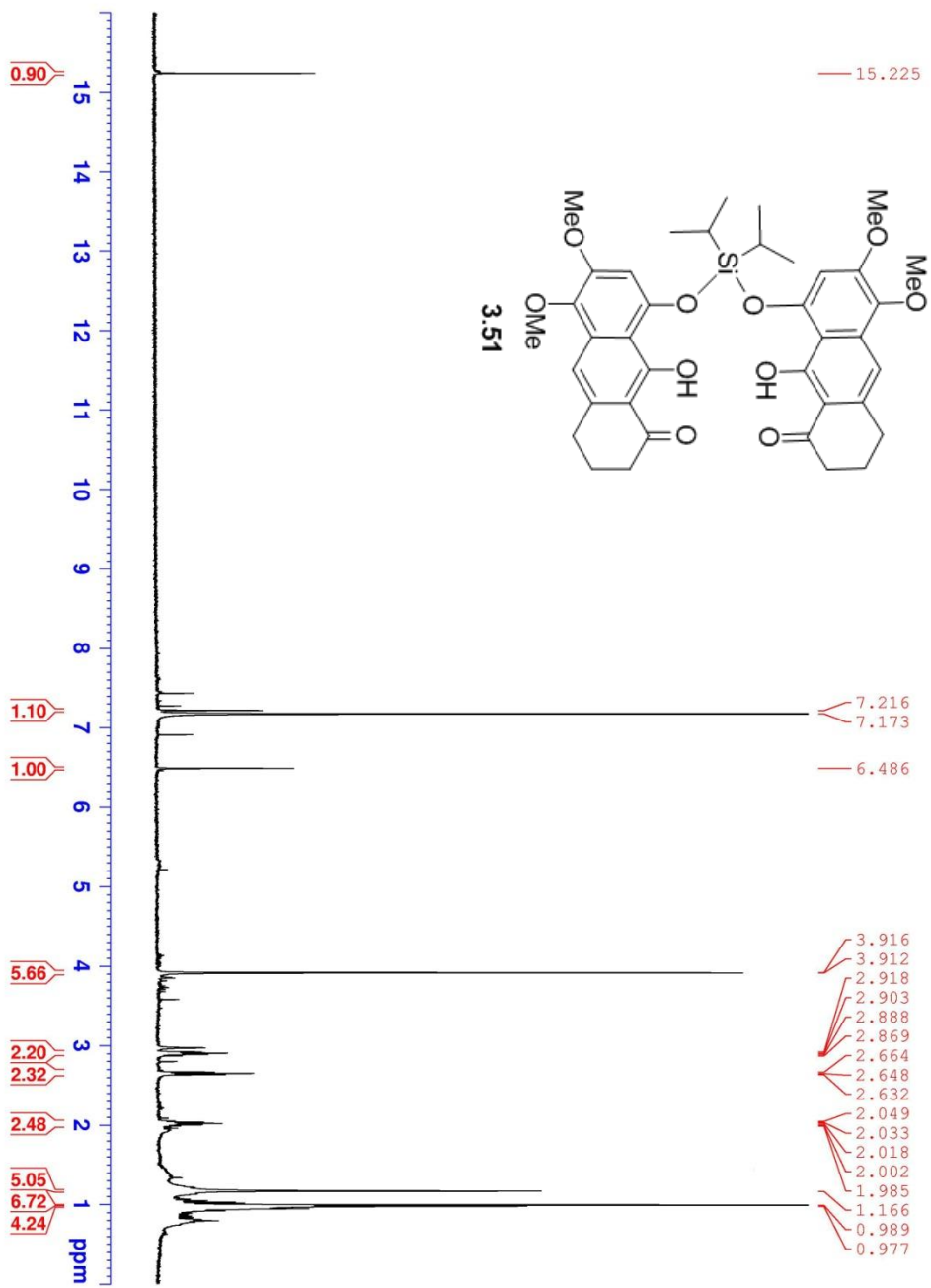


Figure A105. 400 MHz ^1H NMR of **3.51** in CDCl_3 .

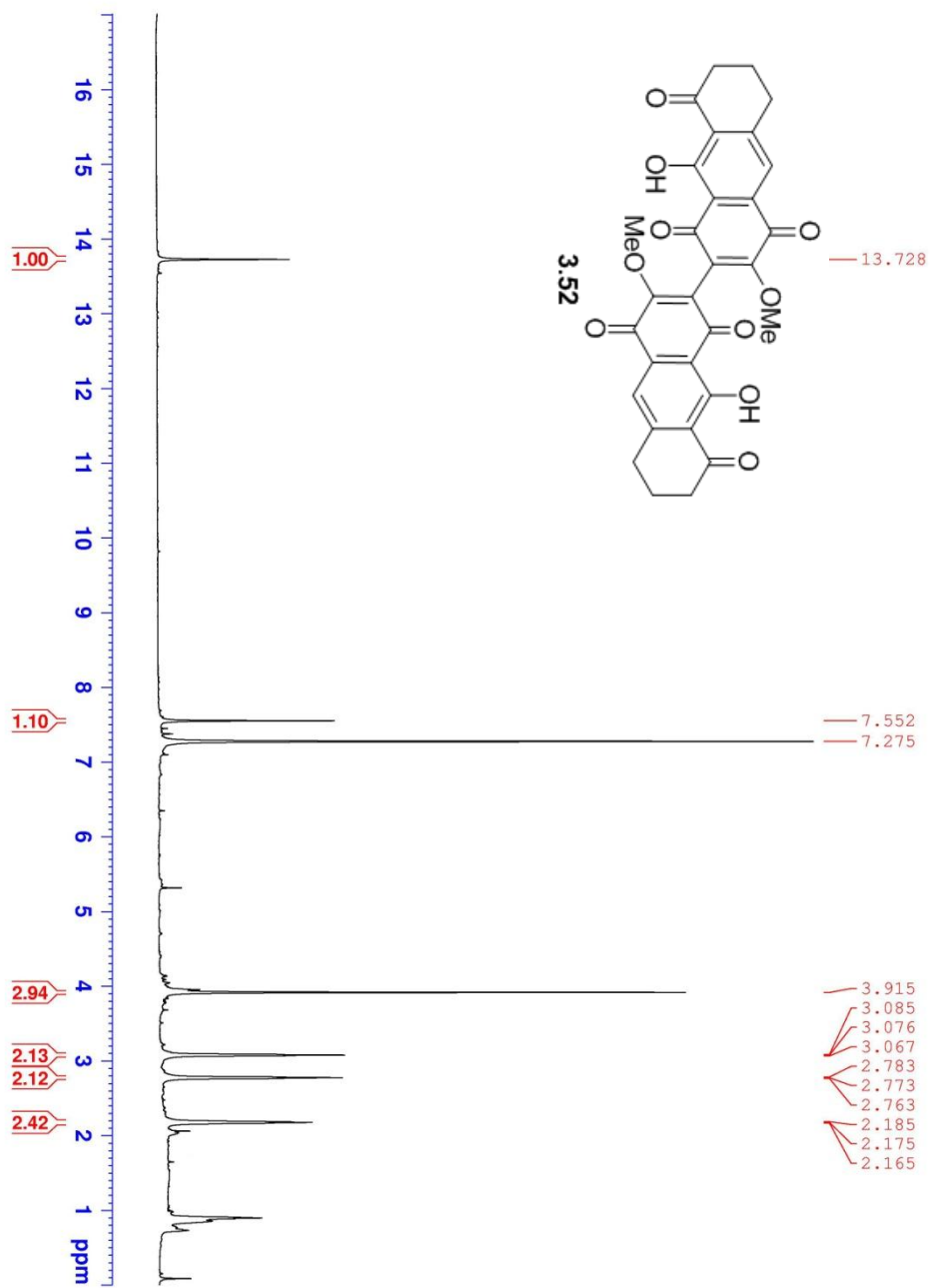


Figure A106. 400 MHz ^1H NMR of **3.52** in CDCl_3 .

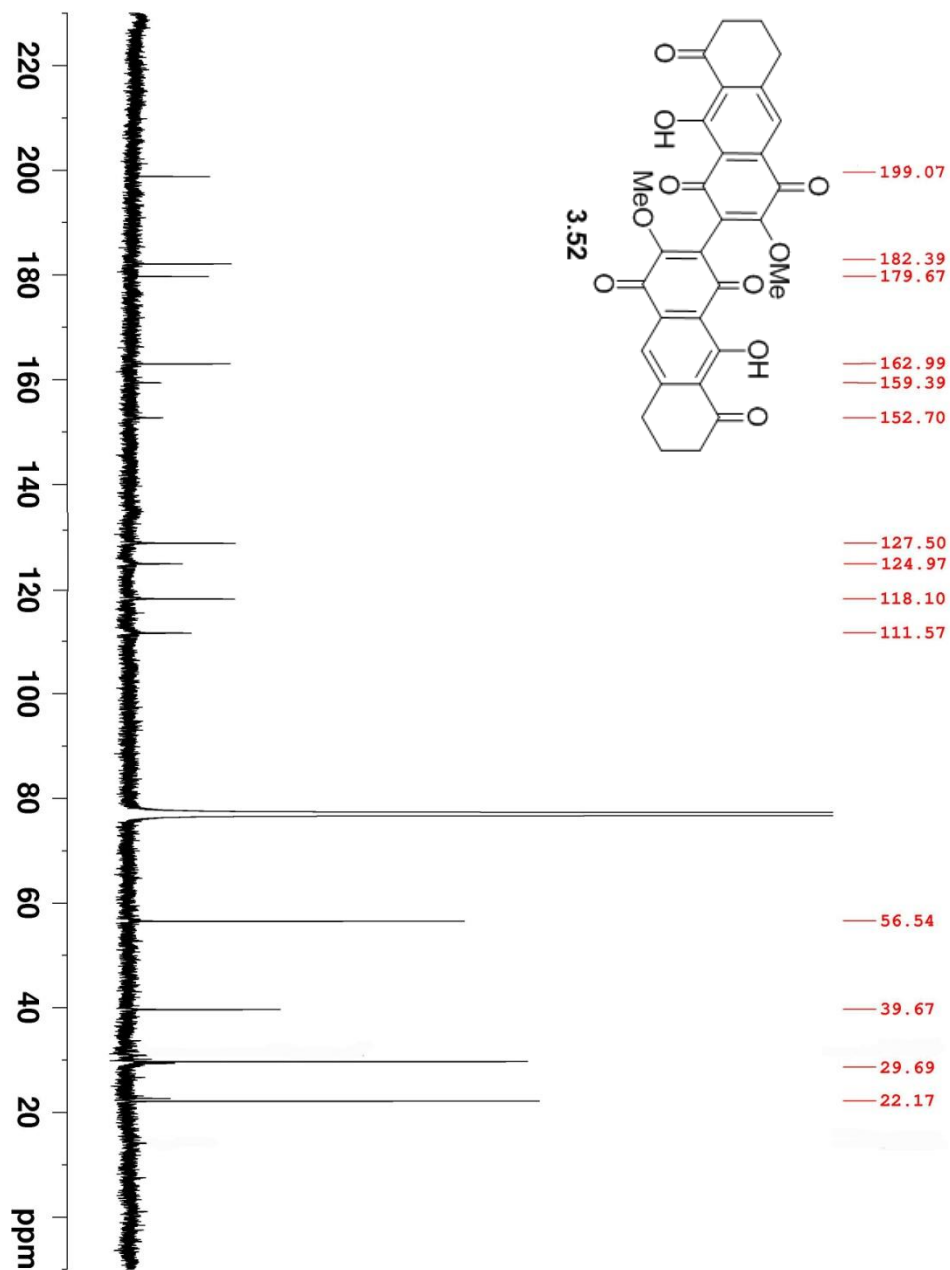


Figure A107. 100 MHz ^{13}C NMR of **3.52** in CDCl_3 .

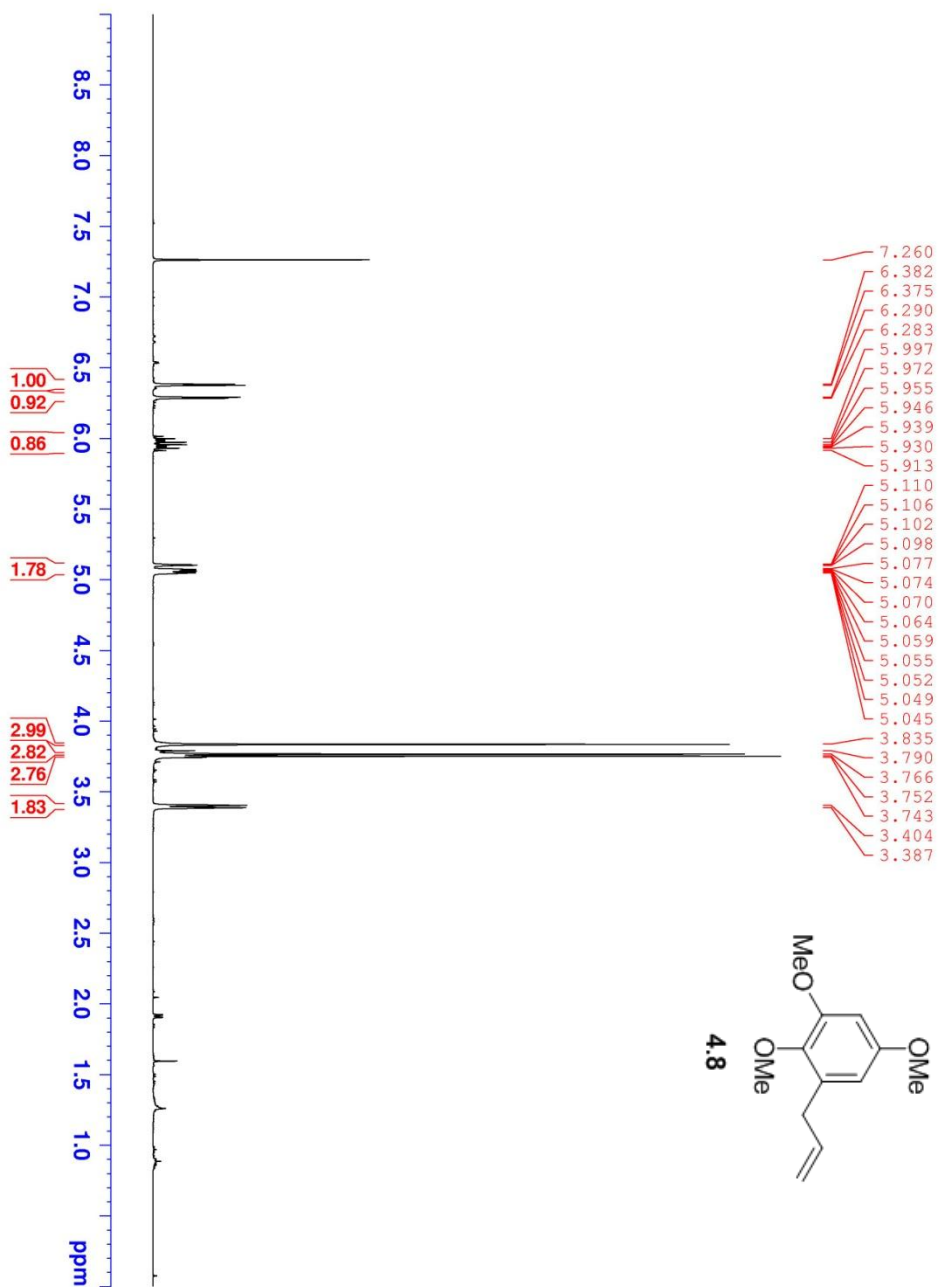


Figure A108. 400 MHz ¹H NMR of **4.8** in CDCl₃.

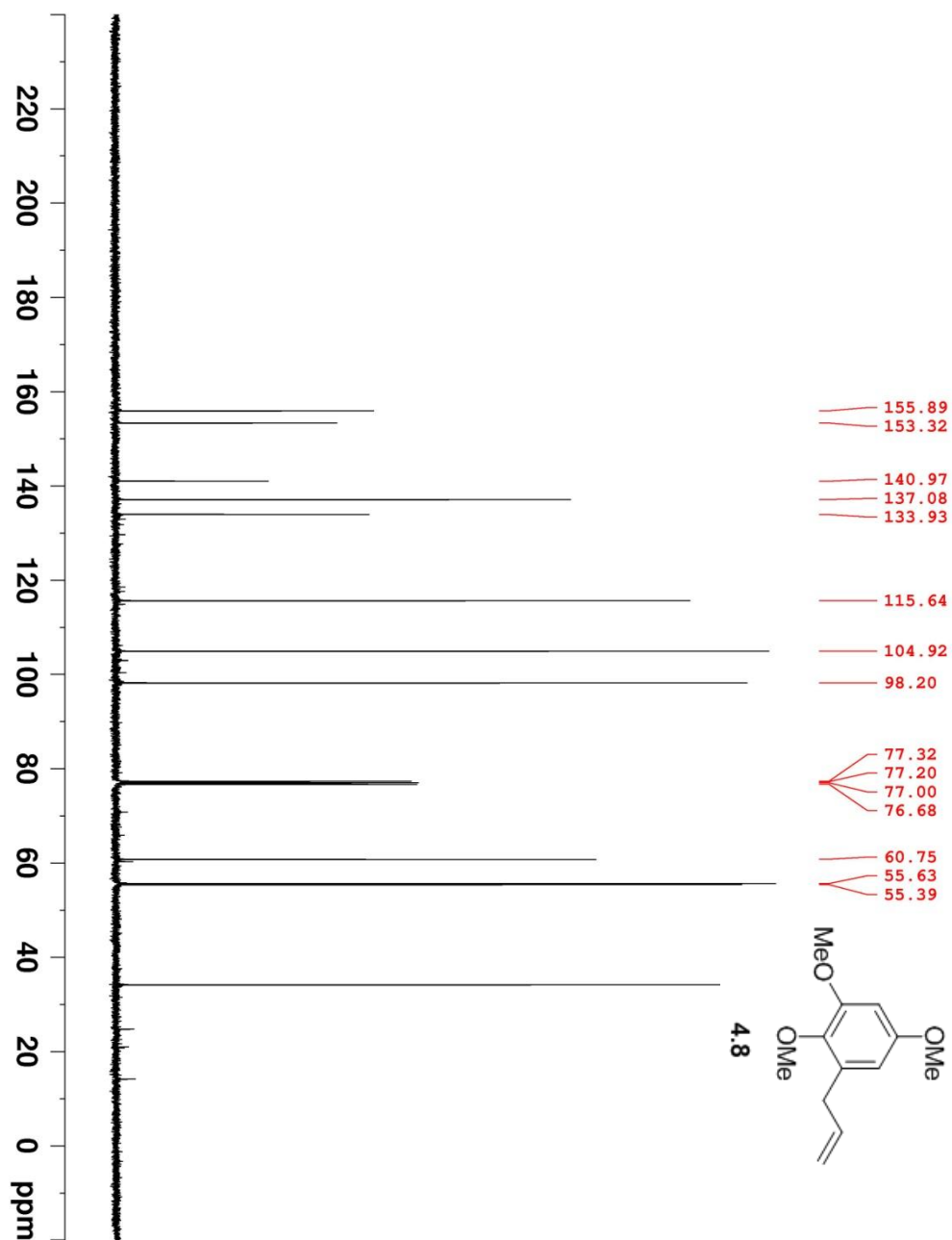


Figure A109. 100 MHz ^{13}C NMR of **4.8** in CDCl_3 .

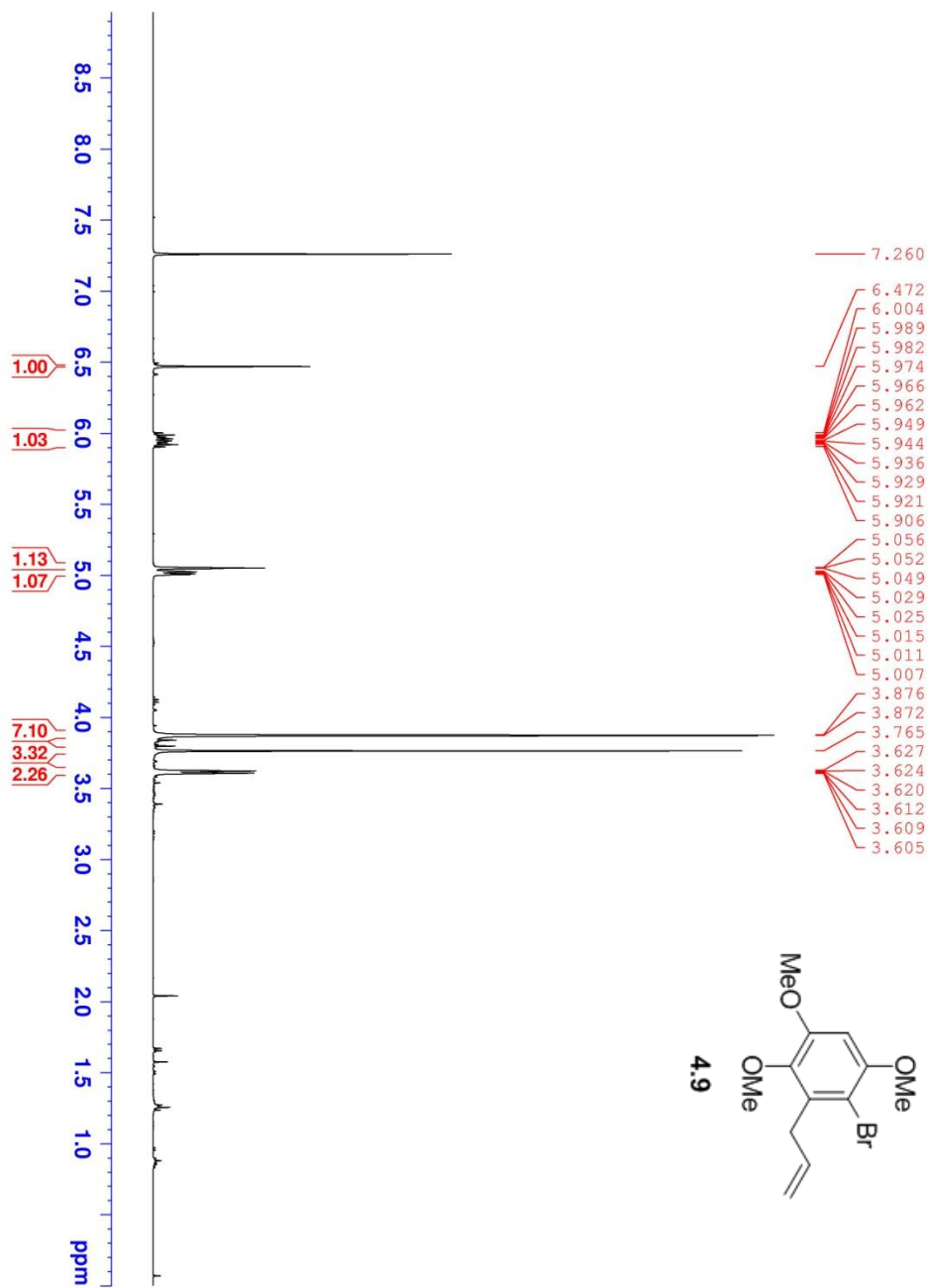


Figure A110. 400 MHz ¹H NMR of **4.9** in CDCl₃.

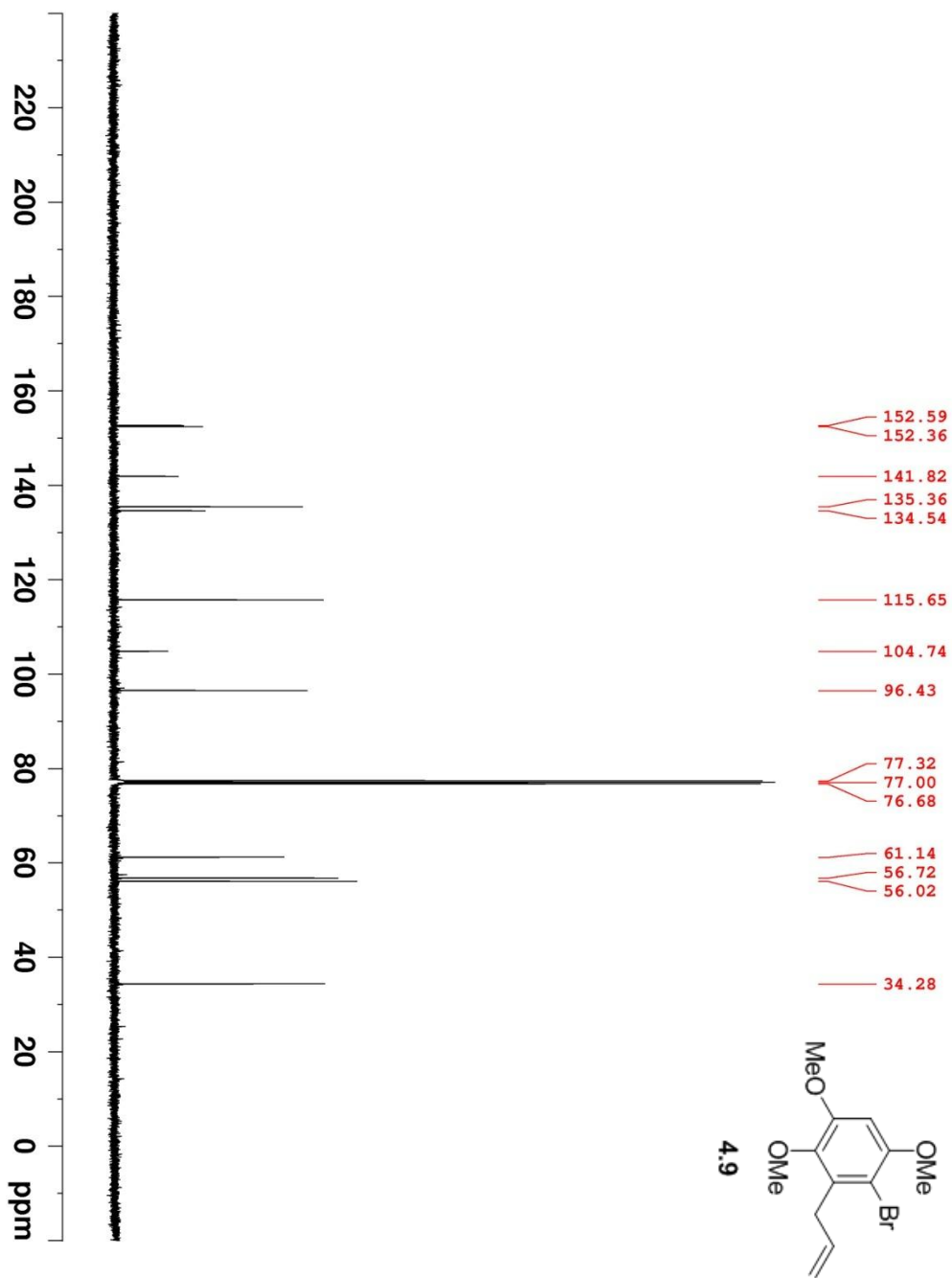


Figure A111. 100 MHz ^{13}C NMR of **4.9** in CDCl_3 .

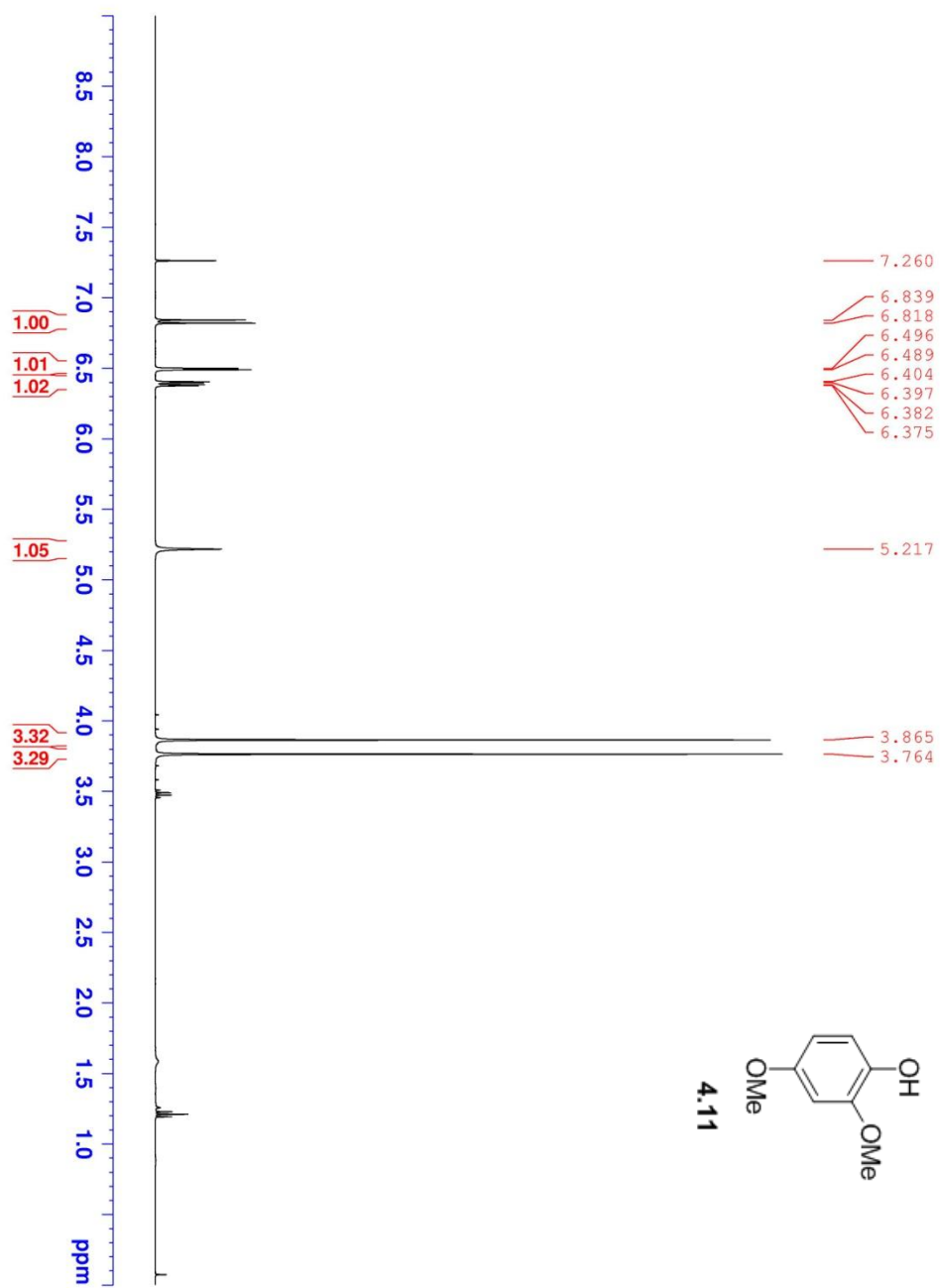


Figure A112. 400 MHz ^1H NMR of **4.11** in CDCl_3 .

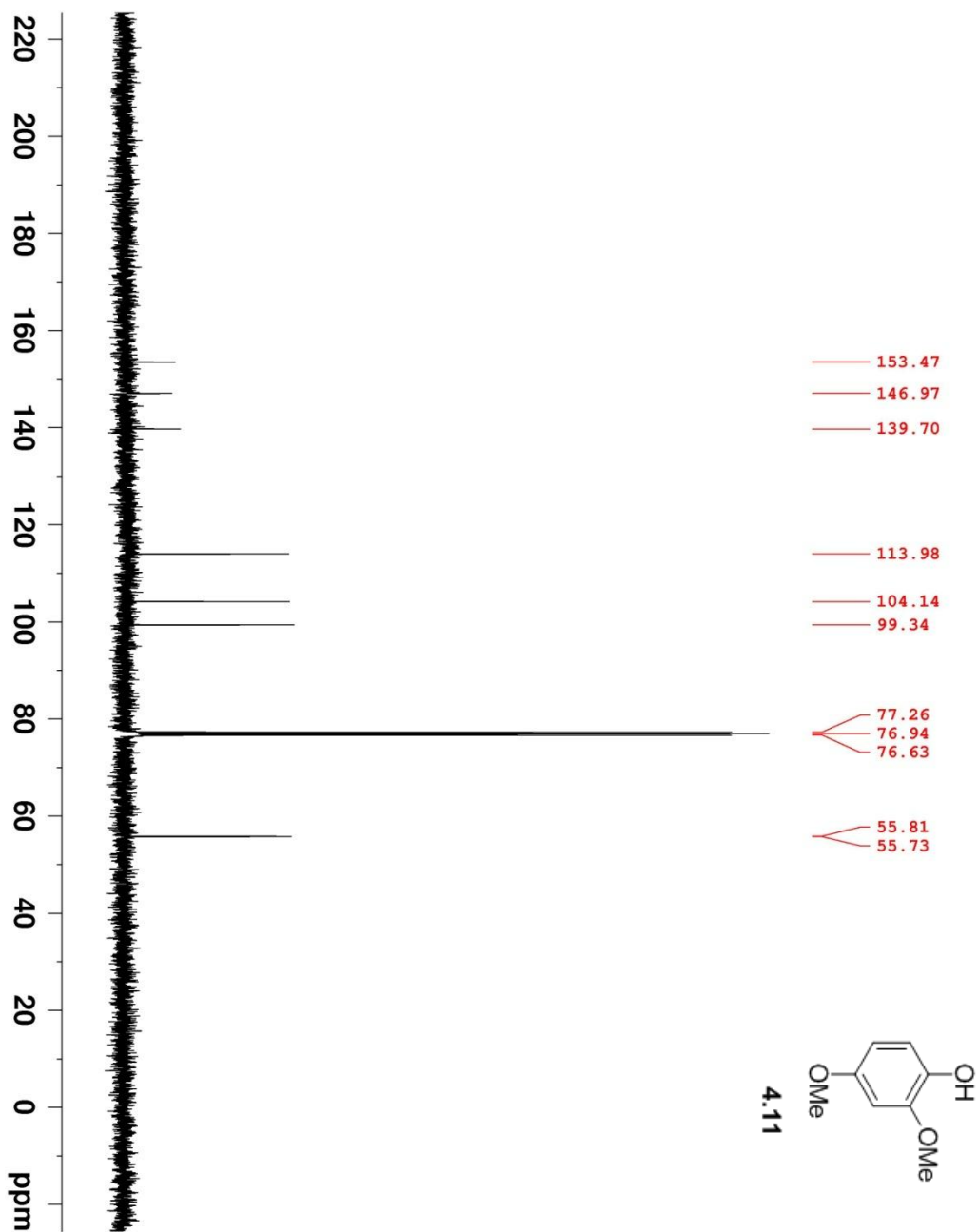


Figure A113. 100 MHz ^{13}C NMR of **4.11** in CDCl_3 .

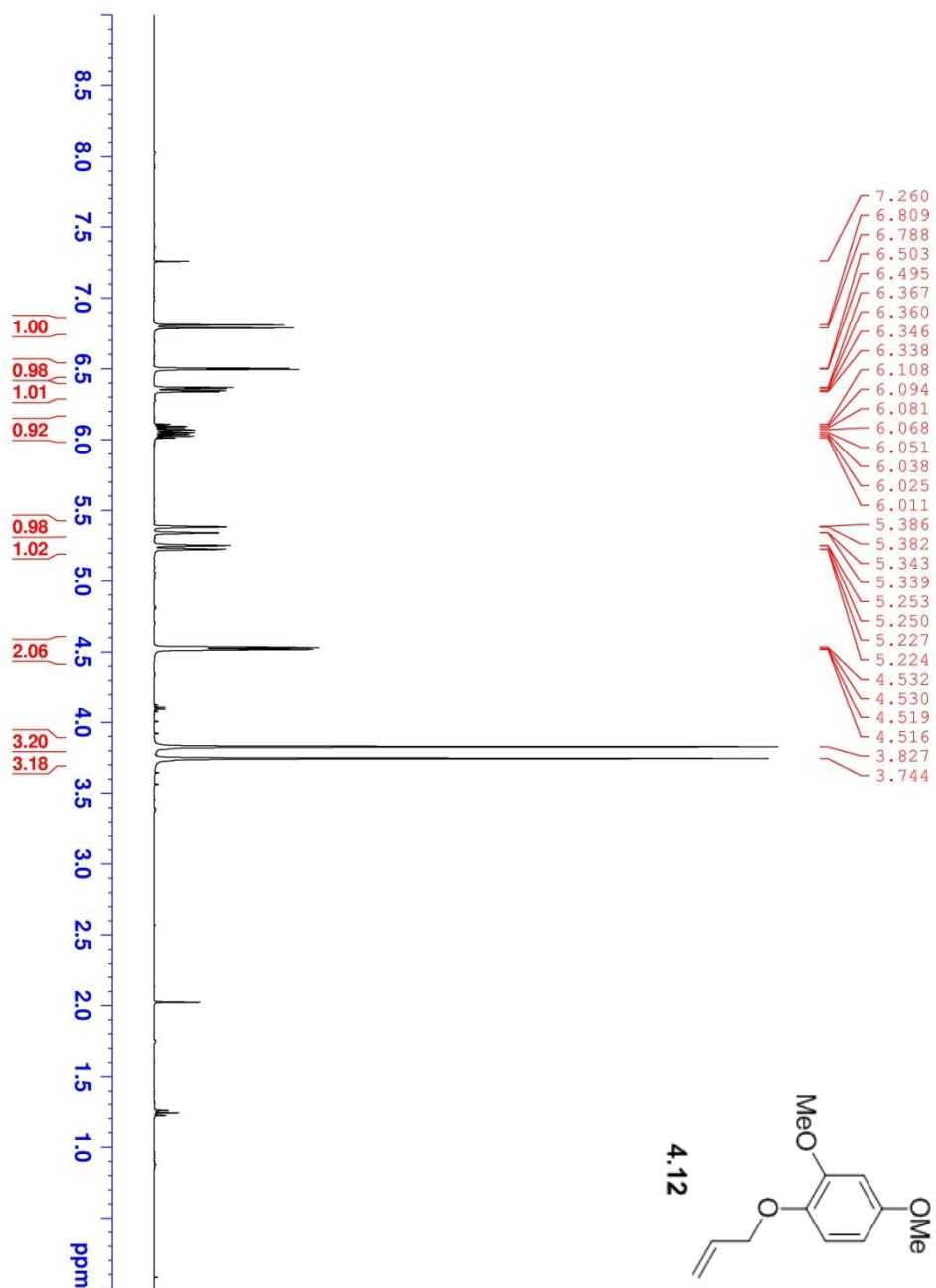


Figure A114. 400 MHz ¹H NMR of **4.12** in CDCl₃.

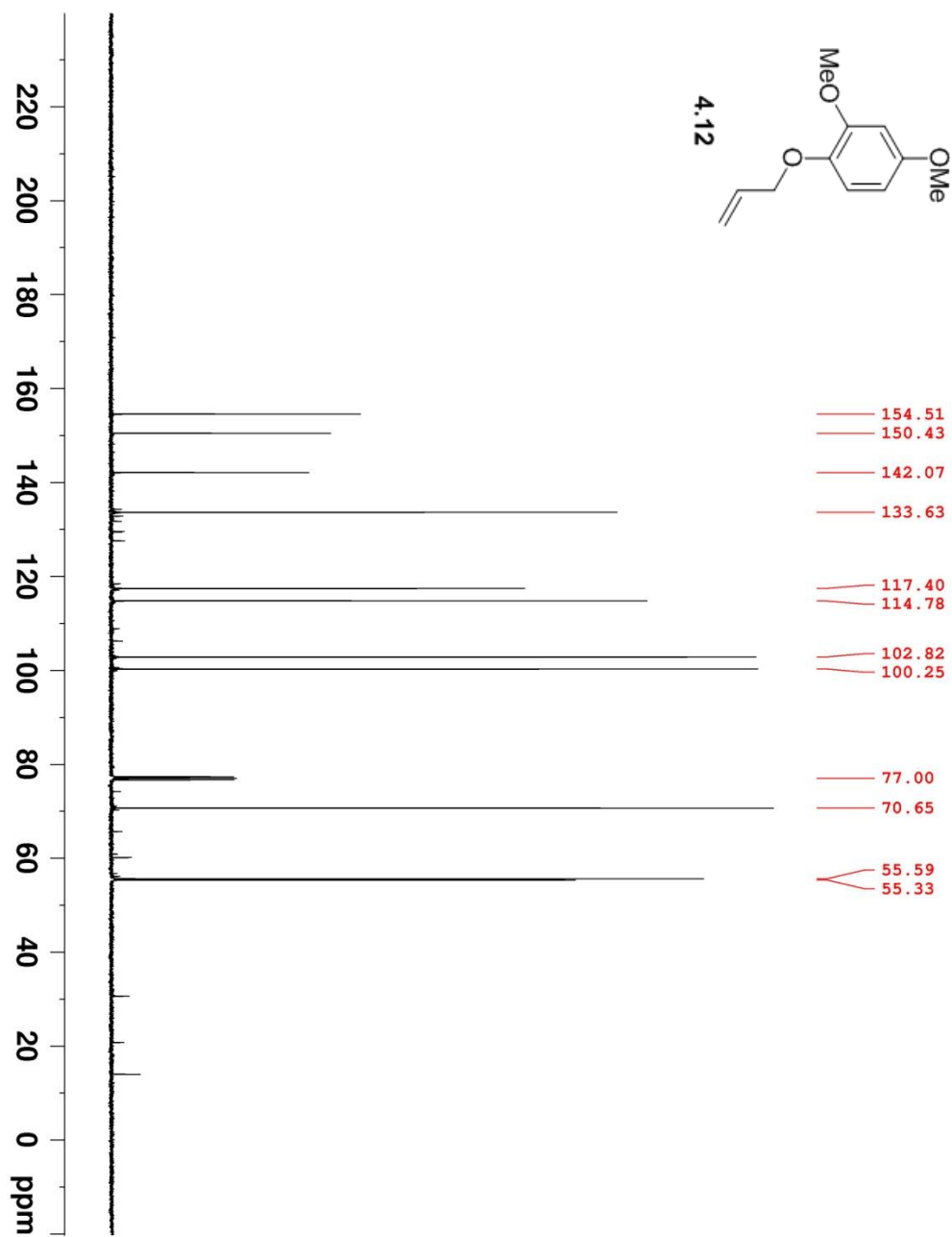


Figure A115. 100 MHz ¹³C NMR of **4.12** in CDCl₃.

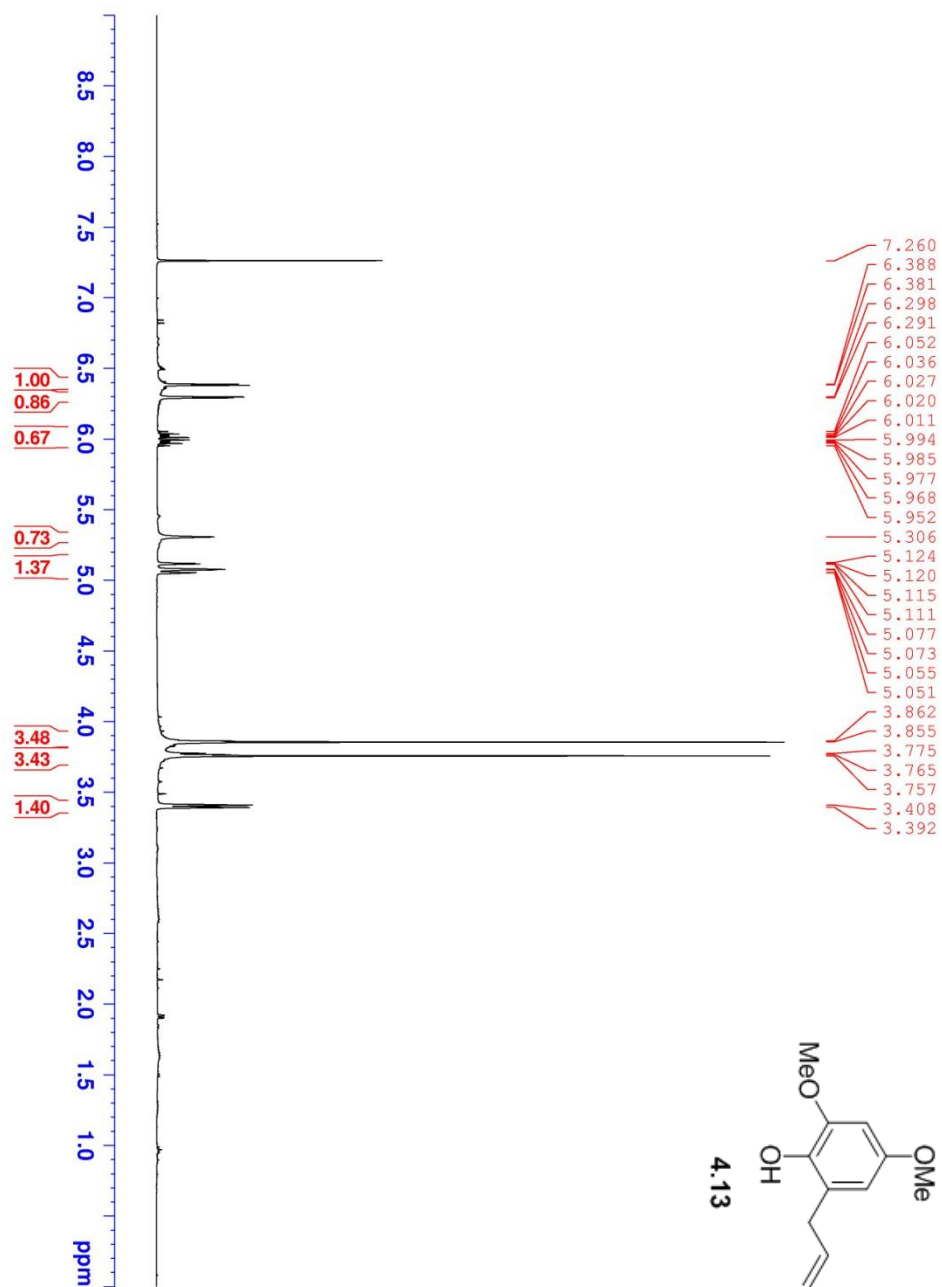


Figure A116. 400 MHz ^1H NMR of **4.13** in CDCl_3 .

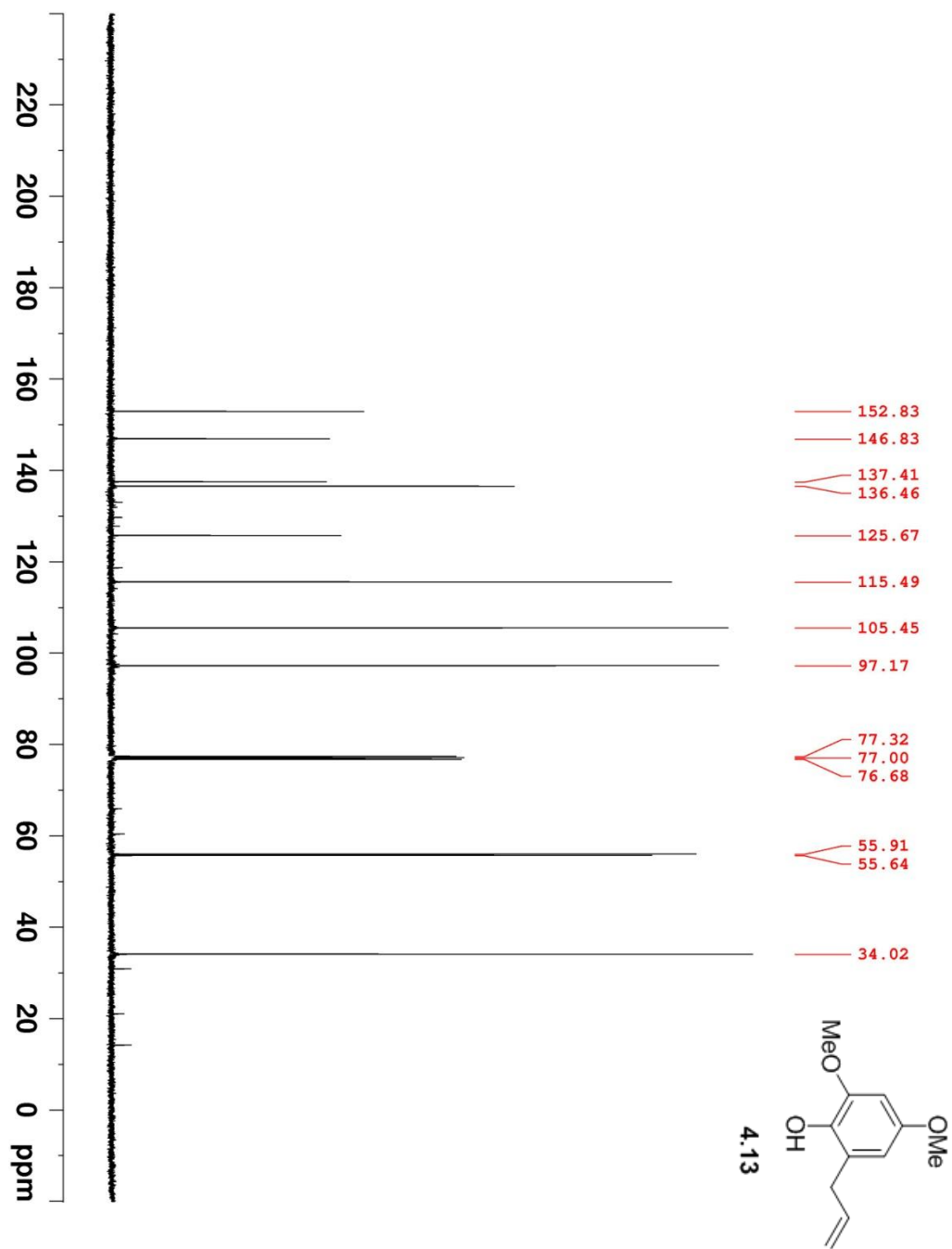


Figure A117. 100 MHz ^{13}C NMR of **4.13** in CDCl_3 .